

The background of the cover features a stylized brain composed of various colored segments (yellow, orange, red, purple, blue, green) arranged in a circular pattern. Overlaid on this brain is a network of white lines connecting small dots, representing a complex system or protein interactions. The top half of the cover has a blue background, while the bottom half is white.

# STRATEGIES AND TOOLS FOR MODULATING PATHOLOGIC PROTEIN SELF-ASSEMBLY IN PROTEINOPATHIES

EDITED BY: Gal Bitan, Sandra Macedo-Ribeiro and Maria Rosário Almeida  
PUBLISHED IN: Frontiers in Molecular Neuroscience



# frontiers

## Frontiers eBook Copyright Statement

The copyright in the text of individual articles in this eBook is the property of their respective authors or their respective institutions or funders. The copyright in graphics and images within each article may be subject to copyright of other parties. In both cases this is subject to a license granted to Frontiers.

The compilation of articles constituting this eBook is the property of Frontiers.

Each article within this eBook, and the eBook itself, are published under the most recent version of the Creative Commons CC-BY licence.

The version current at the date of publication of this eBook is CC-BY 4.0. If the CC-BY licence is updated, the licence granted by Frontiers is automatically updated to the new version.

When exercising any right under the CC-BY licence, Frontiers must be attributed as the original publisher of the article or eBook, as applicable.

Authors have the responsibility of ensuring that any graphics or other materials which are the property of others may be included in the CC-BY licence, but this should be checked before relying on the CC-BY licence to reproduce those materials. Any copyright notices relating to those materials must be complied with.

Copyright and source acknowledgement notices may not be removed and must be displayed in any copy, derivative work or partial copy which includes the elements in question.

All copyright, and all rights therein, are protected by national and international copyright laws. The above represents a summary only. For further information please read Frontiers' Conditions for Website Use and Copyright Statement, and the applicable CC-BY licence.

ISSN 1664-8714

ISBN 978-2-88976-711-3

DOI 10.3389/978-2-88976-711-3

## About Frontiers

Frontiers is more than just an open-access publisher of scholarly articles: it is a pioneering approach to the world of academia, radically improving the way scholarly research is managed. The grand vision of Frontiers is a world where all people have an equal opportunity to seek, share and generate knowledge. Frontiers provides immediate and permanent online open access to all its publications, but this alone is not enough to realize our grand goals.

## Frontiers Journal Series

The Frontiers Journal Series is a multi-tier and interdisciplinary set of open-access, online journals, promising a paradigm shift from the current review, selection and dissemination processes in academic publishing. All Frontiers journals are driven by researchers for researchers; therefore, they constitute a service to the scholarly community. At the same time, the Frontiers Journal Series operates on a revolutionary invention, the tiered publishing system, initially addressing specific communities of scholars, and gradually climbing up to broader public understanding, thus serving the interests of the lay society, too.

## Dedication to Quality

Each Frontiers article is a landmark of the highest quality, thanks to genuinely collaborative interactions between authors and review editors, who include some of the world's best academicians. Research must be certified by peers before entering a stream of knowledge that may eventually reach the public - and shape society; therefore, Frontiers only applies the most rigorous and unbiased reviews.

Frontiers revolutionizes research publishing by freely delivering the most outstanding research, evaluated with no bias from both the academic and social point of view. By applying the most advanced information technologies, Frontiers is catapulting scholarly publishing into a new generation.

## What are Frontiers Research Topics?

Frontiers Research Topics are very popular trademarks of the Frontiers Journals Series: they are collections of at least ten articles, all centered on a particular subject. With their unique mix of varied contributions from Original Research to Review Articles, Frontiers Research Topics unify the most influential researchers, the latest key findings and historical advances in a hot research area! Find out more on how to host your own Frontiers Research Topic or contribute to one as an author by contacting the Frontiers Editorial Office: [frontiersin.org/about/contact](http://frontiersin.org/about/contact)

# STRATEGIES AND TOOLS FOR MODULATING PATHOLOGIC PROTEIN SELF-ASSEMBLY IN PROTEINOPATHIES

Topic Editors:

**Gal Bitan**, University of California, Los Angeles, United States

**Sandra Macedo-Ribeiro**, Universidade do Porto, Portugal

**Maria Rosário Almeida**, Universidade do Porto, Portugal

**Citation:** Bitan, G., Macedo-Ribeiro, S., Almeida, M. R., eds. (2022). Strategies and Tools for Modulating Pathologic Protein Self-Assembly in Proteinopathies. Lausanne: Frontiers Media SA. doi: 10.3389/978-2-88976-711-3

# Table of Contents

- 05    *Prionoid Proteins in the Pathogenesis of Neurodegenerative Diseases***  
Cameron Wells, Samuel E. Brennan, Matt Keon and Nitin K. Saxena
- 29    *Design of a New [PSI<sup>+</sup>]-No-More Mutation in SUP35 With Strong Inhibitory Effect on the [PSI<sup>+</sup>] Prion Propagation***  
Lavrentii G. Danilov, Andrew G. Matveenko, Varvara E. Ryzhkova, Mikhail V. Belousov, Olga I. Poleshchuk, Daria V. Likholetova, Petr A. Sokolov, Nina A. Kasyanenko, Andrey V. Kajava, Galina A. Zhouravleva and Stanislav A. Bondarev
- 43    *Targeting Alpha-Synuclein as a Therapy for Parkinson's Disease***  
Carroll Rutherford Fields, Nora Bengoa-Vergniory and Richard Wade-Martins
- 57    *ZPD-2, a Small Compound That Inhibits  $\alpha$ -Synuclein Amyloid Aggregation and Its Seeded Polymerization***  
Samuel Peña-Díaz, Jordi Pujols, María Conde-Giménez, Anita Čarija, Esther Dalfo, Jesús García, Susanna Navarro, Francisca Pinheiro, Jaime Santos, Xavier Salvatella, Javier Sancho and Salvador Ventura
- 69    *Untangling the Conformational Polymorphism of Disordered Proteins Associated With Neurodegeneration at the Single-Molecule Level***  
Melissa Birol and Ana M. Melo
- 79    *Oligomers Are Promising Targets for Drug Development in the Treatment of Proteinopathies***  
Oxana V. Galzitskaya
- 86    *Protein Aggregation and Dysfunction of Autophagy-Lysosomal Pathway: A Vicious Cycle in Lysosomal Storage Diseases***  
Antonio Monaco and Alessandro Fraldi
- 94    *CNS-Derived Blood Exosomes as a Promising Source of Biomarkers: Opportunities and Challenges***  
Simon Hornung, Suman Dutta and Gal Bitan
- 110    *Islet Amyloid Polypeptide: A Partner in Crime With A $\beta$  in the Pathology of Alzheimer's Disease***  
Ana F. Raimundo, Sofia Ferreira, Ivo C. Martins and Regina Menezes
- 124    *Substrate–Enzyme Interactions in Intramembrane Proteolysis:  $\gamma$ -Secretase as the Prototype***  
Xinyue Liu, Jing Zhao, Yingkai Zhang, Iban Ubarretxena-Belandia, Scott Forth, Raquel L. Lieberman and Chunyu Wang
- 139    *Therapeutic Approaches Targeting Protein Aggregation in Amyotrophic Lateral Sclerosis***  
Ravinder Malik and Martina Wiedau
- 145    *Targeting Amyloidogenic Processing of APP in Alzheimer's Disease***  
Jing Zhao, Xinyue Liu, Weiming Xia, Yingkai Zhang and Chunyu Wang
- 162    *Modulation of  $\beta$ -Amyloid Fibril Formation in Alzheimer's Disease by Microglia and Infection***  
Madeleine R. Brown, Sheena E. Radford and Eric W. Hewitt



**178** ***MIRRAGGE – Minimum Information Required for Reproducible AGGregation Experiments***

Pedro M. Martins, Susanna Navarro, Alexandra Silva, Maria F. Pinto, Zsuzsa Sárkány, Francisco Figueiredo, Pedro José Barbosa Pereira, Francisca Pinheiro, Zuzana Bednarikova, Michał Burdukiewicz, Oxana V. Galzitskaya, Zuzana Gazova, Cláudio M. Gomes, Annalisa Pastore, Louise C. Serpell, Rostislav Skrabana, Vytautas Smirnovas, Mantas Ziaunys, Daniel E. Otzen, Salvador Ventura and Sandra Macedo-Ribeiro

**196** ***Modulation of the Mechanisms Driving Transthyretin Amyloidosis***

Filipa Bezerra, Maria João Saraiva and Maria Rosário Almeida



# Prionoid Proteins in the Pathogenesis of Neurodegenerative Diseases

Cameron Wells, Samuel E. Brennan, Matt Keon and Nitin K. Saxena\*

*Iggy Get Out, Neurodegenerative Section, Darlinghurst, NSW, Australia*

There is a growing body of evidence that prionoid protein behaviors are a core element of neurodegenerative diseases (NDs) that afflict humans. Common elements in pathogenesis, pathological effects and protein-level behaviors exist between Alzheimer's Disease (AD), Parkinson's Disease (PD), Huntington's Disease (HD) and Amyotrophic Lateral Sclerosis (ALS). These extend beyond the affected neurons to glial cells and processes. This results in a complicated system of disease progression, which often takes advantage of protective processes to promote the propagation of pathological protein aggregates. This review article provides a current snapshot of knowledge on these proteins and their intrinsic role in the pathogenesis and disease progression seen across NDs.

**Keywords:** prion, prionoid, neurodegenerative disease, Alzheimer's disease, Parkinson's disease, amyotrophic lateral sclerosis, Huntington's disease

## OPEN ACCESS

### Edited by:

Sandra Macedo-Ribeiro,  
University of Porto, Portugal

### Reviewed by:

Joern R. Steinert,  
University of Leicester,  
United Kingdom  
Alberto Rábano,  
Fundacion Centro De Investigacion  
De Enfermedades Neurologicas,  
Spain

### \*Correspondence:

Nitin K. Saxena  
nitin.saxena@bigpond.com

**Received:** 20 August 2019

**Accepted:** 23 October 2019

**Published:** 12 November 2019

### Citation:

Wells C, Brennan SE, Keon M and  
Saxena NK (2019) Prionoid Proteins  
in the Pathogenesis of  
Neurodegenerative Diseases.  
*Front. Mol. Neurosci.* 12:271.  
doi: 10.3389/fnmol.2019.00271

## INTRODUCTION

Neurodegenerative diseases (NDs) are a range of debilitating conditions, predominantly involving the gradual loss of function and death of cells in the central and peripheral nervous system. Most neurons are incapable of reproducing to replace lost cells, so this damage is often cumulative and permanent. Prionoid disorders are a class of NDs characterized by protein aggregates which propagate *via* template-directed misfolding. Many prominent NDs are now believed to have a basis in prionoid pathology, including Alzheimer's Diseases (AD), Parkinson's Disease (PD), Huntington's Disease (HD) and Amyotrophic Lateral Sclerosis (ALS). Although these diseases express varied etiology and pathology, each demonstrates the degeneration of neurons and gradual loss of neural functions. However, the specific neurons targeted and functions lost vary between diseases. Despite extensive research, our understanding of prionoid disease processes remains limited, and as of today, we have few effective treatments and no cures.

The study of prionoid disorders began with the identification of prions by Prusiner (1982), following decades of study into what had been previously referred to as "slow viruses" (Prusiner, 1982). His research brought several such diseases to the fore, beginning with Scrapie in sheep and later progressing to human prion protein (PrP). He identified prions as a self-templating amyloidogenic state of a normal cellular protein which served as an infectious pathogenic agent (Prusiner, 1994). These represented a novel form of pathology defined not solely by their genetic code, but by the abnormal conformations they take on and confer upon normally ("natively") folded proteins.

The distinction between prions and prionoid proteins has long been a subject of academic discussion. Arguments have been made for various classification and naming conventions, yet no formal conclusion has been reached (discussed in Harbi and Harrison, 2014; Eraña, 2019). In this article, we will use the term “prionoid” to refer to proteins that display prionoid altered states in which they are capable of template-based self-replication and propagation between cells, but which have not demonstrated transmission between individuals.

In this review article, we summarize the current knowledge on prionoid protein disorders. We highlight the underlying mechanisms by which their intercellular transfer is mediated, resulting in pathologic neurodegenerative changes, as well as several proteins involved in neurodegenerative prionoid pathologies. We will specifically explore prionoid mechanisms in the pathologies and pathogenesis of AD (amyloid precursor protein, APP and Tau), HD (Huntingtin, Htt), PD ( $\alpha$ -synuclein), and ALS [Fused in Sarcoma (FUS), Superoxide Dismutase 1 (SOD1), and TAR DNA-Binding Protein 43 (TDP-43)].

## PRIONOID PROTEINS

Prionoid proteins are defined by their ability to misfold into at least one pathological conformation which can be transmitted to native forms of the protein. This templating function has been proposed to be facilitated by the exposure of hydrophobic amino acid side chains that are normally buried in the interior of the protein (Prusiner, 1998; Prusiner et al., 1998). Misfolded prionoid proteins share structures rich in  $\beta$ -sheets, polypeptide structures which render the proteins prone to forming aggregates comprised of protein fibrils (Cushman et al., 2010). These facilitate the development of intracellular aggregates that develop into stable inclusion bodies through the recruitment of native proteins. At the same time, extracellular fibrils can enter and seed aggregation in other cells, enabling intercellular transmissibility.

The specific mechanisms of activity vary between disorders, but they all ultimately lead to the death of a specific set of neurons in the brain. Disentangling the symptoms resulting from loss- or gain-of-function is often difficult, as the major function gained (prionoid protein misfolding) is often accompanied by loss of function (Allison et al., 2017). Leighton and Allison (2016) recently reviewed gain and loss of function mechanisms in AD, HD and ALS. In general, gain-of-function mechanisms include autophagic activation, aggregation, axonal dysfunction, and cellular stress, while loss-of-function entails protein sequestration, synaptic dysfunction and DNA damage. Some symptoms could be the result of either loss- or gain-of-function, such as denervation, mitochondrial dysfunction, excitotoxicity, and oxidative stress.

Immune responses such as the activation of glial cells are an early factor in many prionoid diseases and remain activated for an extended period of time (Sapp et al., 2001; Iannaccone et al., 2012; Liao et al., 2012; Kim et al., 2018). However, these processes are often ineffective, and prionoid proteins linger despite the ongoing activity of autophagic pathways. In the long term, this can result in a shift from a neuroprotective to a persistent neurotoxic environment. This serves to both impede

pathological aggregate clearance and to exert neurotoxic effects (Liddel et al., 2017). It appears likely that the disruption of the neuroprotective-neurotoxic equilibrium through extended immune activation plays a key role in the pathological effects of prionoid disorders.

## PRIONOID NEURODEGENERATIVE DISORDERS AFFLICTING HUMANS

### Alzheimer's Disease (AD)

AD is a neurodegenerative disorder characterized by progressive dementia, developing from subtle memory loss to severe memory loss and behavioral changes. This is caused by the progressive loss of synapses followed by the loss of neurons, particularly in regions of the brain involved in memory. These include the hippocampus, amygdala, entorhinal cortex, parahippocampal region, temporal pole and temporal lobe (Ramos Bernardes da Silva Filho et al., 2017). Most cases are sporadic (cause unknown), although there are rare inherited forms that result from mutations. These mutations are typically associated with the gene encoding APP or in presenilin 1 or 2, enzymes that contribute to the cleaving of APP into A $\beta$ , both of which increase production of A $\beta$  (Selkoe, 2001). The other significant genetic factor is apolipoprotein E (ApoE), with the  $\epsilon$ 4 and  $\epsilon$ 2 alleles increasing and decreasing AD risk respectively (Liu et al., 2013).

There are two major aggregates of prionoid proteins implicated in AD. These are extracellular neuritic plaques composed of amyloid- $\beta$  (A $\beta$ ) peptides and intracellular neurofibrillary tangles (NFTs), cytoplasmic inclusion bodies rich in a hyperphosphorylated form of the tau protein.

### Amyloid- $\beta$

A $\beta$  is a small peptide of 39–42 amino acids in length that is ubiquitously expressed in the central nervous system (CNS). It is formed by the cutting of APP by the enzymes  $\beta$ -secretase (BACE1) and  $\gamma$ -secretase in the membranes of neurons. While not well understood, APP and its isoforms have a broad array of functional roles outside of pathology, including involvement in synaptic plasticity and synaptogenesis, learning and memory, gene transcription and neuroprotection (reviewed in Hiltunen et al., 2009).

A $\beta$  fibrils are toxic to mature neurons at high concentrations, causing dendritic and axonal retraction followed by cell death (Yankner et al., 1990). A $\beta$  fibrils are rapidly cleared from the brains of healthy individuals, with a half-life between 1 and 2.5 h (Savage et al., 1998). However, this clearance is impeded in AD, with A $\beta$  aggregates demonstrating the ability to impair the activity of the ubiquitin-proteasome system (Almeida et al., 2006; Mawuenyega et al., 2010). Varying levels of neurotoxicity are expressed by conformationally different forms of A $\beta$  (Petkova et al., 2005). While A $\beta$ 40 (the peptide form ending at position 40 of APP) is drastically more abundant in the CSF, A $\beta$ 42 is either the major or sole component of neuritic plaques (Miller et al., 1993; Iwatsubo et al., 1994; Gravina et al., 1995). Overexpression of A $\beta$ 40 alone in transgenic mice does not lead to the formation of insoluble aggregates, and mixed aggregates develop more

slowly than those containing A $\beta$ 42 alone (McGowan et al., 2005; Lei and Zhefeng, 2013). As the A $\beta$ 42 variant is significantly more toxic and prone to the formation of amyloid fibrils, this abundance is likely to play a role in AD pathogenesis (Phillips, 2019).

However, it is unlikely that neuritic plaques alone cause AD pathology. Multiple studies have shown a lack of direct correlation between plaque numbers and locations and AD-related damage (Arriagada et al., 1992; Gómez-Isla et al., 1997). He et al. (2018) recently proposed a model of AD pathology in which A $\beta$  is necessary, but not itself a driver of pathological mechanisms. Instead, it creates an environment that promotes seeded tau pathology, and facilitates the accumulation of endogenous tau within nearby dystrophic axons. This increases fibrillization, which becomes a source of secondary tau seeds which can translocate *via* axons and spread pathology through iterative cycles of tau amplification.

A recent study into somatic recombination of APP identified a multitude of sequence variants of this gene, some of which were associated with AD pathogenesis. This study also revealed that AD brains contain three to five times more genetic variants than normal brains (Lee et al., 2018). This increase in variability may contribute to the variety of A $\beta$  isoforms, inhibiting therapeutic activities targeted at only a portion of the A $\beta$  population. Furthermore, it may result in proteins that are significantly more likely to aggregate and contribute to prionoid pathology. This may also contribute to the age-associated increase in AD, as the number of somatic genomic variants likewise increases with age.

## Tau

Tau is a natively unfolded, soluble phosphoprotein. It is a major microtubule-associated protein (MAP) in mature neurons, interacting with tubulin to stabilize microtubules and promote microtubule assembly in the brain (Weingarten et al., 1975; Goedert and Spillantini, 2006). Tau localizes predominantly to axons and neuropil and is not observed in glia (Binder et al., 1985; Trojanowski et al., 1989).

Phosphorylation is integral to the regulation of proper tau function. However, while tau from healthy brains has a ratio of three moles of phosphate: one mole of protein, AD brains have a significantly higher ratio of 8:1 (Köpke et al., 1993). This hyperphosphorylation appears to be a major pathological change in AD, enabling tau to dissociate from microtubules. This both increases tau's mobility and enables it to take on an oligomeric intermediary stage and the fibrillar form which aggregates in NFTs (Grundke-Iqbal et al., 1986). However, these changes do not diminish the levels of soluble cytosolic tau. An overall eightfold increase in hyperphosphorylated tau was reported, suggesting dramatically increased tau production during the course of AD (Khatoon et al., 1992). Furthermore, hyperphosphorylated (but not fibrillar) tau inhibits rather than promotes microtubule assembly by sequestering normal brain tau and microtubule-associated protein 2 (MAP2; Alonso et al., 1994, 2006; Li et al., 2007). This suggests that loss-of-function may be a major pathological process in AD, dramatically reducing the brain's capacity for intracellular transport organelles and cell division.

NFTs spread in an anatomically orderly manner throughout the brain over the course of AD, typically projecting in an anterograde direction from the hippocampus and associated regions (Braak and Braak, 1997; Delacourte et al., 2002; Lace et al., 2009). The majority of the tau fibers which comprise NFTs are coiled helical structures referred to as paired helical filaments (PHFs), although straight filaments also occur (Braak et al., 1986). NFTs emerge in the entorhinal cortex, subiculum of the hippocampal formation and the amygdala early in the disease process. The number of tangles in the neocortex has been positively correlated with disease severity, accumulating in a consistent pattern reflecting the vulnerability of specific areas to AD pathology (Arriagada et al., 1992). However, the neuronal loss does exceed tangle formation by a significant margin, suggesting that it is not the sole contributing factor (Gómez-Isla et al., 1997).

A growing body of evidence suggests that the pre-fibrillar aggregates composed of the oligomeric form of tau have a more significant toxic role, with NFTs being unnecessary for pathology (reviewed in Shafiei et al., 2017). In fact, a transgenic mouse model of human tau demonstrated increased survival in aggregation-prone tau (d'Orange et al., 2018). This suggests a neuroprotective role in which sequestration of neurotoxic oligomeric tau mitigates its damaging effects.

## Parkinson's Disease (PD)

PD manifests as a progressive reduction in conscious muscle control, leading to trembling, stiffness, slowness of movement and a loss of fine motor control. This is caused by selective, progressive degeneration of dopamine-producing neurons in the substantia nigra (Trétiakoff, 1919). Most cases of PD are idiopathic, however, mutations in several genes including the SNCA and parkin genes have been linked with familial forms of the disease.

A current major hypothesis suggests that aggregates develop in the brain stem and anterior olfactory structures several years before the involvement of the substantia nigra. They then propagate along the long unmyelinated axon pathways from the olfactory system and gut, leading to disruption of smell, vagal nerve function and sleep (Braak et al., 2004; Hawkes et al., 2007). However, there have been some observations of some variance in susceptibility of brain regions, temporal order and anatomical distribution, resulting in some opposition to this theory (Burke et al., 2008).

The signature lesions of PD are two types of aggregates in the cytoplasm of dopaminergic neurons; Lewy Bodies (LBs) and Lewy Neurites (LNs). Amyloid forms of ubiquitinated and hyperphosphorylated  $\alpha$ -synuclein are the most abundant protein in LBs and LNs (Uversky, 2007; Braak and Del Tredici, 2008b). These aggregates develop in the cell body and neuronal processes respectively, and form a considerable time prior to the appearance of somatomotor dysfunction (Uversky, 2007). LBs and LNs exhibit a predictable, ascending pattern of progression, suggesting axodendritic transfer between anatomically connected brain regions (Braak and Del Tredici, 2008a). LBs are significantly more abundant in sporadic PD than they are in familial PD (Kotzbauer et al., 2004).

## $\alpha$ -Synuclein

$\alpha$ -synuclein is a small, natively unfolded presynaptic protein. While its precise physiological functions are unknown, it interacts with multiple proteins, lipids, and membranes. It has been suggested to have roles in synaptic maintenance and neurotransmitter release, especially of dopamine (Maroteaux et al., 1988; Clayton and George, 1999; Abeliovich et al., 2000). The absence of  $\alpha$ -synuclein does not significantly impede survival but does suggest that the protein is an essential negative regulator of dopamine neurotransmission (Abeliovich et al., 2000).

The expression of  $\alpha$ -synuclein in PD varies between brain regions. Most  $\alpha$ -syn expression is in the cytosol of excitatory neurons in brain regions affected early in PD such as the olfactory bulb, the dorsal motor nucleus of the vagus and substantia nigra pars compacta. However, some  $\alpha$ -synuclein has been observed in inhibitory synapses of the external plexiform layer of the olfactory bulb, the lateral and medial globus pallidus and the substantia nigra pars reticulata (Taguchi et al., 2016).

Both wild-type and pathological variants of  $\alpha$ -synuclein form amyloid-like fibrils upon prolonged incubation in solution, although the pathological form does so at a higher rate (Conway et al., 2000). In the process of forming these fibrils,  $\alpha$ -synuclein takes on oligomeric forms which later develop into spherical, ring-like and string-like intermediate forms, collectively known as protofibrils. These are soluble structures which gradually coalesce into insoluble fibrils, forming  $\alpha$ -synuclein aggregates. There is evidence that these soluble oligomers are the source of neurotoxicity in PD, disrupting cellular homeostasis and mediating neuronal death (reviewed in Stefanis, 2012). However, it has been noted that even if inclusion bodies are not the main effector of PD pathology they may exert neurotoxic effects including blocking neuronal trafficking in axons and sequestering essential neuronal components.

There is evidence of a synergistic interaction between the Tau protein and  $\alpha$ -synuclein, as co-occurrence leads to accelerated fibrillization of both proteins (Giasson et al., 2003). However, while the proteins co-occur in the same vicinity of LNs, affected neurites typically have either tau or  $\alpha$ -synuclein, but not both (Kotzbauer et al., 2004).

## Huntington's Disease (HD)

HD is a progressive, autosomal dominant neurodegenerative disorder characterized selective neuronal cell death, primarily in the cortex and striatum, leading to motor disturbance, cognitive loss, and psychiatric issues (Vonsattel et al., 1985). The disease typically manifests clinically in people aged 40–50, with pathology worsening over 10–20 years until death.

HD inheritance is driven by mutations in the gene encoding the huntingtin (Htt) protein. The dominant mutation of interest is the repeat expansion of a CAG trinucleotide repeat. In unaffected individuals, the number of repeats varies between 6 and 39, while in individuals with HD the number increases to 36–180 (Rubinshtein et al., 1996; Mangiarini et al., 1997). This leads to the expansion of the polyglutamine (polyQ) tract, leading to the formation of amyloid-like protein aggregates (MacDonald et al., 1993; Scherzinger et al., 1997). Most adult-onset cases have

expansions ranging from 40 to 55 repeats, while expansions of 70 and above have been associated with the juvenile form of the disease (Scherzinger et al., 1997).

## Huntingtin

The function of Htt is not well understood. However, it is essential for development, with disruption resulting in embryonic death in mice (Nasir et al., 1995). N-terminal Htt has demonstrated the ability to shuttle between the cytoplasm and nucleus in a Ran GTPase-dependent manner, interacting with the nuclear export-associated translocated promoter region (Tpr) of the nuclear pore (Cornett et al., 2005). There is evidence for the involvement of Htt in both anterograde and retrograde microtubule-based axonal trafficking, with Htt-associated protein 1 (HAP1) mediating interactions between Htt, microtubule motor proteins and their co-factors (Schulte and Littleton, 2011). These functions are disrupted by the activity of mutant Htt (mHtt), resulting in impaired vesicular and mitochondrial trafficking (Trushina et al., 2004).

Htt is expressed in various parts of the body, including the colon, liver, pancreas, testes and the entirety of the brain. Within the brain, it is focussed on the neurons of the dentate gyrus and pyramidal neurons of the hippocampal formation, cerebellar granule cell layer, cerebellar Purkinje cells and pontine nuclei. While expression does occur in glial cells, the neuronal expression is significantly more prominent (Strong et al., 1993). The protein primarily localizes with vesicles and microtubules, and may function in cytoskeletal anchoring or vesicle transport (DiFiglia et al., 1995; Hoffner et al., 2002).

The expression of the normal and mutant forms of Htt has been shown to be similar in the CNS (Trottier et al., 1995). However, neuronal loss in HD has been found to vary by location. The putamen and caudate nucleus suffer the greatest losses (64 and 57%, respectively), followed by 29–34% in telencephalic white matter and 21–29% in the cerebral cortex (de la Monte et al., 1988). Decreases in the volume of the gray matter (cortex), white matter (axonal fibers) and increases in CSF all begin several years before the onset of symptoms. This change in CSF, in particular, progressed linearly and in association with the number of polyQ repeat expansions (Squitieri et al., 2009). Loss of striatal and white matter volume has been identified as much as 15 years prior to the onset of symptoms, suggesting that preventative treatments must be initiated long before diagnoses can be effectively made (Paulsen et al., 2010).

Pure polyQ segments can be folded into several distinct fiber conformations, which confer different levels of toxicity and consequently neurodegeneration (Nekooki-Machida et al., 2009). This has been used to justify a lack of correlation and in some cases negative correlation, between deposition of Htt aggregates and observed toxicity (Arrasate et al., 2004). It has been proposed that variants with extended  $\beta$ -sheets resulted in modestly toxic or nontoxic effects as a result of “buried” polyQ, which prevented interaction with, and sequestration of, free endogenous proteins (Nekooki-Machida et al., 2009).

Gain of function mechanisms such as increased levels of reactive oxygen species (ROS) and direct toxicity exerted by the polyglutamine repeat expansion appears to be the core



mechanism of pathological toxicity in HD (reviewed in Imarisio et al., 2008). However, this is not likely caused by aggregate formation. Cells with Htt inclusions have, in fact, demonstrated improved survival compared to those without (Arrasate et al., 2004). It may be that aggregates are a protective measure, sequestering toxic oligomers to prevent further cellular damage. A more accurate predictor of neuronal death appears to be levels of diffuse Htt, with several studies arguing that soluble oligomeric forms of polyQ-expanded Htt are the source of HD toxicity (Leitman et al., 2013; Kim et al., 2016). Htt aggregates may instead play a role in toxicity through loss of function mechanisms. While wild-type Htt inhibits excitotoxic neurodegeneration, possibly through the binding of apoptosis-mediator caspase-3 (Leavitt et al., 2006), pathological mutant forms of Htt have been associated with a reduced binding affinity for caspase-3. This can either directly lead to or increase vulnerability to cell death (Zhang et al., 2006). In addition, there is evidence of proteasome sequestration within Htt and polyQ aggregates, facilitating pathology through the inhibition of cellular clearance processes (Holmberg et al., 2004).

## Amyotrophic Lateral Sclerosis (ALS)

ALS is a neurodegenerative disorder characterized by progressive degeneration of muscle function. Symptoms typically involve a combination of lost voluntary muscle control and uncontrolled spasms, with death commonly arising from respiratory failure. In most cases, degeneration is relatively constant until death. Molecular changes have been observed to occur prior to the development of physical symptoms, suggesting that denervation is a more direct symptom of the ALS disease process than cell death (Bertrand et al., 2018).

ALS is atypical in that multiple prionoid proteins have been associated with the disorder, independent from one another. Familial ALS (fALS) has been associated with FUS and SOD1 aggregates. Sporadic ALS (sALS) is predominantly linked to aggregates of TDP-43 and T-cell-restricted intracellular antigen-1 (TIA1). In almost all studies, the accumulation of FUS and TDP-43 in cytoplasmic inclusions has been shown to be mutually exclusive (Mackenzie et al., 2010). This suggests the presence of at least two independent disease pathways.

FUS, TDP-43 and TIA1 each have a “prion-like domain” (PLD). These are low-complexity sequences found in the genetic code of RNA-binding proteins. These sequences are enriched in glycines and uncharged polar amino acids such as asparagine, glutamine, and tyrosine (Couthois et al., 2011; Hennig et al., 2015). They are in either the N- or C-terminals of the protein (the start and end of an amino acid chain respectively). Many genes that encode PLD-containing proteins are essential in mammals, typically having roles in RNA processing (March et al., 2016). Aggregates of RNA-binding proteins are involved in various stages of mRNA processing, storage, and decay. PLDs allow these proteins to “functionally aggregate,” forming higher-order assemblies and cytoplasmic foci such as P-bodies and stress granules (SGs; Gilks et al., 2004; Buchan et al., 2008; Toretzky and Wright, 2014). However, these same aggregates can cause severe cellular damage if protein quality control mechanisms are disrupted, allowing them to propagate unchecked.

## Fused in Sarcoma (FUS)

FUS is an RNA-binding protein that shuttles between the nucleus and cytoplasm (Zinszner et al., 1997). It has functions in transcriptional regulation, RNA homeostasis and rapidly appears at sites of DNA damage, suggesting a role in DNA repair (Bertoletti et al., 1996; Kasyapa et al., 2005; Wang et al., 2013). The protein is a major component of cytoplasmic SGs and results in the co-localization of SGs to autophagosomes (Bosco et al., 2010a).

Most ALS-linked FUS mutations are clustered within the C-terminal domain. Many disrupt the nuclear import of FUS and thus promote cytoplasmic accumulation. The resultant level of cytoplasmic mislocalization has been correlated with ALS disease onset, with stronger mutations resulting in earlier disease onset and more cytoplasmic FUS (Dormann et al., 2010). Mutations in FUS have been observed in fALS and rarely sALS, accounting for 4% and 1% of cases respectively. FUS mutations result in several forms of ALS, with P525L mutations causing juvenile (the early 20s) ALS and R521C and R518K mutations causing a late-onset disease (40s–60s; Deng et al., 2014). Post-mortem tissues from patients with FUS mutations have expressed cytoplasmic aggregates containing FUS in MNs and glial cells (Kwiatkowski et al., 2009). ALS-linked variants of FUS appear to engage different RNAs than wild-type variants, which may contribute to ALS toxicity (Hoell et al., 2011).

According to a yeast model, FUS toxicity requires cytoplasmic aggregation, the presence of a prion-like N-terminal domain and binding of RNA. This suggests that toxicity may be based in the loss-of-function effects of RNA sequestration or otherwise disrupting the activities of RNA (Sun et al., 2011). Glutamine has been observed to promote the formation of toxic oligomers species, and so the high glutamine: asparagine ratio (~6:1) of the FUS PLD may contribute to the fixation of proteins into toxic forms (Halfmann et al., 2011).

## Superoxide Dismutase 1 (SOD1)

SOD1 is one of the most common genes implicated in ALS. While there is no consensus on the proportion of ALS attributed to SOD1 mutations, it is typically held to account for between 13% and 20% of familial ALS and between 0% and 7% of sporadic ALS (Andersen, 2006; Chiò et al., 2008). It is a superoxide radical-scavenging enzyme that natively converts the superoxide anion  $O_2^-$  into  $O_2$  or  $H_2O_2$ , and in doing so clears free radical by-products which cause oxidative stress. It is present in the cytoplasm and nuclei of all cell types.

In its native form, SOD1 is an extremely stable homodimer. However, most ALS-linked SOD1 mutations destabilize the protein. This makes it more likely to expose typically obscured hydrophobic surfaces, increasing vulnerability to partial unfolding and leading to the formation of pathological protein aggregates (Tiwari and Hayward, 2005; Nordlund and Oliveberg, 2008; Münch and Bertolotti, 2010). This is extremely atypical in prion and prionoid pathology, which usually involves a change from instability to stability.

The oxidation appears to be a requirement of SOD1 aggregation, with aggregates lacking oxidants failing to form aggregates at all. The only exception was zinc-deficient

SOD1, which itself produced significantly higher levels of aggregation when oxidated (Rakhit et al., 2002). Aberrant oxidation or post-translational modification of SOD1 has also been observed to promote aggregation in *in vitro* models (Rotunno and Bosco, 2013).

While the pathological activities of mutant SOD1 (mSOD1) are generally considered to have their basis in gain-of-function mechanisms, there is also evidence of lost function. Notably, almost all ALS-associated SOD1 mutations result in a decrease in SOD1 enzyme activity, and SOD1 knockout models demonstrate similar outcomes to ALS (Saccon et al., 2013). These effects include increased oxidative stress, susceptibility to neuron loss following injury and progressive motor neuron degeneration (Reaume et al., 1996; Fischer et al., 2012; Shi et al., 2014).

### TAR DNA-Binding Protein 43 (TDP-43)

TDP-43 is a highly conserved essential RNA-binding ribonucleoprotein. TDP-43 prionoid proteins express ordered, self-perpetuating aggregation transmissible from affected cells to their progeny. Their properties suggest a closer relation to yeast prions than human prion protein (PrP; Polymenidou and Cleveland, 2017).

TDP-43 is the major protein in most ALS-linked cytoplasmic inclusions (Scotter et al., 2015). Increased levels of TDP-43 mRNA have been observed in the motor neurons of both fALS and sALS patients, with TDP-43 aggregates forming in their motor cortices and spinal cords (Arai et al., 2006; Rabin et al., 2010; Qin et al., 2014). The development of TDP-43 inclusions results in increased export of TDP-43 from the nucleus to the cytoplasm, leading to a sustained decrease of nuclear TDP-43 and increased levels of stable TDP-43 mRNAs (Polymenidou and Cleveland, 2017). Upon moving into the cytoplasm, TDP-43 undergoes defective phosphorylation and conformational changes followed by ubiquitination, preventing re-entry into the nuclear compartment (Neumann et al., 2006, 2009; Ayala et al., 2008; Braak et al., 2017). Disruption of intranuclear TDP-43 expression and RNA metabolism, as well as the noxious effects of toxic TDP-43 forms, results in loss of function for affected cells (Neumann et al., 2009; Ratti and Buratti, 2016).

Mutations in TDP-43 appear to either increase aggregation propensity of TDP-43 or promote SG formation, resulting in most patients with TDP-43 mutations developing a classical ALS phenotype (Manghera et al., 2016; Polymenidou and Cleveland, 2017). Cells expressing mutant TDP-43 also form larger SGs, and are incorporated into SGs earlier, than those expressing wild-type TDP-43 (Dewey et al., 2011).

Out of more than 44 ALS-linked mutations in TDP-43, all but 3 are found in the C-terminal PLD (Da Cruz and Cleveland, 2011). Elevated expression of TDP-43 C-terminal fragments containing the PLD has resulted in increased toxicity and aggregation of cytoplasmic TDP-43 in various contexts (King et al., 2012). This suggests that the PLD plays a key role in pathological aggregate formation in ALS. However, Aggregates may also occur due to the supersaturation of TDP-43 and other proteins in MNs (Yerbury et al., 2019) which can undergo liquid-liquid phase separation in the cytoplasm, leading to the

formation of phosphorylated, insoluble aggregates regardless of whether or not mutations are present in TDP-43 (Gasset-Rosa et al., 2019). This may even be a precursor to protein misfolding and self-templating protein aggregation, but there is currently no experimental data to answer this question.

### T-Cell-Restricted Intracellular Antigen-1 (TIA1)

TIA1 is an RNA-binding protein that assembles into membrane-less organelles such as SGs. Seeded TIA1 aggregation through a PLD is a requirement of SG formation (Gilks et al., 2004). TIA1 recruits other mRNAs and proteins to SGs, including TDP-43 and FUS (Polymenidou and Cleveland, 2017). TIA1 may serve to initiate aggregation, facilitated by “scaffolding” proteins and RNA molecules (Deleault et al., 2003).

TIA1 exhibits increased mutation of its PLD in ALS patients. If these mutations are a cause of ALS, it is only in a very small minority of cases (0.5% of sALS, 2% of fALS; Mackenzie et al., 2017). A study by Mackenzie et al. (2017) studied a novel ALS/FTD family and identified the P362L mutation in the PLD of TIA1. Subsequent genetic association analyses revealed a significant increase in the burden of TIA1 PLD mutations in ALS patients relative to controls. Interestingly, the post-mortem neuropathology of five TIA1 mutation carriers clearly showed a consistent pathological signature with numerous round, hyaline, TDP-43-positive inclusions. It appears that the TIA1 mutations significantly increased the propensity of TIA1 protein to undergo phase transition. In live cells, TIA1 mutations delayed SG disassembly and promoted the accumulation of non-dynamic SGs that harbored TDP-43. Moreover, in this study the TDP-43 in SGs apparently became insoluble, impinging on its mobility. These suggest that TIA1 may have a supportive role in TDP-43 pathology, rather than functioning as a sole pathogen.

These TIA1 mutations in ALS/FTD further reinforce the intrinsic role of RNA metabolism, RNA-binding proteins, and SG dynamics in ALS/FTD pathogenesis.

## COMMON PRIONOID FEATURES

### Propagation

The Prionoids function like traditional prions, in that they require both a method of seeding template-based alteration to transform natively conformed proteins into their prionoid form (Figure 1E), and a means of transmission between host neurons (Figure 2).

In AD, it was observed that injection of pathological A $\beta$  brain extracts and homogenates into APP transgenic mice resulted in the development of associated plaques and pathology in a time- and concentration-dependent manner (Meyer-Luehmann et al., 2006). Furthermore, it was found that A $\beta$  can be transmitted between neurons directly *via* interfaces between neurites (Nath et al., 2012). Similarly, Frost et al. (2009) demonstrated that extracellular Tau aggregates, but not monomers, can transmit a misfolded state from the outside to the inside of a cell. These induce fibrillization of intracellular full-length Tau, which is by itself capable of seeding the formation of fibrils composed of recombinant Tau monomers (Friedhoff et al., 1998). Microglia have been found to package defective tau proteins into exosomes,

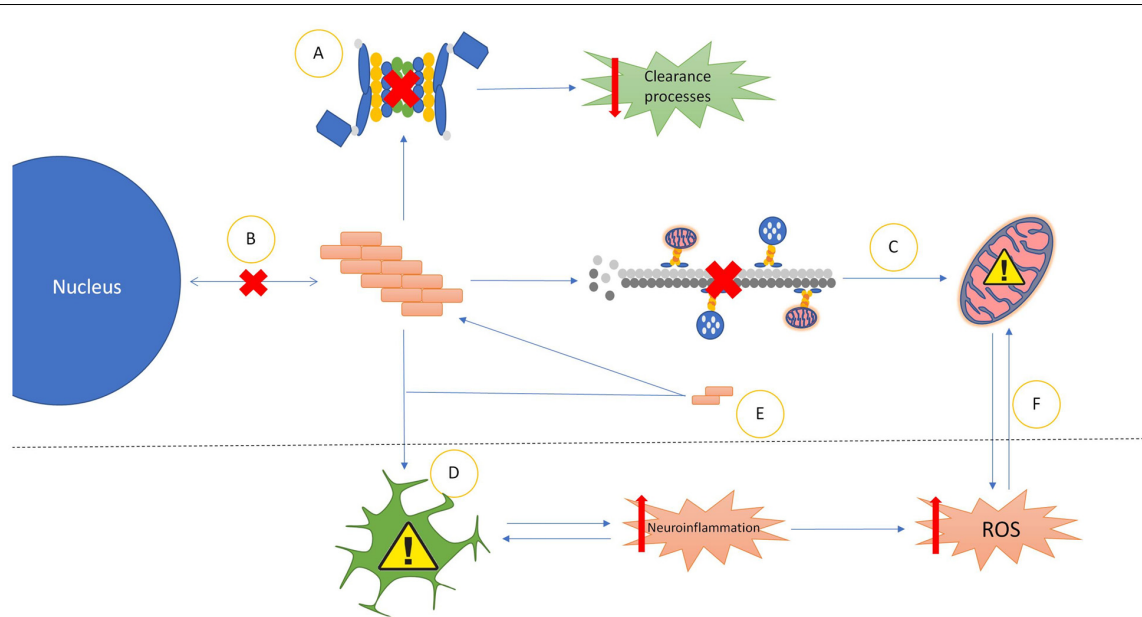


**FIGURE 1 |** Common properties of prionoid disease pathways. **(A)** Most prionoid proteins have been associated with inhibition of the cell's autophagic machinery, particularly the lysosomal autophagy and ubiquitin-proteasome systems. This results in inhibited cellular clearance processes, enabling greater accumulation of aggregates. **(B)** Aggregated proteins often mislocalize into aberrant cellular compartments. In amyotrophic lateral sclerosis (ALS), TAR DNA-binding protein 43 (TDP-43) and fused in sarcoma (FUS) mislocalize from the nucleus to the cytoplasm. Amyloid- $\beta$  in Alzheimer's diseases (AD),  $\alpha$ -synuclein in Parkinson's disease (PD) and mutant superoxide dismutase-1 (mSOD1) in ALS mislocalize into the mitochondria. In Huntington's disease (HD), Huntingtin (Htt) mislocalizes into the nucleus. **(C)** Many Neurodegenerative Disease (ND) processes involve the disruption of microtubule-mediated transport of various cellular components, particularly mitochondria. This often results in incorrect distribution of mitochondria, enhancing mitochondrial dysfunction. **(D)** Glial cells exert various neurotoxic and neuroprotective effects. In NDs these are often either insufficient to control pathological processes or subverted to enhance pathological spread or severity. The most common mechanism of this is increased neuroinflammatory activity, leading to the production of high levels of neurotoxic reactive oxygen species (ROS). The resultant oxidative injury enhances glial activation, compounding the effects of the pathology. **(E)** Soluble oligomeric species of prionoid proteins are often present in the cytoplasm of infected cells. While typically incapable of seeding aggregates, they are recruited to aggregates in order to accelerate their growth. There is evidence that oligomeric prionoids exert neurotoxic effects. Oligomers may contribute to the spread of pathology through uptake by microglia after being exocytosed. **(F)** Dysfunction in mitochondria leads to increased production of neurotoxic ROS. The downstream effects of ROS activity can damage mitochondria, resulting in a self-reinforcing cycle.

nanoscale vesicles secreted by all mammalian cells. While these can act to limit aggregate accumulation within cells, they can also transport the infectious proteins between adjacent brain areas, accelerating the spread of pathological proteins (Asai et al., 2015).

In PD, intracellular transmission of  $\alpha$ -synuclein fibrils, but not monomers, can also seed the formation of LB-like aggregates, actively recruiting and converting soluble endogenous  $\alpha$ -synuclein in the cytoplasm into a misfolded state (Luk et al., 2009). There is evidence that  $\alpha$ -synuclein is secreted into extracellular space by atypical exocytosis processes as a normal part of the protein's life cycle, independent of any pathological processes. However, the amount secreted is elevated in response to cellular defects associated with PD pathogenesis, such as proteasomal and mitochondrial dysfunction. Both monomeric and aggregated  $\alpha$ -synuclein are secreted in this manner (Lee et al., 2005). The internalization of this extracellular  $\alpha$ -synuclein may contribute to the spread of PD, as internalized material seeds aggregation of endogenous  $\alpha$ -synuclein (Hoffmann et al., 2019). However, there is some debate as to the precise mechanism involved in this internalization. Proposed mechanisms include endocytosis, micropinocytosis, and cell surface protein-mediated uptake (reviewed in Rodriguez et al., 2018).

Large, internalized aggregates of Htt polyQ have been observed to bind to cell plasma membranes in culture, forming nuclei that selectively recruit soluble cytoplasmic proteins. These aggregates persist when cells divide, resulting in a heritable, self-sustaining seeding and fragmentation process (Ren et al., 2008). There is also experimental evidence that mHtt may be transmitted across synapses based on transgenic mouse and fly models (Pecho-Vrieseling et al., 2014; Babcock and Ganetzky, 2015). Transmitted Htt can either recruit endogenous Htt monomers and oligomers to propagate seeded aggregation (Herrera et al., 2011) or localize to the nucleus if in possession of a nuclear localization signal. Nuclear localization often leads to cell death. Short peptides with few polyQ repeats are no less toxic than longer peptides, suggesting that the pathological role of polyQ repeats may be in aggregation efficiency rather than toxicity (Yang et al., 2002).

In ALS, both FUS and TDP-43 self-replicate through the actions of their PLDs. Evidence suggests that the C-terminal domain is integral to TDP-43's intrinsic aggregation propensity and is involved in aberrant misfolding, toxicity, recruitment into SGs and aggregate formation (Johnson et al., 2008, 2009; Dewey et al., 2011). While TDP-43 aggregate seeding



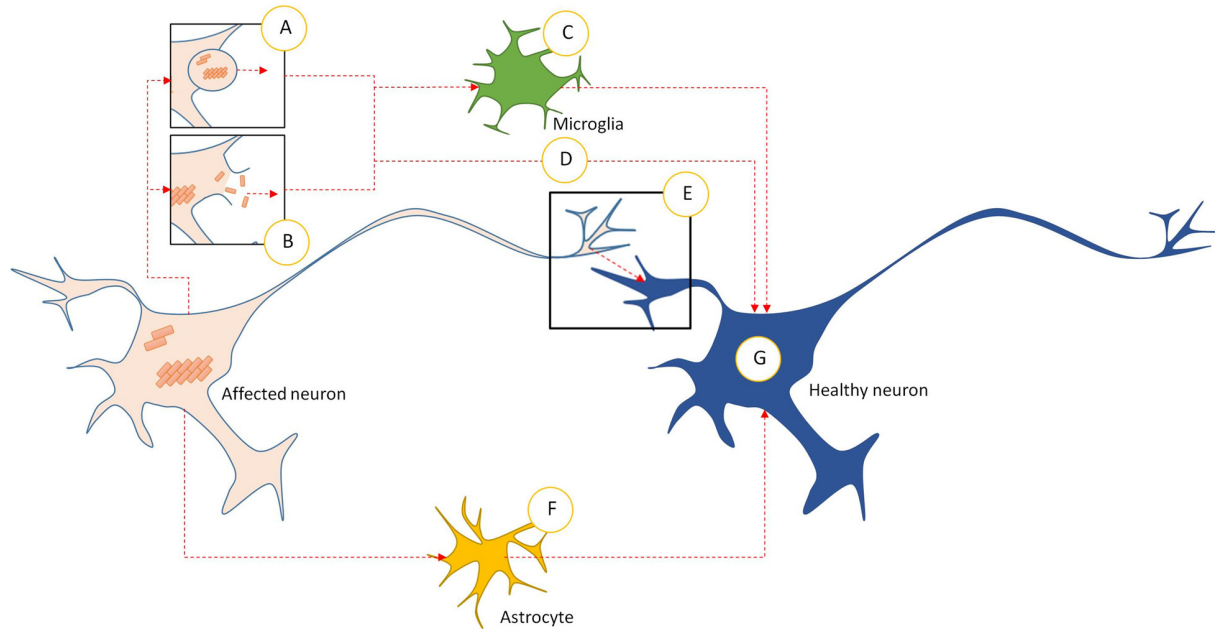


**FIGURE 2 |** Intercellular transmission pathways in prionoid NDs. **(A)** Prionoid aggregates and oligomers are released into the extracellular space through exocytosis. This can occur in normal cells, but may be accelerated during pathology. **(B)** Cell death releases aggregates and oligomers developing within the affected neuron. Some of these are capable of persisting in the extracellular space. **(C)** Microglia phagocytose extracellular aggregates and oligomers. Many pathological processes weaken enzymatic degradation processes, allowing engulfed prionoid material to persist. Some prionoids may be released, either in vesicles or following death of the microglia, facilitating infection of neighboring cells. **(D)** Extracellular aggregates and oligomers can be taken into healthy neurons by unconfirmed processes. These include endocytosis, micropinocytosis and protein-mediated uptake. **(E)** Prionoid material can be transmitted directly across synapses. Alternatively, tunneling nanotubes may facilitate direct transmission between neurons. **(F)** Prionoid material can be internalized by astrocytes, possibly at the synapse or through tunneling nanotubes. Aggregation can progress within the astrocytes, or prionoid material can be transferred to healthy neurons through tunneling nanotubes. **(G)** Once prionoid material has entered a healthy neuron, it can seed pathological aggregation. Aggregates may seed conformational changes in natively conformed proteins, while oligomers may either accelerate the growth of seeded aggregates or infect functional amyloid aggregates.

appears to be mediated by the presence of an RNA scaffold (Deleault et al., 2003), FUS aggregate formation requires both the N-terminal PLD and a C-terminal RGG (glycine-arginine rich) domain. This suggests a more complex, multi-domain process than is observed in TDP-43 pathology (Gitler and Shorter, 2011; Sun et al., 2011). Fibrils of both proteins can seed aggregation *in vitro*, allowing aberrant misfolding and protein accumulation (Furukawa et al., 2011; Nonaka et al., 2013; Nomura et al., 2014).

mSOD1-positive aggregates in human patients and fALS mouse models have shown granule-coated fibrillar morphologies rich in  $\beta$ -sheet structures, which facilitate template-based misfolding of native SOD1 (Kato et al., 2000). In *in vitro* tests, preformed SOD1 aggregates and misfolded proteins have been shown to accelerate or seed aggregation of soluble SOD1 (Chattopadhyay et al., 2008; Chia et al., 2010; Eisenberg and Jucker, 2012). It appears likely that intercellular spread requires the release of aggregates into extracellular space, followed by internalization into other cells by macropinocytosis. This allows the internalized aggregates to seed aggregation of endogenous SOD1 (Münch et al., 2011). The ability to self-propagate through fragments of misfolded fibrils suggests that fibril breakage may be a key part of the self-propagation process (Lee and Kim, 2014).

## Strain-Like Phenomena

One of the most vexing aspects of prionoid pathologies for researchers is the broad range of clinical manifestations which they can produce. While broad categories of symptoms can be sketched out, each case is, for the purposes of medicine, functionally unique. Individuals vary in clinical symptoms, clinical progression, properties and behaviors of aggregates and even brain region specificity. ALS is possibly the best example of this, with multiple accepted and several controversial subtypes based on such factors as the location and age of onset of neurodegeneration and the presence or absence of cognitive symptoms (reviewed in Siddique and Siddique, 2019). Even the definitive boundaries of disorders can be somewhat unclear, as evidenced by the debate as to whether ALS and frontotemporal dementia, a cognitive disorder, share the same disease spectrum.

While there are many hypotheses for the variability of prionoid diseases, one of the most prominent is what we refer to as the “strain hypothesis.” This posits that, much like traditional diseases, prionoid disorders possess sub-species variations. However, rather than being genetic in nature, these variations exist in the conformational states of the prionoid proteins. This results in a broad range of pathological effects despite ostensibly similar aggregates structures. Studies have

observed the presence of such “conformational strains” in aggregates composed of A $\beta$ , tau,  $\alpha$ -synuclein and TDP-43.

A $\beta$  deposits have demonstrated a high level of heterogeneity. Pathological aggregates have been found to form dense-core plaques, diffuse deposits, cerebral amyloid angiopathies, inert deposits, and intracellular aggregates, replicating these conformations in recruited native proteins (Carlo and Stöehr, 2018). While no clear structural predominance has been identified on a population scale, within individuals the non-pathological A $\beta$ 40 isoform has a tendency for one conformation to dominate. Interestingly, pathological A $\beta$ 42 is more structurally heterogeneous and lacks a dominant species (Qiang et al., 2017). There is clear evidence for structural divisions between some pathological subspecies, with rapid-progressing AD possessing distinct A $\beta$ 42 particles that differ in size, display of N-terminal and C-terminal domains, and conformational stability (Cohen et al., 2015). Similarly, there is evidence for structural variance between familial and sporadic AD. FAD patients with mutations in the APP gene were found to test negative to the amyloid-specific PET probe Pittsburgh compound B (PiB), commonly used to detect A $\beta$  in sAD, despite post-mortem analysis showing cerebral amyloid deposits (Scialò et al., 2019).

Studies of tau have provided even greater evidence for this, with Kaufman et al. (2016) identifying and characterizing 18 different tau strains in a cell culture model. Each of these strains resulted in different cellular pathologies when used to inoculate transgenic mice, with distinct cell types and brain regions targeted and different rates of network propagation. There is evidence that different tau fibril types cause part of this variability, resulting in different conformations when grown on fibrils of homogenous or heterogenous 3R or 4R tau isoforms (Soto and Pritzkow, 2018). However, AD has been found to show the highest level of homogeneity when compared to other tauopathies, possible due to the relative predominance of the isoform expressing a 1:1 ratio of 3R and 4R tau (Sanders et al., 2014).

Research into  $\alpha$ -synuclein has found that different environmental factors can alter conformations, such as reduced concentrations of salts causing a change from cylindrical to twisted, ribbon-like structures (Bousset et al., 2013). Truncation of the N-terminal or C-terminal domain can likewise result in conformational differences in  $\alpha$ -synuclein (Guo et al., 2013). Specific conformational strains can also be produced by posttranslational modification, as shown with phosphorylation of serine 129. Phosphorylated fibers demonstrated different morphology compared to wild-type fibers and exerted higher levels of toxicity. However, phosphorylation of other fibers did not lead to changes in fibril morphology, suggesting the involvement of serine 129 in suppressing toxicity (Ma et al., 2016).

We were unable to find significant evidence for conformational strains in HD, although this does not preclude the existence of such phenomena.

While there is a great deal of speculation regarding conformational subtype in ALS due to the broad range of clinical manifestations, this remains mostly conjecture. Tsuji

et al. (2012) demonstrated differing patterns of expression in insoluble material extracted from ALS brain samples through immunoblotting of protease-resistant fragments from three FTL-ALS subtypes. Nonaka et al. (2013) found that transfected cells from brains with specific histopathological subtypes templated the same properties onto wild-type TDP-43, although this was not confirmed to be based on conformational changes. A study into peptide variations also demonstrated some variability, demonstrating that seeding aggregates with different TDP-43 peptides resulted in different phosphorylated C-terminal fragments of TDP-43 and different trypsin-resistant bands. These results were interpreted as suggesting that the variability in TDP-43 peptides allowed them to induce various pathologies, ultimately functioning in a manner similar to prion strains (Shimonaka et al., 2016).

## Persistence and Disrupted Clearance of Protein Aggregates

The formation of misfolded proteins is a normal component of physiological function. As a result, cells possess innate “quality control” mechanisms that either eliminate proteins before aggregation or clear aggregates after they have formed. Schubert et al. (2000) calculated that around one-third of newly synthesized eukaryote proteins were degraded due to misfolding or improper assembly within minutes of synthesis. A growing body of evidence indicates that a core issue in prionoid pathologies is a disruption of this balance, resulting in more misfolded proteins being produced than can be degraded.

Many, but not all, prionoid aggregates are extraordinarily difficult to degrade. This is likely a result of  $\beta$ -sheet structures, sheets of hydrogen-bonded  $\beta$ -strands which are common secondary structures in pathological aggregates (Tyedmers et al., 2010).

The autophagy-lysosome pathway is the key mechanism by which cells actively degrade misfolded proteins and damaged organelles. Macroautophagy (commonly referred to as simply “autophagy”) is a key subset of this. It involves sequestering cytoplasmic materials into double-membraned autophagosome vesicles and fusing them with lysosomes, in which they undergo enzymatic degradation (Ramesh and Pandey, 2017). Several studies have been conducted into autophagy inhibition in the absence of disease-linked mutations, producing symptoms markedly similar to prionoid NDs (Hara et al., 2006; Komatsu et al., 2006; Filimonenko et al., 2007). These include loss of neurons in multiple regions of the brain, particularly cerebellar Purkinje cells and hippocampal pyramidal neurons, and resultant impairment of motor coordination and strength. The studies also observed time-dependent formation of cytoplasmic ubiquitin-positive inclusion bodies in neurons, similar in structure to prionoid pathological inclusions. Komatsu et al. (2006) noted similar proteasome function in healthy and degrading cells, proposing that autophagy had a more significant role in, and was more impaired in, prionoid pathologies.

There is growing evidence for a model of prionoid neurodegenerative disorders in which a primary pathological mechanism is destabilization of the balance between protein misfolding and clearance (**Figure 1A**). This enables abnormal

accumulation of aggregated proteins, enabling escalating neurotoxic effects.

Impeded enzymatic degradation has been noted in both central microglia and peripheral macrophages in AD and affects the clearance of both A $\beta$ 40 and A $\beta$ 42 fibrils (Mawuenyega et al., 2010; Lai and McLaurin, 2012). A $\beta$  accumulation in APP mutants appears to indirectly inhibit activity of the ubiquitin-proteasome system, which may lead to self-reinforcing pathological disruption of autophagy (Almeida et al., 2006). This is a possible explanation for the identification of A $\beta$  aggregates that are able to persist more than 6 months following the cessation of pathological A $\beta$  production (Jankowsky et al., 2005), as well as elevated A $\beta$  levels without a concomitant increase in protein production (Selkoe, 2001).

Inhibition of A $\beta$  and APP production in a transgenic mouse model of AD did not lead to degradation of amyloid aggregates and pools of soluble A $\beta$ 42 but did lead to a rapid decrease in the full-length APP. This resulted in significant improvements in short and long-term spatial and working memory tasks but was ineffective at recovering episodic memory and cognitive flexibility (Melnikova et al., 2013). These results suggest that several symptoms of AD depend upon the continued aggregation of misfolded proteins, while the areas which failed to recover may be affected by existing aggregates or have suffered irreparable damage from early disease processes. The latter explanation is supported by the early and severe effects of AD on areas involved in episodic memory (Gainotti et al., 1998) and cognitive flexibility (Guarino et al., 2019).

Similarly, tau pathology has been associated with decreased autophagic activity. The onset of AD has been associated with a decrease in autophagy-related gene expression, with certain tau isoforms inhibiting lysosome-dependent autophagic processes (reviewed in Hamano et al., 2018). Furthermore, NFTs composed of tau proteins are able to persist after the death of the “host” neuron, forming extracellular “ghost” tangles (Serrano-Pozo et al., 2011).

In PD,  $\alpha$ -synuclein inclusions cannot be effectively degraded either, despite colocalizing with essential components of both the autophagic and proteasomal protein degradation pathways. They persist even after soluble  $\alpha$ -synuclein levels have been substantially reduced, suggesting that once formed, the aggregates have an extremely high resistance to clearance.

Extracellular  $\alpha$ -synuclein internalized by cells has been observed to impair lysosomal activity, resulting in decreased autophagosome clearance in AD patients. This effect was greatest with aggregated  $\alpha$ -synuclein, which more persistently accumulates within recipient cells. Oligomeric intermediates proved to be susceptible to clearance (Lee et al., 2004). Interference with lysosomes, along with other protein quality control systems, has been observed to promote accumulation of  $\alpha$ -synuclein within recipient cells, leading to the formation of inclusion bodies (Desplats et al., 2009). This indicates the potential for a self-reinforcing autophagic inhibition loop, in which internalized  $\alpha$ -synuclein reshapes the cell's immune environment to facilitate further aggregation and consequently, intercellular spread. Macroautophagic inhibition has been observed to contribute to cell death in aggregate-bearing

cells, suggesting a possible role for loss-of-function processes in neurodegeneration (Winslow et al., 2010). Drug-mediated autophagy induction was able to mitigate this inhibitory effect, reducing  $\alpha$ -synuclein accumulation within cells exposed to aggregates (Hoffmann et al., 2019).

Htt fragments containing pathogenic polyQ repeats have been demonstrated to nearly completely inhibit the ubiquitin-proteasome system, a major regulator of autophagy (Bence et al., 2001). This appears to be the result of proteasome sequestration within aggregates of mHtt N-terminal fragments of polyQ expansion proteins, suggesting a pathological role for aggregates outside of direct toxicity. Furthermore, polyQ repeats are themselves resistant to proteasomal degradation, further limiting cellular clearance processes (Holmberg et al., 2004). This proteasomal inhibition has been observed to double the amount of ubiquitinated aggregates, demonstrating significant growth in pathological aggregation in the absence of effective cellular clearance processes (Waelter et al., 2001).

Distinct subsets of aggregates within ALS pathology have also been termed “irreversible.” Their formation typically involves changes to secondary and tertiary structures within the protein monomers of aggregate species (Invernizzi et al., 2012; Prasad et al., 2019). This can require only a small portion of the monomer chains in the aggregate, and during this process, small proteins often undergo a significant increase in  $\beta$ -sheet content. Once this state has been achieved, dissociation becomes extremely difficult. However, some success has been observed with highly concentrated chemical denaturants and high pressures (Amin et al., 2014).

Depletion of healthy TDP-43 has been shown to inhibit expression of the major autophagy component Atg7, likely through destabilization of the Atg7 mRNA. This leads to the impairment of autophagy and facilitates the accumulation of polyubiquitinated proteins (Bose et al., 2011). As such, the prevention of regular TDP-43 function due to disease-associated mutation and the resultant loss of function due to aggregation may contribute to impaired cellular clearance, and thus the spread of pathology.

Mutations in FUS inhibit downstream autophagic activity by reducing the number of omegasomes, a precursor to autophagosomes (Soo et al., 2015). They have also been associated with the accumulation of autophagy substrate p62, which is upregulated when autophagy is inhibited (Mathew et al., 2009). However, p62 itself inhibits the clearance of ubiquitinated proteins, further compromising the ubiquitin-proteasome system (Korolchuk et al., 2009). It also leads to more direct toxic effects, with accumulation leading to aberrant oxidative stress responses and the formation of SGs (Thomas et al., 2013).

## Autophagy Impairment With Aging

The incidence of most NDs increases with age. Concomitantly, the ability of the body to eliminate misfolded proteins declines with age. This decline has been observed in control of the proteostatic network, which maintains proteostasis and the elimination of dysfunctional proteins, as well as many component processes of autophagy, such as autophagosome

induction and fusion with lysosomes (Donati et al., 2001; Massey et al., 2006). Aging also dampens the ability of microglia to respond to stimuli such as  $\alpha$ -synuclein (Bliederhaeuser et al., 2016). Studies of mSOD1 in ALS demonstrated that overexpression of various ALS-linked mutants did not lead to the formation of aggregate deposits (Johnston et al., 2000; Münch et al., 2011). This has led to the proposal of a “latent development” theory, in which many aggregation-promoting mutations are active significantly before symptom onset, with pathological effects held in check by cellular control processes until age-related dysfunction tips the scales. Aging microglia in AD have been observed to become dysfunctional and exhibit decreasing neuroprotective capabilities such as binding and degrading A $\beta$ . However, they retain their ability to produce pro-inflammatory cytokines, allowing a progressive increase in net neurotoxicity (Borchelt et al., 1997; Jankowsky et al., 2001).

The shortening of telomeres may be a factor in this age-related dysfunction. Telomeres modulate DNA stability and shorten through cell replication in the process of aging (Blackburn, 2000). Shortening telomeres are known to be associated with both accelerated synuclein pathology and impaired microglial response (Scheffold et al., 2016). The average length of telomeres is shorter (Forero et al., 2016) and the rate of telomere shortening is faster in neurons, microglia and T-cells from AD patients than in healthy controls, suggesting the involvement of pathological mechanisms (Panossian et al., 2003; Flanary et al., 2007; Liu et al., 2016). Similar findings in ALS models (De Felice et al., 2014; Linkus et al., 2016) suggest that microglial telomere shortening may influence the onset of symptoms in various NDs.

## Protein Mislocalization

Aberrant protein localization is present in many prionoid pathologies. It is typically the result of mutation or alteration of the organelle transport system, either through cargo proteins, transport receptors or general deregulation (Hung and Link, 2011; **Figure 1B**). This can result in pathological effects through either loss of function, in which aberrant localization prevents activity despite maintaining intrinsic function, or toxic gain of function as the protein's typical activity becomes harmful in an aberrant location.

Studies of A $\beta$  have demonstrated abnormal HSP60-mediated translocation of APP to the mitochondria, resulting in increased levels of mitochondrial A $\beta$ . They also observed mislocalization of these mitochondria from axons and dendrites to the soma, and resultant disruption of mitochondrial function (Iijima-Ando et al., 2009; Walls et al., 2012). Following this, A $\beta$  has been reported to impair mitochondrial transport without affecting either mitochondrial function or the cytoskeleton in hippocampal neurons (Rui et al., 2006). The result is mislocalized mitochondria unable to return to their native positions, possibly driving pathological toxicity.

Hoover et al. (2010) found that pseudohyperpolarized tau of the sort observed in AD mislocalized to dendrites and dendritic spines, while phosphorylation-deficient tau block mistargeting. This phosphorylation-mediated mislocalization was concluded to cause early synaptic dysfunction by suppressing

AMPA-mediated synaptic responses. Disruption of postsynaptic targeting and anchoring of glutamate receptors have both been proposed as possible mechanisms (Hoover et al., 2010; Miller et al., 2014).

In HD, N-terminal Htt has demonstrated the ability to shuttle between the cytoplasm and nucleus of cells. The exact mechanism of this shuttling is inconclusive, with possible mechanisms including a nuclear export sequence in Htt and interaction with the nuclear export-associated translocated promoter region (Tpr) of the nuclear pore. Disruption of both systems in HD has been demonstrated to increase nuclear Htt accumulation (Cornett et al., 2005; Zheng et al., 2013). The amphipathic  $\alpha$ -helical membrane-binding domain appears to be required for effective transport between the nucleus and cytoplasm, enabling targeting of vesicles and the endoplasmic reticulum. When disrupted by point mutation, nuclear accumulation and toxicity of mHtt both increased significantly (Atwal et al., 2007).

Mouse models of SOD1 have established that subjects expressing wild-type SOD1 localize to both the cytoplasm and nuclei, while mSOD1 were limited to the cytoplasm. This occurred independently of any mutations in the neurons or astrocytes studied, suggesting that it is a property of the protein rather than the cell (Lee et al., 2015).

Wild-type FUS predominantly resides in the nucleus. However, ALS-linked mutants have been observed to mislocalize to the cytoplasm. The level of mislocalization has been positively correlated with both the onset of ALS and the maturation status of the MNs affected (Higelin et al., 2016). mFUS linked to severe ALS recruits significantly more cytoplasmic FUS into SGs following stress or irradiation than those linked to mild ALS (Higelin et al., 2016). mFUS-expressing cells were also noted to express increased numbers of large, densely packed FUS-positive SGs along neurites (Higelin et al., 2016).

Mutant TDP-43 likewise mislocalizes from the nucleus to the cytoplasm. There is evidence of ubiquitinated TDP-43-containing inclusion bodies in ALS, and evidence of decreased levels of nuclear TDP-43 when such ubiquitinated TDP-43 inclusion bodies are present (Neumann et al., 2006; Geser et al., 2008). Mutant-specific TDP-43 toxicity has been associated with higher levels of cytoplasmic TDP-43 mislocalization, serving as a strong predictor of neuronal death. However, there is evidence that inclusion bodies are not necessary for toxicity, and that their presence is entirely independent of cell death (Barmada et al., 2010). This indicates that the formation of inclusions may be only a method of limiting TDP-43 translocation, rather than a direct effector of pathology.

A study by Archbold et al. (2018) into inhibition and overexpression of nuclear exporters in ALS identified several redundant nuclear export pathways. They observed that inhibition of exportin-1 (XPO1) and depletion of various exportin levels failed to significantly increase levels of nuclear TDP-43, while overexpression of exporters increased nuclear export. It may be that nuclear export is predominantly independent of active export mechanisms. A recent study demonstrated that export is size-dependent, and as a result proposed that export mechanisms are predominantly driven by



passive diffusion (Pinarbasi et al., 2018). They argue that the limited effects of some exporter proteins are due to shuttling of secondary components of SGs; supplementing rather than driving the formation of inclusion bodies.

## Intracellular Transport Dysfunction

A common factor in NDs is the disruption of intracellular transport systems, typically through interference of microtubule-mediated transport (**Figure 1C**). This contributes to the loss-of-function and mislocalization pathologies, particularly with regards to mitochondria. Mitochondrial function is reliant on extensive intracellular transport to meet the cell's energy needs, especially with regards to the maintenance of synapses.

AD is possibly the most involved ND in intracellular transport dysfunction due to the involvement of the MAP tau. This leads to both loss-of-function due to dissociation from microtubules and a gain-of-function inhibition of microtubule assembly in its hyperphosphorylated form (Grundke-Iqbal et al., 1986; Alonso et al., 1994, 2006; Li et al., 2007). There is evidence that this inhibitory activity is the result of tau binding to the “tracks” of the microtubules, slowing anterograde transport (Ebner et al., 1998). A $\beta$  is likewise involved in pathological AD processes. Exposure of cultured hippocampal neurons to soluble A $\beta$  was shown to significantly impair transport of mitochondria along axons in both the retrograde and anterograde directions (Wang et al., 2010). A $\beta$ 42 specifically has demonstrated the ability to induce mitochondrial mislocalization, with fewer in the axons and dendrites and more localized to the soma (Iijima-Ando et al., 2009). This is likely to limit the cell's ability to undergo neurotransmitter Exo- and endocytosis at its synapses, possibly contributing to functional deficits. There is some evidence of pathological synergy between A $\beta$  and tau as well, with the presence of both A $\beta$  and pathologically cleaved tau increasing levels of stationary mitochondria and levels of oxidative stress (Quintanilla et al., 2012).

In HD, the activity of mHtt has been shown to result in disruption of both anterograde and retrograde microtubule-based axonal trafficking of both vesicles and mitochondria. This is accompanied by the retraction of neurites. These effects have been shown to precede entry of mHtt into the nucleus, suggesting that it is an early part of pathology (Trushina et al., 2003). Pathological aggregates in the cytosol have been shown to “immobilize” mitochondria adjacent to them. This process involves the sequestration of wild-type Htt, which is important for fast axonal trafficking, as well as various trafficking motors and mitochondrial components (Trushina et al., 2004; Chang et al., 2006).

Several factors in PD contribute to transport dysfunction. The parkin gene, one of the major sites of mutations in familial PD, is a microtubule-stabilizing protein, and thus a logical target for pathology. However, Yang et al. (2005) found no effect of PD-linked mutations on parkin's interactions with microtubules. Parkin mutations may, however, exert indirect effects on cell stability. Healthy parkin reduces microtubule depolymerization and consequently attenuates the activity of MAP kinase (MAPK), significantly reducing certain toxic mechanisms (Ren et al., 2009).  $\alpha$ -synuclein has also been shown to interact with the

protein tubulin, inducing polymerization of purified tubulin into microtubules. However, the effects of pathological mutations on this process are inconclusive, with some studies suggesting an increase in tubulin polymerization and other impairment (reviewed in Pellegrini et al., 2017).

Research into both fALS and sALS has found a significant role of microtubule-mediated axonal transport in MN survivability. These deficits are believed to be one of the earliest events in ALS. Kinesin and dynein proteins are believed to play a significant role, being directly involved in both anterograde and retrograde transport along with microtubule polymers (reviewed in Burk and Pasterkamp, 2019). Mutations in FUS are particularly involved in the activity of the kinesin family of proteins. Recruitment of the kinesin-1 (KIF1) mRNA and protein within FUS inclusions mediates the mislocalization of specific RNAs from axons. This leads to a loss of detyrosinated glutamate microtubules, and consequently issues with RNA localization. The mechanism of effect appears to not be related to microtubule stability, but rather through targeting the tubulin carboxypeptidase enzyme onto specific microtubules (Yasuda et al., 2017). SOD1 pathology appears more strongly associated with dynein, as MNs from SOD1<sup>G93A</sup> mice display defective dynein-mediated retrograde axonal transport from the embryonic stage (Kieran et al., 2005). There is also evidence for the involvement of the anterograde transport pathway, as studied in a transgenic squid axoplasm model. Activation of p38 MAPK and the consequent phosphorylation of KIF-1, inhibiting transport along microtubules, were implicated in this process (Bosco et al., 2010b). In addition, ALS mSOD1 has been shown to reduce levels of the mitochondrial membrane protein mitochondrial Rho GTPase 1 (Miro1), a master regulator of mitochondrial axonal transport. This results in further inhibition of anterograde axonal transport of mitochondria (Moller et al., 2017). TDP-43 models have demonstrated smaller growth cones and shorter axons than controls, with impaired axonal transport and cytoskeletal disruptions (Baskaran et al., 2018). TDP-43 knockdown and mislocalization have been shown to result in decreased expression of microtubule regulator stathmin-2, which is necessary for normal axonal growth and regeneration (Klim et al., 2019). This may be the result of a polyadenylation site uncovered as a result of altered splicing during TDP-43 deficiency, resulting in a truncated, non-functional mRNA (Melamed et al., 2019). Post-translational stabilization of stathmin-2 has been shown to restore axonal regenerative capabilities (Klim et al., 2019; Melamed et al., 2019).

## Failing Defense Mechanisms Propagate Disease

Another factor which can influence the precarious balance within prionoid pathologies is the subversion of defense mechanisms intended to prevent or slow the diseases' spread. This has been observed in multiple prionoid disorders. Many of these systems involve the ejection of pathological material from stressed cells or transport between regions. These processes can only remain beneficial as long as the proteins, fibrils, and aggregates can be effectively cleared after being removed from already affected

cells. Failure to do so serves as another symptom of the loss of autophagic balance within the CNS in prionoid pathologies.

Reactive astrocytes may propagate A $\beta$  pathology by producing a secretase required for A $\beta$  production (BACE1; Rossner et al., 2005). As A $\beta$  is an upstream activator of astrocytes (Lian et al., 2016), this may result in a cycle in which astrocytes become activated by neuronal A $\beta$  pathology, only to themselves increase the production of A $\beta$ .

In PD, microglia are responsible for phagocytotic  $\alpha$ -synuclein clearance (Lee et al., 2008). However, the microglial activation required to initiate this process has been shown to also lead to inflammatory signaling and production of ROS (Zhang et al., 2005; Jin et al., 2007). This, in turn, facilitates the oxidization of  $\alpha$ -synuclein in nearby neurons, compounding gain-of-function  $\alpha$ -synuclein pathology (Shavali et al., 2006).

The release of  $\alpha$ -synuclein fibers into extracellular space through exocytosis is accelerated under conditions that increase levels of  $\alpha$ -synuclein misfolding, such as mitochondrial and proteasomal dysfunctions (Lee et al., 2005). In adaptive situations, this may serve to limit intracellular aggregation and facilitate extracellular phagocytic clearance processes. However, when the body is incapable of effectively clearing these extracellular proteins as a result of aging or other factors, this process facilitates the spread of infectious fibrils to previously healthy neuronal and glial cells (Cuervo et al., 2004). Once internalized by astrocytes,  $\alpha$ -synuclein pathology can be transmitted between them through tunneling nanotubes (Rostami et al., 2017). This interaction with  $\alpha$ -synuclein oligomers greatly increases opportunities for glial and neuronal exposure, contributing to the spread of the disease. Toll-like receptor 4 (TLR4) appears to mediate inflammatory response to astrocytic  $\alpha$ -synuclein accumulation, increasing ROS production, levels of pro-inflammatory cytokines and microglial phagocytic activity (Fellner et al., 2013; Rannikko et al., 2015).

In ALS, a study of cell-to-cell transfer of mSOD1 in different volumes of culture media indicated that pathological SOD1 transfer is the result of cellular uptake following the expulsion of aggregates by mSOD1-containing cells (Münch et al., 2011).

## Glial Neuroprotective-Neurotoxic Equilibrium

Glial cells, particularly astrocytes and microglia, have a peculiar role in prionoid diseases, in that they exert both neurotoxic and neuroprotective effects. In the context of NDs, glia is predominantly involved in the degradation of aberrant proteins and various pro- and anti-inflammatory processes. There is a great deal of debate as to whether their neuroprotective or neurotoxic activity is more significant, although this is skewed by the tendency of pathological processes to enhance the activity of neurotoxic modalities (Figure 1D). This, in turn, prompts debate as to whether therapies should be targeted at suppressing or enhancing the activities of glial cells.

Astrocytes are specialized glial cells that respond to CNS damage through reactive astrogliosis, a complex graduated continuum of context-dependent changes regulated by various signaling events. Their effects include reversible alteration of

gene expression, cell hypertrophy, and rearrangement of tissue structures into long-lasting astroglial scarring (Sofroniew and Vinters, 2010).

Microglia are the resident macrophage cells of the CNS, functioning as its first and main form of immune defense. While their function is like that of peripheral macrophages, microglia have been found to be more efficient at phagocytosis than their peripheral counterparts (Jin and Yamashita, 2016). In a resting state, they actively probe the CNS for pathological changes, targeting plaques, damaged or unnecessary neurons and synapses, and infectious agents (Gehrmann et al., 1995; Luo and Chen, 2012). However, when activated they take on either the neurotoxic M1 or neuroprotective M2 phenotypes (Li and Zhang, 2016). M1 microglia release pro-inflammatory mediators such as cytokines and chemokines which inhibit phagocytosis, as well as substances such as ROS which promote oxidative stress (Dheen et al., 2007; Sorce et al., 2014; Orihuela et al., 2016). M2 microglia produce anti-inflammatory factors, clearing cellular debris through phagocytosis and releasing various protective and trophic factors (Orihuela et al., 2016; Tang and Le, 2016). However, recent evidence has suggested that microglia exist in a continuum between the M1 and M2 states, exerting various levels of toxic and protective effects. This is supported by data that suggests that the release of the beneficial components of inflammation, such as IGF-1, occurs in mSOD1 microglia in both the pre-symptomatic and end-stages of disease progression (Chiu et al., 2013).

With respect to AD, evidence suggests that astrocytes play a neuroprotective role through uptake and clearance of A $\beta$  aggregates (Pihlaja et al., 2008, 2011). However, this neuroprotective activity is insufficient to clear plaques, as evidenced by the stability of both amyloid plaque burden and plaque size distribution throughout the progression of the disease (Serrano-Pozo et al., 2012). However, astrocytes do preferentially target diffuse A $\beta$  deposits over larger fibrillar aggregates, and so may serve to isolate soluble, neurotoxic A $\beta$  and thus limit collateral damage (Perez-Nievas and Serrano-Pozo, 2018). These neuroprotective activities are diminished over the course of the disease, while neurotoxic effects increase through both the loss of counteractive neurotrophic effects and toxic gain of function (reviewed in Perez-Nievas and Serrano-Pozo, 2018).

The lipid-binding protein apolipoprotein E (APOE) appears to be a necessary component in the astrocytic degradation of A $\beta$  (Koistinaho et al., 2004). The APOE $\epsilon$ 4 allele is the strongest genetic risk factor of AD, with homozygous individuals experiencing an 8–12-fold higher incidence of the disease (Corder et al., 1993). This allele has been found to promote A $\beta$  aggregation (Hyman et al., 1995), formation into soluble oligomers (Hashimoto et al., 2012) and reduces A $\beta$  clearance (Castellano et al., 2011). It has also demonstrated a role in tau pathology, promoting tau-mediated neurodegeneration independent of A $\beta$  pathology (Shi et al., 2017). The strong association between AD and this allele is indicative of a more neurotoxic astrocytic phenotype. Its significance as a risk factor indicates that it may be a driver of AD pathology, allowing neurotoxic elements to overcome natural defense mechanisms. In contrast, the

APOE $\epsilon$ 2 allele exerts a significant protective influence and has been associated with a decreased incidence of AD (Corder et al., 1994). For this reason, upregulation of APOE $\epsilon$ 2 and/or downregulation of APOE $\epsilon$ 4 may serve as valuable therapeutic tools.

Activation of microglia, on the other hand, is largely neurodegenerative in AD. Activated microglia can be induced by pathological proteins such as A $\beta$  under disease conditions, leading to increased production of cytokines and neurotoxins, including ROS, ultimately promoting neurodegeneration (Meda et al., 1995; Coraci et al., 2002).

There is also significant evidence for increased inflammatory activity in PD compared to controls (Lecours et al., 2018). In a mouse model of PD, infected astrocytes were observed to produce A53T mutant  $\alpha$ -synuclein, leading to the induction of severe neurodegeneration (Gu et al., 2010). However, astrocytes have also shown the ability to endocytose  $\alpha$ -synuclein released into the surrounding microenvironment by pathological lesions, sequestering it and inhibiting further infection of neurons (Lee et al., 2010). Microglia are also highly responsive to  $\alpha$ -synuclein deposits. Olanow et al. (2019) showed that dopaminergic neurons implanted into PD patients gradually acquire  $\alpha$ -synuclein aggregates over approximately 14 years, and this aggregation is associated with an increased presence of activated microglia. However, microglia also exhibit both neuroprotective and neurotoxic functions in response to  $\alpha$ -synuclein and may attempt to clear the aggregates or exhibit inflammatory phenotypes (reviewed in Lecours et al., 2018).

HD-associated neurodegeneration has been positively associated with the activation of reactive astrocytes, with mild cases completely lacking reactive astrocytosis (Myers et al., 1991). One factor involved in this is the prevention of glutamate reuptake by reactive astrocytes expressing mHtt, resulting in excitotoxic injury to neurons (Shin et al., 2005). A similar mechanism has also been described in AD (Wang and Reddy, 2017), PD (Ambrosi et al., 2014) and excitotoxicity is suspected to play a role in ALS pathogenesis (King et al., 2016), although the evidence for this is less certain. However, the link between the respective prionoid proteins and glial cells is not as detailed as the other diseases reviewed here. Further research may fully describe this link for the purpose of identifying new therapeutic modalities that function across prionoid NDs by interfering with disease-progressing behaviors of microglia and astrocytes.

Microglia exposed to or expressing mHtt are abnormally reactive to stimuli that prompt an immune response (Björkqvist et al., 2008) and are more toxic to neuronal cells (Crotti et al., 2014). Reactive microglia have been observed in the neostriatum, cortex, globus pallidus and the adjoining white matter of the brains of HD subjects, but not controls. While activation occurred in all levels of pathology, accumulation was greater in cases with more severe neurodegeneration. The processes of these microglia were clearly defined even in low-grade HD, suggesting an early microglial response to changes in the neuropil and axons (Sapp et al., 2001). Transmission of Htt aggregates to microglia through phagocytic activity has been demonstrated in a fly model of HD, enabling seeded aggregation within the microglial cells. While ostensibly neuroprotective, may serve to

impair microglial clearance, and excessive accumulation may facilitate transmission to healthy cells (Pearce et al., 2015).

A rat model of ALS found that selective expression of mTDP-43 in astrocytes led to non-cell-autonomous motor neuron death and consequent denervation atrophy and paralysis. It also led to the activation of astrocytes and microglia (Tong et al., 2013). Interestingly, this rat model also identified a loss of glutamate transporters in the spinal cord of affected animals, although a definitive link with excitotoxic injury was not made.

The interplay between glial cells can shift the balance towards toxic modalities. Activated microglia can cause astrocytes to become neurotoxic reactive astrocytes that produce pro-inflammatory cytokines. This results in the rapid destruction of neurons and oligodendrocytes (Liddel et al., 2017).

There is evidence to suggest that the functions of microglia shift throughout the course of ALS. In a chimeric model with some cells expressing mSOD1, non-neuronal cells that did not express the mutant protein exerted significant neuroprotective effects, delaying neurodegeneration and extending survival (Clement et al., 2003). Similarly, mSOD1-expressing early-activated microglia exhibit higher levels of markers for the neuroprotective M2 state, while end-stage microglia displayed a shift towards the toxic M1 state (Liao et al., 2012; Tang and Le, 2016). As such, impaired microglial accumulation in early disease stages accelerates ND progression, and methods that support early microglial activity may delay prionoid pathology (El Khoury et al., 2007).

Spiller et al. (2018) proposed a biphasic model of microglial activity based on their study of a reversible model of TDP-43 ALS pathology. They observed that while mutant, aggregation-prone TDP-43 was active, there was a significant loss of motor neurons and no significant change to microglia number or activity. However, when the expression of mutant TDP-43 was suppressed, microglia expanded rapidly and specifically cleared TDP-43, allowing the subjects to recover somewhat. This raises the possibility that the constant renewal of prionoid protein aggregates from various sources (glial cells themselves included in some NDs) overwhelms microglia. This may result in a constant state of inflammatory stimulation from stressed neurons, reactive astrocytes or autocrine signals. The sequestration of cellular resources needed for this microglial response may also contribute to the lack of response, suppressing microglial proliferation until aggregation has ceased. Despite evidence from AD and PD showing that microglia can exert neuroprotective effects (Streit, 2005; Chen and Trapp, 2016; Masuch et al., 2016), none have shown this type of temporal response.

## Glia-Mediated Neurotoxicity

Nitric oxide (NO) is a highly diffusible, reactive molecule produced by the nitric oxide synthase (NOS) enzyme. At low concentrations, it is involved in the regulation of metabolic energy levels, neurotransmission, and vasodilation (Thomas et al., 2001). The anionic form of NO, nitroxyl (NO $^-$ ) has also demonstrated some neuroprotective effects, downregulating excessive activity by pathology-associated extrasynaptic N-Methyl-D-aspartate receptors (NMDARs; Kim et al., 1999).



The major pathological effects of NO emerge when co-expressed at high levels with the enzyme complex NADPH oxidase (NOX), which is produced predominantly by microglia. This complex produces the superoxide radical ( $O_2^-$ ) ROS, used for phagocytic pathogen degradation in healthy cells. However, NO and  $O_2^-$  engage in an extremely rapid (almost diffusion-limited) chemical reaction, producing the more neurotoxic ROS peroxynitrite ( $ONOO^-$ ; Rubbo et al., 1994; Mander and Brown, 2005).  $ONOO^-$  causes irreversible nitration or nitrosylation of specific amino acid residues, which induces aberrant protein conformation and function and inhibition of mitochondrial respiration (Hess et al., 2005; Szabó et al., 2007; **Figure 1F**). Nitration of Parkin was noted to initially increase but later decrease Parkin activity, and  $\alpha$ -synuclein nitration was found to contribute to aggregation, increasing resistance to proteolysis as well as reducing lipid binding and solubility in PD (reviewed in Steinert et al., 2010). Nitrosylated proteins have been observed to accumulate in the brains of human ND patients, but not healthy controls (Nakamura and Lipton, 2016). There is evidence that the nitrosylation reaction can result in substantial neuron death, although it is uncertain whether this is a result of this amino acid modification or more direct ROS neurotoxicity (Mander and Brown, 2005). Another cell death process also appears to exist in mSOD1 ALS, as low levels of extracellular NO in mSOD1-expressing MNs, but not non-transgenic or wild-type MNS, activated a self-reinforcing NO upregulation cycle which ended in cell death (Drechsel et al., 2012).

While synaptic activation of NMDA receptors (NMDAR) is protective, extrasynaptic NMDAR activation has been shown to trigger excessive NO production. This is potentially a key pathway in AD, as A $\beta$  oligomers have been shown to hyper stimulate extrasynaptic NMDARs (Talantova et al., 2013; Molokanova et al., 2014).

The inducible NOS isoform (iNOS) has been strongly associated with ND. It is only expressed in astrocytes and microglia following exposure to proinflammatory cytokines and components of pathogens (Mander and Brown, 2005; Saha and Pahan, 2006). Once expressed, iNOS produces sustained high levels of NO, facilitating ROS production (Mander and Brown, 2005). The pro-inflammatory cytokines IL-1 $\beta$  and IFN- $\gamma$  are sufficient to induce iNOS activation in astrocyte cells, while some other cytokines such as TNF- $\alpha$  can sensitive cells to IL-1 $\beta$  and IFN- $\gamma$ -mediated iNOS activation (Trajkovic et al., 2001). iNOS can also be activated by some neurodegenerative toxins. Aggregated A $\beta$  peptides have demonstrated the ability to trigger iNOS activation in primary microglia (Combs et al., 2001). NO-mediated nitration of A $\beta$  also increases its aggregation propensity (reviewed in Kummer et al., 2011), potentially resulting in self-reinforcing pathology. There is also evidence of iNOS activation in HD and ALS, however, the exact inducer has not yet been identified in these diseases (Tabrizi et al., 2000; Barbeito et al., 2004).

## THERAPEUTICS

Prion populations have been shown to adapt to the presence of selection pressures such as anti-prion compounds, developing

heterogeneity even after biological cloning. There is evidence that this variability arises at the conformational level, resulting in quasi-species that can thrive in adverse environments. The most effective replicator dominates, allowing the acquisition of resistance even in the absence of genetic variability (Oelschlegel and Weissmann, 2013). Therapeutic drug design for prions should be carefully considered with this resistance in mind.

Since prions are pure proteins with no genetic material, intuitively one thinks of an antibody as an easy way to clear prion infection. When prion-infected cells in culture were treated with antibodies against PrP, the accumulation of prion protein was reduced (Enari et al., 2001). Similarly in mice, treatment with an antibody against prion protein slowed the onset of disease symptoms (White et al., 2003). Recently, the MRC Prion Unit in London announced the possibility of a human clinical trial of an anti-PrP antibody named PRN100 to treat sporadic Creutzfeldt-Jakob disease, but no details are available yet. Monoclonal antibody trials are also underway for AD but have also met with only limited success (Prins and Scheltens, 2013; van Dyck, 2018). There is also a monoclonal antibody undergoing clinical trial for PD, but the trial is ongoing and the efficacy data are not available yet (Jankovic et al., 2018). Beyond this, new technological approaches aimed at developing antibodies against beta-sheet rich proteins characteristic of prionoid NDs are also underway with promising early results *in vitro* (Goñi et al., 2017; Manoutcharian et al., 2017).

Apart from monoclonal antibodies, many other therapeutic approaches have been developed throughout the years, with limited clinical success (reviewed in Trevitt and Collinge, 2006; Aguzzi et al., 2018). Research suggests that the key to effective therapeutic approaches is not in degrading the highly stable aggregates already formed, but in preventing the development of further pathology. This allows the body to re-establish existent but overwhelmed protective mechanisms, both slowing pathological spread and allowing the recovery of function (Melnikova et al., 2013; Spiller et al., 2018). While some secretase inhibitors such as doxycycline have already experienced significant success in animal models of AD, no such success has been observed in human clinical trials (Molloy et al., 2013). Similarly, inhibitors of the  $\beta$ -secretase BACE1 enzyme which cleaves APP into its A $\beta$  form have been able to lower A $\beta$  levels, but not recover cognitive function (reviewed in Coimbra et al., 2018). However, research is still ongoing as to whether applications at pre-clinical stages may have a stronger positive impact (Voytyuk et al., 2018).

Another target for redressing this pathological imbalance is the enhancement of autophagic processes. Even in the absence of any prionoid proteins, a loss of autophagy can lead to neurodegeneration, suggesting a key role in pathogenesis. Autophagy-enhancing agents such as rapamycin, metformin, and resveratrol have been found to have various positive effects in PD, including increased  $\alpha$ -synuclein clearance and reduced neuronal cell loss (reviewed in Moors et al., 2017). However, these agents are not selective, and many of the agents used are involved in other pathways such as apoptosis, cell growth, and immune responses. This could cause a wide variety of detrimental side effects, limiting clinical application.



However, therapies are in development that target downstream components of the autophagy pathway, which may exhibit more targeted effects (Moors et al., 2017). Extensive studies have been made into inhibitors of mTOR, a complex which inhibits autophagy. One of the most common therapeutic agents is rapamycin, used in ALS, AD and HD treatment, although many others such as resveratrol, BECN1, and calpastatin are being trialed and modeled in various NDs (Towers and Thorburn, 2016; Mandrioli et al., 2018).

Overall, very little has been done in relation to the therapeutic modulation of glial cell activation, which may also clear protein aggregates. We know that sustained inflammation kills neurons and fails to stimulate further clearance of prionoid protein aggregates. Thus, one of the ways to enhance neuroprotection during disease progression in NDs could be by modulating inflammation and subduing the over-activation of glial cells. Our research has observed that while early glial activation is predominantly neuroprotective in nature, this shifts along a continuum towards neurotoxicity through increased inflammation and the production of toxic molecules as diseases progress. If glial activation is to be effectively used as an avenue for therapeutics, more research must be undertaken with regards to both the early identifications of pathological aggregation and determination of when in the disease process the glial response turns from positive to negative. However, even in the absence of such specific mechanistic knowledge, there are some avenues of approach which can be explored.

## REFERENCES

- Abeliovich, A., Schmitz, Y., Farinas, I., Choi-Lundberg, D., Ho, W., Castillo, P., et al. (2000). Mice lacking  $\alpha$ -synuclein display functional deficits in the nigrostriatal dopamine system. *Neuron* 25, 239–252. doi: 10.1016/s0896-6273(00)80886-7
- Aguzzi, A., Lakkaraju, A. K. K., and Frontzek, K. (2018). Toward therapy of human prion diseases. *Annu. Rev. Pharmacol. Toxicol.* 58, 331–351. doi: 10.1146/annurev-pharmtox-010617-052745
- Allison, W. T., DuVal, M. G., Nguyen-Phuoc, K., and Leighton, P. L. A. (2017). Reduced abundance and subverted functions of proteins in prion-like diseases: gained functions fascinate but lost functions affect aetiology. *Int. J. Mol. Sci.* 18:E2223. doi: 10.3390/ijms18102223
- Almeida, C. G., Takahashi, R. H., and Gouras, G. K. (2006).  $\beta$ -amyloid accumulation impairs multivesicular body sorting by inhibiting the ubiquitin-proteasome system. *J. Neurosci.* 26, 4277–4288. doi: 10.1523/JNEUROSCI.5078-05.2006
- Alonso, A. D., Grundke-Iqbal, I., and Iqbal, K. (1994). Role of abnormally phosphorylated tau in the breakdown of microtubules in Alzheimer disease. *Proc. Natl. Acad. Sci. U S A* 91, 5562–5566. doi: 10.1073/pnas.91.12.5562
- Alonso, A. C., Li, B., Grundke-Iqbal, I., and Iqbal, K. (2006). Polymerization of hyperphosphorylated tau into filaments eliminates its inhibitory activity. *Proc. Natl. Acad. Sci. U S A* 103, 8864–8869. doi: 10.1073/pnas.0603214103
- Ambrosi, G., Cerri, S., and Blandini, F. (2014). A further update on the role of excitotoxicity in the pathogenesis of Parkinson's disease. *J. Neural Transm.* 121, 849–859. doi: 10.1007/s00702-013-1149-z
- Amin, S., Barnett, G. V., Pathak, J. A., Roberts, C. J., and Sarangapani, P. S. (2014). Protein aggregation, particle formation, characterization and rheology. *Curr. Opin. Colloid Interface Sci.* 19, 438–449. doi: 10.1016/j.cocis.2014.10.002
- Andersen, P. M. (2006). Amyotrophic lateral sclerosis associated with mutations in the CuZn superoxide dismutase gene. *Curr. Neurol. Neurosci. Rep.* 6, 37–46. doi: 10.1007/s11910-996-0008-9
- Arai, T., Hasegawa, M., Akiyama, H., Ikeda, K., Nonaka, T., Mori, H., et al. (2006). TDP-43 is a component of ubiquitin-positive tau-negative inclusions in frontotemporal lobar degeneration and amyotrophic lateral sclerosis. *Biochem. Biophys. Res. Commun.* 351, 602–611. doi: 10.1016/j.bbrc.2006.10.093
- Archbold, H. C., Jackson, K. L., Arora, A., Weskamp, K., Tank, E. M., Li, X., et al. (2018). TDP43 nuclear export and neurodegeneration in models of amyotrophic lateral sclerosis and frontotemporal dementia. *Sci. Rep.* 8:4606. doi: 10.1038/s41598-018-22858-w
- Arrasate, M., Mitra, S., Schweitzer, E., and Segal, M. F. (2004). Inclusion body formation reduces levels of mutant huntingtin and the risk of neuronal death. *Nature* 431, 805–810. doi: 10.1038/nature02998
- Arriagada, P. V., Growdon, J. H., Hedley-Whyte, E. T., and Hyman, B. T. (1992). Neurofibrillary tangles but not senile plaques parallel duration and severity of Alzheimer's disease. *Neurology* 42, 631–639. doi: 10.1212/wnl.42.3.631
- Asai, H., Ikezu, S., Tsunoda, S., Medalla, M., Luebke, J., Haydar, T., et al. (2015). Depletion of microglia and inhibition of exosome synthesis halt tau propagation. *Nat. Neurosci.* 18, 1584–1593. doi: 10.1038/nn.4132
- Atwal, R. S., Xia, J., Pinchev, D., Taylor, J., Epan, R. M., and Truant, R. (2007). Huntingtin has a membrane association signal that can modulate huntingtin aggregation, nuclear entry and toxicity. *Hum. Mol. Genet.* 16, 2600–2615. doi: 10.1093/hmg/ddm217
- Ayala, Y. M., Zago, P., D'Ambrogio, A., Xu, Y.-F., Petrucelli, L., Buratti, E., et al. (2008). Structural determinants of the cellular localization and shuttling of TDP-43. *J. Cell Sci.* 121, 3778–3785. doi: 10.1242/jcs.038950
- Babcock, D. T., and Ganetzky, B. (2015). Transcellular spreading of huntingtin aggregates in the *Drosophila* brain. *Proc. Natl. Acad. Sci. U S A* 112, E5427–E5433. doi: 10.1073/pnas.1516217112
- Barbeito, L. H., Pehar, M., Cassina, P., Vargas, M. R., Peluffo, H., Viera, L., et al. (2004). A role for astrocytes in motor neuron loss in amyotrophic lateral sclerosis. *Brain Res. Rev.* 47, 263–274. doi: 10.1016/j.brainresrev.2004.05.003
- Barmada, S. J., Skibinski, G., Korb, E., Rao, E. J., Wu, J. Y., and Finkbeiner, S. (2010). Cytoplasmic mislocalization of TDP-43 is toxic to neurons and

## CONCLUDING REMARKS

While these NDs have diverse symptoms, outcomes and prionoid behaviors, their similar mechanisms of action and propagation seem to indicate that they are all different manifestations of the same core pathology. At their cores, they are all indicative of a loss of proteostatic equilibrium. The reduction of protein quality control mechanisms and increase of pathological proteins results in a pathological cascade, producing sinks of cellular resources that eventually lead to dysfunction and death. Perhaps by identifying the common elements within these diverse conditions, a mechanism could be found to disrupt these pathologies before they can develop into the debilitating and lethal conditions they are today.

## AUTHOR CONTRIBUTIONS

NS and MK conceived the article. CW performed most of the research, in addition NS and SB also provided leads to the research. CW produced the first draft of the article. NS and SB performed substantial editing and made contributions of their own to further develop the manuscript.

- enhanced by a mutation associated with familial amyotrophic lateral sclerosis. *J. Neurosci.* 30, 639–649. doi: 10.1523/jneurosci.4988-09.2010
- Baskaran, P., Shaw, C., and Guthrie, S. (2018). TDP-43 causes neurotoxicity and cytoskeletal dysfunction in primary cortical neurons. *PLoS One* 13:e0196528. doi: 10.1371/journal.pone.0196528
- Bence, N. F., Sampat, R. M., and Kopito, R. R. (2001). Impairment of the ubiquitin-proteasome system by protein aggregation. *Science* 292, 1552–1555. doi: 10.1126/science.292.5521.1552
- Bertoletti, A., Lutz, Y., Heard, D., Chambon, P., and Tora, L. (1996). hTAF(II)68, a novel RNA/ssDNA-binding protein with homology to the pro-oncoproteins TLS/FUS and EWS is associated with both TFIID and RNA polymerase II. *EMBO J.* 15, 5022–5031. doi: 10.1002/j.1460-2075.1996.tb00882.x
- Bertrand, A., Wen, J., Rinaldi, D., Houot, M., Sayah, S., Camuzat, A., et al. (2018). Early cognitive, structural and microstructural changes in presymptomatic C9orf72 carriers younger than 40 years. *JAMA Neurol.* 75, 236–245. doi: 10.1001/jamaneurol.2017.4266
- Binder, L. I., Frankfurter, A., and Rebhun, L. I. (1985). The distribution of tau in the mammalian central nervous system. *J. Cell Biol.* 101, 1371–1378. doi: 10.1083/jcb.101.4.1371
- Björkqvist, M., Wild, E. J., Thiele, J., Silvestroni, A., Andre, R., Lahiri, N., et al. (2008). A novel pathogenic pathway of immune activation detectable before clinical onset in Huntington's disease. *J. Exp. Med.* 205, 1869–1877. doi: 10.1084/jem.20080178
- Blackburn, E. H. (2000). Telomere states and cell fates. *Nature* 408, 53–56. doi: 10.1038/35040500
- Bliederhauer, C., Grodzanov, V., Speidel, A., Zondler, L., Ruf, W. P., Bayer, H., et al. (2016). Age-dependent defects of  $\alpha$ -synuclein oligomer uptake in microglia and monocytes. *Acta Neuropathol.* 131, 379–391. doi: 10.1007/s00401-015-1504-2
- Borchelt, D. R., Ratovitski, T., van Lare, J., Lee, M. K., Gonzales, V., Jenkins, N. A., et al. (1997). Accelerated amyloid deposition in the brains of transgenic mice coexpressing mutant presenilin 1 and amyloid precursor proteins. *Neuron* 19, 939–945. doi: 10.1016/s0896-6273(00)80974-5
- Bosco, D. A., Lemay, N., Ko, H., Zhou, H., Burke, C., Kwiatkowski, T., et al. (2010a). Mutant FUS proteins that cause amyotrophic lateral incorporate into stress granules. *Hum. Mol. Genet.* 19, 4160–4175. doi: 10.1093/hmg/ddq335
- Bosco, D. A., Morfini, G., Karabacak, N. M., Song, Y., Gros-Louis, F., Pasinelli, P., et al. (2010b). Wild-type and mutant SOD1 share an aberrant conformation and a common pathogenic pathway in ALS. *Nat. Neurosci.* 13, 1396–1403. doi: 10.1038/nn.2660
- Bose, J. K., Huang, C. C., and Shen, C. K. (2011). Regulation of autophagy by neuropathological protein TDP-43. *J. Biol. Chem.* 286, 44441–44448. doi: 10.1074/jbc.m111.237115
- Bousset, L., Pieri, L., Ruiz-Arlandis, G., Gath, J., Jensen, P. H., Habenstein, B., et al. (2013). Structural and functional characterization of two  $\alpha$ -synuclein strains. *Nat. Commun.* 4:2575. doi: 10.1038/ncomms3575
- Braak, H., and Braak, E. (1997). Frequency of stages of Alzheimer-related lesions in different age categories. *Neurobiol. Aging* 18, 351–357. doi: 10.1016/s0197-4580(97)00052-3
- Braak, H., Braak, E., Grundke-Iqbal, I., and Iqbal, K. (1986). Occurrence of neurofibrillary threads in the senile human brain and in Alzheimer's disease: a third location of paired helical filaments outside of neurofibrillary tangles and neuritic plaques. *Neurosci. Lett.* 65, 351–355. doi: 10.1016/0304-3940(86)90288-0
- Braak, H., and Del Tredici, K. (2008a). Assessing fetal nerve cell grafts in Parkinson's disease. *Nat. Med.* 14, 483–485. doi: 10.1038/nm0508-483
- Braak, H., and Del Tredici, K. (2008b). Invited article: nervous system pathology in sporadic parkinson disease. *Neurology* 70, 1916–1925. doi: 10.1212/01.wnl.0000312279.49272.9f
- Braak, H., Ghebremedhin, E., Rub, U., Bratzke, H., and Del Tredici, K. (2004). Stages in the development of Parkinson's disease-related pathology. *Cell Tissue Res.* 318, 121–134. doi: 10.1007/s00441-004-0956-9
- Braak, H., Neumann, M., Ludolph, A. C., and Del Tredici, K. (2017). Does sporadic amyotrophic lateral sclerosis spread via axonal connectivities. *Neurol. Int. Open* 1, E136–E141. doi: 10.1055/s-0043-111375
- Buchan, J., Muhrlad, D., and Parker, R. (2008). P bodies promote stress granule assembly in *Saccharomyces cerevisiae*. *J. Cell Biol.* 183, 441–455. doi: 10.1083/jcb.200807043
- Burk, K., and Pasterkamp, R. J. (2019). Disrupted neuronal trafficking in amyotrophic lateral sclerosis. *Acta Neuropathol.* 137, 859–877. doi: 10.1007/s00401-019-01964-7
- Burke, R., Dauer, W., and Vonsattel, J. (2008). A critical evaluation of the Braak staging scheme for Parkinson's disease. *Ann. Neurol.* 64, 485–491. doi: 10.1002/ana.21541
- Carlo, C., and Stöhr, J. (2018). A $\beta$  propagation and strains: implications for the phenotypic diversity in Alzheimer's disease. *Neurobiol. Dis.* 109, 191–200. doi: 10.1016/j.nbd.2017.03.014
- Castellano, J. M., Kim, J., Stewart, F. R., Jiang, H., DeMattos, R. B., Patterson, B. W., et al. (2011). Human ApoE isoforms differentially regulate brain amyloid $\beta$  peptide clearance. *Sci. Transl. Med.* 3:89ra57. doi: 10.1126/scitranslmed.3002156
- Chang, D. T. W., Rintoul, G. L., Pandipati, S., and Reynolds, I. J. (2006). Mutant huntingtin aggregates impair mitochondrial movement and trafficking in cortical neurons. *Neurobiol. Dis.* 22, 388–400. doi: 10.1016/j.nbd.2005.12.007
- Chattopadhyay, M., Durazo, A., Sohn, S., Strong, C., Gralla, E., Whitelegge, J., et al. (2008). Initiation and elongation in fibrillation of ALS-linked superoxide dismutase. *Proc. Natl. Acad. Sci. U S A* 105, 18663–18668. doi: 10.1073/pnas.0807058105
- Chen, Z., and Trapp, B. D. (2016). Microglia and neuroprotection. *J. Neurochem.* 136, 10–17. doi: 10.1111/jnc.13062
- Chia, R., Tattum, M., Jones, S., Collinge, J., Fisher, E., and Jackson, G. (2010). Superoxide dismutase 1 and tgSOD1 mouse spinal cord seed fibrils, suggesting a propagative cell death mechanism in amyotrophic lateral sclerosis. *PLoS One* 5:e10627. doi: 10.1371/journal.pone.0010627
- Chiò, J. A., Traynor, J. B., Lombardo, J. F., Fimognari, J. M., Calvo, J. A., Ghiglione, J. P., et al. (2008). Prevalence of SOD1 mutations in the Italian ALS population. *Neurology* 70, 533–537. doi: 10.1212/01.wnl.0000299187.90432.3f
- Chiu, I. M., Morimoto, E. T., Goodarzi, H., Liao, J. T., O'Keefe, S., Phatnani, H. P., et al. (2013). A neurodegeneration-specific gene-expression signature of acutely isolated microglia from an amyotrophic lateral sclerosis mouse model. *Cell Rep.* 4, 385–401. doi: 10.1016/j.celrep.2013.06.018
- Clayton, D. F., and George, J. M. (1999). Synucleins in synaptic plasticity and neurodegenerative disorders. *J. Neurosci. Res.* 58, 120–129. doi: 10.1002/(sici)1097-4547(19991001)58:1<120::aid-jnr12>3.0.co;2-e
- Clement, A. M., Nguyen, M. D., Roberts, E. A., Garcia, M. L., Boillee, S., Rule, M., et al. (2003). Wild-type nonneuronal cells extend survival of SOD1 mutant motor neurons in ALS mice. *Science* 302, 113–117. doi: 10.1126/science.1086071
- Cohen, M. L., Kim, C., Haldiman, T., Elhag, M., Mehndiratta, P., Pichet, T., et al. (2015). Rapidly progressive Alzheimer's disease features distinct structures of amyloid- $\beta$ . *Brain* 138, 1009–1022. doi: 10.1093/brain/awv006
- Coimbra, J. R. M., Marques, D. F. F., Baptista, S. J., Pereira, C. M. F., Moreira, P. I., Dinis, T. C. P., et al. (2018). Highlights in BACE1 inhibitors for Alzheimer's disease treatment. *Front. Chem.* 6:178. doi: 10.3389/fchem.2018.00178
- Combs, C. K., Karlo, J. C., Kao, S. C., and Landreth, G. E. (2001).  $\beta$ -Amyloid stimulation of microglia and monocytes results in TNF $\alpha$ -dependent expression of inducible nitric oxide synthase and neuronal apoptosis. *J. Neurosci.* 21, 1179–1188. doi: 10.1523/jneurosci.21-04-01179.2001
- Conway, K. A., Lee, S., Rochet, J., Ding, T. T., Williamson, R. E., and Lansbury, P. T. (2000). Acceleration of oligomerization, not fibrillization, is a shared property of both  $\alpha$ -synuclein mutations linked to early-onset parkinson's disease: implications for pathogenesis and therapy. *Proc. Natl. Acad. Sci. U S A* 97, 571–576. doi: 10.1073/pnas.97.2.571
- Coraci, I. S., Husemann, J., Berman, J. W., Huette, C., Dufour, J. H., Campanella, G. K., et al. (2002). CD36, a class B scavenger receptor, is expressed on microglia in Alzheimer's disease brains and can mediate production of reactive oxygen species in response to  $\beta$ -amyloid fibrils. *Am. J. Pathol.* 160, 101–112. doi: 10.1016/s0002-9440(10)64354-4
- Corder, E. H., Saunders, A. M., Risch, N. J., Strittmatter, W. J., Schmechel, D. E., Gaskell, P. C. Jr., et al. (1994). Protective effect of apolipoprotein E type 2 allele for late onset Alzheimer disease. *Nat. Genet.* 7, 180–184. doi: 10.1038/ng0694-180
- Corder, E. H., Saunders, A. M., Strittmatter, W. J., Gaskell, P. C., Roses, A. D., and Petricak-Vance, M. A. (1993). Gene dose of apolipoprotein E type 4 allele and the risk of Alzheimer's disease in late onset families. *Science* 261, 921–923. doi: 10.1126/science.8346443

- Cornett, J., Cao, F., Wang, C. E., Ross, C. A., Bates, G. P., Li, S. H., et al. (2005). Polyglutamine expansion of huntingtin impairs its nuclear export. *Nat. Genet.* 37, 198–204. doi: 10.1038/ng1503
- Couthois, J., Hart, M., Shorter, J., DeJesus-Hernandez, M., Erion, R., Oristano, R., et al. (2011). A yeast functional screen predicts new candidate ALS disease genes. *Proc. Natl. Acad. Sci. U S A* 108, 20881–20890. doi: 10.1073/pnas.1109434108
- Crotti, A., Benner, C., Kerman, B. E., Gosselin, D., Lagier-Tourenne, C., Zuccato, C., et al. (2014). Mutant Huntingtin promotes autonomous microglia activation via myeloid lineage-determining factors. *Nat. Neurosci.* 17, 513–521. doi: 10.1038/nn.3668
- Cuervo, A., Stefanis, L., Fredenburg, R., Lansbury, P., and Sulzer, D. (2004). Impaired degradation of mutant  $\alpha$ -synuclein by chaperone-mediated autophagy. *Science* 305, 1292–1295. doi: 10.1126/science.1101738
- Cushman, M., Johnson, B. S., King, O. D., Gitler, A. D., and Shorter, J. (2010). Prion-like disorders: blurring the divide between transmissibility and infectivity. *J. Cell Sci.* 123, 1191–1201. doi: 10.1242/jcs.051672
- d'Orange, M., Aurégan, G., Cheramy, D., Gaudin-Guérif, M., Lieger, S., Guillemer, M., et al. (2018). Potentiating tangle formation reduces acute toxicity of soluble tau species in the rat. *Brain* 141, 535–549. doi: 10.1093/brain/awx342
- Da Cruz, S., and Cleveland, D. (2011). Understanding the role of TDP-43 and FUS/TLS in ALS and beyond. *Curr. Opin. Neurobiol.* 21, 904–919. doi: 10.1016/j.conb.2011.05.029
- De Felice, B., Annunziata, A., Fiorentino, G., Manfellotto, F., D'Alessandro, R., Marino, R., et al. (2014). Telomerase expression in amyotrophic lateral sclerosis (ALS) patients. *J. Hum. Genet.* 59, 555–561. doi: 10.1038/jhg.2014.72
- de la Monte, S. M., Vonsattel, J. P., and Richardson, E. P. (1988). Morphometric demonstration of atrophic changes in the cerebral cortex, white matter, and neostriatum in Huntington's disease. *J. Neuropathol. Exp. Neurol.* 47, 516–525. doi: 10.1097/00005072-198809000-00003
- Delacourte, A., Sergeant, N., Wattez, A., Maurice, C., Lebert, F., Pasquier, F., et al. (2002). Tau aggregation in the hippocampal formation: an ageing or a pathological process? *Exp. Gerontol.* 37, 1291–1296. doi: 10.1016/s0531-5565(02)00141-9
- Deleault, N., Lucassen, R., and Supattapone, S. (2003). RNA molecules stimulate prion protein conversion. *Nature* 425, 717–720. doi: 10.1038/nature01979
- Deng, H., Gao, K., and Jankovic, J. (2014). The role of FUS gene variants in neurodegenerative diseases. *Nat. Rev. Neurol.* 10, 337–348. doi: 10.1038/nrneuro.2014.78
- Desplats, P., Lee, H.-J., Bae, E.-J., Patrick, C., Rockenstein, E., Crews, L., et al. (2009). Inclusion formation and neuronal cell death through neuron-to-neuron transmission of  $\alpha$ -synuclein. *Proc. Natl. Acad. Sci. U S A* 106, 13010–13015. doi: 10.1073/pnas.0903691106
- Dewey, C., Cenik, B., Sephton, C., Dries, D., Mayer, P., Good, S., et al. (2011). TDP-43 is directed to stress granules by sorbitol, a novel physiological osmotic and oxidative stressor. *Mol. Cell. Biol.* 31, 1098–1108. doi: 10.1128/MCB.01279-10
- Dheen, S. T., Kaur, C., and Ling, E. A. (2007). Microglial activation and its implications in the brain diseases. *Curr. Med. Chem.* 14, 1189–1197. doi: 10.2174/092986707780597961
- DiFiglia, M., Sapp, E., Chase, K., Schwarz, C., Meloni, A., Young, C., et al. (1995). Huntingtin is a cytoplasmic protein associated with vesicles in human and rat brain neurons. *Neuron* 14, 1075–1081. doi: 10.1016/0896-6273(95)90346-1
- Donati, A., Cavallini, G., Paradiso, C., Vittorini, S., Pollera, M., Gori, Z., et al. (2001). Age-related changes in the autophagic proteolysis of rat isolated liver cells: effects of antiaging dietary restrictions. *J. Gerontol. A Biol. Sci. Med. Sci.* 56, B375–B383. doi: 10.1093/gerona/56.9.b375
- Dormann, D., Rodde, R., Edbauer, D., Bentmann, E., Fischer, I., Hruscha, A., et al. (2010). ALS-associated fused in sarcoma (FUS) mutations disrupt transportin-mediated nuclear import. *EMBO J.* 29, 2841–2857. doi: 10.1038/emboj.2010.143
- Drechsel, D., Estévez, A., Barbeito, L., and Beckman, J. (2012). Nitric oxide-mediated oxidative damage and the progressive demise of motor neurons in ALS. *Neurotox. Res.* 22, 251–264. doi: 10.1007/s12640-012-9322-y
- Ebner, A., Godemann, R., Stamer, K., and Illenberger, S. (1998). Overexpression of tau protein inhibits kinesin-dependent trafficking of vesicles, mitochondria, and endoplasmic reticulum: implications for Alzheimer's disease. *J. Cell Biol.* 143, 777–794. doi: 10.1083/jcb.143.3.777
- Eisenberg, D., and Jucker, M. (2012). The amyloid state of proteins in human diseases. *Cell* 148, 1188–1203. doi: 10.1016/j.cell.2012.02.022
- El Khoury, J., Toft, M., Hickman, S. E., Means, T. K., Terada, K., Geula, C., et al. (2007). Ccr2 deficiency impairs microglial accumulation and accelerates progression of Alzheimer-like disease. *Nat. Med.* 13, 432–438. doi: 10.1038/nm1555
- Enari, M., Flechsig, E., and Weissmann, C. (2001). Scrapie prion protein accumulation by scrapie-infected neuroblastoma cells abrogated by exposure to a prion protein antibody. *Proc. Natl. Acad. Sci. U S A* 98, 9295–9299. doi: 10.1073/pnas.151242598
- Eraña, H. (2019). The Prion 2018 round tables (II): A $\beta$ , tau,  $\alpha$ -synuclein... are they prions, prion-like proteins, or what? *Prion* 13, 41–45. doi: 10.1080/19336896.2019.1569451
- Fellner, L., Irschick, R., Schanda, K., Reindl, M., Klimaschewski, L., Poewe, W., et al. (2013). Toll-like receptor 4 is required for  $\alpha$ -synuclein dependent activation of microglia and astroglia. *Glia* 61, 349–360. doi: 10.1002/glia.22437
- Filimonenko, M., Stuffers, S., Raiborg, C., Yamamoto, A., Malerod, L., Fisher, E. M., et al. (2007). Functional multivesicular bodies are required for autophagic clearance of protein aggregates associated with neurodegenerative disease. *J. Cell Biol.* 179, 485–500. doi: 10.1083/jcb.200702115
- Fischer, L. R., Li, Y., Asress, S. A., Jones, D. P., and Glass, J. D. (2012). Absence of SOD1 leads to oxidative stress in peripheral nerve and causes a progressive distal motor axonopathy. *Exp. Neurol.* 233, 163–171. doi: 10.1016/j.expneurol.2011.09.020
- Flanary, B. E., Sammons, N. W., Nguyen, C., Walker, D., and Streit, W. J. (2007). Evidence that aging and amyloid promote microglial cell senescence. *Rejuvenation Res.* 10, 61–74. doi: 10.1089/rej.2006.9096
- Forero, D. A., Gonzalez-Giraldo, Y., Lopez-Quintero, C., Castro-Vega, L. J., Barreto, G. E., and Perry, G. (2016). Meta-analysis of telomere length in Alzheimer's disease. *J. Gerontol. A Biol. Sci. Med. Sci.* 71, 1069–1073. doi: 10.1093/gerona/glw053
- Friedhoff, P., von Bergen, M., Mandelkow, E., Davies, P., and Mandelkow, E. (1998). A nucleated assembly mechanism of Alzheimer paired helical filaments. *Proc. Natl. Acad. Sci. U S A* 95, 15712–15717. doi: 10.1073/pnas.95.26.15712
- Frost, B., Jacks, R. L., and Diamond, M. I. (2009). Propagation of tau misfolding from the outside to the inside of a cell. *J. Biol. Chem.* 284, 12845–12852. doi: 10.1074/jbc.M808759200
- Furukawa, Y., Kaneko, K., Watanabe, S., Yamanaka, K., and Nukina, N. (2011). A seeding reaction recapitulates intracellular formation of Sarkosyl-insoluble transactivation response element (TAR) DNA-binding protein-43 inclusions. *J. Biol. Chem.* 286, 18664–18672. doi: 10.1074/jbc.M111.231209
- Gainotti, G., Marra, C., Villa, G., Parlato, V., and Chiarotti, F. (1998). Sensitivity and specificity of some neuropsychological markers of Alzheimer dementia. *Alzheimer Dis. Assoc. Disord.* 12, 152–162. doi: 10.1097/00002093-199809000-00006
- Gasset-Rosa, F., Lu, S., Yu, H., Chen, C., Melamed, Z., Guo, L., et al. (2019). Cytoplasmic TDP-43 de-mixing independent of stress granules drives inhibition of nuclear import, loss of nuclear TDP-43 and cell death. *Neuron* 102, 339.e7–357.e7. doi: 10.1016/j.neuron.2019.02.038
- Gehrmann, J., Matsumoto, Y., and Kreutzberg, G. W. (1995). Microglia: intrinsic immunoreactive cell of the brain. *Brain Res. Rev.* 20, 269–287. doi: 10.1016/0165-0173(94)00015-h
- Geser, F., Brandmeier, N. J., Kwong, L. K., Martinez-Lage, M., Elman, L., McCluskey, L., et al. (2008). Evidence of multisystem disorder in whole-brain map of pathological TDP-43 in amyotrophic lateral sclerosis. *Arch. Neurol.* 65, 636–641. doi: 10.1001/archneur.65.5.636
- Giasson, B., Forman, M., Higuchi, M., Golbe, L., Craves, C., Kotzbauer, P., et al. (2003). Initiation and synergistic fibrillization of tau and  $\alpha$ -synuclein. *Science* 300, 636–640. doi: 10.1126/science.1082324
- Gilks, N., Kedarsha, N., Ayodele, M., Shen, L., Stoecklin, G., Dember, L., et al. (2004). Stress granule assembly is mediated by prion-like aggregation of TIA-1. *Mol. Biol. Cell* 15, 5383–5398. doi: 10.1091/mbc.e04-08-0715
- Gitler, A. D., and Shorter, J. (2011). RNA-binding proteins with prion-like domains in ALS and FTLD-U. *Prion* 5, 179–187. doi: 10.4161/pri.5.3.17230
- Goedert, M., and Spillantini, M. (2006). A century of Alzheimer's disease. *Science* 314, 777–781. doi: 10.1126/science.1132814



- Gómez-Isla, T., Hollister, R., West, H., Mui, S., Growdon, J. H., Petersen, R. C., et al. (1997). Neuronal loss correlates with but exceeds neurofibrillary tangles in Alzheimer's disease. *Ann. Neurol.* 41, 17–24. doi: 10.1002/ana.410410106
- Goñi, F., Martí-Ariza, M., Peyser, D., Herline, K., and Wisniewski, T. (2017). Production of monoclonal antibodies to pathologic  $\beta$ -sheet oligomeric conformers in neurodegenerative diseases. *Sci. Rep.* 7:9881. doi: 10.1038/s41598-017-10393-z
- Gravina, S., Ho, L., Eckman, C., Long, K., Otvos, L., Younkin, L., et al. (1995). Amyloid  $\beta$  protein (A $\beta$ ) in Alzheimer's disease brain: biochemical and immunocytochemical analysis with antibodies specific for forms ending at A $\beta$ 40 or A $\beta$ 42(43). *J. Biol. Chem.* 270, 7013–7016. doi: 10.1074/jbc.270.13.7013
- Grundke-Iqbal, I., Iqbal, K., and Tung, Y. C. (1986). Abnormal phosphorylation of the microtubule-associated protein  $\tau$  (tau) in Alzheimer cytoskeletal pathology. *Proc. Natl. Acad. Sci. U S A* 83, 44913–44917. doi: 10.1073/pnas.83.13.4913
- Gu, X.-L., Long, C.-X., Sun, L., Xie, C., Lin, X., and Cai, H. (2010). Astrocytic expression of Parkinson's disease-related A53T  $\alpha$ -synuclein causes neurodegeneration in mice. *Mol. Brain* 3:12. doi: 10.1186/1756-6606-3-12
- Guarino, A., Favieri, F., Boncompagni, I., Agostini, F., Cantone, M., and Casagrande, M. (2019). Executive functions in alzheimer disease: a systematic review. *Front. Aging Neurosci.* 10:437. doi: 10.3389/fnagi.2018.00437
- Guo, J. L., Covell, D., Daniels, J. P., Iba, M., Stieber, A., Zhang, B., et al. (2013). Distinct  $\alpha$ -synuclein strains differentially promote tau inclusions in neurons. *Cell* 154, 103–117. doi: 10.1016/j.cell.2013.05.057
- Halfmann, R., Alberti, S., Krishnan, R., Lyle, N., O'Donnell, C., King, O., et al. (2011). Opposing effects of glutamine and asparagine govern prion formation by intrinsically disordered proteins. *Mol. Cell* 43, 72–84. doi: 10.1016/j.molcel.2011.05.013
- Hamano, T., Hayashi, K., Shirafuji, N., and Nakamoto, Y. (2018). The implications of autophagy in Alzheimer's disease. *Curr. Alzheimer Res.* 15, 1283–1296. doi: 10.2174/1567205015666181004143432
- Hara, T., Nakamura, K., Matsui, M., Yamamoto, A., Nakahara, Y., Suzuki-Migishima, R., et al. (2006). Suppression of basal autophagy in neural cells causes neurodegenerative disease in mice. *Nature* 441, 885–889. doi: 10.1038/nature04724
- Harbi, D., and Harrison, P. M. (2014). Classifying prion and prion-like phenomena. *Prion* 8:27960. doi: 10.4161/pri.27960
- Hashimoto, T., Serrano-Pozo, A., Hori, Y., Adams, K. W., Takeda, S., Banerji, A. O., et al. (2012). Apolipoprotein E, especially apolipoprotein E4, increases the oligomerization of amyloid  $\beta$  peptide. *J. Neurosci.* 32, 15181–15192. doi: 10.1523/JNEUROSCI.1542-12.2012
- Hawkes, C. H., Del Tredici, K., and Braak, H. (2007). Parkinson's disease: a dual-hit hypothesis. *Neuropathol. Appl. Neurobiol.* 33, 599–614. doi: 10.1111/j.1365-2990.2007.00874.x
- He, Z., Guo, J. L., McBride, J. D., Narasimhan, S., Kim, H., Changolkar, L., et al. (2018). Amyloid- $\beta$  plaques enhance Alzheimer's brain tau-seeded pathologies by facilitating neuritic plaque tau aggregation. *Nat. Med.* 24, 29–38. doi: 10.1038/nm.4443
- Hennig, S., Kong, G., Mannen, T., Sadowska, A., Kobelke, S., Blythe, A., et al. (2015). Prion-like domains in RNA binding proteins are essential for building subnuclear paraspeckles. *J. Cell. Biol.* 210, 529–539. doi: 10.1083/jcb.201504117
- Herrera, F., Tenreiro, S., Miller-Fleming, L., and Outeiro, T. F. (2011). Visualization of cell-to-cell transmission of mutant huntingtin oligomers. *PLoS Curr.* 3:RRN1210. doi: 10.1371/currents.rn1210
- Hess, D. T., Matsumoto, A., Kim, S., Marshall, H. E., and Stamler, J. S. (2005). Protein S-nitrosylation: purview and parameters. *Nat. Rev. Mol. Cell Biol.* 6, 150–166. doi: 10.1038/nrm1569
- Higelin, J., Demestre, M., Putz, S., Delling, J. P., Jacob, C., Lutz, A., et al. (2016). FUS mislocalization and vulnerability to DNA damage in ALS patients derived hiPSCs and aging motoneurons. *Front. Cell. Neurosci.* 10:290. doi: 10.3389/fncel.2016.00290
- Hiltunen, M., van Groen, T., and Jolkonen, J. (2009). Functional roles of amyloid- $\beta$  protein precursor and amyloid- $\beta$  peptides: evidence from experimental studies. *J. Alzheimers Dis.* 18, 401–412. doi: 10.3233/jad-2009-1154
- Hoell, J. I., Larsson, E., Runge, S., Nusbaum, J. D., Duggimpudi, S., Farazi, T. A., et al. (2011). RNA targets of wild-type and mutant FET family proteins. *Nat. Struct. Mol. Biol.* 18, 1428–1431. doi: 10.1038/nsmb.2163
- Hoffmann, A.-C., Minakaki, G., Meges, S., Salvi, R., Savitskiy, S., Kazman, A., et al. (2019). Extracellular aggregated  $\alpha$  synuclein primarily triggers lysosomal dysfunction in neural cells prevented by trehalose. *Sci. Rep.* 9:544. doi: 10.1038/s41598-018-35811-8
- Hoffner, G., Kahlem, P., and Djian, P. (2002). Perinuclear localization of huntingtin as a consequence of its binding to microtubules through an interaction with  $\beta$ -tubulin: relevance to Huntington's disease. *J. Cell Sci.* 115, 941–948.
- Holmberg, C. I., Staniszewski, K. E., Mensah, K. N., Matouschek, A., and Morimoto, R. I. (2004). Inefficient degradation of truncated polyglutamine proteins by the proteasome. *EMBO J.* 23, 4307–4318. doi: 10.1038/sj.emboj.7600426
- Hoover, B. R., Reed, M. N., Su, J., Penrod, R. D., Kotilinek, L. A., Grant, M. K., et al. (2010). Tau mislocalization to dendritic spines mediates synaptic dysfunction independently of neurodegeneration. *Neuron* 68, 1067–1081. doi: 10.1016/j.neuron.2010.11.030
- Hung, M., and Link, W. (2011). Protein localization in disease and therapy. *J. Cell Sci.* 124, 3381–3392. doi: 10.1242/jcs.089110
- Hyman, B., West, H., Rebeck, G., and Buldyrev, S. (1995). Quantitative analysis of senile plaques in Alzheimers disease: observation of log-normal size distribution and molecular epidemiology of differences associated with apolipoprotein E genotype and trisomy 21 (Down syndrome). *Proc. Natl. Acad. Sci. U S A* 92, 3586–3590. doi: 10.1073/pnas.92.8.3586
- Iannaccone, S., Cerami, C., Cerami, M., Garibotto, V., Panzacchi, A., Gelsomino, S., et al. (2012). *In vivo* microglia activation in very early dementia with Lewy bodies, comparison with Parkinson's disease. *Parkinsonism Relat. Disord.* 19, 47–52. doi: 10.1016/j.parkreldis.2013.06.013
- Iijima-Ando, K., Hearn, S. A., Shenton, C., Gatt, A., Zhao, L., Iijima, K., et al. (2009). Mitochondrial mislocalization underlies A $\beta$ 42-induced neuronal dysfunction in a *Drosophila* model of Alzheimer's disease. *PLoS One* 4:e8310. doi: 10.1371/journal.pone.0008310
- Imarisio, S., Carmichael, J., Korolchuk, V., Chen, C. W., Saiki, S., Rose, C., et al. (2008). Huntington's disease: from pathology and genetics to potential therapies. *Biochem. J.* 412, 191–209. doi: 10.1042/BJ20071619
- Invernizzi, G., Papaleo, E., Sabate, R., and Ventura, S. (2012). Protein aggregation: mechanisms and functional consequences. *Int. J. Biochem. Cell Biol.* 44, 1541–1554. doi: 10.1016/j.biocel.2012.05.023
- Iwatsubo, T., Odaka, A., Suzuki, N., Mizusawa, H., Nukina, N., and Ihara, Y. (1994). Visualization of A $\beta$ 42(43) and A $\beta$ 40 in senile plaques with end-specific A $\beta$  monoclonals: Evidence that an initially deposited species is A $\beta$ 42(43). *Neuron* 13, 45–53. doi: 10.1016/0896-6273(94)90458-8
- Jankovic, J., Goodman, I., Safirstein, B., Marmon, T. K., Schenk, D. B., Koller, M., et al. (2018). Safety and tolerability of multiple ascending doses of PRX002/RG7935, an anti- $\alpha$ -synuclein monoclonal antibody, in patients with Parkinson disease: a randomized clinical trial. *JAMA Neurol.* 75, 1206–1214. doi: 10.1001/jamaneurol.2018.1487
- Jankowsky, J., Slunt, H., Gonzales, V., Savonenko, A., Wen, J., Jenkins, N., et al. (2005). Persistent amyloidosis following suppression of A $\beta$  production in a transgenic model of alzheimer disease. *PLoS Med.* 2:e355. doi: 10.1371/journal.pmed.0020355
- Jankowsky, J. L., Slunt, H. H., Ratovitski, T., Jenkins, N. A., Copeland, N. G., and Borchelt, D. R. (2001). Co-expression of multiple transgenes in mouse CNS: a comparison of strategies. *Biomol. Eng.* 17, 157–165. doi: 10.1016/s1389-0344(01)00067-3
- Jin, J., Shie, F. S., Liu, J., Wang, Y., Davis, J., Schantz, A. M., et al. (2007). Prostaglandin E2 receptor subtype 2 (EP2) regulates microglial activation and associated neurotoxicity induced by aggregated  $\alpha$ -synuclein. *J. Neuroinflammation* 4:2. doi: 10.1186/1742-2094-4-2
- Jin, X., and Yamashita, T. (2016). Microglia in central nervous system repair after injury. *J. Biochem.* 159, 491–496. doi: 10.1093/jb/mvw009
- Johnston, J., Dalton, M., Gurney, M., and Kopito, R. (2000). Formation of high molecular weight complexes of mutant Cu, Zn-superoxide dismutase in a mouse model for familial amyotrophic lateral sclerosis. *Proc. Natl. Acad. Sci. U S A* 97, 12571–12576. doi: 10.1073/pnas.220417997
- Johnson, B., McCaffery, J., Lindquist, S., and Gitler, A. (2008). A yeast TDP-43 proteinopathy model: exploring the molecular determinants of TDP-43 aggregation and cellular toxicity. *Proc. Natl. Acad. Sci. U S A* 105, 6439–6444. doi: 10.1073/pnas.0802082105

- Johnson, B., Snead, D., Lee, J., McCaffery, J., Shorter, J., and Gitler, A. (2009). TDP-43 is intrinsically aggregation-prone and amyotrophic lateral sclerosis-linked mutations accelerate aggregation and increase toxicity. *J. Biol. Chem.* 284, 20329–20339. doi: 10.1074/jbc.M109.01026
- Kasyapa, C., Kunapuli, P., and Cowell, J. (2005). Mass spectroscopy identifies the splicing-associated proteins, PSD, hnRNP H3, hnRNP A2/B1 and TLS/FUS as interacting partners of the ZNF198 protein associated with rearrangement in myeloproliferative disease. *Exp. Cell Res.* 309, 78–85. doi: 10.1016/j.yexcr.2005.05.019
- Kato, S., Takikawa, M., Nakashima, K., Hirano, A., Cleveland, D., Kusaka, H., et al. (2000). New consensus research on neuropathological aspects of familial amyotrophic lateral sclerosis with superoxide dismutase 1 (SOD1) gene mutations: inclusions containing SOD1 in neurons and astrocytes. *Amyotroph. Lateral Scler. Other Motor Neuron Disord.* 1, 163–184. doi: 10.1080/14660820050151560
- Kaufman, S. K., Sanders, D. W., Thomas, T. L., Ruchinskas, A. J., Vaquer-Alicea, J., Sharma, A. M., et al. (2016). Tau prion strains dictate patterns of cell pathology, progression rate and regional vulnerability *in vivo*. *Neuron* 92, 796–812. doi: 10.1016/j.neuron.2016.09.055
- Khatoun, S., Grundke-Iqbal, I., and Iqbal, K. (1992). Brain levels of microtubule-associated protein  $\tau$  are elevated in Alzheimer's disease: a radioimmunoslot-blot assay for nanograms of the protein. *J. Neurochem.* 59, 750–753. doi: 10.1111/j.1471-4159.1992.tb09432.x
- Kieran, D., Hafezparast, M., Bohnert, S., Dick, J. R. T., Martin, J., Schiavo, G., et al. (2005). A mutation in dynein rescues axonal transport defects and extends the life span of ALS mice. *J. Cell Biol.* 169, 561–567. doi: 10.1083/jcb.200501085
- Kim, W., Choi, Y., Rayudu, P., Das, P., Asaad, W., Arnelles, D., et al. (1999). Attenuation of NMDA receptor activity and neurotoxicity by nitroxyl anion, NO<sup>-</sup>. *Neuron* 24, 461–469. doi: 10.1016/s0896-6273(00)80859-4
- Kim, Y. E., Hosp, F., Frottin, F., Ge, H., Mann, M., Hayer-Hartl, M., et al. (2016). Soluble oligomers of PolyQ-expanded huntingtin target a multiplicity of key cellular factors. *Mol. Cell* 63, 951–964. doi: 10.1016/j.molcel.2016.07.022
- Kim, Y. S., Jung, H. M., and Yoon, B.-E. (2018). Exploring glia to better understand Alzheimer's disease. *Anim. Cells Syst.* 22, 213–218. doi: 10.1080/19768354.2018.1508498
- King, O. D., Gitler, A. D., and Shorter, J. (2012). The tip of the iceberg: RNA-binding proteins with prion-like domains in neurodegenerative disease. *Brain Res.* 1462, 61–80. doi: 10.1016/j.brainres.2012.01.016
- King, A. E., Woodhouse, A., Kirkcaldie, M. T., and Vickers, J. C. (2016). Excitotoxicity in ALS: overstimulation, or overreaction? *Exp. Neurol.* 275, 162–171. doi: 10.1016/j.expneurol.2015.09.019
- Klim, J. R., Williams, L. A., Limone, F., Guerra San Juan, I., Davis-Dusenberry, B. N., Mordes, D. A., et al. (2019). ALS-implicated protein TDP-43 sustains levels of STMN2, a mediator of motor neuron growth and repair. *Nat. Neurosci.* 22, 167–179. doi: 10.1038/s41593-018-0300-4
- Koistinaho, M., Lin, S., Wu, X., Esterman, M., Koger, D., Hanson, J., et al. (2004). Apolipoprotein E promotes astrocyte colocalization and degradation of deposited amyloid- $\beta$  peptides. *Nat. Med.* 10, 719–826. doi: 10.1038/nm1058
- Komatsu, M., Waguri, S., Chiba, T., Murata, S., Iwata, J.-I., Tanida, I., et al. (2006). Loss of autophagy in the central nervous system causes neurodegeneration in mice. *Nature* 441, 880–884. doi: 10.1038/nature04723
- Köpke, E., Tung, Y. C., Shaikh, S., Alonso, A. C., Iqbal, K., and Grundke-Iqbal, I. (1993). Microtubule-associated protein tau. Abnormal phosphorylation of a non-paired helical filament pool in Alzheimer disease. *J. Biol. Chem.* 268, 24374–24384.
- Korolchuk, V. I., Mansilla, A., Menzies, F. M., and Rubinsztein, D. C. (2009). Autophagy inhibition compromises degradation of ubiquitin-proteasome pathway substrates. *Mol. Cell* 33, 517–527. doi: 10.1016/j.molcel.2009.01.021
- Kotzbauer, P., Giasson, B., Kravitz, A., Golbe, L., Mark, M., Trojanowski, J., et al. (2004). Fibrillization of  $\alpha$ -synuclein and tau in familial Parkinson's disease caused by the A53T  $\alpha$ -synuclein mutation. *Exp. Neurol.* 187, 279–288. doi: 10.1016/j.expneurol.2004.01.007
- Kummer, M. P., Hermes, M., Delekarte, A., Hammerschmidt, T., Kumar, S., Terwel, D., et al. (2011). Nitration of tyrosine 10 critically enhances amyloid  $\beta$  aggregation and plaque formation. *Neuron* 71, 833–844. doi: 10.1016/j.neuron.2011.07.001
- Kwiatkowski, T. J. Jr., Bosco, D. A., Leclerc, A. L., Tamrazian, E., Vanderburg, C. R., Russ, C., et al. (2009). Mutations in the FUS/TLS gene on chromosome 16 cause familial amyotrophic lateral sclerosis. *Science* 323, 1205–1208. doi: 10.1126/science.1166066
- Lace, G., Savva, G., Forster, G., de Silva, R., Brayne, C., Matthews, F., et al. (2009). Hippocampal tau pathology is related to neuroanatomical connections: an ageing population-based study. *Brain* 132, 1324–1334. doi: 10.1093/brain/awp059
- Lai, A. Y., and McLaurin, J. (2012). Clearance of amyloid- $\beta$  peptides by microglia and macrophages: the issue of what, when and where. *Future Neurol.* 7, 165–176. doi: 10.2217/fnl.12.6
- Leavitt, B. R., van Raamsdonk, J. M., Shehadeh, J., Fernandes, H., Murphy, Z., Graham, R. K., et al. (2006). Wild-type huntingtin protects neurons from excitotoxicity. *J. Neurochem.* 96, 1121–1129. doi: 10.1111/j.1471-4159.2005.03605.x
- Lecours, C., Bordeleau, M., Cantin, L., Parent, M., Paolo, T. D., and Tremblay, M.-E. (2018). Microglial implication in Parkinson's disease: loss of beneficial physiological roles or gain of inflammatory functions? *Front. Cell. Neurosci.* 12:282. doi: 10.3389/fncel.2018.00282
- Lee, D., Jeon, G. S., Shim, Y., Seong, S., Lee, K., and Sung, J. (2015). Modulation of SOD1 subcellular localization by transfection with wild- or mutant-type SOD1 in primary neuron and astrocyte cultures from ALS mice. *Exp. Neurobiol.* 24, 226–234. doi: 10.5607/en.2015.24.3.226
- Lee, S., and Kim, H. (2014). Prion-like mechanism in amyotrophic lateral sclerosis: are protein aggregates the key? *Exp. Neurobiol.* 24, 1–7. doi: 10.5607/en.2015.24.1.1
- Lee, H. J., Khoshaghideh, F., Patel, S., and Lee, S. J. (2004). Clearance of  $\alpha$ -synuclein oligomeric intermediates via the lysosomal degradation pathway. *J. Neurosci.* 24, 1888–1896. doi: 10.1523/JNEUROSCI.3809-03.2004
- Lee, H., Patel, S., and Lee, S. (2005). Intravesicular localization and exocytosis of  $\alpha$ -synuclein and its aggregates. *J. Neurosci.* 25, 6016–6024. doi: 10.1523/JNEUROSCI.0692-05.2005
- Lee, M.-H., Siddoway, B., Kaeser, G. E., Segota, I., Rivera, R., Romanow, W. J., et al. (2018). Somatic APP gene recombination in Alzheimer's disease and normal neurons. *Nature* 563, 639–645. doi: 10.1038/s41586-018-0718-6
- Lee, H. J., Suk, J. E., Bae, E. J., and Lee, S. J. (2008). Clearance and deposition of extracellular  $\alpha$ -synuclein aggregates in microglia. *Biochem. Biophys. Res. Commun.* 372, 423–428. doi: 10.1016/j.bbrc.2008.05.045
- Lee, H. J., Suk, J. E., Patrick, C., Bae, E. J., Cho, J. H., Rho, S., et al. (2010). Direct transfer of  $\alpha$ -synuclein from neuron to astroglia causes inflammatory responses in synucleinopathies. *J. Biol. Chem.* 285, 9262–9272. doi: 10.1074/jbc.M109.081125
- Lei, G., and Zhefeng, G. (2013). Alzheimer's A $\beta$ 42 and A $\beta$ 40 peptides form interlaced amyloid. *J. Neurochem.* 126, 305–311. doi: 10.1111/jnc.12202
- Leighton, P. L., and Allison, W. T. (2016). Protein misfolding in prion and prion-like diseases: reconsidering a required role for protein loss-of-function. *J. Alzheimers Dis.* 54, 3–29. doi: 10.3233/jad-160361
- Leitman, J., Ulrich Hartl, F., and Lederkremer, G. Z. (2013). Soluble forms of polyQ-expanded huntingtin rather than large aggregates cause endoplasmic reticulum stress. *Nat. Commun.* 4:2753. doi: 10.1038/ncomms3753
- Li, B., Chohan, M., Grundke-Iqbal, I., and Iqbal, K. (2007). Disruption of microtubule network by Alzheimer abnormally hyperphosphorylated tau. *Acta Neuropathol.* 113, 501–511. doi: 10.1007/s00401-007-0207-8
- Li, T., and Zhang, S. (2016). Microgliosis in the injured brain: infiltrating cells and reactive microglia both play a role. *Neuroscientist* 22, 165–170. doi: 10.1177/1073858415572079
- Lian, H., Litvinchuk, A., Chiang, A. C. A., Aithmitti, N., Jankowsky, J. L., and Zheng, H. (2016). Astrocyte-microglia cross talk through complement activation modulates amyloid pathology in mouse models of Alzheimer's disease. *J. Neurosci.* 36, 577–589. doi: 10.1523/JNEUROSCI.2117-15.2016
- Liao, B., Zhao, W., Beers, D. R., Henkel, J. S., and Appel, S. H. (2012). Transformation from a neuroprotective to a neurotoxic microglial phenotype in a mouse model of ALS. *Exp. Neurol.* 237, 147–152. doi: 10.1016/j.expneurol.2012.06.011
- Liddel, S. A., Guttenplan, K. A., Clarke, L. E., Bennett, F. C., Bohlen, C. J., Schirmer, L., et al. (2017). Neurotoxic reactive astrocytes are induced by activated microglia. *Nature* 541, 481–487. doi: 10.1038/nature21029
- Linkus, B., Wiesner, D., Meßner, M., Karabatsiakakis, A., Scheffold, A., Rudolph, K. L., et al. (2016). Telomere shortening leads to earlier age of onset in ALS mice. *Aging* 8, 382–393. doi: 10.18632/aging.100904

- Liu, Y., Holdbrooks, A. T., De Sarno, P., Rowse, A. L., Yanagisawa, L. L., McFarland, B. C., et al. (2014). Therapeutic efficacy of suppressing the Jak/STAT pathway in multiple models of experimental autoimmune encephalomyelitis. *J. Immunol.* 192, 59–72. doi: 10.4049/jimmunol.1301513
- Liu, M., Huo, Y. R., Wang, C., Liu, S., Liu, S., et al. (2016). Telomere shortening in Alzheimer's disease patients. *Ann. Clin. Lab. Sci.* 46, 260–265.
- Liu, C., Liu, C., Kanekiyo, T., Xu, H., and Bu, G. (2013). Apolipoprotein E and Alzheimer disease: risk, mechanisms and therapy. *Nat. Rev. Neurol.* 9, 106–118. doi: 10.1038/nrneuro.2012.263
- Luk, K., Song, C., O'Brien, P., Stieber, A., Branch, J., Brunden, K., et al. (2009). Exogenous  $\alpha$ -synuclein fibrils seed the formation of Lewy body-like intracellular inclusions in cultured cells. *Proc. Natl. Acad. Sci. U S A* 106, 20051–20056. doi: 10.1073/pnas.0908005106
- Luo, X.-G., and Chen, S.-D. (2012). The changing phenotype of microglia from homeostasis to disease. *Transl. Neurodegener.* 1:9. doi: 10.1186/2047-9158-1-9
- Ma, M., Hu, Z., Zhao, Y., Chen, Y., and Li, Y. (2016). Phosphorylation induces distinct  $\alpha$ -synuclein strain formation. *Sci. Rep.* 6:37130. doi: 10.1038/srep37130
- MacDonald, M. E., Ambrose, C. M., Duyao, M. P., Myers, R. H., Lin, C., Srinidhi, L., et al. (1993). A novel gene containing a trinucleotide repeat that is expanded and unstable on Huntington's disease chromosomes. *Cell* 72, 971–983. doi: 10.1016/0092-8674(93)90585-e
- Mackenzie, I. R., Nicholson, A. M., Sarkar, M., Messing, J., Purice, M. D., Pottier, C., et al. (2017). T1A1 mutations in amyotrophic lateral sclerosis and frontotemporal dementia promote phase separation and alter stress granule dynamics. *Neuron* 95, 808.e9–816.e9. doi: 10.1016/j.neuron.2017.07.025
- Mackenzie, I., Rademakers, R., and Neumann, M. (2010). TDP-43 and FUS in amyotrophic lateral sclerosis and frontotemporal dementia. *Lancet Neurol.* 9, 995–1007. doi: 10.1016/s1474-4422(10)70195-2
- Mander, P., and Brown, G. C. (2005). Activation of microglial NADPH oxidase is synergistic with glial iNOS expression in inducing neuronal death: a dual-key mechanism of inflammatory neurodegeneration. *J. Neuroinflammation* 2:20. doi: 10.1038/s41419-017-0091-7
- Mandrioli, J., D'Amico, R., Zucchi, E., Gessani, A., Fini, N., Fasano, A., et al. (2018). Rapamycin treatment for amyotrophic lateral sclerosis: protocol for a phase II randomized, double-blind, placebo-controlled, multicenter, clinical trial (RAP-ALS trial). *Medicine* 97:e11119. doi: 10.1097/md.0000000000001119
- Manghera, M., Ferguson-Parry, J., and Douville, R. N. (2016). TDP-43 regulates endogenous retrovirus-K viral protein accumulation. *Neurobiol. Dis.* 94, 226–236. doi: 10.1016/j.nbd.2016.06.017
- Mangiarini, L., Sathasivam, K., Mahal, A., Mott, R., Seller, M., and Bates, G. P. (1997). Instability of highly expanded CAG repeats in mice transgenic for the Huntington's disease mutation. *Nat. Genet.* 15, 197–200. doi: 10.1038/ng0297-197
- Manoutcharian, K., Perez-Garmendia, R., and Gevorkian, G. (2017). Recombinant antibody fragments for neurodegenerative diseases. *Curr. Neuropharmacol.* 15, 779–788. doi: 10.2174/1570159x01666160930121647
- March, Z. M., King, O. D., and Shorter, J. (2016). Prion-like domains as epigenetic regulators, scaffolds for subcellular organization and drivers of neurodegenerative disease. *Brain Res.* 1647, 9–18. doi: 10.1016/j.brainres.2016.02.037
- Maroteaux, L., Campanelli, J. T., and Scheller, R. H. (1988). Synuclein: a neuron-specific protein localized to the nucleus and presynaptic nerve terminal. *J. Neurosci.* 8, 2804–2815. doi: 10.1523/JNEUROSCI.08-08-02804.1988
- Massey, A., Kiffin, R., and Cuervo, A. (2006). Autophagic defects in aging: looking for an “emergency exit”? *Cell Cycle* 5, 1292–1296. doi: 10.4161/cc.5.12.2865
- Masuch, A., Shieh, C. H., van Rooijen, N., van Calker, D., and Biber, K. (2016). Mechanism of microglia neuroprotection: involvement of P2X7, TNF $\alpha$ , and valproic acid. *Glia* 64, 76–89. doi: 10.1002/glia.22904
- Mathew, R., Karp, C. M., Beaudoin, B., Vuong, N., Chen, G., Chen, H.-Y., et al. (2009). Autophagy suppresses tumorigenesis through elimination of p62. *Cell* 137, 1062–1075. doi: 10.1016/j.cell.2009.03.048
- Mawuenyega, K. G., Sigurdson, W., Ovod, V., Munsell, L., Kasten, T., Morris, J. C., et al. (2010). Decreased clearance of CNS amyloid- $\beta$  in Alzheimer's disease. *Science* 330:1774. doi: 10.1126/science.1197623
- McGowan, E., Pickford, F., Kim, J., Onstead, L., Eriksen, J., Yu, C., et al. (2005). A $\beta$ 42 is essential for parenchymal and vascular amyloid deposition in mice. *Neuron* 47, 191–199. doi: 10.1016/j.neuron.2005.06.030
- Meda, L., Cassatella, M. A., Szendrei, G. I., Ottvos, L. Jr., Baron, P., Villalba, M., et al. (1995). Activation of microglial cells by  $\beta$ -amyloid protein and interferon- $\gamma$ . *Nature* 374, 647–650. doi: 10.1038/374647a0
- Melamed, Z., López-Erauskin, J., Baughn, M. W., Zhang, O., Drenner, K., Sun, Y., et al. (2019). Premature polyadenylation-mediated loss of stathmin-2 is a hallmark of TDP-43-dependent neurodegeneration. *Nat. Neurosci.* 22, 180–190. doi: 10.1038/s41593-018-0293-z
- Melnikova, T., Fromholt, S., Kim, H., Lee, D., Xu, G., Price, A., et al. (2013). Reversible pathologic and cognitive phenotypes in an inducible model of Alzheimer-amyloidosis. *J. Neurosci.* 33, 3765–3779. doi: 10.1523/JNEUROSCI.4251-12.2013
- Meyer-Luehmann, M., Coomaraswamy, J., Bolmont, T., Kaeser, S., Schaefer, C., Kilger, E., et al. (2006). Exogenous induction of cerebral  $\beta$ -amyloidogenesis is governed by agent and host. *Science* 313, 1781–1784. doi: 10.1126/science.1131864
- Miller, D., Papayannopoulos, I., Styles, J., Bobin, S., Lin, Y., Bieman, K., et al. (1993). Peptide compositions of the cerebrovascular and senile plaque core amyloid deposits of Alzheimer's disease. *Arch. Biochem. Biophys.* 301, 41–52. doi: 10.1006/abbi.1993.1112
- Miller, E. C., Teravskis, P. J., Dummer, B. W., Zhao, X., Haganir, R. L., and Liao, D. (2014). Tau phosphorylation and tau mislocalization mediate soluble A $\beta$  oligomer-induced AMPA glutamate receptor signaling deficits. *Eur. J. Neurosci.* 39, 1214–1224. doi: 10.1111/ejn.12507
- Moller, A., Bauer, C. S., Cohen, R. N., Webster, C. P., and De Vos, K. J. (2017). Amyotrophic lateral sclerosis-associated mutant SOD1 inhibits anterograde axonal transport of mitochondria by reducing Miro1 levels. *Hum. Mol. Genet.* 26, 4668–4679. doi: 10.1093/hmg/ddx348
- Molloy, D. W., Standish, T. I., Zhou, Q., Guyatt, G., and DARAD Study Group. (2013). A multicenter, blinded, randomized, factorial controlled trial of doxycycline and rifampin for treatment of Alzheimer's disease: the DARAD trial. *Int. J. Geriatr. Psychiatry* 28, 463–470. doi: 10.1002/gps.3846
- Molokanova, E., Akhtar, M. W., Sanz-Blasco, S., Tu, S., Piña-Crespo, J. C., Mckercher, S. R., et al. (2014). Differential effects of synaptic and extrasynaptic NMDA receptors on A $\beta$ -induced nitric oxide production in cerebrocortical neurons. *J. Neurosci.* 34, 5023–5028. doi: 10.1523/JNEUROSCI.2907-13.2014
- Moors, T. E., Hoozemans, J. J., Ingrassia, A., Beccari, T., Parnetti, L., Chartier-Harlin, M. C., et al. (2017). Therapeutic potential of autophagy-enhancing agents in Parkinson's disease. *Mol. Neurodegener.* 12:11. doi: 10.1186/s13024-017-0154-3
- Münch, C., and Bertolotti, A. (2010). Exposure of hydrophobic surfaces initiates aggregation of diverse ALS-causing superoxide dismutase-1 mutants. *J. Mol. Biol.* 399, 512–525. doi: 10.1016/j.jmb.2010.04.019
- Münch, C., O'Brien, J., and Bertolotti, A. (2011). Prion-like propagation of mutant superoxide dismutase-1 misfolding in neuronal cells. *Proc. Natl. Acad. Sci. U S A* 108, 3548–3553. doi: 10.1073/pnas.1017275108
- Myers, H. R., Vonsattel, P. J., Paskevich, A. P., Kiely, K. D., Stevens, J. T., Cupples, A. L., et al. (1991). Decreased neuronal and increased oligodendroglial densities in Huntington's disease caudate nucleus. *J. Neuropathol. Exp. Neurol.* 50, 729–742. doi: 10.1097/00005072-199111000-00005
- Nakamura, T., and Lipton, S. A. (2016). Protein S-nitrosylation as a therapeutic target for neurodegenerative diseases. *Trends Pharmacol. Sci.* 37, 73–84. doi: 10.1016/j.tips.2015.10.002
- Nasir, J., Floresco, S. B., O'Kusky, J. R., Diewert, V. M., Richman, J. M., Zeisler, J., et al. (1995). Targeted disruption of the Huntington's disease gene results in embryonic lethality and behavioral and morphological changes in heterozygotes. *Cell* 81, 811–823. doi: 10.1016/0092-8674(95)90542-1
- Nath, S., Agholme, L., Kurudenkandy, F. R., Granseth, B., Marcusson, J., and Hallbeck, M. (2012). Spreading of neurodegenerative pathology via neuron-to-neuron transmission of  $\beta$ -amyloid. *J. Neurosci.* 32, 8767–8777. doi: 10.1523/JNEUROSCI.0615-12.2012
- Nekooki-Machida, Y., Kurosawa, M., Nukina, N., Ito, K., Oda, T., and Tanaka, M. (2009). Distinct conformations of *in vitro* and *in vivo* amyloids of huntingtin-exon1 show different cytotoxicity. *Proc. Natl. Acad. Sci. U S A* 106, 9679–9684. doi: 10.1073/pnas.0812083106
- Neumann, M., Kwong, L., Lee, E., Kremmer, E., Flatley, A., Xu, Y., et al. (2009). Phosphorylation of S409/410 of TDP-43 is a consistent feature in all sporadic and familial of TDP-43 proteinopathies. *Acta Neuropathol.* 117, 137–149. doi: 10.1007/s00401-008-0477-9



- Neumann, M., Sampathu, D. M., Kwong, L. K., Truax, A. C., Micsenyi, M. C., Chou, T. T., et al. (2006). Ubiquitinated TDP-43 in frontotemporal lobar degeneration and amyotrophic lateral sclerosis. *Science* 314, 130–133. doi: 10.1126/science.1134108
- Nomura, T., Watanabe, S., Kaneko, K., Yamanaka, K., Nukina, N., and Furukawa, Y. (2014). Intracellular aggregation of mutant FUS/TLS as a molecular pathomechanism of amyotrophic lateral sclerosis. *J. Biol. Chem.* 289, 1192–1202. doi: 10.1074/jbc.M113.516492
- Nonaka, T., Masuda-Suzukake, M., Arai, T., Hasegawa, Y., Akatsu, H., Obi, T., et al. (2013). Prion-like properties of pathological TDP-43 aggregates from diseased brains. *Cell Rep.* 4, 124–134. doi: 10.1016/j.celrep.2013.06.007
- Nordlund, A., and Oliveberg, M. (2008). SOD1-associated ALS: a promising system for elucidating the origin of protein-misfolding disease. *HFSP J.* 2, 354–364. doi: 10.2976/1.2995726
- Oelschlegel, A. M., and Weissmann, C. (2013). Acquisition of drug resistance and dependence by prions. *PLoS Pathog.* 9:e1003158. doi: 10.1371/journal.ppat.1003158
- Olanow, C. W., Savolainen, M., Chu, Y., Halliday, G., and Kordower, J. (2019). Temporal evolution of microglia and  $\alpha$ -synuclein accumulation following foetal grafting in Parkinson's disease. *Brain* 142, 1690–1700. doi: 10.1093/brain/awz104
- Orihuela, R., McPherson, C. A., and Harry, G. J. (2016). Microglial M1/M2 polarization and metabolic states. *Br. J. Pharmacol.* 173, 649–665. doi: 10.1111/bph.13139
- Panosian, L. A., Porter, V. R., Valenzuela, H. F., Zhu, X., Reback, E., Masterman, D., et al. (2003). Telomere shortening in T cells correlates with Alzheimer's disease status. *Neurobiol. Aging* 24, 77–84. doi: 10.1016/s0197-4580(02)00043-x
- Paulsen, J. S., Nopoulos, P. C., Aylward, E., Ross, C. A., Johnson, H., Magnotta, V. A., et al. (2010). Striatal and white matter predictors of estimated diagnosis for Huntington disease. *Brain Res. Bull.* 82, 201–207. doi: 10.1016/j.brainresbull.2010.04.003
- Pearce, M. M. P., Spartz, E. J., Hong, W., Luo, L., and Kopito, R. R. (2015). Prion-like transmission of neuronal huntingtin aggregates to phagocytic glia in the *Drosophila* brain. *Nat. Commun.* 6:6768. doi: 10.1038/ncomms7768
- Pecho-Vrieseling, E., Rieker, C., Fuchs, S., Bleckmann, D., Esposito, M. S., Botta, P., et al. (2014). Transneuronal propagation of mutant huntingtin contributes to non-cell autonomous pathology in neurons. *Nat. Neurosci.* 17, 1064–1072. doi: 10.1038/nn.3761
- Pellegrini, L., Wetzel, A., Granno, S., Heaton, G., and Harvey, K. (2017). Back to the tubule: microtubule dynamics in Parkinson's disease. *Cell. Mol. Life Sci.* 74, 409–434. doi: 10.1007/s00018-016-2351-6
- Perez-Nievas, B. G., and Serrano-Pozo, A. (2018). Deciphering the astrocyte reaction in Alzheimer's disease. *Front. Aging Neurosci.* 10:114. doi: 10.3389/fnagi.2018.00114
- Petkova, A., Leapman, R., Guo, Z., Yau, W., Mattson, M., and Tycko, R. (2005). Self-propagating, molecular-level polymorphism in Alzheimer's  $\beta$ -amyloid fibrils. *Science* 307, 262–265. doi: 10.1126/science.1105850
- Phillips, J. C. (2019). Why A $\beta$ 42 is much more toxic than A $\beta$ 40. *ACS Chem. Neurosci.* 10, 2843–2847. doi: 10.1021/acscchemneuro.9b00068
- Pihlaja, R., Koistinaho, J., Kauppinen, R., Sandholm, J., Tanila, H., and Koistinaho, M. (2011). Multiple cellular and molecular mechanisms are involved in human A $\beta$  clearance by transplanted adult astrocytes. *Glia* 59, 1643–1657. doi: 10.1002/glia.21212
- Pihlaja, R., Koistinaho, J., Malm, T., Sikkilä, H., Vainio, S., and Koistinaho, M. (2008). Transplanted astrocytes internalize deposited  $\beta$ -amyloid peptides in a transgenic mouse model of Alzheimer's disease. *Glia* 56, 154–163. doi: 10.1002/glia.20599
- Pinarbasi, E. S., Çağatay, T., Fung, H. Y. J., Li, Y. C., Chook, Y. M., and Thomas, P. J. (2018). Active nuclear import and passive nuclear export are the primary determinants of TDP-43 localization. *Sci. Rep.* 8:7083. doi: 10.1038/s41598-018-25008-4
- Polymenidou, M., and Cleveland, D. W. (2017). Biological spectrum of amyotrophic lateral sclerosis prions. *Cold Spring Harb. Perspect. Med.* 7:a024133. doi: 10.1101/cshperspect.a024133
- Prasad, A., Bharathi, V., Sivalingam, V., Girdhar, A., and Patel, B. K. (2019). Molecular mechanisms of TDP-43 misfolding and pathology in amyotrophic lateral sclerosis. *Front. Mol. Neurosci.* 12:25. doi: 10.3389/fnmol.2019.00025
- Prins, N. D., and Scheltens, P. (2013). Treating Alzheimer's disease with monoclonal antibodies: current status and outlook for the future. *Alzheimers Res. Ther.* 5:56. doi: 10.1186/alzrt220
- Prusiner, S. B. (1982). Novel proteinaceous infectious particles cause scrapie. *Science* 216, 136–144. doi: 10.1126/science.6801762
- Prusiner, S. B. (1994). Biology and genetics of prion diseases. *Annu. Rev. Microbiol.* 48, 655–686. doi: 10.1146/annurev.mi.48.100194.003255
- Prusiner, S. B. (1998). Prions. *Proc. Natl. Acad. Sci. U S A* 95, 13363–13383. doi: 10.1073/pnas.95.23.13363
- Prusiner, S. B., Scott, M. R., DeArmond, S. J., and Cohen, F. E. (1998). Prion protein biology. *Cell* 93, 337–348. doi: 10.1016/s0092-8674(00)81163-0
- Qiang, W., Yau, W., Lu, J., Collinge, J., and Tycko, R. (2017). Structural variation in amyloid- $\beta$  fibrils from Alzheimer's disease clinical subtypes. *Nature* 541, 217–221. doi: 10.1038/nature20814
- Qin, H., Lim, L., Wei, Y., and Song, J. (2014). TDP-43 N terminus encodes a novel ubiquitin-like fold and its unfolded form in equilibrium that can be shifted by binding to ssDNA. *Proc. Natl. Acad. Sci. U S A* 111, 18619–18624. doi: 10.1073/pnas.1413994112
- Quintanilla, R. A., Dolan, P. J., Jin, Y. N., and Johnson, G. V. W. (2012). Truncated tau and A $\beta$  cooperatively impair mitochondria in primary neurons. *Neurobiol. Aging* 33, e25–e35. doi: 10.1016/j.neurobiolaging.2011.02.007
- Rabin, S., Kim, J., Baughn, M., Libby, R., Kim, Y., Fan, Y., et al. (2010). Sporadic ALS has compartment-specific aberrant exon splicing and altered cell-matrix adhesion biology. *Hum. Mol. Genet.* 19, 313–338. doi: 10.1093/hmg/ddp498
- Rakhit, R., Cunningham, P., Furtos-Matei, A., Dahan, S., Qi, X., Crow, J., et al. (2002). Oxidation-induced misfolding and aggregation of superoxide dismutase and its implications for amyotrophic lateral sclerosis. *J. Biol. Chem.* 277, 47551–47556. doi: 10.1074/jbc.M207356200
- Ramesh, N., and Pandey, U. B. (2017). Autophagy dysregulation in ALS: when protein aggregates get out of hand. *Front. Mol. Neurosci.* 10:263. doi: 10.3389/fnmol.2017.00263
- Ramos Bernardes da Silva Filho, S., Oliveira Barbosa, J. H., Rondinoni, C., Dos Santos, A. C., Garrido Salmon, C. E., da Costa Lima, N. K., et al. (2017). Neurodegeneration profile of Alzheimer's patients: a brain morphometry study. *Neuroimage Clin.* 15, 15–24. doi: 10.1016/j.nicl.2017.04.001
- Rannikko, E. H., Weber, S. S., and Kahle, P. J. (2015). Exogenous  $\alpha$ -synuclein induces toll-like receptor 4 dependent inflammatory responses in astrocytes. *BMC Neurosci.* 16:57. doi: 10.1186/s12868-015-0192-0
- Ratti, A., and Buratti, E. (2016). Physiological functions and pathobiology of TDP-43 and FUS/TLS proteins. *J. Neurochem.* 138, 95–111. doi: 10.1111/jnc.13625
- Reaume, A. G., Elliott, J. L., Hoffman, E. K., Kowall, N. W., Ferrante, R. J., Siwek, D. F., et al. (1996). Motor neurons in *cu/z*n superoxide dismutase-deficient mice develop normally but exhibit enhanced cell death after axonal injury. *Nat. Genet.* 13, 43–47. doi: 10.1038/ng0596-43
- Ren, Y., Jiang, H., Yang, F., Nakaso, K., and Feng, J. (2009). Parkin protects dopaminergic neurons against microtubule-depolymerizing toxins by attenuating microtubule-associated protein kinase activation. *J. Biol. Chem.* 284, 4009–4017. doi: 10.1074/jbc.M806245200
- Ren, P., Lauckner, J., Kachirskaja, I., Heuser, J., Melki, R., and Kopito, R. (2008). Cytoplasmic penetration and persistent infection of mammalian cells by polyglutamine aggregates. *Nat. Cell Biol.* 11, 219–225. doi: 10.1038/ncb1830
- Rodriguez, L., Marano, M. M., and Tandon, A. (2018). Import and export of misfolded  $\alpha$ -synuclein. *Front. Neurosci.* 12:344. doi: 10.3389/fnins.2018.00344
- Rossner, S., Lange-Dohna, C., Zeitschel, U., and Perez-Polo, J. R. (2005). Alzheimer's disease  $\beta$ -secretase BACE1 is not a neuron-specific enzyme. *J. Neurochem.* 92, 226–234. doi: 10.1111/j.1471-4159.2004.02857.x
- Rostami, J., Holmqvist, S., Lindström, V., Sigvardson, J., Westermark, G. T., Ingelsson, M., et al. (2017). Human astrocytes transfer aggregated  $\alpha$ -synuclein via tunneling nanotubes. *J. Neurosci.* 37, 11835–11853. doi: 10.1523/JNEUROSCI.0983-17.2017
- Rotunno, M., and Bosco, D. (2013). An emerging role for misfolded wild-type SOD1 in sporadic ALS pathogenesis. *Front. Cell. Neurosci.* 7:253. doi: 10.3389/fncel.2013.00253
- Rubbo, H., Radi, R., Trujillo, M., Telleri, R., Kalyanaraman, B., Barnes, S., et al. (1994). Nitric oxide regulation of superoxide and peroxynitrite-dependent lipid peroxidation. *J. Biol. Chem.* 269, 26066–26075.

- Rubinsztein, D. C., Leggo, J., Coles, R., Almqvist, E., Biancalana, V., Cassiman, J. J., et al. (1996). Phenotypic characterization of individuals with 30–40 CAG repeats in the Huntington disease (HD) gene reveals HD cases with 36 repeats and apparently normal elderly individuals with 36–39 repeats. *Am. J. Hum. Genet.* 59, 16–22.
- Rui, Y., Tiwari, P., Xie, Z., and Zheng, J. Q. (2006). Acute impairment of mitochondrial trafficking by  $\beta$ -amyloid peptides in hippocampal neurons. *J. Neurosci.* 26, 10480–10487. doi: 10.1523/JNEUROSCI.3231-06.2006
- Saccon, R., Bunton-Stasyshyn, R., Fisher, E., and Fratta, P. (2013). Is SOD1 loss of function involved in amyotrophic lateral sclerosis? *Brain* 136, 2342–2358. doi: 10.1093/brain/awt097
- Saha, R. N., and Pahan, K. (2006). Regulation of inducible nitric oxide synthase gene in glial cells. *Antioxid. Redox Signal.* 8, 929–947. doi: 10.1089/ars.2006.8.929
- Sanders, D. W., Kaufman, S. K., DeVos, S. L., Sharma, A. M., Mirbaha, H., Li, A., et al. (2014). Distinct tau prion strains propagate in cells and mice and define different tauopathies. *Neuron* 82, 1271–1288. doi: 10.1016/j.neuron.2014.04.047
- Sapp, E., Kegel, K. B., Aronin, N., Hashikawa, T., Uchiyama, Y., Tohyama, K., et al. (2001). Early and progressive accumulation of reactive microglia in the Huntington disease brain. *J. Neuropathol. Exp. Neurol.* 60, 161–172. doi: 10.1093/jnen/60.2.161
- Savage, M. J., Trusko, S. P., Howland, D. S., Pinsker, L. R., Mistretta, S., Reaume, A. G., et al. (1998). Turnover of amyloid  $\beta$ -protein in mouse brain and acute reduction of its level by phorbol ester. *J. Neurosci.* 18, 1743–1752. doi: 10.1523/JNEUROSCI.18-05-01743.1998
- Scheffold, A., Holtman, I. R., Dieni, S., Brouwer, N., Katz, S. F., Jebaraj, B. M., et al. (2016). Telomere shortening leads to an acceleration of synucleinopathy and impaired microglia response in a genetic mouse model. *Acta Neuropathol. Commun.* 4:87. doi: 10.1186/s40478-016-0364-x
- Scherzinger, E., Lurz, R., Turmaine, M., Mangiarini, L., Hollenbach, B., Hasenbank, R., et al. (1997). Huntingtin-encoded polyglutamine expansions form amyloid-like protein aggregates *in vitro* and *in vivo*. *Cell* 90, 549–558. doi: 10.1016/s0092-8674(00)80514-0
- Schubert, U., Antón, L. C., Gibbs, J., Norbury, C. C., Yewdell, J. W., and Bennink, J. R. (2000). Rapid degradation of a large fraction of newly synthesized proteins by proteasomes. *Nature* 404, 770–774. doi: 10.1038/35008096
- Schulte, J., and Littleton, J. T. (2011). The biological function of the Huntingtin protein and its relevance to Huntington's disease pathology. *Curr. Trends Neurol.* 5, 65–78.
- Scialò, C., De Cecco, E., Manganotti, P., and Legname, G. (2019). Prion and prion-like protein strains: deciphering the molecular basis of heterogeneity in neurodegeneration. *Viruses* 11:E261. doi: 10.3390/v11030261
- Scotter, E. L., Chen, H. J., and Shaw, C. E. (2015). TDP-43 proteinopathy and ALS: insights into disease mechanisms and therapeutic targets. *Neurotherapeutics* 12, 352–363. doi: 10.1007/s13311-015-0338-x
- Selkoe, D. J. (2001). Clearing the brain's amyloid cobwebs. *Neuron* 32, 177–180. doi: 10.1016/s0896-6273(01)00475-5
- Serrano-Pozo, A., Frosch, M., Masliah, E., and Hyman, B. (2011). Neuropathological alterations in Alzheimer disease. *Cold Spring Harb. Perspect. Med.* 1:a006189. doi: 10.1101/cshperspect.a006189
- Serrano-Pozo, A. L., Mielke, M. H., Muzitansky, A. J., Gómez-Isla, T. A., Growdon, J. P., Bacska, B. T., et al. (2012). Stable size distribution of amyloid plaques over the course of Alzheimer disease. *J. Neuropathol. Exp. Neurol.* 71, 694–701. doi: 10.1097/nen.0b013e31825e77de
- Shafiei, S. S., Guerrero-Munoz, M. J., and Castillo-Carranza, D. L. (2017). Tau oligomers: cytotoxicity, propagation, and mitochondrial damage. *Front. Aging Neurosci.* 9:83. doi: 10.3389/fnagi.2017.00083
- Shavali, S., Combs, C. K., and Ebadi, M. (2006). Reactive macrophages increase oxidative stress and  $\alpha$ -synuclein nitration during death of dopaminergic neuronal cells in co-culture: relevance to Parkinson's disease. *Neurochem. Res.* 31, 85–94. doi: 10.1007/s11064-005-9233-x
- Shi, Y., Ivannikov, M. V., Walsh, M. E., Liu, Y., Zhang, Y., Jaramillo, C. A., et al. (2014). The lack of *cuznsod* leads to impaired neurotransmitter release, neuromuscular junction destabilization and reduced muscle strength in mice. *PLoS One* 9:e100834. doi: 10.1371/journal.pone.0100834
- Shi, Y., Yamada, K., Liddel, S. A., Smith, S. T., Zhao, L., Luo, W., et al. (2017). ApoE4 markedly exacerbates tau-mediated neurodegeneration in a mouse model of tauopathy. *Nature* 549, 523–527. doi: 10.1038/nature24016
- Shimonaka, S., Nonaka, T., Suzuki, H., Hisanaga, S., and Hasegawa, M. (2016). Templated aggregation of TAR DNA-binding protein of 43 kDa (TDP-43) by seeding with TDP-43 peptide fibrils. *J. Biol. Chem.* 291, 8896–8907. doi: 10.1074/jbc.m115.713552
- Shin, J. Y., Fang, Z. H., Yu, Z. X., Wang, C. E., Li, S. H., and Li, X. J. (2005). Expression of mutant huntingtin in glial cells contributes to neuronal excitotoxicity. *J. Cell Biol.* 171, 1001–1012. doi: 10.1083/jcb.200508072
- Siddique, N., and Siddique, T. (2019). Amyotrophic lateral sclerosis overview, in *GeneReviews® [Internet]*, eds M. P. Adam, H. H. Ardinger, R. A. Pagon, S. E. Wallace, L. J. H. Bean, K. Stephens et al. (Seattle, WA: University of Washington). Available online at: <https://www.ncbi.nlm.nih.gov/books/NBK1450/>. Accessed October 28, 2019.
- Sofroniew, M. V., and Vinters, H. V. (2010). Astrocytes: biology and pathology. *Acta Neuropathol.* 119, 7–35. doi: 10.1007/s00401-009-0619-8
- Soo, K. Y., Sultana, J., King, A. E., Atkinson, R., Warraich, S. T., Sundaramoorthy, V., et al. (2015). ALS-associated mutant FUS inhibits macroautophagy which is restored by overexpression of Rab1. *Cell Death Discov.* 1:15030. doi: 10.1038/cddiscovery.2015.30
- Sorce, S., Nuvolone, M., Keller, A., Falsig, J., Varol, A., Schwarz, P., et al. (2014). The role of the NADPH oxidase NOX2 in prion pathogenesis. *PLoS Pathog.* 10:e1004531. doi: 10.1371/journal.ppat.1004531
- Soto, C., and Pritzkow, S. (2018). Protein misfolding, aggregation, and conformational strains in neurodegenerative diseases. *Nat. Neurosci.* 21, 1332–1340. doi: 10.1038/s41593-018-0235-9
- Spiller, K. J., Restrepo, C. R., Khan, T., Dominique, M. A., Fang, T. C., Canter, R. G., et al. (2018). Microglia-mediated recovery from ALS-relevant motor neuron degeneration in a mouse model of TDP-43 proteinopathy. *Nat. Neurosci.* 21, 329–340. doi: 10.1038/s41593-018-0083-7
- Squitieri, F., Cannella, M., Simonelli, M., Sassone, J., Martino, T., Venditti, E., et al. (2009). Distinct brain volume changes correlating with clinical stage, disease progression rate, mutation size, and age at onset prediction as early biomarkers of brain atrophy in Huntington's disease. *CNS Neurosci. Ther.* 15, 1–11. doi: 10.1111/j.1755-5949.2008.00068.x
- Stefanis, L. (2012).  $\alpha$ -Synuclein in Parkinson's disease. *Cold Spring Harb. Perspect. Med.* 2:a009399. doi: 10.1101/cshperspect.a009399
- Steinert, J. R., Chernova, T., and Forsythe, I. D. (2010). Nitric oxide signaling in brain function, dysfunction, and dementia. *Neuroscientist* 16, 435–452. doi: 10.1177/1073858410366481
- Streit, W. J. (2005). Microglia and neuroprotection: implications for Alzheimer's disease. *Brain Res. Rev.* 48, 234–239. doi: 10.1016/j.brainresrev.2004.12.013
- Strong, T. V., Tagle, D. A., Valdes, J. M., Elmer, L. W., Boehm, K., Swaroop, M., et al. (1993). Widespread expression of the human and rat Huntington's disease gene in brain and nonneural tissues. *Nat. Genet.* 5, 259–265. doi: 10.1038/ng1193-259
- Subramaniam, S., and Federoff, H. (2017). Targeting microglial activation states as a therapeutic avenue in Parkinson's disease. *Front. Aging Neurosci.* 9:176. doi: 10.3389/fnagi.2017.00176
- Sun, Z., Diaz, Z., Fang, X., Hart, M. P., Chesi, A., Shorter, J., et al. (2011). Molecular determinants and genetic modifiers of aggregation and toxicity for the ALS disease protein FUS/TLS. *PLoS Biol.* 9:e1000614. doi: 10.1371/journal.pbio.1000614
- Szabó, S., Ischiropoulos, H., and Radi, R. (2007). Peroxynitrite: biochemistry, pathophysiology and development of therapeutics. *Nat. Rev. Drug Discov.* 6, 662–680. doi: 10.1038/nrd2222
- Tabrizi, S. J., Workman, J., Hart, P. E., Mangiarini, L., Mahal, A., Bates, G., et al. (2000). Mitochondrial dysfunction and free radical damage in the Huntington R6/2 transgenic mouse. *Ann. Neurol.* 47, 80–86. doi: 10.1002/1531-8249(200001)47:1<80::aid-ana13>3.3.co;2-b
- Taguchi, K., Watanabe, Y., Tsujimura, A., and Tanaka, A. (2016). Brain region-dependent differential expression of  $\alpha$ -synuclein. *J. Comp. Neurol.* 524, 1236–1258. doi: 10.1002/cne.23901
- Talantova, M., Sanz-Blasco, S., Zhang, X., Xia, P., Akhtar, M. W., Okamoto, S., et al. (2013). A $\beta$  induces astrocytic glutamate release, extrasynaptic NMDA



- receptor activation, and synaptic loss. *Proc. Natl. Acad. Sci. U S A* 110, E2518–E2527. doi: 10.1073/pnas.1306832110
- Tang, Y., and Le, W. (2016). Differential roles of M1 and M2 microglia in neurodegenerative diseases. *Mol. Neurobiol.* 53, 1181–1194. doi: 10.1007/s12035-014-9070-5
- Thomas, M., Alegre-Abarrategui, J., and Wade-Martins, R. (2013). RNA dysfunction and aggregopathy at the centre of an amyotrophic lateral sclerosis/frontotemporal dementia disease continuum. *Brain* 136, 1345–1460. doi: 10.1093/brain/awt030
- Thomas, D. D., Liu, X., Kantrow, S. P., and Lancaster, J. R. Jr. (2001). The biological lifetime of nitric oxide: implications for the perivascular dynamics of NO and O<sub>2</sub>. *Proc. Natl. Acad. Sci. U S A* 98, 355–360. doi: 10.1073/pnas.011379598
- Tiwari, A., and Hayward, L. (2005). Mutant SOD1 instability: implications for toxicity in amyotrophic lateral sclerosis. *Neurodegener. Dis.* 2, 115–127. doi: 10.1159/000089616
- Tong, J., Huang, C., Bi, F., Wu, Q., Huang, B., Liu, X., et al. (2013). Expression of ALS-linked TDP-43 mutant in astrocytes causes non-cell-autonomous motor neuron death in rats. *EMBO J.* 32, 1917–1926. doi: 10.1038/emboj.2013.122
- Toretsky, J., and Wright, P. (2014). Assemblages: functional units formed by cellular phase separation. *J. Cell Biol.* 206, 579–588. doi: 10.1083/jcb.201404124
- Towers, C. G., and Thorburn, A. (2016). Therapeutic targeting of autophagy. *EBioMedicine* 14, 15–23. doi: 10.1016/j.ebiom.2016.10.034
- Trajkovic, V., Stosic-Grubic, S., Samardzic, T., Markovic, M., Miljkovic, D., Ramic, Z., et al. (2001). Interleukin-17 stimulates inducible nitric oxide synthase activation in rodent astrocytes. *J. Neuroimmunol.* 119, 183–191. doi: 10.1016/s0165-5728(01)00391-5
- Trétiakoff, C. (1919). *Contribution à l'étude de l'anatomie Pathologique du Locus Niger de Sömmerring*. Paris: Jouve.
- Trevitt, C. R., and Collinge, J. (2006). A systematic review of prion therapeutics in experimental models. *Brain* 129, 2241–2265. doi: 10.1093/brain/awl150
- Trojanowski, J. Q., Schuck, T., Schmidt, M. L., and Lee, V. M. (1989). Distribution of tau proteins in the normal human central and peripheral nervous system. *J. Histochem. Cytochem.* 37, 209–215. doi: 10.1177/37.2.2492045
- Trottier, Y., Devys, D., Imbert, G., Sandou, F., An, I., Lutz, Y., et al. (1995). Cellular localisation of the Huntington's disease protein and discrimination of the normal and mutated forms. *Nat. Genet.* 10, 104–110. doi: 10.1038/ng0595-104
- Trushina, E., Dyer, R. B., Badger, J. D. II., Ure, D., Eide, L., Tran, D. D., et al. (2004). Mutant huntingtin impairs axonal trafficking in mammalian neurons *in vivo* and *in vitro*. *Mol. Cell. Biol.* 24, 8195–8209. doi: 10.1128/mcb.24.18.8195-8209.2004
- Trushina, E., Heldebrandt, M. P., Perez-Terzic, C. M., Bortolon, R., Kovtun, I. V., Badger, J. D., et al. (2003). Microtubule destabilization and nuclear entry are sequential steps leading to toxicity in Huntington's disease. *Proc. Natl. Acad. Sci. U S A* 100, 12171–12176. doi: 10.1073/pnas.2034961100
- Tsuji, H., Arai, T., Kametani, F., Nonaka, T., Yamashita, M., Suzukake, M., et al. (2012). Molecular analysis and biochemical classification of TDP-43 proteinopathy. *Brain* 135, 3380–3391. doi: 10.1093/brain/awt230
- Tydemers, J., Treusch, S., Dong, J., McCaffery, J. M., Bevis, B., and Lindquist, S. (2010). Prion induction involves an ancient system for the sequestration of aggregated proteins and heritable changes in prion fragmentation. *Proc. Natl. Acad. Sci. U S A* 107, 8633–8638. doi: 10.1073/pnas.1003895107
- Uversky, V. N. (2007). Neuropathology, biochemistry, and biophysics of  $\alpha$ -synuclein aggregation. *J. Neurochem.* 103, 17–37. doi: 10.1111/j.1471-4159.2007.04764.x
- van Dyck, C. H. (2018). Anti-amyloid- $\beta$  monoclonal antibodies for Alzheimer's disease: pitfalls and promise. *Biol. Psychiatry* 83, 311–319. doi: 10.1016/j.biopsych.2017.08.010
- Vonsattel, J., Myers, R., Stevens, T., Ferrante, R., Bird, E., and Richardson, E. (1985). Neuropathological classification of Huntington's disease. *J. Neuropathol. Exp. Neurol.* 44, 559–577. doi: 10.1097/00005072-198511000-00003
- Voytyuk, I., De Strooper, B., and Chávez-Gutiérrez, L. (2018). Modulation of  $\gamma$ - and  $\beta$ -secretases as early prevention against Alzheimer's disease. *Biol. Psychiatry* 83, 320–327. doi: 10.1016/j.biopsych.2017.08.001
- Waelter, S., Boeddrich, A., Lurz, R., Scherzinger, E., Lueder, G., Lehrach, H., et al. (2001). Accumulation of mutant huntingtin fragments in aggresome-like inclusion bodies as a result of insufficient protein degradation. *Mol. Biol. Cell* 12, 1393–1407. doi: 10.1091/mbc.12.5.1393
- Walls, K. C., Coskun, P., Gallegos-Perez, J. L., Zadourian, N., Freude, K., Rasool, S., et al. (2012). Swedish alzheimer mutation induces mitochondrial dysfunction mediated by HSP60 mislocalization of amyloid precursor protein (APP) and  $\beta$ -amyloid. *J. Biol. Chem.* 287, 30317–30327. doi: 10.1074/jbc.m112.365890
- Wang, W. Y., Pan, L., Su, S. C., Quinn, E. J., Sasaki, M., Jimenez, J. C., et al. (2013). Interaction of FUS and HDAC1 regulates DNA damage response and repair in neurons. *Nat. Neurosci.* 16, 1383–1391. doi: 10.1038/nn.3514
- Wang, X., Perry, G., Smith, M. A., and Zhu, X. (2010). Amyloid- $\beta$ -derived diffusible ligands cause impaired axonal transport of mitochondria in neurons. *Neurodegener. Dis.* 7, 56–59. doi: 10.1159/000283484
- Wang, R., and Reddy, P. H. (2017). Role of glutamate and NMDA receptors in Alzheimer's disease. *J. Alzheimers Dis.* 57, 1041–1048. doi: 10.3233/jad-160763
- Weingarten, M. D., Lockwood, A. H., Hwo, S. Y., and Kirschner, M. W. (1975). A protein factor essential for microtubule assembly. *Proc. Natl. Acad. Sci. U S A* 72, 1858–1862. doi: 10.1073/pnas.72.5.1858
- White, A. R., Enever, P., Tayebi, M., Mushens, R., Linehan, J., Brandner, S., et al. (2003). Monoclonal antibodies inhibit prion replication and delay the development of prion disease. *Nature* 422, 80–83. doi: 10.1038/nature01457
- Winslow, A. R., Chen, C.-W., Corrochano, S., Acevedo-Arozena, A., Gordon, D. E., Peden, A. A., et al. (2010).  $\alpha$ -synuclein impairs macroautophagy: implications for Parkinson's disease. *J. Cell Biol.* 190, 1023–1037. doi: 10.1083/jcb.201003122
- Yang, W., Dunlap, J. R., Andrews, R. B., and Wetzel, R. (2002). Aggregated polyglutamine peptides delivered to nuclei are toxic to mammalian cells. *Hum. Mol. Genet.* 11, 2905–2917. doi: 10.1093/hmg/11.23.2905
- Yang, F., Jiang, Q., Zhao, J., Ren, Y., Sutton, M. D., and Feng, J. (2005). Parkin stabilizes microtubules through strong binding mediated by three independent domains. *J. Biol. Chem.* 280, 17154–17162. doi: 10.1074/jbc.m500843200
- Yankner, B. A., Duffy, L. K., and Kirschner, D. A. (1990). Neurotrophic and neurotoxic effects of amyloid  $\beta$  protein: reversal by tachykinin neuropeptides. *Science* 250, 279–282. doi: 10.1126/science.2218531
- Yasuda, K., Clatterbuck-Soper, S. F., Jackrel, M. E., Shorter, J., and Mili, S. (2017). FUS inclusions disrupt RNA localization by sequestering kinesin-1 and inhibiting microtubule detyrosination. *J. Cell Biol.* 216, 1015–1034. doi: 10.1083/jcb.201608022
- Yerbury, J. J., Ooi, L., Blair, I. P., Ciryam, P., Dobson, C. M., and Vendruscolo, M. (2019). The metastability of the proteome of spinal motor neurons underlies their selective vulnerability in ALS. *Neurosci. Lett.* 704, 89–94. doi: 10.1016/j.neulet.2019.04.001
- Zhang, Y., Leavitt, B. R., van Raamsdonk, J. M., Dragatsis, I., Goldowitz, D., MacDonald, M. E., et al. (2006). Huntingtin inhibits caspase-3 activation. *EMBO J.* 25, 5896–5906. doi: 10.1038/sj.emboj.7601445
- Zheng, Z., Li, A., Holmes, B. B., Marasa, J. C., and Diamond, M. I. (2013). An N-terminal nuclear export signal regulates trafficking and aggregation of huntingtin (Htt) protein exon 1. *J. Biol. Chem.* 288, 6063–6071. doi: 10.1074/jbc.m112.413575
- Zhang, W., Wang, T., Pei, Z., Miller, D. S., Wu, X., Block, M. L., et al. (2005). Aggregated  $\alpha$ -synuclein activates microglia: a process leading to disease progression in Parkinson's disease. *FASEB J.* 19, 533–542. doi: 10.1096/fj.04-2751com
- Zinszner, H., Sok, J., Immanuel, D., Yin, Y., and Ron, D. (1997). TLS (FUS) binds RNA *in vivo* and engages in nucleo-cytoplasmic shuttling. *J. Cell Sci.* 110, 1741–1750.

**Conflict of Interest:** The authors declare that the research was conducted in the absence of any commercial or financial relationships that could be construed as a potential conflict of interest.

Copyright © 2019 Wells, Brennan, Keon and Saksena. This is an open-access article distributed under the terms of the Creative Commons Attribution License (CC BY). The use, distribution or reproduction in other forums is permitted, provided the original author(s) and the copyright owner(s) are credited and that the original publication in this journal is cited, in accordance with accepted academic practice. No use, distribution or reproduction is permitted which does not comply with these terms.



# Design of a New $[PSI^+]$ -No-More Mutation in *SUP35* With Strong Inhibitory Effect on the $[PSI^+]$ Prion Propagation

Lavrentii G. Danilov<sup>1</sup>, Andrew G. Matveenko<sup>1</sup>, Varvara E. Ryzhkova<sup>1</sup>, Mikhail V. Belousov<sup>1,2</sup>, Olga I. Poleshchuk<sup>1</sup>, Daria V. Likholetova<sup>1</sup>, Petr A. Sokolov<sup>3</sup>, Nina A. Kasyanenko<sup>3</sup>, Andrey V. Kajava<sup>4,5</sup>, Galina A. Zhouravleva<sup>1,6\*</sup> and Stanislav A. Bondarev<sup>1,6\*</sup>

<sup>1</sup> Department of Genetics and Biotechnology, St. Petersburg State University, St. Petersburg, Russia, <sup>2</sup> Laboratory for Proteomics of Supra-Organismal Systems, All-Russia Research Institute for Agricultural Microbiology (ARRIAM), St. Petersburg, Russia, <sup>3</sup> Department of Molecular Biophysics and Polymer Physics, St. Petersburg State University, St. Petersburg, Russia, <sup>4</sup> Centre de Recherche en Biologie cellulaire de Montpellier (CRBM), UMR 5237 CNRS, Université Montpellier, Montpellier, France, <sup>5</sup> Institut de Biologie Computationnelle (IBC), Université Montpellier, Montpellier, France, <sup>6</sup> Laboratory of Amyloid Biology, St. Petersburg State University, St. Petersburg, Russia

## OPEN ACCESS

### Edited by:

Maria Rosário Almeida,  
University of Porto, Portugal

### Reviewed by:

Heinrich J. G. Matthies,  
University of Alabama at Birmingham,  
United States

Ilia V. Baskakov,  
University of Maryland, Baltimore,  
United States

### \*Correspondence:

Galina A. Zhouravleva  
zhouravleva@rambler.ru;  
g.zhouravleva@spbu.ru  
Stanislav A. Bondarev  
stanislavspbg@gmail.com;  
s.bondarev@spbu.ru

**Received:** 30 August 2019

**Accepted:** 28 October 2019

**Published:** 19 November 2019

### Citation:

Danilov LG, Matveenko AG, Ryzhkova VE, Belousov MV, Poleshchuk OI, Likholetova DV, Sokolov PA, Kasyanenko NA, Kajava AV, Zhouravleva GA and Bondarev SA (2019) Design of a New  $[PSI^+]$ -No-More Mutation in *SUP35* With Strong Inhibitory Effect on the  $[PSI^+]$  Prion Propagation. *Front. Mol. Neurosci.* 12:274. doi: 10.3389/fnmol.2019.00274

A number of  $[PSI^+]$ -no-more (PNM) mutations, eliminating  $[PSI^+]$  prion, were previously described in *SUP35*. In this study, we designed and analyzed a new PNM mutation based on the parallel in-register  $\beta$ -structure of Sup35 prion fibrils suggested by the known experimental data. In such an arrangement, substitution of non-charged residues by charged ones may destabilize the fibril structure. We introduced Q33K/A34K amino acid substitutions into the Sup35 protein, corresponding allele was called *sup35-M0*. The mutagenized residues were chosen based on ArchCandy *in silico* prediction of high inhibitory effect on the amyloidogenic potential of Sup35. The experiments confirmed that Sup35-M0 leads to the elimination of  $[PSI^+]$  with high efficiency. Our data suggested that the elimination of the  $[PSI^+]$  prion is associated with the decreased aggregation properties of the protein. The new mutation can induce the prion with very low efficiency and is able to propagate only weak  $[PSI^+]$  prion variants. We also showed that Sup35-M0 protein co-aggregates with the wild-type Sup35 *in vivo*. Moreover, our data confirmed the utility of the strategy of substitution of non-charged residues by charged ones to design new mutations to inhibit a prion formation.

**Keywords:**  $[PSI^+]$ , amyloid, ArchCandy, prion, *Saccharomyces cerevisiae*, *SUP35* mutation, superpleated- $\beta$ -structure

## 1. INTRODUCTION

Prions are self-propagating and transmissible protein isoforms that cause fatal neurodegenerative disease in humans or heritable traits in lower eukaryotes. The most known hallmark of almost all prions is a formation of amyloid aggregates (Liebman and Chernoff, 2012). These aggregates have a set of specific properties, such as resistance to detergents and proteases, interaction with dyes Thioflavin T and S, birefringence when stained with the Congo Red dye, and cross- $\beta$ -structure (Baxa et al., 2006). The first discovered prion, PrP<sup>Sc</sup> ("prion protein" scrapie), causes severe

infectious neurodegenerative diseases in mammals (Prusiner, 2013). Discovery of prions in lower eukaryotes (Wickner, 1994) revealed that this phenomenon is widespread and based on common mechanisms. Thus, unicellular organisms such as yeast can be used for investigation of prionization and the data obtained can be extrapolated to mammalian prions (Liebman and Chernoff, 2012).

One of the best-studied prions to date is  $[PSI^+]$ , an isoform of Sup35 protein (Cox, 1965; Wickner, 1994; Wickner et al., 1995), which is a eukaryotic release factor 3 (Stansfield et al., 1995; Zhouravleva et al., 1995). This protein is divided into three domains (N, M, and C) (Kushnirov et al., 1988). The C-terminal part of Sup35 contains four GTP binding sites (Stansfield et al., 1995; Zhouravleva et al., 1995) and it is essential for the cell viability and termination of translation (Ter-Avanesyan et al., 1993). N-domain is required for  $[PSI^+]$  maintenance (Ter-Avanesyan et al., 1994) and formation of stress-inducible condensates (Franzmann et al., 2018). N-domain consists of two parts — the Q/N rich segment (1–39 aa) and the oligopeptide repeats region (OR), containing one incomplete and five complete repeats (40–112 aa) (Kushnirov et al., 1988). The charged M-domain represents an unfolded linker that also affects  $[PSI^+]$  prion maintenance (Liu et al., 2002; Helsen and Glover, 2012).

Cells bearing  $[PSI^+]$  prion have a reduced amount of monomeric Sup35 protein, that increases the frequency of the read-through of premature stop codons (Liebman and Chernoff, 2012). Nonsense mutation *ade1-14*, which lead to the synthesis of a truncated non-functional Ade1 protein and to the inability of cells to synthesize adenine, is often used to test for the nonsense suppression caused by the prion. The accumulation of the adenine biosynthesis intermediate results in the red color of colonies growing on the 1/4 YEPD medium. The appearance of  $[PSI^+]$  prion leads to the suppression of *ade1-14* nonsense mutation and the formation of full-length Ade1. Phenotypically it can be detected by growth on media lacking adenine and the white colony color. This manifestation can vary depending on the structure of Sup35 aggregates (prion variant), templated upon prion propagation. The term “variant” is used hereafter for different prion variants, and “strain” — only for yeast strains. Cells bearing weak variants of the  $[PSI^+]$  prion demonstrate weak growth on adenineless media, *i.e.*, weak nonsense suppression, while the strong  $[PSI^+]$  variants lead to almost complete masking of the *ade1-14* mutant phenotype (Liebman and Chernoff, 2012).

Different approaches may be used for investigation of Sup35 aggregates in  $[PSI^+]$  cells. They can be decorated by transiently overproduced Sup35NM-GFP and visualized with fluorescence microscopy (Osheroich et al., 2004). Sup35 aggregates can also be directly analyzed with biochemical approaches: differential centrifugation, SDD-AGE (Kryndushkin et al., 2003) or modifications of SDS-PAGE (Kushnirov et al., 2006).

Oligopeptide repeats in the Sup35 N-domain significantly affect  $[PSI^+]$  prion maintenance. At least two first ORs are essential for the prion propagation (Liu and Lindquist, 1999; Osheroich et al., 2004; Shkundina et al., 2006). At the same time OR expansion leads to increased fragmentation of Sup35 aggregates, while a decrease in the number of repeats has an

opposite effect (Langlois et al., 2016). Previously, using the T-REKS algorithm (Jorda and Kajava, 2009), we identified an additional OR in the Sup35 N-domain, located from 28 to 40 amino acid residues (Bondarev et al., 2013). The mutation within this OR, named *sup35-M0*, was designed based on the model of a superpleated- $\beta$ -structure, proposed for Sup35 aggregates (Kajava et al., 2004). According to this model, charged amino acid residues located inside the fibril, can destabilize this structure, due to the electrostatic repulsion. In this work, we investigated the effect of this mutation on the prion propagation and properties of Sup35 aggregates.

## 2. MATERIALS AND METHODS

### 2.1. Strains, Media, and Growth Condition

*Saccharomyces cerevisiae* strain 7A-D832 [*psi*<sup>−</sup>] and its isogenic  $[PSI^+]$  derivative 10-7A-D832 (Bondarev et al., 2013) were used in this study unless otherwise specified. Both strains contain the *sup35::TRP1* knockout on the chromosome, compensated by plasmid(s) bearing the *SUP35* gene. For the experiments with protein transformation, the [*psi*<sup>−</sup>] [*pin*<sup>−</sup>] strain 2-OT56 (Matveenko et al., 2016) was used.

Yeast strain 12-D1682, used for the induction of new  $[PSI^+]$  variants, was constructed as follows. Strain GT671 was transformed by pRSU2 plasmid, carrying the *URA3* marker. Transformant with the *Ura*<sup>+</sup>*Leu*<sup>−</sup> phenotype was selected and designated as U-GT671. Yeast strain GT159 (Chernoff et al., 1999) was transformed by the pRSU1 plasmid (Volkov et al., 2002), carrying *LEU2* marker, and mated with the U-GT671 strain. Diploids were selected on SC-Ura-Leu media. Then random ascospore isolates were obtained, and *MATa* *Ura*<sup>−</sup>*Leu*<sup>+</sup> segregant was selected and named 12-D1682 (Table 1). This strain was transformed with a pRS316CUP-NM-GFP plasmid for overproduction of Sup35NM-GFP. The prion induction was performed as described below and seven prion variants were isolated. Clones that lost pRS316CUP-NM-GFP were selected after several passages on YEPD.

Yeast cultures were maintained on the YEPD (yeast extract/peptone/dextrose medium) or synthetic complete minimal medium (SC) (Kaiser et al., 1994). Solid media were prepared with the addition of agar (2%). SC media with 5'-FOA (1 mg/ml) was used for counter-selection of plasmids bearing *URA3* (Kaiser et al., 1994). Nonsense suppression in  $[PSI^+]$  cells was detected by the ability to grow on the SC medium lacking adenine (SC-Ade) or by the colony color on 1/4 YEPD (Eaglestone et al., 2000). Yeast cells were grown at 30°C.

### 2.2. Plasmids

Plasmids bearing the new *sup35* mutation were constructed by site-directed mutagenesis. We amplified the vector using highly processive DNA polymerase (AccuPrime Pfx, Invitrogen) (the primer sequences are available upon request). The vectors pRSU1 (Volkov et al., 2002), pRSU2 (Volkov et al., 2002), pRS316CUP-NM-GFP (Serio et al., 1999), pRS315CUP-NM-GFP and pET-20b-SUP35NM-His<sub>6</sub> (Allen et al., 2005) were used as templates. Next, the PCR mixture was treated with DpnI (Thermo Scientific) to remove the template DNA. Then, this

**TABLE 1** | Strains of *S. cerevisiae* used in this study.

Strain	Genotype	References
7A-D832	<i>MAT<math>\alpha</math> ade1-14(UGA) his7-1(UAA) leu2 lys2-739 trp1 ura3 sup35::TRP1 [pYCH-U2] [psi<sup>-</sup>] [PIN<sup>+</sup>]</i>	Bondarev et al., 2013
10-7A-D832	<i>MAT<math>\alpha</math> ade1-14(UGA) his7-1(UAA) leu2 lys2-739 trp1 ura3 sup35::TRP1 [pYCH-U2] [PSI<sup>+</sup>] [PIN<sup>+</sup>]</i>	Bondarev et al., 2013
2-OT56	<i>MAT<math>\alpha</math> ade1-14(UGA) trp1-289(UG) ura3-52 his3-<math>\Delta</math>200 leu2-3,112 [psi<sup>-</sup>] [pin<sup>-</sup>]</i>	Matveenko et al., 2016
GT159	<i>MAT<math>\alpha</math> ade1-14(UGA) trp1-289(UG) his3 lys2 ura3-52 leu2-3,112 [psi<sup>-</sup>] [PIN<sup>+</sup>]</i>	Chernoff et al., 1999
GT671	<i>MAT<math>\alpha</math> ade1-14(UGA) trp1-289(UG) his3 lys2 ura3-52 leu2-3,112 sup35::HIS3MX [CEN LEU2 SUP35] [psi<sup>-</sup>] [pin<sup>-</sup>]</i>	Gift from Y.O. Chernoff
U-GT671	<i>MAT<math>\alpha</math> ade1-14(UGA) trp1-289(UG) his3 lys2 ura3-52 leu2-3,112 sup35::HIS3MX [pRSU2] [psi<sup>-</sup>] [pin<sup>-</sup>]</i>	This study
12-D1682	<i>MAT<math>\alpha</math> ade1-14(UGA) trp1-289(UG) his3 lys2 ura3-52 leu2-3,112 sup35::HIS3MX [pRSU1] [psi<sup>-</sup>] [PIN<sup>+</sup>]</i>	This study
74-D694	<i>MAT<math>\alpha</math> ade1-14(UGA) trp1-289(UG) ura3-52 his3-<math>\Delta</math>200 leu2-3,112 [psi<sup>-</sup>] [PIN<sup>+</sup>]</i>	Derkatch et al., 1997
P-74-D694	<i>MAT<math>\alpha</math> ade1-14(UGA) trp1-289(UG) ura3-52 his3-<math>\Delta</math>200 leu2-3,112 [PSI<sup>+</sup>] [PIN<sup>+</sup>]</i>	Drozhdova et al., 2016

solution was used for transformation of *E. coli* competent cells. All mutations were verified by sequencing. To construct the pRS315CUP-NM-GFP plasmid, we ligated the region with the *CUP1* promoter, Sup35NM and GFP from pRS316CUP-NM-GFP (Serio et al., 1999) into the polylinker site of the pRS315 plasmid (Sikorski and Hieter, 1989). The region of interest in pRS316CUP-NM-GFP and the polylinker site were digested by *Xho*I and *Sac*I enzymes. Sticky-end ligation was performed with T4 DNA-ligase according to Thermo Scientific protocol. pRS315CG was obtained analogously from pRS316CG (Serio et al., 1999) and pRS315. pR16CUP-NM-yTagRFP-T plasmid was obtained by insertion of the *Xho*I-*Xho*I fragment from pCUP-NM-His<sub>6</sub> (Kiktev et al., 2015) in place of the *Xho*I-*Sal*I fragment of pR16CUP-SFP1C-yTagRFP-T which in turn resulted from the substitution of the *Pst*I-*Pst*I fragment in pR16CUP-SFP1-Cerulean (Matveenko et al., 2016) for the *Pst*I-*Pst*I fragment from pIM35 (Malcova et al., 2016). TagRFP-T is a TagRFP derivative containing one additional substitution (Shaner et al., 2008). All the plasmids are listed in Table 2.

## 2.3. Genetic and Microbiological Procedures

Standard microbiological approaches were used for all manipulations with yeast and bacterial colonies (Sambrook and Fritsch, 1989). Yeast protein transformation was performed as described previously (Tanaka and Weissman, 2006). Direct plasmid shuffle (from wild-type to mutant allele) was performed as follows: the [PSI<sup>+</sup>] *sup35::TRP1* strain with the *SUP35* gene on a *URA3* plasmid was transformed with *LEU2* plasmids bearing the wild-type or mutant *SUP35* alleles. Transformants, selected on SC medium lacking uracil and leucine (SC-Ura-Leu), were tested for suppression of the *ade1-14* mutation to determine the presence of [PSI<sup>+</sup>]. These transformants were replica plated on media with 5'-FOA for counter-selection of the plasmid with *SUP35*, and then on the SC-Leu and SC-Ura media to prove the loss of the plasmid. The suppressor phenotype of the obtained strains was analyzed on SC-Ade or 1/4 YEPD. Reverse plasmid shuffle (from mutant allele to wild-type) was performed as follows: the strains after direct shuffle were transformed with plasmids bearing the wild-type allele. Transformants were selected on SC-Ura-Leu medium and then streaked out on YEPD media to allow spontaneous plasmid loss. Colonies were replica

**TABLE 2** | Plasmids used in this study.

Plasmid	Description	References
pRSU1	<i>LEU2, ampR, PSUP35, SUP35</i>	Volkov et al., 2002
pRSU1-sup35-M0	<i>LEU2, ampR, PSUP35, sup35-M0</i>	This study
pRSU2	<i>URA3, ampR, PSUP35, SUP35</i>	Volkov et al., 2002
pRSU2-sup35-M0	<i>URA3, ampR, PSUP35, SUP35</i>	This study
pRS316CUP-NM-GFP	<i>URA3, ampR, PCUP1, SUP35NM-GFP</i>	Serio et al., 1999
pRS316CUP-NM-M0-GFP	<i>URA3, ampR, PCUP1, SUP35NM-M0-GFP</i>	This study
pET-20b-SUP35NM-His <sub>6</sub>	<i>-, ampR, T7, SUP35NM-His<sub>6</sub></i>	Allen et al., 2005
pET-20b-SUP35NM-M0-His <sub>6</sub>	<i>-, ampR, T7, SUP35NM-M0-His<sub>6</sub></i>	This study
pRS315CUP-NM-GFP	<i>LEU2, ampR, PCUP1, SUP35NM-GFP</i>	This study
pRS315CUP-NM-M0-GFP	<i>LEU2, ampR, PCUP1, SUP35NM-M0-GFP</i>	This study
pRS315	<i>LEU2, ampR</i>	Sikorski and Hieter, 1989
pRS315CG	<i>LEU2, ampR, PCUP1, GFP</i>	This study
pR16CUP-NM-yTagRFP-T	<i>URA3, ampR, PCUP1, SUP35NM-yTagRFP-T</i>	This study
pIM35	<i>URA3, ampR, PMET25, yTagRFP-T</i>	Malcova et al., 2016

For each plasmid, the following characteristics are indicated: yeast selective marker, ("-" — the absence of a yeast selective marker), bacterial selective marker, promoter of the inserted gene, gene of interest. All yeast plasmids in the table are centromeric.

plated on SC-Leu or SC-Ura medium to identify clones which contain only wild-type *SUP35* allele. After selection, the cells were tested for suppression of the *ade1-14* mutation to determine the presence of [PSI<sup>+</sup>].

The [PSI<sup>+</sup>] prion loss and transmission were scored according to the previously described procedure (Afanasyeva et al., 2011) with minor modifications. The [PSI<sup>+</sup>] strain (10-7A-D832) was transformed with a *LEU2* plasmid bearing the *SUP35* or *sup35-M0*. To estimate [PSI<sup>+</sup>] curing, caused by the presence of mutated *sup35* allele, three transformants for each allele were replica plated three times on a medium lacking uracil, then resuspended



in water and plated on 1/4 YEPD medium to obtain single colonies and to reveal the nonsense suppressor phenotype. Then these clones were replica plated on media lacking uracil or leucine. The frequency of prion loss was estimated as a fraction of  $\text{Ura}^+\text{Leu}^-$  [ $\text{PSI}^+$ ] colonies. To determine the efficiency of [ $\text{PSI}^+$ ] transmission from Sup35 to Sup35-M0, 50 transformants for each combination of SUP35 and *sup35-M0* alleles were replica plated three times on medium lacking leucine containing uracil to enable the cells to lose plasmid containing wild-type SUP35. To estimate the efficiency of [ $\text{PSI}^+$ ] transmission, the fraction of  $\text{Ade}^+$  colonies was scored among  $\text{Ura}^-\text{Leu}^+$  isolates.

## 2.4. [ $\text{PSI}^+$ ] Induction

Plasmids bearing SUP35NM-GFP or GFP under control of CUP1 promoter were used for the prion induction. Strains [ $\text{psi}^-$ ][ $\text{PIN}^+$ ] with corresponding plasmids were grown in selective media at 30°C to logarithmic phase. For the induction of CUP1 promoter,  $\text{CuSO}_4$  was added into the media to the final concentration of 100  $\mu\text{M}$  for the 7A-D832 strain or 50  $\mu\text{M}$  for 12-D1682. Before induction and after 24 h, the aliquots of cultures were plated on 1/4 YEPD to count the number of white clones and evaluate the frequency of their appearance. To compare the amounts of Sup35NM for different constructions, other aliquots were taken at the same time points. Cell lysates were obtained with alkaline lysis (Zhang et al., 2011) and subsequently analyzed with SDS-PAGE (Sambrook and Fritsch, 1989). The same cells were used for fluorescence microscopy.

## 2.5. Decoration of Sup35 Aggregates *in vivo*

Two combinations of isogenic strains were used in this experiment: P-74-D694 and 74-D694, or 10-7A-D832 and 7A-D832. The first pair (P-74-D694 and 74-D694) was transformed with plasmids for production of Sup35NM fused with different fluorescent proteins (Sup35NM-TagRFP-T and Sup35NM-GFP with substitutions) and corresponding control constructs (TagRFP-T and GFP). For the TagRFP-T production, cells with plasmid pIM35 were grown overnight in the liquid media lacking methionine. For overproduction of the other constructs with fluorescent proteins,  $\text{CuSO}_4$  was added to a final concentration of 50  $\mu\text{M}$ . The second pair of strains (10-7A-D832 and 7A-D832) was transformed with plasmids for production of Sup35NM-GFP, Sup35NM-M0-GFP or GFP. Overproduction of these proteins was induced by addition of  $\text{CuSO}_4$  to a final concentration of 100  $\mu\text{M}$ . In all cases, the induction time was 4 h.

## 2.6. Propagon Counts

The transformants of 10-7A-D832 with pRS316CUP-NM-GFP and pRS316CUP-NM-M0-GFP were used for the propagon counts. The cells were grown in liquid SC-Ura medium with additional adenine to the early logarithmic phase ( $\text{OD}_{600} = 0.2$ ). Then  $\text{CuSO}_4$  was added to a final concentration of 25  $\mu\text{M}$ . Cells were plated on YEPD supplemented with 3 mM  $\text{GuHCl}$  to obtain single colonies before the addition of  $\text{CuSO}_4$  and after one cell culture division (estimated by  $\text{OD}_{600}$ ). The number of propagons in cells was determined using a previously described colony-based method (Cox et al., 2003).

## 2.7. Fluorescence Microscopy

Cells were gently pelleted (2000–3000 rpm) and resuspended in 50% glycerol. Fluorescence was analyzed using a Zeiss AxioScope.A1 wide-field fluorescence microscope. Images were taken with a QIClick-F-CLR-12 (QImaging) camera using QCAPTURE PRO 7 software.

## 2.8. Protein Analysis

The amount of Sup35 in different strains was quantified using Western Blotting with rabbit polyclonal anti-Sup35 antibodies (Chabelskaya et al., 2004). Monoclonal anti-tubulin antibodies (T6074, Sigma) were used for tubulin detection. Densitometry measurements were performed in ImageJ software (Schneider et al., 2012). SDS-PAGE with additional boiling (Kushnirov et al., 2006) was performed to detect Sup35NM-GFP and Sup35 in the aggregated and soluble fractions. For the analysis of Sup35 amyloid aggregates, SDD-AGE was used (Kryndushkin et al., 2003).

## 2.9. Protein Purification From *Escherichia coli* and Fibril Preparation

For Sup35NM purification, pET-20b-SUP35NM-His<sub>6</sub> (Allen et al., 2005) plasmid or its derivative for Sup35NM-M0 overproduction were used. For protein purification, *E. coli* strain BL21(DE3) was used (Studier and Moffatt, 1986). Overproduction of recombinant proteins was carried out in 2TYa media with 1 mM IPTG. Cultures were grown at 37°C for 6 h. Proteins were purified in denaturing conditions (in the presence of 8 M urea) according to previously published protocols (Glover et al., 1997; Serio et al., 1999). The purification was performed with a two-step procedure with Ni-NTA agarose (Invitrogen) and Q-sepharose (GE Healthcare) columns. Proteins were concentrated with a centrifuge concentrator with molecular weight cutoff of 30 kDa (Millipore).

The obtained Sup35NM proteins were diluted at least 100-fold into fibril assembly buffer (5 mM potassium phosphate pH 7.5, 150 mM NaCl) to a final protein concentration of 0.5 mg/ml. In these conditions, Sup35NM spontaneously forms aggregates. Samples were incubated at 26°C with slow overhead rotation (rotator Bio RS-24, Biosan). To monitor amyloid fibril formation, aliquots were removed every 12 h up to 24 h of incubation. The rate of aggregated protein was estimated by SDS-PAGE with boiled and unboiled samples.

## 2.10. TEM and AFM

For fibrils visualization, Jeol JEM-2100 transmission electron microscope and Bruker Nanoscope V atomic force microscope were used. The negative staining with a 1% aqueous solution of uranyl acetate was used for TEM measurements. Samples were prepared by applying 5  $\mu\text{l}$  of the Sup35NM fibril solution with concentration 0.5 mg/ml on a substrate, followed by washing with distilled water and drying. The fibrils were immobilized on freshly-cleaved mica surface for AFM analysis and formvar coated copper grids for TEM measurements (Sokolov et al., 2018).

## 2.11. Statistical Analysis

To compare the protein amounts the Mann-Whitney *U*-test was used (Mann and Whitney, 1947). The Fisher's exact test (Fisher, 1935) was used to compare the proportion of cells with a particular phenotype. All statistical tests were performed in R (R Core Team, 2018).

## 3. RESULTS

### 3.1. Design of a New *sup35* Mutation

In the previous work, we constructed five mutant *sup35* alleles, each of them leading to substitutions of two consecutive polar residues to charged ones (lysines) in the middle of one of the oligopeptide repeats (OR1 - OR5). Such mutations are incompatible with Sup35p aggregates with superpleated  $\beta$ -structure spanning the ORs with the respective mutations. These mutations were named *sup35<sup>KK</sup>*, and each was designated according to the number of ORs (from *sup35-M1* to *sup35-M5*) (Bondarev et al., 2013). We introduced mutations in all previously known ORs of Sup35 (Kushnirov et al., 1988). However, using T-REKS program, we identified additional repeat upstream of the known ORs (28–40 aa) (Bondarev et al., 2013). To complete the set of *sup35<sup>KK</sup>* alleles, we substituted two residues in the middle of newly identified OR0 (Q33K/A34K) to lysines and designated this mutation *sup35-M0*. The potential effect of this mutation on the Sup35 aggregation was evaluated with ArchCandy program (Ahmed et al., 2015). Previously it was shown that this tool accurately predicts the impact of amino acid substitutions on aggregation properties of a protein (Ahmed et al., 2015; Bondarev et al., 2015; Roche et al., 2017). According to the analysis, *sup35-M0* mutation could significantly decrease the amyloidogenic potential of Sup35 and have the highest effect on this parameter compared to known PNM2 mutation (Doel et al., 1994) and other *sup35<sup>KK</sup>*,

which were shown to eliminate the  $[PSI^+]$  prion (Figure 1) (Bondarev et al., 2013).

### 3.2. The *sup35-M0* Mutation Efficiently Eliminates the $[PSI^+]$ Prion

To analyze the effect of the mutation, we used previously described isogenic  $[PSI^+]$  and  $[psi^-]$  strains with SUP35 deletion compensated by a copy of this gene on a URA3 plasmid (Bondarev et al., 2013). In this system, we can change the alleles of SUP35 by plasmid shuffling. The presence of the nonsense mutation *ade1-14* in these strains allows monitoring the prion propagation by the cell phenotype. As  $[PSI^+]$  strains are able to suppress *ade1-14* mutation, we test for the prion loss by detecting the decrease in growth on medium lacking adenine accompanied by increased accumulation of the red pigment on 1/4 YEPD. To check the effect of *sup35-M0*, we transformed isogenic  $[PSI^+]$  and  $[psi^-]$  strains with a plasmid bearing *sup35-M0* or SUP35 (control). All independent  $[PSI^+]$  transformants bearing the mutant allele demonstrated a significant decrease in nonsense suppression phenotype on 1/4 YEPD (Figure 2A) or SC media without adenine (data not shown). The complete elimination of prion phenotype was observed after loss of the wild-type SUP35 allele (Figure 2A). Yeast cells did not restore nonsense suppressor phenotype after replacement of a mutant allele by the wild-type (Figure 2A) suggesting that *sup35-M0* mutation leads to the  $[PSI^+]$  prion loss.

Elimination of the prion should be accompanied by the elimination of Sup35 aggregates from the cells. We checked for the disappearance of aggregates in the transformants, which lost the wild-type SUP35, with SDD-AGE (Kryndushkin et al., 2003) and did not find Sup35 aggregates in cells bearing only *sup35-M0* (Figure 2B). This fact confirmed our assumption that the mutation eliminates the prion. We also compared the relative amount of the Sup35 protein for strains with the wild-type and

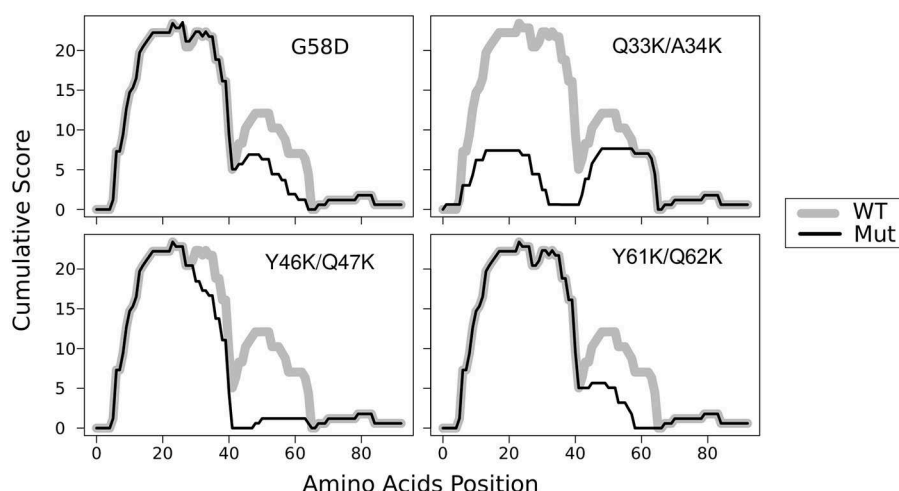


**FIGURE 1 |** Substitutions Q33K/A34K within N-domain of Sup35 decrease the amyloidogenic potential of the protein. The ArchCandy program (Ahmed et al., 2015) was used to predict amyloidogenic properties. Cumulative scores (sum of  $\beta$ -arch scores counted for each amino acid residue) are presented on the plot. WT — wild-type protein; G58D, Q33K/A34K, Y46K/Q47K, and Y61K/Q62K substitutions that correspond to mutations PNM2, *sup35-M0*, -M1, and -M2, respectively.

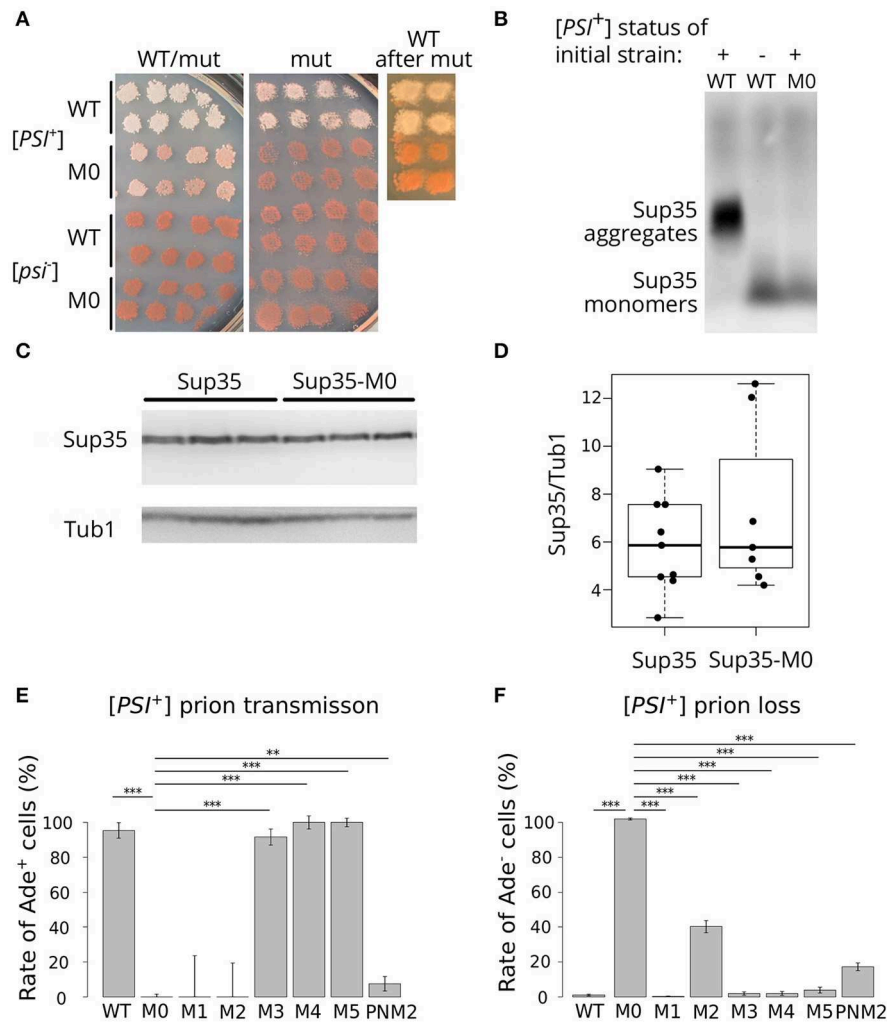


**FIGURE 2 |** *sup35-M0* efficiently and irreversibly eliminates  $[PSI^+]$  prion. **(A)** The phenotype of strains with different combinations of *SUP35* and *sup35-M0* alleles in  $[PSI^+]$  and  $[psi^-]$  strains on 1/4 YEPD is shown (images were taken after 4 days of incubation). Transformants bearing two plasmids with two wild-type alleles or combination of *sup35-M0* and *SUP35* are presented on the panel "WT/mut" (at least 16 transformants were analyzed). The phenotype of cells after the plasmid loss is shown on panel "mut". Finally, *sup35-M0* (or *SUP35* as a control) were replaced with *SUP35* by the reverse plasmid shuffling, phenotype of obtained strains is presented on panel "WT after mut." **(B)** The *sup35-M0* allele leads to the elimination of Sup35 aggregates according to SDD-AGE results. Antibodies against Sup35 were used for Western Blotting. **(C)** Result of Western Blot hybridization after SDS-PAGE analysis of protein lysates from the  $[psi^-]$  strain with mutant or wild-type allele of *SUP35* with anti-Sup35 and anti-Tub1 antibodies. **(D)** The densitometry analysis of Sup35 protein level (ten replicates) revealed no difference in Sup35 protein level in strains with *sup35-M0* compared to *SUP35*. **(E)**  $[PSI^+]$  transmission from the wild-type to the indicated *sup35* allele. Fraction of cells that retained the prion after loss of the wild-type allele is shown on graph. **(F)**  $[PSI^+]$  loss induced by transient expression of the *sup35<sup>KK</sup>* alleles and *PNM2* mutation. Fraction of cells that have lost the prion after the loss of *sup35<sup>KK</sup>* allele is shown. \*\**p*-value < 0.01 and \*\*\**p*-value < 0.001 according to Fisher's exact test.

the mutant *SUP35* allele and found no difference (**Figures 2C,D**), suggesting that the prion loss was not caused by a decreased amount of Sup35.

To compare the effects of the new mutation on the prion replication, we estimated the prion loss and transmission in the presence of *sup35-M0* allele according to special protocols for each parameter [(Afanasieva et al., 2011), see Materials and Methods section for details]. We did not observe cases of prion transmission to the *sup35-M0* allele (**Figure 2E**). At the same time, the rate of  $[PSI^+]$  loss was  $97.12 \pm 0.55\%$  that significantly exceeds the same parameter for other *sup35<sup>KK</sup>* mutations with

a maximum value of  $\sim 40\%$  in case of substitutions within the second OR (**Figure 2F**) (Bondarev et al., 2013). Based on this data we concluded that new mutation very efficiently eliminates the  $[PSI^+]$  prion.

### 3.3. The Sup35NM-M0 Protein Forms Infectious Amyloid Aggregates

The highly efficient loss of the prion caused by *sup35-M0* suggested that Sup35 with amino acid changes Q33K/A34K might be unable to form aggregates and induce  $[PSI^+]$  formation. To check this hypothesis, we constructed plasmids



for purification of the Sup35NM-M0 protein from *E. coli* cells. We chose only the N-terminal part of the protein because it is sufficient for aggregation (Glover et al., 1997). Wild-type Sup35NM protein was used as a control. After 24 h of incubation in nondenaturing conditions, both proteins formed SDS-resistant aggregates, detected by comparing the amount of the proteins in boiled and unboiled samples analyzed with SDS-PAGE (Figure 3A). Using atomic force microscopy (AFM) and transmission electron microscopy (TEM) we investigated the morphology of Sup35NM and Sup35-M0 aggregates and found no detectable difference between them (Figure 3B). To test infectious properties of the obtained fibrils, we used the protein

transformation technique (Tanaka and Weissman, 2006) and demonstrated that aggregates of both proteins were infectious and led to  $[PSI^+]$  appearance (Figure 3C). In all cases, the observed nonsense suppressor phenotype was prion-mediated because it was lost after cell growth on the media with GuHCl (data not shown), which is known to cause the loss of  $[PSI^+]$  (Tuite et al., 1981). At the same time, cells transformed with monomeric protein did not acquire prion phenotype. Thus, charged residues within OR0 in Sup35 do not significantly change its ability to form infectious aggregates *in vitro*.

### 3.4. The *sup35-M0* Allele Can Induce and Propagate the $[PSI^+]$ Prion but With Low Efficiency

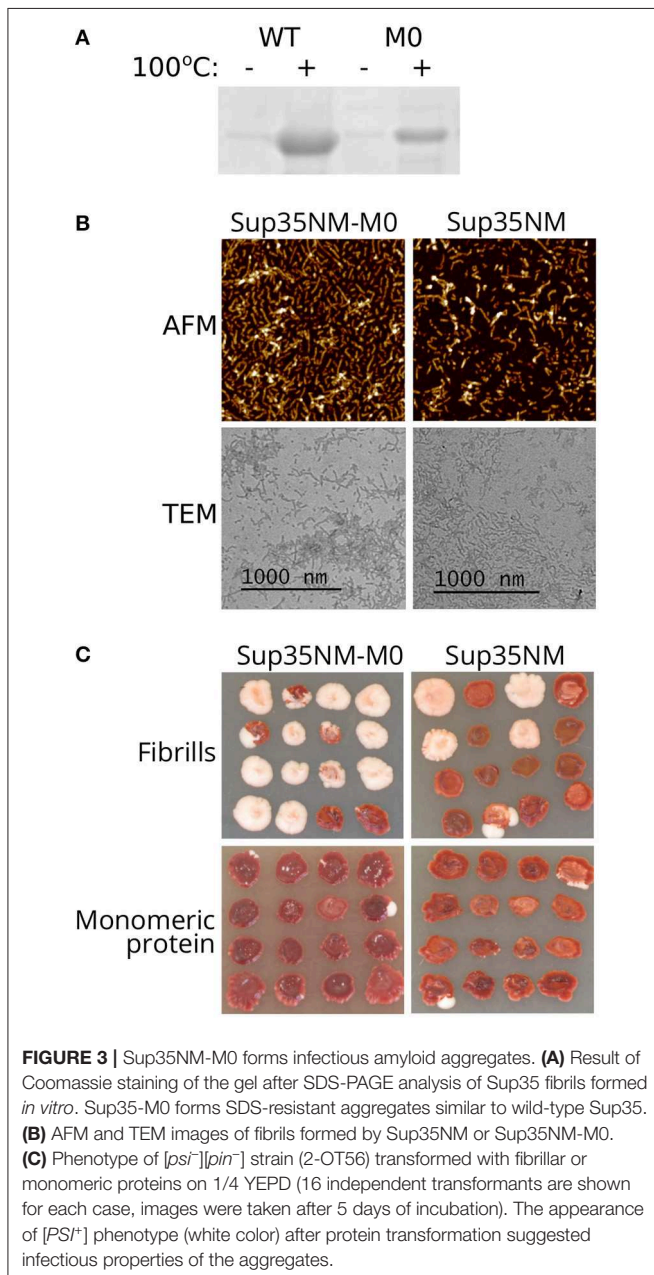
Next, we analyzed the effect of *sup35-M0* allele on the prion induction *in vivo*. The presence of another prion  $[PIN^+]$  is required for  $[PSI^+]$  *de novo* formation in yeast cells (Derkatch et al., 1997). For this experiment  $[psi^-][PIN^+]$  strains (derivatives of 7A-D832 or 12-D1682 bearing SUP35 or *sup35-M0*) were transformed with plasmids for Sup35NM-GFP (positive control), Sup35NM-M0-GFP or GFP (negative control) overproduction. The presence of *sup35-M0* in cells significantly decreased the frequency of  $[PSI^+]$  formation in different yeast strains. Furthermore, the overproduction of Sup35NM-M0-GFP induced  $[PSI^+]$  with very low efficiency (Figures 4A,B). This result allowed us to conclude that investigated substitutions significantly decrease the aggregation propensity of the protein, as was predicted by the ArchCandy program (Figure 1). We also compared patterns of Sup35NM-GFP and Sup35NM-M0-GFP fluorescence upon their overproduction. In all cases, we found that Sup35 aggregates formed during  $[PSI^+]$  induction: rings, ribbons, or dots (Figure 4C), which are detected on the different stages of the prion life cycle (Tyedmers, 2012).

The low frequency of the prion induction upon *sup35NM-M0* overexpression may also be explained by the effect of the mutation on the protein stability. However, the levels of corresponding proteins upon their overproduction are the same (Figures 4D,E), which contradicts this hypothesis.

To check that the cells with nonsense suppressor phenotype and bearing *sup35-M0* were  $[PSI^+]$  we isolated several corresponding clones of 12-D1682. The suppressor phenotype of these clones was preserved after several passages (Figure 4F) and in the absence of the plasmid, used for  $[PSI^+]$  induction, but eliminated after the growth on GuHCl containing media (data not shown). We also found aggregates of Sup35 in all analyzed strains with prion variants (Figure 4G). These results prove the ability of *sup35-M0* to maintain the  $[PSI^+]$  prion. Nevertheless, it should be mentioned that all  $[PSI^+]$  variants formed in presence of *sup35-M0* had weak suppressor phenotype (Figure 4F).

### 3.5. The Sup35-M0 Protein Can Incorporate Into Fibrils of the Wild-Type Protein *in vivo*

We analyzed the ability of the protein with Q33K/A34K substitutions to incorporate into pre-existing Sup35 aggregates *in vivo*. Transient overproduction of Sup35NM fused with fluorescent protein leads to the decoration of existing Sup35





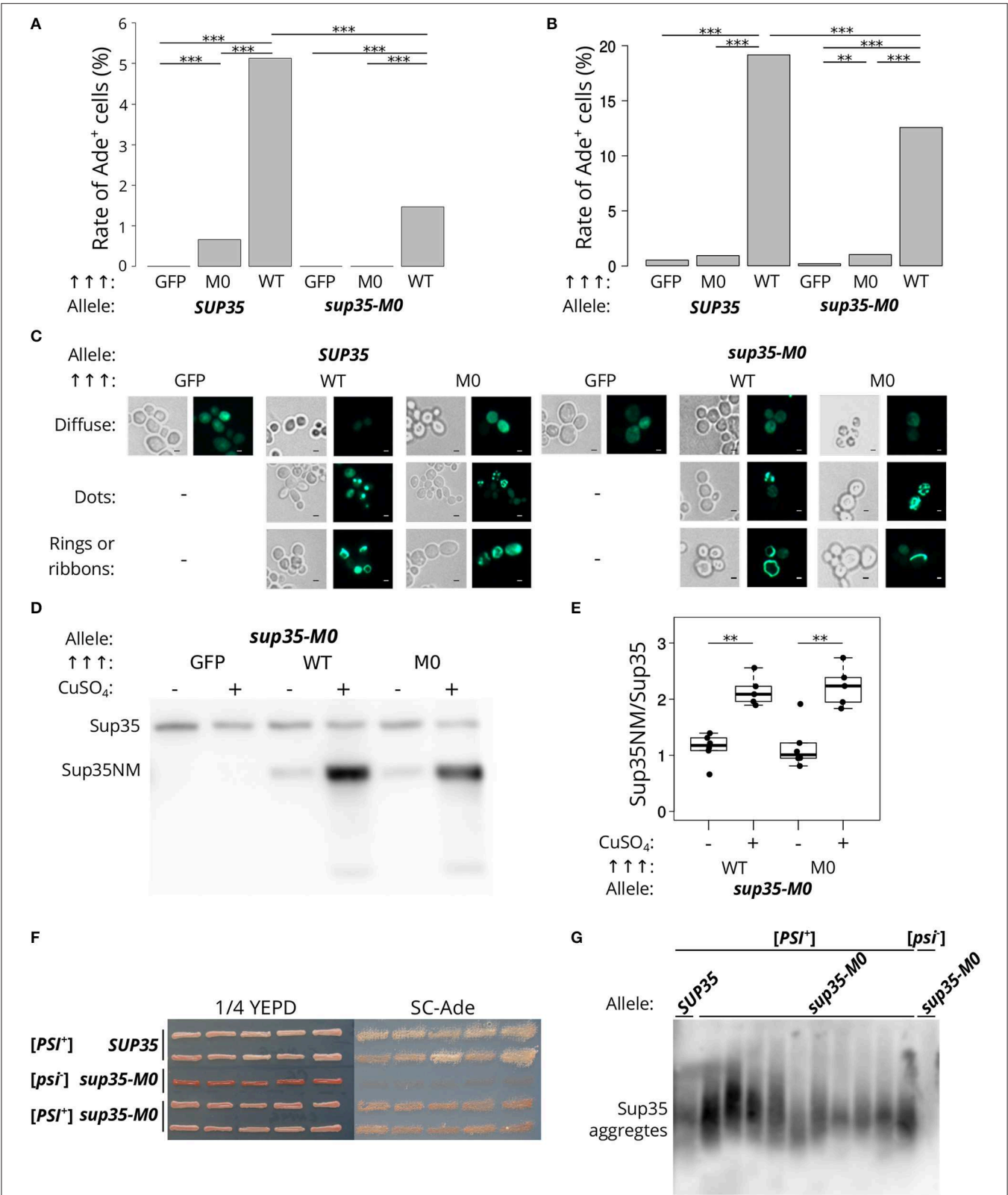


**FIGURE 4** | hereafter was used as a negative control. All constructions were under control of *CUP1* promoter, CuSO<sub>4</sub> was used for the 24 h induction. All experiments were repeated six times. Our results demonstrated that the mutation has a dramatically lower potential to induce  $[PSI^+]$  prion than *SUP35* (\*\**p*-value < 0.001 according to Fisher's exact test). The "Allele" designates allele of full-length *SUP35* present in cells. **(C)** The cells tested on panel A were analyzed with the fluorescence microscopy (scale bar equals 5  $\mu$ m). Various types of prion aggregates (dots, rings, and ribbons) were detected in the presence of both alleles (*SUP35* and *sup35-M0*). **(D)** Results of Western Blot hybridization after SDS-PAGE analysis of protein lysates of strains used for  $[PSI^+]$  induction. **(E)** Densitometry analysis of the Western Blotting. The level of N-terminal domain of Sup35 fused to GFP was normalized to the full-length Sup35-M0 which is unchanged in cells with wild-type and mutant *sup35* allele according to the results presented on the **Figure 2** (\*\**p*-value < 0.01 according to Mann-Whitney *U*-test). **(F)** The nonsense suppressor phenotype of several  $[PSI^+]$  variants induced in presence of *SUP35* or *sup35-M0* in the 12-D1682 strain. Ten independent isolates are shown for each case. Cells were grown for 4 days on 1/4 YEPD and 5 days on SC-Ade. **(G)** The results of SDD-AGE analysis of protein lysates of typical  $[PSI^+]$  variants induced in the presence of *sup35-M0*, antibodies against Sup35 were used for Western Blotting.

aggregates and formation of detectable fluorescent foci in cells (Oshervich et al., 2004).  $[PSI^+][PIN^+]$  and  $[psi^-][PIN^+]$  yeast strains (P-74-D694 and 74-D694, respectively) were transformed with the plasmids for overproduction of Sup35NM fused to a red fluorescent protein, TagRFP-T, in combination with either Sup35NM-GFP, or Sup35NM-M0-GFP, and analyzed with fluorescence microscopy. This experiment showed that the aggregates of Sup35NM and Sup35NM-M0 decorate  $[PSI^+]$  aggregates (**Figure 5A**). One possible explanation of these results is that independently formed Sup35-M0 fibrils might co-localize with the wild-type fibrils, however, colocalization of the fibrils forming *de novo* in  $[psi^-]$  strains seems less likely than co-aggregation of the wild-type and mutant proteins. Then we rechecked the ability of Sup35-M0 to embed into aggregates of the prion variant used in experiments with plasmid shuffle. The isogenic  $[PSI^+][PIN^+]$  and  $[psi^-][PIN^+]$  strains (10-7A-D832 and 7A-D832, respectively) were analyzed for the aggregate formation of Sup35NM-GFP or Sup35NM-M0-GFP. We detected fluorescent foci for both proteins only in  $[PSI^+]$  strain (**Figure 5B**), which suggested the inclusion of the proteins into pre-existing aggregates, rather than *de novo* aggregation of the overproduced proteins. Then the incorporation of Sup35NM-M0 into amyloid aggregates was analyzed with SDS-PAGE with modifications, which allowed to evaluate the distribution of the protein with substitutions between fractions of detergent-resistant aggregates and monomers (**Figure 5C**). The results clearly demonstrated that Sup35NM-M0 was converted into amyloid-like conformation in the investigated  $[PSI^+]$  strain. Taken together these data demonstrated the ability of the Sup35-M0 to incorporate into various Sup35 aggregates *in vivo*.

Incorporation of Sup35-M0 into the existing prion aggregates may have different effects. Previously we proposed that the analogous mutation in the second OR (*sup35-M2*) leads to formation of non-heritable fold and as a result to the prion loss (Bondarev et al., 2013). The main mechanism responsible for the prion transmission is a fragmentation of the prion aggregates by chaperones (Liebman and Chernoff, 2012). An impairment of this process should lead to the decrease in number of prion "seeds," called propagons, and affects the transmission of the prion upon cell division. We analyzed the effect of Sup35NM-M0-GFP production on the propagon number after one generation and found no significant differences compared to Sup35NM-GFP (**Figure 5D**). Thus, we considered that *sup35-M0* has negligible effect on the aggregate fragmentation.

Finally, using phenotypic assay, we investigated the influence of the Sup35NM-M0 incorporation into wild-type Sup35 aggregates on the  $[PSI^+]$  prion properties. One of the effects of increased Sup35 aggregation in  $[PSI^+]$  cells is a reduction in cell viability as overproduction of Sup35NM in  $[PSI^+]$  strains may lead to increased prion-dependent lethality (Derkatch, 1998; Vishveshwara et al., 2009). We checked whether Sup35NM-M0 retained the toxic properties of the wild-type protein. In contrast to Sup35NM-GFP, overexpression of Sup35NM-M0-GFP did not lead to a decrease in cell viability (**Figure 5E**). Overall, our data imply that the mutant Sup35 is able to co-aggregate with the wild-type protein, but their coaggregation may destabilize prion propagation of the native protein.

### 3.6. The Effect of *sup35-M0* Mutation Is Variant-Unspecific

The effect of *sup35* mutations on  $[PSI^+]$  usually depends on the prion variant (Derkatch et al., 1999; King, 2001). We checked whether the effects of *sup35-M0* are variant-specific. We obtained seven new  $[PSI^+]$  prion variants in the strain with a single copy of *SUP35* on the plasmid (see Materials and Methods section for details). These strains had different strengths of the nonsense suppressor phenotype on medium lacking adenine, and differed in size of Sup35 aggregates (**Figures 6A,B**). The replacement of *SUP35* by *sup35-M0* in these strains led to the loss of nonsense suppressor phenotype (**Figure 6C**) and Sup35 aggregates (verified for two investigated strains with SDD-AGE, data not shown). This allowed us to conclude that the *sup35-M0* allele eliminates  $[PSI^+]$  independently of the prion variant.

## 4. DISCUSSION

The N-terminal domain of Sup35 is traditionally subdivided onto QN-rich (1–39 aa) and oligopeptide repeats regions (40–112 aa) (Kushnirov et al., 1988). The minimal region essential for  $[PSI^+]$  propagation was assumed to comprise the first 57 residues, i.e., all QN region and two first ORs (Oshervich et al., 2004; Shkundina et al., 2006). In this work, we described the effects of substitutions (Q33K/A34K) within previously uncharacterized oligopeptide repeat of Sup35 on the  $[PSI^+]$  prion propagation. We designated this new mutation as *sup35-M0* and showed that it is able to eliminate  $[PSI^+]$ . This fact is in good agreement with position of the mutation, as well as the fact, that the majority of known PNM mutations is located within the region which was

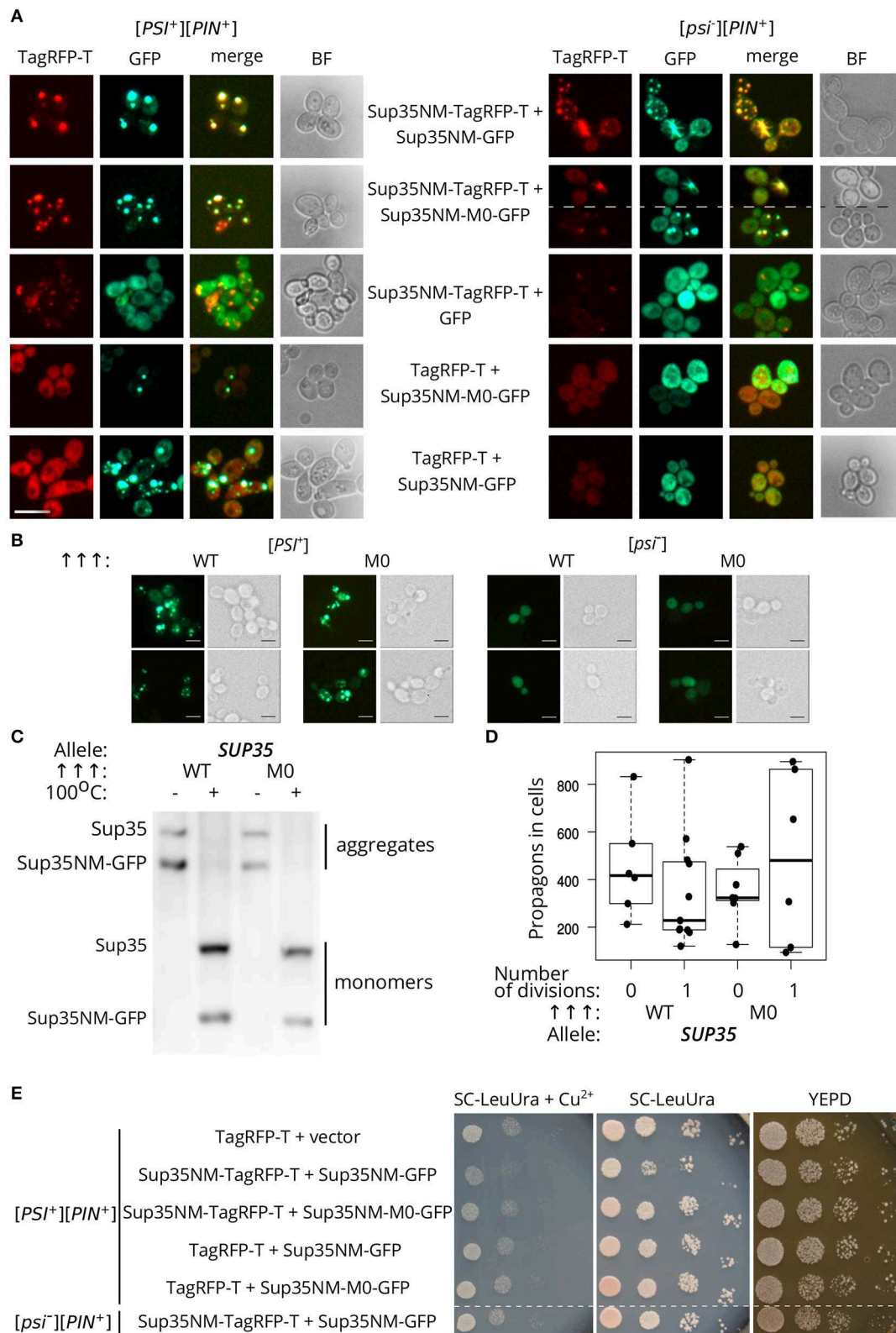


**FIGURE 5 |** The Sup35-M0 protein can incorporate into fibrils of wild-type protein *in vivo*. **(A)** [psi<sup>-</sup>][PIN<sup>+</sup>] (74-D694) and [PSI<sup>+</sup>][PIN<sup>+</sup>] (P-74-D694) yeast strains were transformed with the plasmids for overproduction of Sup35NM-yTagRFP-T, in combination with either Sup35NM-GFP or Sup35NM-M0-GFP. We observed that  
 (Continued)

**FIGURE 5 |** the aggregates of Sup35NM and Sup35NM-M0 colocalize in  $[PSI^+]$ , as well as in  $[psi^-]$  cells (scale bar equals 10  $\mu$ m). **(B)** The transformants of  $[psi^-][PIN^+]$  (7A-D832) and  $[PSI^+][PIN^+]$  (10-7A-D832) with overproduced Sup35NM-GFP (WT), or Sup35NM-M0-GFP (M0) were analyzed with fluorescence microscopy (scale bar equals 5  $\mu$ m). We detected foci of both proteins only in  $[PSI^+]$ , but not in  $[psi^-]$ , strain, which indicates inclusion of the proteins into existing aggregates. **(C)** The result of SDS-PAGE with boiled gel for strains from the panel B was shown. The “Allele” designates allele of full-length SUP35 present in cells. The Sup35NM-GFP (WT) and Sup35NM-M0-GFP (M0) proteins can incorporate into the existing prion aggregates upon transient overproduction in  $[PSI^+]$  strain (both are detected in a fraction of aggregates). **(D)** Production of Sup35NM-M0-GFP does not affect the number of propagons. The cells from the panel B were used to calculate number of propagons before and after mild overproduction of Sup35NM-GFP or Sup35NM-M0-GFP; 25  $\mu$ M CuSO<sub>4</sub> was used for the induction. **(E)** Cells with overproduction of Sup35NM-TagRFP-T together with Sup35-NM-M0-GFP or Sup35NM-GFP were analyzed for prion toxicity. Cells were plated in 10-fold serial dilutions and grown for 2 days on SC-LeuUra + Cu<sup>2+</sup> or YEPD and 4 days on SC-UraLeu. TagRFP-T production was used as a control; vector — pRS315.

shown to be important for  $[PSI^+]$  maintenance (DePace et al., 1998; King, 2001).

The *sup35<sup>KK</sup>* mutations, as it was shown previously, may have different effects on  $[PSI^+]$  propagation (Bondarev et al., 2013). Taken together with current results, we can conclude that proteins with corresponding substitutions within OR0–OR2 eliminate the prion, but can incorporate into pre-existing prion aggregates, induce  $[PSI^+]$  appearance and form amyloid aggregates *in vitro* (Bondarev et al., 2013 and *paper in prep*). Despite these common features only *sup35-M2* and the *sup35-M0* eliminate the prion even in presence of the wild-type allele (Figure 2F). This allows us to speculate that the role of first OR in the prion propagation is different from OR0 or OR2.

The hallmark of *sup35-M0* is the higher efficiency of  $[PSI^+]$  elimination ( $97.12 \pm 0.55\%$ , Figure 2F) compared to the other previously characterized PNM mutations. For example, the prion loss in the presence of *PNM2* or *sup35-M2* mutations reaches 20 and 40%, respectively (Bondarev et al., 2013). The shuffle of SUP35 from *S. cerevisiae* to the homologs from other yeast species (*S. paradoxus*, *S. bayanus*, *S. mikatae*, *S. kudriavzevii*) may also lead to the  $[PSI^+]$  elimination but with lower efficiency than *sup35-M0* (Afanasieva et al., 2011). Furthermore, the prion elimination by the *sup35-M0* mutation can destabilize different  $[PSI^+]$  variants (Figure 6C), while the effects of all previously described PNM mutations were variant-specific (Derkatch et al., 1999; King, 2001). Another specific feature of *sup35-M0* is a very low ability to induce and propagate the prion. Our results suggest that this mutation can maintain only limited number of weak prion variants (Figure 4F).

The strong effect of *sup35-M0* was not linked to the stability of the protein as the relative amounts of wild-type and mutant proteins did not differ (Figures 2C,D). Also, the elimination of the prion in the presence of *sup35-M0* could not be explained by the complete inability of the protein to propagate  $[PSI^+]$ . Sup35NM-M0 can form infectious aggregates *in vitro* (Figure 3C), overproduction of Sup35NM-M0-GFP leads to the prion induction *in vivo*, and, finally, *sup35-M0* can maintain the prion, though, with low efficiency (Figures 4A,B). The low prion induction rate upon overproduction of Sup35NM-M0-GFP and in the presence of *sup35-M0* may be explained by the reduced ability of the soluble protein to aggregate with itself, as was demonstrated for Sup35-M1 and Sup35-M2 (Khan et al., 2018).

It is noteworthy that our experimental results once again illustrate the accuracy of ArchCandy prediction (Ahmed et al., 2015; Bondarev et al., 2015; Roche et al., 2017). We found that *sup35-M0* significantly decreases the frequency of the prion induction *de novo* and has lower prionogenic potential *in vivo* (Figure 4A). These data are in a good agreement with the bioinformatics predictions of ArchCandy, according to which lysines in 33–34 aa positions significantly decrease the amyloidogenic potential of Sup35 protein (Figure 1).

Prion loss caused by a certain SUP35 allele may occur due to different mechanisms. In case of the interspecies barrier, three mechanisms were proposed: the inability of the heterologous protein to incorporate into prion aggregates, the block of aggregation by the protein and formation of the non-heritable fold of aggregates (Afanasieva et al., 2011). Detailed investigation of  $[PSI^+]$  elimination caused by *PNM2* revealed two potential processes that may explain nonheritable properties of aggregates: increased fragmentation leading to solubilization of aggregates and impairment of prion transmission to the daughter cell (DiSalvo et al., 2011; Verges et al., 2011; Pei et al., 2017). We found that Sup35NM-M0 can incorporate into pre-existing Sup35 aggregates *in vivo* (Figures 5B,C), but this does not affect the number of propagons (Figure 5D) and thus the fragmentation of aggregates. It seems that both mechanisms could not explain the effect of *sup35-M0*. We suppose that the prion loss caused by *sup35-M0* is rather linked with the decreased aggregation propensity of the protein, followed by solubilization of aggregates by cellular chaperones. This hypothesis is in good agreement with very low  $[PSI^+]$  induction rate in the presence of *sup35-M0* (Figure 4A) and prediction of the ArchCandy (Figure 1). However, this disagrees with the high efficiency of co-aggregation of Sup35NM-M0 with Sup35 (Figure 5), but we suggest that differences in aggregation rate in this experiment may be hidden due to the overproduction of the protein.

In summary, here we described a new mutation in SUP35, which can efficiently eliminate  $[PSI^+]$  factor in a variant-independent manner. The *sup35-M0* possess very low amyloidogenic potential and can protect cells from the spontaneous appearance of the prion. We suggest that the investigated mutation may be widely used for fast and non-specific elimination of the  $[PSI^+]$  prion or for design of yeast strains which almost never undergo transition to the  $[PSI^+]$  state. Moreover, our discovery may serve as a proof of concept for the design of a prion-eliminating mutations using specific bioinformatic tools. In mammals at least two



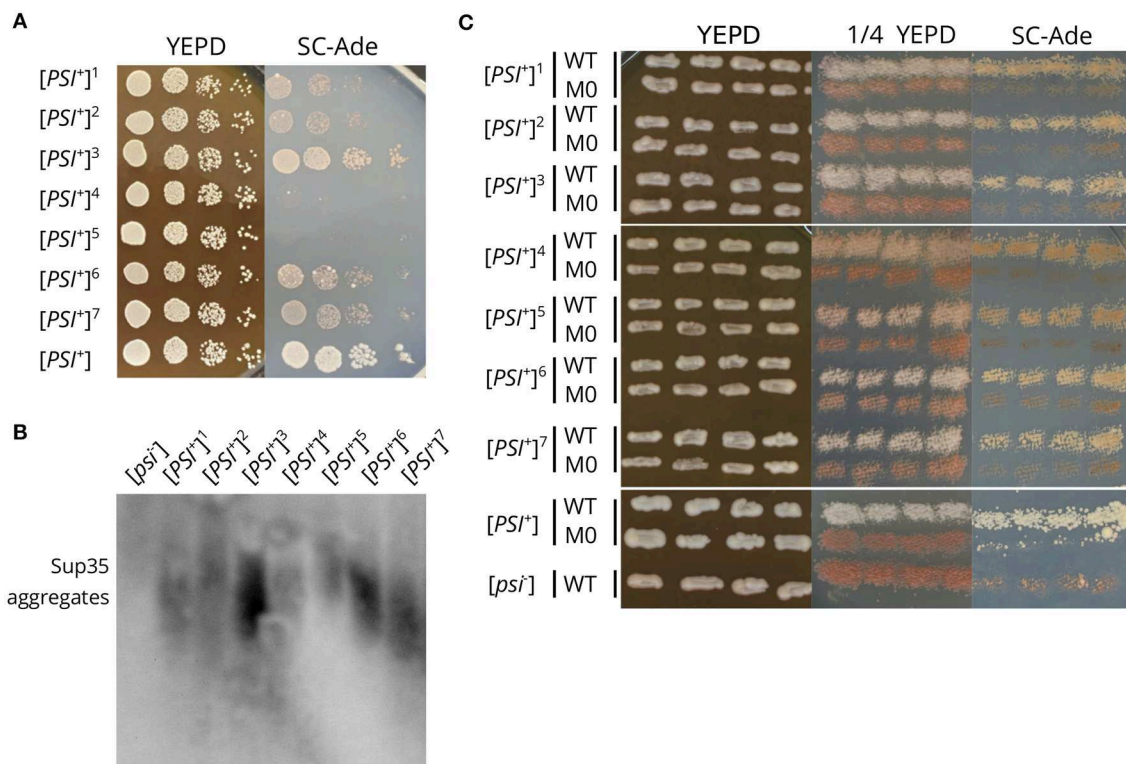


**FIGURE 6 |** The *sup35-M0* mutation destabilizes different *[PSI<sup>+</sup>]* variants. **(A)** The suppressor phenotype of the obtained *[PSI<sup>+</sup>]* variants (designated by numbers 1-7). *[PSI<sup>+</sup>]* designates the 10-7A-D832 strain. Cells were plated in 10-fold serial dilutions and grown for 3 days on YEPD and 5 days on SC-Ade. **(B)** The comparison of Sup35 aggregate size in strains from the panel A. *[psi<sup>-</sup>]* is the 12-D1682 strain. **(C)** The suppressor phenotype of the same strains after the replacement of *SUP35* by *sup35-M0*. Cells were grown for 3 days on YEPD or 1/4 YEPD and 7 days on SC-Ade.

analogous mutations, eliminating the PrP prion in presence of the wild type allele, were described. Both of them lead to substitutions of polar residue to the charged one (Q167R or Q218K) (Zulianello et al., 2000; Perrier et al., 2002), and it was shown that the protein with Q218K substitution decreases formation of PrP amyloid aggregates *in vitro* (Lee et al., 2007). Thus, our study supports the design of analogous mutations that could block propagation of mammalian prion and amyloid proteins and thus may be useful for amyloidosis therapy.

## DATA AVAILABILITY STATEMENT

The datasets generated for this study are available on request to the corresponding author.

## AUTHOR CONTRIBUTIONS

LD, AM, PS, and SB designed the experiments. LD, VR, AM, MB, OP, DL, PS, and SB performed the experiments. LD, VR, AM, PS, and SB prepared figures. LD, AM, and SB wrote original draft. LD, AM, MB, DL, PS, NK, AK, GZ, and SB performed review and editing the manuscript.

## FUNDING

The authors acknowledge St. Petersburg State University for the research grant (id: 28229898, SB, the ArchCandy analysis). This work was also supported by RFBR grants (19-04-00173, GZ, the analysis of *sup35-M0* effects on *[PSI<sup>+</sup>]* propagation; 17-54-150002, GZ, and PRC CNRS grant PRC1524, AK, the *in vitro* experiments; 18-34-00536, AM, the analysis of colocalization of Sup35NM-M0 with the wild-type protein *in vivo*) and RSF grant (18-14-00050, GZ, the analysis of *sup35-M0* effect on the translation termination).

## ACKNOWLEDGMENTS

We are grateful to Yury O. Chernoff and Ivana Malcova for plasmids and strains. We thank Ksenia V. Sukhanova, Anton B. Matiiv, Yury A. Barbitoff and Ekaterina Davydova for critical reading of the manuscript and suggestions. The work was supported by the RRC MCT SPbSU and we thank Maxim Vorobyov, Nikolai Kostin and Alexei Masharskiy from this facility for help with experiments.

## REFERENCES

- Afanasieva, E. G., Kushnirov, V. V., Tuite, M. F., and Ter-Avanesyan, M. D. (2011). Molecular basis for transmission barrier and interference between closely related prion proteins in yeast. *J. Biol. Chem.* 286, 15773–15780. doi: 10.1074/jbc.M110.183889
- Ahmed, A. B., Znassi, N., Château, M.-T., and Kajava, A. V. (2015). A structure-based approach to predict predisposition to amyloidosis. *Alzheimers Dement.* 11, 681–690. doi: 10.1016/j.jalz.2014.06.007
- Allen, K. D., Wegrzyn, R. D., Chernova, T. A., Müller, S., Newnam, G. P., Winslett, P. A., et al. (2005). Hsp70 chaperones as modulators of prion life cycle: novel effects of Ssa and Ssb on the *Saccharomyces cerevisiae* prion [PSI<sup>+</sup>]. *Genetics* 169, 1227–1242. doi: 10.1534/genetics.104.037168
- Baxa, U., Cassese, T., Kajava, A. V., and Steven, A. C. (2006). Structure, function, and amyloidogenesis of fungal prions: filament polymorphism and prion variants. *Adv. Protein. Chem.* 73, 125–180. doi: 10.1016/S0065-3233(06)73005-4
- Bondarev, S. A., Shchepachev, V. V., Kajava, A. V., and Zhouravleva, G. A. (2013). Effect of charged residues in the N-domain of Sup35 protein on prion [PSI<sup>+</sup>] stability and propagation. *J. Biol. Chem.* 288, 28503–28513. doi: 10.1074/jbc.M113.471805
- Bondarev, S. A., Zhouravleva, G. A., Belousov, M. V., and Kajava, A. V. (2015). Structure-based view on [PSI<sup>+</sup>] prion properties. *Prion* 9, 190–199. doi: 10.1080/19336896.2015.1044186
- Chabelskaya, S., Kiktev, D., Inge-Vechtomov, S., Philippe, M., and Zhouravleva, G. (2004). Nonsense mutations in the essential gene *SUP35* of *Saccharomyces cerevisiae* are non-lethal. *Mol. Genet. Genomics* 272, 297–307. doi: 10.1007/s00438-004-1053-1
- Chernoff, Y. O., Newnam, G. P., Kumar, J., Allen, K., and Zink, A. D. (1999). Evidence for a protein mutator in yeast: role of the Hsp70-related chaperone ssb in formation, stability, and toxicity of the [PSI<sup>+</sup>] prion. *Mol. Cell. Biol.* 19, 8103–8112. doi: 10.1128/MCB.19.12.8103
- Cox, B., Ness, F., and Tuite, M. (2003). Analysis of the generation and segregation of propagons: entities that propagate the [PSI<sup>+</sup>] prion in yeast. *Genetics* 165, 23–33.
- Cox, B. S. (1965).  $\psi$ , a cytoplasmic suppressor of super-suppressor in yeast. *Heredity* 20, 505–521.
- DePace, A. H., Santoso, A., Hillner, P., and Weissman, J. S. (1998). A critical role for amino-terminal glutamine/asparagine repeats in the formation and propagation of a yeast prion. *Cell* 93, 1241–1252.
- Derkatch, I. L., Bradley, M. E., and Liebman, S. W. (1998). Overexpression of the *SUP45* gene encoding a Sup35p-binding protein inhibits the induction of the *de novo* appearance of the [PSI<sup>+</sup>] prion. *Proc. Natl. Acad. Sci. U.S.A.* 95, 2400–2405. doi: 10.1073/pnas.95.5.2400
- Derkatch, I. L., Bradley, M. E., Zhou, P., Chernoff, Y. O., and Liebman, S. W. (1997). Genetic and environmental factors affecting the *de novo* appearance of the [PSI<sup>+</sup>] prion in *Saccharomyces cerevisiae*. *Genetics* 147, 507–519.
- Derkatch, I. L., Bradley, M. E., Zhou, P., and Liebman, S. W. (1999). The PNM2 mutation in the prion protein domain of *SUP35* has distinct effects on different variants of the [PSI<sup>+</sup>] prion in yeast. *Curr. Genet.* 35, 59–67.
- DiSalvo, S., Derdowski, A., Pezza, J. A., and Serio, T. R. (2011). Dominant prion mutants induce curing through pathways that promote chaperone-mediated disaggregation. *Nat. Struct. Mol. Biol.* 18, 486–492. doi: 10.1038/nsmb.2031
- Doel, S. M., McCready, S. J., Nierras, C. R., and Cox, B. S. (1994). The dominant PNM2<sup>+</sup> mutation which eliminates the [PSI<sup>+</sup>] factor of *Saccharomyces cerevisiae* is the result of a missense mutation in the *SUP35* gene. *Genetics* 137, 659–670.
- Drozdzova, P. B., Tarasov, O. V., Matveenko, A. G., Radchenko, E. A., Sopova, J. V., Polev, D. E., et al. (2016). Genome sequencing and comparative analysis of *Saccharomyces cerevisiae* strains of the Peterhof genetic collection. *PLoS ONE* 11:e0154722. doi: 10.1371/journal.pone.0154722
- Eaglestone, S. S., Ruddock, L. W., Cox, B. S., Tuite, M. F., and Lindquist, S. L. (2000). Guanidine hydrochloride blocks a critical step in the propagation of the prion-like determinant [PSI<sup>+</sup>] of *Saccharomyces cerevisiae*. *Proc. Natl. Acad. Sci. U.S.A.* 97:240–244. doi: 10.1073/pnas.97.1.240
- Fisher, R. A. (1935). The logic of inductive inference. *J. R. Stat. Soc.* 98:39.
- Franzmann, T. M., Jahnel, M., Pozniakovskiy, A., Mahamid, J., Holehouse, A. S., Nüske, E., et al. (2018). Phase separation of a yeast prion protein promotes cellular fitness. *Science* 359:eaao5654. doi: 10.1126/science.aao5654
- Glover, J. R., Kowal, A. S., Schirmer, E. C., Patino, M. M., Liu, J. J., and Lindquist, S. (1997). Self-seeded fibers formed by Sup35, the protein determinant of [PSI<sup>+</sup>], a heritable prion-like factor of *S. cerevisiae*. *Cell* 89, 811–819.
- Helsen, C. W., and Glover, J. R. (2012). A new perspective on hsp104-mediated propagation and curing of the yeast prion [PSI<sup>+</sup>]. *Prion* 6, 234–239. doi: 10.4161/pri.19913
- Jorda, J., and Kajava, A. V. (2009). T-REKS: identification of tandem REpeats in sequences with a K-meanS based algorithm. *Bioinformatics* 25, 2632–2638. doi: 10.1093/bioinformatics/btp482
- Kaiser, C., Michaelis, S., and Mitchell, A. (1994). *Methods in Yeast Genetics*. New York, NY: Cold Spring Harbour laboratory press.
- Kajava, A. V., Baxa, U., Wickner, R. B., and Steven, A. C. (2004). A model for Ure2p prion filaments and other amyloids: the parallel superpleated  $\beta$ -structure. *Proc. Natl. Acad. Sci. U.S.A.* 101, 7885–7890. doi: 10.1073/pnas.0402427101
- Khan, T., Kandola, T., Wu, J., Venkatesan, S., Ketter, E., Lange, J. J., et al. (2018). Quantifying nucleation *in vivo* reveals the physical basis of prion-like phase behavior. *Mol. Cell.* 71, 155–168. doi: 10.1016/j.molcel.2018.06.016
- Kiktev, D. A., Melomed, M. M., Lu, C. D., Newnam, G. P., and Chernoff, Y. O. (2015). Feedback control of prion formation and propagation by the ribosome-associated chaperone complex. *Mol. Microbiol.* 96, 621–632. doi: 10.1111/mmi.12960
- King, C. Y. (2001). Supporting the structural basis of prion strains: induction and identification of [PSI<sup>+</sup>] variants. *J. Mol. Biol.* 307, 1247–1260. doi: 10.1006/jmbi.2001.4542
- Kryndushkin, D. S., Alexandrov, I. M., Ter-Avanesyan, M. D., and Kushnirov, V. V. (2003). Yeast [PSI<sup>+</sup>] prion aggregates are formed by small Sup35 polymers fragmented by Hsp104. *J. Biol. Chem.* 278, 49636–49643. doi: 10.1074/jbc.M307996200
- Kushnirov, V. V., Alexandrov, I. M., Mitkevich, O. V., Shkundina, I. S., and Ter-Avanesyan, M. D. (2006). Purification and analysis of prion and amyloid aggregates. *Methods* 39, 50–55. doi: 10.1016/j.ymeth.2006.04.007
- Kushnirov, V. V., Ter-Avanesyan, M. D., Telckov, M. V., Surguchov, A. P., Smirnov, V. N., and Inge-Vechtomov, S. G. (1988). Nucleotide sequence of the *SUP2* (*SUP35*) gene of *Saccharomyces cerevisiae*. *Gene* 66, 45–54.
- Langlois, C. R., Pei, F., Sindi, S. S., and Serio, T. R. (2016). Distinct prion domain sequences ensure efficient amyloid propagation by promoting chaperone binding or processing *in vivo*. *PLoS Genet.* 12:e1006417. doi: 10.1371/journal.pgen.1006417
- Lee, C. I., Yang, Q., Perrier, V., and Baskakov, I. V. (2007). The dominant-negative effect of the Q218K variant of the prion protein does not require protein X. *Protein Sci.* 16, 2166–2173. doi: 10.1110/ps.072954607
- Liebman, S. W., and Chernoff, Y. O. (2012). Prions in yeast. *Genetics* 191, 1041–1072. doi: 10.1534/genetics.111.137760
- Liu, J. J., and Lindquist, S. (1999). Oligopeptide-repeat expansions modulate 'protein-only' inheritance in yeast. *Nature* 400, 573–576.
- Liu, J. J., Sondheimer, N., and Lindquist, S. L. (2002). Changes in the middle region of Sup35 profoundly alter the nature of epigenetic inheritance for the yeast prion [PSI<sup>+</sup>]. *Proc. Natl. Acad. Sci. U.S.A.* 99(Suppl. 4), 16446–16453. doi: 10.1073/pnas.252652099
- Malcova, I., Farkasovsky, M., Senohrabkova, L., Vasicova, P., and Hasek, J. (2016). New integrative modules for multicolor-protein labeling and live-cell imaging in *Saccharomyces cerevisiae*. *FEMS Yeast Res.* 16:fow027. doi: 10.1093/femsyr/fow027
- Mann, H. B., and Whitney, D. R. (1947). On a test of whether one of two random variables is stochastically larger than the other. *Ann. Math. Statist.* 18, 50–60.
- Matveenko, A. G., Drozdova, P. B., Belousov, M. V., Moskalenko, S. E., Bondarev, S. A., Barbitoff, Y. A., et al. (2016). *SFPI*-mediated prion-dependent lethality is caused by increased Sup35 aggregation and alleviated by Sis1. *Genes Cells.* 21, 1290–1308. doi: 10.1111/gtc.12444
- Oshervovich, L. Z., Cox, B. S., Tuite, M. F., and Weissman, J. S. (2004). Dissection and design of yeast prions. *PLoS Biol.* 2, 442–451. doi: 10.1371/journal.pbio.0020086
- Pei, F., DiSalvo, S., Sindi, S. S., and Serio, T. R. (2017). A dominant-negative mutant inhibits multiple prion variants through a common mechanism. *PLoS Genet.* 13:e1007085. doi: 10.1371/journal.pgen.1007085
- Perrier, V., Kaneko, K., Safar, J., Vergara, J., Tremblay, P., DeArmond, S. J., et al. (2002). Dominant-negative inhibition of prion replication in transgenic mice. *Proc. Natl. Acad. Sci. U.S.A.* 99, 13079–13084. doi: 10.1073/pnas.182425299

- Prusiner, S. B. (2013). Biology and genetics of prions causing neurodegeneration. *Ann. Rev. Genet.* 47, 601–623. doi: 10.1146/annurev-genet-110711-155524
- R Core Team (2018). *R: A Language and Environment for Statistical Computing*. Vienna: R Foundation for Statistical Computing.
- Roche, D. B., Villain, E., and Kajava, A. V. (2017). Usage of a dataset of NMR resolved protein structures to test aggregation vs. solubility prediction algorithms. *Protein Sci.* 26, 1864–1869. doi: 10.1002/pro.3225
- Sambrook, J., and Fritsch, E., M. T. (1989). *Molecular Cloning: A Laboratory Manual, 2nd Edn.* NY: Cold Spring Harbor Laboratory Press; Cold Spring Harbour.
- Schneider, C. A., Rasband, W. S., and Eliceiri, K. W. (2012). NIH image to ImageJ: 25 years of image analysis. *Nat. Methods* 9, 671–675. doi: 10.1038/nmeth.2089
- Serio, T. R., Cashikar, A. G., Moslehi, J. J., Kowal, A. S., and Lindquist, S. L. (1999). Yeast prion [PSI<sup>+</sup>] and its determinant, Sup35p. *Method. Enzymol.* 309, 649–673.
- Shaner, N. C., Lin, M. Z., McKeown, M. R., Steinbach, P. A., Hazelwood, K. L., Davidson, M. W., and Tsien, R. Y. (2008). Improving the photostability of bright monomeric orange and red fluorescent proteins. *Nat. Methods* 5, 545–551. doi: 10.1038/nmeth.1209
- Shkundina, I. S., Kushnirov, V. V., Tuite, M. F., and Ter-Avanesyan, M. D. (2006). The role of the N-terminal oligopeptide repeats of the yeast Sup35 prion protein in propagation and transmission of prion variants. *Genetics* 172, 827–835. doi: 10.1534/genetics.105.048660
- Sikorski, R. S., and Hieter, P. (1989). A system of shuttle vectors and yeast host strains designed for efficient manipulation of DNA in *Saccharomyces cerevisiae*. *Genetics* 122, 19–27.
- Sokolov, P. A., Bondarev, S. A., Belousov, M. V., Zhouravleva, G. A., and Kasyanenko, N. A. (2018). Sup35Nmp morphology evaluation on Au, Si, formvar and mica surfaces using AFM, SEM and TEM. *J. Struct. Biol.* 201, 5–14. doi: 10.1016/j.jsb.2017.10.006
- Stansfield, I., Jones, K. M., Kushnirov, V. V., Dagkesamanskaya, A. R., Poznyakovski, A., Paushkin, S. V., et al. (1995). The products of the SUP45 (eRF1) and SUP35 genes interact to mediate translation termination in a *Saccharomyces cerevisiae*. *EMBO J.* 14, 4365–4373.
- Studier, F. W., and Moffatt, B. A. (1986). Use of bacteriophage T7 RNA polymerase to direct selective high-level expression of cloned genes. *J. Mol. Biol.* 189, 113–130.
- Tanaka, M., and Weissman, J. S. (2006). An efficient protein transformation protocol for introducing prions into yeast. *Method. Enzymol.* 412, 185–200. doi: 10.1016/S0076-6879(06)12012-1
- Ter-Avanesyan, M. D., Dagkesamanskaya, A. R., Kushnirov, V. V., and Smirnov, V. N. (1994). The SUP35 omnipotent suppressor gene is involved in the maintenance of the non-mendelian determinant [PSI<sup>+</sup>] in the yeast *Saccharomyces cerevisiae*. *Genetics* 137, 671–676.
- Ter-Avanesyan, M. D., Kushnirov, V. V., Dagkesamanskaya, A. R., Didichenko, S. A., Chernoff, Y. O., Inge-Vechtomov, S. G., et al. (1993). Deletion analysis of the SUP35 gene of the yeast *Saccharomyces cerevisiae* reveals two non-overlapping functional regions in the encoded protein. *Mol. Microbiol.* 7, 683–692.
- Tuite, M. F., Mundy, C. R., and Cox, B. S. (1981). Agents that cause a high frequency of genetic change from [PSI<sup>+</sup>] to [psi<sup>-</sup>] in *Saccharomyces cerevisiae*. *Genetics* 98, 691–711.
- Tyedmers, J. (2012). Patterns of [PSI<sup>+</sup>] aggregation allow insights into cellular organization of yeast prion aggregates. *Prion* 6, 191–200. doi: 10.4161/pri.18986
- Verges, K. J., Smith, M. H., Toyama, B. H., and Weissman, J. S. (2011). Strain conformation, primary structure and the propagation of the yeast prion [PSI<sup>+</sup>]. *Nat. Struct. Mol. Biol.* 18, 493–499. doi: 10.1038/nsmb.2030
- Vishveshwara, N., Bradley, M. E., and Liebman, S. W. (2009). Sequestration of essential proteins causes prion associated toxicity in yeast. *Mol. Microbiol.* 73, 1101–1114. doi: 10.1111/j.1365-2958.2009.06836.x
- Volkov, K. V., Aksenova, A. Y., Soom, M. J., Osipov, K. V., Svitin, A. V., Kurischko, C., et al. (2002). Novel non-mendelian determinant involved in the control of translation accuracy in *Saccharomyces cerevisiae*. *Genetics* 160, 25–36.
- Wickner, R. (1994). [URE3] as an altered URE2 protein: evidence for a prion analog in *Saccharomyces cerevisiae*. *Science* 264, 566–569.
- Wickner, R. B., Masison, D. C., and Edsles, H. K. (1995). [PSI<sup>+</sup>] and [URE3] as yeast prions. *Yeast* 11, 1671–1685.
- Zhang, T., Lei, J., Yang, H., Xu, K., Wang, R., and Zhang, Z. (2011). An improved method for whole protein extraction from yeast *Saccharomyces cerevisiae*. *Yeast* 28, 795–798. doi: 10.1002/yea.1905
- Zhouravleva, G., Frolova, L., Le Goff, X., Le Guellec, R., Inge-Vechtomov, S., Kisselev, L., et al. (1995). Termination of translation in eukaryotes is governed by two interacting polypeptide chain release factors, eRF1 and eRF3. *EMBO J.* 14, 4065–4072.
- Zulianello, L., Kaneko, K., Scott, M., Erpel, S., Han, D., Cohen, F. E., et al. (2000). Dominant-negative inhibition of prion formation diminished by deletion mutagenesis of the prion protein. *J. Virol.* 74, 4351–4360. doi: 10.1128/JVI.74.9.4351-4360.2000

**Conflict of Interest:** The authors declare that the research was conducted in the absence of any commercial or financial relationships that could be construed as a potential conflict of interest.

Copyright © 2019 Danilov, Matveenko, Ryzhkova, Belousov, Poleshchuk, Likholetova, Sokolov, Kasyanenko, Kajava, Zhouravleva and Bondarev. This is an open-access article distributed under the terms of the Creative Commons Attribution License (CC BY). The use, distribution or reproduction in other forums is permitted, provided the original author(s) and the copyright owner(s) are credited and that the original publication in this journal is cited, in accordance with accepted academic practice. No use, distribution or reproduction is permitted which does not comply with these terms.



# Targeting Alpha-Synuclein as a Therapy for Parkinson's Disease

Carroll Rutherford Fields<sup>1</sup>, Nora Bengoa-Vergniory<sup>2\*</sup> and Richard Wade-Martins<sup>2\*</sup>

<sup>1</sup>Department of Neuroscience at Johns Hopkins University, Baltimore, MD, United States, <sup>2</sup>Department of Physiology, Oxford Parkinson's Disease Center, Anatomy and Genetics, Oxford, United Kingdom

## OPEN ACCESS

### Edited by:

Maria Rosário Almeida,  
University of Porto, Portugal

### Reviewed by:

Hong Qing,  
Beijing Institute of Technology, China  
Charles Robert Harrington,  
University of Aberdeen,  
United Kingdom  
Philipp Janker Kahle,  
Hertie Institute for Clinical Brain  
Research (HIH), Germany

### \*Correspondence:

Nora Bengoa-Vergniory  
nora.bengoa-  
vergniory@dpag.ox.ac.uk  
Richard Wade-Martins  
richard.wade-martins@dpag.ox.ac.uk

**Received:** 05 September 2019

**Accepted:** 22 November 2019

**Published:** 05 December 2019

### Citation:

Fields CR, Bengoa-Vergniory N and  
Wade-Martins R (2019) Targeting  
Alpha-Synuclein as a Therapy for  
Parkinson's Disease.  
*Front. Mol. Neurosci.* 12:299.  
doi: 10.3389/fnmol.2019.00299

Parkinson's disease (PD) is one of the most common neurodegenerative disorders with a global burden of approximately 6.1 million patients. Alpha-synuclein has been linked to both the sporadic and familial forms of the disease. Moreover, alpha-synuclein is present in Lewy-bodies, the neuropathological hallmark of PD, and the protein and its aggregation have been widely linked to neurotoxic pathways that ultimately lead to neurodegeneration. Such pathways include autophagy/lysosomal dysregulation, synaptic dysfunction, mitochondrial disruption, and endoplasmic reticulum (ER) and oxidative stress. Alpha-synuclein has not only been shown to alter cellular pathways but also to spread between cells, causing aggregation in host cells. Therapeutic approaches will need to address several, if not all, of these angles of alpha-synuclein toxicity. Here we review the current advances in therapeutic efforts for PD that aim to produce a disease-modifying therapy by targeting the spread, production, aggregation, and degradation of alpha-synuclein. These include: receptor blocking strategies whereby putative alpha-synuclein receptors could be blocked inhibiting alpha-synuclein spread, an alpha-synuclein reduction which will decrease the amount alpha-synuclein available for aggregation and pathway disruption, the use of small molecules in order to target alpha-synuclein aggregation, immunotherapy and the increase of alpha-synuclein degradation by increasing autophagy/lysosomal flux. The research discussed here may lead to a disease-modifying therapy that tackles disease onset and progression in the future.

**Keywords:** alpha-synuclein, Parkinson's disease, aggregation, therapy, oligomers, fibrils

## INTRODUCTION

Parkinson's disease (PD) is the second most common neurodegenerative disorder, after Alzheimer's Disease, and the most common movement disorder (Mhyre et al., 2012). PD has a prevalence of approximately 0.5–1% among individuals 65–69 years of age, rising to 1–3% among persons 80 years of age and older (Nussbaum and Ellis, 2003). PD is characterized by motor symptoms including tremor, rigidity, bradykinesia, postural instability, gait and balance impairment and non-motor symptoms such as cognitive decline, autonomic impairment, rapid eye movement behavioral sleep disorder, constipation, and other behavioral disturbances (Stacy, 2011; Obeso et al., 2017). Additionally, its hallmark feature is the accumulation of alpha-synuclein ( $\alpha$ -syn) that results in the formation of proteinaceous cytoplasmic inclusions, known as Lewy-bodies and Lewy neurites



(LBs/LNs; Jakes et al., 1994). Current therapeutic approaches are directed at controlling symptoms and delaying the progression of the disease for as long as possible (Poewe, 2009). Therefore, the development of disease-modifying therapeutics is extremely attractive in experimental and clinical research in PD.

Multiple lines of evidence support the critical importance of  $\alpha$ -syn in PD pathogenesis. The intraneuronal proteinaceous cytoplasmic inclusions now known as LBs, the hallmark of PD, were first described by Lewy in 1912 (Lewy, 1912; Goedert et al., 2013). Several decades later, in 1996, the first link between  $\alpha$ -syn and the PD phenotype was established with the identification of the A53T point mutation on chromosome 4q21-23 (Polymeropoulos et al., 1996). The gene encoding  $\alpha$ -syn (SNCA) was identified the following year (Polymeropoulos et al., 1997). Subsequently,  $\alpha$ -syn was identified as a major component of LBs and LNs (Spillantini et al., 1997). While we have since achieved a greater understanding of PD pathogenesis, the exact mechanisms elucidating the nature of progressive dopaminergic cell loss in the substantia nigra (SN) pars compacta remain to be determined. In this review article, we examine advances in our current understanding of the pivotal role of  $\alpha$ -syn in PD pathogenesis, including pathways implicated in  $\alpha$ -syn toxicity, suggested seeding and propagation mechanisms that underlie cell-to-cell transmission between neighboring neurons, and viability of potential disease-modifying therapeutics targeted against pathological  $\alpha$ -syn species.

## $\alpha$ -Syn

Although the full extent of the physiological function for  $\alpha$ -syn is yet to be revealed and there may be conflicting findings in need of resolution,  $\alpha$ -syn is involved in synaptic activity through regulation of vesicle docking, fusion, and neurotransmitter release (Ghiglieri et al., 2018).  $\alpha$ -syn is an abundant 14 kDa protein consisting of 140 amino acids and comprised of three domains: (1) an N-terminal lipid-binding  $\alpha$ -helix; (2) a non-amyloid-component (NAC); and (3) an acidic C-terminal tail (Lashuel et al., 2013). The N-terminal domain of  $\alpha$ -syn is characterized by a series of seven 11-residue imperfect repeats, each based upon a highly conserved KTKEGV hexameric motif that is also observed in the  $\alpha$ -helical domain of apolipoproteins (Davidson et al., 1998; Bussell and Eliezer, 2003; Bussell et al., 2005). This similar architecture allows  $\alpha$ -syn to mediate lipid interactions in a similar way to how apolipoproteins do, inserting its amphipathic helices into lipid membranes to influence their curvature (Davidson et al., 1998). The central region (residues 61–95), also known as the NAC domain, can form cross  $\beta$ -sheets and consists of a highly hydrophobic sequence underlying its high propensity for aggregation and leading to protofibril and fibril formation (Uéda et al., 1993; Giasson et al., 2001; Tuttle et al., 2016). The predominantly unstructured conformation of  $\alpha$ -syn makes it a target for various post-translational modifications such as phosphorylation. Indeed phosphorylation of Serine 129 in the C-terminal domain of  $\alpha$ -syn has been associated with an increased propensity of aggregate formation (Samuel et al., 2016). A number of studies have reported aberrant accumulation of phosphorylated  $\alpha$ -syn at the Serine-129 residue (pS129) in the brains of PD patients, as well as in animal models

of synucleinopathies (Tenreiro et al., 2014; Oueslati, 2016). While only a small fraction of  $\alpha$ -syn (~4%) is phosphorylated in healthy brains, substantial accumulation of pS129 (~90%) is observed in brains with Lewy pathology, implicating a potentially important association between this posttranslational modification and the accumulation of  $\alpha$ -syn aggregates concomitant with LB formation and neurodegeneration (Fujiwara et al., 2002; Hasegawa et al., 2002). Further insight on the significance of S129 phosphorylation on  $\alpha$ -syn aggregation, LB formation, and neurotoxicity may provide insight into the nature of PD pathogenesis and PD and related disorders. While numerous lines of evidence indicate that monomeric  $\alpha$ -syn is not toxic, several studies highlight  $\alpha$ -syn oligomers and fibrils as the species responsible for  $\alpha$ -syn toxicity (Neumann et al., 2004; Outeiro et al., 2008; Peelaerts et al., 2015), and it has been shown that overexpression or triplication of synuclein is sufficient for  $\alpha$ -syn aggregation to take place (Outeiro et al., 2008; Zambon et al., 2019).

There are conflicting findings on the nature of the native state of  $\alpha$ -syn. Although the majority of studies suggest that cytosolic  $\alpha$ -syn is present within cells as an intrinsically unfolded monomer, alternative hypotheses have proposed that it exists as a tetrameric  $\alpha$ -helical oligomer that is resistant to fibrillization and thus distinct from pathological variants (Bartels et al., 2011; Wang et al., 2011; Fauvet et al., 2012; Burré et al., 2013; Smaldone et al., 2015).  $\alpha$ -Syn can adopt an  $\alpha$ -helical conformation in association with biological membranes or remain in an intrinsically unfolded state in the cytosol, suggesting it has different functions in different subcellular locations depending on its dynamic structure (Eliezer et al., 2001; Ramakrishnan et al., 2006; Ullman et al., 2011). Indeed, a recent investigation lends further support to this notion using chemical crosslinking and FRET experiments to demonstrate that  $\alpha$ -syn multimerizes into a tetrameric complex upon binding cellular membranes and that it is this tetrameric membrane-bound  $\alpha$ -syn that mediates SNAP receptor (SNARE) complex assembly and that functions as a molecular chaperone for these complexes at the presynaptic membrane (Burré et al., 2014). These findings should be interpreted with caution as evidence for tetrameric  $\alpha$ -syn stems from crosslinked samples.

## PATHWAYS IMPLICATED IN TOXICITY OF $\alpha$ -SYN

Disruption of several cellular pathways leads to the loss of dopaminergic neurons in PD, including synaptic vesicle recycling, mitochondrial function, oxidative stress, endoplasmic reticulum (ER) stress, and autophagy-lysosomal pathway (ALP) function (Figure 1). The accumulation of  $\alpha$ -syn into prefibrillar forms, and then its assembly into higher molecular weight aggregates, induces cellular toxicity and maybe the greatest contributor to pathogenesis in PD (Bengoa-Vergniory et al., 2017). The increased cellular toxic burden caused by aggregated  $\alpha$ -syn may arise from overexpression of the protein, genetic multiplication, or impairment to normal protein clearance mechanisms such as autophagy (Alegre-Abarrategui et al., 2019).

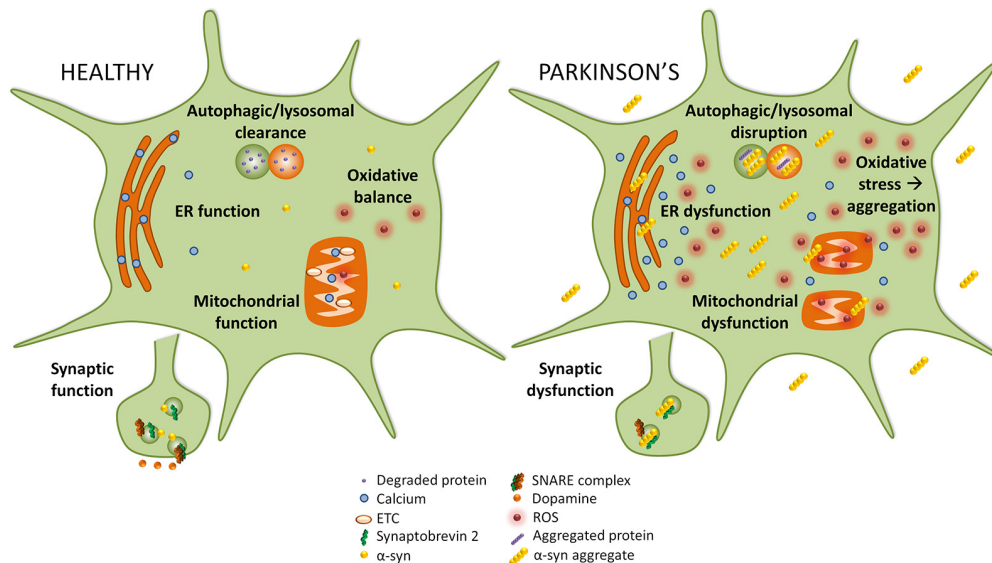


**FIGURE 1 |** Implicated pathways for  $\alpha$ -syn toxicity. To the left, healthy cellular pathways are illustrated, while to the right examples of how these pathways are perturbed in Parkinson's disease (PD) are shown. Under normal circumstances, autophagic and lysosomal clearance degrades protein and other debris in the cell. In PD these pathways are blocked causing an accumulation of aggregated protein that could itself lead to more aggregation. In healthy cells, endoplasmic reticulum (ER) function is preserved, but in PD ER stress leads to calcium efflux into the cytoplasm. While in healthy cells mitochondrial function and oxidative balance are maintained, in PD the electron transport chain (ETC) and mitochondria function are compromised which causes an increase in reactive oxygen species (ROS) that leads to oxidative stress. Finally, in PD  $\alpha$ -syn may interact with synaptobrevin-2, leading to synaptic dysfunction.

## Synaptic Vesicle Impairment

$\alpha$ -syn is typically localized to the presynaptic terminal where it associates with synaptic vesicles and influences membrane curvature (Maroteaux et al., 1988; Wong and Krainc, 2017). There it is known to promote synaptic vesicle fusion and other processes in synaptic-vesicle trafficking through its interactions with the synaptobrevin-2 component of the SNARE (soluble N-ethylmaleimide-sensitive factor attachment protein receptors) complex. Large  $\alpha$ -syn oligomers preferentially bind synaptobrevin-2 and may disrupt SNARE complex assembly, synaptic-vesicle motility, and dopamine release (Burré et al., 2010; Choi et al., 2013). Additionally, loss of  $\alpha$ -syn has been associated with an increase in dopaminergic release (Senior et al., 2008; Anwar et al., 2011), and so the aggregation of  $\alpha$ -syn could also lead to loss of function effects at the synapse.

## Mitochondrial Dysfunction

Dopaminergic neurons are uniquely susceptible to mitochondrial dysfunction due to their high energy demands and increased exposure to oxidative stress (Valente et al., 2004; Ricciardi et al., 2014). The selective vulnerability of these neurons was first recognized following the finding that the mitochondrial neurotoxin 1-methyl-4-phenyl-1,2,3,6-tetrahydropyridine (MPTP) resulted in the cell death of SN DA neurons in humans (Langston et al., 1983). Moreover, MPTP was shown to be toxic to DA neurons in mouse and non-human primate models of PD (Przedborski et al., 2001).  $\alpha$ -Syn oligomers can also inhibit the import of proteins, including some subunits of complex I, into the mitochondria by binding to the translocase of the

outer membrane (TOM20) and inhibiting its interaction with the co-receptor TOM22 (Di Maio et al., 2016). Overexpression of the  $\alpha$ -syn mutants A53T or A30P has been shown to increase the aggregation of  $\alpha$ -syn in human neuroblastoma cells (Parihar et al., 2009). In these cells, immunogold electron transmission microscopy revealed the localization of  $\alpha$ -syn aggregates within the mitochondria of overexpressing cells, which exhibited decreased mitochondrial transmembrane potential and limited cellular respiration concomitant with increased production of reactive oxygen species (ROS). The proximity between the mitochondrial electron transport chain (ETC) and mitochondria DNA (mtDNA) increases the vulnerability of mutations in mtDNA due to ROS, especially during mitochondrial dysfunction, such as in complex I inhibition (Davis et al., 1979). Indeed, mutations in mtDNA or impairment to the ETC cause mitochondrial dysfunction and energy depletion. Damaged mitochondria result in electron leakage, produce increased ROS, and release cytochrome C leading to activation of caspase-3, caspase-9, and other pro-apoptotic factors ultimately leading to cell death (Brustovetsky et al., 2002). Additionally,  $\alpha$ -syn can interfere with mitochondrial membrane fusion and fission, resulting in fragmentation of mitochondria, and it can inhibit mitophagy and complex I activity, and disrupt mitochondrial membrane potential (Cole et al., 2008; Devi et al., 2008; Chen and Chan, 2009). While this review concentrates on PD it is worth noting that oligodendrocytes, which are heavily loaded with pathological glial cytoplasmic inclusions in multiple system atrophy (MSA) patients, are also cells with high endogenous  $\alpha$ -syn and a high metabolic profile. It is interesting to consider

the parallels between these two synucleinopathies and cellular selective vulnerability (Alegre-Abarrategui et al., 2019).

## Oxidative Stress

Failure of the antioxidant proteins regulating ROS levels, like superoxide dismutase (SOD) and glutathione (GSH), results in oxidative stress, which may have deleterious effects inside cells (Indo et al., 2015). Interestingly, the SN appeared to contain twice as much oxidized proteins as compared with the caudate, putamen, and frontal cortex in the post-mortem brains of healthy individuals, suggesting that the increased susceptibility of SN to oxidative stress may contribute to the selective degeneration of nigral DA neurons (Floor and Wetzel, 2002). Unregulated oxidation of intracellular macromolecules and organelles can cause cellular damage and may lead to cell death (Wiseman and Halliwell, 1996; Rego and Oliveira, 2003). As one of the major producers of ROS, mitochondria are particularly vulnerable to oxidative stress-induced cytotoxicity, especially considering mtDNA is not protected by histone proteins as seen in nuclear DNA (Richter et al., 1988). As mentioned above,  $\alpha$ -syn can interfere with translocation of mitochondrial-target proteins, thereby disrupting the proper functioning of the ETC, and leading to elevated levels of intracellular oxidative stress (Di Maio et al., 2016). Interestingly, while  $\alpha$ -syn toxicity is implicated in increasing cellular oxidative stress, it has also been suggested that oxidative stress can induce  $\alpha$ -syn toxicity. Excessive exposure to oxidative stress causes lipid peroxidation of polyunsaturated fatty acids, which in turn leads to the formation of 4-hydroxy-2-nonenal, a product that has been shown to hamper fibrillization of  $\alpha$ -syn and promote the formation of secondary beta sheets and toxic soluble oligomers in a dose-dependent manner (Dexter et al., 1989; Qin et al., 2007; Bae et al., 2013). Incubation of  $\alpha$ -syn with cytochrome c/H<sub>2</sub>O<sub>2</sub> leads to the oxidative stress-induced aggregation of  $\alpha$ -syn by crosslinking  $\alpha$ -syn tyrosine residues through dityrosine bonding (Hashimoto et al., 1999; Ruf et al., 2008). Moreover, colocalization of cytochrome c and  $\alpha$ -syn was reported in the LB of patients with PD (Hashimoto et al., 1999).

## Endoplasmic Reticulum (ER) Stress

The ER is essential for the synthesis, modification, and delivery of proteins to their target sites within the secretory pathway (i.e., Golgi). Overexpressed or mutant  $\alpha$ -syn accumulates within the ER, interfering with protein folding and inducing ER stress, which may contribute to neurodegeneration (Colla et al., 2012). Smith et al. reported that increased ROS levels stemming from ER stress and mitochondrial dysfunction contribute to A53T  $\alpha$ -syn-induced cell death (Smith et al., 2005). Moreover, aggregated  $\alpha$ -syn impairs both the ubiquitin-proteasome system and autophagy, resulting in ER stress and the activation of the unfolded protein response (UPR; Bence et al., 2001; Xu et al., 2005; Kim et al., 2008). Accumulation of  $\alpha$ -syn in the ER results in calcium leakage into the cytosol, which then acts on  $\alpha$ -syn in a feedback-like manner potentiating further aggregation (Volles and Lansbury, 2002; Kaye et al., 2004; Sokolov et al., 2006; Nath et al., 2011). Mitochondria also function in regulating calcium homeostasis. Increased mitochondrial uptake of cytosolic calcium released by the ER generates excessive ROS

(Nunnari and Suomalainen, 2012; Görlach et al., 2015; Paupe and Prudent, 2018). Additionally, the protein folding capacity of the ER operates in an ATP-dependent manner, thus sustained UPR activation promotes increased ROS production.

## Autophagy-Lysosomal Pathway (ALP) Dysfunction

$\alpha$ -Syn overexpression also disrupts autophagy, a cellular process involved in the degradation of damaged organelles, invading microorganisms and aggregated proteins (Wong and Holzbaur, 2015). Impairment of autophagic processes is reported to result in the accumulation of  $\alpha$ -syn and propagation in a prion-like fashion, further potentiating the cellular toxicity of  $\alpha$ -syn pathology. In addition, A53T and A30P  $\alpha$ -syn exhibit a stronger binding affinity for the lysosomal receptor LAMP2A compared with wild-type (WT)  $\alpha$ -syn, so these mutant forms of  $\alpha$ -syn are not efficiently degraded by protein clearance mechanisms, which results in increased  $\alpha$ -syn burden of chaperone-mediated autophagy and inhibits the loading and clearance of other cargo (Cuervo et al., 2004). Moreover,  $\alpha$ -syn overexpression in iPSCs compared with controls reduced the enzymatic activity of multiple lysosomal enzymes, including GCase, which is essential for the proper functioning of the autophagolysosome (Mazzulli et al., 2011, 2016). Mutations in the leucine-rich repeat kinase 2 (LRRK2) protein may also disrupt autophagy and lysosomal function and are the most common cause of familial and sporadic PD. Elevated mutant LRRK2 kinase activity is associated with cytotoxicity (West, 2017). Jeong et al. (2018) demonstrated that dysregulation of downstream Rab substrates of LRRK2 resulted in neurodegeneration of dopaminergic neurons in the mammalian brain. Their findings suggest further study of the Rab GTPases may not only elucidate the processes governing these intercellular membrane dynamics, but also reveal molecules or pathways that can serve as potential targets for therapeutic intervention. Indeed, a recent study showed that the accumulation of phospho- $\alpha$ -syn in a rat rotenone model correlated with ALP dysfunction and that LRRK2 inhibitors could prevent these effects (Di Maio et al., 2018).

## CELL-TO-CELL TRANSMISSION OF $\alpha$ -SYN

$\alpha$ -Syn is proposed to propagate from the peripheral (i.e., enteric) nervous system (PNS) to the central nervous system (CNS) as well as spread *via* a cell-to-cell transmission (Volpicelli-Daley and Brundin, 2018). In 2003, a seminal study published by Braak et al. (2003) introduced a six-stage system for PD based on the observed caudo-rostral pattern of progression of  $\alpha$ -syn pathology, with stage 1 originating in the lower brainstem and stage 6 extending to involve the cortex. According to this theoretical caudo-rostral pattern of progression, the olfactory system, caudal brainstem, and autonomic nervous system were among the earliest areas affected by  $\alpha$ -syn pathology (Braak and Braak stages 1 and 2). This was followed by a significant loss of dopaminergic neurons in the SN (Braak and Braak stages 3 and 4), and subsequent extensive cortical involvement (Braak and Braak stages 5 and 6). Consistent with this hypothesis were the findings that patients who have undergone vagotomy



(Svensson et al., 2015) or appendectomy (Killinger et al., 2018) have reduced risk of developing PD. However, not all cases of sporadic PD exhibit  $\alpha$ -syn pathology as predicted based on the suggested anatomical hierarchy of the caudo-rostral progression pattern of pathology (Burke et al., 2008; Alafuzoff et al., 2009). Additionally, Braak and Braak's staging system does not adequately explain the absence of clinical symptoms in individuals with observable widespread  $\alpha$ -syn pathology at autopsy (Parkkinen et al., 2005; Alafuzoff et al., 2009). A retrospective autopsy series in 30–55% of elderly subjects with widespread Lewy-related pathology (Braak and Braak stages 5 and 6) reported no definite neuropsychiatric symptoms, suggesting considerable cerebral compensatory mechanisms (Jellinger, 2008). Nevertheless, Braak and Braak's model has successfully demonstrated that the  $\alpha$ -syn pathology present in PD is not only restricted to the SN but extends to involve several other brain regions and both the PNS and CNS. Although the precise mechanisms underlying disease progression are yet to be established, pathology could originate in the gut and proceed retrogradely to the brain *via* the vagal nerve or could start in the vagal nerve and extend to the gut *via* anterograde movement (Braak and Del Tredici, 2016; Kim et al., 2019).

Further evidence supporting the hypothesis that  $\alpha$ -syn may self-propagate and spread progressively between interconnected brain regions through a cell-to-cell transmission mechanism came from the pathological analysis of grafted nigral neurons. In 2008, two independent postmortem studies reported that healthy embryonic mesencephalic neurons grafted into the striatum of PD patients developed  $\alpha$ -syn pathology or LB-like structures many years after brain surgery (Kordower et al., 2008; Li et al., 2008). These findings suggested host-to-graft propagation of  $\alpha$ -syn pathology and gave rise to the idea of a “prion-like” transmission mechanism to describe the pathogenic potential of disease progression. In this model, neuron-released aggregated  $\alpha$ -syn in the extracellular space may be internalized by neighboring neurons, where it may act as a seed to induce further misfolding and aggregation of endogenous  $\alpha$ -syn proteins. Repeated subsequent cycles of  $\alpha$ -syn aggregate formation and release are thought to correspond with further disease progression (Brettschneider et al., 2015).

Multiple pre-clinical studies both *in vitro* and *in vivo* have demonstrated strong evidence supporting prion-like propagation and transmission of  $\alpha$ -syn (Spillantini et al., 1998; Prusiner et al., 2015). Desplats et al. (2009) were one of the first studies to demonstrate a cell-to-cell transmission mechanism of  $\alpha$ -syn *in vivo*. The study reported human  $\alpha$ -syn transfer in 15% of the fluorescently labeled mouse neural stem cells transplanted into the hippocampus of  $\alpha$ -syn transgenic mice. In a recent study, injection of nigral LB-enriched fractions containing pathological  $\alpha$ -syn was purified from postmortem PD brains and inoculated into the SN or striatum of WT mice and rhesus macaque monkeys. In both mice and monkeys, intranigral or intrastriatal inoculation of PD-derived LB extracts resulted in progressive nigrostriatal neurodegeneration starting at striatal dopaminergic terminals. At the onset of LB-induced degeneration, host pathological  $\alpha$ -syn diffusely accumulated within nigral neurons and anatomically linked brain regions (Recasens et al., 2014).

Subsequent *in vivo* studies using an injection of recombinant  $\alpha$ -syn aggregates further support the hypothesis of cell-to-cell transmissibility of pathogenic  $\alpha$ -syn. Through injection of  $\alpha$ -syn preformed fibrils (PFFs) into the striatum of transgenic mice, researchers demonstrated the development of Lewy pathology, nigrostriatal degeneration, and importantly expanded our understanding of cell-to-cell transmission by describing the nature of spread in neuroanatomically connected regions: this provided the first evidence that synthetic  $\alpha$ -syn PFFs alone can induce the initiation and propagation of  $\alpha$ -syn pathology *in vivo* (Luk et al., 2012). Furthermore, intracerebral injections of recombinant human or mouse fibrils directly into the SN of C57BL/6J mice or into asymptomatic transgenic mice induced a time-dependent development of extensive  $\alpha$ -syn pathology (Masuda-Suzukake et al., 2013). Similar observations are reported in rats after nigral inoculation with four different structural types of  $\alpha$ -syn assemblies: two distinct strains denoted “fibrils” and “ribbons,”  $\alpha$ -syn oligomers, and brain homogenates from transgenic mice expressing mutant human  $\alpha$ -syn (A30P; Peelaerts et al., 2015). Interestingly, these findings suggest there might be distinct properties to the different strains of  $\alpha$ -syn aggregates associated with PD pathology, including seeding propensity, rate of aggregation, and potential to trigger an inflammatory response.

The evidence of cell-to-cell transmission of pathologic  $\alpha$ -syn in interconnected brain regions suggests a prion-like mechanism of spread. However, a recent study demonstrated that the spread of  $\alpha$ -syn pathology does not always proceed as expected along the connectome, either anterogradely or retrogradely, through a template-recruitment process reminiscent of that observed in prion diseases (Sorrentino et al., 2017). Furthermore, although injected fibrillar human  $\alpha$ -syn induced extensive  $\alpha$ -syn pathology and protein inclusions in A53T transgenic mice, in E46K transgenic mice  $\alpha$ -syn pathology was predominantly localized to the site of injection with no evidence for spread (Sacino et al., 2014). Importantly, it is worth noting that the Mendez et al.'s (2008) study reported no evidence of LB pathology in the surviving grafts 14 years after graft transplantation. Although there is significant evidence supporting the concept of cell-to-cell propagation of  $\alpha$ -syn pathology, there are some discrepancies that need to be taken into consideration, such as differences in the experimental paradigm, starting material for the injection, the injection/graft environment, observational period post-injection, animal models used, and individual differences between PD patients.

## THERAPEUTIC APPROACHES TARGETING $\alpha$ -SYN FOR PD TREATMENT

There is currently no disease-modifying therapies for PD, but medication or surgery can provide palliative treatment directed at controlling symptoms that may substantially improve motor impairments. A systematic division of different strategies to target  $\alpha$ -syn thus separates stabilizing the physiological conformation of  $\alpha$ -syn, decreasing its expression, inhibiting its aggregation, and increasing intracellular clearance, from transmission-directed approaches including inhibiting uptake



by neighboring cells and enhancing extracellular clearance mechanisms (**Figure 2**; Kaufman and Diamond, 2013; Hasegawa et al., 2017).

## Interference With the Prion-Like Spread of $\alpha$ -Syn

Ongoing research seeks to identify disease-modifying agents for PD that will restrict templated conformation changes and transcellular propagation of pathological  $\alpha$ -syn. However, as endogenous  $\alpha$ -syn is necessary in order for  $\alpha$ -syn to spread (Braak et al., 2003; Kordower et al., 2008; Li et al., 2008), it is difficult to only specifically target the spread of  $\alpha$ -syn, and so multiple approaches rely on targeting  $\alpha$ -syn that is associated with its spread, while also partially targeting endogenous  $\alpha$ -syn. An efficient method to regulate transmission would be blocked  $\alpha$ -syn receptors; blocking the LAG3 cell-surface protein, an immune receptor involved in the endocytosis of extracellular aggregated  $\alpha$ -syn (Mao et al., 2016) would be an interesting therapeutic avenue. LAG3-directed antibodies significantly reduce misfolded  $\alpha$ -syn-induced toxicity and transmission (Anderson et al., 2016; Mao et al., 2016). However, LAG3 expression was not associated with modified disease progression in a different study (Liu et al., 2018). One influential study proposed that heparan sulfate proteoglycans on the surfaces of cells can mediate the uptake of amyloid fibrils, including those composed of  $\alpha$ -syn, through endocytosis (Holmes et al., 2013). Thus, limiting the endocytosis of extracellular  $\alpha$ -syn may hamper its pathogenic seeding potential and delay the progression of Lewy pathology. Although it remains unclear how  $\alpha$ -syn escapes the endosome, it has been suggested that compromised endo-lysosomal membrane integrity increases cell susceptibility to  $\alpha$ -syn aggregation after internalization of seeds *via* endocytosis (Jiang et al., 2017). Cell cultures treated with heparin and chloral hydrate, which both disrupt heparan sulfate proteoglycans, suffered a reduction of endocytic uptake of  $\alpha$ -syn (Holmes et al., 2013). Further experiments should be conducted in animal models to identify specific inhibitors of heparan sulfate proteoglycans that can slow the pathology propagation cycle without interfering with essential cellular processes.

A careful study of these and other potential  $\alpha$ -syn receptors is warranted in order to advance  $\alpha$ -syn receptor-blocking therapies.

## Reducing $\alpha$ -Syn Production

Since  $\alpha$ -syn gene duplications and triplications lead to PD, a potential therapeutic approach is to reduce  $\alpha$ -syn production. This reduction of total protein amounts can be achieved with RNA interference (RNAi), using gene-silencing mechanisms to target  $\alpha$ -syn mRNA levels. Indeed, silencing  $\alpha$ -syn has led to neuroprotection *in vitro* upon 1-methyl-4-phenylpyridinium (MPP+) insult (Fountaine and Wade-Martins, 2007). Also, shRNA delivered *via* a lentiviral vector silenced human  $\alpha$ -syn expression in rat striatum, and siRNA directed against  $\alpha$ -syn reduced the expression of endogenous  $\alpha$ -syn after 2 weeks of infusion into the mouse hippocampus (Sapru et al., 2006; Lewis et al., 2008). The success of these studies prompted testing of chronic siRNA infusions directed against  $\alpha$ -syn in squirrel

monkeys (McCormack et al., 2010). Following a unilateral infusion,  $\alpha$ -syn levels were reduced by 40–50% relative to the untreated side. Additionally, experiments in rodent models demonstrated that antisense oligonucleotides (ASOs) safely reduced levels of  $\alpha$ -syn protein expressions and did not affect the normal nigral dopaminergic neuronal function or cause neurodegeneration (Alarcón-Aris et al., 2018). However, a major challenge is that the precise physiological role of  $\alpha$ -syn has not yet been characterized, and thus a therapy aimed at a reduction of its expression could have a significant impact. Indeed, Manfredsson and colleagues reported that the marked reduction (>90%) of  $\alpha$ -syn achieved using viral vectors in rat and non-human primate SN corresponded to nigrostriatal system degeneration (Gorbatyuk et al., 2010; Kanaan and Manfredsson, 2012; Collier et al., 2016). It is essential to determine the degree of reduction necessary to effectively prevent  $\alpha$ -syn accumulation in preclinical trials before this approach is considered viable for further investigation in PD patients. Additionally, careful consideration must be taken regarding the method of delivery, as systemic administration of RNAi or ASOs could potentially act on  $\alpha$ -syn expressed in peripheral tissues. Hence, it is essential to perform further experiments in preclinical trials, especially in non-human primates, to clearly determine preliminary efficacy, tolerability and safety profile of this therapeutic approach, before preparations can be made to move into the clinical stage.

In addition to targeting  $\alpha$ -syn mRNA translation processes, an alternative approach to reduce  $\alpha$ -syn protein expression seeks to interfere with the transcription of the  $\alpha$ -syn gene. A recent study found that  $\beta$ 2-adrenoreceptor (B2AR) agonists (e.g., clenbuterol and salbutamol) could reduce  $\alpha$ -syn gene expression by modulating transcription through altering histone deacetylase (HDAC) activity at the  $\alpha$ -syn gene promoter and enhancer regions, and found that these modifications were neuroprotective in cell line and rodent models (Mittal et al., 2017). Consistent with these findings, a Norwegian epidemiological study reported that treatment with the B2AR salbutamol against asthma corresponded with a reduced lifetime risk of developing PD, whereas the B2AR antagonist propranolol purportedly increased PD risk (Mittal et al., 2017). This report indicates that B2AR agonists may show promise as potential disease-modifying agents that may inhibit  $\alpha$ -syn protein expression at the transcriptional level. Further studies should be pursued in animal models of  $\alpha$ -synucleinopathies to investigate therapeutic implications for PD patients.

## Inhibition of $\alpha$ -Syn Aggregation and Aggregate Reduction

Inhibition of  $\alpha$ -syn aggregation remains an extremely attractive potential target for therapeutic interventions. Heat shock proteins (HSP) act as molecular chaperones that assist nascent polypeptide chains to fold correctly, and thus help prevent protein aggregation events. Klucken et al. (2004) reported the efficacy of HSPs for the reduction of aggregated  $\alpha$ -syn *in vitro* and *in vivo* studies. An interesting point of investigation is how aggregation-prone polypeptides escape protein quality control systems on the way to forming pathological aggregates. Indeed, HSPs may get trapped within aggregates as the rate

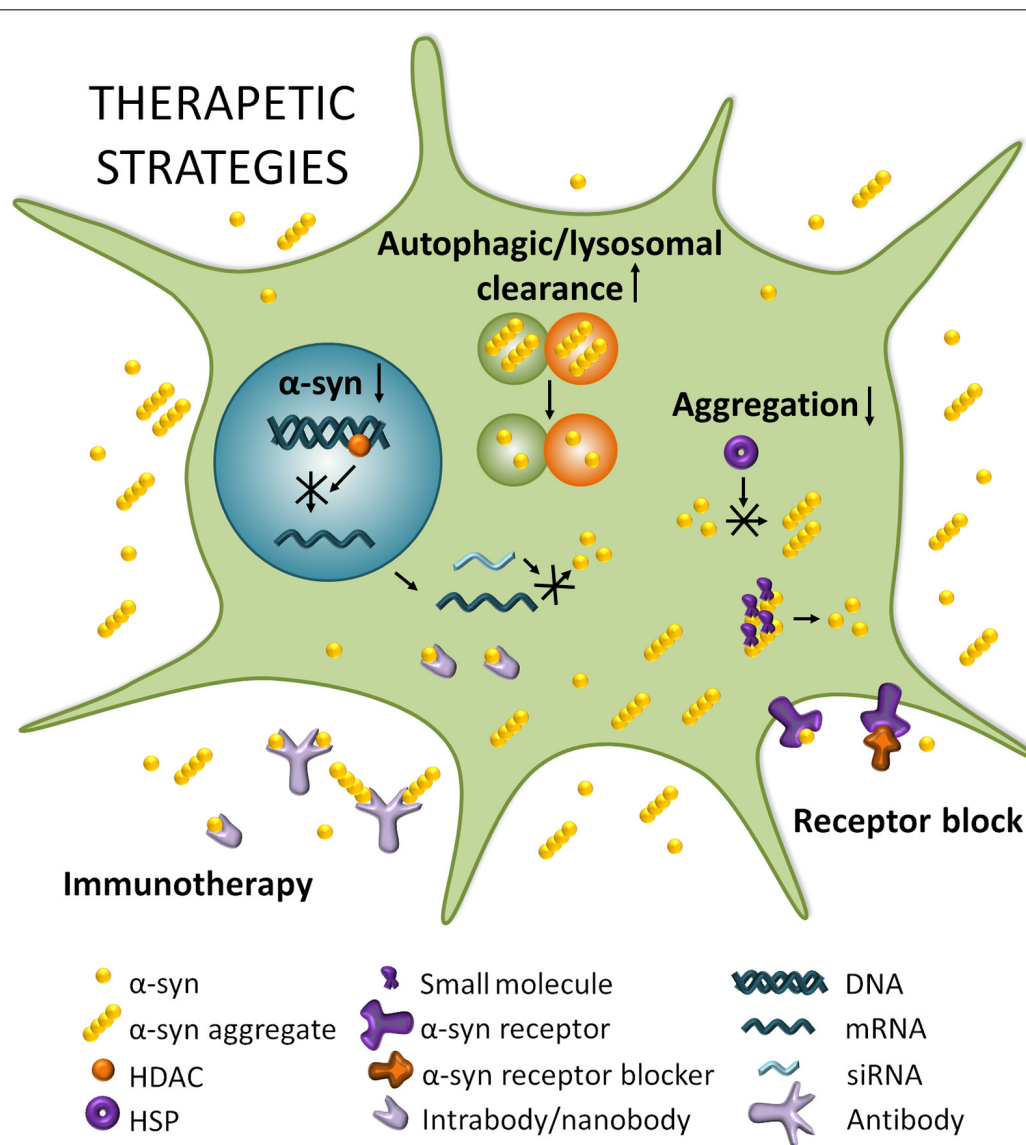


**FIGURE 2 |** Therapeutic strategies for PD. Boosting autophagic/lysosomal clearance is a potential avenue for clearing  $\alpha$ -syn and other aggregating proteins that disrupt cellular homeostasis. Reducing SNCA mRNA by modulating histone deacetylase (HDACs) or through RNA interference (RNAi) strategies can potentially lead to a decrease in expression of  $\alpha$ -syn which is known to result in reduced aggregation and toxicity. Reducing aggregation can be achieved by impeding the multimerization of  $\alpha$ -syn through heat shock proteins (HSPs) for example, or by dissociating existing aggregates with small molecules. Blocking  $\alpha$ -syn entry through receptor blocking would directly target the spread of  $\alpha$ -syn and prevent its transport from cell to cell. Finally, immunotherapy could potentially neutralize  $\alpha$ -syn and/or  $\alpha$ -syn aggregates extracellularly and perhaps even intracellularly in the case of intra/nanobodies.

of the aggregate formation increases with the progression of pathology, thus reducing the availability of these molecular chaperones. The kinetics of aggregation influence the ability of small HSPs to inhibit  $\alpha$ -syn aggregation, and may indicate how these aggregates potentially evade HSP chaperone-action, as the aggregated protein-loads increase the burden on this system (Cox et al., 2016). Therefore, further investigation is needed into mechanisms of regulating HSP expression levels to offer neuroprotection *via* chaperone induction/co-induction.

Another approach to reducing the risk of  $\alpha$ -syn aggregation inside cells utilizes an oligomer modulator called Anle138b

[3-(1,3-benzodioxol-5-yl)-5-(3-bromophenyl)-1H-pyrazole] that inhibits the formation and accumulation of  $\alpha$ -syn oligomers but does not interfere with the level of protein expression (Wagner et al., 2013). Importantly, the compound slowed disease progression in human A30P  $\alpha$ -syn transgenic mice even when treatment started after the onset of disease-related symptoms (Levin et al., 2014). Indeed, both in mouse models of prion disease and in three different PD mouse models, Anle138b strongly inhibited oligomer accumulation, neuronal degeneration, and disease progression (Wagner et al., 2013). Interestingly, binding studies revealed that Anle138b does not

bind the monomeric form of  $\alpha$ -syn, and thus does not interfere with non-aggregated forms of the protein in the physiologic state. Additionally, no detectable toxicity was reported at therapeutic doses and the compound exhibited excellent oral bioavailability and blood-brain barrier (BBB) penetrance. A recent study by Deeg et al. (2015) reported that Anle138b and other diphenyl-pyrazole compounds exhibited significantly increased fluorescence upon binding to fibrillar  $\alpha$ -syn structures, rendering this compound a promising fluorescent biomarker for investigation of aggregation dependent epitopes.

Early *in vitro* studies revealed numerous small molecule inhibitors of  $\alpha$ -syn assembly. Masuda et al. (2006) tested 79 compounds belonging to 12 different chemical classes and found that compounds from seven of these classes (polyphenols, phenothiazines, polyene macrolides, porphyrins, rifamycins, Congo red and its derivatives, and terpenoids) inhibited  $\alpha$ -syn filament assembly. Several molecules including, baicalein, delphinidin, dopamine chloride, and galliccatechin, were of particular interest, as they exhibited strong inhibitory properties against  $\alpha$ -syn filament formation. Soluble  $\alpha$ -syn oligomers formed instead in the presence of inhibitory compounds, probably through binding interactions with the C-terminal, suggesting this may be the mechanism through which filament formation is inhibited. These findings were corroborated by the evidence presented 2 years earlier by Zhu et al. (2004) who showed that baicalein both inhibited the formation of  $\alpha$ -syn fibrils and disaggregated pre-existing  $\alpha$ -syn filaments.

Several other small molecules have been reported to inhibit  $\alpha$ -syn aggregation. Methylthioninium is one such example of an effective aggregation inhibitor of  $\alpha$ -syn fibrillar inclusions both *in vitro* and *in vivo* that also exhibits the potential of rescuing behavioral deficits and ameliorating pathology in transgenic mouse models (Schwab et al., 2018). NPT100-18A interacts with the C-terminal domain of  $\alpha$ -syn, displaces it from the membrane, reducing the formation of  $\alpha$ -syn oligomers, and subsequently reduced neuronal accumulation of  $\alpha$ -syn and decreased markers of cell toxicity. Treatment with NPT100-18A improved motor deficits in mThy1 WT  $\alpha$ -syn transgenic mice in a dose-dependent manner (Wrasidlo et al., 2016). NPT200-11 is another inhibitor of  $\alpha$ -syn aggregation comparable to NPT100-18A, which stabilizes  $\alpha$ -syn conformers and blocks pathological misfolding of the protein. A small randomized, double-blind, single ascending dose phase 1 clinical trial evaluating the safety, tolerability, and pharmacokinetics of NPT200-11 was recently completed (Clinicaltrials.gov Identifier: NCT02606682). A fourth molecule is the human IgG1 fusion protein NPT088 that contains the General Amyloid Interaction Motif (GAIM) and is designed to simultaneously target multiple misfolded proteins. NPT088 treated Thy1-H $\alpha$ -syn mice showed increased tyrosine hydroxylase levels concomitant with a significant reduction in proteinase K-resistant  $\alpha$ -syn (Fisher et al., 2015). A multidose phase 1 clinical trial is currently underway to evaluate the safety and tolerability of NPT088 in patients with probable Alzheimer's disease (NCT03008161).

Molecular tweezers have also been shown to be strong dissociative and anti-aggregation agents (Sinha et al., 2011, 2012). These molecules are relatively small molecules that inhibit

protein interactions; CLR01 has shown great promise *in vitro* inhibiting  $\alpha$ -syn aggregation across multiple studies (Sinha et al., 2012; Acharya et al., 2014; Schrader et al., 2016). CLR01 has shown to be effective at reducing  $\alpha$ -syn-induced cell death *in vitro* and has also been shown to reduce  $\alpha$ -syn proteasomal inhibition in zebrafish (Prabhudesai et al., 2012). This prompted the investigation of the safety of this lysine-specific tweezer in a mammalian system; not only was CLR01 found to be safe and well-tolerated in mice, but it was also shown to cross the BBB, ensuring delivery to the target tissue in subsequent studies (Attar et al., 2014). In a pre-clinical PD mouse model CLR01 was able to reduce motor symptoms and  $\alpha$ -syn-related pathology (Richter et al., 2017), indicating it is an interesting candidate for the treatment of PD. Strengthening this evidence with more pre-clinical research would highlight the case for CLR01 and other molecular tweezers as candidates for PD clinical trials.

Immunotherapy is another promising strategy for the reduction of  $\alpha$ -syn aggregates that is currently in clinical trials. Several studies have reported that both active and passive immunization against  $\alpha$ -syn was neuroprotective in transgenic mouse models of PD (Masliah et al., 2005, 2011; Bae et al., 2013; Sanchez-Guajardo et al., 2013). These findings prompted the first phase 1 clinical trial with PRX002, a humanized IgG1 monoclonal antibody directed against epitopes near the C-terminus of aggregated forms of  $\alpha$ -syn. Results from the phase 1a clinical trial reported a 96.5% reduction in the concentration of free serum  $\alpha$ -syn (Schenk et al., 2017). A multiple-ascending dose study was performed in a phase 1b clinical trial to evaluate the safety and tolerability of PRX002 in idiopathic PD patients (Jankovic et al., 2018). The results of this study demonstrated significant target engagement evidenced by the reduction in free serum  $\alpha$ -syn levels by up to 97% after a single infusion cerebrospinal fluid (CSF) penetration indicated by a dose-dependent increase in CSF PRX002 concentrations. All doses of PRX002 were found to be safe and tolerable, supporting the design of an ongoing phase 2 clinical trial (NCT03100149; Jankovic et al., 2018).

In contrast to PRX002, BIIB054 (Biogen) is a fully human-derived monoclonal antibody directed against the N-terminal epitope of  $\alpha$ -syn that exhibits a high level of specificity for aggregated and fibrillar forms of  $\alpha$ -syn with a more than 800-fold binding affinity for aggregated  $\alpha$ -syn compared with monomeric forms of the protein (Weihofen et al., 2019). BIIB054 treatment was reported to reduce the spread of truncated  $\alpha$ -syn variants to the contralateral cortex and rescued motor impairments by about 50% in  $\alpha$ -syn PFF-inoculated WT mice (Weihofen et al., 2019). A recently-concluded phase 1 clinical trial of a single-ascending dose study of BIIB054 in PD patients and healthy volunteers, reported it was well tolerated at single doses up to 90 mg/kg, had a serum half-life of 28 days, and CSF concentrations achieved in healthy volunteers were 0.2% of those seen in plasma (Brys et al., 2019). Single doses of BIIB054 up to 45 mg/kg were well tolerated in PD patients, and the pharmacokinetic profile was comparable to that seen in healthy volunteers. BIIB054 is currently being evaluated in recently diagnosed PD patients in a multinational phase 2 clinical trial (NCT03318523).

Active immunization approaches have also been previously studied. AFFiRiS, developed AFFITOPE, a vaccine that consists of short synthetic  $\alpha$ -syn peptide fragments. In the recently completed parallel-group phase 1 clinical trial, the AFF008 study series assessed the tolerability and safety of repeated subcutaneous administration of a synthetic  $\alpha$ -syn mimicking epitope called AFFITOPE PD01A in a group of 24 patients randomized to receive either AFFITOPE PD01A low dose or high dose (NCT01568099). Similar results were observed in another phase 1 clinical trial study that used a different synthetic  $\alpha$ -syn mimicking epitope called AFFITOPE PD03A (NCT02267434). At the screening, the average duration of PD after the initial diagnosis was between 1.6–2.3 years. The study design was comparable to that used with AFFITOPE PD01A, with 36 patients randomized to a low dose, high dose, or placebo group. Treatment was found to be safe and well-tolerated at both doses in PD patients. AFFITOPE PD01A elicited a clear dose-dependent immune response against the peptide itself and cross-reactivity against the  $\alpha$ -syn targeted epitope over time. Overall results also reported a significant increase in antibody titer against PD01A. However, there was no significant immunogenicity of AFFITOPE PD03A when compared with controls.

Although antibodies are invaluable tools for synucleinopathy research, their high molecular weight undermines the viability of their therapeutic potential. This is especially important in neurological disorders as the BBB is a formidable obstacle to the systemic treatment of CNS diseases, because it impairs the passage of the vast majority of molecules, including antibodies, to the brain. Therefore, an interesting new avenue of research is that of gene-engineered antibodies called intrabodies and nanobodies, by expressing regions for antibody specificity separate from the full-length antibody. While a major concern about the use of immunotherapy in PD treatment is whether antibodies will have significant brain penetration to achieve sufficient target engagement, these engineered fragments might circumvent that issue, as they have higher brain penetrance and faster clearance. Additionally, because they can be synthesized in large quantities by bacterial or yeast systems, their production can be made more efficient and economical, providing further support for their viability. Zhou et al. (2004) reported scFv fragments, comprised of heavy variable and light variable domains linked by a short, flexible polypeptide sequence, that bind and stabilize monomeric forms of  $\alpha$ -syn, thereby inhibiting the formation of insoluble high-molecular-weight  $\alpha$ -syn species. Moreover, Zha et al. (2016) demonstrated that use of scFv W20 against common epitope of various toxic oligomeric species, reduced  $\alpha$ -syn and mutant huntingtin protein aggregate load in PD and HD transgenic mice, and simultaneously reduced synaptic degeneration, neuroinflammation, and oxidative stress and significantly improved motor and cognitive deficits. Additionally, single domain antibodies called nanobodies might be an alternative to scFvs (Hamers-Casterman et al., 1993). Nanobodies have a higher solubility and a lower molecular weight compared with scFvs, rendering greater brain penetrance due to increased passage through the BBB. Their ability to

recognize unique epitopes with subnanomolar affinity and their high production yield at a relatively low cost make them a useful class of biomolecules for research and therapeutic applications. A study on the nanobody NbSyn87 that has target specificity for residues 118–131 in the C-terminus of  $\alpha$ -syn reported that it binds both monomeric and fibrillar forms of the protein, indicating that the epitope is accessible in the fibrillar state (Guilliams et al., 2013). The length of time of fibrillization influenced the apparent affinities of NbSyn87 for their epitopes. This finding suggests that the epitope on the  $\alpha$ -syn C-terminus undergoes conformational changes during fibrillization and that nanobodies are able to target different, potentially pathogenic forms of aggregated  $\alpha$ -syn.

Although neuro-immunotherapy presents as an elegant tool to inhibit the pathogenic spread of extracellular aggregated  $\alpha$ -syn, the potential associated risks in both active and passive immunization, including systemic side reactions, need to be clearly elucidated. Neurodegenerative disease treatment requires further investigation into the multiple routes of vector administration, including direct injection, injection into the CSF, and intramuscular and intravascular administration. Subsequent studies will need to clearly evaluate the safety and risk associated with more invasive measures that efficiently transduce or treat smaller areas, compared with broader, less-invasive means of distribution associated with limited brain penetrance due to the need to bypass the BBB. Optimization of these technological challenges, including means to either mechanically or biologically bypass the BBB, achieve sufficient antibody levels in CNS to enable adequate target engagement, and direct elimination only against aggregated  $\alpha$ -syn species, are needed to further evaluate important implications for future therapeutics.

## Enhancing Degradation of Intracellular $\alpha$ -Syn Aggregates

Autophagy is suggested to serve a significant role in the intracellular degradation of  $\alpha$ -syn aggregates (Decressac et al., 2013). Once the autophagosome has formed around its target, a lysosome can merge with it, delivering its degradative enzymes to the enclosed, pathogenic cargo. Autophagosome-lysosome fusion events are mediated by Rab GTPases that recruit membrane-tethering complexes to reduce the spatial separation between the two compartments and SNARE proteins that drive the physical fusion of the bilayers (Nakamura and Yoshimori, 2017). Dysfunction of the ALP has been shown to correlate with increased accumulation of intracellular  $\alpha$ -syn aggregates and induce the activation of nonclassical secretory pathways (Poehler et al., 2014). While the presence of intracellular  $\alpha$ -syn aggregates may increase the pathologic burden on host neurons, neuron-released  $\alpha$ -syn aggregates may enhance the cell-to-cell propagation of  $\alpha$ -syn pathology and progression of disease (Lopes da Fonseca et al., 2015). Thus, enhancing autophagic processes may promote increased clearance of pathological  $\alpha$ -syn and alleviate the intracellular burden on host neurons.



The mammalian target of rapamycin (mTOR), a component of protein complexes mTORC1 and mTORC2 are essential for cellular development and tissue regeneration, as well as the regulation of apoptosis and autophagy (Maiese et al., 2013). Rapamycin and its analogs work *via* mTOR inhibition to induce autophagy. This class of drugs has been shown to have neuroprotective effects primarily due to its ability to promote increased clearance of  $\alpha$ -syn through the induction of autophagic processes (Webb et al., 2003; Crews et al., 2010; Bové et al., 2011; Decressac et al., 2013; Maiese et al., 2013). However, rapamycin has limited utility because it lacks specificity, and acts on other essential pathways involved in immunosuppression, and thus is not a viable drug candidate for PD where long-term treatment would be necessary. Due to rapamycin's therapeutic limitations, researchers have investigated other compounds that promote autophagy. For example, trehalose is a sugar molecule present in many organisms that acts through an mTOR-independent pathway, and has been shown to enhance autophagy through increased lysosomal biogenesis, leading to the corresponding increased clearance of protein aggregates (Sarkar et al., 2007). Another strategy to achieve inhibition of mTOR uses a modulator of the mitochondrial pyruvate carrier (MPC) called MSDC-0160 to reduce pyruvate transport into the mitochondria. MSDC-0160 causes alterations in mitochondrial metabolism induced by MPC inhibition that result in mTOR inhibition and upregulation of autophagy in neurons (Ghosh et al., 2016). It has been shown to protect midbrain dopaminergic neurons from MPP<sup>+</sup>-induced cell death and nigral dopaminergic neurons in a "chronic" genetic mouse model of PD, and enhance autophagy in a model of  $\alpha$ -syn-induced toxicity in *C. elegans* (Ghosh et al., 2016). These findings warrant further investigations to determine whether MPC inhibition may present promise as a useful avenue for future therapeutics, and may provide insight into the development of other MPC modulators as potential disease-modifying agents for PD.

## REFERENCES

- Acharya, S., Safaie, B. M., Wongkongkathap, P., Ivanova, M. I., Attar, A., Klärner, F. G., et al. (2014). Molecular basis for preventing  $\alpha$ -synuclein aggregation by a molecular tweezer. *J. Biol. Chem.* 289, 10727–10737. doi: 10.1074/jbc.M113.524520
- Alafuzoff, I., Ince, P. G., Arzberger, T., Al-Sarraj, S., Bell, J., Bodi, I., et al. (2009). Staging/typing of Lewy body related  $\alpha$ -synuclein pathology: a study of the BrainNet europe consortium. *Acta Neuropathol.* 117, 635–652. doi: 10.1007/s00401-009-0523-2
- Alarcón-Aris, D., Recasens, A., Galofré, M., Carballo-Carbajal, I., Zacchi, N., Ruiz-Bronchal, E., et al. (2018). Selective  $\alpha$ -synuclein knockdown in monoamine neurons by intranasal oligonucleotide delivery: potential therapy for Parkinson's disease. *Mol. Ther.* 26, 550–567. doi: 10.1007/s00401-009-0523-2
- Alegre-Abarrategui, J., Brimblecombe, K. R., Roberts, R. F., Velentza-Almpani, E., Tilley, B. S., Bengoa-Vergniory, N., et al. (2019). Selective vulnerability in  $\alpha$ -synucleinopathies. *Acta Neuropathol.* 138, 681–704. doi: 10.1093/med/9780190607166.003.0006
- Anderson, A. C., Joller, N., and Kuchroo, V. K. (2016). Lag-3, Tim-3, and TIGIT: co-inhibitory receptors with specialized functions in immune regulation. *Immunity* 44, 989–1004. doi: 10.1016/j.immuni.2016.05.001

## CONCLUSION

Substantial evidence supports the identification of  $\alpha$ -syn is a key player in the initiation and progression of neurodegeneration in PD pathogenesis. Several pre-clinical therapeutic modalities targeting pathological  $\alpha$ -syn have revealed promising results. Current approaches include treatments designed to inhibit the synthesis, aggregation, or uptake of abnormal  $\alpha$ -syn and enhance extracellular protein clearance mechanisms.  $\alpha$ -syn immunotherapy and small molecule-based dissociation of aggregates have garnered significant interest as potential methods that might slow or halt the progression of the disease. However, further research is needed to optimize our understanding of the clinic-pathological relationship between the various species of  $\alpha$ -syn and the development of PD. While caution is warranted when manipulating global  $\alpha$ -syn levels, we conclude that targeting toxic  $\alpha$ -syn seems a compelling strategy for therapeutic targets in PD.

## AUTHOR CONTRIBUTIONS

CF and NB-V wrote the initial draft. NB-V and RW-M revised and produced the final version of the manuscript.

## FUNDING

Work in the Wade-Martins Laboratory is funded by the Monument Discovery Award from Parkinson's UK (J-1403) and the Michael J Fox Foundation. NB-V holds an Oxford/Celgene Program Fellowship. Parkinson's UK supports open access through the charity open access fund.

## ACKNOWLEDGMENTS

We wish to thank Dr. Siv Vingill and Dr. Sophie Morgan for their critical reading of the manuscript.

- Anwar, S., Peters, O., Millership, S., Ninkina, N., Doig, N., Connor-Robson, N., et al. (2011). Functional alterations to the nigrostriatal system in mice lacking all three members of the synuclein family. *J. Neurosci.* 31, 7264–7274. doi: 10.1523/jneurosci.6194-10.2011
- Attar, A., Chan, W.-T. C., Klärner, F.-G., Schrader, T., and Bitan, G. (2014). Safety and pharmacological characterization of the molecular tweezer CLR01—a broad-spectrum inhibitor of amyloid proteins' toxicity. *BMC Pharmacol. Toxicol.* 15:23. doi: 10.1186/2050-6511-15-23
- Bae, E.-J., Ho, D.-H., Park, E., Jung, J. W., Cho, K., Hong, J. H., et al. (2013). Lipid peroxidation product 4-hydroxy-2-nonenal promotes seeding-capable oligomer formation and cell-to-cell transfer of  $\alpha$ -synuclein. *Antioxid. Redox Signal.* 18, 770–783. doi: 10.1089/ars.2011.4429
- Bartels, T., Choi, J. G., and Selkoe, D. J. (2011).  $\alpha$ -synuclein occurs physiologically as a helically folded tetramer that resists aggregation. *Nature* 477, 107–110. doi: 10.1038/nature10324
- Bence, N. F., Sampat, R. M., and Kopito, R. R. (2001). Impairment of the ubiquitin-proteasome system by protein aggregation. *Science* 292, 1552–1555. doi: 10.1126/science.292.5521.1552
- Bengoa-Vergniory, N., Roberts, R. F., Wade-Martins, R., and Alegre-Abarrategui, J. (2017).  $\alpha$ -synuclein oligomers: a new hope. *Acta Neuropathol.* 134, 819–838. doi: 10.1007/s00401-017-1755-1

- Bové, J., Martínez-Vicente, M., and Vila, M. (2011). Fighting neurodegeneration with rapamycin: mechanistic insights. *Nat. Rev. Neurosci.* 12, 437–452. doi: 10.1038/nrn3068
- Braak, H., and Del Tredici, K. (2016). Potential pathways of abnormal tau and  $\alpha$ -synuclein dissemination in sporadic Alzheimer's and Parkinson's diseases. *Cold Spring Harb. Perspect. Biol.* 8:a023630. doi: 10.1101/cshperspect.a023630
- Braak, H., Del Tredici, K., Rüb, U., de Vos, R. A. I., Jansen Steur, E. N., and Braak, E. (2003). Staging of brain pathology related to sporadic Parkinson's disease. *Neurobiol. Aging* 24, 197–211. doi: 10.1016/s0197-4580(02)00065-9
- Brettschneider, J., Del Tredici, K., Lee, V. M.-Y., and Trojanowski, J. Q. (2015). Spreading of pathology in neurodegenerative diseases: a focus on human studies. *Nat. Rev. Neurosci.* 16, 109–120. doi: 10.1038/nrn3887
- Brustovetsky, N., Brustovetsky, T., Jemmerson, R., and Dubinsky, J. M. (2002). Calcium-induced Cytochrome c release from CNS mitochondria is associated with the permeability transition and rupture of the outer membrane. *J. Neurochem.* 80, 207–218. doi: 10.1046/j.0022-3042.2001.00671.x
- Brys, M., Fanning, L., Hung, S., Ellenbogen, A., Penner, N., Yang, M., et al. (2019). Randomized phase I clinical trial of anti- $\alpha$ -synuclein antibody BIIB054. *Mov. Disord.* 34, 1154–1163. doi: 10.1002/mds.27738
- Burke, R. E., Dauer, W. T., and Vonsattel, J. P. G. (2008). A critical evaluation of the Braak staging scheme for Parkinson's disease. *Ann. Neurol.* 64, 485–491. doi: 10.1002/ana.21541
- Burré, J., Sharma, M., and Südhof, T. C. (2014).  $\alpha$ -synuclein assembles into higher-order multimers upon membrane binding to promote SNARE complex formation. *Proc. Natl. Acad. Sci. U S A* 111, E4274–E4283. doi: 10.1073/pnas.1416598111
- Burré, J., Sharma, M., Tsetsenis, T., Buchman, V., Etherton, M. R., and Südhof, T. C. (2010).  $\alpha$ -synuclein promotes SNARE-complex assembly *in vivo* and *in vitro*. *Science* 329, 1663–1667. doi: 10.1126/science.1195227
- Burré, J., Vivona, S., Diao, J., Sharma, M., Brunger, A. T., and Südhof, T. C. (2013). Properties of native brain  $\alpha$ -synuclein. *Nature* 498, E4–E6; discussion E6–E7. doi: 10.1038/nature12125
- Bussell, R., and Eliezer, D. (2003). A structural and functional role for 11-mer repeats in  $\alpha$ -synuclein and other exchangeable lipid binding proteins. *J. Mol. Biol.* 329, 763–778. doi: 10.1016/s0022-2836(03)00520-5
- Bussell, R., Ramlall, T. F., Eliezer, D., and Eliezer, D. (2005). Helix periodicity, topology and dynamics of membrane-associated  $\alpha$ -synuclein. *Protein Sci.* 14, 862–872. doi: 10.1110/ps.041255905
- Chen, H., and Chan, D. C. (2009). Mitochondrial dynamics—fusion, fission, movement, and mitophagy—in neurodegenerative diseases. *Hum. Mol. Genet.* 18, R169–R176. doi: 10.1093/hmg/ddp326
- Choi, B.-K., Choi, M.-G., Kim, J.-Y., Yang, Y., Lai, Y., Kweon, D.-H., et al. (2013). Large  $\alpha$ -synuclein oligomers inhibit neuronal SNARE-mediated vesicle docking. *Proc. Natl. Acad. Sci. U S A* 110, 4087–4092. doi: 10.1073/pnas.1218421110
- Cole, N. B., Dieuliis, D., Leo, P., Mitchell, D. C., and Nussbaum, R. L. (2008). Mitochondrial translocation of  $\alpha$ -synuclein is promoted by intracellular acidification. *Exp. Cell Res.* 314, 2076–2089. doi: 10.1016/j.yexcr.2008.03.012
- Colla, E., Jensen, P. H., Pletnikova, O., Troncoso, J. C., Glabe, C., and Lee, M. K. (2012). Accumulation of toxic  $\alpha$ -synuclein oligomer within endoplasmic reticulum occurs in  $\alpha$ -synucleinopathy *in vivo*. *J. Neurosci.* 32, 3301–3305. doi: 10.1523/JNEUROSCI.5368-11.2012
- Collier, T. J., Redmond, D. E., Steece-Collier, K., Lipton, J. W., and Manfredsson, F. P. (2016). Is  $\alpha$ -synuclein loss-of-function a contributor to Parkinsonian pathology? Evidence from non-human primates. *Front. Neurosci.* 10:12. doi: 10.3389/fnins.2016.00012
- Cox, D., Selig, E., Griffin, M. D. W., Carver, J. A., and Ecroyd, H. (2016). Small heat-shock proteins prevent  $\alpha$ -synuclein aggregation *via* transient interactions and their efficacy is affected by the rate of aggregation. *J. Biol. Chem.* 291, 22618–22629. doi: 10.1074/jbc.M116.739250
- Crews, L., Spencer, B., Desplats, P., Patrick, C., Paulino, A., Rockenstein, E., et al. (2010). Selective molecular alterations in the autophagy pathway in patients with Lewy body disease and in models of  $\alpha$ -synucleinopathy. *PLoS One* 5:e9313. doi: 10.1371/journal.pone.0009313
- Cuervo, A. M., Dice, J. F., Fredenburg, R., Lansbury, P. T., and Sulzer, D. (2004). Impaired degradation of mutant  $\alpha$ -synuclein by chaperone-mediated autophagy. *Science* 305, 1292–1295. doi: 10.1126/science.1101738
- Davidson, W. S., Jonas, A., Clayton, D. F., and George, J. M. (1998). Stabilization of  $\alpha$ -synuclein secondary structure upon binding to synthetic membranes. *J. Biol. Chem.* 273, 9443–9449. doi: 10.1074/jbc.273.16.9443
- Davis, G. C., Williams, A. C., Markey, S. P., Ebert, M. H., Caine, E. D., Reichert, C. M., et al. (1979). Chronic parkinsonism secondary to intravenous injection of meperidine analogues. *Psychiatry Res.* 1, 249–254. doi: 10.1016/0165-1781(79)90006-4
- Decressac, M., Mattsson, B., Weikop, P., Lundblad, M., Jakobsson, J., and Björklund, A. (2013). TFEB-mediated autophagy rescues midbrain dopamine neurons from  $\alpha$ -synuclein toxicity. *Proc. Natl. Acad. Sci. U S A* 110, E1817–E1826. doi: 10.1073/pnas.1305623110
- Deeg, A. A., Reiner, A. M., Schmidt, F., Schueder, F., Ryazanov, S., Ruf, V. C., et al. (2015). Anle138b and related compounds are aggregation specific fluorescence markers and reveal high affinity binding to  $\alpha$ -synuclein aggregates. *Biochim. Biophys. Acta* 1850, 1884–1890. doi: 10.1016/j.bbagen.2015.05.021
- Desplats, P., Lee, H.-J., Bae, E.-J., Patrick, C., Rockenstein, E., Crews, L., et al. (2009). Inclusion formation and neuronal cell death through neuron-to-neuron transmission of  $\alpha$ -synuclein. *Proc. Natl. Acad. Sci. U S A* 106, 13010–13015. doi: 10.1073/pnas.0903691106
- Devi, L., Raghavendran, V., Prabhu, B. M., Avadhani, N. G., and Anandatheerthavarada, H. K. (2008). Mitochondrial import and accumulation of  $\alpha$ -synuclein impair complex I in human dopaminergic neuronal cultures and Parkinson disease brain. *J. Biol. Chem.* 283, 9089–9100. doi: 10.1074/jbc.m710012200
- Dexter, D. T., Carter, C. J., Wells, F. R., Javoy-Agid, F., Agid, Y., Lees, A., et al. (1989). Basal lipid peroxidation in substantia nigra is increased in Parkinson's disease. *J. Neurochem.* 52, 381–389. doi: 10.1111/j.1471-4159.1989.tb09133.x
- Di Maio, R., Barrett, P. J., Hoffman, E. K., Barrett, C. W., Zharikov, A., Borah, A., et al. (2016).  $\alpha$ -synuclein binds to TOM20 and inhibits mitochondrial protein import in Parkinson's disease. *Sci. Transl. Med.* 8:342ra78. doi: 10.1126/scitranslmed.aaf3634
- Di Maio, R., Hoffman, E. K., Rocha, E. M., Keeney, M. T., Sanders, L. H., De Miranda, B. R., et al. (2018). LRRK2 activation in idiopathic Parkinson's disease. *Sci. Transl. Med.* 10, 1–13. doi: 10.1126/scitranslmed.aar5429
- Eliezer, D., Kutluay, E., Bussell, R., and Browne, G. (2001). Conformational properties of  $\alpha$ -synuclein in its free and lipid-associated states. *J. Mol. Biol.* 307, 1061–1073. doi: 10.1006/jmbi.2001.4538
- Fauvet, B., Mbefo, M. K., Fares, M.-B., Desobry, C., Michael, S., Ardah, M. T., et al. (2012).  $\alpha$ -synuclein in central nervous system and from erythrocytes, mammalian cells and *Escherichia coli* exists predominantly as disordered monomer. *J. Biol. Chem.* 287, 15345–15364. doi: 10.1074/jbc.M111.318949
- Fisher, R. A., Gannon, K. S., Krishnan, R., Levenson, J. M., Tsubery, H., Asp, E., et al. (2015). Discovery, preclinical development and clinical trial approach for NPT088, a general amyloid interaction motif (GAIM)-immunoglobulin fusion. *Alzheimers Dement.* 11:P135. doi: 10.1016/j.jalz.2015.07.051
- Floor, E., and Wetzel, M. G. (2002). Increased protein oxidation in human substantia nigra pars compacta in comparison with basal ganglia and prefrontal cortex measured with an improved dinitrophenylhydrazine assay. *J. Neurochem.* 70, 268–275. doi: 10.1046/j.1471-4159.1998.70010268.x
- Fountaine, T. M., and Wade-Martins, R. (2007). RNA interference-mediated knockdown of  $\alpha$ -synuclein protects human dopaminergic neuroblastoma cells from MPP+ toxicity and reduces dopamine transport. *J. Neurosci. Res.* 85, 351–363. doi: 10.1002/jnr.21125
- Fujiwara, H., Hasegawa, M., Dohmae, N., Kawashima, A., Masliah, E., Goldberg, M. S., et al. (2002).  $\alpha$ -synuclein is phosphorylated in synucleinopathy lesions. *Nat. Cell Biol.* 4, 160–164. doi: 10.1038/ncb748
- Ghiglieri, V., Calabrese, V., and Calabresi, P. (2018).  $\alpha$ -synuclein: from early synaptic dysfunction to neurodegeneration. *Front. Neurol.* 9:295. doi: 10.3389/fneur.2018.00295
- Ghosh, A., Tyson, T., George, S., Hildebrandt, E. N., Steiner, J. A., Madaj, Z., et al. (2016). Mitochondrial pyruvate carrier regulates autophagy, inflammation and neurodegeneration in experimental models of Parkinson's disease. *Sci. Transl. Med.* 8:368ra174. doi: 10.1126/scitranslmed.aag2210
- Giasson, B. I., Murray, I. V., Trojanowski, J. Q., and Lee, V. M. (2001). A hydrophobic stretch of 12 amino acid residues in the middle of  $\alpha$ -synuclein is

- essential for filament assembly. *J. Biol. Chem.* 276, 2380–2386. doi: 10.1074/jbc.m008919200
- Goedert, M., Spillantini, M. G., Del Tredici, K., and Braak, H. (2013). 100 years of Lewy pathology. *Nat. Rev. Neurol.* 9, 13–24. doi: 10.1038/nrneurol.2012.242
- Gorbatyuk, O. S., Li, S., Nash, K., Gorbatyuk, M., Lewin, A. S., Sullivan, L. F., et al. (2010). *In vivo* RNAi-mediated  $\alpha$ -synuclein silencing induces nigrostriatal degeneration. *Mol. Ther.* 18, 1450–1457. doi: 10.1038/mt.2010.115
- Görlach, A., Bertram, K., Hudecova, S., and Krizanov, O. (2015). Calcium and ROS: a mutual interplay. *Redox Biol.* 6, 260–271. doi: 10.1016/j.redox.2015.08.010
- Guilliams, T., El-Turk, F., Buell, A. K., O'Day, E. M., Aprile, F. A., Esbjörner, E. K., et al. (2013). Nanobodies raised against monomeric  $\alpha$ -synuclein distinguish between fibrils at different maturation stages. *J. Mol. Biol.* 425, 2397–2411. doi: 10.1016/j.jmb.2013.01.040
- Hamers-Casterman, C., Atarhouch, T., Muyldermans, S., Robinson, G., Hamers, C., Bajjana Songa, E., et al. (1993). Naturally occurring antibodies devoid of light chains. *Nature* 363, 446–448. doi: 10.1038/363446a0
- Hasegawa, M., Fujiwara, H., Nonaka, T., Wakabayashi, K., Takahashi, H., Lee, V. M.-Y., et al. (2002). Phosphorylated  $\alpha$ -synuclein is ubiquitinated in  $\alpha$ -synucleinopathy lesions. *J. Biol. Chem.* 277, 49071–49076. doi: 10.1074/jbc.M208046200
- Hasegawa, M., Nonaka, T., and Masuda-Suzukake, M. (2017). Prion-like mechanisms and potential therapeutic targets in neurodegenerative disorders. *Pharmacol. Ther.* 172, 22–33. doi: 10.1016/j.pharmthera.2016.11.010
- Hashimoto, M., Takeda, A., Hsu, L. J., Takenouchi, T., and Masliah, E. (1999). Role of cytochrome c as a stimulator of  $\alpha$ -synuclein aggregation in Lewy body disease. *J. Biol. Chem.* 274, 28849–28852. doi: 10.1074/jbc.274.41.28849
- Holmes, B. B., DeVos, S. L., Kfoury, N., Li, M., Jacks, R., Yanamandra, K., et al. (2013). Heparan sulfate proteoglycans mediate internalization and propagation of specific proteopathic seeds. *Proc. Natl. Acad. Sci. U S A* 110, E3138–E3147. doi: 10.1073/pnas.1301440110
- Indo, H. P., Yen, H.-C., Nakanishi, I., Matsumoto, K.-I., Tamura, M., Nagano, Y., et al. (2015). A mitochondrial superoxide theory for oxidative stress diseases and aging. *J. Clin. Biochem. Nutr.* 56, 1–7. doi: 10.3164/jcbs.14-42
- Jakes, R., Spillantini, M. G., and Goedert, M. (1994). Identification of two distinct synucleins from human brain. *FEBS Lett.* 345, 27–32. doi: 10.1016/0014-5793(94)00395-5
- Jankovic, J., Goodman, I., Safirstein, B., Marmon, T. K., Schenk, D. B., Koller, M., et al. (2018). Safety and tolerability of multiple ascending doses of PRX002/RG7935, an anti- $\alpha$ -synuclein monoclonal antibody, in patients with Parkinson disease: a randomized clinical trial. *JAMA Neurol.* 75, 1206–1214. doi: 10.1001/jamaneurol.2018.1487
- Jellinger, K. A. (2008). A critical reappraisal of current staging of Lewy-related pathology in human brain. *Acta Neuropathol.* 116, 1–16. doi: 10.1007/s00401-008-0406-y
- Jeong, G. R., Jang, E.-H., Bae, J. R., Jun, S., Kang, H. C., Park, C.-H., et al. (2018). Dysregulated phosphorylation of Rab GTPases by LRRK2 induces neurodegeneration. *Mol. Neurodegener.* 13:8. doi: 10.1186/s13024-018-0240-1
- Jiang, P., Gan, M., Yen, S.-H., McLean, P. J., and Dickson, D. W. (2017). Impaired endo-lysosomal membrane integrity accelerates the seeding progression of  $\alpha$ -synuclein aggregates. *Sci. Rep.* 7:7690. doi: 10.1038/s41598-017-08149-w
- Kanaan, N. M., and Manfredsson, F. P. (2012). Loss of functional  $\alpha$ -synuclein: a toxic event in Parkinson's disease? *J. Parkinsons Dis.* 2, 249–267. doi: 10.3233/JPD-012138
- Kaufman, S. K., and Diamond, M. I. (2013). Prion-like propagation of protein aggregation and related therapeutic strategies. *Neurotherapeutics* 10, 371–382. doi: 10.1007/s13311-013-0196-3
- Kayed, R., Sokolov, Y., Edmonds, B., McIntire, T. M., Milton, S. C., Hall, J. E., et al. (2004). Permeabilization of lipid bilayers is a common conformation-dependent activity of soluble amyloid oligomers in protein misfolding diseases. *J. Biol. Chem.* 279, 46363–46366. doi: 10.1074/jbc.c400260200
- Killinger, B. A., Madaj, Z., Sikora, J. W., Rey, N., Haas, A. J., Vepa, Y., et al. (2018). The vermiform appendix impacts the risk of developing Parkinson's disease. *Sci. Transl. Med.* 10:ear5280. doi: 10.1126/scitranslmed.aar5280
- Kim, S., Kwon, S.-H., Kam, T.-I., Panicker, N., Karuppagounder, S. S., Lee, S., et al. (2019). Transneuronal propagation of pathologic  $\alpha$ -synuclein from the gut to the brain models Parkinson's disease. *Neuron* 103, 627.e7–641.e7. doi: 10.1016/j.neuron.2019.05.035
- Kim, I., Xu, W., and Reed, J. C. (2008). Cell death and endoplasmic reticulum stress: disease relevance and therapeutic opportunities. *Nat. Rev. Drug Discov.* 7, 1013–1030. doi: 10.1038/nrd2755
- Klucken, J., Shin, Y., Masliah, E., Hyman, B. T., and McLean, P. J. (2004). Hsp70 reduces  $\alpha$ -synuclein aggregation and toxicity. *J. Biol. Chem.* 279, 25497–25502. doi: 10.1074/jbc.M400255200
- Kordower, J. H., Chu, Y., Hauser, R. A., Freeman, T. B., and Olanow, C. W. (2008). Lewy body-like pathology in long-term embryonic nigral transplants in Parkinson's disease. *Nat. Med.* 14, 504–506. doi: 10.1038/nm1747
- Langston, J., Ballard, P., Tetrud, J., and Irwin, I. (1983). Chronic Parkinsonism in humans due to a product of meperidine-analog synthesis. *Science* 219, 979–980. doi: 10.1126/science.6823561
- Lashuel, H. A., Overk, C. R., Oueslati, A., and Masliah, E. (2013). The many faces of  $\alpha$ -synuclein: from structure and toxicity to therapeutic target. *Nat. Rev. Neurosci.* 14, 38–48. doi: 10.1038/nrn3406
- Levin, J., Schmidt, F., Boehm, C., Prix, C., Bötzel, K., Ryazanov, S., et al. (2014). The oligomer modulator anle138b inhibits disease progression in a Parkinson mouse model even with treatment started after disease onset. *Acta Neuropathol.* 127, 779–780. doi: 10.1007/s00401-014-1265-3
- Lewis, J., Melrose, H., Bumcrot, D., Hope, A., Zehr, C., Lincoln, S., et al. (2008). *In vivo* silencing of  $\alpha$ -synuclein using naked siRNA. *Mol. Neurodegener.* 3:19. doi: 10.1186/1750-1326-3-19
- Lewy, F. H. (1912). “Paralysis agitans. I. Pathologische Anatomie,” in *Handbuch der Neurologie*, (Vol. 3) ed. M. Lewandowsky (New York, NY: Springer, Berlin Heidelberg), 920–958.
- Li, J.-Y., Englund, E., Holton, J. L., Soulet, D., Hagell, P., Lees, A. J., et al. (2008). Lewy bodies in grafted neurons in subjects with Parkinson's disease suggest host-to-graft disease propagation. *Nat. Med.* 14, 501–503. doi: 10.1038/nm1746
- Liu, Y., Sorce, S., Nuvolone, M., Domange, J., and Aguzzi, A. (2018). Lymphocyte activation gene 3 (Lag3) expression is increased in prion infections but does not modify disease progression. *Sci. Rep.* 8:14600. doi: 10.1038/s41598-018-32712-8
- Lopes da Fonseca, T., Villar-Piqué, A., and Outeiro, T. F. (2015). The interplay between  $\alpha$ -synuclein clearance and spreading. *Biomolecules* 5, 435–471. doi: 10.3390/biom5020435
- Luk, K. C., Kehm, V. M., Zhang, B., O'Brien, P., Trojanowski, J. Q., and Lee, V. M. Y. (2012). Intracerebral inoculation of pathological  $\alpha$ -synuclein initiates a rapidly progressive neurodegenerative  $\alpha$ -synucleinopathy in mice. *J. Exp. Med.* 209:975. doi: 10.1084/jem.20112457
- Maiese, K., Chong, Z. Z., Shang, Y. C., and Wang, S. (2013). mTOR: on target for novel therapeutic strategies in the nervous system. *Trends Mol. Med.* 19, 51–60. doi: 10.1016/j.molmed.2012.11.001
- Mao, X., Ou, M. T., Karuppagounder, S. S., Kam, T.-I., Yin, X., Xiong, Y., et al. (2016). Pathological  $\alpha$ -synuclein transmission initiated by binding lymphocyte-activation gene 3. *Science* 353:aah3374. doi: 10.1126/science.aah3374
- Maroteaux, L., Campanelli, J. T., and Scheller, R. H. (1988). Synuclein: a neuron-specific protein localized to the nucleus and presynaptic nerve terminal. *J. Neurosci.* 8, 2804–2815. doi: 10.1523/jneurosci.08-08-02804.1988
- Masliah, E., Rockenstein, E., Adame, A., Alford, M., Crews, L., Hashimoto, M., et al. (2005). Effects of  $\alpha$ -synuclein immunization in a mouse model of Parkinson's disease. *Neuron* 46, 857–868. doi: 10.1016/j.neuron.2005.05.010
- Masliah, E., Rockenstein, E., Mante, M., Crews, L., Spencer, B., Adame, A., et al. (2011). Passive immunization reduces behavioral and neuropathological deficits in an  $\alpha$ -synuclein transgenic model of Lewy body disease. *PLoS One* 6:e19338. doi: 10.1371/journal.pone.0019338
- Masuda, M., Suzuki, N., Taniguchi, S., Oikawa, T., Nonaka, T., Iwatsubo, T., et al. (2006). Small molecule inhibitors of  $\alpha$ -synuclein filament assembly. *Biochemistry* 45, 6085–6094. doi: 10.1021/bi0600749
- Masuda-Suzukake, M., Nonaka, T., Hosokawa, M., Oikawa, T., Arai, T., Akiyama, H., et al. (2013). Prion-like spreading of pathological  $\alpha$ -synuclein in brain. *Brain* 136, 1128–1138. doi: 10.1093/brain/awt037
- Mazzulli, J. R., Xu, Y.-H., Sun, Y., Knight, A. L., McLean, P. J., Caldwell, G. A., et al. (2011). Gaucher disease glucocerebrosidase and  $\alpha$ -synuclein form a bidirectional pathogenic loop in synucleinopathies. *Cell* 146, 37–52. doi: 10.1016/j.cell.2011.06.001



- Mazzulli, J. R., Zunke, F., Isacson, O., Studer, L., and Krainc, D. (2016).  $\alpha$ -synuclein-induced lysosomal dysfunction occurs through disruptions in protein trafficking in human midbrain synucleinopathy models. *Proc. Natl. Acad. Sci. U S A* 113, 1931–1936. doi: 10.1073/pnas.1520335113
- McCormack, A. L., Mak, S. K., Henderson, J. M., Bumcrot, D., Farrer, M. J., and Di Monte, D. A. (2010).  $\alpha$ -Synuclein suppression by targeted small interfering RNA in the primate substantia nigra. *PLoS One* 5:e12122. doi: 10.1371/journal.pone.0012122
- Mendez, I., Viñuela, A., Astradsson, A., Mukhida, K., Hallett, P., Robertson, H., et al. (2008). Dopamine neurons implanted into people with Parkinson's disease survive without pathology for 14 years. *Nat. Med.* 14, 507–509. doi: 10.1038/nm1752
- Mhyre, T. R., Boyd, J. T., Hamill, R. W., and Maguire-Zeiss, K. A. (2012). Parkinson's disease. *Subcell. Biochem.* 65, 389–455. doi: 10.1007/978-94-007-5416-4\_16
- Mittal, S., Bjørnevik, K., Im, D. S., Flierl, A., Dong, X., Locascio, J. J., et al. (2017).  $\beta$ 2-adrenoreceptor is a regulator of the  $\alpha$ -synuclein gene driving risk of Parkinson's disease. *Science* 357, 891–898. doi: 10.1126/science.aaf3934
- Nakamura, S., and Yoshimori, T. (2017). New insights into autophagosome-lysosome fusion. *J. Cell Sci.* 130, 1209–1216. doi: 10.1242/jcs.196352
- Nath, S., Goodwin, J., Engelborghs, Y., and Pountney, D. L. (2011). Raised calcium promotes  $\alpha$ -synuclein aggregate formation. *Mol. Cell. Neurosci.* 46, 516–526. doi: 10.1016/j.mcn.2010.12.004
- Neumann, M., Müller, V., Kretschmar, H. A., Haass, C., and Kahle, P. J. (2004). Regional distribution of proteinase K-resistant  $\alpha$ -synuclein correlates with Lewy body disease stage. *J. Neuropathol. Exp. Neurol.* 63, 1225–1235. doi: 10.1093/jnen/63.12.1225
- Nunnari, J., and Suomalainen, A. (2012). Mitochondria: in sickness and in health. *Cell* 148, 1145–1159. doi: 10.1016/j.cell.2012.02.035
- Nussbaum, R. L., and Ellis, C. E. (2003). Alzheimer's disease and Parkinson's disease. *N. Engl. J. Med.* 348, 1356–1364. doi: 10.1056/NEJM2003ra020003
- Obeso, J. A., Stamelou, M., Goetz, C. G., Poewe, W., Lang, A. E., Weintraub, D., et al. (2017). Past, present, and future of Parkinson's disease: a special essay on the 200th anniversary of the shaking palsy. *Mov. Disord.* 32, 1264–1310. doi: 10.1002/mds.27115
- Oueslati, A. (2016). Implication of  $\alpha$ -synuclein phosphorylation at S129 in synucleinopathies: what have we learned in the last decade? *J. Parkinsons Dis.* 6, 39–51. doi: 10.3233/jpd-160779
- Outeiro, T. F., Putcha, P., Tetzlaff, J. E., Spoelgen, R., Koker, M., Carvalho, F., et al. (2008). Formation of toxic oligomeric  $\alpha$ -synuclein species in living cells. *PLoS One* 3:e1867. doi: 10.1371/journal.pone.0001867
- Parihar, M. S., Parihar, A., Fujita, M., Hashimoto, M., and Ghafourifar, P. (2009).  $\alpha$ -Synuclein overexpression and aggregation exacerbates impairment of mitochondrial functions by augmenting oxidative stress in human neuroblastoma cells. *Int. J. Biochem. Cell Biol.* 41, 2015–2024. doi: 10.1016/j.biocel.2009.05.008
- Parkkinen, L., Pirttilä, T., Tervahauta, M., and Alafuzoff, I. (2005). Widespread and abundant  $\alpha$ -synuclein pathology in a neurologically unimpaired subject. *Neuropathology* 25, 304–314. doi: 10.1111/j.1440-1789.2005.00644.x
- Paupe, V., and Prudent, J. (2018). New insights into the role of mitochondrial calcium homeostasis in cell migration. *Biochem. Biophys. Res. Commun.* 500, 75–86. doi: 10.1016/j.bbrc.2017.05.039
- Peelaerts, W., Bousset, L., Van der Perren, A., Moskalyuk, A., Pulizzi, R., Giugliano, M., et al. (2015).  $\alpha$ -Synuclein strains cause distinct synucleinopathies after local and systemic administration. *Nature* 522, 340–344. doi: 10.1038/nature14547
- Poehler, A.-M., Xiang, W., Spitzer, P., May, V. E. L., Meixner, H., Rockenstein, E., et al. (2014). Autophagy modulates SNCA/ $\alpha$ -synuclein release, thereby generating a hostile microenvironment. *Autophagy* 10, 2171–2192. doi: 10.4161/auto.36436
- Poewe, W. (2009). Treatments for Parkinson disease—past achievements and current clinical needs. *Neurology* 72, S65–S73. doi: 10.1212/WNL.0b013e31819908ce
- Polymeropoulos, M. H., Higgins, J. J., Golbe, L. I., Johnson, W. G., Ide, S. E., Di Iorio, G., et al. (1996). Mapping of a gene for Parkinson's disease to chromosome 4q21–q23. *Science* 274, 1197–1199. doi: 10.1126/science.274.5290.1197
- Polymeropoulos, M. H., Lavedan, C., Leroy, E., Ide, S. E., Dehejia, A., Dutra, A., et al. (1997). Mutation in the  $\alpha$ -synuclein gene identified in families with Parkinson's disease. *Science* 276, 2045–2047. doi: 10.1126/science.276.5321.2045
- Prabhudesai, S., Sinha, S., Attar, A., Kotagiri, A., Fitzmaurice, A. G., Lakshmanan, R., et al. (2012). A novel “molecular tweezer” inhibitor of  $\alpha$ -synuclein neurotoxicity *in vitro* and *in vivo*. *Neurotherapeutics* 9, 464–476. doi: 10.1007/s13311-012-0105-1
- Prusiner, S. B., Woerman, A. L., Mordes, D. A., Watts, J. C., Rampersaud, R., Berry, D. B., et al. (2015). Evidence for  $\alpha$ -synuclein prions causing multiple system atrophy in humans with parkinsonism. *Proc. Natl. Acad. Sci. U S A* 112, E5308–E5317. doi: 10.1073/pnas.1514475112
- Przedborski, S., Jackson-Lewis, V., Naini, A. B., Jakowec, M., Petzinger, G., Miller, R., et al. (2001). The parkinsonian toxin 1-methyl-4-phenyl-1,2,3,6-tetrahydropyridine (MPTP): a technical review of its utility and safety. *J. Neurochem.* 76, 1265–1274. doi: 10.1046/j.1471-4159.2001.00183.x
- Qin, Z., Hu, D., Han, S., Reaney, S. H., Di Monte, D. A., and Fink, A. L. (2007). Effect of 4-hydroxy-2-nonenal modification on  $\alpha$ -synuclein aggregation. *J. Biol. Chem.* 282, 5862–5870. doi: 10.1074/jbc.M608126200
- Ramakrishnan, M., Jensen, P. H., and Marsh, D. (2006). Association of R-synuclein and mutants with lipid membranes: spin-label ESR and polarized IR. *Biochemistry* 45, 3386–3395. doi: 10.1021/bi052344d
- Recasens, A., Dehay, B., Bové, J., Carballo-Carbajal, I., Dovero, S., Pérez-Villalba, A., et al. (2014). Lewy body extracts from Parkinson disease brains trigger  $\alpha$ -synuclein pathology and neurodegeneration in mice and monkeys. *Ann. Neurol.* 75, 351–362. doi: 10.1002/ana.24066
- Rego, A. C., and Oliveira, C. R. (2003). Mitochondrial dysfunction and reactive oxygen species in excitotoxicity and apoptosis: implications for the pathogenesis of neurodegenerative diseases. *Neurochem. Res.* 28, 1563–1574. doi: 10.1023/a:1025682611389
- Ricciardi, L., Petrucci, S., Guidubaldi, A., Ialongo, T., Serra, L., Ferraris, A., et al. (2014). Phenotypic variability of PINK1 expression: 12 Years' clinical follow-up of two Italian families. *Mov. Disord.* 29, 1561–1566. doi: 10.1002/mds.25994
- Richter, C., Park, J. W., and Ames, B. N. (1988). Normal oxidative damage to mitochondrial and nuclear DNA is extensive. *Proc. Natl. Acad. Sci. U S A* 85, 6465–6467. doi: 10.1073/pnas.85.17.6465
- Richter, F., Subramaniam, S. R., Magen, I., Lee, P., Hayes, J., Attar, A., et al. (2017). A molecular tweezer ameliorates motor deficits in mice overexpressing  $\alpha$ -synuclein. *Neurotherapeutics* 14, 1107–1119. doi: 10.1007/s13311-017-0544-9
- Ruf, R. A. S., Lutz, E. A., Zigoneanu, I. G., and Pielak, G. J. (2008).  $\alpha$ -Synuclein conformation affects its tyrosine-dependent oxidative aggregation. *Biochemistry* 47, 13604–13609. doi: 1904942
- Sacino, A. N., Brooks, M., Thomas, M. A., McKinney, A. B., McGarvey, N. H., Rutherford, N. J., et al. (2014). Amyloidogenic  $\alpha$ -synuclein seeds do not invariably induce rapid, widespread pathology in mice. *Acta Neuropathol.* 127, 645–665. doi: 10.1007/s00401-014-1268-0
- Samuel, F., Flavin, W. P., Iqbal, S., Pacelli, C., Sri Renganathan, S. D., Trudeau, L.-E., et al. (2016). Effects of serine 129 phosphorylation on  $\alpha$ -synuclein aggregation, membrane association, and internalization. *J. Biol. Chem.* 291, 4374–4385. doi: 10.1074/jbc.M115.705095
- Sanchez-Guajardo, V., Annibali, A., Jensen, P. H., and Romero-Ramos, M. (2013).  $\alpha$ -Synuclein vaccination prevents the accumulation of parkinson disease-like pathologic inclusions in striatum in association with regulatory T cell recruitment in a rat model. *J. Neuropathol. Exp. Neurol.* 72, 624–645. doi: 10.1097/NEN.0b013e31829768d2
- Sapru, M. K., Yates, J. W., Hogan, S., Jiang, L., Halter, J., and Bohn, M. C. (2006). Silencing of human  $\alpha$ -synuclein *in vitro* and in rat brain using lentiviral-mediated RNAi. *Exp. Neurol.* 198, 382–390. doi: 10.1016/j.expneurol.2005.12.024
- Sarkar, S., Davies, J. E., Huang, Z., Tunnacliffe, A., and Rubinsztein, D. C. (2007). Trehalose, a novel mTOR-independent autophagy enhancer, accelerates the clearance of mutant huntingtin and  $\alpha$ -synuclein. *J. Biol. Chem.* 282, 5641–5652. doi: 10.1074/jbc.M609532200
- Schenk, D. B., Koller, M., Ness, D. K., Griffith, S. G., Grundman, M., Zago, W., et al. (2017). First-in-human assessment of PRX002, an anti- $\alpha$ -synuclein monoclonal antibody, in healthy volunteers. *Mov. Disord.* 32, 211–218. doi: 10.1002/mds.26878



- Schrader, T., Bitan, G., and Klärner, F. G. (2016). Molecular tweezers for lysine and arginine-powerful inhibitors of pathologic protein aggregation. *Chem. Commun.* 52, 11318–11334. doi: 10.1039/c6cc04640a
- Schwab, K., Frahm, S., Horsley, D., Rickard, J. E., Melis, V., Goatman, E. A., et al. (2018). A protein aggregation inhibitor, leuco-methylthioninium Bis(Hydromethanesulfonate), decreases  $\alpha$ -synuclein inclusions in a transgenic mouse model of synucleinopathy. *Front. Mol. Neurosci.* 10:447. doi: 10.3389/fnmol.2017.00447
- Senior, S. L., Ninkina, N., Deacon, R., Bannerman, D., Buchman, V. L., Cragg, S. J., et al. (2008). Increased striatal dopamine release and hyperdopaminergic-like behaviour in mice lacking both  $\alpha$ -synuclein and  $\gamma$ -synuclein. *Eur. J. Neurosci.* 27, 947–957. doi: 10.1111/j.1460-9568.2008.06055.x
- Sinha, S., Du, Z., Maiti, P., Klärner, F. G., Schrader, T., Wang, C., et al. (2012). Comparison of three amyloid assembly inhibitors: the sugar scyllo-inositol, the polyphenol epigallocatechin gallate, and the molecular tweezer CLR01. *ACS Chem. Neurosci.* 3, 451–458. doi: 10.1021/cn200133x
- Sinha, S., Lopes, D. H. J., Du, Z., Pang, E. S., Shanmugam, A., Lomakin, A., et al. (2011). Lysine-specific molecular tweezers are broad-spectrum inhibitors of assembly and toxicity of amyloid proteins. *J. Am. Chem. Soc.* 133, 16958–16969. doi: 10.1021/ja206279b
- Smaldone, G., Diana, D., Pollegioni, L., Di Gaetano, S., Fattorusso, R., and Pedone, E. (2015). Insight into conformational modification of  $\alpha$ -synuclein in the presence of neuronal whole cells and of their isolated membranes. *FEBS Lett.* 589, 798–804. doi: 10.1016/j.febslet.2015.02.012
- Smith, W. W., Jiang, H., Pei, Z., Tanaka, Y., Morita, H., Sawa, A., et al. (2005). Endoplasmic reticulum stress and mitochondrial cell death pathways mediate A53T mutant  $\alpha$ -synuclein-induced toxicity. *Hum. Mol. Genet.* 14, 3801–3811. doi: 10.1093/hmg/ddi396
- Sokolov, Y., Kozak, J. A., Kaye, R., Chanturiya, A., Glabe, C., and Hall, J. E. (2006). Soluble amyloid oligomers increase bilayer conductance by altering dielectric structure. *J. Gen. Physiol.* 128, 637–647. doi: 10.1085/jgp.200609533
- Sorrentino, Z. A., Brooks, M. M. T., Hudson, V. III., Rutherford, N. J., Golde, T. E., Giasson, B. I., et al. (2017). Intrastriatal injection of  $\alpha$ -synuclein can lead to widespread synucleinopathy independent of neuroanatomic connectivity. *Mol. Neurodegener.* 12:40. doi: 10.1186/s13024-017-0182-z
- Spillantini, M. G., Crowther, R. A., Jakes, R., Cairns, N. J., Lantos, P. L., and Goedert, M. (1998). Filamentous  $\alpha$ -synuclein inclusions link multiple system atrophy with Parkinson's disease and dementia with Lewy bodies. *Neurosci. Lett.* 251, 205–208. doi: 10.1016/s0304-3940(98)00504-7
- Spillantini, M. G., Schmidt, M. L., Lee, V. M.-Y., Trojanowski, J. Q., Jakes, R., and Goedert, M. (1997).  $\alpha$ -synuclein in lewy bodies. *Nature* 388, 839–840. doi: 10.1038/42166
- Stacy, M. (2011). Nonmotor symptoms in Parkinson's disease. *Int. J. Neurosci.* 121, 9–17. doi: 10.3109/00207454.2011.620196
- Svensson, E., Horváth-Puhó, E., Thomsen, R. W., Djurhuus, J. C., Pedersen, L., Borghammer, P., et al. (2015). Vagotomy and subsequent risk of Parkinson's disease. *Ann. Neurol.* 78, 522–529. doi: 10.1002/ana.24448
- Tenreiro, S., Eckermann, K., and Outeiro, T. F. (2014). Protein phosphorylation in neurodegeneration: friend or foe? *Front. Mol. Neurosci.* 7:42. doi: 10.3389/fnmol.2014.00042
- Tuttle, M. D., Comellas, G., Nieuwkoop, A. J., Covell, D. J., Berthold, D. A., Kloepper, K. D., et al. (2016). Solid-state NMR structure of a pathogenic fibril of full-length human  $\alpha$ -synuclein. *Nat. Struct. Mol. Biol.* 23, 409–415. doi: 10.1038/nsmb.3194
- Ueda, K., Fukushima, H., Masliah, E., Xia, Y., Iwai, A., Yoshimoto, M., et al. (1993). Molecular cloning of cDNA encoding an unrecognized component of amyloid in Alzheimer disease. *Proc. Natl. Acad. Sci. U S A* 90, 11282–11286. doi: 10.1073/pnas.90.23.11282
- Ullman, O., Fisher, C. K., and Stultz, C. M. (2011). Explaining the structural plasticity of  $\alpha$ -synuclein. *J. Am. Chem. Soc.* 133, 19536–19546. doi: 10.1021/ja208657z
- Valente, E. M., Abou-Sleiman, P. M., Caput, V., Muqit, M. M. K., Harvey, K., Gispert, S., et al. (2004). Hereditary early-onset Parkinson's disease caused by mutations in PINK1. *Science* 302, 1158–1160. doi: 10.1126/science.1096284
- Volles, M. J., and Lansbury, P. T. (2002). Vesicle permeabilization by protofibrillar  $\alpha$ -synuclein is sensitive to Parkinson's disease-linked mutations and occurs by a pore-like mechanism. *Biochemistry* 41, 4595–4602. doi: 10.1021/bi0121353
- Volpicelli-Daley, L., and Brundin, P. (2018). Chapter 17 – Prion-like propagation of pathology in Parkinson disease. *Handb. Clin. Neurol.* 153, 321–335. doi: 10.1016/B978-0-444-63945-5.00017-9
- Wagner, J., Ryazanov, S., Leonov, A., Levin, J., Shi, S., Schmidt, F., et al. (2013). Anle138b: a novel oligomer modulator for disease-modifying therapy of neurodegenerative diseases such as prion and Parkinson's disease. *Acta Neuropathol.* 125, 795–813. doi: 10.1007/s00401-013-1114-9
- Wang, W., Perovic, I., Chittuluru, J., Kaganovich, A., Nguyen, L. T. T., Liao, J., et al. (2011). A soluble  $\alpha$ -synuclein construct forms a dynamic tetramer. *Proc. Natl. Acad. Sci. U S A* 108, 17797–17802. doi: 10.1073/pnas.1113260108
- Webb, J. L., Ravikumar, B., Atkins, J., Skepper, J. N., and Rubinsztein, D. C. (2003).  $\alpha$ -Synuclein is degraded by both autophagy and the proteasome. *J. Biol. Chem.* 278, 25009–25013. doi: 10.1074/jbc.m300227200
- Weihofen, A., Liu, Y., Arndt, J. W., Huy, C., Quan, C., Smith, B. A., et al. (2019). Development of an aggregate-selective, human-derived  $\alpha$ -synuclein antibody B1B054 that ameliorates disease phenotypes in Parkinson's disease models. *Neurobiol. Dis.* 124, 276–288. doi: 10.1016/j.nbd.2018.10.016
- West, A. B. (2017). Achieving neuroprotection with LRRK2 kinase inhibitors in Parkinson disease. *Exp. Neurol.* 298, 236–245. doi: 10.1016/j.expneurol.2017.07.019
- Wiseman, H., and Halliwell, B. (1996). Damage to DNA by reactive oxygen and nitrogen species: role in inflammatory disease and progression to cancer. *Biochem. J.* 313, 17–29. doi: 10.1042/bj3130017
- Wong, Y. C., and Holzbaur, E. L. F. (2015). Autophagosome dynamics in neurodegeneration at a glance. *J. Cell Sci.* 128, 1259–1267. doi: 10.1242/jcs.161216
- Wong, Y. C., and Krainc, D. (2017).  $\alpha$ -synuclein toxicity in neurodegeneration: mechanism and therapeutic strategies. *Nat. Med.* 23, 1–13. doi: 10.1038/nm.4269
- Wrasidlo, W., Tsigelny, I. F., Price, D. L., Dutta, G., Rockenstein, E., Schwarz, T. C., et al. (2016). A *de novo* compound targeting  $\alpha$ -synuclein improves deficits in models of Parkinson's disease. *Brain* 139, 3217–3236. doi: 10.1093/brain/aww238
- Xu, C., Bailly-Maitre, B., and Reed, J. C. (2005). Endoplasmic reticulum stress: cell life and death decisions. *J. Clin. Invest.* 115, 2656–2664. doi: 10.1172/jci26373
- Zambon, F., Cherubini, M., Fernandes, H. J. R., Lang, C., Ryan, B. J., Volpato, V., et al. (2019). Cellular  $\alpha$ -synuclein pathology is associated with bioenergetic dysfunction in Parkinson's iPSC-derived dopamine neurons. *Hum. Mol. Genet.* 28, 2001–2013. doi: 10.1093/hmg/ddz038
- Zha, J., Liu, X.-M., Zhu, J., Liu, S.-Y., Lu, S., Xu, P.-X., et al. (2016). A scFv antibody targeting common oligomeric epitope has potential for treating several amyloidoses. *Sci. Rep.* 6:36631. doi: 10.1038/srep36631
- Zhou, C., Emadi, S., Sierks, M. R., and Messer, A. (2004). A human single-chain Fv intrabody blocks aberrant cellular effects of overexpressed  $\alpha$ -synuclein. *Mol. Ther.* 10, 1023–1031. doi: 10.1016/j.ymthe.2004.08.019
- Zhu, M., Rajamani, S., Kaylor, J., Han, S., Zhou, F., and Fink, A. L. (2004). The flavonoid baicalein inhibits fibrillation of  $\alpha$ -synuclein and disaggregates existing fibrils. *J. Biol. Chem.* 279, 26846–26857. doi: 10.1074/jbc.m403129200

**Conflict of Interest:** The authors declare that the research was conducted in the absence of any commercial or financial relationships that could be construed as a potential conflict of interest.

Copyright © 2019 Fields, Bengoa-Vergniory and Wade-Martins. This is an open-access article distributed under the terms of the Creative Commons Attribution License (CC BY). The use, distribution or reproduction in other forums is permitted, provided the original author(s) and the copyright owner(s) are credited and that the original publication in this journal is cited, in accordance with accepted academic practice. No use, distribution or reproduction is permitted which does not comply with these terms.



# ZPD-2, a Small Compound That Inhibits $\alpha$ -Synuclein Amyloid Aggregation and Its Seeded Polymerization

Samuel Peña-Díaz<sup>1,2†</sup>, Jordi Pujols<sup>1,2†</sup>, María Conde-Giménez<sup>3</sup>, Anita Čarija<sup>1,2</sup>, Esther Dalfo<sup>4,5†</sup>, Jesús García<sup>6</sup>, Susanna Navarro<sup>1,2</sup>, Francisca Pinheiro<sup>1,2</sup>, Jaime Santos<sup>1,2</sup>, Xavier Salvatella<sup>6,7</sup>, Javier Sancho<sup>3</sup> and Salvador Ventura<sup>1,2,7\*</sup>

<sup>1</sup> Institut de Biotecnologia i Biomedicina, Universitat Autònoma de Barcelona, Barcelona, Spain, <sup>2</sup> Departament de Bioquímica i Biologia Molecular, Universitat Autònoma de Barcelona, Barcelona, Spain, <sup>3</sup> Department of Biochemistry and Molecular and Cell Biology, Institute for Biocomputation and Physics of Complex Systems (BIFI), University of Zaragoza, Zaragoza, Spain, <sup>4</sup> Faculty of Medicine, M2, Universitat Autònoma de Barcelona, Barcelona, Spain, <sup>5</sup> Faculty of Medicine, University of Vic – Central University of Catalonia, Vic, Spain, <sup>6</sup> Institute for Research in Biomedicine, The Barcelona Institute of Science and Technology, Barcelona, Spain, <sup>7</sup> Catalan Institute for Research and Advance Studies, Barcelona, Spain

## OPEN ACCESS

### Edited by:

Sandra Macedo-Ribeiro,  
University of Porto, Portugal

### Reviewed by:

Yoshitaka Nagai,  
Osaka University, Japan  
Daniel E. Otzen,  
Aarhus University, Denmark

### \*Correspondence:

Salvador Ventura  
salvador.ventura@uab.es

<sup>†</sup> These authors have contributed  
equally to this work

### \*ORCID:

Esther Dalfo  
orcid.org/0000-0003-4677-8515

**Received:** 10 September 2019

**Accepted:** 28 November 2019

**Published:** 17 December 2019

### Citation:

Peña-Díaz S, Pujols J, Conde-Giménez M, Čarija A, Dalfo E, García J, Navarro S, Pinheiro F, Santos J, Salvatella X, Sancho J and Ventura S (2019) ZPD-2, a Small Compound That Inhibits  $\alpha$ -Synuclein Amyloid Aggregation and Its Seeded Polymerization. *Front. Mol. Neurosci.* 12:306. doi: 10.3389/fnmol.2019.00306

$\alpha$ -Synuclein ( $\alpha$ -Syn) forms toxic intracellular protein inclusions and transmissible amyloid structures in Parkinson's disease (PD). Preventing  $\alpha$ -Syn self-assembly has become one of the most promising approaches in the search for disease-modifying treatments for this neurodegenerative disorder. Here, we describe the capacity of a small molecule (ZPD-2), identified after a high-throughput screening, to inhibit  $\alpha$ -Syn aggregation. ZPD-2 inhibits the aggregation of *wild-type*  $\alpha$ -Syn and the A30P and H50Q familial variants *in vitro* at substoichiometric compound:protein ratios. In addition, the molecule prevents the spreading of  $\alpha$ -Syn seeds in protein misfolding cyclic amplification assays. ZPD-2 is active against different  $\alpha$ -Syn strains and blocks their seeded polymerization. Treating with ZPD-2 two different PD *Caenorhabditis elegans* models that express  $\alpha$ -Syn either in muscle or in dopaminergic (DA) neurons substantially reduces the number of  $\alpha$ -Syn inclusions and decreases synuclein-induced DA neurons degeneration. Overall, ZPD-2 is a hit compound worth to be explored in order to develop lead molecules for therapeutic intervention in PD.

**Keywords:** Parkinson's disease,  $\alpha$ -synuclein, amyloid, protein aggregation, aggregation inhibitor, *Caenorhabditis elegans*, neurodegeneration

## INTRODUCTION

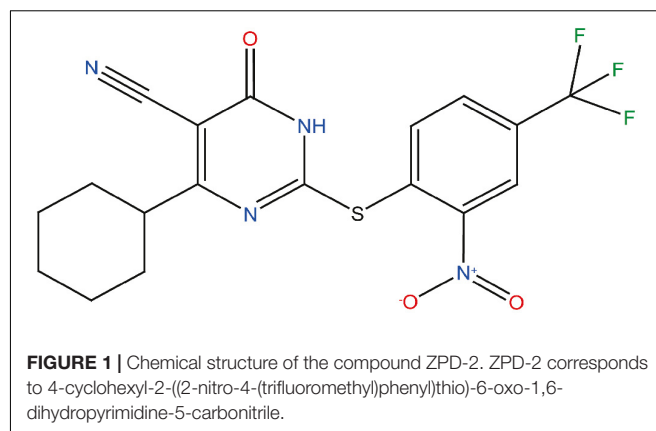
Parkinson's disease (PD) is a neurodegenerative disorder that affects about 0.3% of the population and >1% of people over 60 years of age (4% over 80 years) (Nussbaum and Ellis, 2003; Dexter and Jenner, 2013). It is characterized by the loss of dopaminergic (DA) neurons in *substantia nigra pars compacta*, which compromises the motor capacity of PD-suffering patients, producing tremor, rigidity, and bradykinesia (Marti et al., 2003). Additionally, since the disease spreads to the cerebral cortex (Braak et al., 2003), symptoms could include emotional and cognitive impairment (Marti et al., 2003). Nowadays, treatments are focused on alleviating the above mentioned motor

symptoms, mostly using dopamine replacement by administration of dopamine precursor (L-DOPA), combined with carbidopa, a L-DOPA decarboxylase inhibitor, and/or catechol-O-methyl transferase inhibitors and monoamine oxidase-B inhibitors (Dexter and Jenner, 2013). However, these treatments do not prevent the progression of PD and they lose efficacy as the disease advances.

Parkinson's disease is pathologically characterized by the accumulation of protein aggregates in the neuronal body, Lewy's bodies (LB), and/or fibrils deposited in neuronal processes, Lewy's neurites (LN), of affected neurons (Spillantini et al., 1997). These inclusions are mainly composed of  $\alpha$ -synuclein ( $\alpha$ -Syn), a protein predominantly expressed in the synaptic termination of DA neurons (Bendor et al., 2013). This evidence, together with the identification of mutations in the gene that encodes for this protein (SNCA) as the cause behind familial cases of PD (Polymeropoulos et al., 1997) and the observation that duplications and triplications of the SNCA gene lead to highly penetrant forms of the disease (Singleton et al., 2003; Ibanez et al., 2004) directly connect PD and  $\alpha$ -Syn. In fact, the presence of aggregated  $\alpha$ -Syn in the brain is a common feature of a group of diseases named synucleinopathies, which, in addition to PD, include Dementia with Lewy's bodies (DLB) and multiple system atrophy (MSA), among others (Marti et al., 2003).

In solution,  $\alpha$ -Syn is a 140 amino acid intrinsically disordered protein whose function seems to be related with vesicle trafficking (Bendor et al., 2013). *In vitro* it forms thermodynamically stable amyloid aggregates (Serpell et al., 2000) that can display different conformational features (Li et al., 2018). The formation of amyloids by  $\alpha$ -Syn follows the typical sigmoidal kinetics, reflecting a nucleation-polymerization process (Sabate et al., 2003); although secondary nucleation reactions might also occur (Xue et al., 2010). *In vivo*,  $\alpha$ -Syn assemblies exert a toxic effect (Winner et al., 2011) and could be transmitted from cell to cell in a prion-like manner by seeding native  $\alpha$ -Syn aggregation in previously unaffected neurons (Hansen et al., 2011).

Preventing  $\alpha$ -Syn aggregation seems to hold the potential to achieve significant therapeutic impact. Several strategies have been developed toward this objective: SNCA gene-silencing approaches to decrease the protein levels (McCormack et al., 2010), methods to increase the clearance of aggregated  $\alpha$ -Syn by autophagic and proteasomal machineries (Gao et al., 2019), and molecules intended to avoid the formation and/or propagation of aggregated  $\alpha$ -Syn (Dehay et al., 2015; Hauser, 2015). One of the main limitations of this last strategy is the absence of a well-defined structure of monomeric  $\alpha$ -Syn in solution, due to its intrinsically disordered nature, which hampers the rational design of inhibitors. High-throughput screening protocols have been developed to circumvent this problem (Silva et al., 2011; Levin et al., 2014). A number of promising small molecules have been discovered with this approach, including anle138b (Levin et al., 2014), BIOD303 (Moree et al., 2015), fasudil (Tatenhorst et al., 2016), squalamine (Perni et al., 2017), or SynuClean-D (SCD) (Pujols et al., 2018). In this context, we have developed a robust screening and validation protocol to analyze large chemical libraries in the search for effective inhibitors of  $\alpha$ -Syn aggregation (Pujols et al., 2017). The *in vitro* pipeline



integrates thioflavin-T (Th-T) fluorescence and light scattering measurements, transmission electron microscopy (TEM), and protein misfolding cyclic amplification assays (PMCA). This approach allowed us to identify ZPD-2 (**Figure 1**) as a novel small molecule able to inhibit the aggregation of *wild-type* (WT)  $\alpha$ -Syn, as well as that of the A30P (Kruger et al., 1998) and H50Q (Appel-Cresswell et al., 2013) familial mutants, being active against the seeded polymerization of different  $\alpha$ -Syn strains. The compound displayed low toxicity for neuronal human cells and demonstrated significant inhibitory capacity in two well-established *Caenorhabditis elegans* models of PD (van Ham et al., 2008; Harrington et al., 2012).

## MATERIALS AND METHODS

### Protein Purification

Protein expression and purification of WT  $\alpha$ -Syn and its variants (H50Q and A30P) were carried out as previously described (Pujols et al., 2017) and the resulting purified protein was lyophilized and kept at  $-80^{\circ}\text{C}$  until its use.

### *In vitro* Aggregation of $\alpha$ -Syn

$\alpha$ -Syn was resuspended in sterile PBS and filtered through 0.22  $\mu\text{m}$  membranes to remove small aggregates. Aggregation was performed in a sealed 96-well plate, containing 70  $\mu\text{M}$   $\alpha$ -Syn (WT, A30P or H50Q), 40  $\mu\text{M}$  Th-T in PBS 1 $\times$ , a 1/8" diameter Teflon polyball (Polysciences Europe GmbH, Eppelheim, Germany) and 100  $\mu\text{M}$  ZPD-2 or DMSO (in control samples) in a total volume of 150  $\mu\text{L}$  per well. The plate was incubated at 100 rpm and  $37^{\circ}\text{C}$  after having been fixed in an orbital culture shaker Max-Q 4000 (ThermoScientific, Waltham, MA, United States). Measurements of Th-T fluorescence were done every 2 h in a Victor3.0 Multilabel Reader (PerkinElmer, Waltham, MA, United States), exciting through a 430–450 nm filter and collecting the emission signal with a 480–510 filter. Each assay was done in triplicate. The values of the aggregation kinetics were fitted to the following Eq. 1 (Crespo et al., 2016):

$$\alpha = 1 - \frac{1}{k_b(e^{k_a t} - 1) + 1} \quad (1)$$

where  $k_b$  and  $k_a$  constitute the homogeneous nucleation rate constant and the secondary rate constant (fibril elongation and secondary nucleation), respectively (Crespo et al., 2016).

Titration assays were done by applying different ZPD-2 concentrations (200, 150, 100, 75, 50, 25, and 10  $\mu$ M). Time-dependent assays were developed by adding 100  $\mu$ M of ZPD-2 at different time points after the beginning of the reaction (4, 8, 12, 16, 20, and 24 h). In all cases a fixed concentration of  $\alpha$ -Syn at 70  $\mu$ M was maintained.

Strains were generated as previously described (Bousset et al., 2013; Peelaerts et al., 2015; Carija et al., 2019). Briefly, lyophilized  $\alpha$ -Syn was resuspended in PBS 1 $\times$  and dialyzed for 24 h in a 1:1000 (v/v) ratio with buffer B (50 mM Tris-HCl pH 7.0), or buffer C (50 mM Tris-HCl pH 7.0 supplemented with 150 mM NaCl). Then, the protein was filtered through 0.22  $\mu$ m membrane and incubated at 70  $\mu$ M in presence or absence of 100  $\mu$ M ZPD-2 in a 96-well plate as described above. For the seeding assays,  $\alpha$ -Syn pre-formed fibrils were sonicated for 5 min and then added to the aggregation reaction at ratios of 1% (v/v) for each condition. The plate was then incubated, and Th-T fluorescence measured as previously indicated.

The soluble fraction was obtained for subsequent quantification by centrifuging 300  $\mu$ L of aggregated sample at 16,900  $\times g$  for 90 min. The supernatant was then recovered and loaded into a Tricine-SDS-PAGE gel. Gels were stained with Blue safe. Finally, the density of the  $\alpha$ -Syn bands was calculated using Quantity One software (Bio-Rad, Hercules, CA, United States). Experiments were done at least in triplicate.

## Transmission Electron Microscopy

End-point  $\alpha$ -Syn aggregates incubated for 32 h were collected, diluted 1:10 with PBS 1 $\times$  and sonicated for 5 min. Five microliters of these sonicated samples was placed rapidly on a carbon-coated copper grid and incubated for 5 min. The grids were dried with a filter paper to withdraw the excess of sample and immediately washed twice with miliQ water. Finally, 5  $\mu$ L of 2% (w/v) uranyl acetate was added to the top of the grid and incubated for 2 min. The excess of uranyl acetate was removed with a filter paper and grids were left to air-dry for 10 min. Images were obtained using a TEM Jeol 1400 (Peabody, MA, United States) operating at an accelerating voltage of 120 kV. A minimum of 30 fields were screened per sample, in order to collect representative images.

## Light Scattering

End-point  $\alpha$ -Syn aggregates were collected, placed into a quartz cuvette, and analyzed in a Cary Eclipse Fluorescence Spectrophotometer (Agilent, Santa Clara, CA, United States). The sample was excited at 300 nm and the subsequent scattering at 90° monitored between 280 and 320 nm.

## Protein Misfolding Cyclic Amplification

The PMCA assay was carried out as previously described (Herva et al., 2014). Briefly,  $\alpha$ -Syn was resuspended to a final concentration of 90  $\mu$ M in Conversion Buffer (PBS 1 $\times$ , 1% Triton X-100, 150 mM NaCl), supplemented with Complete Protease Inhibitor Mixture (Roche Applied Science, Penzberg, Germany).

Sixty microliters of this  $\alpha$ -Syn solution was added into 200- $\mu$ L PCR tubes containing 1.0 mm silica beads (Biospec Products, Bartlesville, OK, United States). Samples were exposed to 24-h cycles of 30 s sonication and 30 min incubation at 37°C, using a Misonix 4000 sonicator, at 70% power. After every 24 h-cycle, 1  $\mu$ L of the incubated sample was added to a new PCR-tube containing fresh  $\alpha$ -Syn. This process was repeated for 5 days. In the case of treated samples, ZPD-2 was added in each cycle to the fresh non-sonicated sample to a final concentration of 128  $\mu$ M, which corresponds to the 0.7:1  $\alpha$ -Syn:ZPD-2 ratio of the previous set of aggregation kinetics assays. Untreated samples were prepared adding the same concentration of DMSO (0.26%) present in the treated mixtures. All the reactions were made in triplicate.

At the end of each cycle, 10  $\mu$ L of the incubated samples were diluted 1:10 with 90  $\mu$ L of PBS 1 $\times$ , 40  $\mu$ M Th-T. Th-T fluorescence was measured in a Cary Eclipse Fluorescence Spectrophotometer (Agilent, Santa Clara, CA, United States), exciting at 445 nm and collecting the emission signal between 460 and 600 nm.

## Proteinase K Digestion

For protein digestion, 6  $\mu$ L of Proteinase K (5  $\mu$ g/mL final concentration) was added to 18  $\mu$ L of PMCA aggregated samples and incubated for 30 min at 37°C. After the incubation, 8  $\mu$ L of loading buffer containing 1%  $\beta$ -mercaptoethanol was added and the enzyme was thermally inactivated at 95°C for 10 min. Finally, 7  $\mu$ L of the incubated and stained samples was loaded into a Tricine-SDS-PAGE gel together with unstained Protein Standard markers (ThermoFisher Scientific, Waltham, MA, United States). Gels were stained with Blue safe.

## Nuclear Magnetic Resonance

Expression of  $^{15}$ N-labeled human WT  $\alpha$ -Syn was carried out in *Escherichia coli* BL21 DE3 strain. First, cells were grown in LB medium until an OD<sub>600</sub> of 0.6. The culture was then centrifuged at 3000 rpm for 15 min and the pellets collected and resuspended in 1 L minimal medium, composed of: 768 mL of miliQ water with 1 mL of ampicillin 100 mg/mL, 100  $\mu$ L CaCl<sub>2</sub> 1 M, 2 mL MgSO<sub>4</sub> 2 M, 20 mL glucose 20%, 10 mL vitamins 100 $\times$  (Sigma-Aldrich, Darmstadt, Germany), 200 mL salts M9, and 1 g  $^{15}$ NH<sub>4</sub> (Cambridge Isotope Laboratories, Inc., Tewksbury, MA, United States). Cells were incubated for 1 h at 37°C and 250 rpm. After that, protein expression was induced for 4 h with 1 mM IPTG. Protein was purified as previously described (Pujols et al., 2017).

$^1$ H- $^{15}$ N HSQC spectra were obtained at 20°C on a Bruker 600 MHz NMR spectrometer equipped with a cryoprobe in a mixture containing 70  $\mu$ M  $^{15}$ N-labeled  $\alpha$ -Syn, PBS buffer (pH 7.4), 2.5% d<sub>6</sub>-DMSO, and 10% D<sub>2</sub>O in the absence or in the presence of 100  $\mu$ M ZPD-2.

## Toxicity Assays

Neuroblastoma cells were incubated 24 h in DMEM medium in a 96-well plate before the addition of different concentrations of ZPD-2 (from 1  $\mu$ M to 1 mM). Cells were incubated for 48 h at 37°C and PrestoBlue® reagent



(ThermoFisher Scientific, Waltham, MA, United States) was added to analyze cell death. Treated and untreated cells were incubated with PrestoBlue® for 10 min at 37°C. Finally, fluorescence emission was measured by exciting at 560 nm and collecting at 590 nm.

## Caenorhabditis elegans Assays

### Maintenance

Animals synchronization was carried out by bleaching and overnight hatching in M9 (3 g/L  $\text{KH}_2\text{PO}_4$ , 6 g/L  $\text{Na}_2\text{HPO}_4$ , 5 g/L NaCl, 1 M  $\text{MgSO}_4$ ) buffer. Thus, nematodes were cultured at 20°C on growth media plates (NGM) containing 1 mM  $\text{CaCl}_2$ , 1 mM  $\text{MgSO}_4$ , 5  $\mu\text{g/mL}$  cholesterol, 250 M  $\text{KH}_2\text{PO}_4$  pH 6.0, 17 g/L Agar, and 3 g/L NaCl. Plates were previously seeded with *E. coli OP50* strain. Nematodes were maintained using standard protocols (Brenner, 1974).

### Strains

Strain NL5901, *unc-119(ed3) III; pkIs2386 [Punc-54: $\alpha$ -SYN:YFP; unc-119(+)]* was obtained from the *C. elegans* Genetic Center (CGC). For the  $\alpha$ -Syn-induced DA degeneration analysis, strain UA196 (Harrington et al., 2012), gifted generously by the laboratory of Dr. Guy Caldwell (Department of Biological Science, The University of Alabama, Tuscaloosa, AL, United States), was used; [*sid-1(pk3321); baIn33 (Pdat-1:sid-1, Pmyo-2:mCherry); baIn11 (Pdat-1: $\alpha$ -SYN; Pdat-1:GFP)*]. In the main text, this strain was named *Pdat-1:GFP; Pdat-1: $\alpha$ -SYN*.

### ZPD-2 Administration

After cooled, the autoclaved NGM agar medium (1 mM  $\text{CaCl}_2$ , 1 mM  $\text{MgSO}_4$ , 5  $\mu\text{g/mL}$  cholesterol, 250 M  $\text{KH}_2\text{PO}_4$  pH 6.0, 17 g/L Agar, and 3 g/L NaCl) was enriched with 100  $\mu\text{M}$  of a stock of ZPD-2 in 0.2% DMSO to a final concentration of 10  $\mu\text{M}$ . After 2 days, plates were seeded with 250  $\mu\text{L}$  of *E. coli OP50* with 10  $\mu\text{M}$  of ZPD-2. Nematodes were placed on the plates at larval stages L4 and exposed either to ZPD-2 or DMSO (controls) for 7 days. Daily transfer was done to avoid cross progeny.

### Aggregate Quantification

The number of cellular inclusions was quantified as previously described (van Ham et al., 2008; Munoz-Lobato et al., 2014). Briefly, NL5901 (*Punc-54: $\alpha$ -SYN:YFP*) worms were age-synchronized and left overnight to hatch. Nematodes in phase L1 were cultured and grown into individual NGM plates seeded with *E. coli OP50*. When animals reached L4 developmental stage, they were transferred onto either ZPD-2-treated plates or DMSO-treated plates (negative control). Every day, animals were transferred into a new plate to avoid cross contamination. At stage L4 + 7, the aggregates in the anterior part of every single animal were counted. For each experiment, 30 7-day-old nematodes per treatment were analyzed using a Nikon Eclipse E800 epifluorescence microscope equipped with an Endow GFP HYQ filter cube (Chroma Technology Corp., Bellows Falls, VT, United States) and each experiment was carried out in triplicate. Inclusions could be described as discrete bright structures, with edges

distinguishable from surrounding fluorescence. ImageJ software was used for measuring the number of cellular aggregates considering the area dimensions. For the quantification of  $\alpha$ -syn aggregates in *C. elegans* one single image was taken from each animal. Every image contained among 30–45 stacks (1  $\mu\text{m}$ ) that allowed to detect aggregates at different animal positions. At least 30 animals were imaged for each assayed condition.

### C. elegans Lifespan Analysis

L4-stage synchronized *C. elegans* were exposed to 10  $\mu\text{M}$  of ZPD-2 or DMSO (controls) during lifespan analysis. The worms were classified as alive, dead, or censored every 2 days by determining their movement and response to nose and tail tap. The numbers of alive and dead worms were recorded until all worms perished. The data were plotted as a Kaplan–Meier survival curve and groups compared using a Wilcoxon-test.

### C. elegans Neurodegeneration Assays

Worms were analyzed for  $\alpha$ -Syn-induced DA neurodegeneration as described previously (Harrington et al., 2012). Briefly, 20–30 L4-staged animals were transferred to ZPD-2 – NGM plates and make them grow up to 7 days (L4 + 7 days of development) after which the DA cell death induced by the over-expression of  $\alpha$ -Syn was analyzed by fluorescence. Plates containing only 0.2% DMSO, without ZPD-2, were used as control. Worms were transferred daily to avoid cross contamination.

The six anterior DA neurons (four CEP and two ADE DA neurons) were scored for neurodegeneration according to previously described criteria (Sulston et al., 1975; Harrington et al., 2012). Worms were considered normal when all six anterior DA neurons (four CEP, cephalic, and two ADE, anterior deirid) were present without any visible signs of degeneration. If a worm displayed degeneration in at least one of the six neurons, it was scored as exhibiting degeneration. For each independent experiment, 30 worms of each treatment were examined under a Nikon Eclipse E800 epifluorescence microscope equipped with an Endow GFP HYQ filter cube (Chroma Technology Corp., Bellows Falls, VT, United States).

### Microscopy and Imaging

Animals were placed in a 1 mM solution of sodium azide and mounted with a coverslip on a 4% agarose pad. Animals were visualized with a Nikon Eclipse E800 epifluorescence microscope. The system acquires a series of frames at specific Z-axis position (focal plane) using a Z-axis motor device. Animals were examined at 100 $\times$  magnification to examine  $\alpha$ -Syn-induced DA cell death and at 40 $\times$  to examine  $\alpha$ -Syn apparent aggregate.

### Statistical Analysis

All graphs were generated with GraphPad Prism 6.0 software (GraphPad Software Inc., La Jolla, CA, United States). Data were analyzed by two-way ANOVA Tukey's HSD test using SPSS software version 20.0 (IBM Analytics, Armonk, NY, United States) and *t*-test using GraphPad software version 6.0 (GraphPad Software Inc., La Jolla, CA, United States).

All data are shown as means and standard error of mean (SEM).  $p < 0.05$  was considered statistically significant. In the graphs \*, \*\*, and \*\*\* indicate  $p < 0.05$ ,  $p < 0.01$ , and  $p < 0.001$ , respectively.

## RESULTS

### ZPD-2 Reduces and Delays the Aggregation of Human $\alpha$ -Synuclein *in vitro*

We designed and optimized a screening protocol that allows to follow the aggregation kinetics of  $\alpha$ -Syn by monitoring Th-T fluorescence emission for 32 h. This approach permitted us to study the inhibitory potential of more than 14,000 compounds (Pujols et al., 2017, 2018). The activity of molecules able to reduce significantly the final amount of Th-positive material and/or impact the nucleation or elongation rates of the reaction was further confirmed using light scattering and TEM measurements at the end of the reaction. This allowed us to identify 30 active compounds, most of which seem not to be connected in terms of structure, precluding QSAR studies. We have previously described the properties of SCD a molecule that acts preferentially on top of  $\alpha$ -Syn proto-fibrillar or fibrillar assemblies (Pujols et al., 2018). Here, we describe the properties of ZPD-2 (Figure 1), a compound that differs in its mechanism of action. SCD and ZPD-2 share a benzotrifluoride group, which suggested that it could constitute the minimal inhibitory unit; however, this group is devoid of any anti-aggregation activity by itself (unpublished), indicating that, most likely, it only acts as a framework for the different active groups in the two molecules.

The incubation of 70  $\mu$ M of  $\alpha$ -Syn in the presence and absence of 100  $\mu$ M of ZPD-2 revealed that the compound modulated the protein aggregation, reducing the formation of Th-T positive structures at the end of the reaction by an 80%, while extending  $t_{50}$  by 8 h (Figure 2A). The analysis of the kinetics revealed a reduction in the nucleation rate constant in presence of ZPD-2 ( $k_b = 0.008833$ ) by threefold, when compared to the control reaction ( $k_b = 0.02754$ ). The autocatalytic rate constant was also lower in the treated sample ( $k_a = 0.2432 \text{ h}^{-1}$ ) than in the control ( $k_a = 0.3230 \text{ h}^{-1}$ ). Light scattering measurements at 300 nm confirmed that the observed reduction in Th-T fluorescence corresponds to an effective decrease in the levels of  $\alpha$ -Syn aggregates, with a 67% decrease in the dispersion of light in the presence of ZPD-2 (Figure 2B). TEM images corroborated that the samples incubated with ZPD-2 (Figure 2D) contained less fibrils per field than the non-treated ones (Figure 2C). In good agreement with these data, quantification of soluble  $\alpha$ -Syn at the end of the aggregation reaction indicated that its level was threefold higher in ZPD-2-treated samples (Supplementary Figure S1A).

Further analysis of the inhibition capacity of ZPD-2 indicated that it exhibited a dose-dependent effect, displaying a statistically significant effect even at 10  $\mu$ M (1:7 compound:protein ratio) (Figure 3A), where the final Th-T signal was reduced by 49%.

To address the time window in which ZPD-2 is active, we set up aggregation reactions with a constant amount of ZPD-2 added at different time points after the reaction begins. A time-dependent response was observed (Figure 3B), with a very significant inhibition when ZPD-2 was added at early (4–8 h) and intermediate (12–16 h) times, and a less pronounced effect when it was added at the plateau phase (20–24 h). This indicates that ZPD-2 is mostly active against the species formed early in the aggregation reaction, consistent with its highest impact on the nucleation rate constant  $k_b$ . Importantly, NMR studies using isotopically labeled monomeric and soluble  $\alpha$ -Syn indicated that ZPD-2 does not interact with its native form, since we could not detect any perturbations in chemical shifts or peak intensities in  $\alpha$ -Syn in the presence of a molar excess of the molecule (Supplementary Figure S2).

Several  $\alpha$ -Syn single point mutations are connected with the onset of familial cases of PD (Kruger et al., 1998; Appel-Cresswell et al., 2013). We studied the ability of ZPD-2 to prevent the aggregation of two of the most frequent and aggressive variants, H50Q and A30P. The molecule was also active against these  $\alpha$ -Syn forms in kinetic assays (Figure 4A). According to the relative Th-T signal at the end of the reaction in ZPD-2-treated and non-treated samples, the molecule inhibited the aggregation of A30P and H50Q by 96 and 94%, respectively (Figure 4B).

### ZPD-2 Prevents $\alpha$ -Syn Seeded Aggregation in Protein Misfolding Cyclic Amplification Assays

Protein misfolding cyclic amplification assays, initially developed to study the polymerization and propagation process of the prion protein (Barria et al., 2012; Morales et al., 2012), has been recently adapted for  $\alpha$ -Syn amyloid aggregation (Herva et al., 2014). Essentially, cycles of incubation at 37°C are followed by vigorous sonication in order to allow fibril growth and subsequent fibrillar rupture, thus producing  $\alpha$ -Syn seeds. These preformed seeds are used to trigger the aggregation of fresh protein in the following cycle, amplifying the fibrillar content. At 90  $\mu$ M of  $\alpha$ -Syn, PMCA produced amyloid structures resistant to protease K (PK) digestion, as observed by SDS-PAGE, with the maximum protection arising after four rounds (Figure 5A, middle). Th-T fluorescence measurements of the same samples indicated that this protection correlates with an increasing presence of amyloid-like assemblies (Figure 5B). In sharp contrast, in the presence of ZPD-2, the amount of PK-resistant protein after four rounds is negligible (Figure 5A, right), Th-T fluorescence signal being also significantly low relative to control samples at this stage (Figure 5B). These results suggested that ZPD-2 was strongly interfering with the PMCA-promoted seeding of  $\alpha$ -Syn amyloids. The fact that Th-T decrease becomes significant only at pass 4, likely indicates that the aggregated non PK-resistant species generated at early steps still retain certain Th-T binding ability, since SDS-PAGE analysis indicates that the levels of PK-resistant

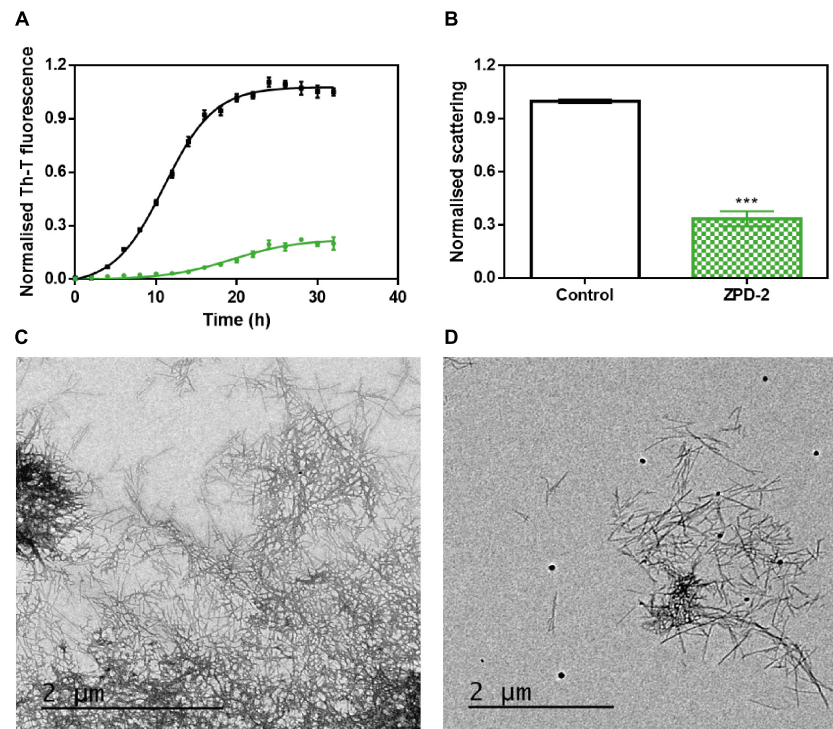


**FIGURE 2 |** ZPD-2 inhibits the aggregation of wild-type  $\alpha$ -synuclein *in vitro*. **(A)** Aggregation kinetics of  $\alpha$ -Syn in absence (black) and presence (green) of ZPD-2. Intensity of Th-T fluorescence is plotted as a function of time. **(B)** Light scattering of end-point aggregates is measured at 300 nm for untreated (white) and ZPD-2-treated samples (green). **(C,D)** Representative TEM images of untreated **(C)** and ZPD-2-treated **(D)** samples. Th-T fluorescence is expressed as normalized means. Final points were obtained at 48 h after the aggregation reaction begin. Error bars are shown as standard errors of mean values, \*\*\* $p < 0.001$ .

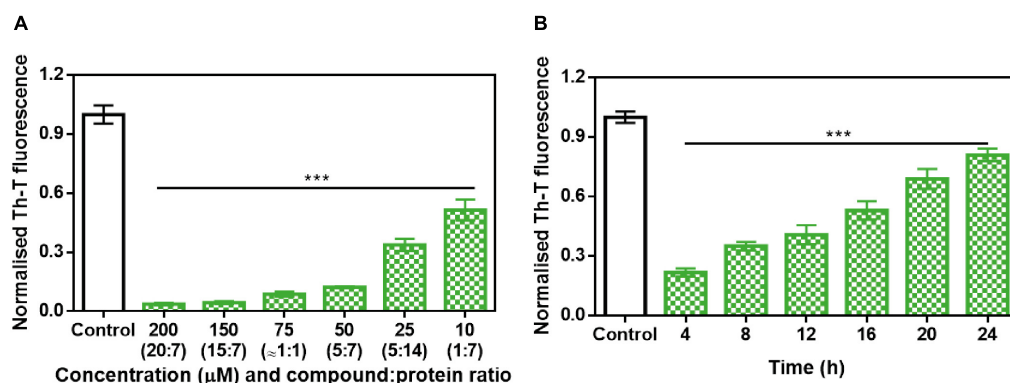


**FIGURE 3 |** Analysis of the inhibitory capacity of ZPD-2. **(A)** Titration of the effect of different concentrations of ZPD-2 on 70 μM  $\alpha$ -Syn aggregation. **(B)** Th-T fluorescence of  $\alpha$ -Syn end-point aggregates after the addition of ZPD-2 at different time points during the aggregation kinetics. Th-T fluorescence is plotted as normalized means. End-points were obtained at 48 h of  $\alpha$ -Syn incubation. Error bars are shown as standard errors of mean values, \*\*\* $p < 0.001$ .

protein is already decreased in treated samples at passes 1–3 (Supplementary Figure S3).

## ZPD-2 Prevents the Aggregation of Different $\alpha$ -Synuclein Amyloid Conformations

The aggregation of  $\alpha$ -Syn has been described to lead to the formation of different amyloid conformations, or strains,

depending on the environmental conditions (Li et al., 2018); a property that has been linked with its spreading in the brain and the manifestation of different synucleinopathies (Peelaerts et al., 2015). We analyzed the capacity of ZPD-2 to prevent the aggregation of  $\alpha$ -Syn into different previously described amyloid conformations (Bousset et al., 2013; Carija et al., 2019). We refer them as strain B (buffer B, 50 mM Tris-HCl pH 7.0) and strain C (buffer C, 50 mM Tris-HCl pH 7.0 supplemented with 150 mM NaCl), to keep the original strain nomenclature. ZPD-2 was

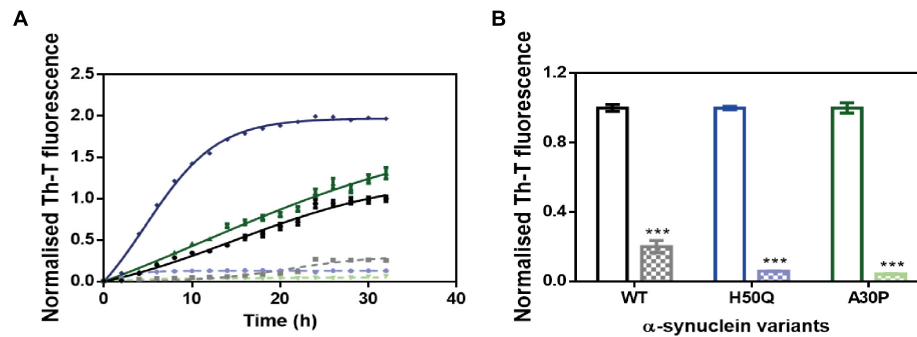


**FIGURE 4 |** ZPD-2 inhibits the aggregation of  $\alpha$ -synuclein familial variants. **(A)** Aggregation kinetics of WT (black), H50Q (blue), and A30P (green) variants of  $\alpha$ -Syn in presence (dotted) and absence (continuous) of ZPD-2, using Th-T as reporter. **(B)** End-point measurements of the aggregation of WT, H50Q, and A30P variants of  $\alpha$ -Syn in presence (dotted) or absence (continuous) of ZPD-2 Th-T fluorescence are expressed as normalized means. Error bars are shown as standard errors of mean values.

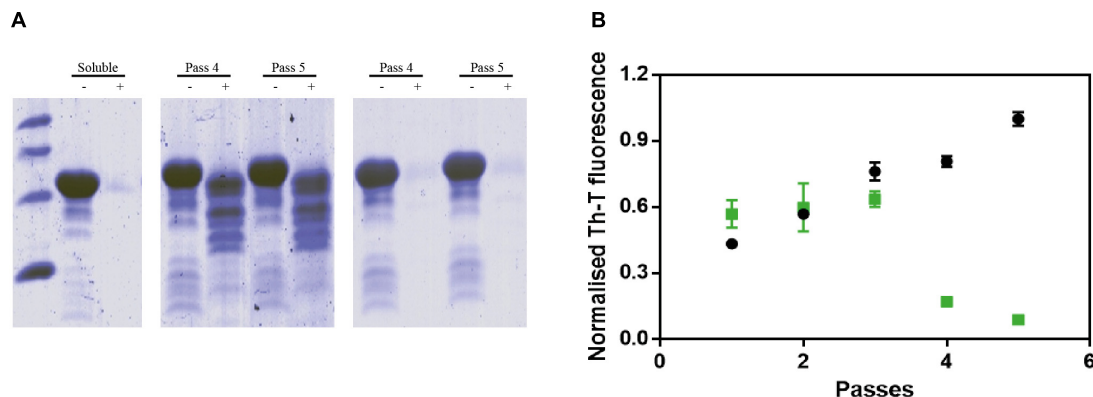


**FIGURE 5 |** PMCA of  $\alpha$ -synuclein in presence of ZPD-2. **(A)** Tricine-SDS-PAGE gels of untreated (middle) and ZPD-2-treated (right) PMCA samples before (–) and after (+) being digested with proteinase K. **(B)** Th-T fluorescence of different PMCA cycles of treated (green) and untreated (black) samples. Soluble  $\alpha$ -Syn and PMCA steps 4 and 5 are shown. Th-T fluorescence is plotted as normalized means. Error bars are shown as standard errors of mean values.

active in both cases (**Figures 6A,E**), inhibiting by up to 90% the formation of the amyloid strains B and C, as monitored by Th-T fluorescence. Light scattering measurements (**Figures 6B,F**) and TEM imaging (**Figures 6C,D,G,H**) and soluble protein quantification at the end of the reaction (**Supplementary Figure S1B**) of the different samples confirmed the inhibitory activity of ZPD-2 against the two strains. Non-fibrillar aggregates might be necessary for fibril formation (obligate), able to convert into fibrils, but not indispensable for fibril formation (on-pathway), or unable of converting directly to fibrils (off-pathway). The difference between the large reduction in Th-T fluorescence promoted by ZPD-2 in strain C aggregation kinetics and the moderate impact the molecule has in light scattering and soluble protein levels might indicate the formation of Th-T negative off-pathway aggregates in these conditions, since they do not evolve into fibrils. However, their size should be rather small, since we did not observe any large amorphous aggregate in ZPD-2-treated samples (**Figure 6H**).

We addressed whether the strong inhibitory capability of ZPD-2 at neutral pH can be overridden by the presence of preformed fibrils able to seed the aggregation reaction. The

addition of 1% (v/v) of seeds effectively accelerated the formation of both B and C strains (**Figures 7A,B**). However, the presence of ZPD-2 abrogates this effect, reducing the final amount of amyloid-like structures in seeded reactions by an 87% for strain B (**Figure 7A**) and a 90% for strain C (**Figure 7B**), according to Th-T fluorescence. Again, light dispersion measured at 300 nm revealed a significant decrease of aggregates by 57 and 70% in the case of strains B and C, respectively (**Figures 7C,D**).

## ZPD-2 Reduces the Formation of $\alpha$ -Synuclein Inclusions in a *C. elegans* Model of PD

We assessed the toxicity of ZPD-2 for human neuroblastoma cells. No significant toxicity was observed when the molecule was added to the cell culture up to 80  $\mu$ M (**Supplementary Figure S4**). We skipped efficacy studies on neuroblastoma cells, because, with more than 20 different compounds analyzed, we could not find a straightforward connection between the potency of the molecules in cell cultures and that in our *C. elegans* models of PD. We first analyzed the effect of ZPD-2 in the *C. elegans*



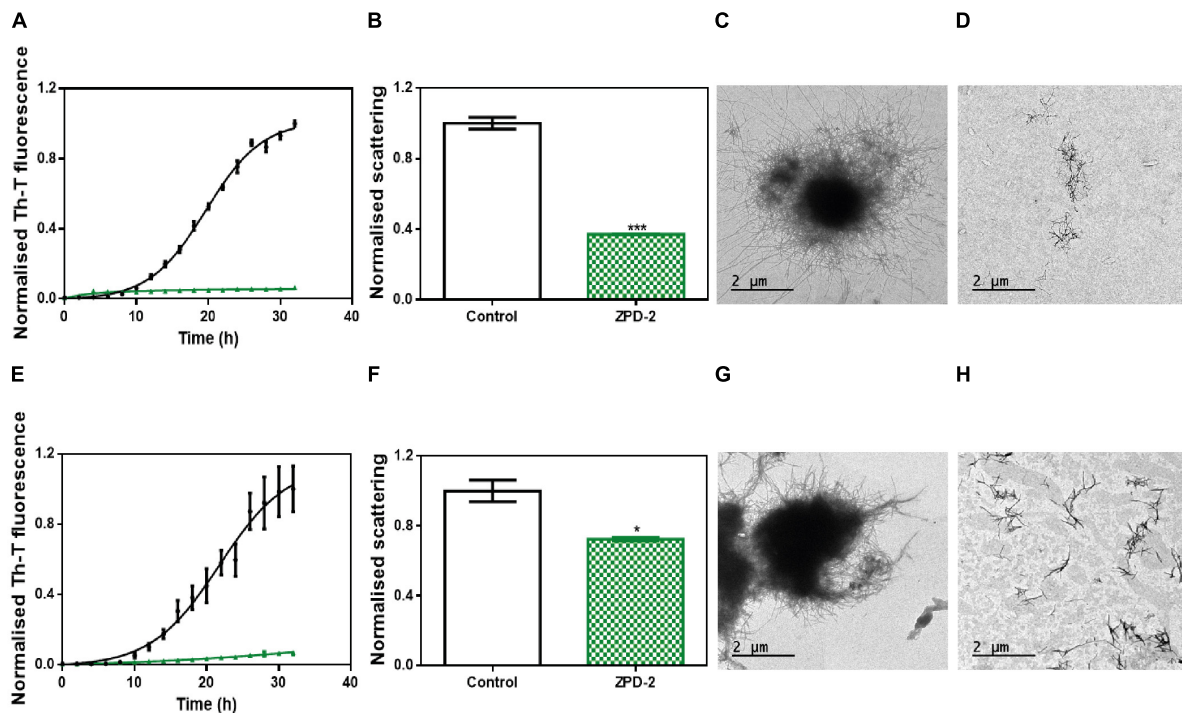


**FIGURE 6 |** ZPD-2 blocks the aggregation of two different  $\alpha$ -synuclein strains. **(A,E)** Aggregation kinetics of  $\alpha$ -Syn strains B **(A)** and C **(E)** in absence (black) and presence (green) of ZPD-2. **(B,F)** Light scattering final point measurements at 300 nm of untreated (white) and ZPD-2-treated samples (green) of strains B **(B)** and C **(F)**. **(C,D,G,H)** Representative TEM images of untreated  $\alpha$ -Syn aggregates **(C,G)** and treated **(D,H)** samples for strains B and C, respectively. Th-T fluorescence is expressed as normalized means. Final points were obtained at 48 h after the aggregation reaction begins. Error bars are shown as standard errors of mean values, where  $p < 0.05$  and  $p < 0.001$  were indicated by \* and \*\*\*, respectively.

strain NL5901. This strain over-expresses human  $\alpha$ -Syn fused to the yellow fluorescent protein (YFP), under the control of the muscular *unc-54* promoter, transgene *phIs2386* (*Punc-54: $\alpha$ -SYN:YFP*). The expression of human  $\alpha$ -Syn in the muscle of this nematode has been successfully used to identify modifier genes (Hamamichi et al., 2008; van Ham et al., 2008). Animals at the fourth larval stage (L4) were incubated in the presence or absence of 10  $\mu$ M ZPD-2 and analyzed at 9 days post-hatching (L4 + 7). These aged worms, which mimic aged PD patients, were then analyzed by epifluorescent microscopy and the number of visible  $\alpha$ -Syn inclusions was quantified (**Figures 8A,B**). In these assays, ZPD-2 moderately, but significantly, reduced the number of apparent aggregates ( $25.7 \pm 1.3$ ) when compared to untreated worms ( $31.8 \pm 1.7$ ) (**Figure 8C**). In addition, worms treated with ZPD-2 showed an increase in their mean lifespan of 14.2%, relative to untreated animals ( $p$ -value = 0.015, Wilcoxon unpaired test) (**Supplementary Figure S5**).

## Neuroprotective Role of ZPD-2 in a *C. elegans* Model of PD

The loss of DA neurons is one of the most important characteristics of PD and an important target in the search for a future treatment for this disorder. *C. elegans* presents a total of four pairs of DA neurons, three of them in the anterior part (CEPD, CEPV, and ADE) and one pair in the posterior part (PDE)

(Sulston et al., 1975). The existence of six anterior DA neurons has been recently used to analyze PD-related processes in a model (strain UA196) that expresses both human  $\alpha$ -Syn and GFP under the control of the dopamine transporter promoter (*Pdat-1:GFP; Pdat-1: $\alpha$ -SYN*) (Kim et al., 2018). Human  $\alpha$ -Syn expression in these DA neurons induces a progressive degeneration process (Cao et al., 2005). At 9 days post-hatching, the number of remaining functional neurons of untreated (**Figure 9A**) and ZPD-2-treated (**Figure 9B**) worms was analyzed. As an average, in control worms 48.1% of DA neurons are non-functional, whereas in treated animals this value decreases to 40.4% ( $p$ -value = 0.038, Wilcoxon unpaired test). Despite the difference between both means is rather low, the distribution of the data indicated a displacement in the DA neurons survival profile (**Figure 9C** and **Supplementary Figure S6**) in the presence of ZPD-2 when compared to the control worms. As a result, there is a significant increase in the number of worms containing more than three functional neurons in the anterior region in the presence of ZPD-2 ( $51.0 \pm 4.8\%$ ) when compared to the controls ( $29.1 \pm 3.1\%$ ) (**Figure 9D**).

## DISCUSSION

Protein aggregation is tightly connected with neurodegenerative disorders such as Alzheimer's and PDs. Immediately after the

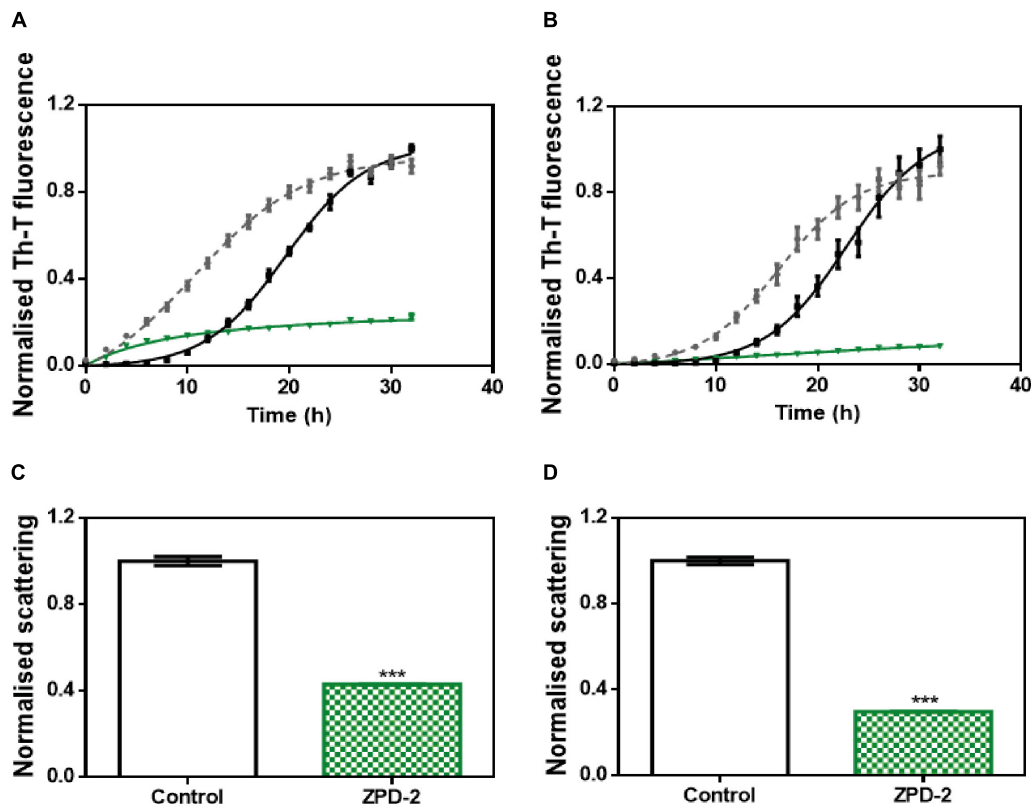


**FIGURE 7 |** Seeding assays with three different strains. (A,B) Aggregation kinetics of  $\alpha$ -Syn, buffer B (50 mM Tris-HCl pH 7.0) (A), or buffer C (50 mM Tris-HCl pH 7.0 supplemented with 150 mM NaCl) (B), reported by Th-T fluorescence, in absence of compounds and seeds (black), in presence of 1% (v/v) of preformed seeds at the specific condition (gray dotted line) and in presence of seeds and 100  $\mu$ M of ZPD-2 (green). Light dispersion of treated (green) and untreated (white) seeded samples at final point of strain B (C) and strain C (D). Error bars are shown as standard errors of mean values, \*\*\* $p$  < 0.001.

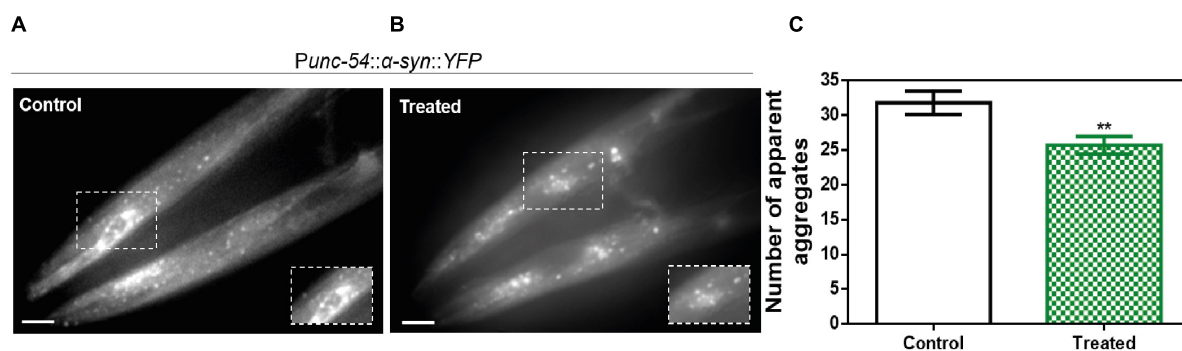


**FIGURE 8 |** *In vivo* anti-aggregational assays in *Caenorhabditis elegans*. Representative images of apparent  $\alpha$ -Syn aggregates in *C. elegans* body wall muscle cells obtained by epifluorescence microscopy of NL5901 worms treated without (A) and with ZPD-2 (B). (C) Quantification of  $\alpha$ -Syn muscle inclusions in the absence (white) and presence of ZPD-2 (green). \*\* $p$  < 0.01.

identification of  $\alpha$ -Syn as the main fibrillar component in LBs and LNs (Spillantini et al., 1997, 1998) it became evident that targeting the aggregation of this protein might hold therapeutic potential (Tatenhorst et al., 2016).

Nevertheless, the absence of a defined three-dimensional structure for the functional state of  $\alpha$ -Syn due to its intrinsically disordered nature makes the rational design of effective inhibitors

that stabilize  $\alpha$ -Syn and thus prevent or delay its aggregation, as it has been successfully done for globular proteins like transthyretin (Bulawa et al., 2012; Sant'Anna et al., 2016), difficult. In this scenario, evaluation of large chemical libraries appears as one of the few strategies we have to discover an effective inhibitor of  $\alpha$ -Syn deposition and, indeed, this approach has already rendered promising molecules (Levin et al., 2014; Moree et al., 2015;

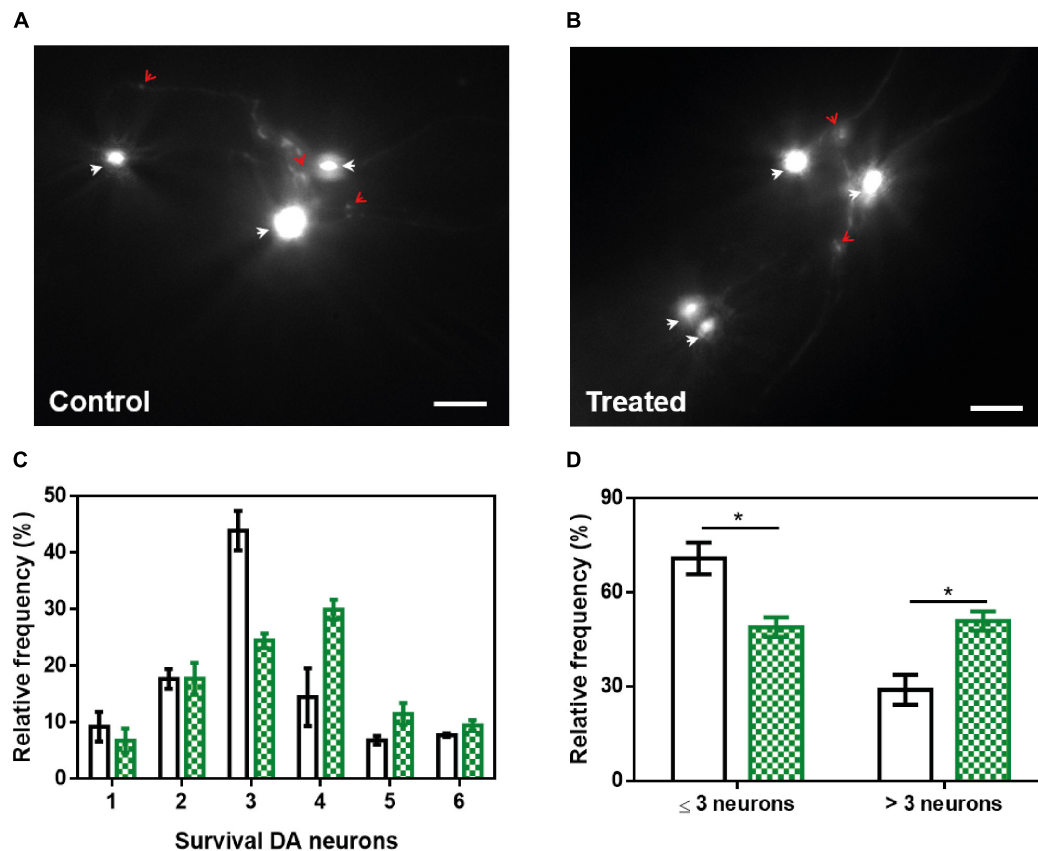


**FIGURE 9 |** Neuroprotective activity of ZPD-2 in a *Caenorhabditis elegans* model of PD. Representative images of GFP and  $\alpha$ -Syn expressing anterior DA neurons in worms treated without (A) and with ZPD-2 (B) for 7 days after L4. Healthy neurons are labeled with white arrows. (C) Distribution of DA surviving neurons in the anterior region of worms. (D) Percentage of worms containing three neurons functional or less and more than three functional neurons after 7 days post-hatching. White bars indicate control samples while the green ones correspond to treated samples. \* $p < 0.05$ .

Tatenhorst et al., 2016; Perni et al., 2017; Pujols et al., 2018). In the present work, we describe the discovery of ZPD-2, a small molecule able to prevent up to 90% the *in vitro* aggregation of WT  $\alpha$ -Syn and of familial mutants of the protein when used in a 0.7:1 (protein:ZPD-2) ratio, delaying also significantly the completion of the reaction. Its inhibitory capacity was confirmed by orthogonal techniques such as light scattering and TEM.

Further analysis demonstrated that ZPD-2 was able to prevent the aggregation in a concentration-dependent manner, with  $\sim 50\%$  inhibition at a 7:1 protein:compound ratio. This, together with solution NMR measurements indicate that ZPD-2 does not interact significantly with soluble monomeric  $\alpha$ -Syn, which suggests that it will not interfere with the functional state of the protein. In addition, the inhibitory potential of ZPD is time-dependent, being more significant at early (0–8 h) stages, in fair contrast with SC-D, a compound we identified in the same screening campaign, whose activity was time-independent, being able to target late species (Pujols et al., 2018). The largest affinity of ZPD-2 for early aggregating species is also inferred from the fact that it mainly impacts the nucleation constant, reducing it by threefold. This might also explain why, at a 0.7:1 ratio, the molecule works well for the A30P (96% inhibition)

and H50Q (94% inhibition) familial variants, provided that both mutations facilitate oligomerization, H50Q favoring also fibrillation (Marvian et al., 2019).

ZPD-2 is able to inhibit the aggregation of  $\alpha$ -Syn under different solution conditions. This ability opens a possibility for its use in different synucleinopathies, where different  $\alpha$ -Syn strains might occur (Bousset et al., 2013; Peelaerts et al., 2015). Importantly, ZPD-2 is one of a few small molecules shown to inhibit efficiently  $\alpha$ -Syn seeded aggregation, where the lag phase of the reaction is shortened or abrogated because the soluble protein can be directly incorporated on top of the preformed fibrillar fragments. This seeding-blocking activity explains why ZPD-2 is so effective preventing the formation of PK-resistant/Th-T-positive species in PMCA assays, which promote both templated seeding and aggregates amplification. This effect might respond to the ability of the compound to either destabilize small aggregates or to prevent their elongation, a property that can be very relevant to prevent the cell-to-cell spreading of misfolded  $\alpha$ -Syn.

ZPD-2 had not detectable toxic effect for neuronal cells at 10  $\mu$ M, a concentration at which it reduces the presence of  $\alpha$ -Syn inclusions in a *C. elegans* model of PD expressing human  $\alpha$ -Syn

in body wall muscle cells and extends lifespan. Not surprisingly, this anti-aggregational activity translates in reduced DA neurons degeneration in a *C. elegans* model that over-expresses human  $\alpha$ -Syn exclusively in these cells, increasing significantly the proportion of animals that keep > 50% of their anterior part DA neurons intact.

## CONCLUSION

In conclusion, ZPD-2 properties make this molecule a promising hit for the sake of developing leads able to tackle  $\alpha$ -Syn aggregation and seeds propagation in PD and, potentially, other synucleinopathies.

## DATA AVAILABILITY STATEMENT

All datasets generated for this study are included in the article/**Supplementary Material**.

## AUTHOR CONTRIBUTIONS

SP-D, JP, XS, JavS, ED, and SV conceived and designed the experiments, and analyzed the results. SP-D, JP, FP, JaiS, and MC-G performed the aggregation assays. AC expressed and purified the H50Q and A30P variants. SP-D and SN performed the PMCA assays. SN performed the toxicity assays. JG and XS performed the NMR assays. SP-D and ED performed the *C. elegans* tests. SP-D, JP, and SV wrote the manuscript.

## FUNDING

SV was supported by the Ministerio de Economía y Competitividad (MINECO) (BIO2016-78310-R), the ICREA (ICREA-Academia 2015) and the Fundación La Marató de TV3 (Ref. 20144330). JavS was supported by the MINECO (BFU2016-78232-P) and the Gobierno de Aragón (E45\_17R). ED was supported by the Instituto de Salud Carlos III (PH613883/ERDF/ESF). JG and XS were supported by the

MINECO (BIO2015-70092-R) and the European Research Council (Contract 648201).

## ACKNOWLEDGMENTS

We thank the Infraestructura Científica y Técnica Singular NMR facility at Centres Científics i Tecnològics de la Universitat de Barcelona for help with NMR, the Servei de Microscòpia at Universitat Autònoma de Barcelona for their help with TEM, and Anna Villar-Pique for help with plasmid construction. The worm strain UA196 used for neurodegeneration assays was a generous gift of Dr. Guy A. Caldwell.

## SUPPLEMENTARY MATERIAL

The Supplementary Material for this article can be found online at: <https://www.frontiersin.org/articles/10.3389/fnmol.2019.00306/full#supplementary-material>

**FIGURE S1** |  $\alpha$ -Synuclein soluble fraction at the end of the aggregation. **(A)** Soluble fraction of  $\alpha$ -Syn when incubated in absence (black) or presence (green) of ZPD-2 in PBS solution. **(B)** Soluble fraction of strains B and C at final point of the aggregation when incubated in presence (green) or absence (black) of ZPD-2.

**FIGURE S2** | Lack of interaction between monomeric  $\alpha$ -synuclein and ZPD-2 assessed by NMR. Superposition of the 1H-15N HSQC NMR spectra of 15N-labeled  $\alpha$ -Syn (70  $\mu$ M) in absence (black) and presence (green) of 100  $\mu$ M of ZPD-2.

**FIGURE S3** | PMCA assay at early stages. Tricine-SDS-PAGE gels of untreated **(middle)** and ZPD-2-treated **(right)** PMCA samples before (–) and after (+) being digested with proteinase K. Soluble  $\alpha$ -Syn and PMCA steps 1–3 are shown.

**FIGURE S4** | Toxicity assays. Analysis of neuronal cells culture survival in presence of different concentration of ZPD-2. Survival is potted as normalized means. Error bars are shown as standard error of means values, where  $p < 0.001$  was indicated by \*\*\*.

**FIGURE S5** | *C. elegans* lifespan analysis. Effect of ZPD-2 treatment (green) on the survival of PD model animals, in comparison with untreated PD worms (black). The data represent the survival ratio (approximately 60–80 animals per group).

**FIGURE S6** | Distribution of functional neurons in the *C. elegans* dopaminergic model. Normal distribution of the remaining functional dopaminergic (DA) neurons in transgenic animals when treated with ZPD-2 (green) or vehicle (gray). The dashed line delimits animals having four or more functional DA neurons.

## REFERENCES

- Appel-Cresswell, S., Vilarino-Guell, C., Encarnacion, M., Sherman, H., Yu, I., Shah, B., et al. (2013). Alpha-synuclein p.H50Q, a novel pathogenic mutation for Parkinson's disease. *Mov. Disord.* 28, 811–813. doi: 10.1002/mds.25421
- Barria, M. A., Gonzalez-Romero, D., and Soto, C. (2012). Cyclic amplification of prion protein misfolding. *Methods Mol. Biol.* 849, 199–212. doi: 10.1007/978-1-61779-551-0\_14
- Bendor, J. T., Logan, T. P., and Edwards, R. H. (2013). The function of alpha-synuclein. *Neuron* 79, 1044–1066. doi: 10.1016/j.neuron.2013.09.004
- Bousset, L., Pieri, L., Ruiz-Arlandis, G., Gath, J., Jensen, P. H., Habenstein, B., et al. (2013). Structural and functional characterization of two alpha-synuclein strains. *Nat. Commun.* 4:2575. doi: 10.1038/ncomms3575
- Braak, H., Del Tredici, K., Rub, U., de Vos, R. A., Jansen Steur, E. N., and Braak, E. (2003). Staging of brain pathology related to sporadic Parkinson's disease. *Neurobiol. Aging* 24, 197–211. doi: 10.1016/s0197-4580(02)00065-9
- Brenner, S. (1974). The genetics of *Caenorhabditis elegans*. *Genetics* 77, 71–94.
- Bulawa, C. E., Connelly, S., Devit, M., Wang, L., Weigel, C., Fleming, J. A., et al. (2012). Tafamidis, a potent and selective transthyretin kinetic stabilizer that inhibits the amyloid cascade. *Proc. Natl. Acad. Sci. U.S.A.* 109, 9629–9634. doi: 10.1073/pnas.1121005109
- Cao, S., Gelwix, C. C., Caldwell, K. A., and Caldwell, G. A. (2005). Torsin-mediated protection from cellular stress in the dopaminergic neurons of *Caenorhabditis elegans*. *J. Neurosci.* 25, 3801–3812. doi: 10.1523/jneurosci.5157-04.2005
- Carija, A., Pinheiro, F., Pujols, J., Bras, I. C., Lazaro, D. F., Santambrogio, C., et al. (2019). Biasing the native alpha-synuclein conformational ensemble towards compact states abolishes aggregation and neurotoxicity. *Redox Biol.* 22:101135. doi: 10.1016/j.redox.2019.101135
- Crespo, R., Villar-Alvarez, E., Taboada, P., Rocha, F. A., Damas, A. M., and Martins, P. M. (2016). What can the kinetics of amyloid fibril formation tell about off-pathway aggregation? *J. Biol. Chem.* 291, 2018–2032. doi: 10.1074/jbc.M115.699348



- Dehay, B., Bourdenx, M., Gorry, P., Przedborski, S., Vila, M., Hunot, S., et al. (2015). Targeting alpha-synuclein for treatment of Parkinson's disease: mechanistic and therapeutic considerations. *Lancet. Neurol.* 14, 855–866. doi: 10.1016/S1474-4422(15)00006-X
- Dexter, D. T., and Jenner, P. (2013). Parkinson disease: from pathology to molecular disease mechanisms. *Free Radic. Biol. Med.* 62, 132–144. doi: 10.1016/j.freeradbiomed.2013.01.018
- Gao, J., Perera, G., Bhadbhade, M., Halliday, G. M., and Dzakmo, N. (2019). Autophagy activation promotes clearance of alpha-synuclein inclusions in fibril-seeded human neural cells. *J. Biol. Chem.* 294, 14241–14256. doi: 10.1074/jbc.RA119.008733
- Hamamichi, S., Rivas, R. N., Knight, A. L., Cao, S., Caldwell, K. A., and Caldwell, G. A. (2008). Hypothesis-based RNAi screening identifies neuroprotective genes in a Parkinson's disease model. *Proc. Natl. Acad. Sci. U.S.A.* 105, 728–733. doi: 10.1073/pnas.0711018105
- Hansen, C., Angot, E., Bergstrom, A. L., Steiner, J. A., Pieri, L., Paul, G., et al. (2011). alpha-Synuclein propagates from mouse brain to grafted dopaminergic neurons and seeds aggregation in cultured human cells. *J. Clin. Invest.* 121, 715–725. doi: 10.1172/JCI43366
- Harrington, A. J., Yacoubian, T. A., Slone, S. R., Caldwell, K. A., and Caldwell, G. A. (2012). Functional analysis of VPS41-mediated neuroprotection in *Caenorhabditis elegans* and mammalian models of Parkinson's disease. *J. Neurosci.* 32, 2142–2153. doi: 10.1523/jneurosci.2606-11.2012
- Hauser, R. A. (2015). alpha-Synuclein in Parkinson's disease: getting to the core of the matter. *Lancet. Neurol.* 14, 785–786. doi: 10.1016/S1474-4422(15)00136-2
- Herva, M. E., Zibae, S., Fraser, G., Barker, R. A., Goedert, M., and Spillantini, M. G. (2014). Anti-amyloid compounds inhibit alpha-synuclein aggregation induced by protein misfolding cyclic amplification (PMCA). *J. Biol. Chem.* 289, 11897–11905. doi: 10.1074/jbc.M113.542340
- Ibanez, P., Bonnet, A. M., Debarges, B., Lohmann, E., Tison, F., Pollak, P., et al. (2004). Causal relation between alpha-synuclein gene duplication and familial Parkinson's disease. *Lancet* 364, 1169–1171. doi: 10.1016/S0140-6736(04)17104-3
- Kim, H., Calatayud, C., Guha, S., Fernandez-Carasa, I., Berkowitz, L., Carballo-Carbajal, I., et al. (2018). The small GTPase RAC1/CED-10 is essential in maintaining dopaminergic neuron function and survival against alpha-synuclein-induced toxicity. *Mol. Neurobiol.* 55, 7533–7552. doi: 10.1007/s12035-018-0881-7
- Kruger, R., Kuhn, W., Muller, T., Woitalla, D., Graeber, M., Kosel, S., et al. (1998). Ala30Pro mutation in the gene encoding alpha-synuclein in Parkinson's disease. *Nat. Genet.* 18, 106–108.
- Levin, J., Schmidt, F., Boehm, C., Prix, C., Botzel, K., Ryazanov, S., et al. (2014). The oligomer modulator anle138b inhibits disease progression in a Parkinson mouse model even with treatment started after disease onset. *Acta Neuropathol.* 127, 779–780. doi: 10.1007/s00401-014-1265-3
- Li, B., Ge, P., Murray, K. A., Sheth, P., Zhang, M., Nair, G., et al. (2018). Cryo-EM of full-length alpha-synuclein reveals fibril polymorphs with a common structural kernel. *Nat. Commun.* 9:3609. doi: 10.1038/s41467-018-05971-2
- Marti, M. J., Tolosa, E., and Campdelacreu, J. (2003). Clinical overview of the synucleinopathies. *Mov. Disord.* 18(Suppl. 6), S21–S27.
- Marvin, A. T., Koss, D. J., Aliakbari, F., Morshedi, D., and Outeiro, T. F. (2019). In vitro models of synucleinopathies: informing on molecular mechanisms and protective strategies. *J. Neurochem.* 150, 535–565. doi: 10.1111/jnc.14707
- McCormack, A. L., Mak, S. K., Henderson, J. M., Bumcrot, D., Farrer, M. J., and Di Monte, D. A. (2010). Alpha-synuclein suppression by targeted small interfering RNA in the primate substantia nigra. *PLoS One* 5:e12122. doi: 10.1371/journal.pone.0012122
- Morales, R., Duran-Aniotz, C., Diaz-Espinoza, R., Camacho, M. V., and Soto, C. (2012). Protein misfolding cyclic amplification of infectious prions. *Nat. Protoc.* 7, 1397–1409. doi: 10.1038/nprot.2012.067
- Moree, B., Yin, G., Lazaro, D. F., Munari, F., Strohaker, T., Giller, K., et al. (2015). Small molecules detected by second-harmonic generation modulate the conformation of monomeric alpha-synuclein and reduce its aggregation in cells. *J. Biol. Chem.* 290, 27582–27593. doi: 10.1074/jbc.M114.636027
- Munoz-Lobato, F., Rodriguez-Palero, M. J., Naranjo-Galindo, F. J., Shephard, F., Gaffney, C. J., Szewczyk, N. J., et al. (2014). Protective role of DJN-27/ERdj5 in *Caenorhabditis elegans* models of human neurodegenerative diseases. *Antioxid. Redox Signal.* 20, 217–235. doi: 10.1089/ars.2012.5051
- Nussbaum, R. L., and Ellis, C. E. (2003). Alzheimer's disease and Parkinson's disease. *N. Engl. J. Med.* 348, 1356–1364.
- Peelaerts, W., Bousset, L., Van der Perren, A., Moskalyuk, A., Pulizzi, R., Giugliano, M., et al. (2015). alpha-Synuclein strains cause distinct synucleinopathies after local and systemic administration. *Nature* 522, 340–344. doi: 10.1038/nature14547
- Perni, M., Galvagnion, C., Maltsev, A., Meisl, G., Muller, M. B., Challa, P. K., et al. (2017). A natural product inhibits the initiation of alpha-synuclein aggregation and suppresses its toxicity. *Proc. Natl. Acad. Sci. U.S.A.* 114, E1009–E1017.
- Polymeropoulos, M. H., Lavedan, C., Leroy, E., Ide, S. E., Dehejia, A., Dutra, A., et al. (1997). Mutation in the alpha-synuclein gene identified in families with Parkinson's disease. *Science* 276, 2045–2047. doi: 10.1126/science.276.5321.2045
- Pujols, J., Pena-Díaz, S., Conde-Giménez, M., Pinheiro, F., Navarro, S., Sancho, J., et al. (2017). High-throughput screening methodology to identify alpha-synuclein aggregation inhibitors. *Int. J. Mol. Sci.* 18:E478. doi: 10.3390/ijms18030478
- Pujols, J., Pena-Díaz, S., Lazaro, D. F., Peccati, F., Pinheiro, F., Gonzalez, D., et al. (2018). Small molecule inhibits alpha-synuclein aggregation, disrupts amyloid fibrils, and prevents degeneration of dopaminergic neurons. *Proc. Natl. Acad. Sci. U.S.A.* 115, 10481–10486. doi: 10.1073/pnas.1804198115
- Sabate, R., Gallardo, M., and Estelrich, J. (2003). An autocatalytic reaction as a model for the kinetics of the aggregation of beta-amyloid. *Biopolymers* 71, 190–195. doi: 10.1002/bip.10441
- Sant'Anna, R., Gallego, P., Robinson, L. Z., Pereira-Henriques, A., Ferreira, N., Pinheiro, F., et al. (2016). Repositioning tolcapone as a potent inhibitor of transthyretin amyloidogenesis and associated cellular toxicity. *Nat. Commun.* 7:10787. doi: 10.1038/ncomms10787
- Serpell, L. C., Berriman, J., Jakes, R., Goedert, M., and Crowther, R. A. (2000). Fiber diffraction of synthetic alpha-synuclein filaments shows amyloid-like cross-beta conformation. *Proc. Natl. Acad. Sci. U.S.A.* 97, 4897–4902. doi: 10.1073/pnas.97.9.4897
- Silva, B., Einarsson, O., Fink, and Uversky, V. (2011). Modulating  $\alpha$ -synuclein misfolding and fibrillation in vitro by agrochemicals. *Res. Rep. Biol.* 2, 43–56.
- Singleton, A. B., Farrer, M., Johnson, J., Singleton, A., Hague, S., Kachergus, J., et al. (2003). alpha-Synuclein locus triplication causes Parkinson's disease. *Science* 302:841. doi: 10.1126/science.1090278
- Spillantini, M. G., Crowther, R. A., Jakes, R., Cairns, N. J., Lantos, P. L., and Goedert, M. (1998). Filamentous alpha-synuclein inclusions link multiple system atrophy with Parkinson's disease and dementia with Lewy bodies. *Neurosci. Lett.* 251, 205–208. doi: 10.1016/S0304-3940(98)00504-7
- Spillantini, M. G., Schmidt, M. L., Lee, V. M., Trojanowski, J. Q., Jakes, R., and Goedert, M. (1997). Alpha-synuclein in lewy bodies. *Nature* 388, 839–840.
- Sulston, J., Dew, M., and Brenner, S. (1975). Dopaminergic neurons in the nematode *Caenorhabditis elegans*. *J. Comp. Neurol.* 163, 215–226.
- Tatenhorst, L., Eckermann, K., Dambeck, V., Fonseca-Ornelas, L., Walle, H., Lopes da Fonseca, T., et al. (2016). Fasudil attenuates aggregation of alpha-synuclein in models of Parkinson's disease. *Acta Neuropathol. Commun.* 4:39. doi: 10.1186/s40478-016-0310-y
- van Ham, T. J., Thijssen, K. L., Breitling, R., Hofstra, R. M., Plasterk, R. H., and Nollen, C. (2008). *elegans* model identifies genetic modifiers of alpha-synuclein inclusion formation during aging. *PLoS Genet.* 4:e1000027. doi: 10.1371/journal.pgen.1000027
- Winner, B., Jappelli, R., Maji, S. K., Desplats, P. A., Boyer, L., Aigner, S., et al. (2011). In vivo demonstration that alpha-synuclein oligomers are toxic. *Proc. Natl. Acad. Sci. U.S.A.* 108, 4194–4199. doi: 10.1073/pnas.1100976108
- Xue, W. F., Hellewell, A. L., Hewitt, E. W., and Radford, S. E. (2010). Fibril fragmentation in amyloid assembly and cytotoxicity: when size matters. *Prion* 4, 20–25. doi: 10.4161/pri.4.1.11378

**Conflict of Interest:** The authors declare that the research was conducted in the absence of any commercial or financial relationships that could be construed as a potential conflict of interest.

Copyright © 2019 Peña-Díaz, Pujols, Conde-Giménez, Čarija, Dalfo, García, Navarro, Pinheiro, Santos, Salvatella, Sancho and Ventura. This is an open-access article distributed under the terms of the Creative Commons Attribution License (CC BY). The use, distribution or reproduction in other forums is permitted, provided the original author(s) and the copyright owner(s) are credited and that the original publication in this journal is cited, in accordance with accepted academic practice. No use, distribution or reproduction is permitted which does not comply with these terms.



# Untangling the Conformational Polymorphism of Disordered Proteins Associated With Neurodegeneration at the Single-Molecule Level

Melissa Birol<sup>1</sup> and Ana M. Melo<sup>2\*</sup>

<sup>1</sup>Department of Chemistry, University of Pennsylvania, Philadelphia, PA, United States, <sup>2</sup>Centro de Química-Física Molecular-IN and iBB-Institute for Bioengineering and Biosciences, Instituto Superior Técnico, Universidade de Lisboa, Lisbon, Portugal

## OPEN ACCESS

### Edited by:

Gal Bitan,  
UCLA David Geffen School of  
Medicine, United States

### Reviewed by:

Abhinav Nath,  
University of Washington,  
United States  
Jianhan Chen,  
University of Massachusetts  
Amherst, United States

### \*Correspondence:

Ana M. Melo  
anamelo@tecnico.ulisboa.pt

**Received:** 01 October 2019

**Accepted:** 29 November 2019

**Published:** 10 January 2020

### Citation:

Birol M and Melo AM  
(2020) Untangling the Conformational  
Polymorphism of Disordered Proteins  
Associated With Neurodegeneration  
at the Single-Molecule Level.  
*Front. Mol. Neurosci.* 12:309.  
doi: 10.3389/fnmol.2019.00309

A large fraction of the human genome encodes intrinsically disordered proteins/regions (IDPs/IDRs) that are involved in diverse cellular functions/regulation and dysfunctions. Moreover, several neurodegenerative disorders are associated with the pathological self-assembly of neuronal IDPs, including tau [Alzheimer's disease (AD)],  $\alpha$ -synuclein [Parkinson's disease (PD)], and huntingtin exon 1 [Huntington's disease (HD)]. Therefore, there is an urgent and emerging clinical interest in understanding the physical and structural features of their functional and disease states. However, their biophysical characterization is inherently challenging by traditional ensemble techniques. First, unlike globular proteins, IDPs lack stable secondary/tertiary structures under physiological conditions and may interact with multiple and distinct biological partners, subsequently folding differentially, thus contributing to the conformational polymorphism. Second, amyloidogenic IDPs display a high aggregation propensity, undergoing complex heterogeneous self-assembly mechanisms. In this review article, we discuss the advantages of employing cutting-edge single-molecule fluorescence (SMF) techniques to characterize the conformational ensemble of three selected neuronal IDPs (huntingtin exon 1, tau, and  $\alpha$ -synuclein). Specifically, we survey the versatility of these powerful approaches to describe their monomeric conformational ensemble under functional and aggregation-prone conditions, and binding to biological partners. Together, the information gained from these studies provides unique insights into the role of *gain* or *loss of function* of these disordered proteins in neurodegeneration, which may assist the development of new therapeutic molecules to prevent and treat these devastating human disorders.

**Keywords:** intrinsically disordered proteins, neurodegenerative diseases, single-molecule FRET, fluorescence correlation spectroscopy, huntingtin exon 1, tau,  $\alpha$ -synuclein

## INTRODUCTION

The classical protein “structure–function” paradigm establishes that proteins fold into a unique ordered 3D structure determined by their amino acid sequence before acquiring a specific biological function (reviewed in Fersht, 2008). However, studies over the last two decades have identified functional proteins lacking a stable secondary and/or tertiary structure, and instead adopting a dynamic ensemble of multiple conformational states (Kriwacki et al., 1996; Wright and Dyson, 1999; Mittag et al., 2010; Babu et al., 2012; Tompa, 2012; van der Lee et al., 2014). These intrinsically disordered proteins and regions (IDPs and IDRs, respectively) are widespread in the human proteome and play critical roles in diverse biological processes, including in transcription and translation, cell cycle, signaling, and transport (Iakoucheva et al., 2002; Wright and Dyson, 2015; Babu, 2016; Tsafou et al., 2018). Their functional diversity is sustained by unique features: (i) quick response to variations in cellular environment; (ii) interaction with multiple binding partners (with high specificity but low affinity) that provides binding promiscuity; and (iii) tight regulation by posttranslational modifications (PTMs) (Babu et al., 2012; Uversky, 2015; Babu, 2016). The misbehavior and misfolding of these naturally flexible proteins or regions can ultimately lead to their dysfunction. Therefore, IDPs/IDRs have been implicated in several devastating human diseases (such as in neurodegeneration and cancer), supporting the emerging “disorder in disorders” (or D<sup>2</sup>) concept (Uversky et al., 2008).

Many severe neurodegenerative disorders are associated with the pathological self-assembly and extra- or intracellular deposition of neuronal IDPs or proteins containing IDRs. These include amyloid- $\beta$  (A $\beta$ ) peptides in Alzheimer’s disease (AD); tau in multiple tauopathies (including AD);  $\alpha$ -synuclein ( $\alpha$ S) in Parkinson’s disease (PD); huntingtin (HTT) in Huntington’s disease (HD); and TAR DNA-binding protein-43 (TDP-43) and fused in sarcoma (FUS) protein in amyotrophic lateral sclerosis and frontotemporal lobar degeneration (FTLD; reviewed in Uversky, 2014, 2015). These neurodegeneration-promoting proteins are fully or locally disordered in their monomeric-unbound state, but surprisingly they display a high tendency to form ordered insoluble aggregates (Uversky, 2014). In addition, accumulated evidence supports that aggregation-prone IDPs/IDRs can cause neurodegeneration through the failure to adopt a functional state (loss of their native functions) and/or gain of abnormal toxic interactions or protein accumulation resulting in toxic oligomers/aggregates (toxic gain of function; Trojanowski and Lee, 2005; Winklhofer et al., 2008). Effective therapies should be designed to restore their biological functions and/or avoid their aggregation at early stages. Therefore, there is an urgent medical interest in understanding these neuronal IDPs/IDRs in normal and disease conditions by: (i) characterizing their functional diversity and structural rearrangements upon interaction with distinct binding partners; and (ii) determining the conformational ensemble of their monomers under conditions that favor aggregation, which are ideal clinical targets. Together, these approaches will provide

insights into the key physical and structural features of these aggregation-prone IDPs/IDRs that trigger gain or loss of function, and ultimately cause neuronal cell death.

Remarkably, single-molecule fluorescence (SMF) methods have enhanced our understanding of IDPs, including amyloid-forming proteins, during the past two decades (reviewed in Brucalé et al., 2014; Schuler et al., 2016). Numerous SMF methodologies have been developed for probing transient oligomeric species and to determine their stoichiometry. These include two-color coincidence detection (TCCD; Cremades et al., 2012), single-molecule Förster resonance energy transfer (smFRET; Shammass et al., 2015), total internal reflection fluorescence microscopy (TIRF)-based approaches (Lv et al., 2015), or single-molecule photobleaching (Zijlstra et al., 2012). In addition, SMF techniques have been successfully used to characterize the complex conformational distribution and plasticity of monomeric IDPs, and molecular interactions with biological partners or aggregation inducers (Banerjee and Deniz, 2014; Lee et al., 2015). While the application of SMF approaches to uncover oligomeric states has been largely debated (Kundel et al., 2018), in this review article, we focus on the use of SMF methods to study the conformational ensemble of monomeric neurodegeneration-promoting IDPs under functional and aggregation-prone conditions. Notably, the low protein concentrations required for these techniques (in the pM or nM range) inhibit the rapid protein self-assembly. In addition, recording behaviors of individual molecules enables the description of dynamic/heterogeneous systems and the detection of coexisting subpopulations, which are not accessible in traditional ensemble and time-averaging methodologies (**Figure 1**; Joo et al., 2008; Schuler and Eaton, 2008; Schuler et al., 2016). From this class of SMF methods, fluorescence correlation spectroscopy (FCS) and smFRET have emerged as powerful and versatile tools.

FCS measures fluorescence-intensity fluctuations arising from the diffusion of a few fluorescent molecules through a small confocal observation volume ( $\sim 1$  fL). These fluorescence fluctuations are then analyzed using the autocorrelation function that quantifies the self-similarity of the signal over several delay times. Commonly, it can provide information in local concentrations, molecular mobility, and/or photophysical properties (Hess et al., 2002). Moreover, FCS allows to determine the overall chain dimensions of proteins (for homogeneous populations) and molecular interactions using the translational diffusion time at a slow time scale and conformational dynamics at fast time scales (Chattopadhyay et al., 2005; Sherman et al., 2008; Melo et al., 2011). In particular, nanosecond FCS in conjugation with smFRET and polymer physics can be used to quantify the reconfiguration time of unfolded polypeptide chains (Soranno et al., 2012). Therefore, FCS has been widely applied to evaluate the hydrodynamic size of monomeric IDPs, internal conformational dynamics, and molecular interactions (**Figure 1**; Crick et al., 2006; Rhoades et al., 2006; Middleton and Rhoades, 2010; Li et al., 2015; Li and Rhoades, 2017).

In addition, smFRET relies on the non-radiative energy transfer from a donor fluorophore to an acceptor fluorophore

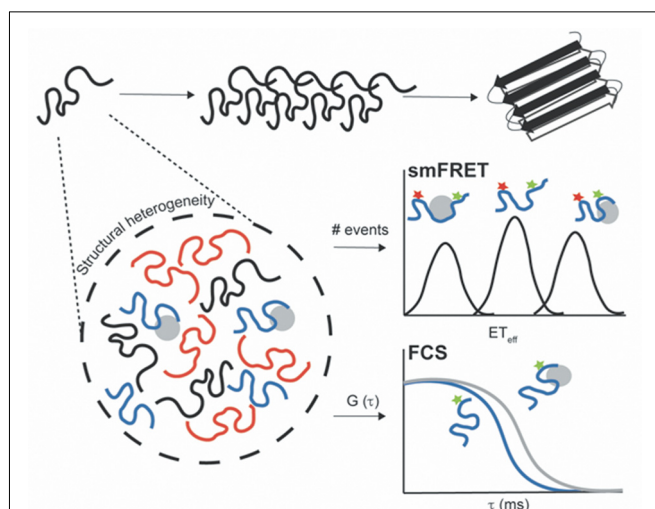


**FIGURE 1 |** Untangling the conformational heterogeneity and molecular interactions of monomeric intrinsically disordered proteins (IDPs) through single-molecule fluorescence (SMF) approaches. Single-molecule Förster resonance energy transfer (smFRET) histogram discriminating between distinct conformational ensembles of double-label protein (donor–acceptor): monomeric free protein in solution and bound states with extended (low  $ET_{eff}$ ) or compacted conformations (high  $ET_{eff}$ ). Fluorescence correlation spectroscopy (FCS) autocorrelation curve reporting on changes in the diffusion time of single-label protein free in solution (blue curve) and upon interaction with aggregation inducers or binding partners (gray curve). The binding results into a shift of the autocorrelation curve to the right (longer translational diffusion times).

through a dipole–dipole coupling mechanism. The efficiency of transfer ( $ET_{eff}$ ) exhibits an inverse sixth power dependence on the interdyne distance, allowing to determine distances on the nanometer scale ( $\sim 2\text{--}10\text{ nm}$ , as a “spectroscopic ruler”; Forster, 1949). Therefore, intramolecular smFRET (both donor and acceptor fluorophores located on same molecule) can evaluate conformational rearrangements and dynamics of proteins (Chen and Rhoades, 2008; Banerjee and Deniz, 2014; Schuler et al., 2016). Several strategies have been applied for site-specific double-labeling IDPs, including the use of cysteine residues and genetically encoded unnatural amino acids (Lemke, 2011). Briefly, in diffusion-based smFRET, fluorescence intensities are recorded for each donor–acceptor labeled protein while it diffuses across a small confocal volume, and subsequently  $ET_{eff}$  values are calculated for each photon burst and plotted as a histogram (Brucal et al., 2014; Schuler et al., 2016). Due to the high structural heterogeneity of IDPs, the Förster equation cannot provide a precise conversion of mean  $ET_{eff}$  values into distances (O’Brien et al., 2009), since there is a wide distribution of donor–acceptor distances (without a single fixed distance). Commonly, several polymer models have been employed to describe the conformational ensemble of IDPs and denatured proteins. These include the Gaussian chain, worm-like chain, or a weighted Flory–Fisk distribution (discussed in detail in Schuler et al., 2016). Remarkably, intramolecular smFRET can report on conformational changes and dynamics of neurodegeneration-promoting IDPs in solution and upon binding to functional partners or aggregation promoters (Figure 1; Ferreon et al.,

2009; Trexler and Rhoades, 2009, 2010; Elbaum-Garfinkle and Rhoades, 2012; Melo et al., 2016, 2017).

In this short review, we focus on the IDPs—huntingtin exon 1 (HTTex1), tau, and  $\alpha S$ —and discuss a series of key SMF studies to characterize their heterogeneous/dynamic monomeric conformational ensemble and also interactions relevant for their function or disease.

## HTTex1 IN HD

HTT is a large multidomain protein (with over 3,000 amino acids and 348 kDa) that is involved in several complex cellular processes, such as in trafficking of vesicles and organelles, transcription regulation, and generally in cellular homeostasis (reviewed in Schulte and Littleton, 2011; Saudou and Humbert, 2016). HTT is of major clinical relevance because the abnormal expansion of the CAG repeat within the first exon of its gene (IT15) is the pathological hallmark of HD (MacDonald et al., 1993). Above a critical threshold of about 37 CAG repeats, it leads to the expression of a mutant HTT protein with an expanded polyglutamine (polyQ) domain, which ultimately forms amyloid-like fibrils and intracellular inclusion bodies (Bates et al., 2014). The aberrant splicing and proteolytic cleavage of mutant proteins result in highly toxic HTT fragments spanning exon 1 (HTTex1; Wellington et al., 2002; Sathasivam et al., 2013), which are sufficient to replicate much of HD’s pathology/progression (Mangiarini et al., 1996). The exact molecular mechanism whereby HTTex1 contributes to neurodegeneration remains elusive, but growing evidence supports that the molecular sources of neurotoxicity inherent to the polyQ expansion are toxic conformations of the monomer and/or oligomers (Nagai et al., 2007; Takahashi et al., 2008). Therefore, considerable effort has been devoted to characterize the conformational features of monomeric polyQ peptides and HTTex1 in solution (reviewed in Wetzel, 2012; Adegboyiro et al., 2017).

HTTex1 consists of a polyQ domain flanked by an N-terminal 17 amino acid segment (N17) and a C-terminal proline-rich region (PRR; Wetzel, 2012; Adegboyiro et al., 2017). Since the age of onset, risk of disease and severity in HD are strongly correlated with the polyQ length (Bates et al., 2014), the early structural studies solely focused on simple synthetic polyQ peptides (with extra lysine residues to improve their solubility). Several circular dichroism (CD) and nuclear magnetic resonance (NMR) studies have shown that simple polyQ sequences regardless of their repeat length are predominantly disordered in solution (Altschuler et al., 1997; Chen et al., 2001; Klein et al., 2007). In a pioneering FCS study, Crick et al. (2006) identified the hydrodynamic radius of monomeric polyQ peptides to obtain insights into their global dimensions and also shapes. The authors measured the average translational diffusion time (proportional to the hydrodynamic radius) of (Gly)–(Gln)<sub>N</sub>–Cys–Lys<sub>2</sub> peptides in solution and assessed how it scales with the chain length. Notably, FCS revealed that: (i) aqueous solution is a “poor solvent” (low scaling exponent with  $\nu = 0.32 \pm 0.02$ ), suggesting that monomeric polyQ sequences adopt a heterogeneous



ensemble of collapsed conformations; and (ii) the absence of sharp structural transitions across the critical polyQ length (no drastic changes in the diffusion time with increasing chain lengths).

A detailed understanding of the structural basis of monomeric mutant HTTex1 is crucial for developing a mechanistic model for HTTex1 toxicity. Current hypotheses describing the toxic structural threshold are largely sustained by indirect evidences. In particular, numerous studies over the last decade support that both flanking regions (PRR and N17) strongly modulate the aggregation of HTTex1 in solution (Thakur et al., 2009; Crick et al., 2013; Shen et al., 2016) and in the presence of biological membranes (Burke et al., 2013). Specifically, in solution, N17 enhances aggregation in a distinct mechanism to that of synthetic polyQ peptides (Thakur et al., 2009), while PRR displays an opposite effect, favoring aggregation-resistant conformations (Bhattacharyya et al., 2006). Together, it supports that the cross-talk between both flanking regions and/or a sharp conformational transition above the pathological polyQ threshold control the HTTex1 cytotoxicity. Nevertheless, there remains controversy due to the absence of single-atom resolution structures of HTTex1 (ones lacking solubilizing tags or stabilizing amino acids). This is due to the high aggregation propensity of HTTex1, the disordered features of the polyQ stretches, and the inherent challenge of recombinant expression and purification of HTTex1. While a recent high-resolution cryo-electron microscopy structure for the full-length HTT protein was reported in a complex with HTT-associated protein 40 (HAP40), the exon 1 region was not solved due to its disordered nature (Guo et al., 2018). Notably, the first single-molecule structural characterization of monomeric HTTex1 in solution was recently provided by a collaborative study from the Lemke, Pappu, and Lashuel groups (Warner et al., 2017). In this elegant study, smFRET was used to determine intramolecular distances within monomeric HTTex1 at pM concentrations, where its self-assembly and phase separation are prevented. Briefly, both an intein-fusion strategy and a semi-synthetic approach were employed to create five polyQ lengths HTTex1 variants (15Q, 23Q, 37Q, 43Q, and 49Q). For each variant, multiple double-labeled smFRET constructs were designed by site-specific labeling at a fixed position in N17 (A2C with Alexa 488 maleimide dye) and variable in PRR (A60C, P70C, P80C, or P90C with Alexa 594 maleimide dye). Remarkably, using smFRET in combination with atomistic simulations, Warner and co-workers proposed that both wild-type (WT) and mutant HTTex1 adopt a “tadpole-like” topology, in which N17 adsorbs on the polyQ tract, making a “globular head,” and the PRR domain forms an extended/semi-flexible chain. Therefore, contrary to previous indirect evidences, smFRET data argue against sharp structural transitions in HTTex1 at pathological polyQ lengths in solution. The authors suggested that the increase of the polyQ surface area with its length promotes: (i) toxic “heterotypic interactions” by increasing the binding sites; and (ii) “homotypic interactions” that ultimately trigger HTTex1 aggregation.

In light of this recent smFRET work, future studies should firstly evaluate whether the toxic polyQ expansion controls the HTTex1 interactome. In particular, FCS or fluorescence cross-correlation spectroscopy (FCCS) will allow to quantify the interaction of WT (as control) and mutant HTTex1 with: (i) biological partners or emerging interacting proteins; (ii) biological membranes with variable lipid composition; and (iii) molecular chaperones. Simultaneously, the characterization of the conformational ensemble of HTTex1 under functional and aggregation-prone conditions through smFRET will provide insights into toxicity relevant conformations.

## TAU IN TAUOPATHIES

Tau is a microtubule-associated protein (MAP) found predominantly in the axons of neurons (Litman et al., 1993; Hirokawa et al., 1996) that plays a critical role in microtubule (MT) assembly/stabilization (Weingarten et al., 1975; Drubin and Kirschner, 1986; Gustke et al., 1994; Trinczek et al., 1995; Goode et al., 2000) and axonal transport (Ebner et al., 1998; Terwel et al., 2002). Its pathological aggregation and deposition are associated with numerous devastating neurodegenerative disorders termed tauopathies, including AD, FTL, chronic traumatic encephalopathy, and Pick’s disease (reviewed in Brunden et al., 2009). Accumulating evidence supports that the disruption of its native function as a MAP can also contribute to these tauopathies (Ballatore et al., 2007; Winklhofer et al., 2008). For instance, the abnormal hyperphosphorylation of tau can promote its self-assembly into toxic oligomers and paired helical filaments (PHFs), as well as reduces tau–MT interaction, resulting in MT destabilization and cell death (reviewed in Johnson and Stoothoff, 2004).

Tau consists of three major functional regions: (1) MT binding region (MTBR) composed of imperfect repeats that directly interacts with MTs/tubulin (Butner and Kirschner, 1991) and forms the core of PHFs (Crowther et al., 1989); (2) a proline-rich domain (PRD) that increases MT-binding/assembly (Gustke et al., 1994); and finally (3) an N-terminal projection domain that controls MT spacing (Chen et al., 1992) and might bind to neuronal plasma membrane (Brandt et al., 1995). In adult human brains, the alternative splicing of a single MAPT gene results in six different isoforms (ranging from 352 to 441 amino acids) that contain up to two N-terminal inserts (0N, 1N, and 2N) and three or four imperfect repeats (3R or 4R) within MTBR.

Tau is a large disordered protein in its monomeric unbound state (Cleveland et al., 1977). The full-length protein is highly demanding for NMR (Mukrasch et al., 2009), and so far, most NMR studies have used MTBR fragments. In a seminal ensemble FRET study, Mandelkow and co-workers identified that tau forms a highly compact structure in solution described by a “paperclip” conformation (Jeganathan et al., 2006). Specifically, this early work revealed that the C-terminus is in close proximity to the N-terminus and the MTBR, but without a measured FRET distance (so higher than 10 nm) between the N-terminus and the MTBR. Recently, the Rhoades Lab used SMF methods to characterize the aggregation-prone structures of tau [in the presence of heparin

(Elbaum-Garfinkle and Rhoades, 2012) and polyphosphates (polyP; Wickramasinghe et al., 2019)] and the functional conformations [with soluble tubulin heterodimers (Elbaum-Garfinkle et al., 2014; Li et al., 2015; Melo et al., 2016)]. Below, we summarize the studies reporting on the conformational transitions undergone by tau relevant to its functional and aggregation-prone states.

Initial smFRET work by Elbaum-Garfinkle and Rhoades redefined the “paperclip” model from ensemble measurements for tau monomer in solution and also characterized its conformational ensemble in the presence of heparin (Elbaum-Garfinkle and Rhoades, 2012). This comprehensive work investigated 12 double-labeled constructs of tau that mapped multiple overlapping regions within the 2N4R isoform (longest tau isoform), and their respective  $ET_{eff}$  were reported for each construct in the absence and presence of heparin. In solution, the overall dimensions of tau diverge from a theoretical random coil protein in a “good solvent.” This is further sustained by intramolecular contacts between the N- and C-termini and also each terminus and the MTBR, which was ascribed to electrostatic effects. Together, smFRET data supported that tau adopts more an “S-shaped” than a “paperclip” topology (Jeganathan et al., 2006; from ensemble FRET) in solution, since the MTBR is in relatively close contact with both termini. The discrepancy is explained, in part, by the use of: (i) a donor–acceptor pair with a small Förster radius; and (ii) the Förster equation to directly convert  $ET_{eff}$  into distances, in ensemble measurements. Notably, the same work also revealed that tau undergoes a two-state conformational transition upon binding to heparin underlined by the pronounced MTBR compaction and the loss of the long-range interactions between the two termini. Moreover, different domains of tau exhibit distinct physical and structural features, and consequently they respond differentially upon heparin binding. In a recent study, Wickramasinghe and co-workers investigated the interaction of tau with the physiologically aggregation inducer, polyP, using FCS and smFRET (Wickramasinghe et al., 2019). Specifically, following a similar approach as described for heparin, smFRET data reported that polyP promotes a local compaction of the MTBR and PRD, with a concomitant decrease in the long-range contacts between both termini. The binding of tau to polyP was further characterized by FCS, revealing that both PRD and MTBR interact with polyP. The conformational changes and aggregation effects depicted were found to strongly correlate with the polyP chain length. Moreover, longer polyP chains were shown to promote intermolecular interactions in tau monomers (working as “intermolecular scaffold”), thus inducing its pathological aggregation.

Most research on tau function has been focused so far on its role in MT dynamic instability and its interaction with stabilized MTs. In addition, ensemble MT polymerization assays (based on scatter measurements) do not provide a detailed description of the first step of MT assembly. Therefore, the molecular mechanism by which tau promotes the polymerization of tubulin into MTs remains poorly understood. The Rhoades Lab has applied SMF methods to describe the largely overlooked

interaction of tau with soluble tubulin heterodimers (the first step of MT assembly mechanism). In a pioneering work, Elbaum-Garfinkle et al. (2014) identified for the first time by FCS that tau binds to soluble tubulin heterodimers (under non MT assembly conditions, with a low concentration of tau and in a buffer lacking GTP), and disease mutations also enhance this interaction. In two subsequent FCS studies, Li et al. (2015) and Li and Rhoades (2017) showed that: (i) tau binds to multiple tubulin heterodimers (Li et al., 2015); and (ii) the C-terminal pseudo-repeat region of tau (adjacent to MTBR) increases the heterogeneity of tau–tubulin complex with further independent binding sites at R2 and R3, in which the size and heterogeneity are strongly linked to tau function (MT polymerization; Li and Rhoades, 2017). The topological features of tau in this heterogeneous/dynamic complex were further investigated by intramolecular smFRET (Melo et al., 2016). These measurements were performed under 100% tubulin binding and a multiprobe approach was again employed for 2N4R and 2N3R tau isoforms. Remarkably, large shifts toward lower mean  $ET_{eff}$  were observed for constructs probing the solution long-range interactions (for both termini and each terminus and the MTBR). This work revealed that tau adopts an overall open structure in this complex, exposing binding sites within the MTBR. Similarly, this expansion is observed upon binding to the MT surface (Sillen et al., 2007) and heparin (Elbaum-Garfinkle and Rhoades, 2012). Surprisingly, smFRET data also showed that the MTBR conserves its global dimensions, while its individual repeats experience local extensions to provide binding to multiple tubulin heterodimers. The extent of conformational changes within the MTBR was larger for two repeat-spanning constructs for both isoforms, also including R3. Contrary to NMR data for tau bound to a single-tubulin dimer (Gigant et al., 2014), no evidence for the U-turn topology adopted by the MTBR was found. Finally, these findings supported that tau forms a “fuzzy complex” with soluble tubulin, in which it retains its flexibility and conformational plasticity as an IDP. However, it remains to be elucidated whether tau can bind simultaneously tubulin and MTs.

In summary, smFRET revealed that the MTBR responds differentially upon interaction with soluble tubulin or heparin/polyP that accounts for distinct conformational ensembles of tau in its tubulin-bound state and aggregation-prone structure, respectively. In addition, it provides a framework to explore the role of PTMs (as hyperphosphorylation) in the conformational ensemble of monomeric tau under functional (“fuzzy complex” with soluble tubulin) and disease conditions. Finally, as recent studies support that tau can undergo liquid–liquid phase separation (LLPS; Hernández-Vega et al., 2017; Zhang et al., 2017; Wegmann et al., 2018), smFRET provides a versatile tool to probe early conformational changes that trigger phase separation (in the presence of molecular crowding and RNA), and to explore the dynamics within the droplet.

## $\alpha$ S IN PD

$\alpha$ S is a small protein (140 amino acids) abundantly expressed in presynaptic terminals of neurons in the human brain

(Maroteaux et al., 1988; Jakes et al., 1994). This protein is intrinsically flexible in solution and, similar to other IDPs, acquires structure upon binding to biological binding partners as lipid membranes (Weinreb et al., 1996; Davidson et al., 1998; Eliezer et al., 2001). While  $\alpha$ S has been associated with several biological activities, including in regulation of synaptic vesicles pools (Murphy et al., 2000; Cabin et al., 2002), neurotransmitter release (Nemani et al., 2010), SNARE complex assembly (Burré et al., 2010), and vesicle trafficking (Cooper et al., 2006; Snead and Eliezer, 2019), the precise function of this protein remains enigmatic and controversial.  $\alpha$ S is the major component of intracellular amyloid deposits known as Lewy bodies and has thus been implicated in the development and pathogenesis of neurodegenerative disorders, such as PD (Polymeropoulos et al., 1997; Spillantini et al., 1998; Goedert, 2001). In particular, biological membranes appear to play a key role in  $\alpha$ S function and dysfunction (reviewed in Snead and Eliezer, 2014).

$\alpha$ S contains three main regions: (1) N-terminal region that mediates binding to lipid membranes; (2) a central hydrophobic non-amyloid  $\beta$ -component (NAC) region responsible for its self-assembly; and (3) a highly negatively charged C-terminus. Several ensemble biophysical methods, including NMR (Eliezer et al., 2001; Bussell and Eliezer, 2003; Chandra et al., 2003; Dedmon et al., 2005), electron paramagnetic resonance (EPR) spectroscopy (Jao et al., 2004; Drescher et al., 2008), and CD (Chandra et al., 2003; Ferreón and Deniz, 2007), have provided valuable insights into the conformational transitions in  $\alpha$ S upon interaction with sodium dodecyl sulfate (SDS) micelles and/or lipid vesicles. In addition, a recent in-cell NMR study revealed that the disordered nature of monomeric  $\alpha$ S is highly conserved in the cytoplasm of mammalian cells (Theillet et al., 2016).

A seminal FCS work from the Webb and Eliezer groups quantified the binding of  $\alpha$ S to large unilamellar vesicles (LUVs) prepared with variable anionic lipid content, showing that electrostatic effects strongly enhance the  $\alpha$ S-lipid interaction (Rhoades et al., 2006). In a subsequent FCS study from the Rhoades lab, this interaction was further explored as a function of different lipid compositions (anionic and saturated lipids), membrane curvature, and PD-associated mutations (Middleton and Rhoades, 2010). This work revealed a preferential binding of  $\alpha$ S to gel-phase liposomes when compared to fluid-phase vesicles. Moreover, it reported on drastic effects of membrane curvature, underlining a stronger affinity of  $\alpha$ S for small unilamellar vesicles (SUVs) over LUVs. Finally, PD-associated mutations presented only minor changes in the molar membrane-partition coefficients compared to the WT protein.

To better understand the disorder-to-order transitions in  $\alpha$ S, several studies have employed SMF methods to identify and resolve multiple coexisting populations and its structural heterogeneity. Pioneering smFRET experiments from the Deniz, Rhoades, and Subramaniam labs provided structural insights into the conformational switching between the broken and extended  $\alpha$ -helical structures adopted by  $\alpha$ S upon binding to SDS micelles and lipid vesicles (Ferreón et al., 2009; Trexler and Rhoades, 2009; Veldhuis et al., 2009). These works were able to distinguish between conflicting reports from ensemble measurements debating the configuration of micelle or lipid

bound  $\alpha$ S (Chandra et al., 2003; Borbat et al., 2006). smFRET identified a broken  $\alpha$ -helical conformation adopted by  $\alpha$ S upon binding to SDS above the critical micelle concentration. Further, the Deniz and Rhoades labs identified that the binding surface curvature strongly modulates the helical topology of  $\alpha$ S. Their works revealed that  $\alpha$ S adopts an extended helical structure upon binding to low-curvature SDS or lipid surfaces, while it assumes a bent-helix conformation on highly curved SDS micelles. Further work from the Deniz group explored the effect of PD-associated mutations on  $\alpha$ S folding by both CD and smFRET measurements (Ferreón et al., 2010). It revealed that A53T, E46K, and C-terminal truncation (residues 1–107) variants display a similar multistate folding behavior to WT protein. However, the A30P mutation (located on the membrane binding region) was found to not adopt an extended conformation at SDS concentrations near or below the critical micelle concentration. A more recent study from the same lab investigated the “two-dimensional (2D) crowding” effect on the structural transitions of  $\alpha$ S at membrane surface (Banerjee et al., 2016). Under high “2D crowding” conditions promoted by the simultaneous membrane binding of  $\alpha$ S and Hsp27 (a lipid-interacting chaperone),  $\alpha$ S was found to adopt an alternative (“hidden”) conformation, which is not highly populated at chaperone-free conditions.

smFRET work from Trexler and Rhoades also probed the aggregation-prone structures of  $\alpha$ S under different aggregation-promoting conditions, such as low pH and in the presence of aggregation inducers (spermine and heparin; Trexler and Rhoades, 2010). Remarkably, this work revealed that the low pH and aggregation inducers promote distinct effects on the  $\alpha$ S structure. Briefly, the C-terminus of  $\alpha$ S was found to structurally collapse at low pH, while minor effects were reported on the N-terminus and the central region of the protein. However, this local compaction of C-terminal region had no significant effect on the overall dimensions of  $\alpha$ S. Meanwhile,  $\alpha$ S binding to both heparin or spermine showed a lack of large-scale structural transitions. In addition, recent work from the Deniz lab used a combination of SMF and ensemble methods to investigate the effect of osmolytes in  $\alpha$ S folding (Moosa et al., 2015). Contrary to the SDS folding pathway, this study supported that  $\alpha$ S follows a two-state transition in the presence of osmolytes, consisting of rapid interconverting conformations of unfolded and force-folded states. The effects obtained for both osmolytes and “2D crowding” support that complex cellular contexts need to be explored in order to describe the physiological folding landscape of  $\alpha$ S. On that note, recent work from the Rhoades lab revealed that cell-surface-exposed glycans are potential cellular interactors of  $\alpha$ S (Birol et al., 2019). This work employed FCS to quantify the interaction of monomer  $\alpha$ S with glycans, and identified these cell exposed glycans as key modulators of  $\alpha$ S internalization in cells.

Together, these works have identified and described the conformational landscape of  $\alpha$ S under diverse conditions (such as membrane-bound state, PD-associated mutations, and the presence of osmolytes and “2D crowding”) and provide an outline in the future to also evaluate the impact of PTMs. In addition, future *in vivo* smFRET measurements could complement in-cell MNR data (although performed at different



concentration range). In particular, it will allow to determine the physical/structural features of  $\alpha$ S under physiological and disease situations and to evaluate *in vivo* conditions promoting the disorder-to-order transition.

## CONCLUSION REMARKS

SMF methods have been recognized as powerful and versatile approaches to investigate the heterogeneous and dynamic nature of neurodegeneration-associated IDPs, including HTTex1, tau, and  $\alpha$ S as discussed in this review article. These cutting-edge techniques have provided valuable insights into: (i) their monomeric states; (ii) the aggregation-prone structures of tau and  $\alpha$ S; (iii) the disorder-to-order transition of  $\alpha$ S upon membrane binding; and finally (iv) the formation of a “fuzzy complex” by tau bound to soluble tubulin. However, the structural interpretation of smFRET data is highly challenging for IDPs due to their heterogeneous and dynamic nature. For IDPs systems, Förster equation does not provide a direct conversation of  $ET_{eff}$  in distances, and polymer physics models have been successfully applied to describe the broad distribution of donor–acceptor distances. Moreover, smFRET requires site-specific double-labeling proteins with small organic dyes through natural/mutated cysteines or genetically encoded unnatural amino acids. Meanwhile, molecular dynamics (MD) simulation provides a valuable tool to rationalize smFRET data, including to describe the dynamic movement of the dye molecule and to consider its linker, and together to provide insights into IDP conformational dynamics.

Most SMF research performed for the discussed proteins has been restricted to *in vitro* studies. As such, native functional

interactions and the associated conformational changes in the cellular context are underinvestigated. Therefore, it is crucial to move SMF methods towards *in vivo* conditions. For smFRET, it requires developing new strategies for *in vivo* labeling proteins, as fluorescent proteins are not suitable. Recent advances by Schuler and colleagues used microinjection to deliver IDPs (recombinant protein labeled *in vitro*) in live mammalian cells and employed a range of SMF techniques (including smFRET) to describe their structural dynamics (König et al., 2015), providing a new avenue to study this challenging class of proteins. We anticipate that adapting a similar approach to the systems discussed in this review article and future advances in SMF tools and application will allow to characterize the conformational ensemble of these neuronal IDPs *in vivo*, and simultaneously reveal and delineate toxic structural transitions associated to their loss of function or aggregation.

## AUTHOR CONTRIBUTIONS

AM conceptualized the manuscript. AM and MB conducted the literature review, drafted the manuscript and revised the manuscript.

## FUNDING

This work was supported by the Fundação para a Ciência e a Tecnologia (FCT, Portugal), Grant PTDC/BIA-BFS/30959/2017 (to AM) and Plataforma Portuguesa de Bioimagem (POCI-01-0145-FEDER-022122). AM is a Junior Researcher under the FCT CEEC-individual call (CEECIND/00884/2017).

## REFERENCES

- Adegbuyiro, A., Sedighi, F., Pilkington, A. W., Groover, S., and Legleiter, J. (2017). Proteins containing expanded polyglutamine tracts and neurodegenerative disease. *Biochemistry* 56, 1199–1217. doi: 10.1021/acs.biochem.6b00936
- Altschuler, E. L., Hud, N. V., Mazrimas, J. A., and Rupp, B. (1997). Random coil conformation for extended polyglutamine stretches in aqueous soluble monomeric peptides. *J. Pept. Res.* 50, 73–75. doi: 10.1111/j.1399-3011.1997.tb00622.x
- Babu, M. M. (2016). The contribution of intrinsically disordered regions to protein function, cellular complexity and human disease. *Biochem. Soc. Trans.* 44, 1185–1200. doi: 10.1042/bst20160172
- Babu, M. M., Kriwacki, R. W., and Pappu, R. V. (2012). Versatility from protein disorder. *Science* 337, 1460–1461. doi: 10.1126/science.1228775
- Ballatore, C., Lee, V. M., and Trojanowski, J. Q. (2007). Tau-mediated neurodegeneration in Alzheimer's disease and related disorders. *Nat. Rev. Neurosci.* 8, 663–672. doi: 10.1038/nrn2194
- Banerjee, P. R., and Deniz, A. A. (2014). Shedding light on protein folding landscapes by single-molecule fluorescence. *Chem. Soc. Rev.* 43, 1172–1188. doi: 10.1039/c3cs60311c
- Banerjee, P. R., Moosa, M. M., and Deniz, A. A. (2016). Two-dimensional crowding uncovers a hidden conformation of  $\alpha$ -synuclein. *Angew. Chem. Int. Ed Engl.* 55, 12789–12792. doi: 10.1002/anie.201606963
- Bates, G., Tabrizi, S., and Jones, L. (2014). *Huntington's Disease*. Oxford: Oxford University Press.
- Bhattacharyya, A., Thakur, A. K., Chellgren, V. M., Thiagarajan, G., Williams, A. D., Chellgren, B. W., et al. (2006). Oligoproline effects on polyglutamine conformation and aggregation. *J. Mol. Biol.* 355, 524–535. doi: 10.1016/j.jmb.2005.10.053
- Birol, M., Wojcik, S. P., Miranker, A. D., and Rhoades, E. (2019). Identification of N-linked glycans as specific mediators of neuronal uptake of acetylated  $\alpha$ -synuclein. *PLoS Biol.* 17:e3000318. doi: 10.1371/journal.pbio.3000318
- Borbat, P., Ramlall, T. F., Freed, J. H., and Eliezer, D. (2006). Inter-helix distances in lysophospholipid micelle-bound  $\alpha$ -synuclein from pulsed ESR measurements. *J. Am. Chem. Soc.* 128, 10004–10005. doi: 10.1021/ja063122l
- Brandt, R., Leger, J., and Lee, G. (1995). Interaction of tau with the neural plasma membrane mediated by tau's amino-terminal projection domain. *J. Cell Biol.* 131, 1327–1340. doi: 10.1083/jcb.131.5.1327
- Brucal, M., Schuler, B., and Samori, B. (2014). Single-molecule studies of intrinsically disordered proteins. *Chem. Rev.* 114, 3281–3317. doi: 10.1021/cr400297g
- Brunden, K. R., Trojanowski, J. Q., and Lee, V. M. (2009). Advances in tau-focused drug discovery for Alzheimer's disease and related tauopathies. *Nat. Rev. Drug Discov.* 8, 783–793. doi: 10.1038/nrd2959
- Burke, K. A., Kauffman, K. J., Umbaugh, C. S., Frey, S. L., and Legleiter, J. (2013). The interaction of polyglutamine peptides with lipid membranes is regulated by flanking sequences associated with huntingtin. *J. Biol. Chem.* 288, 14993–15005. doi: 10.1074/jbc.m112.446237
- Burré, J., Sharma, M., Tsetsenis, T., Buchman, V., Etherton, M. R., and Südhof, T. C. (2010).  $\alpha$ -synuclein promotes SNARE-complex assembly *in vivo* and *in vitro*. *Science* 329, 1663–1667. doi: 10.1126/science.1195227
- Bussell, R. Jr., and Eliezer, D. (2003). A structural and functional role for 11-mer repeats in  $\alpha$ -synuclein and other exchangeable lipid binding proteins. *J. Mol. Biol.* 329, 763–778. doi: 10.1016/s0022-2836(03)00520-5



- Butner, K. A., and Kirschner, M. W. (1991). Tau protein binds to microtubules through a flexible array of distributed weak sites. *J. Cell Biol.* 115, 717–730. doi: 10.1083/jcb.115.3.717
- Cabin, D. E., Shimazu, K., Murphy, D., Cole, N. B., Gottschalk, W., McIlwain, K. L., et al. (2002). Synaptic vesicle depletion correlates with attenuated synaptic responses to prolonged repetitive stimulation in mice lacking  $\alpha$ -synuclein. *J. Neurosci.* 22, 8797–8807. doi: 10.1523/jneurosci.22-20-08797.2002
- Chandra, S., Chen, X., Rizo, J., Jahn, R., and Sudhof, T. C. (2003). A broken  $\alpha$ -helix in folded  $\alpha$ -Synuclein. *J. Biol. Chem.* 278, 15313–15318. doi: 10.1074/jbc.M213128200
- Chattopadhyay, K., Elson, E. L., and Frieden, C. (2005). The kinetics of conformational fluctuations in an unfolded protein measured by fluorescence methods. *Proc. Natl. Acad. Sci. U S A* 102, 2385–2389. doi: 10.1073/pnas.0500127102
- Chen, S., Berthelot, V., Yang, W., and Wetzel, R. (2001). Polyglutamine aggregation behavior *in vitro* supports a recruitment mechanism of cytotoxicity. *J. Mol. Biol.* 311, 173–182. doi: 10.1006/jmbi.2001.4850
- Chen, J., Kanai, Y., Cowan, N. J., and Hirokawa, N. (1992). Projection domains of MAP2 and tau determine spacings between microtubules in dendrites and axons. *Nature* 360, 674–677. doi: 10.1038/360674a0
- Chen, H., and Rhoades, E. (2008). Fluorescence characterization of denatured proteins. *Curr. Opin. Struct. Biol.* 18, 516–524. doi: 10.1016/j.sbi.2008.06.008
- Cleveland, D. W., Hwo, S. Y., and Kirschner, M. W. (1977). Physical and chemical properties of purified tau factor and the role of tau in microtubule assembly. *J. Mol. Biol.* 116, 227–247. doi: 10.1016/0022-2836(77)90214-5
- Cooper, A. A., Gitler, A. D., Cashikar, A., Haynes, C. M., Hill, K. J., Bhullar, B., et al. (2006).  $\alpha$ -synuclein blocks ER-Golgi traffic and Rab1 rescues neuron loss in Parkinson's models. *Science* 313, 324–328. doi: 10.1126/science.1129462
- Cremades, N., Cohen, S. I., Deas, E., Abramov, A. Y., Chen, A. Y., Orte, A., et al. (2012). Direct observation of the interconversion of normal and toxic forms of  $\alpha$ -synuclein. *Cell* 149, 1048–1059. doi: 10.1016/j.cell.2012.03.037
- Crick, S. L., Jayaraman, M., Frieden, C., Wetzel, R., and Pappu, R. V. (2006). Fluorescence correlation spectroscopy shows that monomeric polyglutamine molecules form collapsed structures in aqueous solutions. *Proc. Natl. Acad. Sci. U S A* 103, 16764–16769. doi: 10.1073/pnas.0608175103
- Crick, S. L., Ruff, K. M., Garai, K., Frieden, C., and Pappu, R. V. (2013). Unmasking the roles of N- and C-terminal flanking sequences from exon 1 of huntingtin as modulators of polyglutamine aggregation. *Proc. Natl. Acad. Sci. U S A* 110, 20075–20080. doi: 10.1073/pnas.1320626110
- Crowther, T., Goedert, M., and Wischik, C. M. (1989). The repeat region of microtubule-associated protein tau forms part of the core of the paired helical filament of Alzheimer's disease. *Ann. Med.* 21, 127–132. doi: 10.3109/07853898909149199
- Davidson, W. S., Jonas, A., Clayton, D. F., and George, J. M. (1998). Stabilization of  $\alpha$ -synuclein secondary structure upon binding to synthetic membranes. *J. Biol. Chem.* 273, 9443–9449. doi: 10.1074/jbc.273.16.9443
- Dedmon, M. M., Lindorff-Larsen, K., Christodoulou, J., Vendruscolo, M., and Dobson, C. M. (2005). Mapping long-range interactions in  $\alpha$ -synuclein using spin-label NMR and ensemble molecular dynamics simulations. *J. Am. Chem. Soc.* 127, 476–477. doi: 10.1021/ja044834j
- Drescher, M., Veldhuis, G., van Rooijen, B. D., Milikisyants, S., Subramaniam, V., and Huber, M. (2008). Antiparallel arrangement of the helices of vesicle-bound  $\alpha$ -synuclein. *J. Am. Chem. Soc.* 130, 7796–7797. doi: 10.1021/ja801594s
- Drubin, D. G., and Kirschner, M. W. (1986). Tau protein function in living cells. *J. Cell Biol.* 103, 2739–2746. doi: 10.1083/jcb.103.6.2739
- Ebneth, A., Godemann, R., Stamer, K., Illenberger, S., Trinczek, B., and Mandelkow, E. (1998). Overexpression of tau protein inhibits kinesin-dependent trafficking of vesicles, mitochondria and endoplasmic reticulum: implications for Alzheimer's disease. *J. Cell Biol.* 143, 777–794. doi: 10.1083/jcb.143.3.777
- Elbaum-Garfinkle, S., Cobb, G., Compton, J. T., Li, X. H., and Rhoades, E. (2014). Tau mutants bind tubulin heterodimers with enhanced affinity. *Proc. Natl. Acad. Sci. U S A* 111, 6311–6316. doi: 10.1073/pnas.1315983111
- Elbaum-Garfinkle, S., and Rhoades, E. (2012). Identification of an aggregation-prone structure of tau. *J. Am. Chem. Soc.* 134, 16607–16613. doi: 10.1021/ja305206m
- Eliezer, D., Kutluay, E., Bussell, R. Jr., and Browne, G. (2001). Conformational properties of  $\alpha$ -synuclein in its free and lipid-associated states. *J. Mol. Biol.* 307, 1061–1073. doi: 10.1006/jmbi.2001.4538
- Ferreon, A. C., and Deniz, A. A. (2007).  $\alpha$ -synuclein multistate folding thermodynamics: implications for protein misfolding and aggregation. *Biochemistry* 46, 4499–4509. doi: 10.1021/bi602461y
- Ferreon, A. C., Gambin, Y., Lemke, E. A., and Deniz, A. A. (2009). Interplay of  $\alpha$ -synuclein binding and conformational switching probed by single-molecule fluorescence. *Proc. Natl. Acad. Sci. U S A* 106, 5645–5650. doi: 10.1073/pnas.0809232106
- Ferreon, A. C., Moran, C. R., Ferreon, J. C., and Deniz, A. A. (2010). Alteration of the  $\alpha$ -synuclein folding landscape by a mutation related to Parkinson's disease. *Angew. Chem. Int. Ed Engl.* 49, 3469–3472. doi: 10.1002/anie.201000378
- Fersht, A. R. (2008). From the first protein structures to our current knowledge of protein folding: delights and scepticisms. *Nat. Rev. Mol. Cell Biol.* 9, 650–654. doi: 10.1038/nrm2446
- Forster, T. (1949). Experimentelle und theoretische untersuchung des zwischenmolekularen ubergangs von elektronenanregungsenergie. *Z. Naturforsch. A* 4, 321–327.
- Gigant, B., Landrieu, I., Fauquant, C., Barbier, P., Huvent, I., Wieruszkes, J. M., et al. (2014). Mechanism of Tau-promoted microtubule assembly as probed by NMR spectroscopy. *J. Am. Chem. Soc.* 136, 12615–12623. doi: 10.1021/ja504864m
- Goedert, M. (2001).  $\alpha$ -synuclein and neurodegenerative diseases. *Nat. Rev. Neurosci.* 2, 492–501. doi: 10.1038/35081564
- Goode, B. L., Chau, M., Denis, P. E., and Feinstein, S. C. (2000). Structural and functional differences between 3-repeat and 4-repeat tau isoforms. *J. Biol. Chem.* 275, 38182–38189. doi: 10.1074/jbc.m007489200
- Guo, Q., Bin, H., Cheng, J., Seefelder, M., Engler, T., Pfeifer, G., et al. (2018). The cryo-electron microscopy structure of huntingtin. *Nature* 555, 117–120. doi: 10.1038/nature25502
- Gustke, N., Trinczek, B., Biernat, J., Mandelkow, E. M., and Mandelkow, E. (1994). Domains of tau protein and interactions with microtubules. *Biochemistry* 33, 9511–9522. doi: 10.1021/bi00198a017
- Hernández-Vega, A., Braun, M., Scharrel, L., Jahnel, M., Wegmann, S., Hyman, B. T., et al. (2017). Local nucleation of microtubule bundles through tubulin concentration into a condensed tau phase. *Cell Rep.* 20, 2304–2312. doi: 10.1016/j.celrep.2017.08.042
- Hess, S. T., Huang, S., Heikal, A. A., and Webb, W. W. (2002). Biological and chemical applications of fluorescence correlation spectroscopy: a review. *Biochemistry* 41, 697–705. doi: 10.1021/bi0118512
- Hirokawa, N., Funakoshi, T., Sato-Harada, R., and Kanai, Y. (1996). Selective stabilization of tau in axons and microtubule-associated protein 2C in cell bodies and dendrites contributes to polarized localization of cytoskeletal proteins in mature neurons. *J. Cell Biol.* 132, 667–679. doi: 10.1083/jcb.132.4.667
- Iakoucheva, L. M., Brown, C. J., Lawson, J. D., Obradović, Z., and Dunker, A. K. (2002). Intrinsic disorder in cell-signaling and cancer-associated proteins. *J. Mol. Biol.* 323, 573–584. doi: 10.1016/s0022-2836(02)00969-5
- Jakes, R., Spillantini, M. G., and Goedert, M. (1994). Identification of two distinct synucleins from human brain. *FEBS Lett.* 345, 27–32. doi: 10.1016/0014-5793(94)00395-5
- Jao, C. C., Der-Sarkissian, A., Chen, J., and Langen, R. (2004). Structure of membrane-bound  $\alpha$ -synuclein studied by site-directed spin labeling. *Proc. Natl. Acad. Sci. U S A* 101, 8331–8336. doi: 10.1073/pnas.0400553101
- Jeganathan, S., von Bergen, M., Brutlach, H., Steinhoff, H. J., and Mandelkow, E. (2006). Global hairpin folding of tau in solution. *Biochemistry* 45, 2283–2293. doi: 10.1021/bi0521543
- Johnson, G. V., and Stoothoff, W. H. (2004). Tau phosphorylation in neuronal cell function and dysfunction. *J. Cell Sci.* 117, 5721–5729. doi: 10.1242/jcs.01558
- Joo, C., Balci, H., Ishitsuka, Y., Buranachai, C., and Ha, T. (2008). Advances in single-molecule fluorescence methods for molecular biology. *Annu. Rev. Biochem.* 77, 51–76. doi: 10.1146/annurev.biochem.77.070606.101543
- Klein, F. A. C., Pastore, A., Masino, L., Zeder-Lutz, G., Nierengarten, H., Oulad-Abdelghani, M., et al. (2007). Pathogenic and non-pathogenic polyglutamine tracts have similar structural properties: towards a length-dependent toxicity gradient. *J. Mol. Biol.* 371, 235–244. doi: 10.1016/j.jmb.2007.05.028

- König, I., Zarrine-Afsar, A., Aznauryan, M., Soranno, A., Wunderlich, B., Dingfelder, F., et al. (2015). Single-molecule spectroscopy of protein conformational dynamics in live eukaryotic cells. *Nat. Methods* 12, 773–779. doi: 10.1038/nmeth.3475
- Kriwacki, R. W., Hengst, L., Tennant, L., Reed, S. I., and Wright, P. E. (1996). Structural studies of p21Waf1/Cip1/Sdi1 in the free and Cdk2-bound state: conformational disorder mediates binding diversity. *Proc. Natl. Acad. Sci. U S A* 93, 11504–11509. doi: 10.1073/pnas.93.21.11504
- Kundel, F., Tosatto, L., Whiten, D. R., Wirthensohn, D. C., Horrocks, M. H., and Klenerman, D. (2018). Shedding light on aberrant interactions—a review of modern tools for studying protein aggregates. *FEBS J.* 285, 3604–3630. doi: 10.1111/febs.14409
- Lee, T., Moran-Gutierrez, C. R., and Deniz, A. A. (2015). Probing protein disorder and complexity at single-molecule resolution. *Semin. Cell Dev. Biol.* 37, 26–34. doi: 10.1016/j.semcdb.2014.09.027
- Lemke, E. A. (2011). Site-specific labeling of proteins for single-molecule FRET measurements using genetically encoded ketone functionalities. *Methods Mol. Biol.* 751, 3–15. doi: 10.1007/978-1-61779-151-2\_1
- Li, X. H., Culver, J. A., and Rhoades, E. (2015). Tau binds to multiple tubulin dimers with helical structure. *J. Am. Chem. Soc.* 137, 9218–9221. doi: 10.1021/jacs.5b04561
- Li, X. H., and Rhoades, E. (2017). Heterogeneous tau-tubulin complexes accelerate microtubule polymerization. *Biophys. J.* 112, 2567–2574. doi: 10.1016/j.bpj.2017.05.006
- Litman, P., Barg, J., Rindzoon, L., and Ginzburg, I. (1993). Subcellular localization of tau mRNA in differentiating neuronal cell culture: implications for neuronal polarity. *Neuron* 10, 627–638. doi: 10.1016/0896-6273(93)90165-n
- Lv, Z., Krasnoslobodtsev, A. V., Zhang, Y., Ysselstein, D., Rochet, J. C., Blanchard, S. C., et al. (2015). Direct detection of  $\alpha$ -synuclein dimerization dynamics: single-molecule fluorescence analysis. *Biophys. J.* 108, 2038–2047. doi: 10.1016/j.bpj.2015.03.010
- MacDonald, M. E., Ambrose, C. M., Duyao, M. P., Myers, R. H., Lin, C., Srinidhi, L., et al. (1993). A novel gene containing a trinucleotide repeat that is expanded and unstable on Huntington's disease chromosomes. *Cell* 72, 971–983. doi: 10.1016/0092-8674(93)90585-e
- Mangiarini, L., Sathasivam, K., Seller, M., Cozens, B., Harper, A., Hetherington, C., et al. (1996). Exon 1 of the HD gene with an expanded CAG repeat is sufficient to cause a progressive neurological phenotype in transgenic mice. *Cell* 87, 493–506. doi: 10.1016/S0092-8674(00)81369-0
- Maroteaux, L., Campanelli, J. T., and Scheller, R. H. (1988). Synuclein: a neuron-specific protein localized to the nucleus and presynaptic nerve terminal. *J. Neurosci.* 8, 2804–2815. doi: 10.1523/jneurosci.08-08-02804.1988
- Melo, A. M., Coraor, J., Alpha-Cobb, G., Elbaum-Garfinkle, S., Nath, A., and Rhoades, E. (2016). A functional role for intrinsic disorder in the tau-tubulin complex. *Proc. Natl. Acad. Sci. U S A* 113, 14336–14341. doi: 10.1073/pnas.1610137113
- Melo, A. M., Elbaum-Garfinkle, S., and Rhoades, E. (2017). Insights into tau function and dysfunction through single-molecule fluorescence. *Methods Cell Biol.* 141, 27–44. doi: 10.1016/bs.mcb.2017.06.010
- Melo, A. M., Prieto, M., and Coutinho, A. (2011). The effect of variable liposome brightness on quantifying lipid-protein interactions using fluorescence correlation spectroscopy. *Biochim. Biophys. Acta* 1808, 2559–2568. doi: 10.1016/j.bbame.2011.06.001
- Middleton, E. R., and Rhoades, E. (2010). Effects of curvature and composition on  $\alpha$ -synuclein binding to lipid vesicles. *Biophys. J.* 99, 2279–2288. doi: 10.1016/j.bpj.2010.07.056
- Mittag, T., Kay, L. E., and Forman-Kay, J. D. (2010). Protein dynamics and conformational disorder in molecular recognition. *J. Mol. Recognit.* 23, 105–116. doi: 10.1002/jmr.961
- Moosa, M. M., Ferreon, A. C., and Deniz, A. A. (2015). Forced folding of a disordered protein accesses an alternative folding landscape. *Chemphyschem* 16, 90–94. doi: 10.1002/cphc.201402661
- Mukrasch, M. D., Bibow, S., Korukottu, J., Jeganathan, S., Biernat, J., Griesinger, C., et al. (2009). Structural polymorphism of 441-residue tau at single residue resolution. *PLoS Biol.* 7:e34. doi: 10.1371/journal.pbio.1000034
- Murphy, D. D., Rueter, S. M., Trojanowski, J. Q., and Lee, V. M. (2000). Synucleins are developmentally expressed and  $\alpha$ -synuclein regulates the size of the presynaptic vesicular pool in primary hippocampal neurons. *J. Neurosci.* 20, 3214–3220. doi: 10.1523/jneurosci.20-09-03214.2000
- Nagai, Y., Inui, T., Popiel, H. A., Fujikake, N., Hasegawa, K., Urade, Y., et al. (2007). A toxic monomeric conformer of the polyglutamine protein. *Nat. Struct. Mol. Biol.* 14, 332–340. doi: 10.1038/nsmb1215
- Nemani, V. M., Lu, W., Berge, V., Nakamura, K., Onoa, B., Lee, M. K., et al. (2010). Increased expression of  $\alpha$ -synuclein reduces neurotransmitter release by inhibiting synaptic vesicle recluster after endocytosis. *Neuron* 65, 66–79. doi: 10.1016/j.neuron.2009.12.023
- O'Brien, E. P., Morrison, G., Brooks, B. R., and Thirumalai, D. (2009). How accurate are polymer models in the analysis of Förster resonance energy transfer experiments on proteins? *J. Chem. Phys.* 130:124903. doi: 10.1063/1.3082151
- Polymeropoulos, M. H., Lavedan, C., Leroy, E., Ide, S. E., Dehejia, A., Dutra, A., et al. (1997). Mutation in the  $\alpha$ -synuclein gene identified in families with Parkinson's disease. *Science* 276, 2045–2047. doi: 10.1126/science.276.5321.2045
- Rhoades, E., Ramlall, T. F., Webb, W. W., and Eliezer, D. (2006). Quantification of  $\alpha$ -synuclein binding to lipid vesicles using fluorescence correlation spectroscopy. *Biophys. J.* 90, 4692–4700. doi: 10.1529/biophysj.105.079251
- Sathasivam, K., Neueder, A., Gipson, T. A., Landles, C., Benjamin, A. C., Bondulich, M. K., et al. (2013). Aberrant splicing of HTT generates the pathogenic exon 1 protein in Huntington disease. *Proc. Natl. Acad. Sci. U S A* 110, 2366–2370. doi: 10.1073/pnas.1221891110
- Saudou, F., and Humbert, S. (2016). The biology of Huntingtin. *Neuron* 89, 910–926. doi: 10.1016/j.neuron.2016.02.003
- Schuler, B., and Eaton, W. A. (2008). Protein folding studied by single-molecule FRET. *Curr. Opin. Struct. Biol.* 18, 16–26. doi: 10.1016/j.sbi.2007.12.003
- Schuler, B., Soranno, A., Hofmann, H., and Nettels, D. (2016). Single-molecule FRET spectroscopy and the polymer physics of unfolded and intrinsically disordered proteins. *Annu. Rev. Biophys.* 45, 207–231. doi: 10.1146/annurev-biophys-062215-010915
- Schulte, J., and Littleton, J. T. (2011). The biological function of the Huntingtin protein and its relevance to Huntington's disease pathology. *Curr. Trends Neurol.* 5, 65–78.
- Shammas, S. L., Garcia, G. A., Kumar, S., Kjaergaard, M., Horrocks, M. H., Shivji, N., et al. (2015). A mechanistic model of tau amyloid aggregation based on direct observation of oligomers. *Nat. Commun.* 6:7025. doi: 10.1038/ncomms8025
- Shen, K., Calamini, B., Fauerbach, J. A., Ma, B., Shahmoradian, S. H., Serrano Lachapel, I. L., et al. (2016). Control of the structural landscape and neuronal proteotoxicity of mutant Huntingtin by domains flanking the polyQ tract. *Elife* 18:18065. doi: 10.7554/eLife.18065
- Sherman, E., Itkin, A., Kuttner, Y. Y., Rhoades, E., Amir, D., Haas, E., et al. (2008). Using fluorescence correlation spectroscopy to study conformational changes in denatured proteins. *Biophys. J.* 94, 4819–4827. doi: 10.1529/biophysj.107.120220
- Sillen, A., Barbier, P., Landrieu, I., Lefebvre, S., Wieruszski, J. M., Leroy, A., et al. (2007). NMR investigation of the interaction between the neuronal protein tau and the microtubules. *Biochemistry* 46, 3055–3064. doi: 10.1021/bi061920i
- Snead, D., and Eliezer, D. (2014).  $\alpha$ -synuclein function and dysfunction on cellular membranes. *Exp. Neurobiol.* 23, 292–313. doi: 10.5607/en.2014.23.4.292
- Snead, D., and Eliezer, D. (2019). Intrinsically disordered proteins in synaptic vesicle trafficking and release. *J. Biol. Chem.* 294, 3325–3342. doi: 10.1074/jbc.rev118.006493
- Soranno, A., Buchli, B., Nettels, D., Cheng, R. R., Müller-Späh, S., Pfeil, S. H., et al. (2012). Quantifying internal friction in unfolded and intrinsically disordered proteins with single-molecule spectroscopy. *Proc. Natl. Acad. Sci. U S A* 109, 17800–17806. doi: 10.1073/pnas.1117368109
- Spillantini, M. G., Crowther, R. A., Jakes, R., Hasegawa, M., and Goedert, M. (1998).  $\alpha$ -Synuclein in filamentous inclusions of Lewy bodies from Parkinson's disease and dementia with lewy bodies. *Proc. Natl. Acad. Sci. U S A* 95, 6469–6473. doi: 10.1073/pnas.95.11.6469
- Takahashi, T., Kikuchi, S., Katada, S., Nagai, Y., Nishizawa, M., and Onodera, O. (2008). Soluble polyglutamine oligomers formed prior to inclusion body formation are cytotoxic. *Hum. Mol. Genet.* 17, 345–356. doi: 10.1093/hmg/ddm311

- Terwel, D., Dewachter, I., and Van Leuven, F. (2002). Axonal transport, tau protein, and neurodegeneration in Alzheimer's disease. *Neuromolecular Med.* 2, 151–165. doi: 10.1385/nmm:2:2:151
- Thakur, A. K., Jayaraman, M., Mishra, R., Thakur, M., Chellgren, V. M., Byeon, I.-J., et al. (2009). Polyglutamine disruption of the huntingtin exon1 N-terminus triggers a complex aggregation mechanism. *Nat. Struct. Mol. Biol.* 16, 380–389. doi: 10.1038/nsmb.1570
- Theillet, F. X., Binolfi, A., Bekei, B., Martorana, A., Rose, H. M., Stuiiver, M., et al. (2016). Structural disorder of monomeric  $\alpha$ -synuclein persists in mammalian cells. *Nature* 530, 45–50. doi: 10.1038/nature16531
- Tomba, P. (2012). Intrinsically disordered proteins: a 10-year recap. *Trends Biochem. Sci.* 37, 509–516. doi: 10.1016/j.tibs.2012.08.004
- Trexler, A. J., and Rhoades, E. (2009).  $\alpha$ -synuclein binds large unilamellar vesicles as an extended helix. *Biochemistry* 48, 2304–2306. doi: 10.1021/bi900114z
- Trexler, A. J., and Rhoades, E. (2010). Single molecule characterization of  $\alpha$ -synuclein in aggregation-prone states. *Biophys. J.* 99, 3048–3055. doi: 10.1016/j.bpj.2010.08.056
- Trinczek, B., Biernat, J., Baumann, K., Mandelkow, E. M., and Mandelkow, E. (1995). Domains of tau protein, differential phosphorylation and dynamic instability of microtubules. *Mol. Biol. Cell* 6, 1887–1902. doi: 10.1091/mbc.6.12.1887
- Trojanowski, J. Q., and Lee, V. M. (2005). Pathological tau: a loss of normal function or a gain in toxicity? *Nat. Neurosci.* 8, 1136–1137. doi: 10.1038/nn0905-1136
- Tsafou, K., Tiwari, P. B., Forman-Kay, J. D., Metallo, S. J., and Toretzky, J. A. (2018). Targeting intrinsically disordered transcription factors: changing the paradigm. *J. Mol. Biol.* 430, 2321–2341. doi: 10.1016/j.jmb.2018.04.008
- Uversky, V. N. (2014). The triple power of D<sup>3</sup>: protein intrinsic disorder in degenerative diseases. *Front. Biosci. (Landmark Ed.)* 19, 181–258. doi: 10.2741/4204
- Uversky, V. N. (2015). Intrinsically disordered proteins and their (disordered) proteomes in neurodegenerative disorders. *Front. Aging Neurosci.* 7:18. doi: 10.3389/fnagi.2015.00018
- Uversky, V. N., Oldfield, C. J., and Dunker, A. K. (2008). Intrinsically disordered proteins in human diseases: introducing the D2 concept. *Annu. Rev. Biophys.* 37, 215–246. doi: 10.1146/annurev.biophys.37.032807.125924
- van der Lee, R., Buljan, M., Lang, B., Weatheritt, R. J., Daughdrill, G. W., Dunker, A. K., et al. (2014). Classification of intrinsically disordered regions and proteins. *Chem. Rev.* 114, 6589–6631. doi: 10.1021/cr400525m
- Veldhuis, G., Segers-Nolten, I., Ferlemann, E., and Subramaniam, V. (2009). Single-molecule FRET reveals structural heterogeneity of SDS-bound  $\alpha$ -synuclein. *Chembiochem* 10, 436–439. doi: 10.1002/cbic.200800644
- Warner, J. B. T., Ruff, K. M., Tan, P. S., Lemke, E. A., Pappu, R. V., Lashuel, H. A. (2017). Monomeric huntingtin exon 1 has similar overall structural features for wild-type and pathological polyglutamine lengths. *J. Am. Chem. Soc.* 139, 14456–14469. doi: 10.1021/jacs.7b06659
- Wegmann, S., Eftekharzadeh, B., Tepper, K., Zoltowska, K. M., Bennett, R. E., Dujardin, S., et al. (2018). Tau protein liquid-liquid phase separation can initiate tau aggregation. *EMBO J.* 37:e98049. doi: 10.15252/embj.201798049
- Weingarten, M. D., Lockwood, A. H., Hwo, S. Y., and Kirschner, M. W. (1975). A protein factor essential for microtubule assembly. *Proc. Natl. Acad. Sci. U S A* 72, 1858–1862. doi: 10.1073/pnas.72.5.1858
- Weinreb, P. H., Zhen, W., Poon, A. W., Conway, K. A., and Lansbury, P. T. Jr. (1996). NACP, a protein implicated in Alzheimer's disease and learning, is natively unfolded. *Biochemistry* 35, 13709–13715. doi: 10.1021/bi961799n
- Wellington, C. L., Ellerby, L. M., Gutekunst, C. A., Rogers, D., Warby, S., Graham, R. K., et al. (2002). Caspase cleavage of mutant huntingtin precedes neurodegeneration in Huntington's disease. *J. Neurosci.* 22, 7862–7872. doi: 10.1523/jneurosci.22-18-07862.2002
- Wetzel, R. (2012). Physical chemistry of polyglutamine: intriguing tales of a monotonous sequence. *J. Mol. Biol.* 421, 466–490. doi: 10.1016/j.jmb.2012.01.030
- Wickramasinghe, S. P., Lempart, J., Merens, H. E., Murphy, J., Huettemann, P., Jakob, U., et al. (2019). Polyphosphate initiates tau aggregation through intra- and intermolecular scaffolding. *Biophys. J.* 117, 717–728. doi: 10.1016/j.bpj.2019.07.028
- Winklhofer, K. F., Tatzelt, J., and Haass, C. (2008). The two faces of protein misfolding: gain- and loss-of-function in neurodegenerative diseases. *EMBO J.* 27, 336–349. doi: 10.1038/sj.emboj.7601930
- Wright, P. E., and Dyson, H. J. (1999). Intrinsically unstructured proteins: re-assessing the protein structure-function paradigm. *J. Mol. Biol.* 293, 321–331. doi: 10.1006/jmbi.1999.3110
- Wright, P. E., and Dyson, H. J. (2015). Intrinsically disordered proteins in cellular signalling and regulation. *Nat. Rev. Mol. Cell Biol.* 16, 18–29. doi: 10.1038/nrm3920
- Zhang, X., Lin, Y., Eschmann, N. A., Zhou, H., Rauch, J. N., Hernandez, I., et al. (2017). RNA stores tau reversibly in complex coacervates. *PLoS Biol.* 15:e2002183. doi: 10.1371/journal.pbio.2002183
- Zijlstra, N., Blum, C., Segers-Nolten, I. M., Claessens, M. M., and Subramaniam, V. (2012). Molecular composition of sub-stoichiometrically labeled  $\alpha$ -synuclein oligomers determined by single-molecule photobleaching. *Angew. Chem. Int. Ed. Engl.* 51, 8821–8824. doi: 10.1002/anie.201200813

**Conflict of Interest:** The authors declare that the research was conducted in the absence of any commercial or financial relationships that could be construed as a potential conflict of interest.

Copyright © 2020 Birol and Melo. This is an open-access article distributed under the terms of the Creative Commons Attribution License (CC BY). The use, distribution or reproduction in other forums is permitted, provided the original author(s) and the copyright owner(s) are credited and that the original publication in this journal is cited, in accordance with accepted academic practice. No use, distribution or reproduction is permitted which does not comply with these terms.



# Oligomers Are Promising Targets for Drug Development in the Treatment of Proteinopathies

Oxana V. Galzitskaya<sup>1,2\*</sup>

<sup>1</sup>Laboratory of Bioinformatics and Proteomics, Institute of Protein Research, Russian Academy of Sciences, Pushchino, Russia, <sup>2</sup>Laboratory of the Structure and Function of Muscle Proteins, Institute of Theoretical and Experimental Biophysics, Russian Academy of Sciences, Pushchino, Russia

Currently, there is no effective treatment of proteinopathies, as well as their diagnosis in the early stages of the disease until the first clinical symptoms appear. The proposed model of fibrillation of the A $\beta$  peptide and its fragments not only describes molecular rearrangements, but also offers models of processes that occur during the formation of amyloid aggregates. Since this model is also characteristic of other proteins and peptides, a new potential target for drug development in the treatment of Alzheimer's disease (AD) and other proteinopathies is proposed on the basis of this model. In our opinion, it is oligomers that are promising targets for innovative developments in the treatment of these diseases.

## OPEN ACCESS

### Edited by:

Sandra Macedo-Ribeiro,  
University of Porto, Portugal

### Reviewed by:

Md. Golam Sharoar,  
University of Connecticut Health  
Center, United States  
Vytautas Smirnovas,  
Vilnius University, Lithuania

### \*Correspondence:

Oxana V. Galzitskaya  
ogalzit@vega.protres.ru

**Received:** 24 August 2019

**Accepted:** 16 December 2019

**Published:** 31 January 2020

### Citation:

Galzitskaya OV (2020) Oligomers Are Promising Targets for Drug Development in the Treatment of Proteinopathies. *Front. Mol. Neurosci.* 12:319. doi: 10.3389/fnmol.2019.00319

**Keywords:** amyloid, oligomer, drug, polymorphism, model

## INTRODUCTION

In the process of folding, the protein molecule acquires a unique spatial structure, which is necessary for its biological function. Nevertheless, in cells, there are a number of conditions under which the process of protein folding is disrupted. This leads to the formation of protein oligomers forming insoluble aggregates. A variety of such aggregates are amyloid fibrils. The formation and accumulation of amyloid aggregates in organs and tissues is one of the observed stages of the pathogenesis of diseases, combined into a group of proteinopathies, which includes Alzheimer's disease (AD), Parkinson's disease (PD), type 2 diabetes mellitus, and various systemic amyloidoses (Saha et al., 2000; Hardy and Selkoe, 2002; Caughey and Lansbury, 2003; Chiti and Dobson, 2006; Lesné et al., 2006; Shankar et al., 2008).

Currently, there is no effective therapy for proteinopathies, as well as their diagnosis in the early stages of the disease until the first clinical symptoms appear. In addition, a large number of proteins that are not associated with pathological processes are capable of forming amyloid aggregates and fibrils *in vitro*. This allows us to conclude that the formation of amyloids is a common property of the polypeptide chain (Fändrich and Dobson, 2002). It is also known that amyloid fibrils formed by the same protein can have a high degree of polymorphism (Fändrich et al., 2009). Therefore, the study of the molecular mechanism of the pathogenesis of amyloidosis is one of the urgent and important tasks of modern medicine and molecular biology.



## THE EFFECTIVENESS OF DRUG THERAPY

It is extremely alarming that the inefficiency of modern methods of treatment is associated with failures in the development of new drugs for the treatment of AD. The proportion of successful treatment attempts created by drugs during the decade from 2002 to 2012 is 0.4% (Ousset et al., 2014).

Cholinesterase Inhibitors (ChEIs) are a common form of drug treatment of AD, and the three most effective drugs are donepezil, galantamine, and rivastigmine. Side effects when using these drugs are different, but none of them contributes to a significant improvement in cognitive function in patients (Birks, 2006). There is evidence that prolonged exposure to these drugs even accelerates AD (Lu and Tune, 2003). In addition, they effectively increase the level of acetylcholine available for neurotransmission. Memantine is an alternative approved drug that only mildly inhibits the glutamatergic system by binding to N-methyl-D-aspartate receptors (NMDARs; Glasgow et al., 2017), which reduce excess  $\text{Ca}^{2+}$  in postsynaptic neurons associated with neurodegenerative diseases (Parsons et al., 2013). Glutamate receptors of the central nervous system play a key role in ensuring the plasticity of neurons and the processes of memory consolidation (under normal conditions). Hyperactivation of the N-methyl-D-aspartate (NMDA) subtype of these receptors leads to the development of neurotoxicity.

Memantine is also effective in combination with ChEIs (Tariot et al., 2004). Non-specific treatments for AD used include antidepressants, such as selective serotonin reuptake inhibitors fluoxetine and paroxetine, which can combine well with ChEI (Aboukhatwa et al., 2010). Other symptoms of AD, such as anxiety and psychosis, may be affected by drugs such as anxiolytics, oxazepam or antipsychotics, risperidone (Ballard and Waite, 2006). Although these drugs are considered effective in the treatment of AD, they nevertheless affect only the symptoms of the disease.

From the point of view of drug targets in the treatment of AD,  $\alpha$ -,  $\beta$ - and  $\gamma$ -secretases are studied, which are involved in APP proteolysis to the A $\beta$  peptide. As mentioned above, the disruption of the aggregation of the A $\beta$  peptide can lead to the prevention of plaque formation (Yang et al., 2019). There are several targets associated with the degradation of the A $\beta$  peptide, one of which is neprilysin (Hornung et al., 2019). There are targets that regulate the expression of APP in patients with AD. It is also necessary to include targets related to the phosphorylation and aggregation of tau protein in this incomplete list.

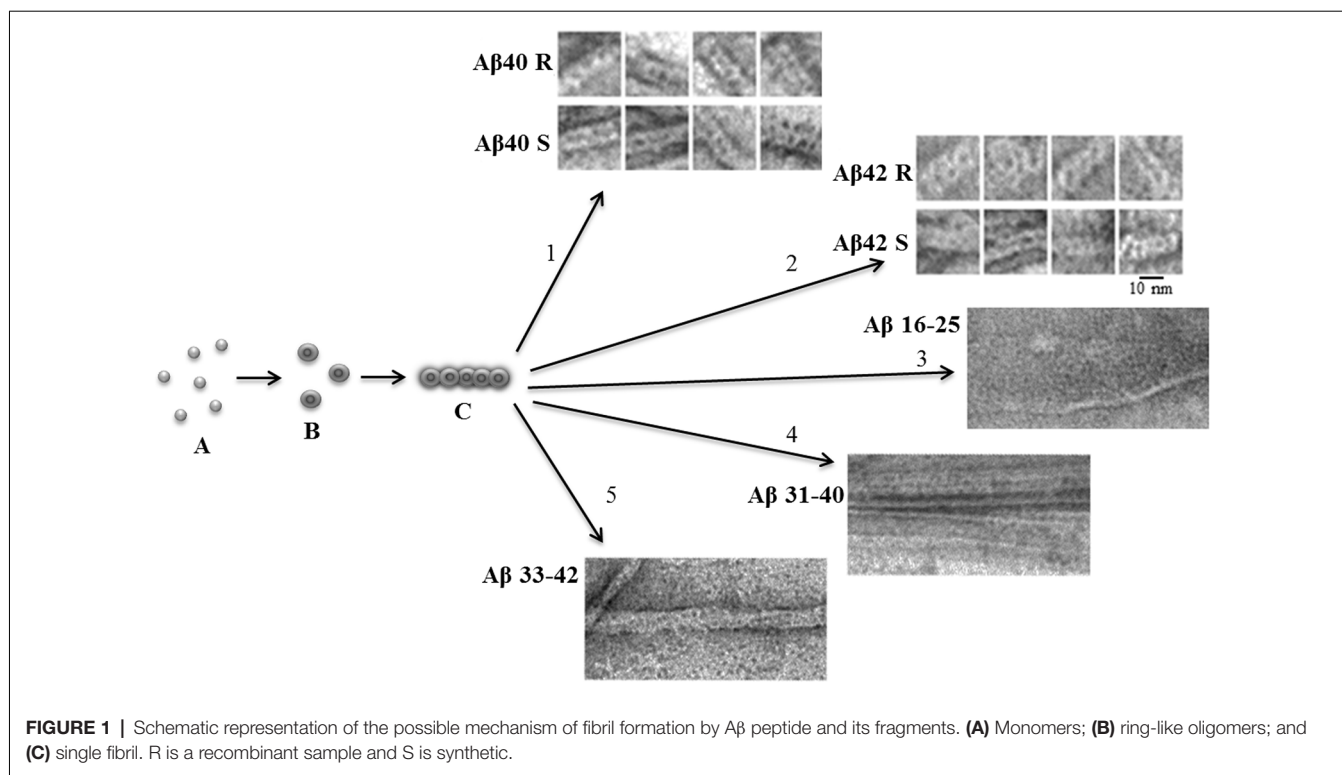
As for  $\beta$ -secretase (BACE1), there are many studies on its inhibition, including docking of a number of flavonoids (Shimmyo et al., 2008), as well as a number of studies on virtual screening (Huang et al., 2005; John et al., 2011); later high-throughput screening (in combination with pharmacophore modeling to clarify), which revealed the reasons for the inhibition of this enzyme (Muthusamy et al., 2013). Studies of mutant forms of BACE1 in mice indicate that there may be serious side effects when inhibiting this particular enzyme. In particular, such effects can be neurodegeneration, which is a serious problem (Yan and Vassar, 2014). As regards

$\gamma$ -secretase, this intramembrane protein is involved not only in the APP proteolysis but also in a number of other processes (Minter et al., 2005). It is clear that inhibition of this enzyme leads to a decrease in the amount of A $\beta$  peptide (He et al., 2010). The situation is complicated by another protein,  $\beta$ -arrestin 2, which apparently regulates  $\gamma$ -secretase, and thus, inhibition of this enzyme can reduce the formation of A $\beta$  peptide plaques (Thathiah et al., 2013). Since the formation of the A $\beta$  peptide is a sequential process from the APP precursor protein that requires the sequential participation of BACE1 and  $\gamma$ -secretase, combination therapy, including both BACE1 inhibitor and  $\gamma$ -secretase modulator, will be more effective than an individual treatment of each individual enzyme during the formation of A $\beta$  peptide (Strömberg et al., 2015).

## AMYLOID FIBRILS AND OLIGOMERS

There are two competing hypotheses about the cause of AD: one of them is the amyloid hypothesis (Tanzi and Bertram, 2005). It is based on the idea that the amyloid A $\beta$  peptide, instead of being synthesized and participating in metabolism, begins to accumulate in the brain and form aggregates in the form of plaques. The accumulation of the peptide leads to pathology, expressed in the death of neuron cells and the appearance of plaques containing this protein. Genetic data are also a source of confirmation of this hypothesis. The A $\beta$  peptide precursor protein (APP) gene is located on chromosome 21, and trisomy of this chromosome in Down syndrome is the reason that AD is often observed in patients with Down syndrome (Masters et al., 1985; Maltsev et al., 2011), which in this case indicates the genetic basis of AD disease. Simple proteolysis is required to convert the A $\beta$  peptide precursor protein (APP) to the A $\beta$  peptide. It should be mentioned that no correlation was found between amyloid plaque formation and neuronal loss (Schmitz et al., 2004). The so-called “channel” hypothesis of AD, first proposed in 1993, states: that oligomers of amyloidogenic proteins make pores into the membrane that causes the influx of  $\text{Ca}^{2+}$  ions, an imbalance of ions of other metals, oxidative stress, and finally cell death (Arispe et al., 1993). The second hypothesis is associated with modifications of tau protein. Hyperphosphorylation of tau protein associated with microtubules leads to pathology of neural tangles. Recent studies have shown that there is a connection between these two hypotheses (Small and Duff, 2008; Jin et al., 2011; Maltsev et al., 2014). In addition to this, misfolding of the A $\beta$  peptide and tau protein is observed, which leads to their uncontrolled aggregation. Observation of the pathological process shows that misfolding is distributed from local points by the prion-like mechanism for both tau and A $\beta$  peptide (Bloom, 2014). For tau protein, the formation of polymorphic particles was shown by NMR analysis (Mukrasch et al., 2009).

In the last decade, several researchers have attempted to describe oligomeric particles, which are possibly the precursors of the formation of amyloid fibrils. The direct interest in oligomeric particles is due to the fact that, for example, in the case of AD, oligomers formed by the A $\beta$  peptide are found in the brain tissues of patients suffering from this disease (Roher et al.,



1996). A similar role of oligomers (nanomers and dodecamers) was noted in many studies since such particles have the highest toxicity compared to dimers, trimers, and tetramers. More and more facts indicate that in the pathogenesis of neurodegenerative diseases, it is the oligomers, and not the mature fibrils, that pose the greatest danger. Thus, it has recently been demonstrated that oligomers formed by the Aβ(1–42) peptide have a damaging effect on the blood-brain barrier, thereby disrupting brain homeostasis (Brkic et al., 2015).

It is believed that amyloid fibrils are specifically ordered aggregates characterized by the presence of a secondary structure of a certain type—a cross-β structure, in which β-sheets are parallel to the axis of fibril (Makin and Serpell, 2005). In the formation of amyloid aggregates by globular proteins, only part of their amino acid sequence is involved in the formation of the cross-β structure. The introduction of amino acid substitutions into these regions (amyloidogenic region) may affect the ability of the protein to form amyloid fibrils. The determination of amyloidogenic regions is necessary to understand the mechanism of amyloid aggregation and the pathogenesis of neurodegenerative diseases (Selivanova et al., 2016c; Surin et al., 2016).

In addition, it currently remains difficult to establish the spatial structure of fibrillar aggregates due to the limited capabilities of individual physicochemical methods. For example, the structure of amyloid fibrils can be determined using the method of solid-state NMR spectroscopy, however, this method is very time-consuming and ambiguous in the interpretation of the obtained data. Also, despite the fact that amyloidogenic proteins and peptides are

the objects of study by a large number of researchers, and the appearance of a large number of publications at the moment there is no general model that describes the molecular mechanism of the formation of amyloid aggregates and fibrils (Fändrich et al., 2011). Protofibrils are not yet available on images from a cryogenic sample, and therefore high-resolution cryo-EM reconstructions from fibrils represent the average values of multiple conformations of protofilaments (Gremer et al., 2017). In this case, averaging as high-resolution information of individual protofilaments, as well as conformational variability in flexible regions, are lost (Seuring et al., 2018).

Using bioinformatics approaches and modern physicochemical methods, we studied the formation of amyloid aggregates of the Aβ(1–40), Aβ(1–42) peptides and their fragments, and a model is proposed that describes the mechanism of the structural organization of amyloid fibrils (Suvorina et al., 2015; Selivanova et al., 2016a,b,c, 2018a,b; Galzitskaya and Selivanova, 2017; Galzitskaya et al., 2018a,b; Galzitskaya, 2019).

Based on the developed kinetic model of amyloid formation, the sizes of primary and secondary nucleus of fibril formation were calculated for two isoforms of the Aβ peptide (Dovidchenko et al., 2014, 2016). Thus, for the Aβ(1–40) peptide, it was found that the size of the primary nucleus is two monomers, and for Aβ(1–42) three monomers. In this case, the size of the secondary nucleus for the Aβ(1–40) peptide is one monomer, and for Aβ(1–42) it is two monomers. Based on the obtained data, a structural model of the primary oligomer underlying the dodecamer was proposed (Dovidchenko et al., 2016).

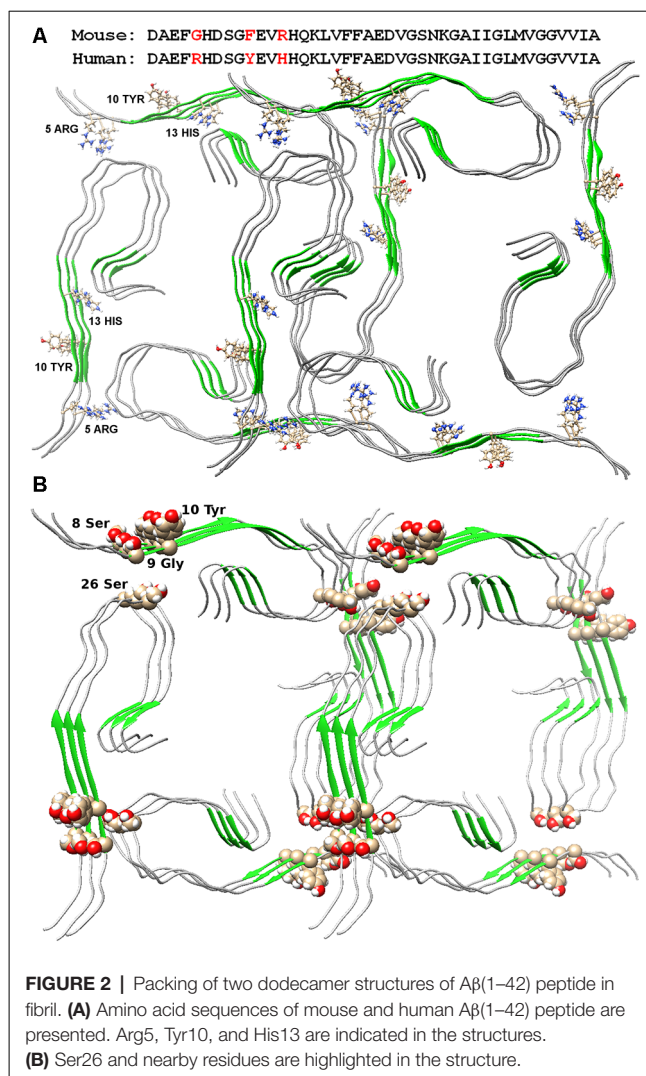
It was shown by electron microscopy that the key structural element, which is the building block for the formation of amyloid fibrils, is a ring-like oligomer consisting of approximately 12 monomers for A $\beta$ (1–40) and A $\beta$ (1–42) peptides. The diameter of such an oligomer is 8–9 nm, and the height about 3 nm. The inner diameter of the ring oligomer is 3–4 nm. Ring-like oligomers are stacked in a fibril on a ring-to-ring or more frequently ring-on-ring basis with a slight overlap. Oligomers of this type are observed in electron micrographs from the moment when the amyloid formation process begins, and their number gradually decreases. Oligomers interact with each other not only on a ring-to-ring basis but can also attached to the side surface of fibrils due to lateral interactions, thereby increasing its thickness.

We have proposed an oligomer structure for the A $\beta$  peptide and its fragments, which are very different from each other. The A $\beta$  peptide oligomer consists of three primary oligomers that form a ring-like structure in a cross-section. Twelve monomers (56 kDa) form a tubular cylinder with an internal diameter of about 3–4 nm, and the salt bridges stabilize this oligomer: Arg5–Glu22 is formed between the primary oligomers, and Asp23–Lys28 is formed inside the monomeric structure. The regular sizes of the structures observed upon application of these oligomers are present on X-ray diffraction patterns (this is the meridional reflection at 53Å and the equatorial reflection at 55Å). In the case of oligomer for the fragments of A $\beta$  peptide, such an oligomer is formed from 48 peptides that form 12  $\beta$ -sheets arranged in a tubular cylinder with outer and inner diameters of 6 and 2 nm, respectively (Galzitskaya et al., 2018b).

An important characteristic of amyloid fibrils formed by A $\beta$ (1–40) and A $\beta$ (1–42) peptides is their polymorphism. The model of aggregation of amyloid fibrils that we have proposed is valuable in that it explains this polymorphism. In this case, this is due to a change in the association of oligomers during amyloidogenesis (Figure 1). The structure of the oligomer itself is determined by the amino acid sequence of the monomers. A vivid example of this can be demonstrated by the example of A $\beta$ (1–40) and A $\beta$ (1–42) isoforms and amyloidogenic fragments of the A $\beta$  peptide. The constructions of oligomers differ in the structure of the complex and physicochemical properties (Dovidchenko et al., 2014; Galzitskaya and Selivanova, 2017; Selivanova et al., 2018b; Galzitskaya, 2019; Figure 1).

To determine the amyloidogenic regions of the protein polypeptide chain that form intermolecular interactions in amyloid fibrils, an approach was used consisting in the limited proteolysis of mature fibrils and subsequent determination of the amino acid sequence of the obtained peptides using high-resolution mass spectrometry (Selivanova et al., 2016c; Surin et al., 2016; Galzitskaya et al., 2018b).

The data obtained using the approach described above allowed us not only to find out what structural transformations a protein or peptide molecule undergoes in the process of fibril formation, but also to confirm the described model of amyloid formation for A $\beta$ (1–40) and A $\beta$ (1–42) peptides. It should be noted that the experimentally determined amyloidogenic fragments coincided with the predicted sites using the FoldAmyloid program (Garbuzynskiy et al., 2010).



## WHY DO NOT MICE GET ALZHEIMER'S DISEASE? A POSSIBLE ORGANIZATION OF THE OLIGOMERIC STRUCTURE MAY PROVIDE AN ANSWER TO THIS QUESTION

Recent evidence suggests that soluble A $\beta$  peptide oligomers are a major cause of synaptic dysfunction and memory loss in AD. To further address this uncertainty, the neurotoxicity of various isoforms of A $\beta$  peptide was analyzed at the cellular level. The results showed that A $\beta$ (1–42) can form oligomers much faster than A $\beta$ (1–40) oligomers, while A $\beta$ (1–43) and A $\beta$ (1–42) exhibit the highest level of neurotoxicity (Fu et al., 2017).

The EM images clearly show that fibrils are built from oligomeric structures for both the A $\beta$  peptide and its fragments (Figure 1). The structure of A $\beta$ (1–42) fibril, determined using cryo-electron microscopy, does not coincide with the EM images presented in the Supplementary: when increasing the EM images, it is clear that the fibril does not consist of endless beta-sheets



obtained using the processing program cryo-EM, and the fibril is constructed of oligomeric structures laid in the same way as in our model (Gremer et al., 2017).

The possible organization of the oligomeric structure may answer the question, why mice do not have AD? In the mouse A $\beta$  peptide, Gly is located instead of Arg5, thereby violating the salt bridge, a bond that stabilizes the layers of primary oligomers. And the presence of Arg13 instead of His13 only prevents the formation of such an oligomer structure. Thus, the replacement of three amino acids at the N-terminus of the murine A $\beta$  peptide results in no signs of AD in mice (**Figure 2A**). The deletion of Glu22 (Osaka mutant) causes enhanced oligomerization of the A $\beta$  peptide, but not fibrillogenesis (Tomiya et al., 2008). Again, a salt bridge cannot form, a bond stabilizing the monomeric form of the A $\beta$  peptide. Ala2Thr mutation (Jonsson et al., 2012) can slow down A $\beta$  fibrillogenesis (Lin et al., 2017), but at the same time, Ala2Val mutation (Di Fede et al., 2009) accelerates A $\beta$  fibrillogenesis and is associated with the early onset of AD (Messa et al., 2014), since such mutation leads to stabilization of the N-terminal part of the peptide. English mutation (Janssen et al., 2003) His6Arg promotes fibrillogenesis, enhances cytotoxicity, and increases the average size of A $\beta$  oligomers (Ono et al., 2010). It should be noted that for only a few mutants, the model structure of monomer packing in amyloid fibril was obtained.

Five developed antibodies (Gantenerumab, Solanezumab, Aducanumab, Bapineuzumab, Crenezumab) did not reach clinical stage 3. This means that there was a misconception (vision) of the structure of the amyloid against which antibodies were developed. Among the ensemble of oligomers, it is necessary to single out the “correct” oligomer, which is involved in the construction of fibrils. And as we now understand, such an oligomer should be just 56 kDa dodecamer. It is just stable compared with the primary oligomer—tetramer. Murakami (2014) presents in his article a picture with a large pool of oligomers that will participate in the construction of fibrils. But if we take into account that the fibril is built from specific building material, then all the other oligomers should not interest us as a target.

The Ser26Glu mutation was detected in the A $\beta$  peptide (a message from S. Linse at the Amyloid 2019 conference in Lund), which does not lead to cross-seeding, which means that the structures from which the fibrils are built for the wild type and mutant shape are different (Tran et al., 2017). From the point of view of existing structures, such a mutation should not affect the fibril structure in any way, since in both structures of 2016 and 2017, this residue looks at the solvent (Wälti et al., 2016; Gremer et al., 2017). Only in our model, this mutation will prevent the formation of an oligomeric particle, and most likely,

the mutant form will have a completely different structure of the building block—the oligomer, so the process of cross-seeding is impossible (**Figure 2B**).

## CONCLUSIONS

The study of the reasons and development of neurodegenerative diseases is an important and urgent task of modern medicine. The prevalence of these diseases is from 5 to 15%, depending on the age of the patient. It should also be noted that the spread of this group of diseases is also an acute social problem, since these diseases reduce the quality and life of patients. As a rule, such diseases are diagnosed in the late stages of development, when patients develop the impaired cognitive function. At the moment, the etiology and pathogenesis of various neurodegenerative diseases and proteinopathies are only being clarified, there are almost no diagnostic methods at an early stage of the disease and attempts to develop an effective method of treatment have practically no results. This is a direct consequence of a lack of understanding of key events in the molecular mechanism of the pathogenesis of neurodegenerative diseases and proteinopathies.

Our proposed model of fibrillation of A $\beta$  peptide and its fragments not only describes molecular rearrangements, but also offers models of processes that occur during the formation of amyloid aggregates. In addition, we offer a new potential target for drug development in the treatment of AD. In our opinion, it is “correct” oligomeric complexes that are promising targets for innovative developments in the treatment of this disease.

## DATA AVAILABILITY STATEMENT

The datasets generated for this study are available on request to the corresponding author.

## AUTHOR CONTRIBUTIONS

The author confirms being the sole contributor of this work and has approved it for publication.

## FUNDING

The study was funded by the Russian Science Foundation (grants #18-14-00321 and 14-14-00536).

## ACKNOWLEDGMENTS

We are grateful to A.V. Glyakina for assistance in the preparation of the manuscript, O.M. Selivanova, and A.K. Surin for their help in obtaining EM and mass spectrometry analysis.

## REFERENCES

- Aboukhatwa, M., Dosanjh, L., and Luo, Y. (2010). Antidepressants are a rational complementary therapy for the treatment of Alzheimer's disease. *Mol. Neurodegener.* 5:10. doi: 10.1186/1750-1326-5-10
- Arispe, N., Rojas, E., and Pollard, H. B. (1993). Alzheimer disease amyloid  $\beta$  protein forms calcium channels in bilayer membranes: blockade by tromethamine and aluminum. *Proc. Natl. Acad. Sci. U S A* 90, 567–571. doi: 10.1073/pnas.90.2.567
- Ballard, C., and Waite, J. (2006). The effectiveness of atypical antipsychotics for the treatment of aggression and psychosis in Alzheimer's disease. *Cochrane Database Syst. Rev.* 4:CD003476. doi: 10.1002/14651858.CD003476.pub2
- Birks, J. (2006). Cholinesterase inhibitors for Alzheimer's disease. *Cochrane Database Syst. Rev.* 1:CD005593. doi: 10.1002/14651858.CD005593



- Bloom, G. S. (2014). Amyloid- $\beta$  and tau: the trigger and bullet in Alzheimer disease pathogenesis. *JAMA Neurol.* 71, 505–508. doi: 10.1001/jamaneurol.2013.5847
- Brkic, M., Balusu, S., Van Wouterghem, E., Gorlé, N., Benilova, I., Kremer, A., et al. (2015). Amyloid- $\beta$  oligomers disrupt blood-CSF barrier integrity by activating matrix metalloproteinases. *J. Neurosci.* 35, 12766–12778. doi: 10.1523/JNEUROSCI.0006-15.2015
- Caughey, B., and Lansbury, P. T. (2003). Protofibrils, pores, fibrils, and neurodegeneration: separating the responsible protein aggregates from the innocent bystanders. *Annu. Rev. Neurosci.* 26, 267–298. doi: 10.1146/annurev.neuro.26.010302.081142
- Chiti, F., and Dobson, C. M. (2006). Protein misfolding, functional amyloid, and human disease. *Annu. Rev. Biochem.* 75, 333–366. doi: 10.1146/annurev.biochem.75.101304.123901
- Di Fede, G., Catania, M., Morbin, M., Rossi, G., Suardi, S., Mazzoleni, G., et al. (2009). A recessive mutation in the APP gene with dominant-negative effect on amyloidogenesis. *Science* 323, 1473–1477. doi: 10.1126/science.1168979
- Dovidchenko, N. V., Finkelstein, A. V., and Galzitskaya, O. V. (2014). How to determine the size of folding nuclei of protofibrils from the concentration dependence of the rate and lag-time of aggregation. I. Modeling the amyloid protofibril formation. *J. Phys. Chem. B* 118, 1189–1197. doi: 10.1021/jp4083294
- Dovidchenko, N. V., Glyakina, A. V., Selivanova, O. M., Grigorashvili, E. I., Suvorina, M. Y., Dzhus, U. F., et al. (2016). One of the possible mechanisms of amyloid fibrils formation based on the sizes of primary and secondary folding nuclei of A $\beta$ 40 and A $\beta$ 42. *J. Struct. Biol.* 194, 404–414. doi: 10.1016/j.jsb.2016.03.020
- Fändrich, M., and Dobson, C. M. (2002). The behaviour of polyamino acids reveals an inverse side chain effect in amyloid structure formation. *EMBO J.* 21, 5682–5690. doi: 10.1093/emboj/cdf573
- Fändrich, M., Meinhardt, J., and Grigorieff, N. (2009). Structural polymorphism of Alzheimer A $\beta$  and other amyloid fibrils. *Prion* 3, 89–93. doi: 10.4161/pri.3.2.8859
- Fändrich, M., Schmidt, M., and Grigorieff, N. (2011). Recent progress in understanding Alzheimer's  $\beta$ -amyloid structures. *Trends Biochem. Sci.* 36, 338–345. doi: 10.1016/j.tibs.2011.02.002
- Fu, L., Sun, Y., Guo, Y., Chen, Y., Yu, B., Zhang, H., et al. (2017). Comparison of neurotoxicity of different aggregated forms of A $\beta$ 40, A $\beta$ 42 and A $\beta$ 43 in cell cultures. *J. Pept. Sci.* 23, 245–251. doi: 10.1002/psc.2975
- Galzitskaya, O. (2019). New mechanism of amyloid fibril formation. *Curr. Protein Pept. Sci.* 20, 630–640. doi: 10.2174/1389203720666190125160937
- Galzitskaya, O. V., Galushko, E. I., and Selivanova, O. M. (2018a). Studies of the process of amyloid formation by A $\beta$  peptide. *Biochemistry* 83, S62–S80. doi: 10.1134/S0006297918140079
- Galzitskaya, O. V., Surin, A. K., Glyakina, A. V., Rogachevsky, V. V., and Selivanova, O. M. (2018b). Should the treatment of amyloidosis be personified? Molecular mechanism of amyloid formation by A $\beta$  peptide and its fragments. *J. Alzheimers Dis. Rep.* 2, 181–199. doi: 10.3233/ADR-180063
- Galzitskaya, O. V., and Selivanova, O. M. (2017). Rosetta stone for amyloid fibrils: the key role of ring-like oligomers in amyloidogenesis. *J. Alzheimers Dis.* 59, 785–795. doi: 10.3233/jad-170230
- Garbuzynski, S. O., Lobanov, M. Y., and Galzitskaya, O. V. (2010). FoldAmyloid: a method of prediction of amyloidogenic regions from protein sequence. *Bioinformatics* 26, 326–332. doi: 10.1093/bioinformatics/btp691
- Glasgow, N. G., Povysheva, N. V., Azofeifa, A. M., and Johnson, J. W. (2017). Memantine and ketamine differentially alter NMDA receptor desensitization. *J. Neurosci.* 37, 9686–9704. doi: 10.1523/jneurosci.1173-17.2017
- Gremer, L., Schölzel, D., Schenk, C., Reinartz, E., Labahn, J., Ravelli, R. B. G., et al. (2017). Fibril structure of amyloid- $\beta$ (1–42) by cryo-electron microscopy. *Science* 358, 116–119. doi: 10.1126/science.aao2825
- Hardy, J., and Selkoe, D. J. (2002). The amyloid hypothesis of Alzheimer's disease: progress and problems on the road to therapeutics. *Science* 297, 353–356. doi: 10.1126/science.1072994
- He, G., Luo, W., Li, P., Remmers, C., Netzer, W. J., Hendrick, J., et al. (2010).  $\gamma$ -secretase activating protein is a therapeutic target for Alzheimer's disease. *Nature* 467, 95–98. doi: 10.1038/nature09325
- Hornung, K., Zampar, S., Engel, N., Klafki, H., Liepold, T., Bayer, T. A., et al. (2019). N-terminal truncated A $\beta$ 4–42 is a substrate for neprilysin degradation *in vitro* and *in vivo*. *J. Alzheimers Dis.* 67, 849–858. doi: 10.3233/JAD-181134
- Huang, D., Lüthi, U., Kolb, P., Edler, K., Cecchini, M., Audetat, S., et al. (2005). Discovery of cell-permeable non-peptide inhibitors of  $\beta$ -secretase by high-throughput docking and continuum electrostatics calculations. *J. Med. Chem.* 48, 5108–5111. doi: 10.1021/jm050499d
- Janssen, J. C., Beck, J. A., Campbell, T. A., Dickinson, A., Fox, N. C., Harvey, R. J., et al. (2003). Early onset familial Alzheimer's disease: mutation frequency in 31 families. *Neurology* 60, 235–239. doi: 10.1212/01.wnl.0000042088.22694.e3
- Jin, M., Shepardson, N., Yang, T., Chen, G., Walsh, D., and Selkoe, D. J. (2011). Soluble amyloid  $\beta$ -protein dimers isolated from Alzheimer cortex directly induce Tau hyperphosphorylation and neuritic degeneration. *Proc. Natl. Acad. Sci. U S A* 108, 5819–5824. doi: 10.1073/pnas.1017033108
- John, S., Thangapandian, S., Sakkiath, S., and Lee, K. W. (2011). Potent BACE-1 inhibitor design using pharmacophore modeling, *in silico* screening and molecular docking studies. *BMC Bioinformatics* 12:S28. doi: 10.1186/1471-2105-12-s1-s28
- Jonsson, T., Atwal, J. K., Steinberg, S., Snaedal, J., Jonsson, P. V., Bjornsson, S., et al. (2012). A mutation in APP protects against Alzheimer's disease and age-related cognitive decline. *Nature* 488, 96–99. doi: 10.1038/nature11283
- Lesné, S., Koh, M. T., Kotilinek, L., Kaye, R., Glabe, C. G., Yang, A., et al. (2006). A specific amyloid- $\beta$  protein assembly in the brain impairs memory. *Nature* 440, 352–357. doi: 10.1038/nature04533
- Lin, T.-W., Chang, C.-F., Chang, Y.-J., Liao, Y.-H., Yu, H.-M., and Chen, Y.-R. (2017). Alzheimer's amyloid- $\beta$  A2T variant and its N-terminal peptides inhibit amyloid- $\beta$  fibrillization and rescue the induced cytotoxicity. *PLoS One* 12:e0174561. doi: 10.1371/journal.pone.0174561
- Lu, C., and Tune, L. E. (2003). Chronic exposure to anticholinergic medications adversely affects the course of Alzheimer disease. *Am. J. Geriatr. Psychiatry* 11, 458–461. doi: 10.1176/appi.ajgp.11.4.458
- Makin, O. S., and Serpell, L. C. (2005). X-ray diffraction studies of amyloid structure. *Methods Mol. Biol.* 299, 67–80. doi: 10.1385/1-59259-874-9:067
- Maltsev, A. V., Bystryak, S., and Galzitskaya, O. V. (2011). The role of  $\beta$ -amyloid peptide in neurodegenerative diseases. *Ageing Res. Rev.* 10, 440–452. doi: 10.1016/j.arr.2011.03.002
- Maltsev, A. V., Santockyte, R., Bystryak, S., and Galzitskaya, O. V. (2014). Activation of neuronal defense mechanisms in response to pathogenic factors triggering induction of amyloidosis in Alzheimer's disease. *J. Alzheimers Dis.* 40, 19–32. doi: 10.3233/jad-131562
- Masters, C. L., Simms, G., Weinman, N. A., Multhaup, G., McDonald, B. L., and Beyreuther, K. (1985). Amyloid plaque core protein in Alzheimer disease and Down syndrome. *Proc. Natl. Acad. Sci. U S A* 82, 4245–4249. doi: 10.1073/pnas.82.12.4245
- Messa, M., Colombo, L., del Favero, E., Cantù, L., Stoilova, T., Cagnotto, A., et al. (2014). The peculiar role of the A2V mutation in amyloid- $\beta$  (A $\beta$ ) 1–42 molecular assembly. *J. Biol. Chem.* 289, 24143–24152. doi: 10.1074/jbc.m114.576256
- Minter, L. M., Turley, D. M., Das, P., Shin, H. M., Joshi, I., Lawlor, R. G., et al. (2005). Inhibitors of  $\gamma$ -secretase block *in vivo* and *in vitro* T helper type 1 polarization by preventing Notch upregulation of Tbx21. *Nat. Immunol.* 6, 680–688. doi: 10.1038/ni1209x
- Mukrasch, M. D., Bibow, S., Korukottu, J., Jeganathan, S., Biernat, J., Griesinger, C., et al. (2009). Structural polymorphism of 441-residue tau at single residue resolution. *PLoS Biol.* 7:e34. doi: 10.1371/journal.pbio.1000034
- Murakami, K. (2014). Conformation-specific antibodies to target amyloid  $\beta$  oligomers and their application to immunotherapy for Alzheimer's disease. *Biosci. Biotechnol. Biochem.* 78, 1293–1305. doi: 10.1080/09168451.2014.940275
- Muthusamy, K., Singh, K. D., Chinnasamy, S., Nagamani, S., Krishnasamy, G., Thiagarajan, C., et al. (2013). High throughput virtual screening and E-pharmacophore filtering in the discovery of new BACE-1 inhibitors. *Interdiscip. Sci.* 5, 119–126. doi: 10.1007/s12539-013-0157-x
- Ono, K., Condron, M. M., and Teplow, D. B. (2010). Effects of the English (H6R) and Tottori (D7N) familial Alzheimer disease mutations on amyloid  $\beta$ -protein assembly and toxicity. *J. Biol. Chem.* 285, 23186–23197. doi: 10.1074/jbc.m109.086496
- Ousset, P.-J., Cummings, J., Delrieu, J., Legrand, V., Prins, N., Winblad, B., et al. (2014). Is Alzheimer's disease drug development broken? What must be improved. *J. Prev. Alzheimers Dis.* 1, 40–45. doi: 10.14283/jpad.2014.19

- Parsons, C. G., Danysz, W., Dekundy, A., and Pulte, I. (2013). Memantine and cholinesterase inhibitors: complementary mechanisms in the treatment of Alzheimer's disease. *Neurotox. Res.* 24, 358–369. doi: 10.1007/s12640-013-9398-z
- Roher, A. E., Chaney, M. O., Kuo, Y. M., Webster, S. D., Stine, W. B., Haverkamp, L. J., et al. (1996). Morphology and toxicity of A $\beta$ -(1–42) dimer derived from neuritic and vascular amyloid deposits of Alzheimer's disease. *J. Biol. Chem.* 271, 20631–20635. doi: 10.1074/jbc.271.34.20631
- Saha, A. R., Ninkina, N. N., Hanger, D. P., Anderton, B. H., Davies, A. M., and Buchman, V. L. (2000). Induction of neuronal death by  $\alpha$ -synuclein. *Eur. J. Neurosci.* 12, 3073–3077. doi: 10.1046/j.1460-9568.2000.00210.x
- Schmitz, C., Rutten, B. P. F., Pielen, A., Schäfer, S., Wirths, O., Tremp, G., et al. (2004). Hippocampal neuron loss exceeds amyloid plaque load in a transgenic mouse model of Alzheimer's disease. *Am. J. Pathol.* 164, 1495–1502. doi: 10.1016/s0002-9440(10)63235-x
- Selivanova, O. M., Gorbunova, E. Y., Mustaeva, L. G., Grigorashvili, E. I., Suvorina, M. Y., Surin, A. K., et al. (2016a). Peptide A $\beta$ (16–25) forms nanofilms in the process of its aggregation. *Biochemistry* 81, 755–761. doi: 10.1134/S0006297916070129
- Selivanova, O. M., Grigorashvili, E. I., Suvorina, M. Y., Dzhus, U. F., Nikulin, A. D., Marchenkov, V. V., et al. (2016b). X-ray diffraction and electron microscopy data for amyloid formation of A $\beta$ 40 and A $\beta$ 42. *Data Brief* 8, 108–113. doi: 10.1016/j.dib.2016.05.020
- Selivanova, O. M., Surin, A. K., Marchenkov, V. V., Dzhus, U. F., Grigorashvili, E. I., Suvorina, M. Y., et al. (2016c). The mechanism underlying amyloid polymorphism is opened for Alzheimer's disease amyloid- $\beta$  peptide. *J. Alzheimers Dis.* 54, 821–830. doi: 10.3233/jad-160405
- Selivanova, O. M., Rogachevsky, V. V., Syrin, A. K., and Galzitskaya, O. V. (2018a). Molecular mechanism of amyloid formation by A $\beta$  peptide: review of own works. *Biomed. Khim.* 64, 94–109. doi: 10.18097/pbmc20186401094
- Selivanova, O. M., Surin, A. K., Ryzhykau, Y. L., Glyakina, A. V., Suvorina, M. Y., Kuklin, A. I., et al. (2018b). To be fibrils or to be nanofilms? oligomers are building blocks for fibril and nanofilm formation of fragments of A $\beta$  peptide. *Langmuir* 34, 2332–2343. doi: 10.1021/acs.langmuir.7b03393
- Seuring, C., Ayyer, K., Filippaki, E., Barthelmess, M., Longchamp, J.-N., Ringler, P., et al. (2018). Femtosecond X-ray coherent diffraction of aligned amyloid fibrils on low background graphene. *Nat. Commun.* 9:1836. doi: 10.1038/s41467-018-04116-9
- Shankar, G. M., Li, S., Mehta, T. H., Garcia-Munoz, A., Shepardson, N. E., Smith, I., et al. (2008). Amyloid- $\beta$  protein dimers isolated directly from Alzheimer's brains impair synaptic plasticity and memory. *Nat. Med.* 14, 837–842. doi: 10.1038/nm1782
- Shimmyo, Y., Kihara, T., Akaike, A., Niidome, T., and Sugimoto, H. (2008). Flavonols and flavones as BACE-1 inhibitors: structure-activity relationship in cell-free, cell-based and *in silico* studies reveal novel pharmacophore features. *Biochim. Biophys. Acta* 1780, 819–825. doi: 10.1016/j.bbagen.2008.01.017
- Small, S. A., and Duff, K. (2008). Linking A $\beta$  and tau in late-onset Alzheimer's disease: a dual pathway hypothesis. *Neuron* 60, 534–542. doi: 10.1016/j.neuron.2008.11.007
- Strömberg, K., Eketjäll, S., Georgievskaya, B., Tunblad, K., Eliason, K., Olsson, F., et al. (2015). Combining an amyloid- $\beta$  (A $\beta$ ) cleaving enzyme inhibitor with a  $\gamma$ -secretase modulator results in an additive reduction of A $\beta$  production. *FEBS J.* 282, 65–73. doi: 10.1111/febs.13103
- Surin, A. K., Grigorashvili, E. I., Suvorina, M. Y., Selivanova, O. M., and Galzitskaya, O. V. (2016). Determination of regions involved in amyloid fibril formation for A $\beta$ (1–40) peptide. *Biochemistry* 81, 762–769. doi: 10.1134/S0006297916070130
- Suvorina, M. Y., Selivanova, O. M., Grigorashvili, E. I., Nikulin, A. D., Marchenkov, V. V., Surin, A. K., et al. (2015). Studies of polymorphism of amyloid- $\beta$  42 peptide from different suppliers. *J. Alzheimers Dis.* 47, 583–593. doi: 10.3233/JAD-150147
- Tanzi, R. E., and Bertram, L. (2005). Twenty years of the Alzheimer's disease amyloid hypothesis: a genetic perspective. *Cell* 120, 545–555. doi: 10.1016/j.cell.2005.02.008
- Tariot, P. N., Farlow, M. R., Grossberg, G. T., Graham, S. M., McDonald, S., Gergel, I., et al. (2004). Memantine treatment in patients with moderate to severe Alzheimer disease already receiving donepezil: a randomized controlled trial. *JAMA* 291, 317–324. doi: 10.1001/jama.291.3.317
- Thathiah, A., Horré, K., Snellinx, A., Vandeweyer, E., Huang, Y., Ciesielska, M., et al. (2013).  $\beta$ -arrestin 2 regulates A $\beta$  generation and  $\gamma$ -secretase activity in Alzheimer's disease. *Nat. Med.* 19, 43–49. doi: 10.1038/nm.3023
- Tomiyama, T., Nagata, T., Shimada, H., Teraoka, R., Fukushima, A., Kanemitsu, H., et al. (2008). A new amyloid  $\beta$  variant favoring oligomerization in Alzheimer's-type dementia. *Ann. Neurol.* 63, 377–387. doi: 10.1002/ana.21321
- Tran, J., Chang, D., Hsu, F., Wang, H., and Guo, Z. (2017). Cross-seeding between A $\beta$ 40 and A $\beta$ 42 in Alzheimer's disease. *FEBS Lett.* 591, 177–185. doi: 10.1002/1873-3468.12526
- Wälti, M. A., Ravotti, F., Arai, H., Glabe, C. G., Wall, J. S., Böckmann, A., et al. (2016). Atomic-resolution structure of a disease-relevant A $\beta$ (1–42) amyloid fibril. *Proc. Natl. Acad. Sci. U S A* 113, E4976–E4984. doi: 10.1073/pnas.1600749113
- Yan, R., and Vassar, R. (2014). Targeting the  $\beta$  secretase BACE1 for Alzheimer's disease therapy. *Lancet Neurol.* 13, 319–329. doi: 10.1016/S1474-4422(13)70276-X
- Yang, T., Dang, Y., Ostaszewski, B., Mengel, D., Steffen, V., Rabe, C., et al. (2019). Target engagement in an Alzheimer trial: crenesumab lowers amyloid  $\beta$  oligomers in cerebrospinal fluid. *Ann. Neurol.* 86, 215–224. doi: 10.1002/ana.25513

**Conflict of Interest:** The author declares that the research was conducted in the absence of any commercial or financial relationships that could be construed as a potential conflict of interest.

Copyright © 2020 Galzitskaya. This is an open-access article distributed under the terms of the Creative Commons Attribution License (CC BY). The use, distribution or reproduction in other forums is permitted, provided the original author(s) and the copyright owner(s) are credited and that the original publication in this journal is cited, in accordance with accepted academic practice. No use, distribution or reproduction is permitted which does not comply with these terms.



# Protein Aggregation and Dysfunction of Autophagy-Lysosomal Pathway: A Vicious Cycle in Lysosomal Storage Diseases

Antonio Monaco<sup>1</sup> and Alessandro Fraldi<sup>1,2\*</sup>

<sup>1</sup> Telethon Institute of Genetics and Medicine, Pozzuoli, Italy, <sup>2</sup> Department of Translational Medicine, University of Naples "Federico II," Naples, Italy

## OPEN ACCESS

### Edited by:

Sandra Macedo-Ribeiro,  
University of Porto, Portugal

### Reviewed by:

Sabine Hilfiker,  
Spanish National Research Council,  
Spain

Cleio Nobrega,  
University of Algarve, Portugal

### \*Correspondence:

Alessandro Fraldi  
fraldi@tigem.it

**Received:** 16 December 2019

**Accepted:** 24 February 2020

**Published:** 11 March 2020

### Citation:

Monaco A and Fraldi A (2020)  
Protein Aggregation and Dysfunction  
of Autophagy-Lysosomal Pathway:  
A Vicious Cycle in Lysosomal Storage  
Diseases.  
*Front. Mol. Neurosci.* 13:37.  
doi: 10.3389/fnmol.2020.00037

Many neurodegenerative conditions are characterized by the deposition of protein aggregates (mainly amyloid-like) in the central nervous system (CNS). In post-mitotic CNS cells protein aggregation causes cytotoxicity by interfering with various cellular functions. Mutations in different genes may directly cause protein aggregation. However, genetic factors together with aging may contribute to the onset of protein aggregation also by affecting cellular degradative functions, in particular the autophagy-lysosomal pathway (ALP). Increasing body of evidence show that ALP dysfunction and protein aggregation are functionally interconnected and induce each other during neurodegenerative processes. We will summarize the findings supporting these concepts by focusing on lysosomal storage diseases (LSDs), a class of metabolic inherited conditions characterized by global lysosomal dysfunction and often associated to a severe neurodegenerative course. We propose a model by which the inherited lysosomal defects initiate aggregate-prone protein deposition, which, in turns, worsen ALP degradation function, thus generating a vicious cycle, which boost neurodegenerative cascades.

**Keywords:** lysosome, lysosomal storage disease, autophagy, amyloid aggregation, molecular therapy of neurodegenerative diseases

## PROTEIN AGGREGATION IN NEURODEGENERATION DISEASES

A hallmark of many neurodegenerative diseases is the progressive formation of insoluble protein aggregates that, in most cases, are composed by amyloidogenic proteins (Chiti and Dobson, 2006). Indeed, under different stress conditions, several intrinsically disordered proteins (normally soluble) misfold and undergo structural changes and self-assembly that ultimately lead to their aggregation into insoluble deposits, referred to as amyloids (Dobson, 2003). Amyloid deposits are characterized by a fibrillar morphology and a cross- $\beta$  structure, whereby intermolecular main-chain hydrogen bonding acts as one major stabilizing interaction (Chiti and Dobson, 2006). Although in some neurodegenerations (e.g., in the polyglutamine diseases; see below) aggregation *per se* could be not the cause of the observed neurotoxicity, generally, amyloid aggregation

represents a therapeutic target for neurological conditions since it can cause cytotoxicity either by directly interfering with various cellular functions or because the aggregates sequester other proteins, which play essential cellular functions (Ciechanover and Kwon, 2015; Gallardo et al., 2016). Nevertheless, the mechanisms underlying neurotoxicity driven by amyloid deposition are not completely understood.

Amyloid deposits found in neurodegenerative diseases are often characterized by one main component; however, in some neurodegenerative conditions several amyloidogenic proteins may contribute to amyloid deposition (Table 1). Alzheimer's disease (AD), the most common neurodegenerative disorder is characterized by deposition of amyloid plaques, whose main component is the amyloid-beta (A $\beta$ ) protein (Goedert and Spillantini, 2006).  $\alpha$ -Synuclein accumulation and aggregation within Lewy bodies and neurites of the CNS in the form of amyloid fibrils plays a central role in the pathophysiology of Parkinson's disease (PD) and in a subset of neurodegenerative conditions known as dementias with Lewy bodies (Spillantini et al., 1997). Polyglutamine (polyQ) expansions in unrelated proteins and consequent intracellular accumulation of the mutant protein in inclusion bodies is the underlying cause of a number of inherited rare neurodegenerative disorders, including Huntington's disease (HD) (polyQ expansion in the huntingtin protein), spinal and bulbar muscular atrophy (SBMA) (polyQ expansion in the androgen receptor protein), and some forms of spinocerebellar ataxias (polyQ expansion in ataxin protein) (Perutz, 1999). Neurofibrillary tangles, which consists of fibrillar aggregates of hyperphosphorylated tau protein, are commonly seen in aging and AD brain and are correlated with decline of brain functions in these conditions (Goedert and Spillantini, 2006). Frontotemporal dementia (FTD), another neuropathy with protein aggregation has also been associated with toxic intracellular aggregates of hyperphosphorylated tau (Lee et al., 2001). Interestingly, some forms of FTD are negative for tau

inclusions, while are positive for inclusions containing misfolded TAR DNA-binding protein 43 (TDP-43) (Kwong et al., 2007). TDP-43 inclusions are also found in the amyotrophic lateral sclerosis (ALS), the most common forms of motor neuron disease (Kwong et al., 2007). Aggregate containing the carboxy terminal fragment of APP (APP- $\beta$ CTF) have been found in Down Syndrome, a neurodevelopmental disorder with pathological features common to the early onset forms of AD (Ying et al., 2019). Amyloid aggregates containing misfolded prion protein (PrP) cause the so-called prion diseases, a group of rare neurodegenerative conditions characterized by the capability of misfolded PrP to transmit their pathological shape onto normal variants of the same protein (Aguzzi and Heikenwelder, 2006). The accumulation of different unrelated misfolded proteins, including the neuronal intermediate filaments (NFs), is a hallmark of the Charcot-Marie-Tooth disease, the most common inherited neuromuscular disease (Theocharopoulou and Vlamos, 2015; Didonna and Opal, 2019). Aggregates containing NFs are frequently observed also in other motor neuron diseases. Lysosomal storage diseases (LSDs) are a group of metabolic diseases caused by inherited defects in lysosomal or non-lysosomal proteins leading to lysosomal storage and global dysfunction often associated with neurodegeneration (Schultz et al., 2011; Platt et al., 2012, 2018). In several LSDs the primary storage caused by the specific inherited lysosomal defect is associated to the deposition of amyloidogenic proteins. Accumulation of  $\alpha$ -synuclein has been shown to trigger neurotoxicity through aggregation-dependent mechanisms in Gaucher disease, a severe neurological LSD belonging to the sphingolipidoses, a family of LSDs characterized by primary lipid storage (Mazzulli et al., 2011).  $\alpha$ -Synuclein aggregation and neurofibrillary tangles have been observed also in other sphingolipidoses, such as the Niemann-Pick and the Krabbe diseases (Suzuki et al., 1995; Saito et al., 2004; Smith et al., 2014). Accumulation and amyloidogenic processing of an oversialylated APP in lysosomes, and extracellular release of A $\beta$  peptides have been observed in a mouse model of sialidosis, an LSDs caused by the deficiency of the lysosomal sialidase NEU1 (Annunziata et al., 2013). Accumulation of APP- $\beta$ CTF was found in GM1 gangliosidosis, an LSD characterized by primary lysosomal storage of GM1 ganglioside in neurons (Zha et al., 2004). Mucopolysaccharidoses (MPS) are a family of LSDs with primary storage of glycosaminoglycans (GAGs) due to the deficiency of lysosomal enzymes required for GAG stepwise degradation (Clarke, 2008). Amyloid aggregation has been observed in different types of MPSs, including the MPS type IIIA, one of the most common and severe form of neurodegenerative LSD (Ginsberg et al., 1999; Hamano et al., 2008; Ohmi et al., 2009; Martins et al., 2015; Beard et al., 2017; Sambri et al., 2017; Monaco et al., 2020). In particular, by studying a mouse model of MPS-IIIa, we have shown that brain deposition of  $\alpha$ -synuclein together with other amyloidogenic proteins including tau, A $\beta$ , and PrP trigger neurodegenerative processes by both loss-of-function (LOF) (Sambri et al., 2017) and gain of toxic function mechanisms (Monaco et al., 2020) (see next sections for further discussion).

**TABLE 1 |** Protein aggregation in neurodegenerative diseases.

Neurodegenerative disease	Aggregating protein/s
Alzheimer's disease	A $\beta$ , tau
Parkinson's disease	$\alpha$ -syn, tau
Dementia with Lewy bodies (DLB)	$\alpha$ -syn
PolyQ expansion diseases (Huntington's, others)	PolyQ expanded proteins (PolyQ htt, others)
Frontotemporal dementia (FTD)	TDP-43, tau
Amyotrophic lateral sclerosis (ALS)	TDP-43
Prion diseases	PrP
Charcot-Marie-Tooth disease	NFs and other misfolded proteins
Down syndrome	APP- $\beta$ -CTF
Lysosomal storage diseases	
Mucopolysaccharidoses	Multiple amyloid proteins ( $\alpha$ -syn, A $\beta$ , tau, PrP)
Gaucher disease	$\alpha$ -syn
Krabbe, NPC-1	$\alpha$ -syn, tau
GM1 gangliosidoses	APP- $\beta$ -CTF
Sialidosis	APP, A $\beta$



## FACTORS DETERMINING PROTEIN AGGREGATION

There are two main factors that cause protein aggregation in neurodegenerative diseases: Gain-of-function (GOF) dominant mutations in genes encoding aggregate-prone proteins and the decline of cellular degradation functions, in particular of the autophagy-lysosomal system (Figure 1).

### GOF Mutations in Genes Encoding Aggregate-Prone Proteins

Protein aggregation may be directly caused by dominant GOF mutations in gene encoding aggregate-prone proteins or precursors of aggregate-prone proteins. GOF mutations in the gene encoding huntingtin lead to polyQ expansion and huntingtin aggregation, thus causing HD (Perutz, 1999). In the AD, ~5% of the forms are Mendelian and are caused by mutations in the genes encoding the amyloid precursor protein (*APP*) and presenilin1/2 (*PSEN1/2*). These genes are directly involved in the “amyloidogenic cascade” by which the APP protein is sequentially cleaved and processed to generate aggregate-prone A $\beta$  peptides (Hardy and Selkoe, 2002). While *PSEN1/2* mutations increase the activity of  $\gamma$ -secretase that enhances A $\beta$  peptides production, GOF mutations in *APP* gene increase the generation of A $\beta$  peptides either by making APP a better substrate for its processing or by changing the biophysical properties of the A $\beta$  peptide, thus rendering it more likely to aggregate. Among the rare Mendelian forms of PD a number of cases are associated with dominant GOF mutations in the gene encoding  $\alpha$ -synuclein (*SNCA*), which lead to the abnormal aggregation of the protein (Bras et al., 2015). Some GOF mutations in the *PRNP* gene (encoding the PrP protein)

produce altered misfolded-prone versions of PrP, thus causing prion disease (Beck et al., 2010). Genetic studies identified GOF mutations in the *MAPT* gene encoding tau protein in some familial cases of the FTD (Rainero et al., 2017). GOF mutations in the *TARDBP* gene (encoding TDP-43) are associated with FTD and ALS (Kwong et al., 2007). In Down syndrome the extra gene copy of *APP* gene (on chromosome 21) leads to increased production of APP- $\beta$ CTF (Ying et al., 2019). Finally, several GOF mutations in unrelated genes have been found to cause misfolding and accumulation of the corresponding proteins in Charcot–Marie–Tooth disease (Braathen, 2012).

### Decline of the Autophagy-Lysosomal Pathway

In many neurodegenerative conditions protein aggregation may occur without specific GOF mutations in genes encoding aggregate-prone proteins. In these conditions protein aggregation is associated to the decline of cellular degradative functions, specifically of the autophagy-lysosomal pathway (ALP) (Figure 1). ALP is a major process for degrading intracellular macromolecules and generating energy or building blocks to make other macromolecules. ALP relies on the engulfment of cargos to be degraded (macromolecules or damaged organelles) in double-membrane vesicles (autophagosomes), which, therefore, fuse with endosomes/lysosomes to form autolysosomes, where autophagosome contents are degraded by lysosomal enzymes (Yu et al., 2018). ALP plays a key role in protein homeostasis and in the clearance of protein aggregates (processes that are particularly important in non-dividing neurons). Therefore, ALP dysfunction may determine/contribute to the toxic aggregation in neurodegenerative conditions (Nixon, 2013; Fraldi et al., 2016). Accordingly, mice KO for key ALP

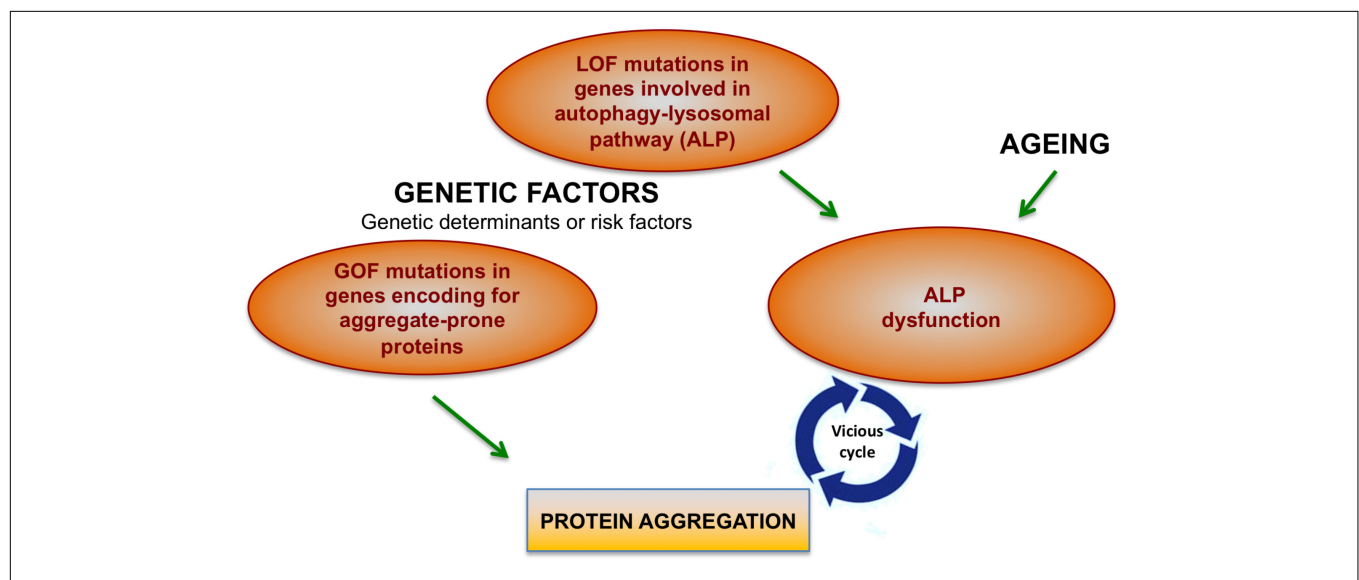


**FIGURE 1 |** Factors contributing to protein aggregation in neurodegenerative conditions. Mutations in different genes may directly cause protein aggregation. However, genetic factors together with aging may contribute to the onset of protein aggregation also by affecting cellular degradative functions, in particular the autophagy-lysosomal pathway (ALP). Increasing body of evidence show that ALP dysfunction and protein aggregation are functionally and closely interconnected and induce each other during neurodegenerative processes.

components exhibit neuronal accumulation of aggregate-prone proteins and neurodegeneration (Hara et al., 2006; Komatsu et al., 2006). Furthermore, in the case of A $\beta$  aggregation, it has been reported that the functionality of endo-lysosomal recycling trafficking is critical for determining the amyloidogenic cascade (Rajendran and Annaert, 2012; Das et al., 2013) and, therefore, any detrimental effect on the endo-lysosomal transport results in alterations of A $\beta$  production (Nixon, 2017).

Autophagy-lysosomal pathway decline may be caused by genetic factors (LOF – mutations inherited in a dominant or recessive fashion), environmental factors (mainly aging) which are known to impact on degradative capability of cells (Nixon et al., 2008) or by protein aggregation itself (see next paragraph). Therefore, genetic factors trigger protein aggregation in neurodegenerative diseases either directly (GOF mutations in gene encoding aggregate-prone proteins) or indirectly (LOF mutations in ALP genes). Importantly, genetic factors can represent either the genetic determinant or a risk factor that contributes to neurodegenerative conditions (**Figure 1**).

Lysosomal storage diseases are the paradigm of neurodegenerative diseases associated to ALP dysfunction caused by genetic factors (Fraldi et al., 2016). Indeed, in LSDs LOF mutations in lysosomal hydrolases or in proteins involved in lysosomal biology cause lysosomal storage and global dysfunction associated to the impairment of the autophagy flux (Lieberman et al., 2012; Platt et al., 2012). A number of AD patients carrying LOF mutations in *PSEN1* show lysosomal and autophagic dysfunction (Lee et al., 2010). Lysosome dysfunction in these patients can be explained by two different mechanisms, one involving defects in the lysosomal acidification machinery and the other in lysosomal Ca<sup>+2</sup> homeostasis (Coen et al., 2012; Lee et al., 2015). Some Mendelian forms of PD are caused by mutations in ALP genes. Mutations in *ATP13A2* encoding a component of the lysosomal acidification machinery (ATPase type 13A2) are associated with lysosomal dysfunction and defective autophagosome clearance in PD (Ramirez et al., 2006). PD caused by mutations in the *LRRK2* gene showed lysosomal stress and accumulation of abnormal autophagosomes (reviewed in Jin and Klionsky, 2014). PD with mutations in *VPS35* is associated to defects in the retrograde transport between endosomes and the trans-Golgi network (Zimprich et al., 2011). Mutations in *PINK* (PTEN-induced putative kinase) or *PARKIN* (PD protein) genes cause PD forms characterized by defective mitophagy (Geisler et al., 2010). Dysfunction of ALP has been associated with specific mutations also in ALS (Song et al., 2012) and in CMT disease (Lee et al., 2012; BasuRay et al., 2013). LOF mutations in the genes whose products are involved in endo-lysosomal function (such as *CHMP2B*, *progranulin*, and *TMEM106B* genes) have been identified as the causative factors in familial forms of FTD (Rainero et al., 2017).

Mutations in ALP genes may also represent risk/predisposing factors for disease pathogenesis. Interestingly, in PD many ALP gene mutations represent risk factors when they are in heterozygosis, while cause a specific LSD when they are in homozygosis, thus providing a strong genetic evidence linking between PD and LSDs (Shachar et al., 2011; Robak et al., 2017). The most known example of this genetic link is

provided by the *GBA* gene encoding for the glucocerebrosidase (GCase), a lysosomal enzyme involved in the degradation of glucosylceramide. When *GBA* is mutated in homozygosis causes the Gaucher's diseases, while when it is mutated in heterozygosis represents a major risk factor for PD (Sidransky et al., 2009).

## PROTEIN AGGREGATION MAY AFFECT ALP GENERATING A VICIOUS CYCLE IN NEURODEGENERATIVE DISEASES

As discussed in the previous section, ALP dysfunction may contribute to the toxic aggregation in neurodegenerative diseases. On the other hand, mounting evidence also show that protein aggregation itself may affect ALP, thus generating a vicious cycle, which boost protein aggregation and toxicity (**Figure 1**). Although mechanisms underlying these processes are still poorly understood, these indirect pathways may explain why ALP became dysfunctional in neurodegenerative conditions caused by GOF mutations in aggregate-prone proteins.

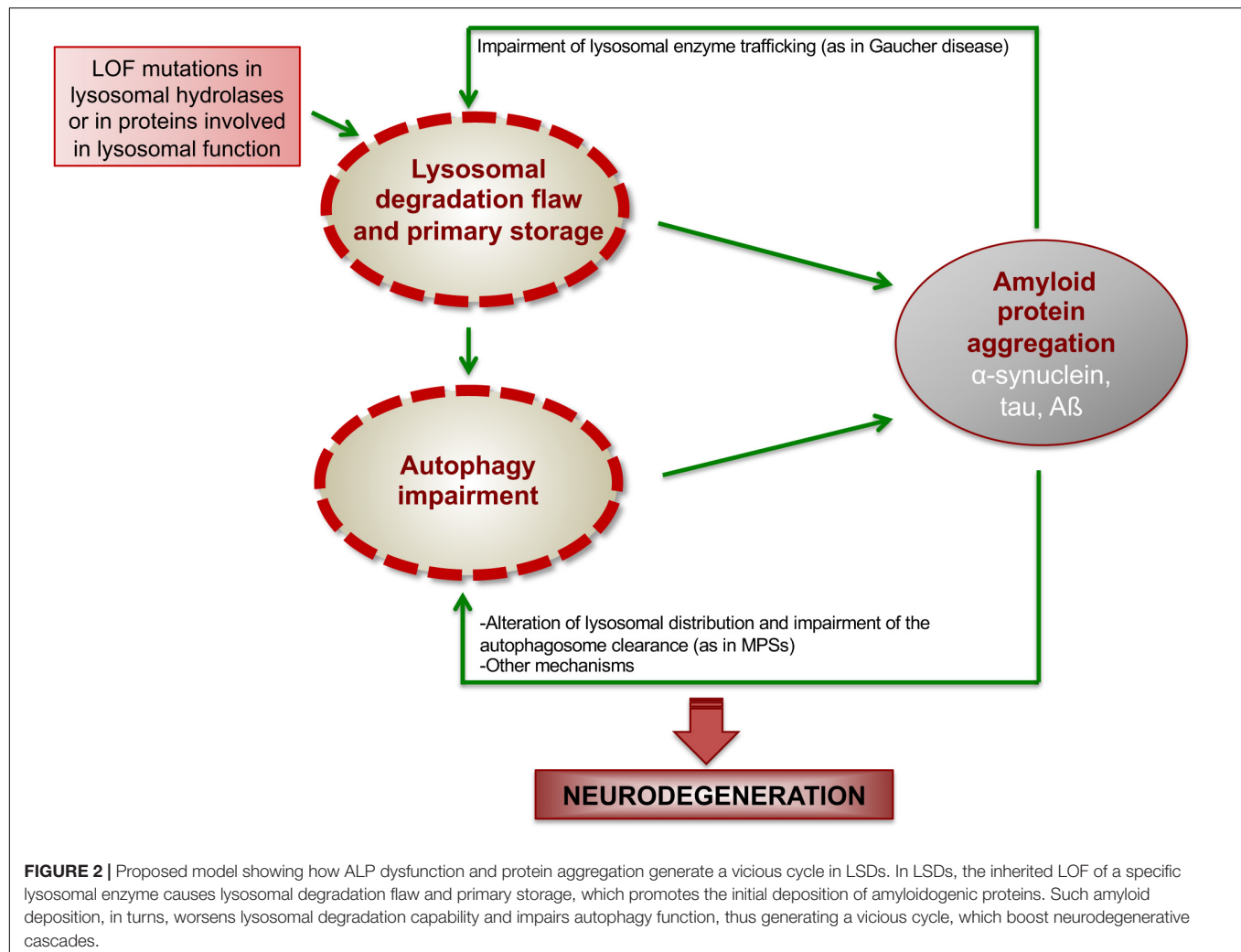
### How Protein Aggregation Affect ALP

Different works have shown that the aggregated forms of  $\alpha$ -synuclein can bind the lysosome, thus impairing the chaperone-mediated autophagy, a selective autophagy pathway for degradation of cytosolic proteins (Cuervo et al., 2004; Martinez-Vicente et al., 2008) or inducing lysosomal rupture (Freeman et al., 2013). Moreover,  $\alpha$ -synuclein overexpression may compromise ALP by inhibiting autophagy initiation via Rab1a inhibition (Winslow et al., 2010). In addition,  $\alpha$ -synuclein toxicity has been reported to be associated with a progressive decline in markers of lysosome function due to cytoplasmic retention of TFEB, a master transcription factor regulating lysosomal biogenesis and function (Settembre et al., 2011; Decressac et al., 2013). Similarly, the polyglutamine-expanded androgen receptor (polyQ-AR) associated to SBMA, interferes with TFEB transactivation, which accounts for autophagic flux defects present in SBMA motor neuron-like cells (Cortes et al., 2014). Abnormal toxic polyQ expansions of htt protein may affect the efficiency of autophagy by inhibiting cargo recognition by autophagosomes (Martinez-Vicente et al., 2010) and/or by inhibiting autophagosome biogenesis and transport (Wong and Holzbaur, 2014; Rui et al., 2015). In Down syndrome increased production of APP- $\beta$ CTF has been shown to impair lysosomal acidification and function (Ying et al., 2019).

## The Paradigm of Lysosomal Storage Diseases

The interplay between ALP dysfunction, protein aggregation, and neurodegenerative processes is well represented in LSDs (**Figure 2**). Here, we will provide some key examples of LSDs in which the mechanisms underlying this interconnection have been studied more in depth.

In Gaucher disease lower levels of GCase in the lysosomes lead to the increased accumulation of glucosylceramide, which stabilizes soluble oligomeric  $\alpha$ -synuclein intermediates that, in



turn, are converted into amyloid fibrils (Mazzulli et al., 2011). The accumulation of  $\alpha$ -synuclein inhibits the trafficking of newly synthesized GCase from ER to Golgi, thus reducing the amount of functional GCase in the lysosomes and further amplifying glucosylceramide accumulation. Therefore, the loss of GCase creates a positive feedback loop of reduced lysosomal function and  $\alpha$ -synuclein accumulation that ultimately leading to neurodegeneration (Mazzulli et al., 2011).

As discussed above several MPSs show the presence of amyloidogenic protein aggregates in the brain. Nevertheless, the neuropathogenic relevance of these amyloid deposits in the context of MPSs and the underlying mechanisms remain largely unexplored. Recently, we have demonstrated that  $\alpha$ -synuclein accumulates as neuronal insoluble aggregates in a mouse model of MPS-IIIa, and showed that this accumulation depletes synaptic  $\alpha$ -synuclein, contributing to neurodegeneration by a LOF mechanism (Sambri et al., 2017). Further studies in MPS-IIIa mice have showed that  $\alpha$ -synuclein progressively accumulates together with other amyloid proteins, including PrP, tau, and A $\beta$  mostly into the lysosomes of neuronal cell bodies, thus exerting a gain of neurotoxic function by affecting ALP

(Monaco et al., 2020). Indeed, inhibiting amyloid aggregation in MPS-IIIa mice by using CLR01, a “molecular tweezer” that acts as a broad-spectrum inhibitor of protein self-assembly (Attar and Bitan, 2014) reduced lysosomal enlargement and re-activates autophagy, thus ameliorating neurodegenerative signs (Monaco et al., 2020). Mechanistically, our preliminary data in MPS-IIIa mouse brain indicate that the build-up of multiple amyloid proteins into the lysosomes of neurons leads to lysosomal clustering in cell body and to the concomitant depletion of the axonal pool of lysosomes, which are critical for autophagosome encountering and clearance. As a consequence, LAMP1-negative autophagosomes massively accumulate in the cell periphery and axons. Therefore, our data suggest a model in which amyloid aggregation impairs the autophagic flux in neurons by disrupting normal lysosomal distribution and, thus preventing lysosomes to encounter and fuse with autophagosomes. Importantly, a similar neuropathogenic link between amyloid deposition and ALP is likely to occur also in other MPSs showing both amyloid deposition (see previous section) and autophagy impairment (Pierzynowska et al., 2019). Furthermore, in addition to the inhibition of lysosomal-mediated

clearance of autophagosomes, other mechanisms (such as those discussed above) may contribute to amyloid-induced autophagy impairment in MPSs. Nevertheless, an open question is: if amyloid accumulation accounts for autophagy degradative dysfunction, what triggers initial deposition of amyloid proteins in the MPS brain? In the case of Gaucher disease it has been demonstrated that the primary storage of glucosylceramide stabilizes  $\alpha$ -synuclein intermediates, promoting amyloid fibrils deposition (Mazzulli et al., 2011). It is likely that the primary storage of other sphingolipids may trigger amyloid aggregation in other forms of sphingolipidoses where, indeed, amyloid protein deposition has been observed (see the previous section). Similarly, GAGs could initiate and stabilize amyloid deposition in the case of MPSs. Supporting this hypothesis, it has been reported that GAGs provide a scaffold promoting amyloid aggregation (Iannuzzi et al., 2015; Liu et al., 2016).

In summary, findings in Gaucher disease and MPSs suggest a model in which primary lysosomal storage due to the inherited lysosomal deficiency triggers initial amyloid deposition, which, in turns, affect lysosomal functions, including autophagy degradation, thus generating a vicious loop between ALP and amyloid deposition, which boost neurodegeneration (Figure 2).

## CONCLUSION

The interplay between protein aggregation and ALP dysfunction is crucial in driving neurodegenerative processes in a number of neurological conditions, among which LSDs represent the paradigm. In LSDs genetic factors directly cause the failure in lysosomal degradation function and the storage of undegraded materials into the lysosome. Although the underlying mechanisms are still unclear, it is likely that the primary storage due to the inherited lysosomal defect may promote the initial deposition of amyloidogenic proteins into the

lysosomal compartment. Such compartmentalized deposition, in turns, worsens autophagy-lysosomal degradation capability of neurons through different mechanisms that may involve reduced trafficking of lysosomal enzymes to the lysosomes (as in the case of Gaucher diseases), impaired autophagosome clearance (as we demonstrated in MPSs) and, likely, others. These mechanisms generate a vicious loop that boost neurodegenerative processes in LSDs, thus allowing, on the other hand, the possibility to identify new attractive therapeutic targets to treat these severe neurological conditions.

## DATA AVAILABILITY STATEMENT

The datasets generated for this study are available on request to the corresponding author.

## ETHICS STATEMENT

The animal studies were conducted in accordance with the guidelines of the Animal Care and Use Committee of TIGEM in Naples and authorized by the Italian Ministry of Health.

## AUTHOR CONTRIBUTIONS

AF conceived and wrote the manuscript. AM contributed to conceiving the manuscript and co-wrote the manuscript. All authors listed approved it for publication.

## FUNDING

We acknowledge the Cure Sanfilippo Foundation (Grant to AF) and the Telethon Foundation (Grant to AF).

## REFERENCES

- Aguzzi, A., and Heikenwalder, M. (2006). Pathogenesis of prion diseases: current status and future outlook. *Nat. Rev. Microbiol.* 4, 765–775. doi: 10.1038/nrmicro1492
- Annunziata, I., Patterson, A., Helton, D., Hu, H., Moshiah, S., Gomero, E., et al. (2013). Lysosomal NEU1 deficiency affects amyloid precursor protein levels and amyloid-beta secretion via deregulated lysosomal exocytosis. *Nat. Commun.* 4:2734. doi: 10.1038/ncomms3734
- Attar, A., and Bitan, G. (2014). Disrupting self-assembly and toxicity of amyloidogenic protein oligomers by “molecular tweezers” – from the test tube to animal models. *Curr. Pharm. Des.* 20, 2469–2483. doi: 10.2174/13816128113199990496
- BasuRay, S., Mukherjee, S., Romero, E. G., Seaman, M. N., and Wandinger-Ness, A. (2013). Rab7 mutants associated with Charcot-Marie-Tooth disease cause delayed growth factor receptor transport and altered endosomal and nuclear signaling. *J. Biol. Chem.* 288, 1135–1149. doi: 10.1074/jbc.M112.417766
- Beard, H., Hassiotis, S., Gai, W. P., Parkinson-Lawrence, E., Hopwood, J. J., and Hemsley, K. M. (2017). Axonal dystrophy in the brain of mice with Sanfilippo syndrome. *Exp. Neurol.* 295, 243–255. doi: 10.1016/j.expneurol.2017.06.010
- Beck, J. A., Poulter, M., Campbell, T. A., Adamson, G., Uphill, J. B., Guerreiro, R., et al. (2010). PRNP allelic series from 19 years of prion protein gene sequencing at the MRC Prion Unit. *Hum. Mutat.* 31, E1551–E1563. doi: 10.1002/humu.21281
- Braathen, G. J. (2012). Genetic epidemiology of Charcot-Marie-Tooth disease. *Acta Neurol. Scand. Suppl.* 126, iv–22. doi: 10.1111/ane.12013
- Bras, J., Guerreiro, R., and Hardy, J. (2015). SnapShot: genetics of Parkinson's disease. *Cell* 160, 570–570.e1. doi: 10.1016/j.cell.2015.01.019
- Chiti, F., and Dobson, C. M. (2006). Protein misfolding, functional amyloid, and human disease. *Annu. Rev. Biochem.* 75, 333–366. doi: 10.1146/annurev.biochem.75.101304.123901
- Ciechanover, A., and Kwon, Y. T. (2015). Degradation of misfolded proteins in neurodegenerative diseases: therapeutic targets and strategies. *Exp. Mol. Med.* 47:e147. doi: 10.1038/emmm.2014.117
- Clarke, L. A. (2008). The mucopolysaccharidoses: a success of molecular medicine. *Expert Rev. Mol. Med.* 10:e1. doi: 10.1017/S1462399408000550
- Coen, K., Flannagan, R. S., Baron, S., Carraro-Lacroix, L. R., Wang, D., Vermeire, W., et al. (2012). Lysosomal calcium homeostasis defects, not proton pump defects, cause endo-lysosomal dysfunction in PSEN-deficient cells. *J. Cell Biol.* 198, 23–35. doi: 10.1083/jcb.201201076
- Cortes, C. J., Miranda, H. C., Frankowski, H., Batlevi, Y., Young, J. E., Le, A., et al. (2014). Polyglutamine-expanded androgen receptor interferes with TFEB to elicit autophagy defects in SBMA. *Nat. Neurosci.* 17, 1180–1189. doi: 10.1038/nn.3787



- Cuervo, A. M., Stefanis, L., Fredenburg, R., Lansbury, P. T., and Sulzer, D. (2004). Impaired degradation of mutant alpha-synuclein by chaperone-mediated autophagy. *Science* 305, 1292–1295. doi: 10.1126/science.1101738
- Das, U., Scott, D. A., Ganguly, A., Koo, E. H., Tang, Y., and Roy, S. (2013). Activity-induced convergence of APP and BACE-1 in acidic microdomains via an endocytosis-dependent pathway. *Neuron* 79, 447–460. doi: 10.1016/j.neuron.2013.05.035
- Decressac, M., Mattsson, B., Weikop, P., Lundblad, M., Jakobsson, J., and Bjorklund, A. (2013). TFEB-mediated autophagy rescues midbrain dopamine neurons from alpha-synuclein toxicity. *Proc. Natl. Acad. Sci. U.S.A.* 110, E1817–E1826. doi: 10.1073/pnas.1305623110
- Didonna, A., and Opal, P. (2019). The role of neurofilament aggregation in neurodegeneration: lessons from rare inherited neurological disorders. *Mol. Neurodegener.* 14:19. doi: 10.1186/s13024-019-0318-4
- Dobson, C. M. (2003). Protein folding and misfolding. *Nature* 426, 884–890. doi: 10.1038/nature02261
- Fraldi, A., Klein, A. D., Medina, D. L., and Settembre, C. (2016). Brain disorders due to lysosomal dysfunction. *Annu. Rev. Neurosci.* 39, 277–295. doi: 10.1146/annurev-neuro-070815-14031
- Freeman, D., Cedillos, R., Choyke, S., Lukic, Z., McGuire, K., Marvin, S., et al. (2013). Alpha-synuclein induces lysosomal rupture and cathepsin dependent reactive oxygen species following endocytosis. *PLoS One* 8:e62143. doi: 10.1371/journal.pone.0062143
- Gallardo, R., Ramakers, M., De Smet, F., Claes, F., Khodaparast, L., Khodaparast, L., et al. (2016). De novo design of a biologically active amyloid. *Science* 354:aah4949. doi: 10.1126/science.aah4949
- Geisler, S., Holmstrom, K. M., Treis, A., Skujat, D., Weber, S. S., Fiesel, F. C., et al. (2010). The PINK1/Parkin-mediated mitophagy is compromised by PD-associated mutations. *Autophagy* 6, 871–878. doi: 10.4161/auto.6.7.13286
- Ginsberg, S. D., Galvin, J. E., Lee, V. M., Rorke, L. B., Dickson, D. W., Wolfe, J. H., et al. (1999). Accumulation of intracellular amyloid-beta peptide (A beta 1-40) in mucopolysaccharidosis brains. *J. Neuropathol. Exp. Neurol.* 58, 815–824. doi: 10.1097/00005072-199908000-4
- Goedert, M., and Spillantini, M. G. (2006). A century of Alzheimer's disease. *Science* 314, 777–781. doi: 10.1126/science.1132814
- Hamano, K., Hayashi, M., Shioda, K., Fukatsu, R., and Mizutani, S. (2008). Mechanisms of neurodegeneration in mucopolysaccharidoses II and IIIB: analysis of human brain tissue. *Acta Neuropathol.* 115, 547–559. doi: 10.1007/s00401-007-0325-3
- Hara, T., Nakamura, K., Matsui, M., Yamamoto, A., Nakahara, Y., Suzuki-Migishima, R., et al. (2006). Suppression of basal autophagy in neural cells causes neurodegenerative disease in mice. *Nature* 441, 885–889. doi: 10.1038/nature04724
- Hardy, J., and Selkoe, D. J. (2002). The amyloid hypothesis of Alzheimer's disease: progress and problems on the road to therapeutics. *Science* 297, 353–356. doi: 10.1126/science.1072994
- Iannuzzi, C., Irace, G., and Sirangelo, I. (2015). The effect of glycosaminoglycans (GAGs) on amyloid aggregation and toxicity. *Molecules* 20, 2510–2528. doi: 10.3390/molecules20022510
- Jin, M., and Klionsky, D. J. (2014). Regulation of autophagy: modulation of the size and number of autophagosomes. *FEBS Lett.* 588, 2457–2463. doi: 10.1016/j.febslet.2014.06.015
- Komatsu, M., Waguri, S., Chiba, T., Murata, S., Iwata, J., Tanida, I., et al. (2006). Loss of autophagy in the central nervous system causes neurodegeneration in mice. *Nature* 441, 880–884. doi: 10.1038/nature04723
- Kwong, L. K., Neumann, M., Sampathu, D. M., Lee, V. M., and Trojanowski, J. Q. (2007). TDP-43 proteinopathy: the neuropathology underlying major forms of sporadic and familial frontotemporal lobar degeneration and motor neuron disease. *Acta Neuropathol.* 114, 63–70. doi: 10.1007/s00401-007-0226-5
- Lee, J. H., McBrayer, M. K., Wolfe, D. M., Haslett, L. J., Kumar, A., Sato, Y., et al. (2015). Presenilin 1 maintains lysosomal Ca(2+) homeostasis via TRPML1 by regulating vATPase-mediated lysosome acidification. *Cell Rep.* 12, 1430–1444. doi: 10.1016/j.celrep.2015.07.050
- Lee, J. H., Yu, W. H., Kumar, A., Lee, S., Mohan, P. S., Peterhoff, C. M., et al. (2010). Lysosomal proteolysis and autophagy require presenilin 1 and are disrupted by Alzheimer-related PS1 mutations. *Cell* 141, 1146–1158. doi: 10.1016/j.cell.2010.05.008
- Lee, S. M., Chin, L. S., and Li, L. (2012). Charcot-Marie-Tooth disease-linked protein SIMPLE functions with the ESCRT machinery in endosomal trafficking. *J. Cell Biol.* 199, 799–816. doi: 10.1083/jcb.201204137
- Lee, V. M., Goedert, M., and Trojanowski, J. Q. (2001). Neurodegenerative tauopathies. *Annu. Rev. Neurosci.* 24, 1121–1159. doi: 10.1146/annurev.neuro.24.1.1121
- Lieberman, A. P., Puertollano, R., Raben, N., Slaugenhaupt, S., Walkley, S. U., and Ballabio, A. (2012). Autophagy in lysosomal storage disorders. *Autophagy* 8, 719–730. doi: 10.4161/auto.19469
- Liu, C. C., Zhao, N., Yamaguchi, Y., Cirrito, J. R., Kanekiyo, T., Holtzman, D. M., et al. (2016). Neuronal heparan sulfates promote amyloid pathology by modulating brain amyloid-beta clearance and aggregation in Alzheimer's disease. *Sci. Transl. Med.* 8:332ra44. doi: 10.1126/scitranslmed.aad3650
- Martinez-Vicente, M., Tallozy, Z., Kaushik, S., Massey, A. C., Mazzulli, J., Mosharov, E. V., et al. (2008). Dopamine-modified alpha-synuclein blocks chaperone-mediated autophagy. *J. Clin. Invest.* 118, 777–788. doi: 10.1172/JCI32806
- Martinez-Vicente, M., Tallozy, Z., Wong, E., Tang, G., Koga, H., Kaushik, S., et al. (2010). Cargo recognition failure is responsible for inefficient autophagy in Huntington's disease. *Nat. Neurosci.* 13, 567–576. doi: 10.1038/nn.2528
- Martins, C., Hulkova, H., Dridi, L., Dormoy-Raclet, V., Grigoryeva, L., Choi, Y., et al. (2015). Neuroinflammation, mitochondrial defects and neurodegeneration in mucopolysaccharidosis III type C mouse model. *Brain* 138(Pt 2), 336–355. doi: 10.1093/brain/awu355
- Mazzulli, J. R., Xu, Y. H., Sun, Y., Knight, A. L., McLean, P. J., Caldwell, G. A., et al. (2011). Gaucher disease glucocerebrosidase and alpha-synuclein form a bidirectional pathogenic loop in synucleinopathies. *Cell* 146, 37–52. doi: 10.1016/j.cell.2011.06.001
- Monaco, A., Maffia, V., Sorrentino, N., Sambri, I., Ezhova, Y., Giuliano, T., et al. (2020). The amyloid self-assembly inhibitor CLR01 relieves autophagy and ameliorates neuropathology in a severe lysosomal storage disease. *Mol. Ther.* doi: 10.1016/j.ymthe.2020.02.005 [Epub ahead of print].
- Nixon, R. A. (2013). The role of autophagy in neurodegenerative disease. *Nat. Med.* 19, 983–997. doi: 10.1038/nm.3232
- Nixon, R. A. (2017). Amyloid precursor protein and endosomal-lysosomal dysfunction in Alzheimer's disease: inseparable partners in a multifactorial disease. *FASEB J.* 31, 2729–2743. doi: 10.1096/fj.201700359
- Nixon, R. A., Yang, D. S., and Lee, J. H. (2008). Neurodegenerative lysosomal disorders: a continuum from development to late age. *Autophagy* 4, 590–599. doi: 10.4161/auto.6259
- Ohmi, K., Kudo, L. C., Ryazantsev, S., Zhao, H. Z., Karsten, S. L., and Neufeld, E. F. (2009). Sanfilippo syndrome type B, a lysosomal storage disease, is also a tauopathy. *Proc. Natl. Acad. Sci. U.S.A.* 106, 8332–8337. doi: 10.1073/pnas.0903223106
- Perutz, M. F. (1999). Glutamine repeats and neurodegenerative diseases: molecular aspects. *Trends Biochem. Sci.* 24, 58–63. doi: 10.1016/s0968-0004(98)01350-4
- Pierzynowska, K., Gaffke, L., Podlacha, M., Brokowska, J., and Wegrzyn, G. (2019). Mucopolysaccharidosis and autophagy: controversies on the contribution of the process to the pathogenesis and possible therapeutic applications. *Neuromol. Med.* 22, 25–30. doi: 10.1007/s12017-019-08559-1
- Platt, F. M., Boland, B., and van der Spoel, A. C. (2012). The cell biology of disease: lysosomal storage disorders: the cellular impact of lysosomal dysfunction. *J. Cell Biol.* 199, 723–734. doi: 10.1083/jcb.201208152
- Platt, F. M., d'Azzo, A., Davidson, B. L., Neufeld, E. F., and Tift, C. J. (2018). Lysosomal storage diseases. *Nat. Rev. Dis. Primers* 4:27. doi: 10.1038/s41572-018-0025-4
- Rainero, I., Rubino, E., Michelerio, A., D'Agata, F., Gentile, S., and Pinassi, L. (2017). Recent advances in the molecular genetics of frontotemporal lobar degeneration. *Funct. Neurol.* 32, 7–16. doi: 10.11138/fneur/2017.32.1.007
- Rajendran, L., and Annaert, W. (2012). Membrane trafficking pathways in Alzheimer's disease. *Traffic* 13, 759–770. doi: 10.1111/j.1600-0854.2012.01332.x
- Ramirez, A., Heimbach, A., Grundemann, J., Stiller, B., Hampshire, D., Cid, L. P., et al. (2006). Hereditary parkinsonism with dementia is caused by mutations in ATP13A2, encoding a lysosomal type 5 P-type ATPase. *Nat. Genet.* 38, 1184–1191. doi: 10.1038/ng1884
- Robak, L. A., Jansen, I. E., van Rooij, J., Uitterlinden, A. G., Kraaij, R., Jankovic, J., et al. (2017). Excessive burden of lysosomal storage disorder gene variants in Parkinson's disease. *Brain* 140, 3191–3203. doi: 10.1093/brain/awx285

- Rui, Y. N., Xu, Z., Patel, B., Chen, Z., Chen, D., Tito, A., et al. (2015). Huntingtin functions as a scaffold for selective macroautophagy. *Nat. Cell Biol.* 17, 262–275. doi: 10.1038/ncb3101
- Saito, Y., Suzuki, K., Hulette, C. M., and Murayama, S. (2004). Aberrant phosphorylation of alpha-synuclein in human Niemann-Pick type C1 disease. *J. Neuropathol. Exp. Neurol.* 63, 323–328. doi: 10.1093/jnen/63.4.323
- Sambri, I., D'Alessio, R., Ezhova, Y., Giuliano, T., Sorrentino, N. C., Cacace, V., et al. (2017). Lysosomal dysfunction disrupts presynaptic maintenance and restoration of presynaptic function prevents neurodegeneration in lysosomal storage diseases. *EMBO Mol. Med.* 9, 112–132. doi: 10.15252/emmm.201606965
- Schultz, M. L., Tecedor, L., Chang, M., and Davidson, B. L. (2011). Clarifying lysosomal storage diseases. *Trends Neurosci.* 34, 401–410. doi: 10.1016/j.tins.2011.05.006
- Settembre, C., Di Malta, C., Polito, V. A., Garcia Arencibia, M., Vetrini, F., Erdin, S., et al. (2011). TFEB links autophagy to lysosomal biogenesis. *Science* 332, 1429–1433. doi: 10.1126/science.1204592
- Shachar, T., Lo Bianco, C., Recchia, A., Wiessner, C., Raas-Rothschild, A., and Futerman, A. H. (2011). Lysosomal storage disorders and Parkinson's disease: Gaucher disease and beyond. *Mov. Disord.* 26, 1593–1604. doi: 10.1002/mds.23774
- Sidransky, E., Nalls, M. A., Aasly, J. O., Aharon-Peretz, J., Annesi, G., Barbosa, E. R., et al. (2009). Multicenter analysis of glucocerebrosidase mutations in Parkinson's disease. *N. Engl. J. Med.* 361, 1651–1661. doi: 10.1056/NEJMoa0901281
- Smith, B. R., Santos, M. B., Marshall, M. S., Cantuti-Castelvetri, L., Lopez-Rosas, A., Li, G., et al. (2014). Neuronal inclusions of alpha-synuclein contribute to the pathogenesis of Krabbe disease. *J. Pathol.* 232, 509–521. doi: 10.1002/path.4328
- Song, C. Y., Guo, J. F., Liu, Y., and Tang, B. S. (2012). Autophagy and its comprehensive impact on ALS. *Int. J. Neurosci.* 122, 695–703. doi: 10.3109/00207454.2012.714430
- Spillantini, M. G., Schmidt, M. L., Lee, V. M., Trojanowski, J. Q., Jakes, R., and Goedert, M. (1997). Alpha-synuclein in Lewy bodies. *Nature* 388, 839–840. doi: 10.1038/42166
- Suzuki, K., Parker, C. C., Pentchev, P. G., Katz, D., Ghetti, B., D'Agostino, A. N., et al. (1995). Neurofibrillary tangles in Niemann-Pick disease type C. *Acta Neuropathol.* 89, 227–238. doi: 10.1007/bf00309338
- Theocharopoulou, G., and Vlamos, P. (2015). Modeling protein misfolding in charcot-marie-tooth disease. *Adv. Exp. Med. Biol.* 820, 91–102. doi: 10.1007/978-3-319-09012-2\_7
- Winslow, A. R., Chen, C. W., Corrochano, S., Acevedo-Arozena, A., Gordon, D. E., Peden, A. A., et al. (2010). alpha-Synuclein impairs macroautophagy: implications for Parkinson's disease. *J. Cell Biol.* 190, 1023–1037. doi: 10.1083/jcb.201003122
- Wong, Y. C., and Holzbaur, E. L. (2014). The regulation of autophagosome dynamics by huntingtin and HAP1 is disrupted by expression of mutant huntingtin, leading to defective cargo degradation. *J. Neurosci.* 34, 1293–1305. doi: 10.1523/JNEUROSCI.1870-13.2014
- Ying, J., Sato, Y., Im, E., Berg, M., Bordi, M., Darji, S., et al. (2019). Lysosomal dysfunction in Down syndrome is APP-dependent and mediated by APP-betaCTF (C99). *J. Neurosci.* 39, 5255–5268. doi: 10.1523/JNEUROSCI.0578-19.2019
- Yu, L., Chen, Y., and Tooze, S. A. (2018). Autophagy pathway: cellular and molecular mechanisms. *Autophagy* 14, 207–215. doi: 10.1080/15548627.2017.1378838
- Zha, Q., Ruan, Y., Hartmann, T., Beyreuther, K., and Zhang, D. (2004). GM1 ganglioside regulates the proteolysis of amyloid precursor protein. *Mol. Psychiatry* 9, 946–952. doi: 10.1038/sj.mp.4001509
- Zimprich, A., Benet-Pages, A., Struhal, W., Graf, E., Eck, S. H., Offman, M. N., et al. (2011). A mutation in VPS35, encoding a subunit of the retromer complex, causes late-onset Parkinson disease. *Am. J. Hum. Genet.* 89, 168–175. doi: 10.1016/j.ajhg.2011.06.008

**Conflict of Interest:** The authors declare that the research was conducted in the absence of any commercial or financial relationships that could be construed as a potential conflict of interest.

Copyright © 2020 Monaco and Fraldi. This is an open-access article distributed under the terms of the Creative Commons Attribution License (CC BY). The use, distribution or reproduction in other forums is permitted, provided the original author(s) and the copyright owner(s) are credited and that the original publication in this journal is cited, in accordance with accepted academic practice. No use, distribution or reproduction is permitted which does not comply with these terms.



# CNS-Derived Blood Exosomes as a Promising Source of Biomarkers: Opportunities and Challenges

Simon Hornung<sup>1†</sup>, Suman Dutta<sup>1</sup> and Gal Bitan<sup>1,2,3\*</sup>

<sup>1</sup> Department of Neurology, David Geffen School of Medicine, University of California, Los Angeles, Los Angeles, CA, United States, <sup>2</sup> Brain Research Institute, University of California, Los Angeles, Los Angeles, CA, United States, <sup>3</sup> Molecular Biology Institute, University of California, Los Angeles, Los Angeles, CA, United States

## OPEN ACCESS

### Edited by:

Ashok K. Shetty,  
Texas A&M University College of  
Medicine, United States

### Reviewed by:

Madhu LN,  
Texas A&M University, United States  
Esperanza González,  
CIC bioGUNE, Spain

### \*Correspondence:

Gal Bitan  
gbitan@mednet.ucla.edu

### †Present address:

Simon Hornung,  
Division of Peptide Biochemistry,  
Technical University of Munich,  
Freising, Germany

**Received:** 25 November 2019

**Accepted:** 24 February 2020

**Published:** 19 March 2020

### Citation:

Hornung S, Dutta S and Bitan G  
(2020) CNS-Derived Blood Exosomes  
as a Promising Source of Biomarkers:  
Opportunities and Challenges.  
Front. Mol. Neurosci. 13:38.  
doi: 10.3389/fnmol.2020.00038

Eukaryotic cells release different types of extracellular vesicles (EVs) including exosomes, ectosomes, and microvesicles. Exosomes are nanovesicles, 30–200 nm in diameter, that carry cell- and cell-state-specific cargo of proteins, lipids, and nucleic acids, including mRNA and miRNA. Recent studies have shown that central nervous system (CNS)-derived exosomes may carry amyloidogenic proteins and facilitate their cell-to-cell transfer, thus playing a critical role in the progression of neurodegenerative diseases, such as tauopathies and synucleinopathies. CNS-derived exosomes also have been shown to cross the blood-brain-barrier into the bloodstream and therefore have drawn substantial attention as a source of biomarkers for various neurodegenerative diseases as they can be isolated via a minimally invasive blood draw and report on the biochemical status of the CNS. However, although isolating specific brain-cell-derived exosomes from the blood is theoretically simple and the approach has great promise, practical details are of crucial importance and may compromise the reproducibility and utility of this approach, especially when different laboratories use different protocols. In this review we discuss the role of exosomes in neurodegenerative diseases, the usefulness of CNS-derived blood exosomes as a source of biomarkers for these diseases, and practical challenges associated with the methodology of CNS-derived blood exosomes and subsequent biomarker analysis.

**Keywords:** biomarker, exosome, extracellular vesicle (EV), neurodegenerative diseases, Alzheimer' disease, Parkinson's and related diseases, ALS

## INTRODUCTION

Eukaryotic cells release a variety of extracellular vesicles (EVs), including microvesicles, ectosomes, oncosomes, and exosomes. EVs can be shed directly from the plasma membrane, e.g., ectosomes, or can be released upon fusion of multivesicular bodies (MVBs) with the plasma membrane (Colombo et al., 2014; Coleman and Hill, 2015; Lööv et al., 2016). Exosomes are formed via the latter process by the inward budding of the endosomal membrane, creating MVBs that contain intraluminal vesicles (ILVs). The formation of ILVs is regulated tightly and in many cases depends on endosomal sorting complex required for transport (ESCRT) proteins, and on tetraspanins, including CD9, CD63, and CD81. Alternatively, ILVs can form by ESCRT-independent mechanisms, e.g., by a

process mediated by ceramides (van Niel et al., 2011; Perez-Hernandez et al., 2013; Colombo et al., 2014; Thompson et al., 2016). Fusion of MVBs with the plasma membrane leads to the release of ILVs as exosomes, ranging from 30 to 200 nm in diameter (Paulaitis et al., 2018), into the extracellular space where they can be taken up by recipient cells (**Figure 1**; Coleman and Hill, 2015; Lööv et al., 2016; Thompson et al., 2016). The precise details of the uptake mechanisms of exosomes into recipient cells are not known. In general, exosomes can be taken up by non-specific endocytotic mechanisms, such as macropinocytosis and micropinocytosis, or by more specific, receptor-dependent pathways involving integrins (Hoshino et al., 2015), proteoglycans (Christianson et al., 2013), T cell immunoglobulins, and mucin-domain-containing protein 4 (Tim4) (Miyanishi et al., 2007). Moreover, exosomes can fuse directly with the plasma membrane releasing their cargo into the cytosol of the recipient cell (**Figure 1**; Montecalvo et al., 2012; Mathieu et al., 2019).

Transmission electron microscopy (TEM) images of negatively stained exosomes initially indicated a cup-shaped morphology, yet later cryo-electron microscopy images of unfixed exosomes, including in a study by Banizs et al., comparing negative-stain EM and unstained cryo-EM of the same exosome preparation, showed a spherical shape, suggesting that the cup-shaped morphology might have resulted from the fixation process in conventional TEM (**Figure 2**; Théry et al., 2006; Raposo and Stoorvogel, 2013; Banizs et al., 2014).

Exosomes are produced and released by virtually all cell types, including different brain cells, such as neurons, astrocytes, microglia, and oligodendrocytes (Potolicchio et al., 2005; Fauré et al., 2006; Krämer-Albers et al., 2007; Bianco et al., 2009; Dutta et al., 2018; Goetzl et al., 2018; Xia et al., 2019). The nomenclature used in the field is somewhat problematic. Isolation of pure exosomes requires the use of methods such as a sucrose cushion, a density gradient, size-exclusion chromatography, or sequential ultracentrifugation and filtration steps and the resulting vesicles must be characterized thoroughly for their size, morphology, and biochemical characteristics (Lötvall et al., 2014). However, because exosomes are the main type of vesicle in preparations including other types of extracellular vesicles, many authors have used the terms extracellular vesicles and exosomes interchangeably. For simplicity, here we also use the term “exosomes” inclusively when discussing papers that did not go through the rigorous isolation protocols and characterization needed to establish the identity of pure exosome preparation. The reader should keep in mind that in many cases, the preparations described as exosomes may contain also small amounts of other extracellular vesicles.

Originally, exosomes were believed to be a disposal mechanism of unwanted membranes and proteins during the maturation process of reticulocytes into erythrocytes (Pan, 1985). Recent studies have demonstrated that exosomes have multiple additional roles including spreading various proteins, DNA, mRNA, miRNA, and other non-coding RNAs from cell to cell, often depending on the physiological state of the parent cell (Valadi et al., 2007; Guescini et al., 2010; Montecalvo et al., 2012; Cai et al., 2013; Budnik et al., 2016;

Sardar Sinha et al., 2018). In the central nervous system (CNS), exosomes play critical physiological roles in intercellular communication, maintenance of myelination, synaptic plasticity, antigen presentation, and trophic support to neurons. Under pathological conditions, especially in proteinopathies, there is an increase in the use of this machinery for disposal of accumulating, unwanted biomolecules (Krämer-Albers et al., 2007; Antonucci et al., 2012; Lee et al., 2012; Budnik et al., 2016; Goetzl et al., 2016; Thompson et al., 2016). In particular, disposal of unwanted cellular components via exosomes occurs to assist when other cellular clearance mechanisms, such as the proteasome and autophagy-lysosome system, gradually fail in eliminating aggregated amyloidogenic proteins (Alvarez-Erviti et al., 2011; Ihara et al., 2012; Urbanelli et al., 2013; Fussi et al., 2018; Miranda and Di Paolo, 2018). Under such conditions, CNS-derived exosomes have been shown to be involved in prion-like, cell-to-cell spread of amyloidogenic proteins, including A $\beta$ , tau,  $\alpha$ -synuclein, and TDP-43 (Bellingham et al., 2012; Vingtdeux et al., 2012; Feiler et al., 2015; Polanco et al., 2016).

The role of exosomes in exporting amyloidogenic proteins from brain cells in neurodegenerative proteinopathies has been demonstrated in recent years by multiple groups who showed that CNS-derived exosomes may be enriched in amyloidogenic proteins, such as tau and hyperphosphorylated tau in Alzheimer's disease (AD) and other tauopathies (Clavaguera et al., 2009; Liu et al., 2012; Vella et al., 2016), monomeric and oligomeric amyloid  $\beta$ -protein (A $\beta$ ) in AD (Fiandaca et al., 2015; Sardar Sinha et al., 2018), and  $\alpha$ -synuclein in Parkinson's disease (PD) (Danzer et al., 2012).

Exosomes have been isolated successfully from human serum and plasma (Caby et al., 2005; Fiandaca et al., 2015), cerebrospinal fluid (CSF) (Vella et al., 2008), saliva (Ogawa et al., 2008; Michael et al., 2010), and urine (Pisitkun et al., 2004). Characterization of exosomes isolated from human serum and plasma has demonstrated similarities in vesicle size, shape, concentration, and presence of exosomal markers suggesting that serum and plasma are equally useful for isolation of blood exosomes (Soares Martins et al., 2018). Multiple exosomal surface markers have been reported and are routinely used to identify exosomes, including the tetraspanins CD9, CD63, and CD81, ALG 2-interacting protein X (ALIX), tumor susceptibility gene 101 protein (TSG101) and ESCRT proteins (Théry et al., 2002; Dutta et al., 2015; Thompson et al., 2016). Exosomes can cross the blood-brain-barrier (BBB) making them a highly attractive source of biomarkers originating in the CNS that could be isolated from the blood (Alvarez-Erviti et al., 2011; Zheng et al., 2017). The ability to cross the BBB in the opposite direction potentially can make exosomes useful for delivering drugs and biomolecules into the brain (Luan et al., 2017; Rashed et al., 2017) though this topic is beyond the scope of our review. Rather, we focus on exosomes that cross the BBB from the CNS into the blood and discuss the role of CNS-derived exosomes in different neurodegenerative disorders, biomarker opportunities, and the technological challenges associated with isolation of CNS-derived blood exosomes.



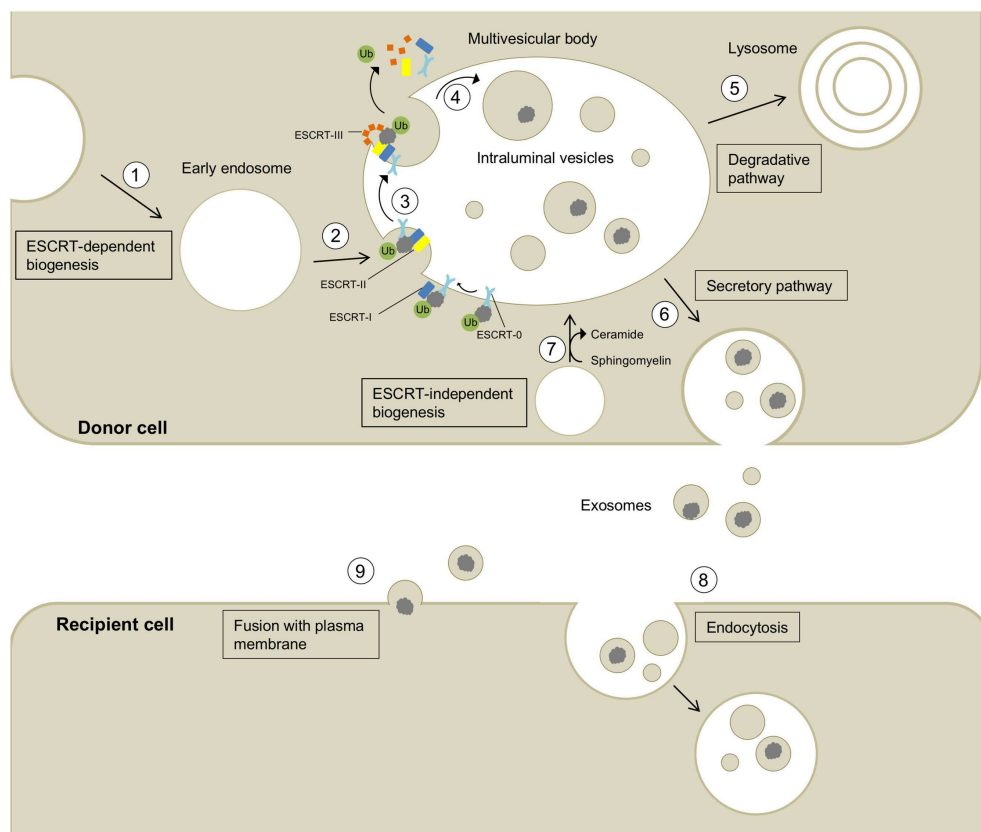


**FIGURE 1 |** Biogenesis, secretion, and uptake of exosomes and their cargo. (1) Invagination of the cell membrane leads to the formation of early endosomes. (2) ESCRT-0 recognizes and binds ubiquitinated proteins and further recruits ESCRT-I (including the exosomal marker TSG101) and ESCRT-II to this complex. (3) ESCRT-III is a transient protein complex that plugs the inward budding vesicle to avoid the escape of the cargo during scission. Alix recruits deubiquitinases to ESCRT-III, which remove ubiquitin from cargo proteins (Budnik et al., 2016). ESCRT proteins detach from the membrane and are released into the cytoplasm. (4) The formed intraluminal vesicle contains the cargo protein and can either be (5) degraded in lysosomes or (6) secreted into the extracellular space. (7) The formation of intraluminal vesicles can occur via ESCRT-independent pathways and is promoted by higher levels of ceramides in the lipid membrane (Budnik et al., 2016). Exosomes released into the extracellular space can be taken up by recipient cells by endocytosis (8) or fusion with the plasma membrane (9) allowing the transport of cargo between different cells and body parts.

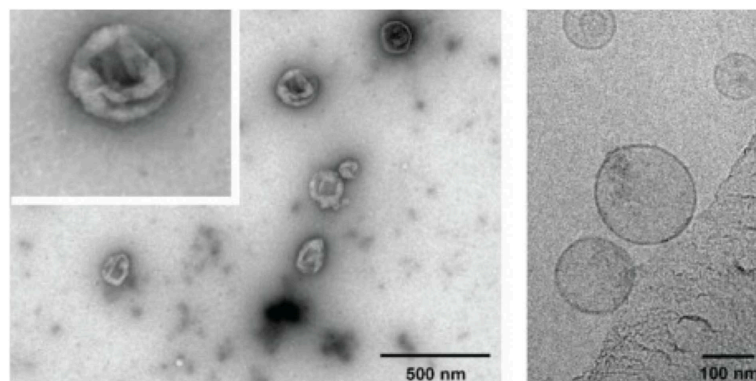


**FIGURE 2 |** Electron micrographs of exosomes. Exosomes were isolated from cultured primary endothelial cells. Left: exosomes were stained with uranyl acetate and embedded as whole mount preparations in methylcellulose. The image shows a cup-shaped morphology and heterogeneous sizes ranging from 30 to 100 nm. Right: Exosomes were analyzed by cryoelectron microscopy without chemical fixation or contrasting. Exosomes appear as round membranous structures. Adapted from panels B and C in Figure 1 of Banizs et al., © 2014, originally published in International Journal of Nanomedicine (Dovepress). <https://doi.org/10.2147/IJN.S64267>.

## ROLE OF CNS EXOSOMES IN NEURODEGENERATIVE DISORDERS

Exosomes have been shown to play a crucial role in the pathology of various neurodegenerative diseases, including AD, PD, amyotrophic lateral sclerosis (ALS), frontotemporal dementia (FTD), and prion diseases (Thompson et al., 2016; Shi et al., 2019). In addition, multiple groups have begun using exosomes as a source of biomarkers for these diseases. The most common fluid biomarkers are listed in **Table 1**. Some of these biomarkers already have been analyzed in exosomes in one or more diseases, whereas others have been measured in biofluids but not yet in exosomes. This section summarizes briefly the current state of research into the role of exosomes in these diseases whereas the subsequent section discusses their use as a source of biomarkers originating in the CNS.

**TABLE 1** | List of potential fluid biomarkers for diagnosis of neurodegenerative diseases.

Disease	Biomarker	Biofluids	References
AD	A $\beta$ 42, pT181-tau, pS396-tau, total-tau	Neuronal exosomes isolated from blood, CSF	Tapiola et al., 2009; Fianadaca et al., 2015; Goetzl et al., 2016; Winston et al., 2016; Jia et al., 2019
PD	$\alpha$ -synuclein, DJ-1	Neuronal exosomes isolated from blood, CSF	Shi et al., 2014; Dutta et al., 2018; Zhao et al., 2019
Prion diseases	PrP, tau, 14-3-3	CSF	Otto et al., 1997; Llorens et al., 2018
FTD	A $\beta$ 42, total tau, pT181-tau, pS396-tau, NfL	Neuronal exosomes isolated from blood, CSF	Irwin et al., 2013; Fianadaca et al., 2015; Abu-Rumeileh et al., 2018; Goossens et al., 2018
ALS	TDP-43, NfL, phospho-NfH	CSF, plasma, serum	Kasai et al., 2009; Noto et al., 2011; Boylan et al., 2013; Hosokawa et al., 2014; Lehnert et al., 2014; Lu et al., 2015; Oeckl et al., 2016

AD, Alzheimer's disease; A $\beta$ 42, Amyloid  $\beta$ -protein 1-42; CSF, Cerebrospinal fluid; FTD, Frontotemporal dementia; NfH, Neurofilament heavy chain; NfL, Neurofilament light chain; PD, Parkinson's disease; PrP, Prion protein; pS396-Tau, Tau phosphorylated at S396; pT181-Tau, Tau phosphorylated at T181; TDP-43, transactive response DNA-binding protein 43 kDa.

## Alzheimer's Disease

The pathology of AD is characterized by the aggregation of A $\beta$  in senile plaques and of hyperphosphorylated tau in neurofibrillary tangles. Accumulation and spread of the latter lesion in susceptible brain regions correlate with a progressive cognitive decline (Rajendran et al., 2006; Guix et al., 2018). Different roles of exosomes related to both A $\beta$  and tau pathologies in AD have been reported in several studies. Rajendran et al. demonstrated that in HeLa and Neuroblastoma 2a (N2a) cells, sequential cleavage of the amyloid  $\beta$ -protein precursor (APP) by  $\beta$ -secretase occurs intracellularly in early endosomes, where it may be directed subsequently to MVBs and secreted into the extracellular space in exosomes after fusion of the MVB with the plasma membrane. Possibly supporting this idea, the authors showed that the exosomal marker Alix was enriched in the vicinity of senile plaques in the AD brain, whereas the brain of a patient with PD or of a healthy control subject stained negatively for plaques and for Alix (Rajendran et al., 2006).

Other studies have shown that exosomes isolated from neuronal cell cultures accelerated the aggregation of A $\beta$ , suppressed the formation of toxic A $\beta$  oligomers, and facilitated the uptake of A $\beta$  by microglia (Yuyama et al., 2008, 2012). A protective role of exosomes in AD pathogenesis was proposed based on the finding that exosomes isolated from human CSF or brain samples sequestered oligomeric A $\beta$  in the brain (An et al., 2013). The importance of the originating cell type for the physiological effect of exosomes was highlighted by Dinkins et al. who showed that exosomes isolated from astrocytes, in contrast to neuronal exosomes, interfered with the uptake of A $\beta$  in a mixed glial cell culture. However, similar to neuronal exosomes, astrocytic exosomes promoted A $\beta$  aggregation (Yuyama et al., 2012; Dinkins et al., 2014). Recently, it has been found that N2a cells carrying the autosomal-dominant Swedish form of APP (KM670/671NL) secreted exosomes containing A $\beta$  and C-terminal fragments of APP whereas cells expressing wild-type APP secreted exosomes that contained the APP C-terminal fragments but not A $\beta$ . Furthermore, APP and its C-terminal fragments were specifically sorted into exosomes lacking the tetraspanin protein CD63, demonstrating that neuroblastoma cells secrete distinct populations of exosomes containing different cargos and targeting specific cell types (Laulagnier et al., 2018).

Pathologic forms of tau have been shown to spread via exosomes among different cells (Polanco et al., 2016). A study by Clavaguera et al. demonstrated the spreading of the frontotemporal-dementia-associated form P301S-tau from mouse brain extracts to different brain regions after injection into the hippocampus and the overlying cerebral cortex of transgenic mice expressing wild-type human tau (Clavaguera et al., 2009). The authors did not comment on the potential involvement of exosomes in the spread of tau pathology yet several subsequent publications provided strong evidence for the presence of tau in CNS-derived exosomes and the contribution of such exosomes to the spread of the pathology. Tau and hyperphosphorylated tau have been identified in exosomes isolated from human CSF (Saman et al., 2012; Guix et al., 2018), human plasma and

serum (Fiandaca et al., 2015; Guix et al., 2018), brain tissue of transgenic rTg4510 mice (Polanco et al., 2016), and conditioned medium of M1C cells (Saman et al., 2012). Further evidence for a role of exosomes in the transmission of tau has been provided by the findings that microglia secrete and phagocytose exosomal tau and that inhibition of exosome synthesis reduced tau propagation in mouse and cellular model systems (Asai et al., 2015). Exosomes also may contribute to the interplay between A $\beta$  and tau in AD. In a recent study, Aulston et al. demonstrated that treatment with EVs (presumably mostly exosomes), isolated from induced pluripotent stem-cell (iPSC)-derived neuronal cultures generated from a patient harboring the familial-AD-associated A246E of presenilin-1, which increases the A $\beta$ 42/A $\beta$ 40 ratio, induced tau phosphorylation in wild type C57BL/6 mouse brain (Aulston et al., 2019). Taken together, there is already substantial evidence for the contribution of exosomes to AD pathology, both in spreading the pathology in the brain and potentially in modulating A $\beta$  aggregation. However, this is a developing field and elucidating the precise mechanisms and implications of exosome involvement in AD will require further investigation.

## Parkinson's Disease

The neuropathological hallmark of PD is the accumulation and aggregation of  $\alpha$ -synuclein in intracellular inclusions termed Lewy bodies (LBs) and Lewy neurites.  $\alpha$ -Synuclein also is the main component of pathological aggregates in related disorders called synucleinopathies, including dementia with Lewy bodies and multiple system atrophy (Spillantini et al., 1998). Several lines of evidence indicate participation of exosomes in the intercellular spread of  $\alpha$ -synuclein in the brain. Patients with PD that received transplants of either embryonic nigral neurons (Kordower et al., 2008) or fetal mesencephalic dopaminergic neurons (Li et al., 2008) developed Lewy body-like inclusions in these grafts over a period of 11–16 years, which stained positive for  $\alpha$ -synuclein. These findings might be attributed to the prion-like spread of  $\alpha$ -synuclein pathology from disease-affected host neurons to the grafts, but also to other factors, such as an unfavorable microenvironment, lack of appropriate trophic signaling, or immune reactions (Kordower et al., 2008; Li et al., 2008). Following up on these initial studies, Hansen et al. explored intercellular  $\alpha$ -synuclein transfer in disease propagation using cellular co-culture model systems and transgenic mice. They found that extracellular  $\alpha$ -synuclein was taken up by recipient cells via endocytosis and interacted with intracellular  $\alpha$ -synuclein. They also demonstrated the *in-vivo* transfer of  $\alpha$ -synuclein between host and grafted cells in a mouse model overexpressing human  $\alpha$ -synuclein, though this model was not suitable for detecting the potential involvement of exosomes in the transfer (Hansen et al., 2011).

Newly synthesized  $\alpha$ -synuclein can be secreted rapidly via unconventional exocytosis and has been found in the lumen of cellular vesicles. Importantly, this intravesicular  $\alpha$ -synuclein is more prone to aggregation and is secreted from the cells (Lee, 2005). Proteasomal and mitochondrial dysfunction and other cellular defects associated with PD pathogenesis lead to increased secretion of monomeric and aggregated forms of  $\alpha$ -synuclein (Lee, 2005). Emmanouilidou et al. provided the first evidence

for exosomal secretion of  $\alpha$ -synuclein in a calcium-dependent manner in SH-SY5Y cells. Conditioned medium containing exosomal  $\alpha$ -synuclein has been shown to reduce the viability of recipient neurons, suggesting that secretion of  $\alpha$ -synuclein contributed to the spreading of PD pathology (Emmanouilidou et al., 2010). Additionally, lysosomal dysfunction is believed to accelerate exosomal  $\alpha$ -synuclein release and propagation to surrounding cells (Alvarez-Erviti et al., 2011).

By using a novel protein-fragment-complementation assay, Danzer et al. identified oligomeric  $\alpha$ -synuclein species in exosomes in the conditioned medium of human H4 neuroglioma cells and primary cortical neurons. Moreover, they determined that  $\alpha$ -synuclein oligomers were present both on the outside and the inside of exosomes, and suggested that  $\alpha$ -synuclein could be secreted through different pathways as it was found both free and in association with exosomes (Danzer et al., 2012). In the presence of exosomes,  $\alpha$ -synuclein was more prone to aggregation and exosome-associated  $\alpha$ -synuclein was taken up more efficiently by cells in culture than free  $\alpha$ -synuclein, further supporting a role for exosomes in the intercellular transfer of  $\alpha$ -synuclein (Danzer et al., 2012; Grey et al., 2015). A recent study showed that phosphorylated  $\alpha$ -synuclein concentration in saliva exosomes was higher in patients with PD than in healthy individuals. The authors also observed a higher abundance of neuronal exosomes in the saliva of patients with PD, which they speculated could reflect increased salivary secretion of exosomes from neuronal endings in salivary glands (Rani et al., 2019).

## Frontotemporal Dementia (FTD) and Amyotrophic Lateral Sclerosis (ALS)

Frontotemporal dementia is a heterogeneous disorder that causes progressive changes in behavior, language, memory, executive control, and motor functions (Olney et al., 2017). It is characterized pathologically by atrophy of the frontal lobe and often involves accumulation of different forms of aberrantly post-translationally modified and aggregated tau in the brain of affected individuals. In addition, FTD can be characterized pathologically by cellular inclusions of the transactive response DNA-binding protein 43 kDa (TDP-43) (Turner et al., 2017), a feature it shares with ALS, which is a distinct neurodegenerative disease affecting motor neurons in the brain and spinal cord. In fact, FTD and ALS appear to be on a spectrum and some patients display mixed phenotypes of both diseases (Kawakami et al., 2019). However, each disease also can present without involvement of the other one and unlike TDP-43, which is shared by both diseases, mutations in certain proteins are associated with either FTD or ALS, but not both. For example, mutations in the superoxide dismutase 1 (SOD1) gene lead to familial forms of ALS but not FTD (Münch et al., 2011). The FTD-ALS clinical spectrum correlates not only with TDP-43 inclusions in neuronal and glial cells, but also with the observation that hexanucleotide-repeat expansion of the C9orf72 gene can lead to ALS, FTD, or a mixed clinical presentation of both diseases (Neumann et al., 2006; Turner et al., 2017).

SOD1 was the first gene discovered to cause familial ALS and the most studied cause of ALS. The presence of SOD1

in exosomes secreted from motor-neuron-like NSC-34 cells overexpressing human wild-type or mutant SOD1 provided the first evidence for the secretion and cell-to-cell transmission of SOD1 in the context of ALS (Gomes et al., 2007). Using a similar cell model, misfolded, mutant, or wild-type human SOD1 was shown to be transmitted between cells both as free protein aggregates and through exosomal transport. In addition, misfolding of human, wild-type SOD1 was propagated in HEK293 cells via exosomes in conditioned media over several passages and was transferred to cultured transgenic mouse primary spinal cord neurons expressing human wild-type SOD1 (Grad et al., 2014). Immunoelectron microscopy using the misfolded-SOD1-specific antibody 3H1 (Pickles et al., 2016; Atlasi et al., 2018) demonstrated that the majority of SOD1 aggregates were present on the exterior of exosomes isolated from the conditioned medium of cultured NSC-34 cells (Grad et al., 2014).

Like SOD1, TDP-43 might be secreted in exosomes, facilitating a prion-like spread of its misfolded species, though to our knowledge, this has not yet been demonstrated directly. Treatment of SH-SY5Y cells expressing TDP-43 with brain extracts of buffer-insoluble proteins from patients with ALS showed that the TDP-43 concentration was increased significantly in exosomes isolated from the conditioned medium compared to untreated cells, whereas the concentration level of the exosomal marker CD63 did not differ between the fractions suggesting that there was no change in exosome concentration (Nonaka et al., 2013). A study by Feiler et al. used a protein-complementation assay allowing the researchers to quantify TDP-43 in HEK-293 cells. Western blot analysis showed the presence of myc-tagged exogenous and endogenous TDP-43 in exosomes of cells transfected with myc-TDP-43. The study showed that exosomal TDP-43 was taken up preferentially by recipient cells and exerted higher toxicity than free TDP-43 (Feiler et al., 2015).

A study by Iguchi et al. provided further support for exosomal transport of TDP-43 using exosomes from the cell-culture medium of N2a cells. Cells expressing mutant forms of human TDP-43 or a fragment thereof secreted the respective protein forms in their exosomes. TDP-43 also was detected in purified exosomes from primary cortical neurons of transgenic C57BL/6 mice expressing human TDP-43<sup>A315T</sup> but not from primary astrocytes or microglia (Iguchi et al., 2016). The pathological relevance of exosomal TDP-43 was highlighted by the presence of TDP-43 in exosomes isolated from frozen post-mortem temporal cortices of patients who died of sporadic ALS, in which TDP-43 concentration levels were increased compared to exosomes from brains of healthy controls. Treatment of N2a cells overexpressing human TDP-43 with GW4869 or siRNA silencing Rab27A to reduce exosome secretion (Ostrowski et al., 2010) resulted in increased intracellular levels of insoluble TDP-43 aggregates (Iguchi et al., 2016). The studies presented above suggest that TDP-43 is secreted via exosomes in the human brain and that the exosomes are involved in the spread of TDP-43 pathology, common to ALS and FTD, yet a conclusive demonstration of these processes is still not available.

## Prion Diseases

Transmissible prion encephalopathies, such as Creutzfeldt-Jakob disease, scrapie, and bovine spongiform encephalopathy are characterized by misfolding of the normal prion protein PrP<sup>c</sup> into the aggregation-prone form PrP<sup>Sc</sup> (Prusiner, 1982, 1991). The first suggestion of an association of misfolded prion protein with exosomes came from a ME7 scrapie-infected mouse model in which PrP<sup>Sc</sup> was identified in late-endosome-like organelles from brain homogenates, which were obtained by sequential centrifugation steps using a Nycodenz<sup>®</sup> density gradient. Analysis of these fractions by dot blot, western blot, and double-labeled immunogold electron microscopy identified the endosome-lysosome markers cathepsin B, mannose 6-phosphate receptor, ubiquitin-protein conjugates, and  $\beta$ -glucuronidase (Arnold et al., 1995). Because ILVs, the direct precursors of exosomes, are formed in late endosomes (Stoorvogel et al., 2002), the presence of PrP<sup>Sc</sup> in these organelles may suggest a possible localization of PrP<sup>Sc</sup> in exosomes.

Based on multiple analysis methods, including western blot, mass spectrometry, and morphological analysis, a later study found strong evidence supporting this possibility. PrP<sup>c</sup> and PrP<sup>Sc</sup> were found to be actively released into the extracellular space by PrP-expressing Rov cells before and after infection with sheep PrP<sup>Sc</sup>. Importantly, the study showed that exosomes containing PrP<sup>Sc</sup> were infectious to other cells, suggesting a contribution of exosomes to the intercellular spread of prions *in-vivo* (Fevrier et al., 2004). Further support for this hypothesis came from studies reporting exosomal secretion of the endogenous prion protein by cultured primary rat cortical cells (Fauré et al., 2006), mouse hypothalamic neuronal GT1-7 cells (Vella et al., 2007), and mouse N2a cells (Alais et al., 2008; Veith et al., 2009). Additionally, exosomes derived from these cells were shown to introduce prions into uninfected recipient cells (Vella et al., 2007; Alais et al., 2008) and induce prion disease when inoculated in mice (Vella et al., 2007). The relationship between exosome release and intercellular prion transport was investigated also by Guo et al. who observed that stimulation of exosome release by treatment with the ionophore monensin (Savina et al., 2003) led to an increase in prion infectivity, whereas inhibition of exosome release using GW4869 (Guo et al., 2015) decreased prion transmission between rabbit kidney epithelial (RK13) and mouse GT1-7 cells (Guo et al., 2016).

In contrast to other neurodegenerative disorders, wherein only a small fraction of the offending proteins are released in exosomes, exosomes may be a major pathway for the spread of pathological proteoforms in prion diseases (Arellano-Anaya et al., 2015; Stuendl et al., 2016). Arellano-Anaya et al. (2015) showed that strains of PrP<sup>Sc</sup> from three different species were secreted into the culture medium of RK13 cells and were present in fractions containing exosomal markers and at typical densities of exosomes. Moreover, it was shown that these exosomal prion proteins retained their infectivity (Arellano-Anaya et al., 2015). Pan et al. observed that prion proteins were secreted in exosomes upon inhibition of cyclophilins by the immunosuppressive agent cyclosporine A, which usually leads to an accumulation of aggregated PrP<sup>Sc</sup> and its deposition in aggresomes in N2a and



Chinese hamster ovary cells (Pan et al., 2018). The presented studies strongly indicate that different prion protein species are secreted via exosomes and therefore contribute, possibly to a high extent, to the spread of the misfolded, pathogenic protein in prion diseases.

## CNS-DERIVED EXOSOMES AS A SOURCE OF BIOMARKERS FOR NEURODEGENERATIVE DISEASES

Blood biomarkers are highly sought-after in the field of neurodegenerative diseases. They offer important advantages relative to expensive imaging modalities or the invasive lumbar puncture required for analysis of CSF biomarkers. However, drawbacks such as inconsistent results from different research groups and weak or non-existent correlation with disease severity or with CSF-derived or imaging biomarkers have hampered progress in this direction (Mehta and Adler, 2016; Lashley et al., 2018; Zhao et al., 2019). The relatively poor performance of blood-based biomarkers reflects the disconnect between the brain biochemistry and the blood composition, which is maintained by the BBB to protect the brain. As CNS-derived exosomes can cross the BBB into the blood and can be isolated from the blood, measurement of biomarkers in them offers an attractive solution for these issues.

The groups of Zhang at University of Washington, Seattle and Goetzl at University of California, San Francisco have pioneered this field establishing isolation protocols for neuronal exosomes, which were used as a novel source for neurodegenerative-disease biomarkers. Neuronal exosomes were obtained by immunoprecipitation using antibodies targeting the neuronal marker proteins NCAM or L1CAM (see section Isolation of CNS-Derived Blood Exosomes). NCAM is a neuronal cell adhesion protein that belongs to the immunoglobulin superfamily and is involved in cell-cell and cell-matrix interactions. L1CAM is an axonal glycoprotein that plays an important role in nervous-system development and its mutations cause neurological syndromes known as CRASH.

Using this methodology, Fiandaca et al. (2015) determined the levels of total tau, pT181-tau, pS396-tau and A $\beta$ 42 in neuronal exosomes in a cohort comprising patients with AD, patients with FTD, and matching cognitively normal control subjects. They found significantly higher levels of all four biomarkers in patients with AD and of pT181-tau and A $\beta$ 42 in patients with FTD compared to healthy controls. Impressively, their final model classified 96.4% of patients with AD and 87.5% of patients with FTD correctly and predicted the development of AD up to 10 years before the onset of clinical symptoms (Fiandaca et al., 2015).

Further analysis of neuronal exosomes obtained from the same cohort, demonstrated that levels of cathepsin D, LAMP-1, and ubiquitinated proteins, which are involved in the proteasomal and lysosomal degradation pathways, were significantly higher in patients with AD than in those with FTD. Similar to their initial study, the authors found that the concentration levels of the investigated proteins in neuronal

exosomes from patients with AD were significantly distinct from those in age- and sex-matched healthy controls up to 10 years before the diagnosis (Goetzl et al., 2015). The results suggested that neuronal lysosomal dysfunction is an early event in the development of AD and may be useful as a predictive biomarker in prospective studies.

A following study by the Rissman group found that plasma-derived neuronal exosomal levels of pT181-tau, pS396-tau, and A $\beta$ 42 were increased, whereas the post-synaptic protein neurogranin and repressor element 1-silencing transcription factor (REST) levels were decreased in patients with AD or with mild cognitive impairment (MCI) converting to AD compared to normal subjects and patients with stable MCI that did not convert to AD (Winston et al., 2016). These promising results suggest that alterations of these neuronal-exosomal biomarkers could predict the conversion from MCI to AD.

An adaptation of the original procedure for isolation of neuronal exosomes allowed Goetzl et al. to enrich astrocyte-derived exosomes from plasma and subsequent analysis of biomarkers in these exosomes (Goetzl et al., 2016). Astrocyte-derived exosomes from patients with AD, patients with FTD, and healthy controls showed up to 20-fold higher levels of  $\beta$ -site amyloid  $\beta$ -protein precursor-cleaving enzyme 1,  $\gamma$ -secretase, A $\beta$ 42, soluble APP $\alpha$  and APP $\beta$ , glial-derived neurotrophic factor, pT181-tau, and pS396-tau compared to the concentrations measured in neuronal exosomes. Moreover, concentration levels of A $\beta$ 42 in astrocytic exosomes were lower in AD samples compared to the concentrations in healthy control samples, whereas pT181-tau, pS396-tau, and A $\beta$ 42 concentration in neuronal exosomes were significantly higher than in the control samples (Goetzl et al., 2016). In a recent study, Rissman's group showed that plasma-derived neuronal and astrocytic exosomes from patients with mild traumatic brain injury (mTBI) contained high levels of A $\beta$ 42 and low levels of neurogranin compared to healthy individuals with no history of TBI, suggesting that injury-associated proteins in these exosomes could be used as biomarkers for mTBI (Winston et al., 2019).

The Zhang group analyzed  $\alpha$ -synuclein in neuronal exosomes from a large cohort of 267 patients with PD and 215 healthy controls and found that  $\alpha$ -synuclein concentrations in the isolated exosomes were higher in the PD group compared to the control group. Although the diagnostic performance of neuronal exosomal  $\alpha$ -synuclein was moderate (receiver operating characteristic (ROC) analysis AUC = 0.654, sensitivity = 70.1%, specificity = 52.9%), a significant cross-sectional correlation of neuronal exosomal  $\alpha$ -synuclein was found with disease severity (Shi et al., 2014), suggesting that if a similar correlation were observed longitudinally, this biomarker could be useful for measuring PD progression and outcome measures of clinical trials. In a follow-up study, the same group demonstrated that tau protein levels in neuronal exosomes were elevated in patients with PD but not in patients with AD (Shi et al., 2016). In a longitudinal study, Wang et al. tested the utility of plasma  $\alpha$ -synuclein and CNS-derived exosomal  $\alpha$ -synuclein at baseline and in 2-year follow-up samples in a cohort comprising 256 individuals who might be at risk of PD. Their data showed that an increase in plasma  $\alpha$ -synuclein at baseline and at follow-up

could predict progression of cognitive decline in a subgroup of people with an increased PD risk, evidenced by hyposmia and reduced dopamine transporter imaging. In contrast, a decrease of  $\alpha$ -synuclein in exosomes was associated with worsening of cognitive performance (Wang et al., 2018).

Recently, the protocol developed by Goetzl et al. was used by another group to determine the levels of DJ-1 and  $\alpha$ -synuclein in neuronal exosomes from 39 patients with PD and 40 healthy controls (Zhao et al., 2019). Both, DJ-1 and  $\alpha$ -synuclein were significantly higher in neuronal exosomes from patients with PD than in those from healthy controls whereas no significant differences were observed in total plasma, in agreement with the previous study by Shi et al. (2014). As in the previous study, ROC analysis yielded only a moderate discrimination between patients with PD and healthy controls even when both biomarkers were combined (Zhao et al., 2019).

In another new study, A $\beta$ 42, total tau, and pT181-tau were analyzed in two cohorts consisting of patients with AD, patients with amnesic MCI (aMCI), and healthy controls (Jia et al., 2019). The study included a discovery stage cohort comprising 28 patients with AD, 25 patients with aMCI, and 29 healthy controls, and a larger validation cohort consisting of 73 patients with AD, 71 patients with aMCI, and 72 healthy controls. The authors compared the biomarker concentration levels in the neuronal exosomes to the concentration of the same biomarkers in the CSF of all subjects. The data in both the discovery and validation cohorts showed that all three assessed biomarkers—A $\beta$ 42, total tau, and pT181-tau in neuronal exosomes were highest in patients with AD, significantly lower in patients with aMCI, and lowest in healthy controls. Encouragingly, the level of each exosomal biomarker showed a strong correlation with the respective CSF biomarker, suggesting that the measurement of these biomarkers in the neuronal exosomes could replace CSF analysis (Jia et al., 2019). A comprehensive summary of the studies described in this section is shown in **Table 2**.

These studies demonstrate the potential of CNS-derived blood exosomes as a source of diagnostic, prognostic, and progression biomarkers for neurodegenerative diseases. In addition to blood products, exosomes obtained from other biofluids, such as CSF and saliva, also have been used for diagnostic purposes (Yoo et al., 2018; Cao et al., 2019). Obtaining saliva from patients is less invasive than obtaining blood and saliva is easier to process because it does not coagulate. However, as a source of biomarkers in neurodegenerative (and systemic) diseases, saliva has been studied much less than plasma or serum, likely because variability and risk of contamination in saliva compared to blood are higher (Han et al., 2018; Cao et al., 2019). In contrast, the fidelity of biomarkers measured in CNS-derived blood exosomes as representing biochemical changes in the CNS has been found to be similar to that of CSF biomarkers, suggesting that the same level of confidence can be achieved using a substantially less invasive procedure. This is important in particular for measurement of treatment efficacy in clinical trials where multiple tests often are required during the trial. Similar to CSF biomarker studies, the data also suggest that biomarker panels likely will provide better diagnostic or prognostic power than single biomarkers (Fiandaca et al., 2015; Goetzl et al., 2016;

Shi et al., 2016; Winston et al., 2016). A particular advantage of biomarker analysis in CNS-derived blood exosomes compared to CSF is the ability to compare the biomarkers in exosomes originating in different cell types.

## ISOLATION OF CNS-DERIVED BLOOD EXOSOMES

Numerous methods for isolation of exosomes have been reported, including protocols based on ultracentrifugation, filtration, precipitation, immuno-affinity capture, and microfluidics arrays (Contreras-Naranjo et al., 2017; Doyle and Wang, 2019; Zhang et al., 2019). However, only a minority of the reported methods can yield a sufficient number of exosomes when starting from a typical patient sample, e.g., 0.5 mL, if the goal is to isolate subsequently CNS-derived exosomes for biomarker analysis. Therefore, we focus here on isolation methods that have been used successfully for isolating CNS-derived blood exosomes followed by biomarker analysis. For more general reviews on exosome isolation techniques (see Li et al., 2017; Doyle and Wang, 2019).

The use of blood plasma as a source of exosomes requires the addition of EDTA or heparin to prevent clotting and subsequent separation of plasma by centrifugation (e.g., 15 min at 2,500 g) (Goetzl et al., 2015). To isolate exosomes from human plasma, thrombin needs to be added to the plasma samples prior to proceeding with the actual isolation. Alternatively, serum can be obtained by allowing the blood to clot for 15–20 min at room temperature before separating the serum by centrifugation and the serum then can be used directly for exosome isolation. Addition of protease and phosphatase inhibitors to the samples and maintaining the clotting time consistent for all the samples under study is crucial for preventing degradation or modification of exosomal ingredients, especially those present in minute concentrations (Fiandaca et al., 2015; Goetzl et al., 2015). Additional precautionary measures should be taken for measurement of  $\alpha$ -synuclein in CNS-derived exosomes isolated from the blood as minute quantities of erythrocytic  $\alpha$ -synuclein released upon hemolysis can contaminate the sample.

A side-by-side comparison of the protocols developed by the two first groups pioneering this field, the Zhang and Goetzl groups, is shown in **Figure 3**. The Zhang group was the first to describe a method for isolating CNS-derived exosomes from mouse and human plasma. Their approach used anti-L1CAM antibodies immobilized on superparamagnetic microbeads for immuno-capture of CNS-derived exosomes directly from plasma diluted 1:3 in phosphate-buffered saline without prior isolation of total exosomes (**Figure 3A**). They incubated diluted plasma samples with anti-L1CAM antibody-coated epoxy beads for 24 h with gentle rotation before proceeding to exosome release or lysis.

In the work of Goetzl and co-workers, the process included an initial polymer-assisted precipitation of extracellular vesicles from serum or plasma followed by immunoprecipitation using antibodies specific for NCAM or L1CAM to enrich CNS neuronal exosomes (**Figure 3B**; Fiandaca et al., 2015). They

**TABLE 2 |** Selected publications analyzing biomarkers in CNS-derived blood exosomes.

Exosome isolation method	Validation methods	Study cohort	Analyzed biomarkers	Outcome	References
Immunocapture using anti-L1CAM antibody-coated M-270 Dynabeads	TEM, Western blot	PD: 267 HC: 215	Neuronal exosomal $\alpha$ -synuclein	$\alpha$ -synuclein: PD $\uparrow$ , Correlation with disease severity	Shi et al., 2014
Exosome precipitation and immunocapture using biotinylated anti-NCAM or anti-L1CAM antibodies and streptavidin-agarose resin	NTA	AD: 57 AC: 57 FTD: 16 FTC: 16 AD (preclinical and after AD diagnosis): 24	Neuronal exosomal A $\beta$ 42, total tau, pT181-tau, pS396-tau	A $\beta$ 42, total-tau, pT181-tau, pS396-tau: AD $\uparrow$ A $\beta$ 42, pT181-tau: FTD $\uparrow$ A $\beta$ 42, pT181-tau, pS396-tau: Preclinical AD $\uparrow$ compared to AC, AD $\uparrow$ compared to preclinical AD and AC	Fiandaca et al., 2015
Exosome precipitation and immunocapture using biotinylated anti-L1CAM antibody and streptavidin-polyacrylamide resin	NTA	AD: 26 AC: 26 FTD: 16 FTC: 16 AD (preclinical and after AD diagnosis): 20	Neuronal exosomal Cathepsin D, LAMP-1, Ubiquitin, HSP-70	Cathepsin D, LAMP-1, ubiquitinated proteins: AD $\uparrow$ compared to AC and FTD HSP70: AD $\downarrow$ compared to AC, FTD $\downarrow$ compared to FTC and AD Cathepsin D: FTD $\uparrow$ compared to FTC Cathepsin D, LAMP-1, ubiquitinated proteins: preclinical AD $\uparrow$ , AD $\uparrow$ compared to AC HSP70: preclinical AD $\downarrow$ , AD $\downarrow$ compared to AC	Goetzl et al., 2015
Exosome precipitation and immunocapture using biotinylated anti-L1CAM antibody and streptavidin-polyacrylamide resin	TEM, NTA	AD: 10 MCI: 20 MCI to AD converter: 20 HC: 10	Neuronal exosomal A $\beta$ 42, pT181-tau, pS396-tau	A $\beta$ 42, pT181-tau, pS396-tau: AD $\uparrow$ , MCI to AD converter $\uparrow$ both compared to MCI and HC NRGN, REST: AD $\downarrow$ , MCI to AD converter $\downarrow$ both compared to MCI and HC	Winston et al., 2016
Exosome precipitation and immunocapture by biotinylated anti-GLAST or anti-L1CAM antibodies and streptavidin-agarose resin	NTA	AD: 12 AC: 10 FTD: 14 FTC: 10	Neuronal and astrocytic exosomal BACE-1, $\gamma$ -secretase, sAPP $\alpha$ , sAPP $\beta$ , Septin-8, GDNF, A $\beta$ 42, pT181-tau, pS396-tau	BACE-1, sAPP $\beta$ : AD $\uparrow$ , FTD n.s. GDNF: AD/MCI $\downarrow$ , FTD n.s. BACE-1, $\gamma$ -secretase, A $\beta$ 42, sAPP $\alpha$ , sAPP $\beta$ , GDNF, pT181-tau, pS396-tau: ADE of all groups $\uparrow$ compared to NDE	Goetzl et al., 2016
Immunocapture using anti-L1CAM antibody-coated M-270 Dynabeads	TEM, Western Blot, NTA	PD: 91 AD: 106 HC: 106	Neuronal exosomal total tau	Total-tau: PD $\uparrow$ compared to AD and HC Correlation to disease duration and CSF tau in PD	Shi et al., 2016
Immunocapture using anti-L1CAM antibody-coated M-270 Dynabeads	Not determined	Normosmia/ no DAT reduction: 80 Hyposmia/ no DAT reduction: 133 Hyposmia/ DAT reduction: 43	Total plasma and neuronal exosomal $\alpha$ -synuclein	Total- $\alpha$ -synuclein: Hyposmic/ DAT reduction $\uparrow$ at baseline and longitudinally NDE $\alpha$ -synuclein: Hyposmic/ DAT reduction $\downarrow$ longitudinally Correlation with cognitive function and DAT imaging	Wang et al., 2018
Exosome precipitation and immunocapture by biotinylated anti-L1CAM antibody and streptavidin-agarose resin	TEM	PD: 39 HC: 40	Neuronal exosomal DJ-1 and $\alpha$ -synuclein	DJ-1 and $\alpha$ -synuclein: PD $\uparrow$ compared to HC	Zhao et al., 2019

(Continued)

**TABLE 2 |** Selected publications analyzing biomarkers in CNS-derived blood exosomes.

Exosome isolation method	Validation methods	Study cohort	Analyzed biomarkers	Outcome	References
Exosome precipitation and immunocapture by biotinylated anti-NCAM antibody and streptavidin-agarose resin	TEM, Western blot	Discovery stage: AD: 28 aMCI: 25 HC: 29 Validation stage: AD: 73 aMCI: 71 HC: 72	Neuronal exosomal A $\beta$ 42, total-tau, pT181 tau	A $\beta$ 42, total-tau, pT181-tau: aMCI $\uparrow$ compared to HC, AD $\uparrow$ compared to aMCI and HC Exosomal biomarker correlate with respective CSF biomarker	Jia et al., 2019
Exosome precipitation and immunocapture by biotinylated anti-L1CAM or anti-GLAST antibodies immobilized on streptavidin-coated magnetic beads	FACS	mTBI: 19 HC: 20	Neuronal and astrocytic exosomal A $\beta$ 40, A $\beta$ 42, NRG1, NfL, total tau, pT181-tau, pS396-tau	A $\beta$ 42: mTBI $\uparrow$ NRG1: mTBI $\downarrow$ A $\beta$ 40, total-tau, NfL, pT181-tau, pS396-tau: mTBI n.d. or n.s.	Winston et al., 2019

$\uparrow$ , increased;  $\downarrow$ , decreased; AC, Alzheimer's disease control; AD, Alzheimer's disease; ADE, astrocyte-derived exosomes; aMCI, amnesic mild cognitive impairment; A $\beta$ 40, amyloid  $\beta$ -protein 1-40; A $\beta$ 42, amyloid  $\beta$ -protein 1-42; BACE-1,  $\beta$ -site amyloid precursor protein-cleaving enzyme 1; CSF, cerebrospinal fluid; DAT, dopamine transporter; FACS, fluorescence activated cell sorting; FTC, frontotemporal dementia control; FTD, frontotemporal dementia; GDNF, glial-derived neurotrophic factor; GLAST, glutamate aspartate transporter; HC, healthy control; HSP70, heat shock protein 70; L1CAM, L1-cell adhesion molecule; LAMP-1, lysosomal-associated membrane protein 1; MCI, mild cognitive impairment; MOG, myelin oligodendrocyte glycoprotein; mTBI, mild traumatic brain injury; n.d., not detectable; n.s., not significant; NCAM, neuronal cell adhesion molecule; NDE, neuron-derived exosomes; NfL, neurofilament light; NRG1, neurogranin; NTA, nanoparticles tracking analysis; PD, Parkinson's disease; pS396-tau, tau phosphorylated at S396; pT181-tau, tau phosphorylated at T181; REST, repressor element 1-silencing transcription factor; sAPP $\alpha$ / $\beta$ , soluble amyloid precursor protein  $\alpha$ / $\beta$ ; TEM, transmission electron microscopy; TRPS, tunable resistive pulse sensing.

first incubated serum or thromboplastin-D-treated plasma samples with the non-specific PEG-based ExoQuick exosome precipitation solution to obtain a pellet of total exosomes, which was resuspended and the incubated with biotinylated anti-human NCAM or L1CAM antibodies to enrich neuronal exosomes by subsequent immunoprecipitation using a streptavidin-coated polyacrylamide resin (Goetzl et al., 2015). Similar approaches were used later by the groups of Kapogiannis, Rissman, and others (Winston et al., 2016; Doyle and Wang, 2019).

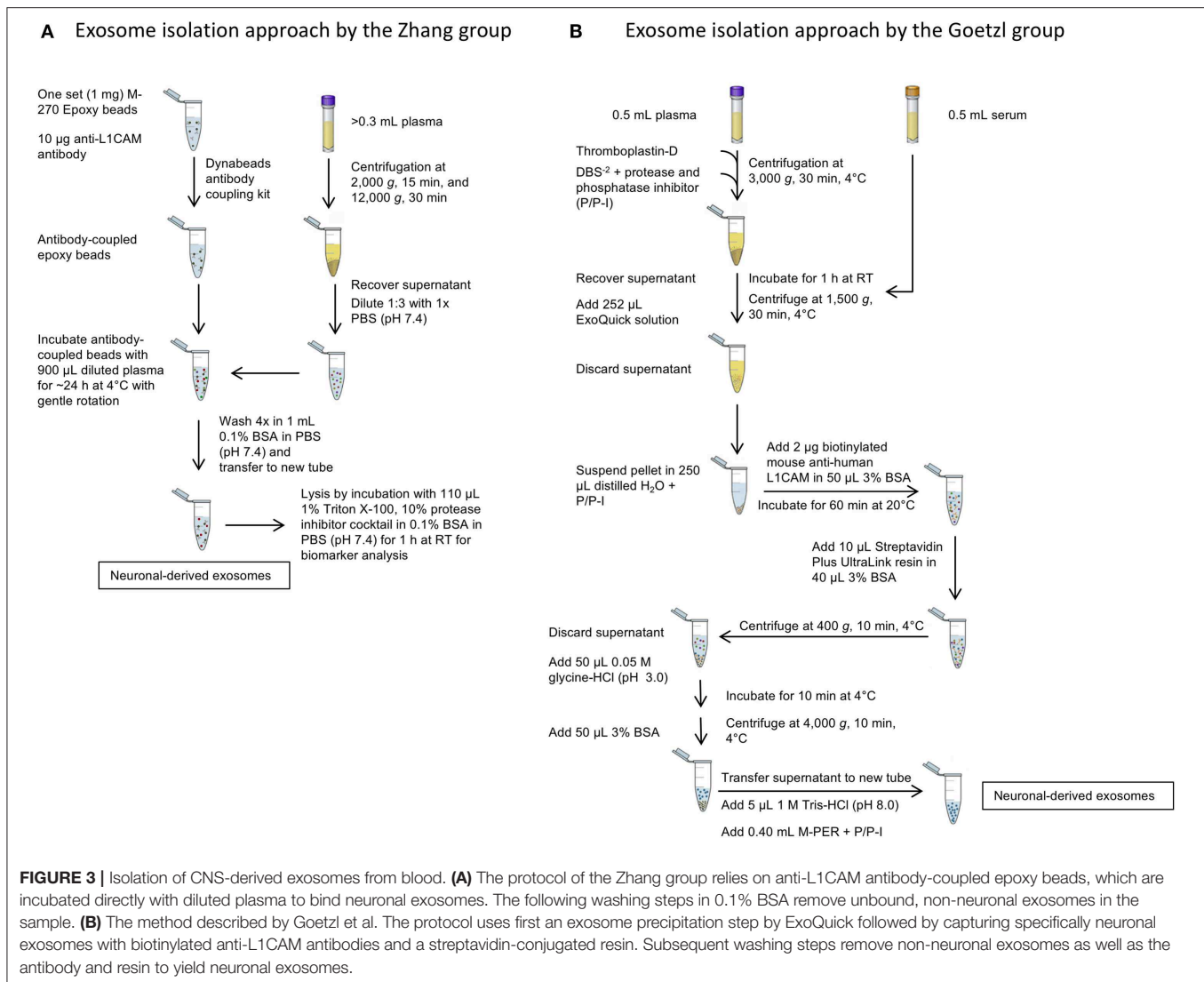
After capturing the exosomes by antibody-coated beads, according to both groups' protocols the beads are washed and the NCAM/L1CAM-positive exosomes can be eluted, e.g., for morphological analysis and for measurement of exosome number and size using methods, such as Nanoparticle Tracking Analysis (NTA), Tunable Resistive Pulse Sensing (TRPS) or Microfluidic Resistive Pulse Sensing (MRPS) (Shi et al., 2014; Goetzl et al., 2016; Winston et al., 2016; Jia et al., 2019; Yan et al., 2019). Alternatively, the exosomes may be lysed on the beads by treatment with different buffers, such as Mammalian Protein Extraction Reagent (M-PER) (Fiandaca et al., 2015; Goetzl et al., 2015) or other detergent-containing buffers for different downstream analyses and biomarker measurement (Shi et al., 2014, 2016; Wang et al., 2018). The methods used in different studies and the measured candidate biomarkers in CNS-derived blood exosomes for different neurological diseases and conditions are summarized in **Table 2**. The reported methods for isolation of CNS-derived exosomes from blood samples share wide similarities and differ mainly in the type of solid support used to immobilize the respective antibodies in the immunoprecipitation step. Although to date no study has compared side-by-side the different approaches, the efficiency

and specificity of each method likely depends mainly on the specificity of the used antibody.

Adaptations of the protocol of Goetzl et al. have subsequently been applied for the isolation of astrocyte-derived blood exosomes using an anti-GLutamate ASpartate Transporter (GLAST) antibody (Goetzl et al., 2016, 2018). Our group was the first to successfully isolate oligodendrocyte-derived blood exosomes using anti-myelin oligodendrocyte glycoprotein (MOG) antibody coupled to magnetic Dynabeads (Dutta et al., 2018). A challenge in such studies is to confirm that the isolated exosomes indeed originated in the cell type intended. Such confirmation can be achieved using dot blots or western blots using antibodies against specific protein markers of the cells of origin. For example, enolase 2 or glutamate ionotropic receptor AMPA type subunit 1 (GRIA1) may be used to identify neuronal exosomes, glial fibrillary acidic protein (GFAP) for astrocytic exosomes, and myelin proteolipid protein for oligodendroglial exosomes. The challenge in such experiments is due to the low abundance of exosomes released specifically from these cell types into the blood (Doyle and Wang, 2019), which in our experience is  $\leq 1\%$  of the total serum/plasma exosomes. To address this challenge one must either isolate the exosomes starting with relatively large starting volumes of serum/plasma or use detection methods with higher sensitivity than those of dot blots or western blots.

It is also important to note that immunoprecipitation using NCAM or L1CAM does not provide exclusively CNS neuronal exosomes. NCAM and L1CAM are enriched in, but are not restricted to, neurons. They also may be present in microvesicles other than exosomes though no information exists currently regarding this possibility. According to the





human protein atlas (<https://www.proteinatlas.org>), L1CAM is expressed mainly in the CNS, peripheral nervous system (PNS), and in distal renal tubules whereas NCAM is mainly observed in the CNS, PNS, adrenal gland, heart, and peptic cells. Proteomic analysis of L1CAM-captured exosomes from plasma showed higher concentrations of several CNS marker proteins, including phosphorylated tau, neuron-specific enolase, microtubule associated protein 2, neurofilament light chain (NfL), and L1CAM than in total exosome samples (i.e., before enrichment of neuronal exosomes) (Mustapic et al., 2017), suggesting that the majority of the exosomes indeed originated in CNS neurons. Nonetheless, the field should continue searching for, and testing, more specific markers that will allow isolation of purer exosome populations of CNS neurons and other cell types. Moreover, as different neurological diseases affect different brain regions, markers specific to a brain region or a neuron type, e.g., dopaminergic neurons for PD, may be developed in the future and allow biomarker analysis that would offer higher level of precision than general neuronal markers.

## CURRENT CHALLENGES AND FUTURE PERSPECTIVES

Extensive research in the last two decades has demonstrated that exosomes play a role in both physiological and pathological states of cells in the CNS. These vesicles function as intercellular communicators and serve as a vehicle for disposal of unwanted biological material. By carrying aggregated amyloidogenic proteins from cell to cell, exosomes contribute to the spread of these pathologic proteoforms in various neurodegenerative disorders. Impairment of the lysosomal and/or proteasomal pathways has been reported to increase disposal of pathogenic proteins via exosomes, contributing to disease spread in the CNS. However, the mechanisms involved in this process, the uptake of the released exosomes by specific recipient cells, the involvement of receptors and the impact of the lipid composition in the exosome membrane in these processes are yet to be elucidated.

Numerous studies have examined biofluid biomarkers for neurodegenerative diseases (Table 1). In AD, the most consistent

biomarkers have been A $\beta$ 42, total tau, pT181-tau, and pS396-tau measured in CSF and more recently in neuronal exosomes (Tapiola et al., 2009; Fiandaca et al., 2015; Goetzl et al., 2016; Winston et al., 2016; Jia et al., 2019). The same biomarker panel has been shown to distinguish FTD from AD and healthy controls in multiple studies mostly using CSF as a biomarker source. In addition, although NfL is elevated in most neurodegenerative diseases, it was found to be significantly higher in FTD than in AD (Irwin et al., 2013; Fiandaca et al., 2015; Abu-Rumeileh et al., 2018; Goossens et al., 2018). DJ-1 and  $\alpha$ -synuclein have been shown to be promising biomarkers in the diagnosis of PD. Results from studies involving neuronal exosomes have been demonstrated to be reproducible for  $\alpha$ -synuclein (Shi et al., 2014; Dutta et al., 2018; Zhao et al., 2019) and for different forms of A $\beta$  and tau (Fiandaca et al., 2015; Goetzl et al., 2016; Winston et al., 2016; Jia et al., 2019), and the acquired data in the neuronal exosomes correlated to those obtained from CSF samples (Jia et al., 2019). Increased CSF levels of tau and 14-3-3 proteins and decreased concentration levels of total PrP were found to be potential biomarkers for prion diseases (Otto et al., 1997; Llorens et al., 2018). NfL and phosphorylated forms of the neurofilament heavy chain have been shown consistently to be increased in the CSF, plasma, and serum of patients with ALS in several single- and multi-center studies (Boylan et al., 2013; Lehnert et al., 2014; Lu et al., 2015; Oeckl et al., 2016). However, NfL is associated with many neurodegenerative diseases and is likely to be more useful as an indicator of disease progression rather than diagnosis (Olsson et al., 2019; Preische et al., 2019). Therefore, TDP-43 measured in CSF may constitute a more promising biomarker for ALS as it was demonstrated to be a main component in the disease pathology (Neumann et al., 2006) and its concentration levels are elevated in patients with ALS compared to healthy controls (Kasai et al., 2009) and patients of other neurodegenerative or inflammatory diseases (Table 1; Noto et al., 2011; Hosokawa et al., 2014). Nevertheless, there is still a need for more specific biomarkers obtained through minimally invasive means for diagnosing patients reliably, ideally in early disease stages, monitor their disease progression, and evaluate clinical-trial outcomes. Similar needs exist for many rare neurodegenerative and neuromuscular diseases, many of which are genetic (e.g., ataxias, myotonic dystrophies) and can be diagnosed based on identifying the relevant mutant gene, but without reliable progression biomarkers, conducting successful clinical trials is a major challenge. Investigating new sources, such as CNS-derived exosomes, promises to generate robust biomarkers for neurodegenerative diseases through simple blood tests.

CNS-derived exosomes isolated from blood also have been shown to be a useful source of biomarkers for other neurological conditions, including stroke (Chen et al., 2016) and TBI (Winston et al., 2019), and for following brain processes that are not easily accessible, such as adult hippocampal neurogenesis (AHN) (Luarte et al., 2017). The enrichment of exosomes derived from specific brain cell types, such as neurons, astrocytes, and recently oligodendrocytes by immuno-capture likely will provide a more specific and useful source of diagnostic and progression

biomarkers compared to plasma or serum themselves or total exosomes isolated from these biofluids. The fourth brain-cell type, microglia, presents a unique challenge because microglia share surface markers, which potentially could be used to distinguish their exosomes from the other brain-cell types, with peripheral monocytes and macrophages. In the absence of a unique microglial marker presented on the exosomal membrane, isolation of microglial exosomes from blood currently is not possible.

An important practical challenge in the methodology discussed above is the limited sample volume typically available from biobanks or providing clinics and the minute number of CNS-derived exosomes in such samples, necessitating the use of high-sensitivity detection methods, such as single molecule array (SIMOA, Quanterix, USA), electrochemiluminescence ELISA (Meso Scale Discovery, USA) or Immuno magnetic reduction (MagQu, Taiwan). Another potential difficulty, discussed more in personal communication than represented in the published literature, is the reproducibility of biomarker analysis in CNS-derived exosomes. The challenges are both the exosome-isolation process itself, which requires a high level of expertise and precision, and the characterization of the subsequent assays, which must be done for each assay separately using multiple independent exosome preparations for establishing acceptable intra- and inter-experiment coefficients of variation. There is still a need for reproducible, standardized protocols for isolation of exosomes and subsequent analysis of biomarkers of interest. Nonetheless, the examples discussed above demonstrate that exosome populations enriched from specific brain cell-types hold potential as a promising source of biomarkers for different neurodegenerative disorders and it will be particularly interesting to compare biomarkers in exosomes from different cell types side-by-side in the same samples. Finally, a major difficulty specific for development of diagnostic biomarkers for many neurodegenerative diseases is the absence of samples from patients with a validated diagnosis. To develop this field further, the establishment of biobanks containing pathologically validated samples from patients with neurodegenerative diseases and healthy controls is essential.

## AUTHOR CONTRIBUTIONS

SH, SD, and GB conceived and wrote the manuscript.

## FUNDING

We are grateful for funding from Team Parkinson/Parkinson Alliance, American Parkinson Disease Association Pilot Award, MSA Coalition grant 2017-10-007, NIH/NINDS R01 grant NS107596, California Department of Public Health grant 18-10926, The Alzheimer's Association, The Michael J. Fox Foundation, Weston Brain Institute, and Alzheimer's Research UK Biomarkers Across Neurodegenerative Diseases (BAND 3) grant 17990, CurePSP grant 665-2019-07, and The Michael J. Fox Foundation grant 18303.

## REFERENCES

- Abu-Rumeileh, S., Mometto, N., Bartoletti-Stella, A., Polisch, B., Oppi, F., Poda, R., et al. (2018). Cerebrospinal fluid biomarkers in patients with frontotemporal dementia spectrum: a single-center study. *J. Alzheimers Dis.* 66, 551–563. doi: 10.3233/JAD-180409
- Alais, S., Simoes, S., Baas, D., Lehmann, S., Raposo, G., Darlix, J. L., et al. (2008). Mouse neuroblastoma cells release prion infectivity associated with exosomal vesicles. *Biol. Cell.* 100, 603–618. doi: 10.1042/BC20080025
- Alvarez-Erviti, L., Seow, Y., Schapira, A. H., Gardiner, C., Sargent, I. L., Wood, M. J. A., et al. (2011). Lysosomal dysfunction increases exosome-mediated  $\alpha$ -synuclein release and transmission. *Neurobiol. Dis.* 42, 360–367. doi: 10.1016/j.nbd.2011.01.029
- An, K., Klyubin, L., Kim, Y., Jung, J., Mably, A. J., O'Dowd, S. T., et al. (2013). Exosomes neutralize synaptic plasticity-disrupting activity of A $\beta$  assemblies *in vivo*. *Mol. Brain* 6:47. doi: 10.1186/1756-6606-6-47
- Antonucci, F., Turola, E., Riganti, L., Caleo, M., Gabrielli, M., Perrotta, C., et al. (2012). Microvesicles released from microglia stimulate synaptic activity via enhanced sphingolipid metabolism: Microglial MVs increase sphingolipid metabolism in neurons. *EMBO J.* 31, 1231–1240. doi: 10.1038/emboj.2011.489
- Arellano-Anaya, Z. E., Huor, A., Leblanc, P., Lehmann, S., Provansal, M., Raposo, G., et al. (2015). Prion strains are differentially released through the exosomal pathway. *Cell. Mol. Life Sci.* 72, 1185–1196. doi: 10.1007/s00018-014-1735-8
- Arnold, J. E., Tipler, C., Laszlo, L., Hope, J., Landon, M., and Mayer, R. J. (1995). The abnormal isoform of the prion protein accumulates in late-endosome-like organelles in scrapie-infected mouse brain. *J. Pathol.* 176, 403–411. doi: 10.1002/path.1711760412
- Asai, H., Ikezu, S., Tsunoda, S., Medalla, M., Luebke, J., Haydar, T., et al. (2015). Depletion of microglia and inhibition of exosome synthesis halt tau propagation. *Nat. Neurosci.* 18, 1584–1593. doi: 10.1038/nn.4132
- Atlasi, R. S., Malik, R., Corrales, C. I., Tzeplaff, L., Whitelegge, J. P., Cashman, N. R., et al. (2018). Investigation of Anti-SOD1 antibodies yields new structural insight into SOD1 misfolding and surprising behavior of the antibodies themselves. *ACS Chem. Biol.* 13, 2794–2807. doi: 10.1021/acschembio.8b00729
- Aulston, B., Liu, Q., Mante, M., Florio, J., Rissman, R. A., and Yuan, S. H. (2019). Extracellular vesicles isolated from familial Alzheimer's disease neuronal cultures induce aberrant tau phosphorylation in the wild-type mouse brain. *J. Alzheimers Dis.* 72, 575–585. doi: 10.3233/JAD-190656
- Banizs, A. B., Huang, T., Dryden, K., Berr, S. S., Stone, J. R., Nakamoto, R. K., et al. (2014). *In vitro* evaluation of endothelial exosomes as carriers for small interfering ribonucleic acid delivery. *Int. J. Nanomed.* 9, 4223–4230. doi: 10.2147/IJN.S64267
- Bellingham, S. A., Guo, B. B., Coleman, B. M., and Hill, A. F. (2012). Exosomes: vehicles for the transfer of toxic proteins associated with neurodegenerative diseases? *Front. Physiol.* 3:124. doi: 10.3389/fphys.2012.00124
- Bianco, F., Perrotta, C., Novellino, L., Francolini, M., Riganti, L., Menna, E., et al. (2009). Acid sphingomyelinase activity triggers microparticle release from glial cells. *EMBO J.* 28, 1043–1054. doi: 10.1038/emboj.2009.45
- Boylan, K. B., Glass, J. D., Crook, J. E., Yang, C., Thomas, C. S., Desaro, P., et al. (2013). Phosphorylated neurofilament heavy subunit (pNF-H) in peripheral blood and CSF as a potential prognostic biomarker in amyotrophic lateral sclerosis. *J. Neurol. Neurosurg. Psychiatr.* 84, 467–472. doi: 10.1136/jnnp-2012-303768
- Budnik, V., Ruiz-Cañada, C., and Wendler, F. (2016). Extracellular vesicles round off communication in the nervous system. *Nat. Rev. Neurosci.* 17, 160–172. doi: 10.1038/nrn.2015.29
- Caby, M.-P., Lankar, D., Vincendeau-Scherrer, C., Raposo, G., and Bonnerot, C. (2005). Exosomal-like vesicles are present in human blood plasma. *Int. Immunol.* 17, 879–887. doi: 10.1093/intimm/dxh267
- Cai, J., Han, Y., Ren, H., Chen, C., He, D., Zhou, L., et al. (2013). Extracellular vesicle-mediated transfer of donor genomic DNA to recipient cells is a novel mechanism for genetic influence between cells. *J. Mol. Cell Biol.* 5, 227–238. doi: 10.1093/jmcb/mjt011
- Cao, Z., Wu, Y., Liu, G., Jiang, Y., Wang, X., Wang, Z., et al. (2019).  $\alpha$ -Synuclein in salivary extracellular vesicles as a potential biomarker of Parkinson's disease. *Neurosci. Lett.* 696, 114–120. doi: 10.1016/j.neulet.2018.12.030
- Chen, C. C., Liu, L., Ma, F., Wong, C. W., Guo, X. E., Chacko, J. V., et al. (2016). Elucidation of exosome migration across the blood-brain barrier model *in vitro*. *Cell. Mol. Bioeng.* 9, 509–529. doi: 10.1007/s12195-016-0458-3
- Christianson, H. C., Svensson, K. J., van Kuppevelt, T. H., Li, J. P., and Belting, M. (2013). Cancer cell exosomes depend on cell-surface heparan sulfate proteoglycans for their internalization and functional activity. *Proc. Natl. Acad. Sci. U.S.A.* 110, 17380–17385. doi: 10.1073/pnas.1304266110
- Clavaguera, F., Bolmont, T., Crowther, R. A., Abramowski, D., Frank, S., Probst, A., et al. (2009). Transmission and spreading of tauopathy in transgenic mouse brain. *Nat. Cell Biol.* 11, 909–913. doi: 10.1038/ncb1901
- Coleman, B. M., and Hill, A. F. (2015). Extracellular vesicles – their role in the packaging and spread of misfolded proteins associated with neurodegenerative diseases. *Semin. Cell Dev. Biol.* 40, 89–96. doi: 10.1016/j.semcdb.2015.02.007
- Colombo, M., Raposo, G., and Théry, C. (2014). Biogenesis, Secretion, and intercellular interactions of exosomes and other extracellular vesicles. *Annu. Rev. Cell Dev. Biol.* 30, 255–289. doi: 10.1146/annurev-cellbio-101512-122326
- Contreras-Naranjo, J. C., Wu, H. J., and Ugaz, V. M. (2017). Microfluidics for exosome isolation and analysis: enabling liquid biopsy for personalized medicine. *Lab. Chip* 17, 3558–3577. doi: 10.1039/c7lc00592j
- Danzer, K. M., Kranich, L. R., Ruf, W. P., Cagsal-Getkin, O., Winslow, A. R., Zhu, L., et al. (2012). Exosomal cell-to-cell transmission of  $\alpha$ -synuclein oligomers. *Mol. Neurodegener.* 7:42. doi: 10.1186/1750-1326-7-42
- Dinkins, M. B., Dasgupta, S., Wang, G., Zhu, G., and Bieberich, E. (2014). Exosome reduction *in vivo* is associated with lower amyloid plaque load in the 5XFAD mouse model of Alzheimer's disease. *Neurobiol. Aging* 35, 1792–1800. doi: 10.1016/j.neurobiolaging.2014.02.012
- Doyle, L. M., and Wang, M. Z. (2019). Overview of extracellular vesicles, their origin, composition, purpose, and methods for exosome isolation and analysis. *Cells* 8:E727. doi: 10.3390/cells8070727
- Dutta, S., Reamtong, O., Panvongsa, W., Kitdumrongthum, S., Janpipatkul, K., Sangvanich, P., et al. (2015). Proteomics profiling of cholangiocarcinoma exosomes: a potential role of oncogenic protein transferring in cancer progression. *Biochim. Biophys. Acta.* 1852, 1989–1999. doi: 10.1016/j.bbadis.2015.06.024
- Dutta, S., del Rosario, I., Paul, K., Palma, J. A., Perlman, S. L., Poon, W. W., et al. (2018).  $\alpha$ -Synuclein in brain-derived blood exosomes distinguishes multiple system atrophy from parkinson's disease. *Ann. Neurol.* 84, S191–S191.
- Emmanouilidou, E., Melachroinou, K., Roumeliotis, T., Garbis, S. D., Ntzouni, M., Margaritis, L. H., et al. (2010). Cell-produced  $\alpha$ -synuclein is secreted in a calcium-dependent manner by exosomes and impacts neuronal survival. *J. Neurosci.* 30, 6838–6851. doi: 10.1523/JNEUROSCI.5699-09.2010
- Fauré, J., Lachenal, G., Court, M., Hirrlinger, J., Chatellard-Causse, C., Blot, B., et al. (2006). Exosomes are released by cultured cortical neurones. *Mol. Cell. Neurosci.* 31, 642–648. doi: 10.1016/j.mcn.2005.12.003
- Feiler, M. S., Strobel, B., Freischmidt, A., Helfrich, A. M., Kappel, J., Brewer, B. M., et al. (2015). TDP-43 is intercellularly transmitted across axon terminals. *J. Cell Biol.* 211, 897–911. doi: 10.1083/jcb.201504057
- Fevrier, B., Vilette, D., Archer, F., Loew, D., Faigle, W., Vidal, M., et al. (2004). Cells release prions in association with exosomes. *Proc. Natl. Acad. Sci. U.S.A.* 101, 9683–9688. doi: 10.1073/pnas.0308413101
- Fiandaca, M. S., Kapogiannis, D., Mapstone, M., Boxer, A., Eitan, E., Schwartz, J. B., et al. (2015). Identification of preclinical Alzheimer's disease by a profile of pathogenic proteins in neurally derived blood exosomes: a case-control study. *Alzheimers Dement.* 11, 600–607. doi: 10.1016/j.jalz.2014.06.008
- Fussi, N., Höllerhage, M., Chakraborty, T., Nykänen, N.-P., Rösler, T. W., Koeglspenger, T., et al. (2018). Exosomal secretion of  $\alpha$ -synuclein as protective mechanism after upstream blockage of macroautophagy. *Cell Death Dis.* 9:757. doi: 10.1038/s41419-018-0816-2
- Goetzl, E. J., Boxer, A., Schwartz, J. B., Abner, E. L., Petersen, R. C., Miller, B. L., et al. (2015). Altered lysosomal proteins in neural-derived plasma exosomes in preclinical Alzheimer disease. *Neurology* 85, 40–47. doi: 10.1212/WNL.0000000000001702
- Goetzl, E. J., Mustapic, M., Kapogiannis, D., Eitan, E., Lobach, I. V., Goetzl, L., et al. (2016). Cargo proteins of plasma astrocyte-derived exosomes in Alzheimer's disease. *FASEB J.* 30, 3853–3859. doi: 10.1096/fj.201600756R
- Goetzl, E. J., Schwartz, J. B., Abner, E. L., Jicha, G. A., and Kapogiannis, D. (2018). High complement levels in astrocyte-derived exosomes of Alzheimer disease. *Ann. Neurol.* 83, 544–552. doi: 10.1002/ana.25172

- Gomes, C., Keller, S., Altevogt, P., and Costa, J. (2007). Evidence for secretion of Cu,Zn superoxide dismutase via exosomes from a cell model of amyotrophic lateral sclerosis. *Neurosci. Lett.* 428, 43–46. doi: 10.1016/j.neulet.2007.09.024
- Goossens, J., Bjerke, M., Van Mossevelde, S., Van den Bossche, T., Goeman, J., De Vil, B., et al. (2018). Diagnostic value of cerebrospinal fluid tau, neurofilament, and progranulin in definite frontotemporal lobar degeneration. *Alzheimers Res. Ther.* 10:31. doi: 10.1186/s13195-018-0364-0
- Grad, L. I., Yerbury, J. J., Turner, B. J., Guest, W. C., Pokrishevsky, E., O'Neill, M. A., et al. (2014). Intercellular propagated misfolding of wild-type Cu/Zn superoxide dismutase occurs via exosome-dependent and -independent mechanisms. *Proc. Natl. Acad. Sci. U.S.A.* 111, 3620–3625. doi: 10.1073/pnas.1312245111
- Grey, M., Dunning, C. J., Gaspar, R., Grey, C., Brundin, P., Sparr, E., et al. (2015). Acceleration of  $\alpha$ -Synuclein Aggregation by Exosomes. *J. Biol. Chem.* 290, 2969–2982. doi: 10.1074/jbc.M114.585703
- Guescini, M., Genedani, S., Stocchi, V., and Agnati, L. F. (2010). Astrocytes and Glioblastoma cells release exosomes carrying mtDNA. *J. Neural Transm.* 117, 1–4. doi: 10.1007/s00702-009-0288-8
- Guix, F., Corbett, G., Cha, D., Mustapic, M., Liu, W., Mengel, D., et al. (2018). Detection of aggregation-competent tau in neuron-derived extracellular vesicles. *Int. J. Mol. Sci.* 19:E663. doi: 10.3390/ijms19030663
- Guo, B. B., Bellingham, S. A., and Hill, A. F. (2015). The neutral sphingomyelinase pathway regulates packaging of the prion protein into exosomes. *J. Biol. Chem.* 290, 3455–3467. doi: 10.1074/jbc.M114.605253
- Guo, B. B., Bellingham, S. A., and Hill, A. F. (2016). Stimulating the release of exosomes increases the intercellular transfer of prions. *J. Biol. Chem.* 291, 5128–5137. doi: 10.1074/jbc.M115.684258
- Han, Y., Jia, L., Zheng, Y., and Li, W. (2018). Salivary exosomes: emerging roles in systemic disease. *Int. J. Biol. Sci.* 14, 633–643. doi: 10.7150/ijbs.25018
- Hansen, C., Angot, E., Bergström, A.-L., Steiner, J. A., Pieri, L., Paul, G., et al. (2011).  $\alpha$ -Synuclein propagates from mouse brain to grafted dopaminergic neurons and seeds aggregation in cultured human cells. *J. Clin. Invest.* 121, 715–725. doi: 10.1172/JCI43366
- Hoshino, A., Costa-Silva, B., Shen, T. L., Rodrigues, G., Hashimoto, A., Tesic Mark, M., et al. (2015). Tumour exosome integrins determine organotropic metastasis. *Nature* 527, 329–335. doi: 10.1038/nature15756
- Hosokawa, M., Arai, T., Yamashita, M., Tsuji, H., Nonaka, T., Masuda-Suzukake, M., et al. (2014). Differential diagnosis of amyotrophic lateral sclerosis from Guillain-Barre syndrome by quantitative determination of TDP-43 in cerebrospinal fluid. *Int. J. Neurosci.* 124, 344–349. doi: 10.3109/00207454.2013.848440
- Iguchi, Y., Eid, L., Parent, M., Soucy, G., Bareil, C., Riku, Y., et al. (2016). Exosome secretion is a key pathway for clearance of pathological TDP-43. *Brain* 139, 3187–3201. doi: 10.1093/brain/aww237
- Ihara, Y., Morishima-Kawashima, M., and Nixon, R. (2012). The ubiquitin-proteasome system and the autophagic-lysosomal system in alzheimer disease. *Cold Spring Harb. Perspect. Med.* 2:a006361. doi: 10.1101/cshperspect.a006361
- Irwin, D. J., Trojanowski, J. Q., and Grossman, M. (2013). Cerebrospinal fluid biomarkers for differentiation of frontotemporal lobar degeneration from Alzheimer's disease. *Front. Aging Neurosci.* 5:6. doi: 10.3389/fnagi.2013.00006
- Jia, L., Qiu, Q., Zhang, H., Chu, L., Du, Y., Zhang, J., et al. (2019). Concordance between the assessment of A $\beta$ 42, T-tau, and P-T181-tau in peripheral blood neuronal-derived exosomes and cerebrospinal fluid. *Alzheimers Dement.* 15, 1071–1080. doi: 10.1016/j.jalz.2019.05.002
- Kasai, T., Tokuda, T., Ishigami, N., Sasayama, H., Foulds, P., Mitchell, D. J., et al. (2009). Increased TDP-43 protein in cerebrospinal fluid of patients with amyotrophic lateral sclerosis. *Acta Neuropathol.* 117, 55–62. doi: 10.1007/s00401-008-0456-1
- Kawakami, I., Arai, T., and Hasegawa, M. (2019). The basis of clinicopathological heterogeneity in TDP-43 proteinopathy. *Acta Neuropathol.* 138, 751–770. doi: 10.1007/s00401-019-02077-x
- Kordower, J. H., Chu, Y., Hauser, R. A., Freeman, T. B., and Olanow, C. W. (2008). Lewy body-like pathology in long-term embryonic nigral transplants in Parkinson's disease. *Nat. Med.* 14, 504–506. doi: 10.1038/nm1747
- Krämer-Albers, E.-M., Bretz, N., Tenzer, S., Winterstein, C., Möbius, W., Berger, H., et al. (2007). Oligodendrocytes secrete exosomes containing major myelin and stress-protective proteins: trophic support for axons? *Proteomics Clin. Appl.* 1, 1446–1461. doi: 10.1002/prca.200700522
- Lashley, T., Schott, J. M., Weston, P., Murray, C. E., Wellington, H., Keshavan, A., et al. (2018). Molecular biomarkers of Alzheimer's disease: progress and prospects. *Dis. Model. Mech.* 11:dm031781. doi: 10.1242/dmm.031781
- Laulagnier, K., Javale, C., Hemming, F. J., Chivet, M., Lachenal, G., Blot, B., et al. (2018). Amyloid precursor protein products concentrate in a subset of exosomes specifically endocytosed by neurons. *Cell. Mol. Life Sci.* 75, 757–773. doi: 10.1007/s00018-017-2664-0
- Lee, H.-J. (2005). Intravesicular localization and exocytosis of  $\alpha$ -synuclein and its aggregates. *J. Neurosci.* 25, 6016–6024. doi: 10.1523/JNEUROSCI.0692-05.2005
- Lee, Y., Morrison, B. M., Li, Y., Lengacher, S., Farah, M. H., Hoffman, P. N., et al. (2012). Oligodendroglia metabolically support axons and contribute to neurodegeneration. *Nature* 487, 443–448. doi: 10.1038/nature11314
- Lehnert, S., Costa, J., de Carvalho, M., Kirby, J., Kuzma-Kozakiewicz, M., Morelli, C., et al. (2014). Multicentre quality control evaluation of different biomarker candidates for amyotrophic lateral sclerosis. *Amyotroph. Lateral Scler. Frontotemp. Degener.* 15, 344–350. doi: 10.3109/21678421.2014.884592
- Li, J.-Y., Englund, E., Holton, J. L., Soulet, D., Hagell, P., Lees, A. J., et al. (2008). Lewy bodies in grafted neurons in subjects with Parkinson's disease suggest host-to-graft disease propagation. *Nat. Med.* 14, 501–503. doi: 10.1038/nm1746
- Li, P., Kaslan, M., Lee, S. H., Yao, J., and Gao, Z. (2017). Progress in exosome isolation techniques. *Theranostics* 7, 789–804. doi: 10.7150/thno.18133
- Liu, L., Drouet, V., Wu, J. W., Witter, M. P., Small, S. A., Clelland, C., et al. (2012). Trans-Synaptic spread of tau pathology *in vivo*. *PLoS ONE* 7:e31302. doi: 10.1371/journal.pone.0031302
- Llorens, F., Barrio, T., Correia, A., Villar-Pique, A., Thune, K., Lange, P., et al. (2018). cerebrospinal fluid prion disease biomarkers in pre-clinical and clinical naturally occurring scrapie. *Mol. Neurobiol.* 55, 8586–8591. doi: 10.1007/s12035-018-1014-z
- Lööv, C., Scherzer, C. R., Hyman, B. T., Breakefield, X. O., and Ingelsson, M. (2016).  $\alpha$ -synuclein in extracellular vesicles: functional implications and diagnostic opportunities. *Cell. Mol. Neurobiol.* 36, 437–448. doi: 10.1007/s10571-015-0317-0
- Lötvall, J., Hill, A. F., Hochberg, F., Buzas, E. I., Di Vizio, D., Gardiner, C., et al. (2014). Minimal experimental requirements for definition of extracellular vesicles and their functions: a position statement from the international society for extracellular vesicles. *J. Extracell. Vesicles.* 3:26913. doi: 10.3402/jev.v3.26913
- Lu, C.-H., Macdonald-Wallis, C., Gray, E., Pearce, N., Petzold, A., Norgren, N., et al. (2015). Neurofilament light chain: a prognostic biomarker in amyotrophic lateral sclerosis. *Neurology* 84, 2247–2257. doi: 10.1212/WNL.0000000000001642
- Luan, X., Sansanaphongpricha, K., Myers, I., Chen, H., Yuan, H., and Sun, D. (2017). Engineering exosomes as refined biological nanoplateforms for drug delivery. *Acta Pharmacol. Sin.* 38, 754–763. doi: 10.1038/aps.2017.12
- Luarte, A., Cisternas, P., Caviedes, A., Batiz, L. F., Lafourcade, C., Wyneken, U., et al. (2017). Astrocytes at the hub of the stress response: potential modulation of neurogenesis by miRNAs in astrocyte-derived exosomes. *Stem Cells Int.* 2017:1719050. doi: 10.1155/2017/1719050
- Mathieu, M., Martin-Jaular, L., Lavieu, G., and Thery, C. (2019). Specificities of secretion and uptake of exosomes and other extracellular vesicles for cell-to-cell communication. *Nat. Cell Biol.* 21, 9–17. doi: 10.1038/s41556-018-0250-9
- Mehta, S. H., and Adler, C. H. (2016). Advances in biomarker research in Parkinson's Disease. *Curr. Neurol. Neurosci. Rep.* 16:7. doi: 10.1007/s11910-015-0607-4
- Michael, A., Bajracharya, S., Yuen, P., Zhou, H., Star, R., Illei, G., et al. (2010). Exosomes from human saliva as a source of microRNA biomarkers: microRNA biomarkers in salivary exosomes. *Oral Dis.* 16, 34–38. doi: 10.1111/j.1601-0825.2009.01604.x
- Miranda, A. M., and Di Paolo, G. (2018). Endolysosomal dysfunction and exosome secretion: implications for neurodegenerative disorders. *Cell Stress* 2, 115–118. doi: 10.15698/cst2018.05.136
- Miyaniishi, M., Tada, K., Koike, M., Uchiyama, Y., Kitamura, T., and Nagata, S. (2007). Identification of Tim4 as a phosphatidylserine receptor. *Nature* 450, 435–439. doi: 10.1038/nature06307
- Montecalvo, A., Larregina, A. T., Shufesky, W. J., Beer Stolz, D., Sullivan, M. L. G., Karlsson, J. M., et al. (2012). Mechanism of transfer of functional



- microRNAs between mouse dendritic cells via exosomes. *Blood* 119, 756–766. doi: 10.1182/blood-2011-02-338004
- Münch, C., O'Brien, J., and Bertolotti, A. (2011). Prion-like propagation of mutant superoxide dismutase-1 misfolding in neuronal cells. *Proc. Natl. Acad. Sci. U.S.A.* 108, 3548–3553. doi: 10.1073/pnas.1017275108
- Mustapic, M., Eitan, E., Werner, J. K. Jr., Berkowitz, S. T., Lazaropoulos, M. P., Tran, J., et al. (2017). Plasma extracellular vesicles enriched for neuronal Origin: a potential window into brain pathologic processes. *Front. Neurosci.* 11:278. doi: 10.3389/fnins.2017.00278
- Neumann, M., Sampathu, D. M., Kwong, L. K., Truax, A. C., Micsenyi, M. C., Chou, T. T., et al. (2006). Ubiquitinated TDP-43 in Frontotemporal lobar degeneration and amyotrophic lateral sclerosis. *Science* 314, 130–133. doi: 10.1126/science.1134108
- Nonaka, T., Masuda-Suzukake, M., Arai, T., Hasegawa, Y., Akatsu, H., Obi, T., et al. (2013). Prion-like properties of pathological TDP-43 aggregates from diseased brains. *Cell Rep.* 4, 124–134. doi: 10.1016/j.celrep.2013.06.007
- Noto, Y., Shibuya, K., Sato, Y., Kanai, K., Misawa, S., Sawai, S., et al. (2011). Elevated CSF TDP-43 levels in amyotrophic lateral sclerosis: specificity, sensitivity, and a possible prognostic value. *Amyotroph. Lateral Scler.* 12, 140–143. doi: 10.3109/17482968.2010.541263
- Oeckl, P., Järdel, C., Salachas, F., Lamari, F., Andersen, P. M., Bowser, R., et al. (2016). Multicenter validation of CSF neurofilaments as diagnostic biomarkers for ALS. *Amyotroph. Lateral Scler. Frontotemp. Degener.* 17, 404–413. doi: 10.3109/21678421.2016.1167913
- Ogawa, Y., Kanai-Azuma, M., Akimoto, Y., Kawakami, H., and Yanoshita, R. (2008). Exosome-like vesicles with dipeptidyl peptidase IV in human saliva. *Biol. Pharm. Bull.* 31, 1059–1062. doi: 10.1248/bpb.31.1059
- Olney, N. T., Spina, S., and Miller, B. L. (2017). Frontotemporal dementia. *Neurol. Clin.* 35, 339–374. doi: 10.1016/j.ncl.2017.01.008
- Olsson, B., Portelius, E., Cullen, N. C., Sandelius, A., Zetterberg, H., Andreasson, U., et al. (2019). Association of cerebrospinal fluid neurofilament light protein levels with cognition in patients with dementia, motor neuron disease, and movement disorders. *JAMA Neurol.* 76, 318–325. doi: 10.1001/jamaneurol.2018.3746
- Ostrowski, M., Carmo, N. B., Krumeich, S., Fanget, I., Raposo, G., Savina, A., et al. (2010). Rab27a and Rab27b control different steps of the exosome secretion pathway. *Nat. Cell Biol.* 12, 19–30. doi: 10.1038/ncb2000
- Otto, M., Wiltfang, J., Tümani, H., Zerr, I., Lantsch, M., Kornhuber, J., et al. (1997). Elevated levels of tau-protein in cerebrospinal fluid of patients with creutzfeldt-jakob disease. *Neurosci. Lett.* 225, 210–212. doi: 10.1016/S0304-3940(97)00215-2
- Pan, B. T. (1985). Electron microscopic evidence for externalization of the transferrin receptor in vesicular form in sheep reticulocytes. *J. Cell Biol.* 101, 942–948. doi: 10.1083/jcb.101.3.942
- Pan, I., Roitenberg, N., and Cohen, E. (2018). Vesicle-mediated secretion of misfolded prion protein molecules from cyclosporin A-treated cells. *FASEB J.* 32, 1479–1492. doi: 10.1096/fj.201700598RRR
- Paulaitis, M., Agarwal, K., and Nana-Sinkam, P. (2018). Dynamic scaling of exosome sizes. *Langmuir* 34, 9387–9393. doi: 10.1021/acs.langmuir.7b04080
- Perez-Hernandez, D., Gutiérrez-Vázquez, C., Jorge, I., López-Martín, S., Ursa, A., Sánchez-Madrid, F., et al. (2013). The intracellular interactome of tetraspanin-enriched microdomains reveals their function as sorting machineries toward exosomes. *J. Biol. Chem.* 288, 11649–11661. doi: 10.1074/jbc.M112.445304
- Pickles, S., Semmler, S., Broom, H. R., Destroismaisons, L., Legroux, L., Arbour, N., et al. (2016). ALS-linked misfolded SOD1 species have divergent impacts on mitochondria. *Acta Neuropathol. Commun.* 4:43. doi: 10.1186/s40478-016-0313-8
- Pisitkun, T., Shen, R.-F., and Knepper, M. A. (2004). Identification and proteomic profiling of exosomes in human urine. *Proc. Natl. Acad. Sci. U.S.A.* 101, 13368–13373. doi: 10.1073/pnas.0403453101
- Polanco, J. C., Scicluna, B. J., Hill, A. F., and Götz, J. (2016). Extracellular vesicles isolated from the brains of rTg4510 mice seed tau protein aggregation in a threshold-dependent manner. *J. Biol. Chem.* 291, 12445–12466. doi: 10.1074/jbc.M115.709485
- Potolichio, I., Carven, G. J., Xu, X., Stipp, C., Riese, R. J., Stern, L. J., et al. (2005). Proteomic analysis of Microglia-Derived exosomes: metabolic role of the aminopeptidase CD13 in neuropeptide catabolism. *J. Immunol.* 175, 2237–2243. doi: 10.4049/jimmunol.175.4.2237
- Preisiche, O., Schultz, S. A., Apel, A., Kuhle, J., Kaeser, S. A., Barro, C., et al. (2019). Serum neurofilament dynamics predicts neurodegeneration and clinical progression in presymptomatic Alzheimer's disease. *Nat. Med.* 25, 277–283. doi: 10.1038/s41591-018-0304-3
- Prusiner, S. B. (1982). Novel proteinaceous infectious particles cause scrapie. *Science* 216, 136–144. doi: 10.1126/science.6801762
- Prusiner, S. B. (1991). Molecular biology of prion diseases. *Science* 252, 1515–1522. doi: 10.1126/science.1675487
- Rajendran, L., Honsho, M., Zahn, T. R., Keller, P., Geiger, K. D., Verkade, P., et al. (2006). Alzheimer's disease  $\beta$ -amyloid peptides are released in association with exosomes. *Proc. Natl. Acad. Sci. U.S.A.* 103, 11172–11177. doi: 10.1073/pnas.0603838103
- Rani, K., Mukherjee, R., Singh, E., Kumar, S., Sharma, V., Vishwakarma, P., et al. (2019). Neuronal exosomes in saliva of Parkinson's disease patients: a pilot study. *Parkinsonism Relat. Disord.* 67, 21–23. doi: 10.1016/j.parkreldis.2019.09.008
- Raposo, G., and Stoorvogel, W. (2013). Extracellular vesicles: Exosomes, microvesicles, and friends. *J. Cell Biol.* 200, 373–383. doi: 10.1083/jcb.201211138
- Rashed, H. M., Bayraktar, E. K., Helal, G., Abd-Ellah, M., Amero, P., et al. (2017). Exosomes: from garbage bins to promising therapeutic targets. *Int. J. Mol. Sci.* 18:E538. doi: 10.3390/ijms18030538
- Saman, S., Kim, W., Raya, M., Visnick, Y., Miro, S., Saman, S., et al. (2012). Exosome-associated tau is secreted in tauopathy models and is selectively phosphorylated in cerebrospinal fluid in early Alzheimer disease. *J. Biol. Chem.* 287, 3842–3849. doi: 10.1074/jbc.M111.277061
- Sardar Sinha, M., Ansell-Schultz, A., Civitelli, L., Hildesjö, C., Larsson, M., Lannfelt, L., et al. (2018). Alzheimer's disease pathology propagation by exosomes containing toxic amyloid-beta oligomers. *Acta Neuropathol.* 136, 41–56. doi: 10.1007/s00401-018-1868-1
- Savina, A., Furlan, M., Vidal, M., and Colombo, M. I. (2003). Exosome release is regulated by a calcium-dependent mechanism in K562 cells. *J. Biol. Chem.* 278, 20083–20090. doi: 10.1074/jbc.M301642200
- Shi, M., Kovac, A., Korff, A., Cook, T. J., Ginghina, C., Bullock, K. M., et al. (2016). CNS tau efflux via exosomes is likely increased in Parkinson's disease but not in Alzheimer's disease. *Alzheimers Dement.* 12, 1125–1131. doi: 10.1016/j.jalz.2016.04.003
- Shi, M., Liu, C., Cook, T. J., Bullock, K. M., Zhao, Y., Ginghina, C., et al. (2014). Plasma exosomal  $\alpha$ -synuclein is likely CNS-derived and increased in Parkinson's disease. *Acta Neuropathol.* 128, 639–650. doi: 10.1007/s00401-014-1314-y
- Shi, M., Sheng, L., Stewart, T., Zabetian, C. P., and Zhang, J. (2019). New windows into the brain: central nervous system-derived extracellular vesicles in blood. *Prog. Neurobiol.* 175, 96–106. doi: 10.1016/j.pneurobio.2019.01.005
- Soares Martins, T., Catita, J., Martins Rosa, I. A. B., da Cruz e Silva, O., and Henriques, A. G. (2018). Exosome isolation from distinct biofluids using precipitation and column-based approaches. *PLoS ONE* 13:e0198820. doi: 10.1371/journal.pone.0198820
- Spillantini, M. G., Crowther, R. A., Jakes, R., Cairns, N. J., Lantos, P. L., and Goedert, M. (1998). Filamentous  $\alpha$ -synuclein inclusions link multiple system atrophy with Parkinson's disease and dementia with Lewy bodies. *Neurosci. Lett.* 251, 205–208. doi: 10.1016/S0304-3940(98)00504-7
- Stoorvogel, W., Kleijmeer, M. J., Geuze, H. J., and Raposo, G. (2002). The biogenesis and functions of exosomes. *Traffic* 3, 321–330. doi: 10.1034/j.1600-0854.2002.30502.x
- Stuendl, A., Kunadt, M., Kruse, N., Bartels, C., Moebius, W., Danzer, K. M., et al. (2016). Induction of  $\alpha$ -synuclein aggregate formation by CSF exosomes from patients with Parkinson's disease and dementia with lewy bodies. *Brain* 139, 481–494. doi: 10.1093/brain/awv346
- Tapiola, T., Alafuzoff, I., Herukka, S.-K., Parkkinen, L., Hartikainen, P., Soininen, H., et al. (2009). Cerebrospinal fluid  $\beta$ -amyloid 42 and tau proteins as biomarkers of alzheimer-type pathologic changes in the brain. *Arch. Neurol.* 66, 382–389. doi: 10.1001/archneurol.2008.596
- Théry, C., Amigorena, S., Raposo, G., and Clayton, A. (2006). Isolation and characterization of exosomes from cell culture supernatants and biological fluids. *Curr. Protoc. Cell Biol.* 30:3.22. doi: 10.1002/0471143030.cb0322s30
- Théry, C., Zitvogel, L., and Amigorena, S. (2002). Exosomes: composition, biogenesis and function. *Nat. Rev. Immunol.* 2, 569–579. doi: 10.1038/nri855

- Thompson, A. G., Gray, E., Heman-Ackah, S. M., Mäger, I., Talbot, K., Andaloussi, S. E., et al. (2016). Extracellular vesicles in neurodegenerative disease - pathogenesis to biomarkers. *Nat. Rev. Immunol.* 12, 346–357. doi: 10.1038/nrneurol.2016.68
- Turner, M. R., Al-Chalabi, A., Chio, A., Hardiman, O., Kiernan, M. C., Rohrer, J. D., et al. (2017). Genetic screening in sporadic ALS and FTD. *J. Neurol. Neurosurg. Psychiatr.* 88, 1042–1044. doi: 10.1136/jnnp-2017-315995
- Urbanelli, L., Magini, A., Buratta, S., Brozzi, A., Sagini, K., Polchi, A., et al. (2013). Signaling pathways in exosomes biogenesis, secretion and fate. *Genes* 4, 152–170. doi: 10.3390/genes4020152
- Valadi, H., Ekström, K., Bossios, A., Sjöstrand, M., Lee, J. J., and Lötvall, J. O. (2007). Exosome-mediated transfer of mRNAs and microRNAs is a novel mechanism of genetic exchange between cells. *Nat. Cell Biol.* 9, 654–659. doi: 10.1038/ncb1596
- van Niel, G., Charrin, S., Simoes, S., Romao, M., Rochin, L., Saftig, P., et al. (2011). The tetraspanin CD63 regulates ESCRT-Independent and -dependent endosomal sorting during melanogenesis. *Dev. Cell* 21, 708–721. doi: 10.1016/j.devcel.2011.08.019
- Veith, N. M., Plattner, H., Stuermer, C. A. O., Schulz-Schaeffer, W. J., and Bürkle, A. (2009). Immunolocalisation of PrPSc in scrapie-infected N2a mouse neuroblastoma cells by light and electron microscopy. *Eur. J. Cell Biol.* 88, 45–63. doi: 10.1016/j.ejcb.2008.08.001
- Vella, L., Hill, A., and Cheng, L. (2016). Focus on extracellular vesicles: exosomes and their role in protein trafficking and biomarker potential in Alzheimer's and Parkinson's Disease. *Int. J. Mol. Sci.* 17:173. doi: 10.3390/ijms17020173
- Vella, L., Sharples, R., Lawson, V., Masters, C., Cappai, R., and Hill, A. (2007). Packaging of prions into exosomes is associated with a novel pathway of PrP processing. *J. Pathol.* 211, 582–590. doi: 10.1002/path.2145
- Vella, L. J., Greenwood, D. L. V., Cappai, R., Scheerlinck, J.-P. Y., and Hill, A. F. (2008). Enrichment of prion protein in exosomes derived from ovine cerebral spinal fluid. *Vet. Immunol. Immunopathol.* 124, 385–393. doi: 10.1016/j.vetimm.2008.04.002
- Vingtdeux, V., Sergeant, N., and Buée, L. (2012). Potential contribution of exosomes to the prion-like propagation of lesions in Alzheimer's disease. *Front. Physiol.* 3:229. doi: 10.3389/fphys.2012.00229
- Wang, H., Atik, A., Stewart, T., Ghingina, C., Aro, P., Kerr, K. F., et al. (2018). Plasma  $\alpha$ -synuclein and cognitive impairment in the Parkinson's associated risk syndrome: a pilot study. *Neurobiol. Dis.* 116, 53–59. doi: 10.1016/j.nbd.2018.04.015
- Winston, C. N., Goetzl, E. J., Akers, J. C., Carter, B. S., Rockenstein, E. M., Galasko, D., et al. (2016). Prediction of conversion from mild cognitive impairment to dementia with neuronally derived blood exosome protein profile. *Alzheimers Dement.* 3, 63–72. doi: 10.1016/j.dadm.2016.04.001
- Winston, C. N., Romero, H. K., Ellisman, M., Naus, S., Julovich, D. A., Conger, T., et al. (2019). Assessing neuronal and astrocyte derived exosomes from individuals with mild traumatic brain injury for markers of neurodegeneration and cytotoxic activity. *Front. Neurosci.* 13:1005. doi: 10.3389/fnins.2019.01005
- Xia, Y., Zhang, G., Han, C., Ma, K., Guo, X., Wan, F., et al. (2019). Microglia as modulators of exosomal  $\alpha$ -synuclein transmission. *Cell Death Dis.* 10:174. doi: 10.1038/s41419-019-1404-9
- Yan, Z., Dutta, S., Liu, Z., Yu, X., Mesgarzadeh, N., Ji, F., et al. (2019). A Label-Free Platform for identification of exosomes from different sources. *ACS Sensors* 4, 488–497. doi: 10.1021/acssensors.8b01564
- Yoo, Y. K., Lee, J., Kim, H., Hwang, K. S., Yoon, D. S., and Lee, J. H. (2018). Toward Exosome-Based neuronal diagnostic devices. *Micromachines* 9:E634. doi: 10.3390/mi9120634
- Yuyama, K., Sun, H., Mitsutake, S., and Igarashi, Y. (2012). Sphingolipid-modulated exosome secretion promotes clearance of amyloid- $\beta$  by microglia. *J. Biol. Chem.* 287, 10977–10989. doi: 10.1074/jbc.M111.324616
- Yuyama, K., Yamamoto, N., and Yanagisawa, K. (2008). Accelerated release of exosome-associated GM1 ganglioside (GM1) by endocytic pathway abnormality: another putative pathway for GM1-induced amyloid fibril formation. *J. Neurochem.* 105, 217–224. doi: 10.1111/j.1471-4159.2007.05128.x
- Zhang, P., Zhou, X., He, M., Shang, Y., Tetlow, A. L., Godwin, A. K., et al. (2019). Ultrasensitive detection of circulating exosomes with a 3D-nanopatterned microfluidic chip. *Nat. Biomed. Eng.* 3, 438–451. doi: 10.1038/s41551-019-0356-9
- Zhao, Z.-H., Chen, Z.-T., Zhou, R.-L., Zhang, X., Ye, Q.-Y., and Wang, Y.-Z. (2019). Increased DJ-1 and  $\alpha$ -synuclein in plasma neural-derived exosomes as potential markers for Parkinson's disease. *Front. Aging Neurosci.* 10:438. doi: 10.3389/fnagi.2018.00438
- Zheng, T., Pu, J., Chen, Y., Mao, Y., Guo, Z., Pan, H., et al. (2017). Plasma exosomes spread and cluster around  $\beta$ -Amyloid plaques in an animal model of Alzheimer's disease. *Front. Aging Neurosci.* 9:12. doi: 10.3389/fnagi.2017.00012

**Conflict of Interest:** The authors declare that the research was conducted in the absence of any commercial or financial relationships that could be construed as a potential conflict of interest.

Copyright © 2020 Hornung, Dutta and Bitan. This is an open-access article distributed under the terms of the Creative Commons Attribution License (CC BY). The use, distribution or reproduction in other forums is permitted, provided the original author(s) and the copyright owner(s) are credited and that the original publication in this journal is cited, in accordance with accepted academic practice. No use, distribution or reproduction is permitted which does not comply with these terms.



# Islet Amyloid Polypeptide: A Partner in Crime With A $\beta$ in the Pathology of Alzheimer's Disease

Ana F. Raimundo<sup>1,2,3†</sup>, Sofia Ferreira<sup>1,2†</sup>, Ivo C. Martins<sup>4\*</sup> and Regina Menezes<sup>1,2,3\*</sup>

<sup>1</sup> iBET - Instituto de Biologia Experimental e Tecnológica, Oeiras, Portugal, <sup>2</sup> CEDOC - Chronic Diseases Research Center, Faculdade de Ciências Médicas, Universidade Nova de Lisboa, Lisbon, Portugal, <sup>3</sup> ITQB-NOVA, Instituto de Tecnologia Química e Biológica António Xavier, Universidade Nova de Lisboa, Oeiras, Portugal, <sup>4</sup> Instituto de Medicina Molecular, Faculdade de Medicina, Universidade de Lisboa, Lisbon, Portugal

## OPEN ACCESS

### Edited by:

Maria Rosário Almeida,  
University of Porto, Portugal

### Reviewed by:

Fernando Peña-Ortega,  
National Autonomous University of  
Mexico, Mexico  
Cong Liu,  
University of Chinese Academy of  
Sciences, China

### \*Correspondence:

Ivo C. Martins  
ivomartins@medicina.ulisboa.pt  
Regina Menezes  
rmenezes@ibet.pt;  
regina.menezes@nms.unl.pt

<sup>†</sup>These authors have contributed  
equally to this work

**Received:** 21 November 2019

**Accepted:** 20 February 2020

**Published:** 20 March 2020

### Citation:

Raimundo AF, Ferreira S, Martins IC  
and Menezes R (2020) Islet Amyloid  
Polypeptide: A Partner in Crime With  
A $\beta$  in the Pathology of Alzheimer's  
Disease. *Front. Mol. Neurosci.* 13:35.  
doi: 10.3389/fnmol.2020.00035

Diabetes affects hundreds of millions of patients worldwide. Despite the advances in understanding the disease and therapeutic options, it remains a leading cause of death and of comorbidities globally. Islet amyloid polypeptide (IAPP), or amylin, is a hormone produced by pancreatic  $\beta$ -cells. It contributes to the maintenance of glucose physiological levels namely by inhibiting insulin and glucagon secretion as well as controlling adiposity and satiation. IAPP is a highly amyloidogenic polypeptide forming intracellular aggregates and amyloid structures that are associated with  $\beta$ -cell death. Data also suggest the relevance of unprocessed IAPP forms as seeding for amyloid buildup. Besides the known consequences of hyperamylinemia in the pancreas, evidence has also pointed out that IAPP has a pathological role in cognitive function. More specifically, IAPP was shown to impair the blood–brain barrier; it was also seen to interact and co-deposit with amyloid beta peptide (A $\beta$ ), and possibly with Tau, within the brain of Alzheimer's disease (AD) patients, thereby contributing to diabetes-associated dementia. In fact, it has been suggested that AD results from a metabolic dysfunction in the brain, leading to its proposed designation as type 3 diabetes. Here, we have first provided a brief perspective on the IAPP amyloidogenic process and its role in diabetes and AD. We have then discussed the potential interventions for modulating IAPP proteotoxicity that can be explored for therapeutics. Finally, we have proposed the concept of a “diabetes brain phenotype” hypothesis in AD, which may help design future IAPP-centered drug development strategies against AD.

**Keywords:** A $\beta$ -42, Alzheimer's disease, amylin, diabetes, IAPP, protein aggregation

## INTRODUCTION

Amyloidogenesis is a process by which peptides spontaneously self-assemble into higher order structures, namely oligomers, protofibrils, and mature amyloid fibrils (Martins et al., 2008; Maurer-Stroh et al., 2010; Hauser et al., 2014). These mature amyloid fibrils are highly ordered structures with fibrillar aggregates derived from different amyloidogenic amino acid sequences that share common features (Maurer-Stroh et al., 2010). The current consensus is that the amyloid fibrils are not the main cause of toxicity (Martins et al., 2008; Kuperstein et al., 2010; Hauser et al., 2014). This seems to be mostly down to precursor oligomers and protofibrils, which are associated with a number of the so-called amyloid diseases, including type 2 diabetes mellitus (T2DM), Alzheimer's

disease (AD), Parkinson's disease, and cataracts (Hauser et al., 2014; Cremades and Dobson, 2018).

T2DM, the most prevalent type of diabetes, is an islet amyloid polypeptide (IAPP)-associated pathology (Cukierman et al., 2005; Westermark et al., 2011; Yang and Song, 2013). Dementia also represents a major public concern, affecting 50 million people worldwide. AD, the most common form of dementia in North America (Alzheimer's Association, 2016; Bondi et al., 2017; Lane et al., 2018), is associated with amyloid beta peptide 42 (A $\beta$ -42) (Martins et al., 2008; Kuperstein et al., 2010). The amyloid hypothesis on AD pathology is, however, called into question by the undeniable role of Tau aggregation and other important players, as has been reviewed (Makin, 2018).

There is much evidence to support the close association between T2DM and AD. IAPP (also known as amylin) and A $\beta$ -42 were proven to co-deposit, contributing to AD onset and progression (Jackson et al., 2013; Wijesekara et al., 2017). In addition, it the molecular interaction between Tau and IAPP was recently proved (Arya et al., 2019). At last, AD is associated with insulin resistance and an imbalance of glucose levels in the brain (Cukierman et al., 2005; Yang and Song, 2013), earning the designation of type 3 diabetes (T3DM) (de la Monte, 2014; Kandimalla et al., 2017; Leszek et al., 2017). Given these links, we have reviewed the mechanisms of IAPP dysfunction in diabetes and dementia, particularly in AD, thus adding to the recent view of multi-factorial contributions to both diseases. Furthermore, we have also discussed the potential interventions for modulating IAPP proteotoxicity that can be explored for therapeutics, encouraging new venues for treatment.

## IAPP AND DIABETES

Diabetes mellitus (DM) is one of the major causes of premature illness and mortality worldwide (Federation, 2009). High blood glucose levels and glucose intolerance, as a consequence of a defective insulin production/secretion by pancreatic  $\beta$  cells ( $\beta$ -cells) or insulin sensitivity (Stumvoll et al., 2005; Tan et al., 2019), are the typical clinical features of the disease. In T2DM, impairment and loss of  $\beta$ -cell mass has been associated with diverse pathological phenomena, including glucolipotoxicity, islet cholesterol accumulation, and islet inflammation (Poitout and Robertson, 2002; Ishikawa et al., 2008; Brunham et al., 2010; Donath and Shoelson, 2011). Equally important are the current views that regard IAPP dyshomeostasis, intracellular accumulation of IAPP oligomers, and IAPP amyloid deposition in the islets of Langerhans as detrimental events in  $\beta$ -cell dysfunction and disease (Kanatsuka et al., 2018).

IAPP is a 37-amino acid neuroendocrine hormone that plays an important role in regulating metabolism and glucose homeostasis (Figure 1A). In circulation, IAPP and insulin act as synergistic partners: they stimulate the uptake of blood glucose into muscle and fat tissues and inhibit the endogenous glucose output from the liver, thus stabilizing the blood sugar levels in post-meal conditions (Zhang et al., 2016). Physiologically, IAPP also reduces the secretion of nutrient-stimulated glucagon, regulates gastric emptying and satiation (Lutz, 2010; Akter et al.,

2016), and regulates blood pressure while having an effect on the renin-angiotensin system (Wookey et al., 1998).

IAPP and insulin are co-secreted and processed by proprotein convertase (PC) 1/3, PC 2, and carboxypeptidase E (Yonemoto et al., 2008). During its biogenesis, IAPP is synthesized as an 89-residue preprohormone (Sanke et al., 1988). Its signal peptide is cleaved throughout the transport into the endoplasmic reticulum (ER) to form proIAPP (Akter et al., 2016), which is then processed in the late Golgi complex. To yield the mature active form of the hormone, IAPP suffers amidation of the C-terminal end, and a disulphide bond is formed between cysteines at positions two and seven (Westermark et al., 2011; Akter et al., 2016; Bower and Hay, 2016). Once produced, mature IAPP is co-packaged with insulin in secretory granules of  $\beta$ -cells to then be co-released in response to glucose (Kahn et al., 1993; Gedulin et al., 1997; Zhang et al., 2016). In a pre-diabetes/diabetes phenotypes, the increased production of insulin is accompanied by augmented IAPP levels (Kahn et al., 1991; Mulder et al., 1996). The overload and impairment of  $\beta$ -cell processing machinery leads to the accumulation of unprocessed IAPP forms (Westermark et al., 2000; Paulsson et al., 2006). These events, together with the overwhelming of the ER, generate a feed-forward cycle that promotes IAPP oligomerization, fibril formation, and  $\beta$ -cell injury. Elevated proIAPP levels and amyloid deposition in  $\beta$ -cells lacking PC1/3 and PC2 (Marzban et al., 2006), as well as the presence of proIAPP in intracellular fibrils (Paulsson et al., 2006), corroborate this idea. Despite this, the role of unprocessed IAPP forms in the disease is not fully understood.

Under pathological conditions, increased IAPP expression and the generation of aberrant IAPP intermediates favor misfolding, which leads to the formation of toxic aggregates through a seeding-nucleation model, similar to prion replication (Mukherjee et al., 2017). As misfolded molecules accumulate, they build up into intracellular oligomers and larger amyloid fibrils, which deposit in surrounding tissues, thus disrupting the normal islet architecture and functioning (Zhang et al., 2016). Deposits of aggregated IAPP are present in the pancreas of about 90% of T2DM patients, thus representing a histopathological hallmark of the disease (Westermark and Grimelius, 1973; Mukherjee et al., 2017). Corroborating the toxicity of these aggregates in diabetes, the IAPP allele S20G, which raises IAPP aggregation propensity (Sakagashira et al., 2000), has been associated with premature onset diabetes and has accelerated the decline of endogenous insulin secretion when compared to non-S20G T2DM individuals (Morita et al., 2011). Moreover, a transgenic mice model expressing human IAPP (hIAPP) spontaneously developed amyloidosis, showing impaired insulin production,  $\beta$ -cell loss, and fasting hyperglycemia (Janson et al., 1996).

Although the link between IAPP aggregation and  $\beta$ -cell loss seems to be convincing, there are some questions that remain poorly understood, including (a) the initiation site and triggers of amyloid formation, (b) the mechanisms of IAPP-mediated toxicity in  $\beta$ -cell death, and (c) the nature of toxic IAPP species (Kanatsuka et al., 2018). Initially, mature amyloid fibrils were presumed to be the pathological structures (Lorenzo and



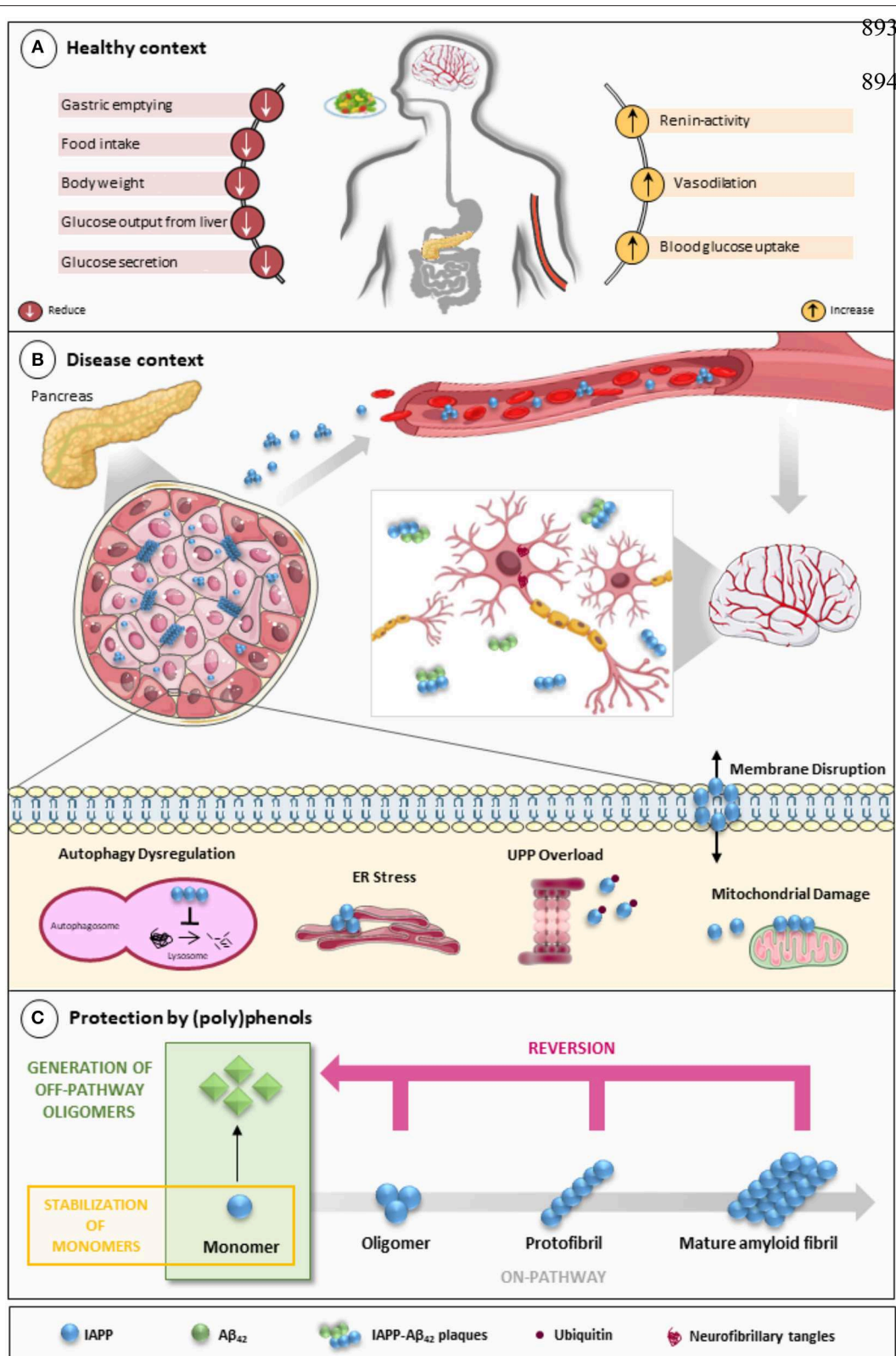


**FIGURE 1 |** IAPP on physiological and pathological contexts and (poly)phenols-mediated protection. **(A)** In healthy conditions, IAPP is co-secreted with insulin to regulate glucose metabolism and homeostasis in a post-meal condition. Several functions are attributed to IAPP: slowing down gastric emptying, thereby reducing food intake and body weight; reducing glucose output from liver and glucagon secretion; and stimulating the renin-angiotensin system, vasodilation, and

(Continued)

**FIGURE 1 |** blood glucose uptake. **(B)** In disease conditions, IAPP pathological species deposit in the pancreas and in brain microvasculature where they induce the injury of small vessels and reach the brain parenchyma. In the brain environment, IAPP forms heterogeneous deposits with A $\beta$  molecules increasing neurotoxicity. Proteostasis imbalance caused by A $\beta$ /IAPP and tau may promote a set of molecular changes that culminate in glucose homeostasis dysregulation, cell death, and neurodegeneration. The molecular pathways of  $\beta$ -cell dysfunction are depicted: autophagy dysregulation; ER stress; UPP overload; membrane instability; and mitochondrial damage. **(C)** Protection mediated by (poly)phenols is associated with the stabilization of IAPP monomers, the remodeling of amyloids, protofibrils, and toxic oligomers to non-fibrillogenic “off-pathway” oligomers and monomers. A $\beta$ , Amyloid beta; ER, Endoplasmic Reticulum; IAPP, Islet Amyloid Polypeptide; Ub, Ubiquitin; UPP, Ubiquitin Proteasome Pathway.

Yankner, 1996), however, the current consensus is that toxicity is mostly associated with soluble oligomers and protofibrils, which may act as the trigger agents for  $\beta$ -cell depletion and diabetes onset (Haataja et al., 2008; Zhao et al., 2009; Zhang et al., 2016).

Oligomeric IAPP species form ion-leaking pores in the cell membranes (Gurlo et al., 2010; Li et al., 2016b), leading to enhanced membrane fluidity, calcium dysregulation, and decreased cell viability (Huang et al., 2010). IAPP oligomers have also been found within disturbed mitochondrial membranes in transgenic hIAPP mice and T2DM patients (Gurlo et al., 2010). Unstable mitochondrial membrane potential induced by toxic oligomers is thought to be involved in the overproduction of reactive oxygen species (ROS), which are currently considered to be potential initiators of IAPP toxicity (Konarkowska et al., 2005). ER stress and impairment of proteasome function have also been associated with hIAPP-induced toxicity (Casas et al., 2007; Gurlo et al., 2010), however, in studies with cultured islets producing IAPP at more physiological levels, ER stress was not detected (Hull et al., 2009).

In heterozygous *hIAPP*<sup>+</sup> mice with  $\beta$  cell-specific *Atg7* deficiency (*hIAPP*<sup>+</sup>*Atg7* <sup>$\Delta\beta$ cell</sup> mice), the accumulation of toxic oligomers, the loss of  $\beta$ -cells, and diabetes development is linked to autophagy disruption, and this is suggestive of a role for autophagy in IAPP toxicity (Kim et al., 2014). Moreover, inhibition of lysosomal degradation in HIP (hIAPP transgenic) rats increases hIAPP-mediated toxicity, whereas autophagy stimulation protects  $\beta$ -cells against hIAPP-induced apoptosis (Rivera et al., 2011). Chronic inflammation is also observed in local and systemic amyloidosis due to the activation of the NLRP3 inflammasome by hIAPP aggregates (Masters et al., 2010). A general view of IAPP pathological mechanisms is given in **Figure 1B**.

## IAPP PATHOLOGY IN THE BRAIN

AD was considered for a long period to be caused by A $\beta$  amyloidogenesis and/or Tau aggregation (Makin, 2018). Indeed, the presence of extracellular A $\beta$ -42 amyloid plaques and intracellular aggregates of hyperphosphorylated Tau are the classical diagnostic markers of the disease (Glenner et al., 1984; Gotz, 2001; Gong et al., 2003). A $\beta$  exists mainly in two forms, A $\beta$ -40 and A $\beta$ -42, composed of 40 and 42 amino acids, respectively, and the increase of the A $\beta$ -42/A $\beta$ -40 ratio is strongly correlated with AD severity (Kuperstein et al., 2010). Given the importance of these players in disease pathophysiology, AD research has been so focused on them that other possible agents have been somewhat overlooked.

More recently, IAPP has emerged as a novel player in AD pathology (de la Monte and Wands, 2008; Wijesekara et al., 2017; Norwitz et al., 2019; Qiu et al., 2019). Notwithstanding, the mechanisms by which IAPP contributes to AD pathology are still unclear and deserve further enquiry. It is known that IAPP and A $\beta$  interact with each other and that IAPP promotes A $\beta$  aggregation in a seeding-like manner, leading to the formation of cross-seeded oligomers (Andreetto et al., 2010; Rezaei-Ghaleh et al., 2011; Yan et al., 2014; Hu et al., 2015; Bakou et al., 2017; Moreno-Gonzalez et al., 2017; Ge et al., 2018; Armiento et al., 2019). Interestingly, an aggregation blocker mimicking IAPP has been proven to work against A $\beta$  (Yan et al., 2007).

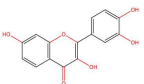
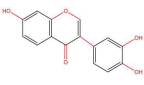
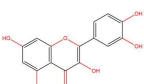
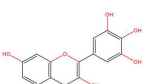
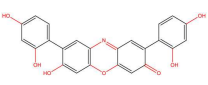
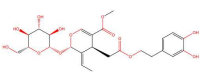
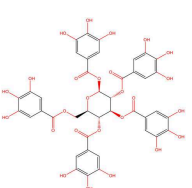
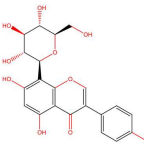
Hyperamylinemia has been pointed out as a possible trigger for IAPP misfolding and aggregation, which may cause damage in the brain (Jackson et al., 2013) and other organs by various mechanisms that include the toxic gain-of-function of IAPP aggregates and the loss of IAPP physiological functions (Westermarck et al., 2011; Despa et al., 2012, 2014). In addition, IAPP dyshomeostasis may affect other organs, particularly the brain, in A $\beta$ -42-dependent and -independent manners. This is illustrated by studies showing that IAPP deposition impairs brain function regardless of A $\beta$ -42 pathology (Srodulski et al., 2014) and that the brain of AD patients can also have IAPP deposits, alone or in the presence of A $\beta$ -42 (Fawver et al., 2014), even if clinical signs of diabetes are absent (Jackson et al., 2013; Oskarsson et al., 2015). A remarkable aspect is the fact that the IAPP analog pramlintide is able to have a neuroprotective effect, both in AD pathogenesis as well as on cognition in general (Adler et al., 2014). This is in line with observations that the key regions involved in A $\beta$ -42-IAPP interaction—the interface amino acid residues—are at the same time high-affinity binding sites in both the cross- and self-aggregation of these molecules (Andreetto et al., 2010). Pramlintide possibly modulates these interactions by preventing them or promoting the formation of biologically inactive fibrils. However, the *in silico* cross seeding of A $\beta$ -42 and IAPP fibril-like oligomers still needs to be complemented with further experimental evidence to support this hypothesis (Berhanu et al., 2013). In addition to A $\beta$ -42, it was also reported that the major component of cerebrovascular plaques in the AD brain, the A $\beta$ -40, can cross-seed IAPP fibrillization, suggesting that these two peptides might populate states that cross-interact (O’Nuallain et al., 2004). Other mechanisms by which IAPP dyshomeostasis exacerbates A $\beta$ -42 toxicity in the brain may include ROS generation (Jhamandas and MacTavish, 2004; Lim et al., 2010) and the breakdown of insulin degrading enzyme activity, which is responsible for insulin, IAPP, and A $\beta$  degradation (Kurochkin and Goto, 1994; McDermott and Gibson, 1997).

**TABLE 1** | Effect of (poly)phenols on the aggregation of human IAPP.

Phenolic compound	Experimental model	Mechanism of action	References
<b>Baicalein</b> 	<ul style="list-style-type: none"> <li>Cell-free</li> <li>Cell-free</li> <li>INS-1 rat pancreatic <math>\beta</math>-cell line exposed to hIAPP aggregates</li> </ul>	<ul style="list-style-type: none"> <li>Inhibits the formation of <math>\beta</math>-sheet structures</li> <li>Inhibits IAPP amyloid formation</li> <li>Neutralizes IAPP-induced cytotoxicity in a dose depend manner</li> </ul>	Mirhashemi, 2012 Velander et al., 2016
<b>Curcumin</b> 	<ul style="list-style-type: none"> <li>Cell-free</li> <li>Cell-free</li> <li>Cell-free</li> <li>INS-1 rat pancreatic <math>\beta</math>-cell line exposed to hIAPP aggregates</li> </ul>	<ul style="list-style-type: none"> <li>Modulates IAPP self-assembly by unfolding <math>\alpha</math>-helix structures</li> <li>Induces the dissociation of amyloid fibrils</li> <li>Alters the morphology and conformation of IAPP aggregates</li> <li>Protects cells against amyloid-induced toxicity</li> </ul>	Sparks et al., 2012 Shoval et al., 2008 Daval et al., 2010
<b>ECG</b> 	<ul style="list-style-type: none"> <li>Cell-free</li> </ul>	<ul style="list-style-type: none"> <li>Reduces the rate constants of first nucleation step of amyloid fibril formation, inhibiting the first stages of this process</li> </ul>	Kamihira-Ishijima et al., 2012
<b>EGCG</b> 	<ul style="list-style-type: none"> <li>Cell-free</li> <li>Cell-free</li> <li>Cell-free</li> <li>Cell-free</li> <li>Cell-free</li> <li>Cell-free</li> <li>Cell-free</li> <li>Cell-free</li> <li>Cell-free</li> <li>INS-1 rat pancreatic <math>\beta</math>-cell line exposed to hIAPP aggregates</li> <li>RIPHAT transgenic mice expressing hIAPP (sub-chronic administration)</li> </ul>	<ul style="list-style-type: none"> <li>Binds to specific conformers within an ensemble of IAPP monomers, affecting the oligomerization process and fibril assembly</li> <li>Delays the formation of <math>\beta</math>-sheet containing IAPP aggregates</li> <li>Stabilizes non-fibrillar large aggregates during fibrillogenesis</li> <li>Inhibits the formation of IAPP-NH<sub>2</sub> fibrils</li> <li>Promotes the generation of IAPP-NH<sub>2</sub> amorphous aggregates</li> <li>Remodels IAPP fibrils, but does not fully resolubilize them to unstructured monomers</li> <li>Presents an amyloid remodeling activity that is dependent on its auto-oxidation</li> <li>Destabilizes IAPP oligomers</li> <li>Breaks the initial ordered pattern of two polymers, decreases their <math>\beta</math>-sheet content, and enlarges their conformational space</li> <li>Acts as an efficient amyloid inhibitor, especially in bulk solution</li> <li>Does not disaggregate amyloid fibrils at a phospholipid interface</li> <li>Binds to IAPP and induces the formation of amorphous aggregates</li> <li>Disaggregates preformed amyloid fibrils derived from IAPP</li> <li>Protect cells against IAPP-induced cytotoxicity</li> <li>Reduces the amount of IAPP fibrils in the pancreas but does not alter the disease clinical signs</li> </ul>	Young et al., 2014a Suzuki et al., 2012 Xu et al., 2017 Cao and Raleigh, 2012 Palhano et al., 2013 Wang et al., 2014 Engel et al., 2012 Franko et al., 2018 Meng et al., 2010 Franko et al., 2018
<b>EGCG/Al(III)</b> <b>EGCG:Zn(II) complex</b>	<ul style="list-style-type: none"> <li>Cell-free</li> <li>Cell-free</li> <li>RIN-5F rat pancreatic <math>\beta</math>-cell line exposed to hIAPP aggregates</li> </ul>	<ul style="list-style-type: none"> <li>Inhibits IAPP fibrillation</li> <li>Suppresses IAPP amyloid aggregation, both in the presence and absence of a lipid membranes</li> <li>Promotes the stabilization of a helical structure of IAPP</li> <li>Suppresses the cellular toxicity mediated by IAPP</li> </ul>	Xu et al., 2016 Lee et al., 2019
<b>Ferulic acid</b> 	<ul style="list-style-type: none"> <li>Cell-free</li> </ul>	<ul style="list-style-type: none"> <li>Represses IAPP amyloid formation</li> </ul>	Mirhashemi, 2012

(Continued)

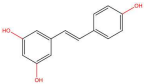
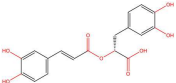
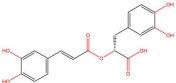
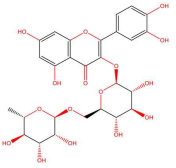
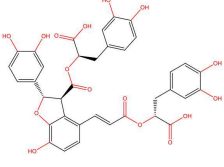
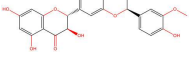
TABLE 1 | Continued

Phenolic compound	Experimental model	Mechanism of action	References
<b>Fisetin</b> 	<ul style="list-style-type: none"> <li>Cell-free</li> </ul>	<ul style="list-style-type: none"> <li>Inhibits the formation of <math>\beta</math>-sheet structures</li> </ul>	Aarabi and Mirhashemi, 2017
<b>Genistein</b> 	<ul style="list-style-type: none"> <li>Cell-free</li> <li>RIN-5F rat pancreatic <math>\beta</math>-cell line exposed to hIAPP aggregates</li> </ul>	<ul style="list-style-type: none"> <li>Prevents the conformational transition of IAPP monomers to <math>\beta</math>-sheet structures</li> <li>Decreases amyloid fibrillization</li> <li>Interferes with self-aggregation of IAPP oligomers</li> <li>Reduces IAPP cytotoxicity</li> <li>Increases cell viability, decreases cell apoptosis, and reduces cell membrane leakage</li> </ul>	Ren et al., 2018
<b>Morin</b> 	<ul style="list-style-type: none"> <li>Cell-free</li> <li>Cell-free</li> </ul>	<ul style="list-style-type: none"> <li>Inhibits the generation of IAPP aggregates</li> <li>Promotes the disaggregation of preformed fibrils</li> <li>Inhibits insulin aggregation and prevents conformational changes</li> <li>Changes the morphology, solvent accessible surface area, and the secondary structure of IAPP pentamer</li> </ul>	Noor et al., 2012  Wang et al., 2015b
<b>Myricetin</b> 	<ul style="list-style-type: none"> <li>Cell-free</li> <li>PC12 rat adrenal gland cell line exposed to hIAPP aggregates</li> </ul>	<ul style="list-style-type: none"> <li>Inhibits IAPP fibrillogenesis</li> <li>Reduces IAPP-induced cytotoxicity</li> </ul>	Zelus et al., 2012
<b>O4, orcein-related small molecule</b> 	<ul style="list-style-type: none"> <li>Cell-like system (using artificial crowding agents Ficoll 70 and sucrose)</li> </ul>	<ul style="list-style-type: none"> <li>Generates globular, amorphous off-pathway assemblies, inhibiting the polymerization of mature IAPP fibrils</li> </ul>	Gao et al., 2015
<b>Oleuropein aglycone</b> 	<ul style="list-style-type: none"> <li>Cell-free</li> <li>RIN-5F rat pancreatic <math>\beta</math>-cell line exposed to hIAPP aggregates</li> <li>INS-1 rat pancreatic <math>\beta</math>-cell line exposed to hIAPP aggregates</li> </ul>	<ul style="list-style-type: none"> <li>Favors the generation of off-pathway IAPP species</li> <li>Reduces IAPP cytotoxicity</li> <li>Promotes glucose-stimulated insulin secretion</li> <li>Stimulates the ERK/MAPK signaling pathway</li> <li>Inhibits the cytotoxicity mediated by IAPP amyloids</li> </ul>	Rigacci et al., 2010  Wu et al., 2017
<b>PGG</b> 	<ul style="list-style-type: none"> <li>Cell-free</li> <li>PC12 rat adrenal gland cell line exposed to hIAPP aggregates</li> </ul>	<ul style="list-style-type: none"> <li>Inhibits IAPP aggregation and amyloid-based fiber formation</li> <li>Prevents the toxicity of IAPP oligomers</li> </ul>	Bruno et al., 2013
<b>Quercetin</b> 	<ul style="list-style-type: none"> <li>RIN-5F rat pancreatic <math>\beta</math>-cell line exposed to hIAPP aggregates</li> </ul>	<ul style="list-style-type: none"> <li>Modulates the aggregation propensity of IAPP</li> <li>Protects cells from IAPP cytotoxicity</li> <li>Reduces oxidative damage</li> </ul>	López et al., 2016

(Continued)

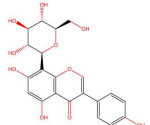


TABLE 1 | Continued

Phenolic compound	Experimental model	Mechanism of action	References
<b>Resveratrol</b> 	<ul style="list-style-type: none"> <li>Cell-free</li> <li>Cell-free</li> <li>Cell-free</li> <li>Cell-free</li> <li>POPG model membrane</li> <li>INS-1 rat pancreatic <math>\beta</math>-cell line exposed to hIAPP aggregates</li> <li>INS-1 rat pancreatic <math>\beta</math>-cell line exposed to hIAPP aggregates</li> <li>INS-1 rat pancreatic <math>\beta</math>-cell line expressing hIAPP</li> </ul>	<ul style="list-style-type: none"> <li>Stabilizes IAPP off-pathway oligomers</li> <li>Inhibits the stacking of IAPP oligomers, avoiding its aggregation and accumulation</li> <li>Promotes conformational changes of hIAPP1 pentamer (alters secondary structures, order degree, and morphology)</li> <li>Inhibits IAPP aggregation in the presence of aggregation-fostering negatively charged lipid interfaces</li> <li>Promotes the generation of secondary structures (sheets and helices)</li> <li>Perturbs the interaction between IAPP and negative charged membranes</li> <li>Arrests IAPP fibril generation and associated cytotoxic effects at an early stage</li> <li>Generates off-pathway non-toxic IAPP conformations</li> <li>Enhances cell survival</li> <li>Decreases amyloid deposition and restores insulin secretion, though only when autophagy is not blocked</li> </ul>	<p>Nedumpully-Govindan et al., 2016</p> <p>Jiang et al., 2011</p> <p>Wang et al., 2015a</p> <p>Evers et al., 2009</p> <p>Lolicato et al., 2015</p> <p>Radovan et al., 2009</p> <p>Mishra et al., 2009</p> <p>Lv et al., 2019</p>
<b>Resveratrol derivate</b> 	<ul style="list-style-type: none"> <li>POPC/POPS model membrane</li> </ul>	<ul style="list-style-type: none"> <li>Eliminates amyloid growth and associated-membrane damage</li> </ul>	<p>Sciacca et al., 2018</p>
<b>Rosmarinic acid</b> 	<ul style="list-style-type: none"> <li>Cell-free</li> </ul>	<ul style="list-style-type: none"> <li>Represses IAPP amyloidogenic aggregates by opening the <math>\beta</math>-sheet conformation of these structures</li> <li>Reduces IAPP-mediated toxicity</li> </ul>	<p>Zheng and Lazo, 2018</p>
<b>Rutin</b> 	<ul style="list-style-type: none"> <li>Cell-free</li> <li>FVB/NJ transgenic mice expressing hIAPP</li> <li>SH-SY5Y human neuroblastoma cell line exposed to hIAPP aggregates</li> <li>BV-2 mouse microglial cell line exposed to hIAPP aggregates</li> </ul>	<ul style="list-style-type: none"> <li>Inhibits IAPP misfolding, disaggregates IAPP oligomers and reverts IAPP conformation toward the physiological state</li> <li>Slows diabetes progression</li> <li>Inhibits IAPP aggregation and reduces IAPP-induced neurotoxicity and oxidative stress</li> <li>Reduces the production of ROS and NO</li> <li>Attenuates mitochondrial damage</li> <li>Inhibits IAPP aggregation and reduces IAPP-induced neurotoxicity</li> <li>Increases GSH/GSSG ratio</li> <li>Reduces the production of MDA, GSSG and pro-inflammatory cytokines (TNF-<math>\alpha</math> and IL-1<math>\beta</math>)</li> </ul>	<p>Aitken et al., 2017</p> <p>Yu et al., 2015</p>
<b>Salvianolic acid B</b> 	<ul style="list-style-type: none"> <li>INS-1 rat pancreatic <math>\beta</math>-cell line exposed to hIAPP aggregates</li> </ul>	<ul style="list-style-type: none"> <li>Suppresses membrane permeabilization, mitochondrial impairment, and cytotoxicity induced by IAPP</li> <li>Inhibits the formation of lower order oligomers and fibrils</li> </ul>	<p>Cheng et al., 2013</p>
<b>Silibinin</b> 	<ul style="list-style-type: none"> <li>Cell-free</li> <li>Cell-free</li> </ul>	<ul style="list-style-type: none"> <li>Binds to specific conformers within an ensemble of IAPP monomers, affecting the oligomerization process and fibril assembly</li> <li>Favors the 3+ IAPP monomer preventing oligomerization</li> <li>Disaggregates preformed fibrils into small off-pathway oligomers</li> </ul>	<p>Young et al., 2014a</p> <p>Young et al., 2014b</p>

(Continued)

TABLE 1 | Continued

	<ul style="list-style-type: none"> <li>Cell-free</li> <li>INS-1 rat pancreatic <math>\beta</math>-cell line exposed to hIAPP aggregates</li> <li>INS-1 rat pancreatic <math>\beta</math>-cell line exposed to hIAPP aggregates</li> <li>INS-1 rat pancreatic <math>\beta</math>-cell line exposed to hIAPP aggregates</li> </ul>	<ul style="list-style-type: none"> <li>Inhibits IAPP fibrillization through the suppression of toxic IAPP oligomerization</li> <li>Reduces IAPP cytotoxicity in a dose-dependent manner</li> <li>Enhances estrogen receptors phosphorylation, leading to downregulation of ROS/RNS production induced by IAPP/A<math>\beta</math>-42</li> <li>Protects cells from IAPP-induced apoptosis through activation of GLP-1R/PKA signaling</li> </ul>	<p>Cheng et al., 2012</p> <p>Yang et al., 2019a</p> <p>Yang et al., 2019b</p>
<b>8-<math>\beta</math>-d-Glucopyranosylgenistein</b> 	<ul style="list-style-type: none"> <li>Cell-free</li> <li>STZ-induced diabetic rats</li> </ul>	<ul style="list-style-type: none"> <li>Interacts with IAPP oligomers, preventing amyloid fibrillization</li> <li>Normalizes fasting hyperglycemia</li> <li>Ameliorates excessive post-prandial glucose excursions</li> <li>Increases <math>\beta</math>-cell sensitivity and insulin secretion</li> </ul>	Jesus et al., 2014

A(III), Aluminum III; A $\beta$ , Amyloid beta; ECG, Epicatechin-3-Gallate; EGCG, Epigallocatechin-3-Gallate; ERK, Extracellular-Signal-Regulated Kinase; FVB/NJ, Friend Virus B NIH Jackson; GLP-1R, Glucagon-like Peptide-1 Receptor; GSH, Glutathione; GSSG, Glutathione disulfide; hIAPP, Human Islet Amyloid Polypeptide; hIAPP-NH<sub>2</sub>, Amidated Human Islet Amyloid Polypeptide; IL-1 $\beta$ , Interleukin-1beta; MAPK, Mitogen Activated Protein Kinase; MDA, Malondialdehyde; NO, Nitric Oxide; PGG, Pentagalloyl Glucose; PKA, Protein Kinase A; POPC, 2-oleoyl-1-palmitoyl-sn-glycero-3-phosphocholine; POPG, 2-oleoyl-1-palmitoyl-sn-glycero-3-glycerol; POPS, 1-palmitoyl-2-oleoyl-sn-glycero-3-phospho-L-serine; RNS, Reactive Nitrogen Species; ROS, Reactive Oxygen Species; STZ-induced diabetic rat, Streptozotocin-induced diabetic rat; TNF- $\alpha$ , Tumor Necrosis Factor-alpha; Zn(II), Zinc II.

As IAPP produced in the pancreas was shown to cross the blood–brain barrier (Banks et al., 1995; Banks and Kastin, 1998) and to act on brain receptors, another important aspect of IAPP pathophysiology in the brain is its role in neuronal network function. Therefore, the effects of IAPP on neuronal and glial cells have been investigated (Chaitanya et al., 2011; Xi et al., 2019). As the primary site of IAPP action, the *area postrema* (AP) is the brain structure best characterized in terms of IAPP effects. While IAPP was shown to promote the formation of AP neuronal projections in neonatal rodents, in adult Wistar rats, IAPP injections were reported (1) to affect genes controlling neurogenesis, particularly *NeuroD1*, (2) to increase the number of newly proliferated AP-cells, and (3) to promote differentiation of these cells into neurons (Liberini et al., 2016). A study to investigate the mechanism by which IAPP modulates neuronal excitability in AP neurons in rat brainstem slices revealed that IAPP induced changes in excitatory responses of neurons not displaying the hyperpolarization-activated cation current. Furthermore, this study revealed that IAPP receptors were mainly located on presynaptic glutamatergic terminals connecting these neurons and that IAPP can increase glutamate release enough to cause cell firing (Fukuda et al., 2013). Likewise, hIAPP was shown to cause a dose-dependent membrane depolarization and an increase in firing frequency in neurons of the diagonal band of Broca, a cholinergic basal forebrain nucleus, in rats (Li and Li, 2012). Hence, IAPP dysregulation may have important implications in neuronal function. IAPP receptors were also proven to be mediators of the deleterious actions of A $\beta$ -42 in human neurons (Jhamandas et al., 2011). In this sense, amylin receptors are seen as potential targets for AD therapies (Fu et al., 2017).

AD is also considered a metabolic disease to a large extent. It is clear that the brain loses its capacity to deal with glucose and to respond to insulin and insulin-like growth factor (IGF)

(Rivera et al., 2005; Liu et al., 2011; Talbot et al., 2012). The inability to respond to insulin and IGF leads to brain “starvation” and neuronal loss (de la Monte et al., 2009; de la Monte, 2012). Moreover, reducing the activity of the insulin/IGF signaling cascade seems to protect from AD-like neurodegeneration in nematodes, possibly by promoting more densely packed (and less toxic) amyloid fibrils (Cohen and Goedert, 2004; El-Ami et al., 2014). Thus, the link between AD and insulin/IGF exists, but it is not easy to decipher. However, some of the mechanisms involved are becoming clear. For example, the kinases that promote Tau phosphorylation, causing cell death, become increasingly activated due to insulin resistance (Schubert et al., 2003, 2004). Then, A $\beta$ -42 and its precursor protein levels also increase in the brain as a result of insulin resistance (Messier and Teutenberg, 2005). One can state that, what could be called the “brain diabetes phenotype,” i.e., increased resistance to insulin and to IGF, can result in the appearance of classical AD molecular biomarkers. Besides these clear links between diabetes and AD-related peptides and proteins, the physiological functioning of insulin and IGF promotes neuronal growth, differentiation, and the formation of synapses, the lack of which is associated with dementia (Takeda et al., 2010; Westwood et al., 2014). Overall, insulin and IGF are required for synaptic plasticity and are necessary for the cognitive function, the mechanisms of which are only partially explained (Qiu et al., 1998; Wickelgren, 1998; Zhao and Alkon, 2001). Oxidative stress is also associated with AD and diabetes as well as advanced glycation end products (Ramasamy et al., 2011; Silveira et al., 2019).

Although studies focusing on IAPP, insulin, and IGF are stimulating and may lead to exciting developments, one must be careful to draw definitive conclusions regarding multi-factorial diseases such as AD, even if it has been analyzed through the prism of the glucose metabolism. The road to a treatment for AD is full of failed starts and drug-development pipeline failures even

if one (partially) understands the mechanism involved (Berhanu et al., 2013). The fact that aging implies reductions in insulin and IAPP release (Dechenes et al., 1998) provides important clues that, in retrospect, should not have been overlooked for so long (Despa and Decarli, 2013). The most powerful process may be related to IGF-I, which has been shown to protect and rescue hippocampal neurons from A $\beta$ -42 neurotoxicity and IAPP-induced toxicity, as a two-in-one solution. This was already reported over 20 years ago (Doré et al., 1997), but, inexplicably, it was somewhat ignored. This is no longer the case: the role of IAPP in AD is not overlooked, as IAPP is even seen as the second amyloid of AD pathology, a promising approach to understand IAPP in relation to AD (Fawver et al., 2014). A curious finding is that A $\beta$ -42 directly activates the amylin-3 receptor subtype, which may have major implications in AD pathology (Fu et al., 2012) as well as in the “brain diabetes phenotype” that we have proposed here. Moreover, it may also explain why pramlintide, which acts on rat and human amylin receptors (Gingell et al., 2014), can be protective in AD. Interestingly, A $\beta$ -42 expressed on human neurons can bind to amylin receptors (Jhamandas et al., 2011), thereby triggering activation of apoptotic genes, as IAPP does (Jhamandas and Mactavish, 2012). The activity of these molecules on the brain may lead to neuronal death, particularly in AD patients, thus explaining their phenotypic profiles (Kawarabayashi et al., 2001; Dubois et al., 2016; Li and Huang, 2016; Li et al., 2016a).

## STRATEGIES FOR REDUCING IAPP PROTEOTOXICITY USING NATURAL COMPOUNDS

The links between IAPP and AD have not gone unnoticed, with some authors presenting relevant reviews on the topic and hinting at possible therapeutic strategies (Despa and Decarli, 2013; Jackson et al., 2013; Bharadwaj et al., 2017; Mietlicki-Baase, 2018). The role of IAPP is undeniably relevant in both diabetes and AD. Therefore, attempting to modulate the oligomerization process or block its cytotoxicity is an appealing venue for therapeutic strategies. Different approaches have been attempted to block protein aggregation (Figure 1C). Efforts have been made to interfere with the oligomerization process itself by (i) stabilizing the monomer, (ii) remodeling small oligomers from a fibrillogenic to non-fibrillogenic form, thereby creating “off-pathway” oligomers, and (iii) reverting fibrils to monomers or other intermediate species (Pithadia et al., 2016; Table 1). Another strategy is to revert the pathological effects of oligomers in cellular homeostasis, such as ER stress, mitochondrial damage, cell membrane permeabilization, autophagy impairment, inflammation, and  $\beta$ -cell death (Kiriya and Nochi, 2018).

The pleiotropic action of (poly)phenols toward chronic diseases, particularly diabetes, is well-documented (Bahadoran et al., 2013; Panickar, 2013; Jasmin and Jaitak, 2019; Silveira et al., 2019). Most importantly, (poly)phenols have been linked to the inhibition of aggregation of proteins such as IAPP and A $\beta$ -42 (Pithadia et al., 2016; Sequeira and Poppitt, 2017; Dhoulfi et al., 2018). It has been shown that different classes of (poly)phenols

may interfere with different steps of the oligomerization process (Ladiwala et al., 2011). The lower toxicity of these compounds compared to synthetic molecules gives them an advantage as future therapeutics. However, there is an urgent need for the validation of their therapeutic potential in pre-clinical studies, as most of the evidences derives from cell-free and *in vitro* assays (Table 1).

Epigallocatechin gallate (EGCG) and resveratrol are the most-studied compounds. EGCG has been proved to remodel IAPP oligomers, create “off-pathway” intermediates, and prevent monomers from shifting into  $\beta$ -sheet structures, a critical step in early-stage aggregation processes (Bieschke et al., 2010; Young et al., 2014a; Nedumpully-Govindan et al., 2016). Resveratrol has also been suggested as an inhibitor of both IAPP and A $\beta$ -42 pathological effects. It was reported to lower intracellular and secreted levels of A $\beta$ -42 and also to stimulate intracellular degradation (Marambaud et al., 2005). However, resveratrol seems to be less effective than EGCG and inefficient in preventing amyloid formation (Tu et al., 2015). In addition, (poly)phenols have an important role in reducing oligomer-induced cytotoxicity by modulating oxidative stress (Chakrabarti et al., 2013), inflammation (Apetz et al., 2014), and autophagy (Rigacci et al., 2015). A compilation of (poly)phenols as bioactive components modulating IAPP toxicity is given in Table 1.

## CONCLUDING REMARKS

This study shows how an “old story” can originate groundbreaking knowledge and create new venues for a therapeutic approach. The first high-impact paper describing IAPP as a relevant factor for T2DM was published in 1994 (Lorenzo et al., 1994). Since then, even though it took a long time for this field to be pursued, knowledge has come a long way. It is now clear that direct brain microvascular injury, leading to white matter disease, is unequivocally originated by elevated IAPP levels in diabetes (Ly et al., 2017), further supporting the “diabetes brain phenotype” hypothesis that we have proposed here.

This change of approach is as cutting-edge as the finding that amyloid fibrils precursors, but not the amyloid fibrils themselves, are the cause of toxicity (Martins et al., 2008). We believe that this study, and others that reflect on the role of IAPP in AD in an unbiased manner (Mietlicki-Baase, 2018) complemented by further experiments, will certainly pave the road to future IAPP-centered drug development strategies against AD, as we considering it as the result of a “diabetes brain phenotype.” Such a view will certainly yield major therapeutic advances.

## AUTHOR CONTRIBUTIONS

AR and SF wrote the manuscript. IM wrote and revised the manuscript. RM designed the layout and wrote and revised the manuscript.

## FUNDING

We acknowledge iNOVA4Health—UID/Multi/04462/2019, a program financially supported by Fundação para a Ciência

e Tecnologia/Ministério da Educação e Ciência, through national funds and co-funded by FEDER under the PT2020 Partnership Agreement. Funding from the INTERFACE Programme, through the Innovation, Technology and Circular Economy Fund (FITEC) is gratefully acknowledged. This study was also supported by FCT via PTDC/BIA-MOL31104/2017

and UID/Multi/04462/2019-SubProj iNOVA4Health 44 to RM and PD/BD/135504/2018 to AR. Sociedade Portuguesa de Diabetologia for the Nuno Castelo-Branco Prize—2016, attributed to RM, was also acknowledged. IM acknowledges FCT-MCTES Program Concurso de Estímulo ao Emprego Científico (CEECIND/01670/2017).

## REFERENCES

- Aarabi, M. H., and Mirhashemi, S. M. (2017). To estimate effective anti-amyloidogenic property of melatonin and fisetin and their actions to destabilize amyloid fibrils. *Pak. J. Pharm. Sci.* 30, 1589–1593.
- Adler, B. L., Yarchoan, M., Hwang, H. M., Louneva, N., Blair, J. A., Palm, R., et al. (2014). Neuroprotective effects of the amylin analogue pramlintide on Alzheimer's disease pathogenesis and cognition. *Neurobiol. Aging* 35, 793–801. doi: 10.1016/j.neurobiolaging.2013.10.076
- Aitken, J. F., Loomes, K. M., Riba-Garcia, I., Unwin, R. D., Pijic, G., Phillips, A. S., et al. (2017). Rutin suppresses human-amylin/hIAPP misfolding and oligomer formation *in-vitro*, and ameliorates diabetes and its impacts in human-amylin/hIAPP transgenic mice. *Biochem. Biophys. Res. Commun.* 482, 625–631. doi: 10.1016/j.bbrc.2016.11.083
- Akter, R., Cao, P., Noor, H., Ridgway, Z., Tu, L.-H., Wang, H., et al. (2016). Islet amyloid polypeptide: structure, function, and pathophysiology. *J. Diabetes Res.* 2016:2798269. doi: 10.1155/2016/2798269
- Alzheimer's Association (2016). 2016 Alzheimer's disease facts and figures. *Alzheimers Dement.* 12, 459–509. doi: 10.1016/j.jalz.2016.03.001
- Andreotto, E., Yan, L. M., Tatarek-Nossol, M., Velkova, A., Frank, R., and Kapurniotu, A. (2010). Identification of hot regions of the A $\beta$ -IAPP interaction interface as high-affinity binding sites in both cross- and self-association. *Angew. Chem. Int. Ed. Engl.* 49, 3081–3085. doi: 10.1002/anie.200904902
- Apetz, N., Munch, G., Govindaraghavan, S., and Gyengesi, E. (2014). Natural compounds and plant extracts as therapeutics against chronic inflammation in Alzheimer's disease—a translational perspective. *CNS Neurol. Disord. Drug Targets* 13, 1175–1191. doi: 10.2174/1871527313666140917110635
- Armiento, V., Spanopoulou, A., and Kapurniotu, A. (2019). Peptide-based molecular strategies to interfere with protein misfolding, aggregation, and cell degeneration. *Angew. Chem. Int. Ed. Engl.* 59, 3372–84. doi: 10.1002/anie.201906908
- Arya, S., Claud, S. L., Cantrell, K. L., and Bowers, M. T. (2019). Catalytic prion-like cross-talk between a key Alzheimer's disease tau-fragment r3 and the type 2 diabetes peptide IAPP. *ACS Chem. Neurosci.* 10, 4757–4765. doi: 10.1021/acscchemneuro.9b00516
- Bahadoran, Z., Mirmiran, P., and Azizi, F. (2013). Dietary polyphenols as potential nutraceuticals in management of diabetes: a review. *J. Diabetes. Metab. Disord.* 12:43. doi: 10.1186/2251-6581-12-43
- Bakou, M., Hille, K., Kracklauer, M., Spanopoulou, A., Frost, C. V., Malideli, E., et al. (2017). Key aromatic/hydrophobic amino acids controlling a cross-amyloid peptide interaction versus amyloid self-assembly. *J. Biol. Chem.* 292, 14587–14602. doi: 10.1074/jbc.M117.774893
- Banks, W. A., and Kastin, A. J. (1998). Differential permeability of the blood-brain barrier to two pancreatic peptides: insulin and amylin. *Peptides* 19, 883–889. doi: 10.1016/S0196-9781(98)00018-7
- Banks, W. A., Kastin, A. J., Maness, L. M., Huang, W., and Jaspan, J. B. (1995). Permeability of the blood-brain barrier to amylin. *Life Sci.* 57, 1993–2001. doi: 10.1016/0024-3205(95)02197-Q
- Berhanu, W. M., Yaşar, F., and Hansmann, U. H. E. (2013). *In silico* cross seeding of A $\beta$  and amylin fibril-like oligomers. *ACS Chem. Neurosci.* 4, 1488–1500. doi: 10.1021/cn400141x
- Bharadwaj, P., Wijesekara, N., Liyanapathirana, M., Newsholme, P., Ittner, L., Fraser, P., et al. (2017). The link between type 2 diabetes and neurodegeneration: roles for amyloid-beta, amylin, and tau proteins. *J. Alzheimers Dis.* 59, 421–432. doi: 10.3233/JAD-161192
- Bieschke, J., Russ, J., Friedrich, R. P., Ehrnhoefer, D. E., Wobst, H., Neugebauer, K., et al. (2010). EGCG remodels mature alpha-synuclein and amyloid-beta fibrils and reduces cellular toxicity. *Proc. Natl. Acad. Sci. U.S.A.* 107, 7710–7715. doi: 10.1073/pnas.0910723107
- Bondi, M. W., Edmonds, E. C., and Salmon, D. P. (2017). Alzheimer's disease: past, present, and future. *J. Int. Neuropsychol. Soc.* 23, 818–831. doi: 10.1017/S135561771700100X
- Bower, R. L., and Hay, D. L. (2016). Amylin structure-function relationships and receptor pharmacology: implications for amylin mimetic drug development. *Br. J. Pharmacol.* 173, 1883–1898. doi: 10.1111/bph.13496
- Brunham, L. R., Kruit, J. K., Hayden, M. R., and Verchere, C. B. (2010). Cholesterol in beta-cell dysfunction: the emerging connection between HDL cholesterol and type 2 diabetes. *Curr. Diab. Rep.* 10, 55–60. doi: 10.1007/s11892-009-0090-x
- Bruno, E., Pereira, C., Roman, K. P., Takiguchi, M., Kao, P. Y., Nogaj, L. A., et al. (2013). IAPP aggregation and cellular toxicity are inhibited by 1,2,3,4,6-penta-O-galloyl-beta-D-glucose. *Amyloid* 20, 34–38. doi: 10.3109/13506129.2012.762761
- Cao, P., and Raleigh, D. P. (2012). Analysis of the inhibition and remodeling of islet amyloid polypeptide amyloid fibers by flavanols. *Biochemistry* 51, 2670–2683. doi: 10.1021/bi2015162
- Casas, S., Gomis, R., Gribble, F. M., Altirriba, J., Knuutila, S., and Novials, A. (2007). Impairment of the ubiquitin-proteasome pathway is a downstream endoplasmic reticulum stress response induced by extracellular human islet amyloid polypeptide and contributes to pancreatic beta-cell apoptosis. *Diabetes* 56, 2284–2294. doi: 10.2337/db07-0178
- Chaitanya, G. V., Cromer, W. E., Wells, S. R., Jennings, M. H., Couraud, P. O., Romero, I. A., et al. (2011). Gliovascular and cytokine interactions modulate brain endothelial barrier *in vitro*. *J. Neuroinflammation* 8:162. doi: 10.1186/1742-2094-8-162
- Chakrabarti, S., Sinha, M., Thakurta, I. G., Banerjee, P., and Chattopadhyay, M. (2013). Oxidative stress and amyloid beta toxicity in Alzheimer's disease: intervention in a complex relationship by antioxidants. *Curr. Med. Chem.* 20, 4648–4664. doi: 10.2174/09298673113209990152
- Cheng, B., Gong, H., Li, X., Sun, Y., Chen, H., Zhang, X., et al. (2013). Salvianolic acid B inhibits the amyloid formation of human islet amyloid polypeptide and protects pancreatic beta-cells against cytotoxicity. *Proteins* 81, 613–621. doi: 10.1002/prot.24216
- Cheng, B., Gong, H., Li, X., Sun, Y., Zhang, X., Chen, H., et al. (2012). Silibinin inhibits the toxic aggregation of human islet amyloid polypeptide. *Biochem. Biophys. Res. Commun.* 419, 495–499. doi: 10.1016/j.bbrc.2012.02.042
- Cohen, P., and Goedert, M. (2004). GSK3 inhibitors: development and therapeutic potential. *Nat. Rev. Drug Discov.* 3, 479–487. doi: 10.1038/nrd1415
- Cremades, N., and Dobson, C. M. (2018). The contribution of biophysical and structural studies of protein self-assembly to the design of therapeutic strategies for amyloid diseases. *Neurobiol. Dis.* 109(Pt B), 178–190. doi: 10.1016/j.nbd.2017.07.009
- Cukierman, T., Gerstein, H. C., and Williamson, J. D. (2005). Cognitive decline and dementia in diabetes—systematic overview of prospective observational studies. *Diabetologia* 48, 2460–2469. doi: 10.1007/s00125-005-0023-4
- Daval, M., Bedrood, S., Gurlo, T., Huang, C. J., Costes, S., Butler, P. C., et al. (2010). The effect of curcumin on human islet amyloid polypeptide misfolding and toxicity. *Amyloid* 17, 118–128. doi: 10.3109/13506129.2010.530008
- de la Monte, S. M. (2012). Contributions of brain insulin resistance and deficiency in amyloid-related neurodegeneration in Alzheimer's disease. *Drugs* 72, 49–66. doi: 10.2165/11597760-000000000-00000
- de la Monte, S. M. (2014). Type 3 diabetes is sporadic Alzheimers disease: mini-review. *Eur. Neuropsychopharmacol.* 24, 1954–1960. doi: 10.1016/j.euroneuro.2014.06.008



- de la Monte, S. M., Longato, L., Tong, M., and Wands, J. R. (2009). Insulin resistance and neurodegeneration: roles of obesity, type 2 diabetes mellitus and non-alcoholic steatohepatitis. *Curr. Opin. Investig. Drugs* 10, 1049–1060.
- de la Monte, S. M., and Wands, J. R. (2008). Alzheimer's disease is type 3 diabetes-evidence reviewed. *J. Diabetes Sci. Technol.* 2, 1101–1113. doi: 10.1177/193229680800200619
- Dechenes, C. J., Verchere, C. B., Andrikopoulos, S., and Kahn, S. E. (1998). Human aging is associated with parallel reductions in insulin and amylin release. *Am. J. Physiol.* 275, E785–91. doi: 10.1152/ajpendo.1998.275.5.E785
- Despa, F., and Decarli, C. (2013). Amylin: what might be its role in Alzheimer's disease and how could this affect therapy? *Expert Rev. Proteomics* 10, 403–405. doi: 10.1586/14789450.2013.841549
- Despa, S., Margulies, K. B., Chen, L., Knowlton, A. A., Havel, P. J., Taegtmeier, H., et al. (2012). Hyperamylinemia contributes to cardiac dysfunction in obesity and diabetes: a study in humans and rats. *Circ. Res.* 110, 598–608. doi: 10.1161/CIRCRESAHA.111.258285
- Despa, S., Sharma, S., Harris, T. R., Dong, H., Li, N., Chiamvimonvat, N., et al. (2014). Cardioprotection by controlling hyperamylinemia in a “humanized” diabetic rat model. *J. Am. Heart Assoc.* 3:e001015. doi: 10.1161/JAHA.114.001015
- Dhouafli, Z., Cuanalo-Contreras, K., Hayouni, E. A., Mays, C. E., Soto, C., and Moreno-Gonzalez, I. (2018). Inhibition of protein misfolding and aggregation by natural phenolic compounds. *Cell Mol. Life Sci.* 75, 3521–3538. doi: 10.1007/s00018-018-2872-2
- Donath, M. Y., and Shoelson, S. E. (2011). Type 2 diabetes as an inflammatory disease. *Nat. Rev. Immunol.* 11, 98–107. doi: 10.1038/nri2925
- Doré, S., Kar, S., and Quirion, R. (1997). Insulin-like growth factor I protects and rescues hippocampal neurons against  $\beta$ -amyloid- and human amylin-induced toxicity. *Proc. Natl. Acad. Sci. U.S.A.* 94, 4772–4777. doi: 10.1073/pnas.94.9.4772
- Dubois, B., Padovani, A., Scheltens, P., Rossi, A., and Dell'Agnello, G. (2016). Timely diagnosis for Alzheimer's disease: a literature review on benefits and challenges. *J. Alzheimers Dis.* 49, 617–631. doi: 10.3233/JAD-150692
- El-Ami, T., Moll, L., Carvalhal Marques, F., Volovik, Y., Reuveni, H., and Cohen, E. (2014). A novel inhibitor of the insulin/IGF signaling pathway protects from age-onset, neurodegeneration-linked proteotoxicity. *Aging Cell* 13, 165–174. doi: 10.1111/acel.12171
- Engel, M. F., vandenAkker, C. C., Schleegeer, M., Velikov, K. P., Koenderink, G. H., and Bonn, M. (2012). The polyphenol EGCG inhibits amyloid formation less efficiently at phospholipid interfaces than in bulk solution. *J. Am. Chem. Soc.* 134, 14781–14788. doi: 10.1021/ja3031664
- Evers, F., Jeworrek, C., Tiemeyer, S., Weise, K., Sellin, D., Paulus, M., et al. (2009). Elucidating the mechanism of lipid membrane-induced IAPP fibrillogenesis and its inhibition by the red wine compound resveratrol: a synchrotron X-ray reflectivity study. *J. Am. Chem. Soc.* 131, 9516–9521. doi: 10.1021/ja8097417
- Fawcett, J. N., Ghiwot, Y., Koola, C., Carrera, W., Rodriguez-Rivera, J., Hernandez, C., et al. (2014). Islet amyloid polypeptide (IAPP): a second amyloid in Alzheimer's disease. *Curr. Alzheimer Res.* 11, 928–940. doi: 10.2174/1567205011666141107124538
- Federation ID. (2009). *IDF Diabetes Atlas, 4th Edn.* Montreal, CA: International Diabetes Federation.
- Franko, A., Rodriguez Camargo, D. C., Böddrich, A., Garg, D., Rodriguez Camargo, A., Rathkolb, B., et al. (2018). Epigallocatechin gallate (EGCG) reduces the intensity of pancreatic amyloid fibrils in human islet amyloid polypeptide (hIAPP) transgenic mice. *Sci. Rep.* 8:1116. doi: 10.1038/s41598-017-18807-8
- Fu, W., Patel, A., Kimura, R., Soudy, R., and Jhamandas, J. H. (2017). Amylin receptor: a potential therapeutic target for Alzheimer's disease. *Trends Mol. Med.* 23, 709–720. doi: 10.1016/j.molmed.2017.06.003
- Fu, W., Ruangkittisakul, A., MacTavish, D., Shi, J. Y., Ballanyi, K., and Jhamandas, J. H. (2012). Amyloid beta (A $\beta$ ) peptide directly activates amylin-3 receptor subtype by triggering multiple intracellular signaling pathways. *J. Biol. Chem.* 287, 18820–18830. doi: 10.1074/jbc.M111.331181
- Fukuda, T., Hirai, Y., Maezawa, H., Kitagawa, Y., and Funahashi, M. (2013). Electrophysiologically identified presynaptic mechanisms underlying amylinergic modulation of area postrema neuronal excitability in rat brain slices. *Brain Res.* 1494, 9–16. doi: 10.1016/j.brainres.2012.11.051
- Gao, M., Estel, K., Seeliger, J., Friedrich, R. P., Dogan, S., Wanker, E. E., et al. (2015). Modulation of human IAPP fibrillation: cosolutes, crowders and chaperones. *Phys. Chem. Chem. Phys.* 17, 8338–8348. doi: 10.1039/C4CP04682J
- Ge, X., Yang, Y., Sun, Y., Cao, W., and Ding, F. (2018). Islet amyloid polypeptide promotes amyloid-beta aggregation by binding-induced helix-unfolding of the amyloidogenic core. *ACS Chem. Neurosci.* 9, 967–975. doi: 10.1021/acschemneuro.7b00396
- Gedulin, B. R., Rink, T. J., and Young, A. A. (1997). Dose-response for glucagonostatic effect of amylin in rats. *Metabolism* 46, 67–70. doi: 10.1016/S0026-0495(97)90170-0
- Gingell, J. J., Burns, E. R., and Hay, D. L. (2014). Activity of pramlintide, rat and human amylin but not Abeta1-42 at human amylin receptors. *Endocrinology* 155, 21–26. doi: 10.1210/en.2013-1658
- Glenner, G. G., Wong, C. W., Quaranta, V., and Eanes, E. D. (1984). The amyloid deposits in Alzheimer's disease: their nature and pathogenesis. *Appl. Pathol.* 2, 357–369.
- Gong, Y., Chang, L., Viola, K. L., Lacor, P. N., Lambert, M. P., Finch, C. E., et al. (2003). Alzheimer's disease-affected brain: presence of oligomeric A $\beta$  ligands (ADDLs) suggests a molecular basis for reversible memory loss. *Proc. Natl. Acad. Sci. U.S.A.* 100, 10417–10422. doi: 10.1073/pnas.1834302100
- Gotz, J. (2001). Tau and transgenic animal models. *Brain Res. Brain Res. Rev.* 35, 266–286. doi: 10.1016/S0165-0173(01)00055-8
- Gurlo, T., Ryazantsev, S., Huang, C.-j., Yeh, M. W., Reber, H. A., Hines, O. J., et al. (2010). Evidence for proteotoxicity in beta cells in type 2 diabetes: toxic islet amyloid polypeptide oligomers form intracellularly in the secretory pathway. *Am. J. Pathol.* 176, 861–869. doi: 10.2353/ajpath.2010.090532
- Haataja, L., Gurlo, T., Huang, C. J., and Butler, P. C. (2008). Islet amyloid in type 2 diabetes, and the toxic oligomer hypothesis. *Endocr. Rev.* 29, 303–316. doi: 10.1210/er.2007-0037
- Hauser, C. A., Maurer-Stroh, S., and Martins, I. C. (2014). Amyloid-based nanosensors and nanodevices. *Chem. Soc. Rev.* 43, 5326–5345. doi: 10.1039/C4CS00082J
- Hu, R., Zhang, M., Chen, H., Jiang, B., and Zheng, J. (2015). Cross-seeding interaction between beta-amyloid and human islet amyloid polypeptide. *ACS Chem. Neurosci.* 6, 1759–1768. doi: 10.1021/acschemneuro.5b00192
- Huang, C.-J., Gurlo, T., Haataja, L., Costes, S., Daval, M., Ryazantsev, S., et al. (2010). Calcium-activated calpain-2 is a mediator of beta cell dysfunction and apoptosis in type 2 diabetes. *J. Biol. Chem.* 285, 339–348. doi: 10.1074/jbc.M109.024190
- Hull, R. L., Zraika, S., Udayasankar, J., Aston-Mourney, K., Subramanian, S. L., and Kahn, S. E. (2009). Amyloid formation in human IAPP transgenic mouse islets and pancreas, and human pancreas, is not associated with endoplasmic reticulum stress. *Diabetologia* 52, 1102–1111. doi: 10.1007/s00125-009-1329-4
- Ishikawa, M., Iwasaki, Y., Yatoh, S., Kato, T., Kumadaki, S., Inoue, N., et al. (2008). Cholesterol accumulation and diabetes in pancreatic beta-cell-specific SREBP-2 transgenic mice: a new model for lipotoxicity. *J. Lipid. Res.* 49, 2524–2534. doi: 10.1194/jlr.M800238-JLR200
- Jackson, K., Barisone, G. A., Diaz, E., Jin, L. W., DeCarli, C., and Despa, F. (2013). Amylin deposition in the brain: a second amyloid in Alzheimer disease? *Ann. Neurol.* 74, 517–526. doi: 10.1002/ana.23956
- Janson, J., Soeller, W. C., Roche, P. C., Nelson, R. T., Torchia, A. J., Kreutter, D. K., et al. (1996). Spontaneous diabetes mellitus in transgenic mice expressing human islet amyloid polypeptide. *Proc. Natl. Acad. Sci. U.S.A.* 93, 7283–7288. doi: 10.1073/pnas.93.14.7283
- Jasmin, and Jaitak, V. (2019). A review on molecular mechanism of flavonoids as antidiabetic agents. *Mini. Rev. Med. Chem.* 19, 762–786. doi: 10.2174/1389557519666181227153428
- Jesus, A. R., Dias, C., Matos, A. M., de Almeida, R. F. M., Viana, A. S., Marcelo, F., et al. (2014). Exploiting the therapeutic potential of 8- $\beta$ -d-glucopyranosylgenistein: synthesis, antidiabetic activity, and molecular interaction with islet amyloid polypeptide and amyloid  $\beta$ -peptide (1–42). *J. Med. Chem.* 57, 9463–9472. doi: 10.1021/jm501069h
- Jhamandas, J. H., Li, Z., Westaway, D., Yang, J., Jassar, S., and MacTavish, D. (2011). Actions of  $\beta$ -amyloid protein on human neurons are expressed through the amylin receptor. *Am. J. Pathol.* 178, 140–149. doi: 10.1016/j.ajpath.2010.11.022
- Jhamandas, J. H., and MacTavish, D. (2004). Antagonist of the amylin receptor blocks beta-amyloid toxicity in rat cholinergic basal forebrain neurons. *J. Neurosci.* 24, 5579–5584. doi: 10.1523/JNEUROSCI.1051-04.2004

- Jhamandas, J. H., and Mactavish, D. (2012).  $\beta$ -Amyloid protein (A $\beta$ ) and human amylin regulation of apoptotic genes occurs through the amylin receptor. *Apoptosis* 17, 37–47. doi: 10.1007/s10495-011-0656-3
- Jiang, P., Li, W., Shea, J. E., and Mu, Y. (2011). Resveratrol inhibits the formation of multiple-layered  $\beta$ -sheet oligomers of the human islet amyloid polypeptide segment 22–27. *Biophys. J.* 100, 1550–1558. doi: 10.1016/j.bpj.2011.02.010
- Kahn, S. E., Fujimoto, W. Y., D'Alessio, D. A., Ensink, J. W., and Porte, D. Jr. (1991). Glucose stimulates and potentiates islet amyloid polypeptide secretion by the B-cell. *Horm. Metab. Res.* 23, 577–580. doi: 10.1055/s-2007-1003759
- Kahn, S. E., Verchere, C. B., D'Alessio, D. A., Cook, D. L., and Fujimoto, W. Y. (1993). Evidence for selective release of rodent islet amyloid polypeptide through the constitutive secretory pathway. *Diabetologia* 36, 570–573. doi: 10.1007/BF02743276
- Kamihira-Ishijima, M., Nakazawa, H., Kira, A., Naito, A., and Nakayama, T. (2012). Inhibitory mechanism of pancreatic amyloid fibril formation: formation of the complex between tea catechins and the fragment of residues 22–27. *Biochemistry* 51, 10167–10174. doi: 10.1021/bi3012274
- Kanatsuka, A., Kou, S., and Makino, H. (2018). Correction to: IAPP/amylin and betacell failure: implication of the risk factors of type 2 diabetes. *Diabetol. Int.* 9, 143–157. doi: 10.1007/s13340-018-0363-1
- Kandimalla, R., Thirumala, V., and Reddy, P. H. (2017). Is Alzheimer's disease a Type 3 Diabetes? A critical appraisal. *Biochim. Biophys. Acta Mol. Basis. Dis.* 1863, 1078–1089. doi: 10.1016/j.bbdis.2016.08.018
- Kawarabayashi, T., Younkin, L. H., Saido, T. C., Shoji, M., Ashe, K. H., and Younkin, S. G. (2001). Age-dependent changes in brain, CSF, and plasma amyloid (beta) protein in the Tg2576 transgenic mouse model of Alzheimer's disease. *J. Neurosci.* 21, 372–381. doi: 10.1523/JNEUROSCI.21-02-00372.2001
- Kim, J., Cheon, H., Taek Jeong, Y., Quan, W., Kim, K., Min Cho, J., et al. (2014). Amyloidogenic peptide oligomer accumulation in autophagy-deficient  $\beta$  cells induces diabetes. *J. Clin. Invest.* 124, 3311–3324. doi: 10.1172/JCI69625
- Kiriya, Y., and Nohi, H. (2018). Role and cytotoxicity of amylin and protection of pancreatic islet beta-cells from amylin cytotoxicity. *Cell* 7:95. doi: 10.3390/cells7080095
- Konarkowska, B., Aitken, J. F., Kistler, J., Zhang, S., and Cooper, G. J. (2005). Thiol reducing compounds prevent human amylin-evoked cytotoxicity. *FEBS J.* 272, 4949–4959. doi: 10.1111/j.1742-4658.2005.04903.x
- Kuperstein, I., Broersen, K., Benilova, I., Rozenski, J., Jonckheere, W., Debulpaep, M., et al. (2010). Neurotoxicity of Alzheimer's disease A $\beta$  peptides is induced by small changes in the A $\beta$ 42 to A $\beta$ 40 ratio. *EMBO J.* 29, 3408–3420. doi: 10.1038/emboj.2010.211
- Kurochkin, I. V., and Goto, S. (1994). Alzheimer's beta-amyloid peptide specifically interacts with and is degraded by insulin degrading enzyme. *FEBS Lett.* 345, 33–37. doi: 10.1016/0014-5793(94)00387-4
- Ladiwala, A. R., Dordick, J. S., and Tessier, P. M. (2011). Aromatic small molecules remodel toxic soluble oligomers of amyloid beta through three independent pathways. *J. Biol. Chem.* 286, 3209–3218. doi: 10.1074/jbc.M110.173856
- Lane, C. A., Hardy, J., and Schott, J. M. (2018). Alzheimer's disease. *Eur. J. Neurol.* 25, 59–70. doi: 10.1111/ene.13439
- Lee, Y. H., Lin, Y., Cox, S. J., Kinoshita, M., Sahoo, B. R., Ivanova, M., et al. (2019). Zinc boosts EGCG's hIAPP amyloid Inhibition both in solution and membrane. *Biochim. Biophys. Acta Proteins Proteom.* 1867, 529–536. doi: 10.1016/j.bbapap.2018.11.006
- Leszek, J., Trypka, E., Tarasov, V. V., Ashraf, G. M., and Aliev, G. (2017). Type 3 diabetes mellitus: a novel implication of Alzheimers disease. *Curr. Top. Med. Chem.* 17, 1331–1335. doi: 10.2174/1568026617666170103163403
- Li, W., and Huang, E. (2016). An update on type 2 diabetes mellitus as a risk factor for dementia. *J. Alzheimers Dis.* 53, 393–402. doi: 10.3233/JAD-160114
- Li, W., Wang, T., and Xiao, S. (2016a). Type 2 diabetes mellitus might be a risk factor for mild cognitive impairment progressing to Alzheimer's disease. *Neuropsychiatr. Dis. Treat.* 12, 2489–2495. doi: 10.2147/NDT.S111298
- Li, X., Wan, M., Gao, L., and Fang, W. (2016b). Mechanism of inhibition of human islet amyloid polypeptide-induced membrane damage by a small organic fluorogen. *Sci. Rep.* 6:21614. doi: 10.1038/srep21614
- Li, Z. M., and Li, X. F. (2012). Functional coupling reactions of human amylin receptor and nicotinic acetylcholine receptors in rat brain neurons. *Acta Psychol. Sin.* 44, 69–74.
- Liberini, C. G., Borner, T., Boyle, C. N., and Lutz, T. A. (2016). The satiating hormone amylin enhances neurogenesis in the area postrema of adult rats. *Mol. Metab.* 5, 834–843. doi: 10.1016/j.molmet.2016.06.015
- Lim, Y. A., Rhein, V., Baysang, G., Meier, F., Poljak, A., Raftery, M. J., et al. (2010). Abeta and human amylin share a common toxicity pathway via mitochondrial dysfunction. *Proteomics* 10, 1621–1633. doi: 10.1002/pmic.200900651
- Liu, Y., Liu, F., Grundke-Iqbal, I., Iqbal, K., and Gong, C. X. (2011). Deficient brain insulin signalling pathway in Alzheimer's disease and diabetes. *J. Pathol.* 225, 54–62. doi: 10.1002/path.2912
- Lolicato, F., Raudino, A., Milardi, D., and La Rosa, C. (2015). Resveratrol interferes with the aggregation of membrane-bound human-IAPP: a molecular dynamics study. *Eur. J. Med. Chem.* 92, 876–881. doi: 10.1016/j.ejmech.2015.01.047
- López, L. C., Varela, O., Navarro, S., Carrodegua, J. A., Sanchez de Groot, N., Ventura, S., et al. (2016). Benzbromarone, quercetin, and folic acid inhibit amylin aggregation. *Int. J. Mol. Sci.* 17, 964. doi: 10.3390/ijms17060964
- Lorenzo, A., Razzaboni, B., Weir, G. C., and Yankner, B. A. (1994). Pancreatic islet cell toxicity of amylin associated with type-2 diabetes mellitus. *Nature* 368, 756–760. doi: 10.1038/368756a0
- Lorenzo, A., and Yankner, B. A. (1996). Amyloid fibril toxicity in Alzheimer's disease and diabetes. *Ann. N. Y. Acad. Sci.* 777, 89–95. doi: 10.1111/j.1749-6632.1996.tb34406.x
- Lutz, T. A. (2010). The role of amylin in the control of energy homeostasis. *Am. J. Physiol. Regul. Integr. Comp. Physiol.* 298, R1475–R1484. doi: 10.1152/ajpregu.00703.2009
- Lv, W., Zhang, J., Jiao, A., Wang, B., Chen, B., and Lin, J. (2019). Resveratrol attenuates hIAPP amyloid formation and restores the insulin secretion ability in hIAPP-INS1 cell line via enhancing autophagy. *Can. J. Physiol. Pharmacol.* 97, 82–89. doi: 10.1139/cjpp-2016-0686
- Ly, H., Verma, N., Wu, F., Liu, M., Saatman, K. E., Nelson, P. T., et al. (2017). Brain microvascular injury and white matter disease provoked by diabetes-associated hyperamylinemia. *Ann. Neurol.* 82, 208–222. doi: 10.1002/ana.24992
- Makin, S. (2018). The amyloid hypothesis on trial. *Nature* 559, S4–S7. doi: 10.1038/d41586-018-05719-4
- Marambaud, P., Zhao, H., and Davies, P. (2005). Resveratrol promotes clearance of Alzheimer's disease amyloid-beta peptides. *J. Biol. Chem.* 280, 37377–37382. doi: 10.1074/jbc.M508246200
- Martins, I. C., Kuperstein, I., Wilkinson, H., Maes, E., Vanbrabant, M., Jonckheere, W., et al. (2008). Lipids revert inert Abeta amyloid fibrils to neurotoxic protofibrils that affect learning in mice. *EMBO J.* 27, 224–233. doi: 10.1038/sj.emboj.7601953
- Marzban, L., Rhodes, C. J., Steiner, D. F., Haataja, L., Halban, P. A., and Verchere, C. B. (2006). Impaired NH<sub>2</sub>-terminal processing of human proislet amyloid polypeptide by the prohormone convertase PC2 leads to amyloid formation and cell death. *Diabetes* 55, 2192–2201. doi: 10.2337/db05-1566
- Masters, S. L., Dunne, A., Subramanian, S. L., Hull, R. L., Tannahill, G. M., Sharp, F. A., et al. (2010). Activation of the NLRP3 inflammasome by islet amyloid polypeptide provides a mechanism for enhanced IL-1 $\beta$  in type 2 diabetes. *Nat. Immunol.* 11, 897–904. doi: 10.1038/ni.1935
- Maurer-Stroh, S., Debulpaep, M., Kummerer, N., Lopez de la Paz, M., Martins, I. C., Reumers, J., et al. (2010). Exploring the sequence determinants of amyloid structure using position-specific scoring matrices. *Nat. Methods* 7, 237–242. doi: 10.1038/nmeth.1432
- McDermott, J. R., and Gibson, A. M. (1997). Degradation of Alzheimer's beta-amyloid protein by human and rat brain peptidases: involvement of insulin-degrading enzyme. *Neurochem. Res.* 22, 49–56. doi: 10.1023/A:1027325304203
- Meng, F., Abedini, A., Plesner, A., Verchere, C. B., and Raleigh, D. P. (2010). The flavanol (-)-epigallocatechin 3-gallate inhibits amyloid formation by islet amyloid polypeptide, disaggregates amyloid fibrils, and protects cultured cells against IAPP-induced toxicity. *Biochemistry* 49, 8127–8133. doi: 10.1021/bi100939a
- Messier, C., and Teutenberg, K. (2005). The role of insulin, insulin growth factor, and insulin-degrading enzyme in brain aging and Alzheimer's disease. *Neural. Plast.* 12, 311–328. doi: 10.1155/NP.2005.311
- Mietlicki-Baase, E. G. (2018). Amylin in Alzheimer's disease: pathological peptide or potential treatment? *Neuropharmacology* 136(Pt B), 287–297. doi: 10.1016/j.neuropharm.2017.12.016
- Mirhashemi, S. M. (2012). To evaluate likely anti-amyloidogenic property of ferulic acid and baicalin against human islet amyloid polypeptide aggregation, *in vitro* study. *Afr. J. Pharm. Pharmacol.* 6, 671–676. doi: 10.5897/AJPP12.033
- Mishra, R., Sellin, D., Radovan, D., Gohlke, A., and Winter, R. (2009). Inhibiting islet amyloid polypeptide fibril formation by the red wine compound resveratrol. *Chembiochem* 10, 445–449. doi: 10.1002/cbic.200800762

- Moreno-Gonzalez, I., Edwards Iii, G., Salvadores, N., Shah Nawaz, M., Diaz-Espinoza, R., and Soto, C. (2017). Molecular interaction between type 2 diabetes and Alzheimer's disease through cross-seeding of protein misfolding. *Mol. Psychiatry* 22, 1327–1334. doi: 10.1038/mp.2016.230
- Morita, S., Sakagashira, S., Ueyama, M., Shimajiri, Y., Furuta, M., and Sanke, T. (2011). Progressive deterioration of insulin secretion in Japanese type2 diabetic patients in comparison with those who carry the S20G mutation of the islet amyloid polypeptide gene: a long-term follow-up study. *J. Diabetes Investig.* 2, 287–292. doi: 10.1111/j.2040-1124.2011.00102.x
- Mukherjee, A., Morales-Scheiing, D., Salvadores, N., Moreno-Gonzalez, I., Gonzalez, C., Taylor-Presse, K., et al. (2017). Induction of IAPP amyloid deposition and associated diabetic abnormalities by a prion-like mechanism. *J. Exp. Med.* 214, 2591–2610. doi: 10.1084/jem.20161134
- Mulder, H., Ahren, B., and Sundler, F. (1996). Islet amyloid polypeptide and insulin gene expression are regulated in parallel by glucose *in vivo* in rats. *Am. J. Physiol.* 271(6 Pt 1), E1008–E1014. doi: 10.1152/ajpendo.1996.271.6.E1008
- Nedumpully-Govindan, P., Kakinien, A., Pilkington, E. H., Davis, T. P., Chun Ke, P., and Ding, F. (2016). Stabilizing Off-pathway oligomers by polyphenol nanoassemblies for iapp aggregation inhibition. *Sci. Rep.* 6:19463. doi: 10.1038/srep19463
- Noor, H., Cao, P., and Raleigh, D. P. (2012). Morin hydrate inhibits amyloid formation by islet amyloid polypeptide and disaggregates amyloid fibers. *Protein Sci.* 21, 373–382. doi: 10.1002/pro.2023
- Norwitz, N. G., Mota, A. S., Norwitz, S. G., and Clarke, K. (2019). Multi-Loop model of alzheimer disease: an integrated perspective on the Wnt/GSK3 $\beta$ , alpha-synuclein, and type 3 diabetes hypotheses. *Front. Aging Neurosci.* 11:184. doi: 10.3389/fnagi.2019.00184
- O'Nuallain, B., Williams, A. D., Westermark, P., and Wetzal, R. (2004). Seeding specificity in amyloid growth induced by heterologous fibrils. *J. Biol. Chem.* 279, 17490–17499. doi: 10.1074/jbc.M311300200
- Oskarsson, M. E., Paulsson, J. F., Schultz, S. W., Ingelsson, M., Westermark, P., and Westermark, G. T. (2015). *In vivo* seeding and cross-seeding of localized amyloidosis: a molecular link between type 2 diabetes and Alzheimer disease. *Am. J. Pathol.* 185, 834–846. doi: 10.1016/j.ajpath.2014.11.016
- Palhano, F. L., Lee, J., Grimster, N. P., and Kelly, J. W. (2013). Toward the molecular mechanism(s) by which EGCG treatment remodels mature amyloid fibrils. *J. Am. Chem. Soc.* 135, 7503–7510. doi: 10.1021/ja3115696
- Panickar, K. S. (2013). Effects of dietary polyphenols on neuroregulatory factors and pathways that mediate food intake and energy regulation in obesity. *Mol. Nutr. Food Res.* 57, 34–47. doi: 10.1002/mnfr.2012.00431
- Paulsson, J. F., Andersson, A., Westermark, P., and Westermark, G. T. (2006). Intracellular amyloid-like deposits contain unprocessed pro-islet amyloid polypeptide (proIAPP) in beta cells of transgenic mice overexpressing the gene for human IAPP and transplanted human islets. *Diabetologia* 49, 1237–1246. doi: 10.1007/s00125-006-0206-7
- Pithadia, A., Brender, J. R., Fierke, C. A., and Ramamoorthy, A. (2016). Inhibition of IAPP aggregation and toxicity by natural products and derivatives. *J. Diabetes Res.* 2016:2046327. doi: 10.1155/2016/2046327
- Poitout, V., and Robertson, R. P. (2002). Minireview: Secondary beta-cell failure in type 2 diabetes—a convergence of glucotoxicity and lipotoxicity. *Endocrinology* 143, 339–342. doi: 10.1210/endo.143.2.8623
- Qiu, Q., Lin, X., Sun, L., Zhu, M. J., Wang, T., Wang, J. H., et al. (2019). Cognitive decline is related to high blood glucose levels in older Chinese adults with the ApoE  $\epsilon$ 3/ $\epsilon$ 3 genotype. *Transl. Neurodegener.* 8:12. doi: 10.1186/s40035-019-0151-2
- Qiu, W. Q., Walsh, D. M., Ye, Z., Vekrellis, K., Zhang, J., Podlisny, M. B., et al. (1998). Insulin-degrading enzyme regulates extracellular levels of amyloid beta-protein by degradation. *J. Biol. Chem.* 273, 32730–32738. doi: 10.1074/jbc.273.49.32730
- Radovan, D., Opitz, N., and Winter, R. (2009). Fluorescence microscopy studies on islet amyloid polypeptide fibrillation at heterogeneous and cellular membrane interfaces and its inhibition by resveratrol. *FEBS Lett.* 583, 1439–1445. doi: 10.1016/j.febslet.2009.03.059
- Ramasamy, R., Yan, S. F., and Schmidt, A. M. (2011). Receptor for AGE (RAGE): signaling mechanisms in the pathogenesis of diabetes and its complications. *Ann. N. Y. Acad. Sci.* 1243, 88–102. doi: 10.1111/j.1749-6632.2011.06320.x
- Ren, B., Liu, Y., Zhang, Y., Cai, Y., and Gong, X. (2018). Genistein: a dual inhibitor of both amyloid beta and human islet amylin peptides. *ACS Chem. Neurosci.* 9, 1215–1224. doi: 10.1021/acschemneuro.8b00039
- Rezaei-Ghaleh, N., Andreotto, E., Yan, L. M., Kapurniotu, A., and Zweckstetter, M. (2011). Interaction between amyloid beta peptide and an aggregation blocker peptide mimicking islet amyloid polypeptide. *PLoS ONE* 6:e20289. doi: 10.1371/journal.pone.0020289
- Rigacci, S., Guidotti, V., Bucciantini, M., Parri, M., Nediani, C., Cerbai, E., et al. (2010). Oleuropein aglycon prevents cytotoxic amyloid aggregation of human amylin. *J. Nutr. Biochem.* 21, 726–735. doi: 10.1016/j.jnutbio.2009.04.010
- Rigacci, S., Miceli, C., Nediani, C., Berti, A., Cascella, R., Pantano, D., et al. (2015). Oleuropein aglycone induces autophagy via the AMPK/mTOR signalling pathway: a mechanistic insight. *Oncotarget* 6, 35344–35357. doi: 10.18632/oncotarget.6119
- Rivera, E. J., Goldin, A., Fulmer, N., Tavares, R., Wands, J. R., and de la Monte, S. M. (2005). Insulin and insulin-like growth factor expression and function deteriorate with progression of Alzheimer's disease: link to brain reductions in acetylcholine. *J. Alzheimers Dis.* 8, 247–268. doi: 10.3233/JAD-2005-8304
- Rivera, J. F., Gurlo, T., Daval, M., Huang, C. J., Matveyenko, A. V., Butler, P. C., et al. (2011). Human-IAPP disrupts the autophagy/lysosomal pathway in pancreatic  $\beta$ -cells: protective role of p62-positive cytoplasmic inclusions. *Cell Death Differ.* 18, 415–426. doi: 10.1038/cdd.2010.111
- Sakagashira, S., Hiddinga, H. J., Tateishi, K., Sanke, T., Hanabusa, T., Nanjo, K., et al. (2000). S20G mutant amylin exhibits increased *in vitro* amyloidogenicity and increased intracellular cytotoxicity compared to wild-type amylin. *Am. J. Pathol.* 157, 2101–2109. doi: 10.1016/S0002-9440(10)64848-1
- Sanke, T., Bell, G. I., Sample, C., Rubenstein, A. H., and Steiner, D. F. (1988). An islet amyloid peptide is derived from an 89-amino acid precursor by proteolytic processing. *J. Biol. Chem.* 263, 17243–17246.
- Schubert, M., Brazil, D. P., Burks, D. J., Kushner, J. A., Ye, J., Flint, C. L., et al. (2003). Insulin receptor substrate-2 deficiency impairs brain growth and promotes tau phosphorylation. *J. Neurosci.* 23, 7084–7092. doi: 10.1523/JNEUROSCI.23-18-07084.2003
- Schubert, M., Gautam, D., Surjo, D., Ueki, K., Baudler, S., Schubert, D., et al. (2004). Role for neuronal insulin resistance in neurodegenerative diseases. *Proc. Natl. Acad. Sci. U.S.A.* 101, 3100–3105. doi: 10.1073/pnas.0308724101
- Sciaccia, M. F. M., Chillemi, R., Sciuto, S., Greco, V., Messineo, C., Kotler, S. A., et al. (2018). A blend of two resveratrol derivatives abolishes hIAPP amyloid growth and membrane damage. *Biochim. Biophys. Acta Biomembr.* 1860, 1793–1802. doi: 10.1016/j.bbamem.2018.03.012
- Sequeira, I. R., and Poppitt, S. D. (2017). Unfolding novel mechanisms of polyphenol flavonoids for better glycaemic control: targeting pancreatic Islet Amyloid Polypeptide (IAPP). *Nutrients* 9:788. doi: 10.3390/nu9070788
- Shoval, H., Weiner, L., Gazit, E., Levy, M., Pinchuk, I., and Lichtenberg, D. (2008). Polyphenol-induced dissociation of various amyloid fibrils results in a methionine-independent formation of ROS. *Biochim. Biophys. Acta* 1784, 1570–1577. doi: 10.1016/j.bbapap.2008.08.007
- Silveira, A. C., Dias, J. P., Santos, V. M., Oliveira, P. F., Alves, M. G., Rato, L., et al. (2019). The action of polyphenols in diabetes mellitus and alzheimer's disease: a common agent for overlapping pathologies. *Curr. Neuropharmacol.* 17, 590–613. doi: 10.2174/1570159X16666180803162059
- Sparks, S., Liu, G., Robbins, K. J., and Lazo, N. D. (2012). Curcumin modulates the self-assembly of the islet amyloid polypeptide by disassembling alpha-helix. *Biochem. Biophys. Res. Commun.* 422, 551–555. doi: 10.1016/j.bbrc.2012.05.013
- Srodulski, S., Sharma, S., Bachstetter, A. B., Brelsfoard, J. M., Pascual, C., Xie, X. S., et al. (2014). Neuroinflammation and neurologic deficits in diabetes linked to brain accumulation of amylin. *Mol. Neurodegener.* 9:30. doi: 10.1186/1750-1326-9-30
- Stumvoll, M., Goldstein, B. J., and van Haeften, T. W. (2005). Type 2 diabetes: principles of pathogenesis and therapy. *Lancet* 365, 1333–1346. doi: 10.1016/S0140-6736(05)61032-X
- Suzuki, Y., Brender, J. R., Hartman, K., Ramamoorthy, A., and Marsh, E. N. G. (2012). Alternative pathways of human islet amyloid polypeptide aggregation distinguished by (19)f nuclear magnetic resonance-detected kinetics of monomer consumption. *Biochemistry* 51, 8154–8162. doi: 10.1021/bi3012548
- Takeda, S., Sato, N., Uchio-Yamada, K., Sawada, K., Kunieda, T., Takeuchi, D., et al. (2010). Diabetes-accelerated memory dysfunction via cerebrovascular



- inflammation and A $\beta$  deposition in an Alzheimer mouse model with diabetes. *Proc. Natl. Acad. Sci. U.S.A.* 107, 7036–7041. doi: 10.1073/pnas.1000645107
- Talbot, K., Wang, H. Y., Kazi, H., Han, L. Y., Bakshi, K. P., Stucky, A., et al. (2012). Demonstrated brain insulin resistance in Alzheimer's disease patients is associated with IGF-1 resistance, IRS-1 dysregulation, and cognitive decline. *J. Clin. Invest.* 122, 1316–1338. doi: 10.1172/JCI59903
- Tan, S. Y., Mei Wong, J. L., Sim, Y. J., Wong, S. S., Mohamed Elhassan, S. A., Tan, S. H., et al. (2019). Type 1 and 2 diabetes mellitus: a review on current treatment approach and gene therapy as potential intervention. *Diabetes Metab. Syndr.* 13, 364–372. doi: 10.1016/j.dsx.2018.10.008
- Tu, L. H., Young, L. M., Wong, A. G., Ashcroft, A. E., Radford, S. E., and Raleigh, D. P. (2015). Mutational analysis of the ability of resveratrol to inhibit amyloid formation by islet amyloid polypeptide: critical evaluation of the importance of aromatic-inhibitor and histidine-inhibitor interactions. *Biochemistry* 54, 666–676. doi: 10.1021/bi501016r
- Velander, P., Wu, L., Ray, W. K., Helm, R. F., and Xu, B. (2016). Amylin amyloid inhibition by flavonoid baicalein: key roles of its vicinal dihydroxyl groups of the catechol moiety. *Biochemistry* 55, 4255–4258. doi: 10.1021/acs.biochem.6b00578
- Wang, Q., Guo, J., Jiao, P., Liu, H., and Yao, X. (2014). Exploring the influence of EGCG on the beta-sheet-rich oligomers of human islet amyloid polypeptide (hIAPP1-37) and identifying its possible binding sites from molecular dynamics simulation. *PLoS ONE* 9:e94796. doi: 10.1371/journal.pone.0094796
- Wang, Q., Ning, L., Niu, Y., Liu, H., and Yao, X. (2015a). Molecular mechanism of the inhibition and remodeling of human islet amyloid polypeptide (hIAPP(1-37)) oligomer by resveratrol from molecular dynamics simulation. *J. Phys. Chem. B* 119, 15–24. doi: 10.1021/jp507529f
- Wang, Q., Zhou, S., Wei, W., Yao, X., Liu, H., and Hu, Z. (2015b). Computational insights into the inhibition and destabilization of morin on the oligomer of full-length human islet amyloid polypeptide. *Phys. Chem. Chem. Phys.* 17, 29103–29112. doi: 10.1039/C5CP03991F
- Westermarck, G. T., Steiner, D. F., Gebre-Medhin, S., Engstrom, U., and Westermarck, P. (2000). Pro islet amyloid polypeptide (ProIAPP) immunoreactivity in the islets of Langerhans. *Ups J. Med. Sci.* 105, 97–106. doi: 10.1517/03009734000000057
- Westermarck, P., Andersson, A., and Westermarck, G. T. (2011). Islet amyloid polypeptide, islet amyloid, and diabetes mellitus. *Physiol. Rev.* 91, 795–826. doi: 10.1152/physrev.00042.2009
- Westermarck, P., and Grimelius, L. (1973). The pancreatic islet cells in insular amyloidosis in human diabetic and non-diabetic adults. *Acta Pathol. Microbiol. Scand. A* 81, 291–300. doi: 10.1111/j.1699-0463.1973.tb03538.x
- Westwood, A. J., Beiser, A., Decarli, C., Harris, T. B., Chen, T. C., He, X.-M., et al. (2014). Insulin-like growth factor-1 and risk of Alzheimer dementia and brain atrophy. *Neurology* 82, 1613–1619. doi: 10.1212/WNL.0000000000000382
- Wickelgren, I. (1998). Tracking insulin to the mind. *Science* 280, 517–519. doi: 10.1126/science.280.5363.517
- Wijesekara, N., Ahrens, R., Sabale, M., Wu, L., Ha, K., Verdile, G., et al. (2017). Amyloid-beta and islet amyloid pathologies link Alzheimer's disease and type 2 diabetes in a transgenic model. *FASEB J.* 31, 5409–5418. doi: 10.1096/fj.201700431R
- Wookey, P. J., Cao, Z., and Cooper, M. E. (1998). Interaction of the renal amylin and renin-angiotensin systems in animal models of diabetes and hypertension. *Miner. Electrolyte Metab.* 24, 389–399. doi: 10.1159/000057400
- Wu, L., Velander, P., Liu, D., and Xu, B. (2017). Olive component oleuropein promotes beta-cell insulin secretion and protects beta-cells from amylin amyloid-induced cytotoxicity. *Biochemistry* 56, 5035–5039. doi: 10.1021/acs.biochem.7b00199
- Xi, X. X., Sun, J., Chen, H. C., Chen, A. D., Gao, L. P., Yin, J., et al. (2019). High-fat diet increases amylin accumulation in the hippocampus and accelerates brain aging in hIAPP transgenic mice. *Front. Aging Neurosci.* 11:225. doi: 10.3389/fnagi.2019.00225
- Xu, Z. X., Ma, G. L., Zhang, Q., Chen, C. H., He, Y. M., Xu, L. H., et al. (2017). Inhibitory mechanism of epigallocatechin gallate on fibrillation and aggregation of amidated human islet amyloid polypeptide. *Chemphyschem* 18, 1611–1619. doi: 10.1002/cphc.201700057
- Xu, Z. X., Zhang, Q., Ma, G. L., Chen, C. H., He, Y. M., Xu, L. H., et al. (2016). Influence of aluminium and ecgc on fibrillation and aggregation of human islet amyloid polypeptide. *J. Diabetes Res.* 2016:1867059. doi: 10.1155/2016/1867059
- Yan, L. M., Velkova, A., and Kapurniotu, A. (2014). Molecular characterization of the hetero-assembly of  $\beta$ -amyloid peptide with islet amyloid polypeptide. *Curr. Pharm. Des.* 20, 1182–1191. doi: 10.2174/13816128113199990064
- Yan, L. M., Velkova, A., Tarek-Nossol, M., Andreetto, E., and Kapurniotu, A. (2007). IAPP mimic blocks Abeta cytotoxic self-assembly: cross-suppression of amyloid toxicity of Abeta and IAPP suggests a molecular link between Alzheimer's disease and type II diabetes. *Angew. Chem. Int. Ed. Engl.* 46, 1246–1252. doi: 10.1002/anie.200604056
- Yang, J., Sun, Y., Xu, F., Liu, W., Hayashi, T., Hattori, S., et al. (2019a). Silibinin protects rat pancreatic  $\beta$ -cell through up-regulation of estrogen receptors' signaling against amylin- or A $\beta$ <sub>1–42</sub> -induced reactive oxygen species/reactive nitrogen species generation. *Phytother. Res.* 33, 998–1009. doi: 10.1002/ptr.6293
- Yang, J., Sun, Y., Xu, F., Liu, W., Mai, Y., Hayashi, T., et al. (2019b). Silibinin ameliorates amylin-induced pancreatic beta-cell apoptosis partly via upregulation of GLP-1R/PKA pathway. *Mol. Cell Biochem.* 452, 83–94. doi: 10.1007/s11010-018-3414-9
- Yang, Y., and Song, W. (2013). Molecular links between Alzheimer's disease and diabetes mellitus. *Neuroscience* 250, 140–150. doi: 10.1016/j.neuroscience.2013.07.009
- Yonemoto, I. T., Kroon, G. J. A., Dyson, H. J., Balch, W. E., and Kelly, J. W. (2008). Amylin propeptide processing generates progressively more amyloidogenic peptides that initially sample the helical state. *Biochemistry* 47, 9900–9910. doi: 10.1021/bi800828u
- Young, L. M., Cao, P., Raleigh, D. P., Ashcroft, A. E., and Radford, S. E. (2014a). Ion mobility spectrometry-mass spectrometry defines the oligomeric intermediates in amylin amyloid formation and the mode of action of inhibitors. *J. Am. Chem. Soc.* 136, 660–670. doi: 10.1021/ja406831n
- Young, L. M., Saunders, J. C., Mahood, R. A., Revell, C. H., Foster, R. J., Tu, L.-H., et al. (2014b). Screening and classifying small-molecule inhibitors of amyloid formation using ion mobility spectrometry-mass spectrometry. *Nat. Chem.* 7, 73–81. doi: 10.1038/nchem.2129
- Yu, X. L., Li, Y. N., Zhang, H., Su, Y. J., Zhou, W. W., Zhang, Z. P., et al. (2015). Rutin inhibits amylin-induced neurocytotoxicity and oxidative stress. *Food Funct.* 6, 3296–3306. doi: 10.1039/C5FO00500K
- Zelus, C., Fox, A., Calciano, A., Faridian, B. S., Nogaj, L. A., and Moffet, D. A. (2012). Myricetin inhibits Islet Amyloid Polypeptide (IAPP) Aggregation and rescues living mammalian cells from IAPP toxicity. *Open Biochem. J.* 6, 66–70. doi: 10.2174/1874091X01206010066
- Zhang, X.-X., Pan, Y.-H., Huang, Y.-M., and Zhao, H.-L. (2016). Neuroendocrine hormone amylin in diabetes. *World J. Diabetes* 7, 189–197. doi: 10.4239/wjd.v7.i9.189
- Zhao, H. L., Sui, Y., Guan, J., He, L., Gu, X. M., Wong, H. K., et al. (2009). Amyloid oligomers in diabetic and nondiabetic human pancreas. *Transl. Res.* 153, 24–32. doi: 10.1016/j.trsl.2008.10.009
- Zhao, W. Q., and Alkon, D. L. (2001). Role of insulin and insulin receptor in learning and memory. *Mol. Cell Endocrinol.* 177, 125–134. doi: 10.1016/S0303-7207(01)00455-5
- Zheng, Q., and Lazo, N. D. (2018). Mechanistic studies of the inhibition of insulin fibril formation by rosmarinic acid. *J. Phys. Chem. B* 122, 2323–2331. doi: 10.1021/acs.jpcc.8b00689

**Conflict of Interest:** The authors declare that the research was conducted in the absence of any commercial or financial relationships that could be construed as a potential conflict of interest.

Copyright © 2020 Raimundo, Ferreira, Martins and Menezes. This is an open-access article distributed under the terms of the Creative Commons Attribution License (CC BY). The use, distribution or reproduction in other forums is permitted, provided the original author(s) and the copyright owner(s) are credited and that the original publication in this journal is cited, in accordance with accepted academic practice. No use, distribution or reproduction is permitted which does not comply with these terms.





# Substrate–Enzyme Interactions in Intramembrane Proteolysis: $\gamma$ -Secretase as the Prototype

Xinyue Liu<sup>1</sup>, Jing Zhao<sup>1</sup>, Yingkai Zhang<sup>2</sup>, Iban Ubarretxena-Belandia<sup>3,4</sup>, Scott Forth<sup>1,5</sup>, Raquel L. Lieberman<sup>6</sup> and Chunyu Wang<sup>1,5,7\*</sup>

<sup>1</sup>Center for Biotechnology and Interdisciplinary Studies, Rensselaer Polytechnic Institute, Troy, NY, United States,

<sup>2</sup>Department of Chemistry, New York University, New York, NY, United States, <sup>3</sup>Instituto Biofisika (UPV/EHU, CSIC),

University of the Basque Country, Leioa, Spain, <sup>4</sup>Ikerbasque, Basque Foundation for Science, Bilbao, Spain, <sup>5</sup>Department of

Biological Sciences, Rensselaer Polytechnic Institute, Troy, NY, United States, <sup>6</sup>School of Chemistry and Biochemistry,

Georgia Institute of Technology, Atlanta, GA, United States, <sup>7</sup>Department of Chemistry and Chemical Biology, Rensselaer

Polytechnic Institute, Troy, NY, United States

## OPEN ACCESS

### Edited by:

Maria Rosário Almeida,  
University of Porto, Portugal

### Reviewed by:

Homira Behbahani,  
Karolinska Institutet (KI), Sweden  
Hong Qing,  
Beijing Institute of Technology, China

### \*Correspondence:

Chunyu Wang  
wangc5@rpi.edu

**Received:** 19 December 2019

**Accepted:** 03 April 2020

**Published:** 19 May 2020

### Citation:

Liu X, Zhao J, Zhang Y,  
Ubarretxena-Belandia I, Forth S,  
Lieberman RL and Wang C  
(2020) Substrate–Enzyme  
Interactions in Intramembrane  
Proteolysis:  $\gamma$ -Secretase as the  
Prototype.  
*Front. Mol. Neurosci.* 13:65.  
doi: 10.3389/fnmol.2020.00065

Intramembrane-cleaving proteases (I-CLiPs) catalyze the hydrolysis of peptide bonds within the transmembrane regions of membrane protein substrates, releasing bioactive fragments that play roles in many physiological and pathological processes. Based on their catalytic mechanism and nucleophile, I-CLiPs are classified into metallo-, serine, aspartyl, and glutamyl proteases. Presenilin is the most prominent among I-CLiPs, as the catalytic subunit of  $\gamma$ -secretase (GS) complex responsible for cleaving the amyloid precursor protein (APP) and Notch, as well as many other membrane substrates. Recent cryo-electron microscopy (cryo-EM) structures of GS provide new details on how presenilin recognizes and cleaves APP and Notch. First, presenilin transmembrane helix (TM) 2 and 6 are dynamic. Second, upon binding to GS, the substrate TM helix is unwound from the C-terminus, resulting in an intermolecular  $\beta$ -sheet between the substrate and presenilin. The transition of the substrate C-terminus from  $\alpha$ -helix to  $\beta$ -sheet is proposed to expose the scissile peptide bond in an extended conformation, leaving it susceptible to protease cleavage. Despite the astounding new insights in recent years, many crucial questions remain unanswered regarding the inner workings of  $\gamma$ -secretase, however. Key unanswered questions include how the enzyme recognizes and recruits substrates, how substrates are translocated from an initial docking site to the active site, how active site aspartates

**Abbreviations:** I-CLiPs, intramembrane-cleaving proteases; GS,  $\gamma$ -secretase; APP, amyloid precursor protein; cryo-EM, cryo-electron microscopy; SREBPs, sterol regulatory element-binding proteins; AD, Alzheimer's disease; S2P, site-2-protease; S1P, site-1-protease; TM, transmembrane helix; IAP, intramembrane aspartate protease; PS, presenilin; SPP, signal peptide peptidase; TMD, transmembrane domain; PSH, presenilin homolog; NTF, amino-terminal fragment; CTF, carboxy-terminal fragment; SANS, small angle neutron scattering; Rce1, Ras and a-factor converting enzyme 1; MmRce1, *Methanococcus maripaludis* homolog of Rce1; ZMPSTE24, zinc metallopeptidase STE24; A $\beta$ , amyloid- $\beta$  peptide; APPTM, transmembrane domain of APP; C99, C-terminal fragment containing 99 amino acid residues; AICD, APP intracellular domain; FAD, familial Alzheimer's disease; PSEN1 and PSEN2, presenilin 1 and 2 genes; NICD, Notch intracellular domain; NCT, nicastrin; APH-1, anterior pharynx-defective 1; PEN-2, presenilin enhancer 2; DpNCT, *Dictyostelium purpureum* homolog of nicastrin; HsNCT, human nicastrin; ECD, extracellular domain; CSP, chemical shift perturbation; GSIs,  $\gamma$ -secretase inhibitors; dUVR, deep-ultraviolet resonance Raman spectra.

recruit and coordinate catalytic water, and the nature of the mechanisms of processive trimming of the substrate and product release. Answering these questions will have important implications for drug discovery aimed at selectively reducing the amyloid load in Alzheimer's disease (AD) with minimal side effects.

**Keywords:** I-CLiPs,  $\gamma$ -secretase, substrate, interaction, Alzheimer's disease

## FOUR CLASSES OF INTRAMEMBRANE-CLEAVING PROTEASES

Intramembrane-cleaving proteases (I-CLiPs, also called IMPAS) carry out regulated intramembrane proteolysis (RIP). They hydrolyze peptide bonds buried inside the membrane lipid bilayer (Brown et al., 2000) and release bioactive fragments (Haze et al., 1999; Niwa et al., 1999; Lal and Caplan, 2011; Lichtenthaler et al., 2011). Numerous I-CLiP substrates have been discovered, including the sterol regulatory element-binding proteins (SREBPs; Brown and Goldstein, 1997), the membrane receptor Notch (Selkoe and Kopan, 2003), and the amyloid precursor protein (APP; Annaert and De Strooper, 1999). I-CLiPs therefore play crucial roles in a variety of biological processes, including embryonic development, immune responses, and normal function of the nervous system. In addition, I-CLiPs contribute to many diseases such as cancer and Alzheimer's disease (AD; Winter-Vann and Casey, 2005; Lichtenthaler et al., 2011; Dusterhöft et al., 2017).

Based on their catalytic mechanisms, I-CLiPs are classified into four families: rhomboid serine proteases (Wu et al., 2006), S2P-metalloproteases (Feng et al., 2007), di-aspartyl proteases (Fluhrer et al., 2009), and glutamyl proteases (Manolaridis et al., 2013). Although six classes of soluble proteases are known, I-CLiPs using cysteine or threonine as catalytic residue have not yet been identified. In the 3D structures of I-CLiPs, the polar catalytic residues are located well below the membrane surface, shielded from hydrophobic membrane environment by surrounding transmembrane helices (TMs), whereas water molecules are readily accessible to the catalytic residues through a hydrophilic chamber or channel.

### Serine I-CLiPs

Rhomboids constitute a large superfamily of serine I-CLiPs, which are involved in developmental signaling in *Drosophila* (Wasserman and Freeman, 1997), host invasion of protozoan parasites (Sibley, 2013), and human diseases such as cancer and neurodegeneration (Bergbold and Lemberg, 2013; Dusterhöft et al., 2017). Rhomboids have been intensely studied as model I-CLiP and also for their biological importance (see an excellent review by Strisovsky et al., 2009; Tichá et al., 2018). The rhomboid fold is composed of six TMs named TM1 to TM6 (Figure 1A). The catalytic dyad, serine (on TM4) and histidine (on TM6), is located at a V-shaped cavity accessible to the aqueous phase at a distance of 10–12 Å below the membrane surface (Wang et al., 2006; Wu et al., 2006; Ben-Shem et al., 2007; Figure 1A). During intramembrane proteolysis, the histidine activates the catalytic serine for a nucleophilic

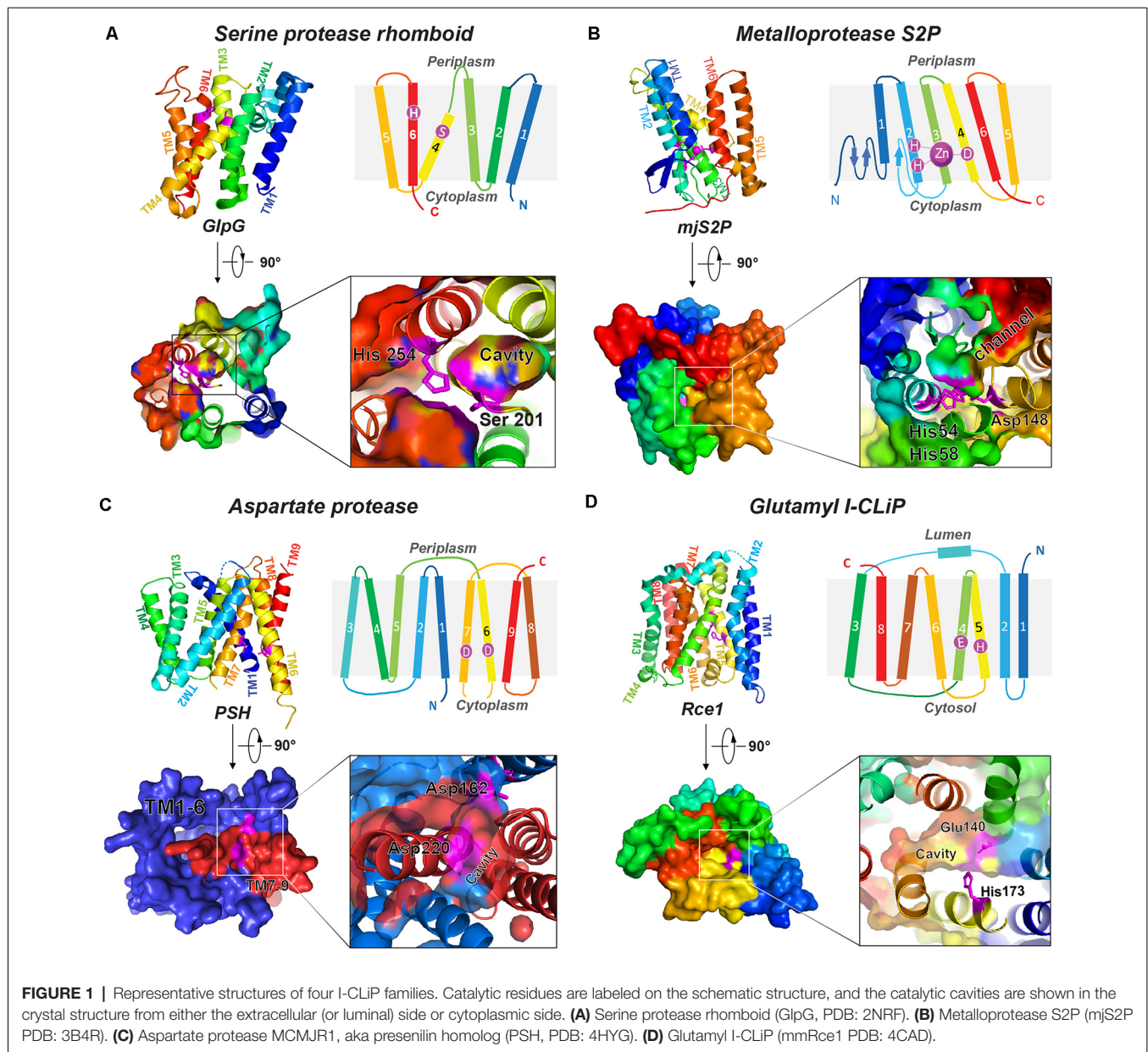
attack on substrates (Lemieux et al., 2007). Rhomboids recognize the helical TMs and a linear segment adjacent to the TMs of their substrates (Strisovsky et al., 2009). Structural and modeling studies proposed that the TMs of the substrates may bind the rhomboid at the interface of TM2 and TM5, where TM5 plays the role of the substrate gate (Baker et al., 2007; Xue and Ha, 2013; Zoll et al., 2014; Shokhen and Albeck, 2017). Binding studies reveal a role of allostery in catalysis. Dimerization of rhomboids is required for the formation of an exosite and subsequent allosteric substrate binding and activation (Arutyunova et al., 2014).

### Metalloproteases

Site-2 proteases (S2Ps) constitute another family of metalloproteases, which activate membrane-bound transcription factors through RIP. S2Ps have been well studied in the context of cholesterol metabolism, with a zinc ion at its active site (Sun et al., 2016). After site-1 protease (S1P) cleavage, S2P cleaves SREBPs. The N-terminus of SREBP is then released and enters the nucleus to activate genes for biosynthesis and uptake of cholesterol (Sakai et al., 1996; Brown and Goldstein, 1997). An X-ray structure of *Methanocaldococcus jannaschii* S2P (mjS2P; Figure 1B), an S2P ortholog, revealed six TMs and three  $\beta$ -strands. The zinc ion,  $\sim 14$  Å below the membrane surface, is coordinated by two histidine residues in an HEXXH motif ("H" is histidine, "E" is glutamate, and "X" is any amino acid) in TM2 and an aspartate in TM4 (Feng et al., 2007). Two conformations were identified: an open state and a closed state (Figure 2A). In the closed conformation, water accesses zinc via a polar channel open to the cytoplasmic side. In the open conformation, the TM1 and TM6 are separated by 10–12 Å, forming a cleft for substrate entry and positioning the catalytic zinc towards the substrate (Figure 2B).

### Di-Aspartyl Proteases

Di-aspartyl intramembrane proteases are characterized by a pair of catalytic aspartates. One of their catalytic aspartates is contained within the signature GXGD motif ("G" is glycine, "X" is any amino acid, and "D" is aspartate; Steiner et al., 2000; Fluhrer et al., 2009). Di-aspartyl intramembrane proteases are involved in many fundamental processes such as cell differentiation, development, immune surveillance, and virus maturation. This family has two key members: presenilin (PS) and signal peptide peptidase (SPP; Weihofen et al., 2002). PS is the catalytic subunit of  $\gamma$ -secretase (GS; Wolfe et al., 1999; Li et al., 2000), which cleaves Notch and APP transmembrane domain (TMD; Francis et al., 2002; Haass and Steiner, 2002), among over 90 substrates (Beel and Sanders, 2008). PS homologs (PSHs) can also cleave APP at the two major cleavage sites



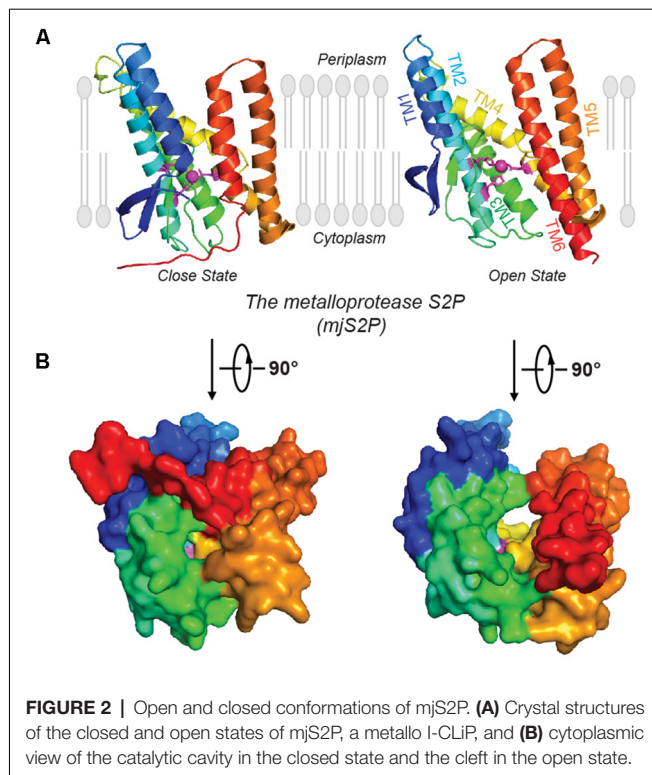
of PS (Torres-Arancivia et al., 2010; Naing et al., 2018a): the  $\gamma$ -site and the  $\epsilon$ -site, generating A $\beta$ 42 and A $\beta$ 48, respectively (Naing et al., 2018a). A  $\sim 3.3$ -Å resolution crystal structure of an ortholog from *Methanoculleus marisnigri* (MCMJR1) showed nine TMs (Figure 1C) with TM1–TM6 equivalent to the amino-terminal fragment [N-terminal fragment (NTF)] and TM7–TM9 equivalent to the C-terminal fragment (CTF) of PS formed by autoproteolysis of GS (Li et al., 2013). TM1–TM6 tilt at angles of 15–35° away from the lipid membrane surface and form a horseshoe-shaped structure surrounding the CTF TMs. The active site aspartates (Asp 162 on TM6 and Asp 220 on TM7) are located in a cavity accessible from the cytoplasmic side, approximately 8 Å from the membrane surface. The structure of MCMJR1 characterized by small angle neutron scattering

(SANS) is smaller than the crystal structure, indicating that the enzyme may be more compact in solution (Naing et al., 2018b).

## Glutamyl Proteases

Ras converting enzyme 1 (Rce1) is a glutamate intramembrane protease (Manolaridis et al., 2013) found in the endoplasmic reticulum. Rce1 carries out posttranslational modifications of proteins with a C-terminus CAAX motif (“C” is cysteine, “A” is an aliphatic amino acid, and “X” is any amino acid residue; Figure 3; Boyartchuk et al., 1997). Substrates of Rce1 include Ras and prelamin A. Rce1 cleavage of these substrates is necessary for their function. The posttranslational modifications of CAAX proteins include cysteine isoprenylation, –AAX release, and methylation of the exposed C-terminal





carboxyl of isoprenylcysteine (**Figure 3**; Schmidt et al., 1998). The Rce1 is the prenyl endopeptidase responsible for the release of the C-terminal –AAX peptide. These modifications are required for proper localization of the Ras protein (Michaelson et al., 2005) and can affect various signaling pathways during differentiation, proliferation, and oncogenesis (Winter-Vann and Casey, 2005; Christiansen et al., 2011). A crystal structure of the Rce1 ortholog from *Methanococcus maripaludis* (MmRce1) reveals eight TMs (**Figure 1D**; Manolaridis et al., 2013). TMs 4–7 form a conical cavity with an opening towards the cytosol, allowing solvent access and prenylated substrate accommodation. The catalytic dyad, a glutamate and a histidine, is located in the cavity approximately 10 Å away from the membrane surface.

Finally, a hybrid I-CLiP, ZMPSTE24, is a zinc metalloprotease that matures lamin A, a nuclear scaffold protein, through recognizing a CAAX motif (Pendás et al., 2002). Mutations in ZMPSTE24 are associated with premature aging, such as in Hutchinson–Guilford progeria syndrome (HGPS; Navarro et al., 2014). ZMPSTE24 resides in the inner nuclear membrane and is also known as farnesylated-protein converting enzyme 1 (FACE-1), and Ste24 in yeast. After farnesylation of the C-terminal CAAX motif, prelamin A is cleaved by either Rce1 or ZMPSTE24, and then the C-terminal cysteine residue is carboxymethylated (**Figure 3**). ZMPSTE24 further cleaves a 15-residue CTF, resulting in mature lamin and its release from the nuclear membrane. In progeroid conditions caused by ZMPSTE24 mutation, farnesylated and methylated prelamin accumulates in the nuclear membrane. ZMPSTE24 contains an extraordinary intramembrane chamber, large enough to

accommodate a ~10-kDa protein or ~450 water molecules (Pryor et al., 2013). The active site residues are facing the chamber, with an arrangement almost identical to bacterial thermolysin.

## GS IN HEALTH AND DISEASE

GS is reported to cleave over 90 substrates (Beel and Sanders, 2008). Conversely, aberrant GS cleavage is associated with many diseases, including cancer, skin disorder, and neurodegenerative diseases (Shih and Wang, 2007; Kelleher and Shen, 2010). Here, we highlight the two most prominent GS substrates, APP and Notch, which are involved in AD and cancer, respectively.

### GS and AD

Amyloid plaques are a hallmark of AD pathology, which are mainly composed of aggregated amyloid- $\beta$  (A $\beta$ ) peptides. A $\beta$  deposits have been proposed as the initial trigger in the decade-long progression towards neurodegeneration in AD (Tanzi and Bertram, 2005), which leads to tau pathology and eventually widespread neuroinflammation. A $\beta$  peptides are produced from APP by the consecutive action of two proteases,  $\beta$ -secretase and GS.  $\beta$ -Secretase sheds the ectodomain of APP, generating C99 and the N-terminus of the subsequent A $\beta$  species (Mullard, 2017). GS is the I-CLiP that cleaves within the TM of APP (APPTM), releasing different lengths of A $\beta$  peptides into the extracellular matrix or endosome lumen (Qi-Takahara et al., 2005; Takami et al., 2009). Longer A $\beta$  peptides (e.g., A $\beta$ 42 and A $\beta$ 43) are particularly prone to aggregation.

There are two APP processing pathways (**Figure 4**). In the non-amyloidogenic pathway, APP is first cleaved by  $\alpha$ -secretase to generate C83, and further cleavage of GS can no longer generate A $\beta$ . In the amyloidogenic pathway, APP is first cleaved by  $\beta$ -secretase to generate a membrane-bound CTF containing 99 amino acid residues (C99). C99 is then the substrate of GS to generate A $\beta$ , the pathogenic peptide for AD (Lichtenthaler et al., 2011), while the APP intracellular domain (AICD) is liberated into the cytoplasm (Haass and Steiner, 2002).  $\beta$ -Secretase and GS both localize to the lipid rafts of cell or organellar membranes, and cholesterol plays an important role in the enzyme activity (Tun et al., 2002; Urano et al., 2005). The observation of different lengths of A $\beta$  peptides suggests a successive C-terminal trimming mechanism of GS after the initial  $\epsilon$ -cleavage (Qi-Takahara et al., 2005; Takami et al., 2009). In addition to A $\beta$ 40 and A $\beta$ 42, A $\beta$ 38, A $\beta$ 43, A $\beta$ 45, A $\beta$ 46, and A $\beta$ 48 are also identified. Starting from two initial  $\epsilon$ -cleavage sites  $\epsilon$ 48 and  $\epsilon$ 49, A $\beta$ 40, A $\beta$ 43, and A $\beta$ 46 are generated from A $\beta$ 49 through successive shedding of tripeptides. Non-translational state GS inhibitors (GSI), DAPT and Compound E, suppress intracellular A $\beta$ 40 production while increasing A $\beta$ 43 and in turn A $\beta$ 46 levels (Qi-Takahara et al., 2005). A $\beta$ 45, A $\beta$ 42, and A $\beta$ 38 are generated from A $\beta$ 48 (**Figure 4**). These two product lines have been established using LC-MS/MS (Takami et al., 2009). The stepwise cleavage sites are named  $\epsilon$ 48/ $\epsilon$ 49,  $\zeta$ 45/ $\zeta$ 46,  $\zeta$ 42/ $\zeta$ 43, and  $\gamma$ 38/ $\gamma$ 40 (Lichtenthaler et al., 2011; De Strooper and Chávez Gutiérrez, 2015; Langosch and Steiner, 2017).



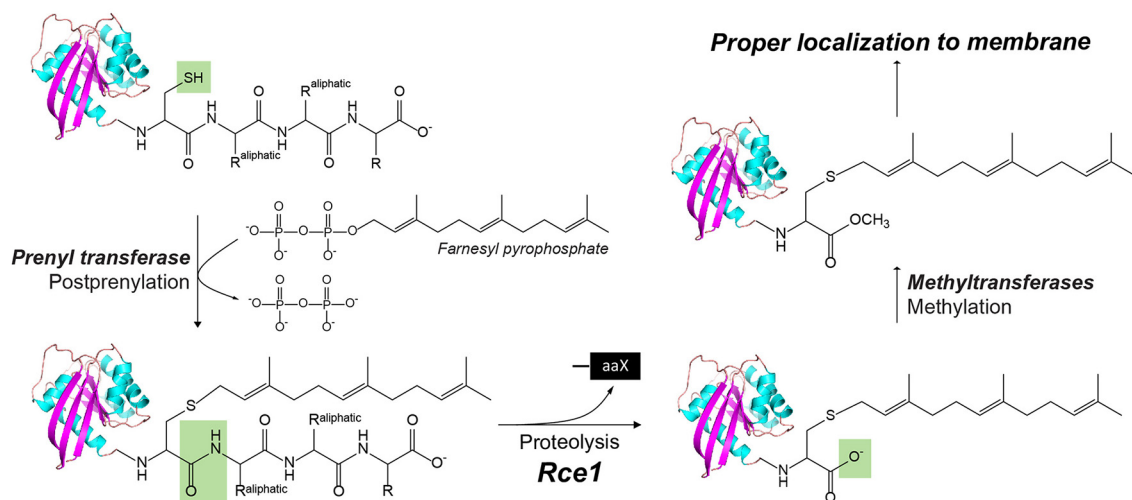


**FIGURE 3 |** The posttranslational modification of proteins with a C-terminus CAAX motif by Rce1, a glutamyl IMP. In CaaX, “C” is cysteine, “A” is an aliphatic amino acid, and “X” is any amino acid. The posttranslational modifications of CAAX proteins include the cysteine isoprenylation, the –aaX release, and carboxyl methylation of the exposed isoprenylcysteine. The Rce1 is the prenyl endopeptidase for the release of the C-terminal –aaX peptide. These modifications are required for proper localization of the Ras to the membrane.

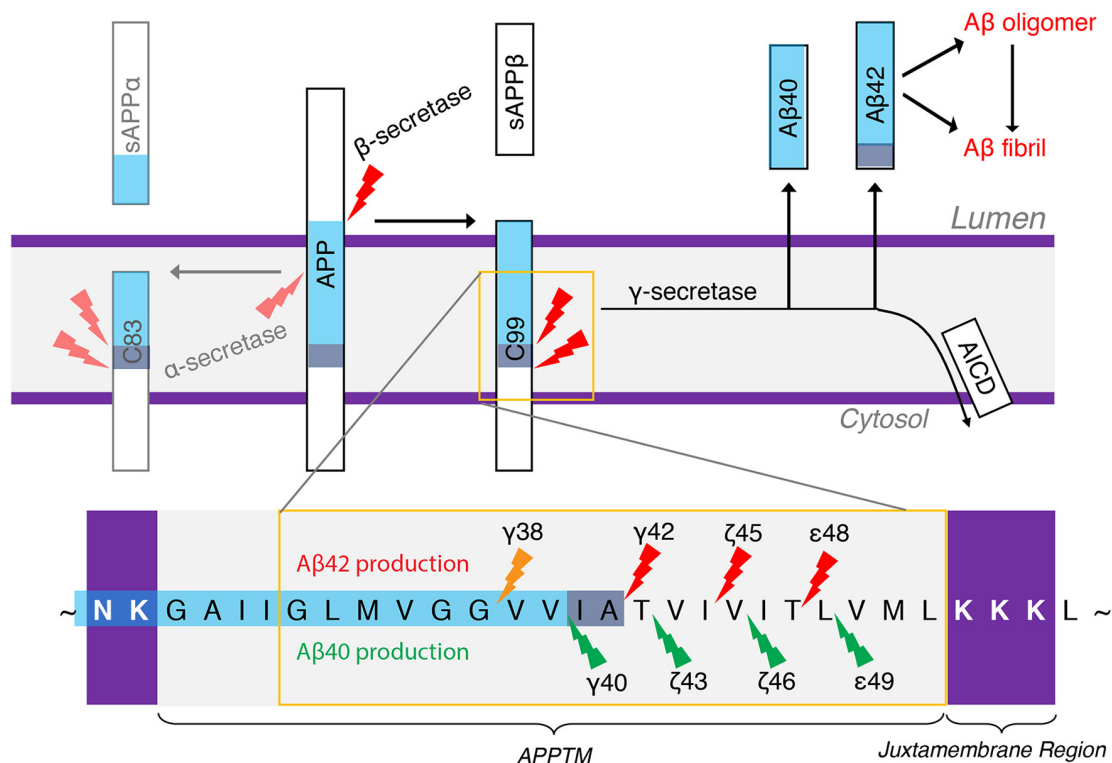


**FIGURE 4 |** The generation of Aβ40 and Aβ42 from amyloid precursor protein (APP). α-Secretase and β-secretase are the sheddases generating C83 and C99 from APP, respectively. γ-secretase (GS) is the I-CLIP that carries out intramembrane proteolysis of C99 to generate Aβ, a pathogenic peptide in Alzheimer's disease (AD).

Aβ peptides can aggregate into oligomers and fibrils. Longer Aβ forms, such as Aβ42 and Aβ43, are especially prone to aggregation and are therefore much more toxic (Makin,

2018). Mutations in APP on chromosome 21q (Levy et al., 1990; Goate et al., 1991; Tanzi and Bertram, 2005; Bertram et al., 2010) and in PS 1 and 2 genes (PSEN1 and PSEN2,

respectively) on chromosomes 14 and 1 (Levy-Lahad et al., 1995; Rogaev et al., 1995; Sherrington et al., 1995) can cause early-onset familial Alzheimer's disease (FAD), characterized by an increased A $\beta$ 42/A $\beta$ 40 ratio biochemically. The most common FAD mutations occur in PS, underlining the important biological role for GS. The successive cleavage of the APP substrates progressively destabilizes the GS–A $\beta$ <sub>n</sub> complex with the shortening of the A $\beta$ <sub>n</sub>. It has been shown that PSEN mutations will further destabilize the A $\beta$ <sub>n</sub>–GS complex, resulting in the release of longer A $\beta$ <sub>n</sub> (Szaruga et al., 2017) and raising the A $\beta$ 42/A $\beta$ 40 ratio.

As a GS substrate, the local conformation and dynamics of APPTM contribute to the observed cleavage sites. A right-handed APPTM helical dimer was characterized by nuclear magnetic resonance (NMR) in solution (Figure 5A). In the same study, FAD mutations V44M and V44A within APPTM were found to selectively expose the T48 site for fast solvent exchange. This may promote T48 for the initial  $\epsilon$ -cleavage over L49 and consequently shift cleavage preference towards A $\beta$ 42 production (Chen et al., 2014).

## GS and Notch Signaling

Notch signaling is involved in neurogenesis, synapse growth and plasticity, and neuronal death in vertebrates (Kopan and Ilagan, 2009). The Notch receptor is a single-span membrane protein like APP. For Notch-1, the TMD is from residues Ala1732 to Ser1757, terminated by a cluster of basic residues: 1758RKRRR<sub>1762</sub>, similar to the APP intracellular juxtamembrane region 724KKK<sub>726</sub> (Deatherage et al., 2017; Figures 5A,B). In the Notch signaling pathway, Notch precursors are cleaved by a furin-like convertase at Site-1 (S1), generating the mature Notch receptor, a 2,500-residue membrane protein. The shedding of the Notch ectodomain following S1 cleavage is carried out by ADAM, a metalloprotease, which is referred to as Site-2 (S2) cleavage. After shedding, the Notch receptor undergoes cleavage by GS, which, like APP, is Processive (van Tetering and Vooijs, 2011). For Notch-1, the initial cleavage, which is called the Site-3 (S3) cleavage, mainly occurs at Val1754 (Figure 5B), releasing a large Notch intracellular domain (NICD; Deatherage et al., 2017). The NICD translocates to the nucleus, forming an activator complex (Kitagawa, 2015). The processive cleavage stops at Site-4 (S4), mainly at Ala1742, and an extracellular domain (ECD) peptide (N $\beta$ ) terminating at residue 1741 is released (Deatherage et al., 2017). PS1 mutations associated with FAD also cause a shift in the N $\beta$  cleavage site, in a similar manner to A $\beta$  (Okochi et al., 2006).

## Targeting GS for AD Drug Discovery

A major theme in AD drug discovery is to reduce amyloid by inhibiting GS. To date, however, clinical trials of GSIs have failed due to severe side effects and worsening cognitive functions in patients. The so-called Notch-sparing APP-selective inhibitors, which preferentially inhibit APP cleavage over Notch by GS, did not show reduced toxicity (Crump et al., 2012; Tong et al., 2012). Another strategy in AD drug discovery is to develop GS modulators (GSM), which bias GS activity towards generating shorter, less toxic A $\beta$  peptides (Bursavich et al., 2016). Given

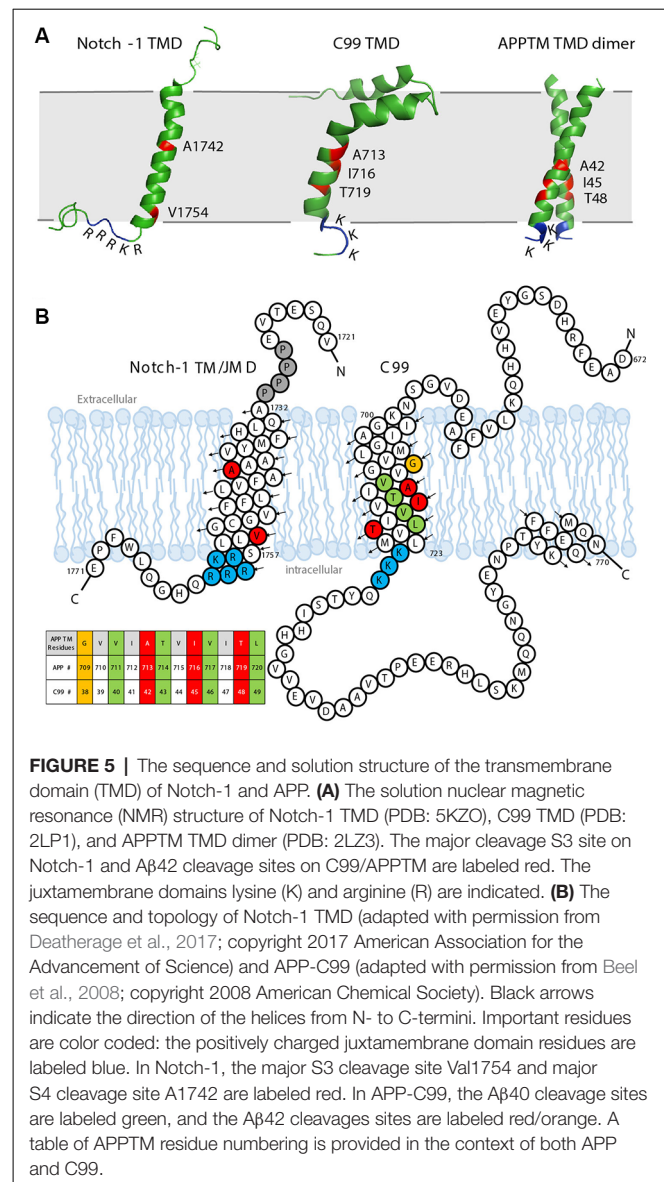


**FIGURE 5 |** The sequence and solution structure of the transmembrane domain (TMD) of Notch-1 and APP. **(A)** The solution nuclear magnetic resonance (NMR) structure of Notch-1 TMD (PDB: 5KZO), C99 TMD (PDB: 2LP1), and APPTM TMD dimer (PDB: 2LZ3). The major cleavage S3 site on Notch-1 and A $\beta$ 42 cleavage sites on C99/APPTM are labeled red. The juxtamembrane domains lysine (K) and arginine (R) are indicated. **(B)** The sequence and topology of Notch-1 TMD (adapted with permission from Deatherage et al., 2017; copyright 2017 American Association for the Advancement of Science) and APP-C99 (adapted with permission from Beel et al., 2008; copyright 2008 American Chemical Society). Black arrows indicate the direction of the helices from N- to C-termini. Important residues are color coded: the positively charged juxtamembrane domain residues are labeled blue. In Notch-1, the major S3 cleavage site Val1754 and major S4 cleavage site Ala1742 are labeled red. In APP-C99, the A $\beta$ 40 cleavage sites are labeled green, and the A $\beta$ 42 cleavage sites are labeled red/orange. A table of APPTM residue numbering is provided in the context of both APP and C99.

the complexity of the role of GS in biology beyond Notch and APP, it is imperative that the molecular details of GS interactions with substrates be understood to inform an effective strategy for discovering disease-modifying drugs in AD.

## STRUCTURES OF APO GS AND ITS SUBUNITS

There are four essential components of GS: PS (also abbreviated as PSEN), nicastrin (NCT), anterior pharynx-defective 1 (APH-1), and PS enhancer 2 (PEN-2; Kimberly et al., 2003; Figure 6A). The catalytic subunit, PS, consists of nine TMs with two catalytic aspartates, Asp257 and Asp385, located in TM6 and TM7, respectively (Wolfe et al., 1999; Li et al., 2013; Bai et al., 2015b). GS is matured and activated only after PS undergoes autoproteolysis, cleaving itself between TM6 and TM7 and

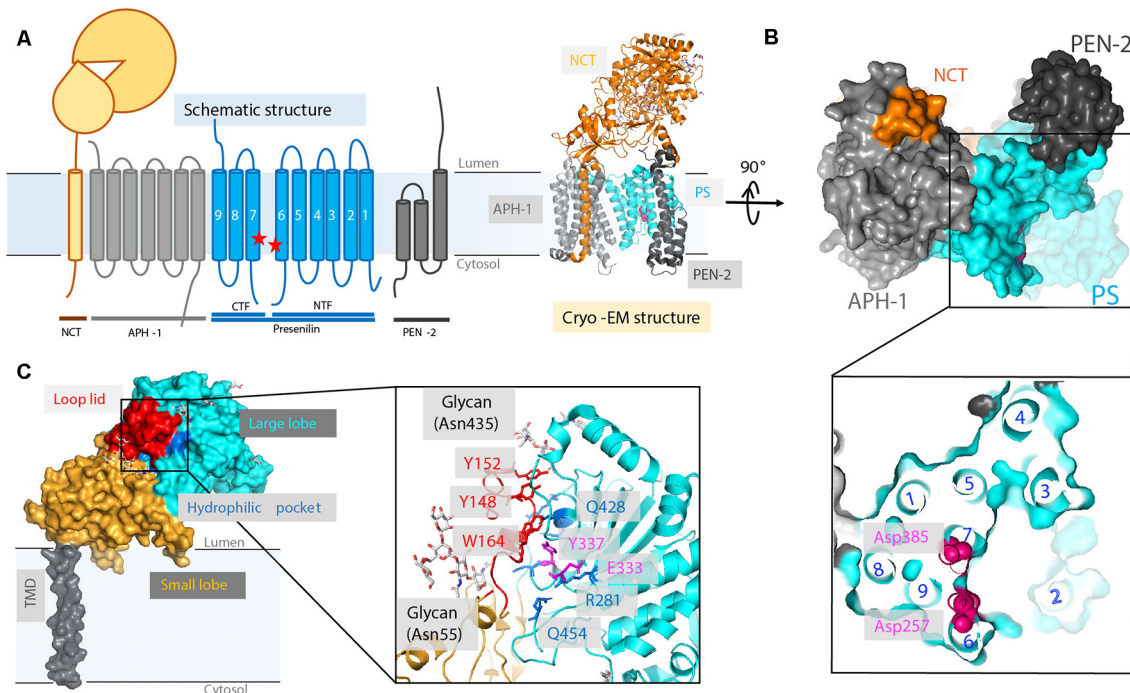


**FIGURE 6 |** High-resolution cryo-electron microscopy (cryo-EM) structure of apo  $\gamma$ -secretase (GS; PDB: 5A63). **(A)** Schematics of GS complex. **(B)** The horseshoe shape arrangement of the GS TMs, with two catalytic aspartates located on the convex side of the transmembrane helix (TM) horseshoe: Asp257 on TM6 and Asp385 on TM7. The location of TM2 is drawn based on a bound-state GS structure (PDB: 5FN3). **(C)** The cryo-EM structure of a nicastrin subunit; a close-up view of the hydrophilic pocket is shown.

dividing PS into an NTF and a CTF (Thinakaran et al., 1996; Knappenberger et al., 2004). NCT, which has a large, heavily glycosylated ECD and a single TM segment (Xie et al., 2014), is involved in the initial binding of substrate and likely inhibits the docking of substrates with long N-termini prior to the action of a sheddase. APH-1 contains seven TMs and is mainly responsible for the assembly, scaffolding, and stabilization of the GS complex (Brunkan et al., 2005). PEN-2, composed of three TMs is required for PS autoproteolysis and stabilizes PS NTF and CTF (Luo et al., 2003; Prokop et al., 2004). Although these four components are sufficient for performing cleavage, additional proteins are possibly involved in the modulation of the GS cleavage activity (Wakabayashi et al., 2009). For example, TMP21, a member of the p24 cargo protein family, is reported to be a component of PS complexes and regulates GS cleavage (Chen et al., 2006).

### X-Ray Structure of a PSH From *Methanoculleus marisnigri* JR1 (MCMJR1)

A PS ortholog was discovered from *Methanoculleus marisnigri* JR1 (Torres-Arancivia et al., 2010), and its X-ray structure (Figure 1) was solved soon thereafter (Li et al., 2013). The two catalytic aspartate residues are  $\sim 9\text{--}10$  Å apart. This distance is too far for the coordination of a catalytic water when compared to soluble aspartate proteases. In pepsin, the two catalytic aspartates are  $\sim 3$  Å away from each other, and in

HIV protease, the two catalytic aspartates are only 2.3 Å apart (Kovalevsky et al., 2007; Weber et al., 2013). Several explanations may account for the MCMJR1 structure being in an inactive conformation. Limited proteolysis was used during crystallization, which likely removed linker regions between TMs that in turn allow new motions to occur. Another possibility is that the apo state of the enzyme is an inactive conformation, and substrate binding triggers a conformational change to move the two aspartate residues closer together to carry out catalysis, as suggested by structures of GS (see below and Bai et al., 2015a).

### X-Ray Structure of the NCT Homolog From *Dictyostelium purpureum* (DpNCT)

The structure of NCT was first solved for a eukaryotic homolog from *Dictyostelium purpureum* (DpNCT), which shares 40% sequence identity with human NCT (HsNCT). The 1.95-Å resolution crystal structure reveals a large ECD and a single TM helix (Xie et al., 2014). The ECD of DpNCT contains a large lobe and a small lobe, interacting with each other through numerous van der Waals contacts at the center of the interface and 11 hydrogen bonds at the periphery of the interface. A pocket in the large lobe is surrounded by hydrophilic side chains, which may be responsible for anchoring hydrophilic N-termini of the substrates such as APP and Notch. An extended loop from the small lobe forms a lid that hovers above the pocket, likely gating



substrate entry. Conformational changes are needed for substrate recruitment (Li et al., 2014; Xie et al., 2014).

## Cryo-Electron Microscopy Structure of GS

After intensive cryo-electron microscopy (cryo-EM) efforts (Lu et al., 2014; Sun et al., 2015), a 3.4-Å map of GS was obtained with excellent main-chain connectivity and discernable side-chain features (Bai et al., 2015b; **Figures 6A,B**). Among the 20 TMs identified, TM2 of PS1 shows the highest degree of flexibility. Except for TM2 and TM6, the other 18 TMs were observed with good side-chain density, including the seven TMs of APH-1, the other seven TMs of PS1, the three TMs of PEN-2, and the lone TM of NCT. Overall, the TMs form a horseshoe shape (Bai et al., 2015b; Sun et al., 2015), with PS1 and APH-1 at the center and PEN-2 and NCT at the tips of the horseshoe. The two catalytic residues (Asp257 and Asp385 of PS1) are on the convex side of the TM horseshoe (**Figure 6B**). The cryo-EM structure of PS solved here is largely superimposable with the PSH from MCMJR1. The ECD of NCT directly interacts with PEN-2. The TMs predominantly interact through van der Waals contacts among hydrophobic side chains.

The flexibility of PS1 TM2 and TM6 seen in the cryo-EM structure suggests a pathway for the substrate entrance and conformational changes during substrate docking and translocation. Masked classification of the apo-state GS cryo-EM dataset revealed three major classes of conformations (**Figure 7**; Bai et al., 2015a). In class 1, TM2 from PS1 is ordered, and there is unassigned density corresponding to a kinked  $\alpha$ -helix, which may be a fortuitously co-purified cellular substrate or product. In class 2, the TM2 helix could be also observed but not well defined. In class 3, no substrate or TM2 could be observed. PEN-2 rotates away from PS1, together with PS1 TM3 and TM4, while PS1 TM5/TM6 move towards the extracellular/luminal space and TM6 rotates towards TM7. In the cryo-EM structure of GS in complexes with the peptidomimetic inhibitor DAPT (Bai et al., 2015a), the conformation of PS1 is very similar to class 1. Both PS1 TM2 and the linkers between TM2 and TM1 and TM2 and TM3 become ordered in the presence of DAPT, as well as part of the long linker between TM6 and TM7. TM6 displays a kink near the active site, forming a hydrophobic binding pocket with TM2, TM3, TM5, and TM7 for DAPT, the same pocket that APP and Notch substrates occupy revealed by later cryo-EM structures (see “Interaction of GS With Substrates” section). Crucial structural features and interactions of PS1 are listed in **Table 1**.

The cryo-EM structure of GS also reveals new details regarding HsNCT (Bai et al., 2015b; **Figure 6C**). First, the residues involved in GS substrate recognition, Glu333 and Tyr337, are located in a hydrophilic pocket. Charged arginine residues (Arg281, Arg285, Arg429, and Arg432) in this buried pocket may also mediate specific hydrogen bonding and salt bridges for substrate recruitment. Second, 11 glycosylation sites were identified on the large lobe. This heavy glycosylation likely contributes to substrate recruitment (Shah et al., 2005) and in ECD folding and stability. Two glycans on Asn55 and Asn435 from the large lobe flank the lid from the small lobe.

## INTERACTION OF GS WITH SUBSTRATES

Several interaction models have been put forth to explain the successive cleavage of APP substrate by GS [see “GS and AD” section]. First, a “piston model” was proposed in which APP-C99 remains in a helical conformation but shifts successively downward towards the active site of PS (Takagi et al., 2010). However, downward shifting of the substrate may make it harder for the product to be released as processive cleavage progresses. Second, a substrate “bending model” was put forward based on C99 TM backbone dynamics and the bend of a co-purified substrate observed in the class I cryo-EM structure of GS. In this model, C99 presents the scissile bond by bending the TM helix (Scharnagl et al., 2014; Langosch et al., 2015). Lastly, as elaborated in this section, growing evidence supports a substrate TM unwinding model to generate the scissile peptide bond in extended conformation, favoring the extended  $\beta$ -strand conformation that binds productively to the active site of proteases (Madala et al., 2010).

## Docking Site Mapping by Nuclear Magnetic Resonance (NMR)

Solution NMR has been utilized to probe substrate docking of APPTM, using PS orthologs that are catalytically active towards the TM segment of APP (APPTM). Chemical shift perturbation (CSP) showed that juxtamembrane regions of APPTM mediate its docking to MCMJR1. The largest CSP occurred at residues K28 and K54 of APPTM (**Figure 8**), likely mediating electrostatic interactions with the MCMJR1 (Clemente et al., 2018). Binding of the substrate to MCMJR1 decreased the magnitude of amide proton chemical shifts  $\delta_H$  at the C-terminal half of the substrate APPTM. Because amide  $\delta_H$  has a strong positive correlation with hydrogen bond strength, the pattern of decreasing  $\delta_H$  indicates that the docking to the enzyme weakens helical hydrogen bonds and unwinds the substrate TM helix around the initial  $\epsilon$ -cleavage site. The APPTM V44M substitution linked to FAD caused more CSP and helical unwinding around the  $\epsilon$ -cleavage site. MAMRE50, another archaeal ortholog of PSH, which cleaved APPTM at a higher rate, also caused more CSP and helical unwinding in APPTM than in MCMJR1. These data suggest that docking of the substrate TM helix and helix unwinding are coupled in intramembrane proteolysis by PS and its ortholog, and FAD mutations can modify enzyme–substrate interaction.

## Interaction Mapping by Photoaffinity Cross-Linking

A comprehensive mapping of the interaction between APP C99 and GS at residue resolution was accomplished by photoaffinity mapping (Fukumori and Steiner, 2016). Sixty-eight His-tagged C99 constructs containing photo-active amino acid *para*-benzoyl-L-phenylalanine (Bpa) substitution, from residues D1 to D68, were produced. After incubation with CHAPSO-solubilized GS and UV irradiation, the Bpa residue photo-cross-linked with nearby GS residues, within  $\sim 3$  Å. Cross-linked substrates and GS components were isolated by



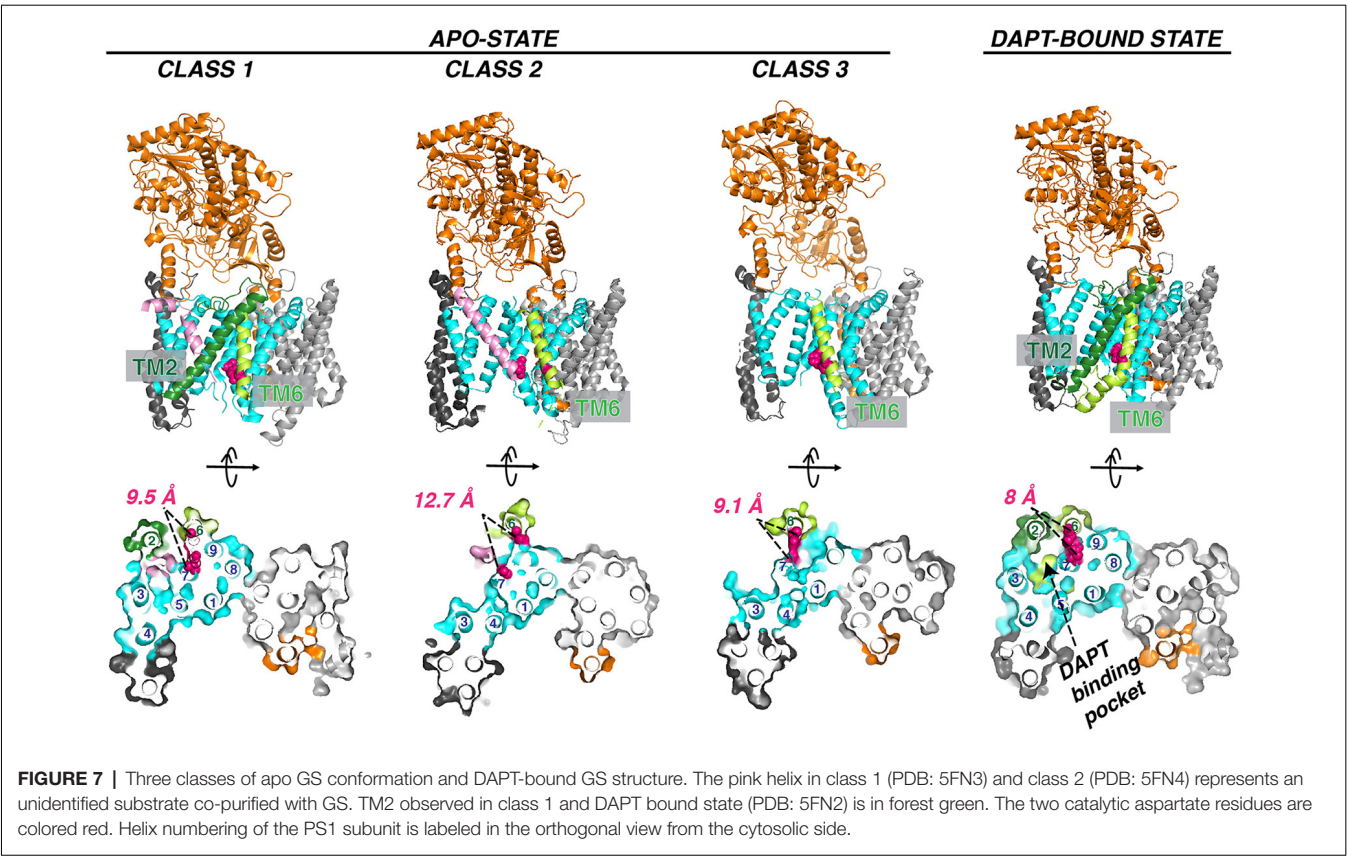


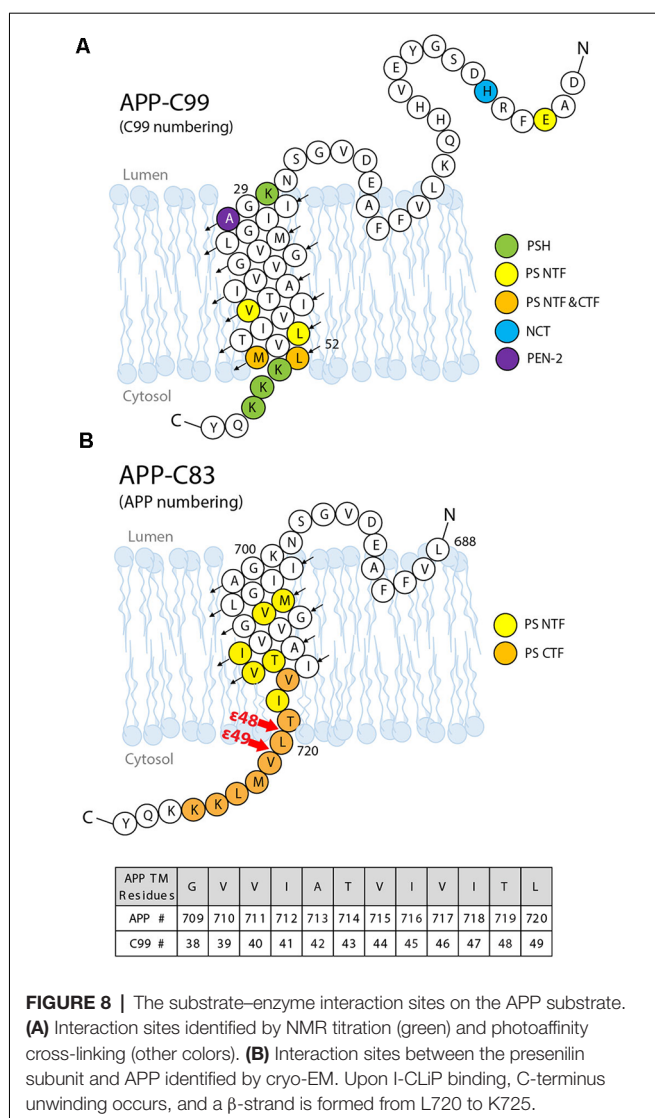
**TABLE 1 |** Function and motifs in the transmembrane domains (TM) and loops (L) of PS1.

		Residue#	Motifs	Function	References
NTF	TM1	G78-V103	-	Interaction with NCT	Bai et al. (2015a,b)
	L1	S104-E123	-	Hydrophilic for substrate recognition	Takagi-Niidome et al. (2015)
	TM2	T124-C158	-	Most dynamic TM; lateral gating of TMD substrate entry	Bai et al. (2015a,b)
	TM3	Y159-A192	-	Interaction with PEN-2	Bai et al. (2015a)
	TM4	V193-G217	NF motif (204NF205)	Interaction with PEN-2	Kim and Sisodia (2005)
	TM5	P218-P242	-	Hot spot for FAD mutation	Bai et al. (2015a)
	TM6	E243-Q276	-	Lateral gating of TMD substrate entry	Bai et al. (2015a)
CTF	L6	E277-L381	Catalytic aspartate (D257)	Active site aspartate	Bai et al. (2015a,b)
	TM7	G382-A398	Endoproteolysis region	$\gamma$ -Secretase autocleavage site	Bai et al. (2015a)
	TM8	T399-K429	GxGD motif (382GLGD385)	Peptide bond cleavage and substrate selectivity	Bai et al. (2015a)
	TM9	K430-I467	-	Interaction with APH-1	Steiner et al. (2000)
			PAL motif (433PAL435)	PS1 endoproteolysis and $\gamma$ -secretase activity	Sato et al. (2008)
			Hydrophobic C-terminus (465FYI467)	Interaction with a hydrophobic pocket in APH-1	Bai et al. (2015a)

Values for age represent the mean  $\pm$  standard deviation. Odds ratios (O.R.) are normalized to APOE- $\epsilon$ 3 and non-APOJ-C, making these values “1”. Risk scores shown are sums of the natural log of the odds ratios. Non-APOE- $\epsilon$ 4 group includes APOE- $\epsilon$ 2 carriers that have O.R. of 0.6.

Ni-NTA affinity pulldown followed by dissociation of GS for photoaffinity mapping. Photoaffinity mapping showed that APP C99 residues Val44, Leu49, Met51, and Leu52 are cross-linked to PS1 NTF, representing major substrate–enzyme interaction sites. Cross-linking at an exosite was also observed. C99 Glu3 was cross-linked to PS1 NTF, most likely through interaction with the loop L1 between TM1 and TM2. His6 and Ala30 cross-linked with NCT and PEN-2, respectively. Ala30 is not close to PEN-2 in the cryo-EM structure of the GS–APP complex, indicating

that major conformation changes occur during substrate–GS interaction. Met51 and Leu52 also cross-linked to PS1 CTF (Figure 8), as expected. To distinguish between interactions for substrate recruitment and for cleavage, “substrate-binding chase” experiments were carried out: first, C99 “binding” and cross-linking to GS were performed at 4°C to inhibit enzyme cleavage, followed by a 37°C cleavage “chase” experiment. When the substrate was cross-linked with PS1 NTF, it could be cleaved under 37°C and could also be inhibited by GSIs. However, when the substrate and NCT/PEN-2 are cross-linked, the substrate



cannot be cleaved, indicating that exosite cross-linking blocked the substrate passage from the GS exosite to the active site. Furthermore, the cross-linking of PS1 NTF was suppressed by GSIs while cross-linking involving PEN-2 was increased with GSI's presence. These data further confirmed the existence of a substrate docking site distinct from the active site. In summary, these studies show that the GS substrate binds to GS in two steps: first, the substrate binds to the exosite, likely formed by NCT, PEN-2, and NTF, and then the substrate translocates to the active site formed by PS1 NTF/CTF. Compared with the interaction sites identified in the cryo-EM structure of the GS–APP complex (Zhou et al., 2019; **Figure 8B**), this photoaffinity mapping showed additional interaction sites during substrate docking and translocation.

## Biophysical Studies of Substrate TM Unwinding

Solid-state NMR revealed that the TM helix of C99 unravels downstream of the  $\epsilon$ -sites (Sato et al., 2009). Under isotopic

labeling, deep-ultraviolet resonance Raman (dUVR) spectra of Gurken, a substrate for GlpG rhomboid and MCMJR1 (Torres-Arancivia et al., 2010), displays both  $\alpha$ -helical and  $3_{10}$ -helical geometry;  $3_{10}$ -helical unwinding was observed during binding to the enzyme (Brown et al., 2018). When the  $3_{10}$ -helical content was suppressed using a proline-to-alanine mutation, binding was not affected, but cleavage was inhibited. This result is consistent with the fact that the initial docking site is distinct from the active site proposed for GS (Fukumori and Steiner, 2016) and rhomboids (Arutyunova et al., 2014). As mentioned above, hydrogen bond weakening and helical unwinding in the APPTM C-terminus upon binding to MCMJR1 were also observed in solution NMR (Clemente et al., 2018).

## Cryo-EM Structure of GS in Complex With Notch and APP

The unwinding of the substrate TM helix at the carboxyl terminus was confirmed in cryo-EM structures of human GS in complex with mouse Notch-100 (Yang et al., 2019) and APP-C83 fragment (Zhou et al., 2019). To stabilize the GS–substrate complexes, disulfide-cross-linked GS–APP/Notch complexes were generated with human GS containing an active site mutation (PS1-Q112C/D385A, PEN-2, APH-1aL, and NCT) and APP-C83 (V695C; Zhou et al., 2019) or Notch-100 (P1728C; Yang et al., 2019). In the highest-resolution (2.6–2.7 Å) complex structure, TM6 extends to having two helices (TM6 and TM6a; **Figure 9**); TM2 and the loop between TM6/TM7 of PS are more ordered compared to free GS (Bai et al., 2015b).

The structures reveal that the C-termini of both APP and Notch adopt a  $\beta$ -strand conformation, forming an intermolecular, antiparallel  $\beta$ -sheet with two induced  $\beta$ -strands from PS1 NTF (TM6) and CTF (TM7). In this  $\beta$ -strand mode, the cleavage sites on substrate TM are in a more extended conformation and become more exposed. The  $\epsilon$ -cleavage sites (residues T719 and L720) in APPTM are fully extended (**Figure 9D**), as is the S3 cleavage sites (V1754) at the C-terminal part of Notch TM (**Figure 9C**).

Additional details of the participation of the NCT ECD in substrate recruitment (Xie et al., 2014) were revealed in the complex structures. In addition to the hydrophilic pocket reported in DpNCT (Xie et al., 2014), another hydrophilic pocket (Ser651, Arg652, Lys654, and Asp655) located at the small lobe near the membrane was identified (**Figure 9A**). A short helix of Notch-100 is inserted into the hydrophilic pocket (Yang et al., 2019). Kinetic data showed that the binding affinity between GS and Notch is driven by TMD interaction and that the affinity decreases with increasing ectodomain length and structure (Bolduc et al., 2016). Substrates with longer ectodomains could only be efficiently cleaved after disrupting the NCT fold. The steric hindrance of NCT likely contributes to the selectivity of the GS substrate.

## OPEN QUESTIONS AND FUTURE DIRECTIONS

Despite the tremendous progress detailed above, our molecular picture of GS remains far from complete. We do not know

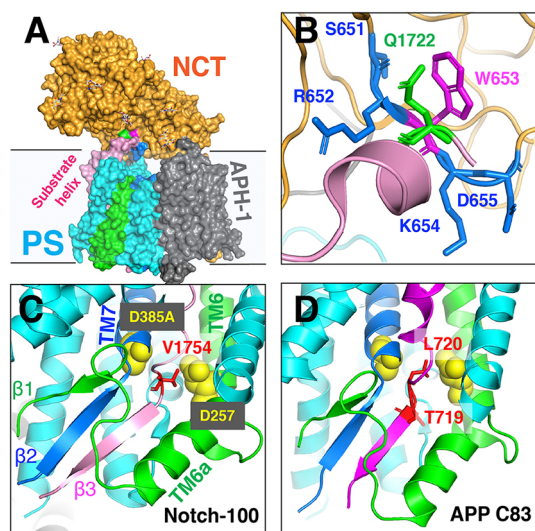


**FIGURE 9** | The cryo-EM structure of the GS-substrate complex with Notch-100 and APP-C83. Nicastrin (NCT) is colored orange and PS1 cyan. TM6 and TM7 from PS1 are colored green and blue, respectively. Substrates are in pink/magenta. **(A)** The overall complex structure. **(B)** A close-up view of the NCT hydrophilic pocket interacting with the Notch substrate. Q1722 is on Notch-100. 651SRWKD655 is on NCT. **(C)** The intermolecular  $\beta$ -sheet around Notch-100 C-terminal cleavage sites. TM6 extends to two helices (TM6/TM6a). The hybrid  $\beta$ -sheet consists of  $\beta$ 1 from TM6,  $\beta$ 2 from TM7, and  $\beta$ 3 from the substrate. Two catalytic aspartates are at the S3 cleavage site. **(D)** A similar hybrid  $\beta$ -sheet between APP-C83 and PS1 TM6/TM7. The  $\epsilon$ -cleavage sites are in extended conformation.

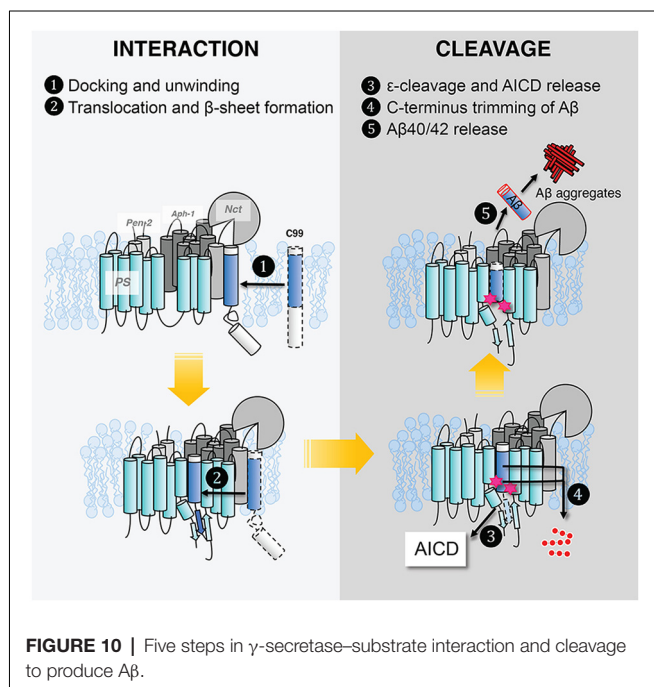


**FIGURE 10** | Five steps in  $\gamma$ -secretase-substrate interaction and cleavage to produce A $\beta$ .

the effect of the lipid composition of the lipid bilayer, hence how the cellular location of APP affects GS cleavage and how FAD mutations affect A $\beta$  production and increase the

A $\beta$ 42/A $\beta$ 40 ratio. We still do not have full clarity on how GS interacts with its substrate. In **Figure 10**, we outline the major steps of APP C99 interaction with GS, which ultimately results in the production of A $\beta$ , a pathogenic peptide in AD. In each step, there are many important, unanswered questions:

1. C99 docks to the GS exosite, coupled with helical unwinding near the initial cleavage site (Clemente et al., 2018). However, we do not know the molecular identity of the exosite. Most likely the exosite is not too far from the active site and may be composed of both NCT, TM2, and loop 1 of PS. The exosite may be mapped by blocking substrate entry into the GS active site using an active site GSI. Disulfide gates may be engineered to probe the exosite and substrate translocation pathway, as was carried out with rhomboids (Baker et al., 2007).
2. From the exosite, C99 translocates to the enzyme active site, forming an intermolecular  $\beta$ -sheet with PS (Zhou et al., 2019). We do not know the pathway of substrate translocation, partly because we do not know the exact substrate docking site. TM2 and TM6 are the most dynamic TMs in PS1 and therefore are mostly likely involved in the lateral gating mechanism of substrate translocation. The detailed dynamics of substrate translocation can be elucidated by combining the power of molecular dynamics simulations and cutting-edge experimental structural determination methods for membrane proteins.
3. Initial  $\epsilon$ -cleavage occurs at T48 or L49, releasing the AICD and forming A $\beta$ 48 or A $\beta$ 49, precursor peptides of the A $\beta$ 42 or A $\beta$ 42 production line, respectively. Here, the catalytic mechanism is not known, nor how the two active site aspartates coordinate a catalytic water molecule to facilitate hydrolysis. In all of the solved structures of GS and MCMJR1, the catalytic aspartates appear to be too far away from each other to coordinate a catalytic water. Thus, we have yet to capture the conformation of the GS active site in a catalytically competent state. Because of the stability of hybrid  $\beta$ -sheet at the C-terminus of C83, a large conformational change is needed for reducing this intermolecular interaction to facilitate the release of AICD. How this happens also remains an open question.
4. Following  $\epsilon$ -cleavage, carboxypeptidase activity of GS trims A $\beta$ 48/A $\beta$ 49 processively (**Figure 10**), shedding tripeptides to produce A $\beta$ 42 and A $\beta$ 40. The mechanism of processive cleavage is not known. Based on biochemical evidence, Wolfe et al. proposed a tripeptide binding pocket in the GS active site for P1'P2'P3' (Wolfe, 2020), which is not obvious in the GS-C83 complex. How the active site aspartates get to the next cleavage site on the substrate, as well as the driving force for this process, is not clear. It is straightforward to speculate that it involves concerted conformational changes and dynamics in both GS and the substrate. The catalytic aspartates in PS may move towards more N-terminal cleavage sites in APPTM while GS continues to unwind the substrate. The timing of AICD release and C-terminal trimming is not clear, for example, whether they are concurrent, sequential, or of



random order. We suggest that MD simulations will be extremely helpful in providing clues for experimentalists in this area.

5. Finally, following processive cleavage by GS, the shorter and more hydrophilic A $\beta$  fragment dissociates from the enzyme and exits the membrane. The mechanism of A $\beta$  peptide or AICD release has been little studied. What are the kinetics and pathway of A $\beta$  release? How does it involve NCT and other components of GS? During processive cleavage, A $\beta$  fragments may either be released or undergo one more step of trimming (e.g., A $\beta$ 42 is released vs. A $\beta$ 42 is cut down to A $\beta$ 38). How is this bifurcation in the A $\beta$  production pathway determined mechanistically? Both equilibrium (Szaruga et al., 2017) and kinetic stability of the A $\beta$ /GS complex might be critical determinants in this situation. Answers to these questions have important implications for the design and discovery of new GSIs and selective GSIs.

Given the recent structural insights, an intriguing question for AD drug discovery is whether selective GSIs can be designed or discovered. Yang et al. (2019) pointed out several distinct pockets in the GS-C83 complex that have different shapes and dimensions compared with the GS-Notch complex (Zhou et al., 2019), which may be targeted for rational drug design. However, it is important to note that GS is highly dynamic, and binding pockets can stretch and/or shrink. Thus, for selective GSI, we may still need to rely on docking coupled with

long-time-course MD simulation, high-throughput (HT), or ultra-HT methods such as DNA encoded libraries which enable screening of tens of billions of compounds in a single test tube (Satz, 2018).

## CONCLUSION

There has been tremendous progress in the structural and mechanistic investigation of the substrate-enzyme interaction in intramembrane proteolysis, especially in light of the recent cryo-EM structures of GS-C83 and GS-Notch complexes. In particular, cryo-EM revealed the formation of a hybrid, intermolecular  $\beta$ -sheet between GS and its substrates, which is consistent with numerous biochemical and biophysical studies. However, our knowledge of how GS interacts with its substrates, which is crucial for developing selective amyloid reduction agents, remains far from complete.

## AUTHOR CONTRIBUTIONS

XL and CW prepared the text and figures. JZ, YZ, IU-B, SF, and RL edited and revised the manuscript.

## FUNDING

This work was supported by a grant NS109926 to CW from the National Institute of Neurological Disorders and Stroke (NINDS), and a grant to RL from NSF MCB-1817796.

## REFERENCES

- Annaert, W., and De Strooper, B. (1999). Presenilins: molecular switches between proteolysis and signal transduction. *Trends Neurosci.* 22, 439–443. doi: 10.1016/s0166-2236(99)01455-1
- Arutyunova, E., Panwar, P., Skiba, P. M., Gale, N., Mak, M. W., and Lemieux, M. J. (2014). Allosteric regulation of rhomboid intramembrane proteolysis. *EMBO J.* 33, 1869–1881. doi: 10.15252/embj.201488149
- Bai, X.-C., Rajendra, E., Yang, G., Shi, Y., and Scheres, S. H. W. (2015a). Sampling the conformational space of the catalytic subunit of human  $\gamma$ -secretase. *Elife* 4:e11182. doi: 10.7554/eLife.11182
- Bai, X.-C., Yan, C., Yang, G., Lu, P., Ma, D., Sun, L., et al. (2015b). An atomic structure of human  $\gamma$ -secretase. *Nature* 525, 212–217. doi: 10.1038/nature14892
- Baker, R. P., Young, K., Feng, L., Shi, Y., and Urban, S. (2007). Enzymatic analysis of a rhomboid intramembrane protease implicates transmembrane helix 5 as the lateral substrate gate. *Proc. Natl. Acad. Sci. U S A* 104, 8257–8262. doi: 10.1073/pnas.0700814104
- Beel, A. J., Mobley, C. K., Kim, H. J., Tian, F., Hadziselimovic, A., Jap, B., et al. (2008). Structural studies of the transmembrane C-terminal domain of the amyloid precursor protein (APP): does APP function as a cholesterol sensor? *Biochemistry* 47, 9428–9446. doi: 10.1021/bi800993c
- Beel, A. J., and Sanders, C. R. (2008). Substrate specificity of  $\gamma$ -secretase and other intramembrane proteases. *Cell. Mol. Life Sci.* 65, 1311–1334. doi: 10.1007/s00018-008-7462-2
- Ben-Shem, A., Fass, D., and Bibi, E. (2007). Structural basis for intramembrane proteolysis by rhomboid serine proteases. *Proc. Natl. Acad. Sci. U S A* 104, 462–466. doi: 10.1073/pnas.0609773104
- Bergbold, N., and Lemberg, M. K. (2013). Emerging role of rhomboid family proteins in mammalian biology and disease. *Biochim. Biophys. Acta* 1828, 2840–2848. doi: 10.1016/j.bbame.2013.03.025
- Bertram, L., Lill, C. M., and Tanzi, R. E. (2010). The genetics of Alzheimer disease: back to the future. *Neuron* 68, 270–281. doi: 10.1016/j.neuron.2010.10.013
- Bolduc, D. M., Montagna, D. R., Gu, Y., Selkoe, D. J., and Wolfe, M. S. (2016). Nicastrin functions to sterically hinder  $\gamma$ -secretase-substrate interactions driven by substrate transmembrane domain. *Proc. Natl. Acad. Sci. U S A* 113, E509–E518. doi: 10.1073/pnas.1512952113
- Boyartchuk, V. L., Ashby, M. N., and Rine, J. (1997). Modulation of Ras and a-factor function by carboxyl-terminal proteolysis. *Science* 275, 1796–1800. doi: 10.1126/science.275.5307.1796
- Brown, M. C., Abdine, A., Chavez, J., Schaffner, A., Torres-Arancivia, C., Lada, B., et al. (2018). Unwinding of the substrate transmembrane helix in intramembrane proteolysis. *Biophys. J.* 114, 1579–1589. doi: 10.1016/j.bpj.2018.01.043
- Brown, M. S., and Goldstein, J. L. (1997). The SREBP pathway: regulation of cholesterol metabolism by proteolysis of a membrane-bound transcription factor. *Cell* 89, 331–340. doi: 10.1016/s0092-8674(00)80213-5
- Brown, M. S., Ye, J., Rawson, R. B., and Goldstein, J. L. (2000). Regulated intramembrane proteolysis: a control mechanism conserved from bacteria to humans. *Cell* 100, 391–398. doi: 10.1016/s0092-8674(00)80675-3
- Brunkan, A. L., Martinez, M., Walker, E. S., and Goate, A. M. (2005). Presenilin endoproteolysis is an intramolecular cleavage. *Mol. Cell. Neurosci.* 29, 65–73. doi: 10.1016/j.mcn.2004.12.012
- Bursavich, M. G., Harrison, B. A., and Blain, J.-F. (2016).  $\gamma$  secretase modulators: new Alzheimer's drugs on the horizon? *J. Med. Chem.* 59, 7389–7409. doi: 10.1021/acs.jmedchem.5b01960
- Chen, W., Gamache, E., Rosenman, D. J., Xie, J., Lopez, M. M., Li, Y.-M., et al. (2014). Familial Alzheimer's mutations within APPTM increase A $\beta$ 42 production by enhancing accessibility of  $\epsilon$ -cleavage site. *Nat. Commun.* 5:3037. doi: 10.1038/ncomms4037
- Chen, F., Hasegawa, H., Schmitt-Ulms, G., Kawarai, T., Bohm, C., Katayama, T., et al. (2006). TMP21 is a presenilin complex component that modulates  $\gamma$ -secretase but not  $\epsilon$ -secretase activity. *Nature* 440, 1208–1212. doi: 10.1038/nature04667
- Christiansen, J. R., Kolandaivelu, S., Bergo, M. O., and Ramamurthy, V. (2011). RAS-converting enzyme 1-mediated endoproteolysis is required for trafficking



- of rod phosphodiesterase 6 to photoreceptor outer segments. *Proc. Natl. Acad. Sci. U S A* 108, 8862–8866. doi: 10.1073/pnas.1103627108
- Clemente, N., Abdine, A., Ubarretxena-Belandia, I., and Wang, C. (2018). Coupled transmembrane substrate docking and helical unwinding in intramembrane proteolysis of amyloid precursor protein. *Sci. Rep.* 8:12411. doi: 10.1038/s41598-018-30015-6
- Crump, C. J., Castro, S. V., Wang, F., Pozdnyakov, N., Ballard, T. E., Sisodia, S. S., et al. (2012). BMS-708,163 targets presenilin and lacks notch-sparing activity. *Biochemistry* 51, 7209–7211. doi: 10.1021/bi301137h
- De Strooper, B., and Chávez Gutiérrez, L. (2015). Learning by failing: ideas and concepts to tackle  $\gamma$ -secretases in Alzheimer's disease and beyond. *Annu. Rev. Pharmacol. Toxicol.* 55, 419–437. doi: 10.1146/annurev-pharmtox-010814-124309
- Deatherage, C. L., Lu, Z., Kroncke, B. M., Ma, S., Smith, J. A., Voehler, M. W., et al. (2017). Structural and biochemical differences between the Notch and the amyloid precursor protein transmembrane domains. *Sci. Adv.* 3:e1602794. doi: 10.1126/sciadv.1602794
- Düsterhöft, S., Künzel, U., and Freeman, M. (2017). Rhomboid proteases in human disease: mechanisms and future prospects. *Biochim. Biophys. Acta Mol. Cell Res.* 1864, 2200–2209. doi: 10.1016/j.bbamcr.2017.04.016
- Feng, L., Yan, H., Wu, Z., Yan, N., Wang, Z., Jeffrey, P. D., et al. (2007). Structure of a site-2 protease family intramembrane metalloprotease. *Science* 318, 1608–1612. doi: 10.1126/science.1150755
- Fluhrer, R., Steiner, H., and Haass, C. (2009). Intramembrane Proteolysis by signal peptide peptidases: a comparative discussion of GXGD-type aspartyl proteases. *J. Biol. Chem.* 284, 13975–13979. doi: 10.1074/jbc.R800040200
- Francis, R., McGrath, G., Zhang, J., Ruddy, D. A., Sym, M., Apfeld, J., et al. (2002). Aph-1 and pen-2 are required for notch pathway signaling,  $\gamma$ -secretase cleavage of  $\beta$ APP and presenilin protein accumulation. *Dev. Cell* 3, 85–97. doi: 10.1016/s1534-5807(02)00189-2
- Fukumori, A., and Steiner, H. (2016). Substrate recruitment of  $\gamma$ -secretase and mechanism of clinical presenilin mutations revealed by photoaffinity mapping. *EMBO J.* 35, 1628–1643. doi: 10.15252/embj.201694151
- Goate, A., Chartier-Harlin, M.-C., Mullan, M., Brown, J., Crawford, F., Fidani, L., et al. (1991). Segregation of a missense mutation in the amyloid precursor protein gene with familial Alzheimer's disease. *Nature* 349, 704–706. doi: 10.1038/349704a0
- Li, X., Dang, S., Yan, C., Gong, X., Wang, J., and Shi, Y. (2013). Structure of a presenilin family intramembrane aspartate protease. *Nature* 493, 56–61. doi: 10.1038/nature11801
- Haass, C., and Steiner, H. (2002). Alzheimer disease  $\gamma$ -secretase: a complex story of GxGD-type presenilin proteases. *Trends Cell Biol.* 12, 556–562. doi: 10.1016/s0962-8924(02)02394-2
- Haze, K., Yoshida, H., Yanagi, H., Yura, T., and Mori, K. (1999). Mammalian transcription factor ATF6 is synthesized as a transmembrane protein and activated by proteolysis in response to endoplasmic reticulum stress. *Mol. Biol. Cell* 10, 3787–3799. doi: 10.1091/mbc.10.11.3787
- Kelleher, R. J., and Shen, J. (2010).  $\gamma$ -secretase and human disease. *Science* 330, 1055–1056. doi: 10.1126/science.1198668
- Kim, S. H., and Sisodia, S. S. (2005). Evidence that the “NF” motif in transmembrane domain 4 of presenilin 1 is critical for binding with PEN-2. *J. Biol. Chem.* 280, 41953–41966. doi: 10.1074/jbc.M509070200
- Kimberly, W. T., LaVoie, M. J., Ostaszewski, B. L., Ye, W., Wolfe, M. S., and Selkoe, D. J. (2003).  $\gamma$ -Secretase is a membrane protein complex comprised of presenilin, nicastrin, aph-1, and pen-2. *Proc. Natl. Acad. Sci. U S A* 100, 6382–6387. doi: 10.1073/pnas.1037392100
- Kitagawa, M. (2015). Notch signalling in the nucleus: roles of Mastermind-like (MAML) transcriptional coactivators. *J. Biochem.* 159, 287–294. doi: 10.1093/jb/mvv123
- Knappenberger, K. S., Tian, G., Ye, X., Sobotka-Briner, C., Ghanekar, S. V., Greenberg, B. D., et al. (2004). Mechanism of  $\gamma$ -secretase cleavage activation: is  $\gamma$ -secretase regulated through autoinhibition involving the presenilin-1 exon 9 loop? *Biochemistry* 43, 6208–6218. doi: 10.1016/j.mechmachtheory.2004
- Kopan, R., and Ilagan, M. X. G. (2009). The canonical notch signaling pathway: unfolding the activation mechanism. *Cell* 137, 216–233. doi: 10.1016/j.cell.2009.03.045
- Kovalevsky, A. Y., Chumanevich, A. A., Liu, F., Louis, J. M., and Weber, I. T. (2007). Caught in the Act: the 1.5 Å resolution crystal structures of the HIV-1 protease and the I54V mutant reveal a tetrahedral reaction intermediate. *Biochemistry* 46, 14854–14864. doi: 10.1021/bi700822g
- Lal, M., and Caplan, M. (2011). Regulated intramembrane proteolysis: signaling pathways and biological functions. *Physiology* 26, 34–44. doi: 10.1152/physiol.00028.2010
- Langosch, D., Scharnagl, C., Steiner, H., and Lemberg, M. K. (2015). Understanding intramembrane proteolysis: from protein dynamics to reaction kinetics. *Trends Biochem. Sci.* 40, 318–327. doi: 10.1016/j.tibs.2015.04.001
- Langosch, D., and Steiner, H. (2017). Substrate processing in intramembrane proteolysis by  $\gamma$ -secretase—the role of protein dynamics. *Biol. Chem.* 398, 441–453. doi: 10.1515/hsz-2016-0269
- Lemieux, M. J., Fischer, S. J., Cherney, M. M., Bateman, K. S., and James, M. N. G. (2007). The crystal structure of the rhomboid peptidase from *Haemophilus influenzae* provides insight into intramembrane proteolysis. *Proc. Natl. Acad. Sci. U S A* 104, 750–754. doi: 10.1073/pnas.0609981104
- Levy, E., Carman, M., Fernandez-Madrid, I., Power, M., Lieberburg, I., van Duinen, S., et al. (1990). Mutation of the Alzheimer's disease amyloid gene in hereditary cerebral hemorrhage, Dutch type. *Science* 248, 1124–1126. doi: 10.1126/science.2111584
- Levy-Lahad, E., Wasco, W., Poorkaj, P., Romano, D., Oshima, J., Pettingell, W., et al. (1995). Candidate gene for the chromosome 1 familial Alzheimer's disease locus. *Science* 269, 973–977. doi: 10.1126/science.7638622
- Li, Y., Lu, S. H.-J., Tsai, C.-J., Bohm, C., Qamar, S., Dodd, R. B., et al. (2014). Structural interactions between inhibitor and substrate docking sites give insight into mechanisms of human PS1 complexes. *Structure* 22, 125–135. doi: 10.1016/j.str.2013.09.018
- Li, Y. M., Xu, M., Lai, M. T., Huang, Q., Castro, J. L., DiMuzio-Mower, J., et al. (2000). Photoactivated  $\gamma$ -secretase inhibitors directed to the active site covalently label presenilin 1. *Nature* 405, 689–694. doi: 10.1038/35015085
- Lichtenthaler, S. F., Haass, C., and Steiner, H. (2011). Regulated intramembrane proteolysis—lessons from amyloid precursor protein processing. *J. Neurochem.* 117, 779–796. doi: 10.1111/j.1471-4159.2011.07248.x
- Lu, P., Bai, X., Ma, D., Xie, T., Yan, C., Sun, L., et al. (2014). Three-dimensional structure of human  $\gamma$ -secretase. *Nature* 512, 166–170. doi: 10.1038/nature13567
- Luo, W., Wang, H., Li, H., Kim, B. S., Shah, S., Lee, H.-J., et al. (2003). PEN-2 and APH-1 coordinately regulate proteolytic processing of presenilin 1. *J. Biol. Chem.* 278, 7850–7854. doi: 10.1074/jbc.C200648200
- Madala, P. K., Tyndall, J. D. A., Nall, T., and Fairlie, D. P. (2010). Update 1 of: proteases universally recognize  $\beta$  strands in their active sites. *Chem. Rev.* 110, PR1–PR31. doi: 10.1021/cr900368a
- Makin, S. (2018). The amyloid hypothesis on trial. *Nature* 559, S4–S7. doi: 10.1038/d41586-018-05719-4
- Manolaridis, I., Kulkarni, K., Dodd, R. B., Ogasawara, S., Zhang, Z., Bineva, G., et al. (2013). Mechanism of farnesylated CAAX protein processing by the intramembrane protease Rce1. *Nature* 504, 301–305. doi: 10.1038/nature12754
- Michaelson, D., Ali, W., Chiu, V. K., Bergo, M., Silletti, J., Wright, L., et al. (2005). Postprenylation CAAX processing is required for proper localization of Ras but not Rho GTPases. *Mol. Biol. Cell* 16, 1606–1616. doi: 10.1091/mbc.e04-11-0960
- Mullard, A. (2017). BACE inhibitor bust in Alzheimer trial. *Nat. Rev. Drug Discov.* 16:155. doi: 10.1038/nrd.2017.43
- Naing, S.-H., Kalyoncu, S., Smalley, D. M., Kim, H., Tao, X., George, J. B., et al. (2018a). Both positional and chemical variables control *in vitro* proteolytic cleavage of a presenilin ortholog. *J. Biol. Chem.* 293, 4653–4663. doi: 10.1074/jbc.ra117.001436
- Naing, S.-H., Oliver, R. C., Weiss, K. L., Urban, V. S., and Lieberman, R. L. (2018b). Solution structure of an intramembrane aspartyl protease via small angle neutron scattering. *Biophys. J.* 114, 602–608. doi: 10.1016/j.bpj.2017.12.017
- Navarro, C. L., Esteves-Vieira, V., Courrier, S., Boyer, A., Duong Nguyen, T., Huong, L. T. T., et al. (2014). New ZMPSTE24 (FACE1) mutations in patients affected with restrictive dermopathy or related progeroid syndromes and mutation update. *Eur. J. Hum. Genet.* 22, 1002–1011. doi: 10.1038/ejhg.2013.258
- Niwa, M., Sidrauski, C., Kaufman, R. J., and Walter, P. (1999). A role for presenilin-1 in nuclear accumulation of ire1 fragments and induction of the mammalian unfolded protein response. *Cell* 99, 691–702. doi: 10.1016/s0092-8674(00)81667-0

- Okochi, M., Fukumori, A., Jiang, J., Itoh, N., Kimura, R., Steiner, H., et al. (2006). Secretion of the Notch-1 A $\beta$ -like peptide during Notch signaling. *J. Biol. Chem.* 281, 7890–7898. doi: 10.1074/jbc.m513250200
- Pendás, A. M., Zhou, Z., Cadiñanos, J., Freije, J. M. P., Wang, J., Hultenby, K., et al. (2002). Defective prelamins A processing and muscular and adipocyte alterations in Zmpste24 metalloproteinase-deficient mice. *Nat. Genet.* 31, 94–99. doi: 10.1038/ng871
- Prokop, S., Shirotani, K., Edbauer, D., Haass, C., and Steiner, H. (2004). Requirement of PEN-2 for stabilization of the presenilin N-/C-terminal fragment heterodimer within the  $\gamma$ -secretase complex. *J. Biol. Chem.* 279, 23255–23261. doi: 10.1074/jbc.m401789200
- Pryor, E. E., Horanyi, P. S., Clark, K. M., Fedoriw, N., Connelly, S. M., Koszelak-Rosenblum, M., et al. (2013). Structure of the integral membrane protein CAAX protease Ste24p. *Science* 339, 1600–1604. doi: 10.1126/science.1232048
- Qi-Takahara, Y., Morishima-Kawashima, M., Tanimura, Y., Dolios, G., Hirotsu, N., Horikoshi, Y., et al. (2005). Longer forms of amyloid  $\beta$  protein: implications for the mechanism of intramembrane cleavage by  $\gamma$ -secretase. *J. Neurosci.* 25, 436–445. doi: 10.1523/JNEUROSCI.1575-04.2005
- Rogaev, E. I., Sherrington, R., Rogaeva, E. A., Levesque, G., Ikeda, M., Liang, Y., et al. (1995). Familial Alzheimer's disease in kindreds with missense mutations in a gene on chromosome 1 related to the Alzheimer's disease type 3 gene. *Nature* 376, 775–778. doi: 10.1038/376775a0
- Sakai, J., Duncan, E. A., Rawson, R. B., Hua, X., Brown, M. S., and Goldstein, J. L. (1996). Sterol-regulated release of SREBP-2 from cell membranes requires two sequential cleavages, one within a transmembrane segment. *Cell* 85, 1037–1046. doi: 10.1016/s0092-8674(00)81304-5
- Takami, M., Nagashima, Y., Sano, Y., Ishihara, S., Morishima-Kawashima, M., Funamoto, S., et al. (2009).  $\gamma$ -secretase: successive tripeptide and tetrapeptide release from the transmembrane domain of -carboxyl terminal fragment. *J. Neurosci.* 29, 13042–13052. doi: 10.1523/JNEUROSCI.2362-09.2009
- Sato, C., Takagi, S., Tomita, T., and Iwatsubo, T. (2008). The C-terminal PAL motif and transmembrane domain 9 of presenilin 1 are involved in the formation of the catalytic pore of the  $\gamma$ -secretase. *J. Neurosci.* 28, 6264–6271. doi: 10.1523/JNEUROSCI.1163-08.2008
- Sato, T., Tang, T.-C., Reubins, G., Fei, J. Z., Fujimoto, T., Kienlen-Campard, P., et al. (2009). A helix-to-coil transition at the -cut site in the transmembrane dimer of the amyloid precursor protein is required for proteolysis. *Proc. Natl. Acad. Sci. U S A* 106, 1421–1426. doi: 10.1073/pnas.0812261106
- Satz, A. L. (2018). What do you get from DNA-encoded libraries? *ACS Med. Chem. Lett.* 9, 408–410. doi: 10.1021/acsmchemlett.8b00128
- Scharnagl, C., Pester, O., Hornburg, P., Hornburg, D., Götz, A., and Langosch, D. (2014). Side-chain to main-chain hydrogen bonding controls the intrinsic backbone dynamics of the amyloid precursor protein transmembrane helix. *Biophys. J.* 106, 1318–1326. doi: 10.1016/j.bpj.2014.02.013
- Schmidt, W. K., Tam, A., Fujimura-Kamada, K., and Michaelis, S. (1998). Endoplasmic reticulum membrane localization of Rce1p and Ste24p, yeast proteases involved in carboxyl-terminal CAAX protein processing and amino-terminal a-factor cleavage. *Proc. Natl. Acad. Sci. U S A* 95, 11175–11180. doi: 10.1073/pnas.95.19.11175
- Selkoe, D., and Kopan, R. (2003). Notch And Presenilin: regulated intramembrane proteolysis links development and degeneration. *Annu. Rev. Neurosci.* 26, 565–597. doi: 10.1146/annurev.neuro.26.041002.131334
- Shah, S., Lee, S. F., Tabuchi, K., Hao, Y. H., Yu, C., LaPlant, Q., et al. (2005). Nicastrin functions as a  $\gamma$ -secretase-substrate receptor. *Cell* 122, 435–447. doi: 10.1016/j.cell.2005.05.022
- Sherrington, R., Rogaev, E. I., Liang, Y., Rogaeva, E. A., Levesque, G., Ikeda, M., et al. (1995). Cloning of a gene bearing missense mutations in early-onset familial Alzheimer's disease. *Nature* 375, 754–760. doi: 10.1038/375754a0
- Shih, I. M., and Wang, T. L. (2007). Notch signaling,  $\gamma$ -secretase inhibitors, and cancer therapy. *Cancer Res.* 67, 1879–1882. doi: 10.1158/0008-5472.CAN-06-3958
- Shokhen, M., and Albeck, A. (2017). How does the exosite of rhomboid protease affect substrate processing and inhibition? *Protein Sci.* 26, 2355–2366. doi: 10.1002/pro.3294
- Sibley, L. D. (2013). The roles of intramembrane proteases in protozoan parasites. *Biochim. Biophys. Acta* 1828, 2908–2915. doi: 10.1016/j.bbamem.2013.04.017
- Steiner, H., Kostka, M., Romig, H., Basset, G., Pesold, B., Hardy, J., et al. (2000). Glycine 384 is required for presenilin-1 function and is conserved in bacterial polytopic aspartyl proteases. *Nat. Cell Biol.* 2, 848–851. doi: 10.1038/35041097
- Strisovsky, K., Sharpe, H. J., and Freeman, M. (2009). Sequence-specific intramembrane proteolysis: identification of a recognition motif in rhomboid substrates. *Mol. Cell* 36, 1048–1059. doi: 10.1016/j.molcel.2009.11.006
- Sun, L., Li, X., and Shi, Y. (2016). Structural biology of intramembrane proteases: mechanistic insights from rhomboid and S2P to  $\gamma$ -secretase. *Curr. Opin. Struct. Biol.* 37, 97–107. doi: 10.1016/j.sbi.2015.12.008
- Sun, L., Zhao, L., Yang, G., Yan, C., Zhou, R., Zhou, X., et al. (2015). Structural basis of human  $\gamma$ -secretase assembly. *Proc. Natl. Acad. Sci. U S A* 112, 6003–6008. doi: 10.1073/pnas.1506242112
- Szaruga, M., Munteanu, B., Lismont, S., Veugelen, S., Horré, K., Mercken, M., et al. (2017). Alzheimer's-causing mutations shift A $\beta$  length by destabilizing  $\gamma$ -secretase-A $\beta$ n interactions. *Cell* 170, 443.e14–456.e14. doi: 10.1016/j.cell.2017.07.004
- Takagi, S., Tominaga, A., Sato, C., Tomita, T., and Iwatsubo, T. (2010). Participation of transmembrane domain 1 of presenilin 1 in the catalytic pore structure of the  $\gamma$ -secretase. *J. Neurosci.* 30, 15943–15950. doi: 10.1523/JNEUROSCI.3318-10.2010
- Takagi-Niidome, S., Sasaki, T., Osawa, S., Sato, T., Morishima, K., Cai, T., et al. (2015). Cooperative roles of hydrophilic loop 1 and the c-terminus of presenilin 1 in the substrate-gating mechanism of  $\gamma$ -secretase. *J. Neurosci.* 35, 2646–2656. doi: 10.1523/JNEUROSCI.3164-14.2015
- Tanzi, R. E., and Bertram, L. (2005). Twenty years of the Alzheimer's disease amyloid hypothesis: a genetic perspective. *Cell* 120, 545–555. doi: 10.1016/j.cell.2005.02.008
- Thinakaran, G., Borchelt, D. R., Lee, M. K., Slunt, H. H., Spitzer, L., Kim, G., et al. (1996). Endoproteolysis of presenilin 1 and accumulation of processed derivatives *in vivo*. *Neuron* 17, 181–190. doi: 10.1016/s0896-6273(00)80291-3
- Tichá, A., Collis, B., and Strisovsky, K. (2018). The rhomboid superfamily: structural mechanisms and chemical biology opportunities. *Trends Biochem. Sci.* 43, 726–739. doi: 10.1016/j.tibs.2018.06.009
- Tong, G., Wang, J. S., Sverdlow, O., Huang, S. P., Slemmon, R., Croop, R., et al. (2012). Multicenter, randomized, double-blind, placebo-controlled, single-ascending dose study of the oral  $\gamma$ -secretase inhibitor BMS-708163 (Avagacestat): tolerability profile, pharmacokinetic parameters, and pharmacodynamic markers. *Clin. Ther.* 34, 654–667. doi: 10.1016/j.clinthera.2012.01.022
- Torres-Arancibia, C., Ross, C. M., Chavez, J., Assur, Z., Dolios, G., Mancina, F., et al. (2010). Identification of an archaeal presenilin-like intramembrane protease. *PLoS One* 5:e13072. doi: 10.1371/journal.pone.0013072
- Tun, H., Marlow, L., Pinnix, L., Kinsey, R., and Sambamurti, K. (2002). Lipid rafts play an important role in A $\beta$  biogenesis by regulating the  $\beta$ -secretase pathway. *J. Mol. Neurosci.* 19, 31–35. doi: 10.1007/s12031-002-0007-5
- Urano, Y., Hayashi, I., Isoo, N., Reid, P. C., Shibasaki, Y., Noguchi, N., et al. (2005). Association of active  $\gamma$ -secretase complex with lipid rafts. *J. Lipid Res.* 46, 904–912. doi: 10.1194/jlr.M400333-JLR200
- van Tetering, G., and Vooijs, M. (2011). Proteolytic cleavage of notch: “HIT and RUN”. *Curr. Mol. Med.* 11, 255–269. doi: 10.2174/156652411795677972
- Wakabayashi, T., Craessaerts, K., Bammens, L., Bentahir, M., Borgions, F., Herdewijn, P., et al. (2009). Analysis of the  $\gamma$ -secretase interactome and validation of its association with tetraspanin-enriched microdomains. *Nat. Cell Biol.* 11, 1340–1346. doi: 10.1038/ncb1978
- Wang, Y., Zhang, Y., and Ha, Y. (2006). Crystal structure of a rhomboid family intramembrane protease. *Nature* 444, 179–180. doi: 10.1038/nature05255
- Wasserman, J. D., and Freeman, M. (1997). Control of EGF receptor activation in Drosophila. *Trends Cell Biol.* 7, 431–436. doi: 10.1016/s0962-8924(97)01143-4
- Weber, I. T., Waltman, M. J., Mustyakimov, M., Blakeley, M. P., Keen, D. A., Ghosh, A. K., et al. (2013). Joint X-ray/neutron crystallographic study of HIV-1 protease with clinical inhibitor amprenavir: insights for drug design. *J. Med. Chem.* 56, 5631–5635. doi: 10.1021/jm400684f

- Weihofen, A., Binns, K., Lemberg, M. K., Ashman, K., and Martoglio, B. (2002). Identification of signal peptide peptidase, a presenilin-type aspartic protease. *Science* 296, 2215–2218. doi: 10.1126/science.1070925
- Winter-Vann, A. M., and Casey, P. J. (2005). Post-prenylation-processing enzymes as new targets in oncogenesis. *Nat. Rev. Cancer* 5, 405–412. doi: 10.1038/nrc1612
- Wolfe, M. S. (2020). Substrate recognition and processing by  $\gamma$ -secretase. *Biochim. Biophys. Acta Biomembr.* 1862:183016. doi: 10.1016/j.bbamem.2019.07.004
- Wolfe, M. S., Xia, W., Ostaszewski, B. L., Diehl, T. S., Kimberly, W. T., and Selkoe, D. J. (1999). Two transmembrane aspartates in presenilin-1 required for presenilin endoproteolysis and  $\gamma$ -secretase activity. *Nature* 398, 513–517. doi: 10.1038/19077
- Wu, Z., Yan, N., Feng, L., Oberstein, A., Yan, H., Baker, R. P., et al. (2006). Structural analysis of a rhomboid family intramembrane protease reveals a gating mechanism for substrate entry. *Nat. Struct. Mol. Biol.* 13, 1084–1091. doi: 10.1038/nsmb1179
- Xie, T., Yan, C., Zhou, R., Zhao, Y., Sun, L., Yang, G., et al. (2014). Crystal structure of the  $\gamma$ -secretase component nicastrin. *Proc. Natl. Acad. Sci. U S A* 111, 13349–13354. doi: 10.1073/pnas.1414837111
- Xue, Y., and Ha, Y. (2013). Large lateral movement of transmembrane helix S5 is not required for substrate access to the active site of rhomboid intramembrane protease. *J. Biol. Chem.* 288, 16645–16654. doi: 10.1074/jbc.m112.438127
- Yang, G., Zhou, R., Zhou, Q., Guo, X., Yan, C., Ke, M., et al. (2019). Structural basis of Notch recognition by human  $\gamma$ -secretase. *Nature* 565, 192–197. doi: 10.1038/s41586-018-0813-8
- Zhou, R., Yang, G., Guo, X., Zhou, Q., Lei, J., and Shi, Y. (2019). Recognition of the amyloid precursor protein by human  $\gamma$ -secretase. *Science* 363:eaaw0930. doi: 10.1126/science.aaw0930
- Zoll, S., Stanchev, S., Began, J., Škerle, J., Lepšík, M., Peclinovská, L., et al. (2014). Substrate binding and specificity of rhomboid intramembrane protease revealed by substrate-peptide complex structures. *EMBO J.* 33, 2408–2421. doi: 10.15252/embj.201489367

**Conflict of Interest:** The authors declare that the research was conducted in the absence of any commercial or financial relationships that could be construed as a potential conflict of interest.

Copyright © 2020 Liu, Zhao, Zhang, Ubarretxena-Belandia, Forth, Lieberman and Wang. This is an open-access article distributed under the terms of the Creative Commons Attribution License (CC BY). The use, distribution or reproduction in other forums is permitted, provided the original author(s) and the copyright owner(s) are credited and that the original publication in this journal is cited, in accordance with accepted academic practice. No use, distribution or reproduction is permitted which does not comply with these terms.



# Therapeutic Approaches Targeting Protein Aggregation in Amyotrophic Lateral Sclerosis

**Ravinder Malik and Martina Wiedau\***

*Department of Neurology, David Geffen School of Medicine, University of California, Los Angeles, Los Angeles, CA, United States*

Amyotrophic lateral sclerosis (ALS) is a debilitating neurodegenerative disease that targets motor neurons (MNs) in the brain and spinal cord. It leads to gradual loss of motor signals to muscles leading to atrophy and weakness. Most patients do not survive for more than 3–5 years after disease onset. Current ALS treatments provide only a small delay of disease progression. Therefore, it is of utmost importance to explore new therapeutic approaches. One of the major hindrances in achieving this goal is poor understanding of causes of the disease. ALS has complex pathophysiological mechanisms in its genetic and sporadic forms. Protein aggregates are a common hallmark of ALS regardless of cause making protein pathways attractive therapeutic targets in ALS. Here, we provide an overview of compounds in different stages of pharmacological development and their protein pathway targets.

**Keywords:** Lou Gehrig's disease, protein misfolding, superoxide dismutase, C9ORF72 DPRs, motor neuron disease, proteinopathies, proteostasis

## OPEN ACCESS

### Edited by:

Sandra Macedo-Ribeiro,  
University of Porto, Portugal

### Reviewed by:

Nadia D'Ambrosi,  
University of Rome Tor Vergata, Italy  
Amit Mishra,  
Indian Institute of Technology  
Jodhpur, India

### \*Correspondence:

Martina Wiedau  
mwiedau@mednet.ucla.edu

**Received:** 16 December 2019

**Accepted:** 08 May 2020

**Published:** 09 June 2020

### Citation:

Malik R and Wiedau M (2020)  
Therapeutic Approaches Targeting  
Protein Aggregation in Amyotrophic  
Lateral Sclerosis.  
*Front. Mol. Neurosci.* 13:98.  
doi: 10.3389/fnmol.2020.00098

## INTRODUCTION

Amyotrophic lateral sclerosis (ALS) or Lou Gehrig's disease is the most common motor neuron (MN) disease. It is a progressive and fatal neurodegenerative disease, which affects both upper MNs in the motor cortex and lower MNs in brain stem and the anterior spinal cord (Ravits and La Spada, 2009). ALS patients experience muscle cramps, fasciculations, progressive muscle atrophy and weakness, hyperactive reflexes, difficulty with speech, chewing, and swallowing. Ultimately, the breathing muscles are affected leading to respiratory failure (Borasio and Miller, 2001). The average age of disease onset is 55 years (Naruse et al., 2019). More than half of all patients do not live more than 3–4 years after diagnosis, 20% live 5 years or more, and only 10% live more than 10 years. Men are at a 1.2 times higher risk to get the disease as compared to women. Other possible risk factors include genetics, aging, and environmental factors such as toxins, metals, smoking, traumatic head injury, and infections (Seals et al., 2016a; Spencer et al., 2019). Military veterans are approximately twice as likely to develop ALS compared to the average prevalence (Seals et al., 2016b). So far only two drugs are approved by the Federal Drug Administration (FDA) to treat ALS: riluzole and edaravone. These drugs provide limited relief and slow disease progression by a few months. There is no known therapy that can halt the disease. The exact mechanism of the disease is still unknown. Research studies suggest that multiple phenomena can be involved such as protein misfolding and aggregation, impairment of protein trafficking, oxidative stress, RNA dysmetabolism, failure of protein clearance machinery, and imbalance in protein homeostasis (Blokhuys et al., 2013; Parakh and Atkin, 2016; Ramesh and Pandey, 2017; McAlary et al., 2019). Sporadic forms comprise about



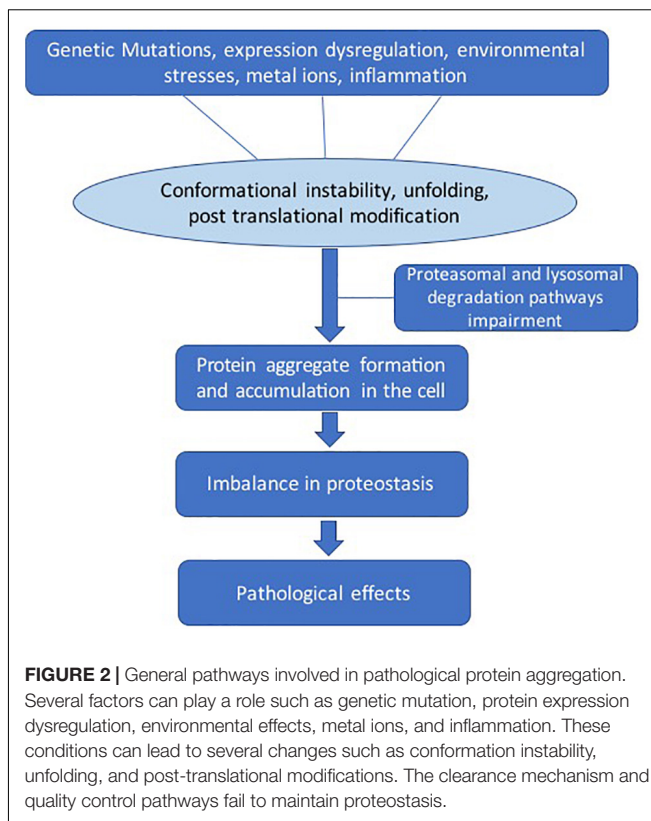
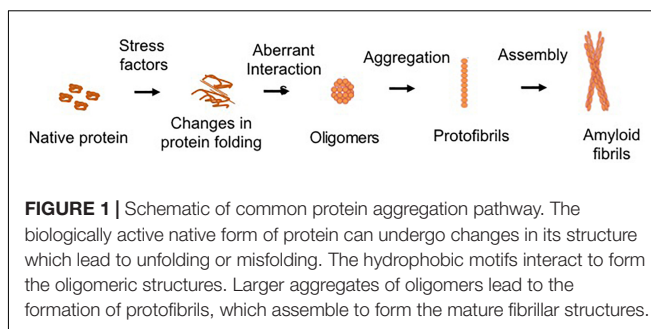
90–95% of all cases. Familial ALS (fALS) accounts for 5–10% of all cases in the United States (Mehta et al., 2018) involving genes such as superoxide dismutase 1 (SOD1), Chromosome 9 open reading frame 72 (C9ORF72), tar-DNA binding protein 43 (TDP-43), and fused in sarcoma (FUS) (Chen et al., 2013; Brenner and Weishaupt, 2019).

Protein aggregation is an important feature of ALS pathology. Amyloid deposits from different proteins such as TDP-43, C9ORF72 dipeptide repeats (DPRs), phosphorylated high molecular weight neurofilament protein (pNFH), rho guanine nucleotide exchange factor (RGNF), and FUS have been detected in ALS MNs (Blokhuis et al., 2013). These aberrant protein deposits may be toxic to the cells, leading to neurodegeneration and are potential targets for therapeutic interventions. In this review, we focus on proteins which form MN aggregates implicated in ALS pathology. Multiple promising efforts to therapeutically target these proteins, either by specific approaches, e.g., interaction modulators or through small molecules or via indirect and/or wide-ranging methods, e.g., by protein degradation pathway regulators or by antisense, are highlighted. We discuss examples of emerging and promising therapeutic candidates at their different stages of development (Table 1).

## DEFINING PROTEIN AGGREGATION

Protein aggregation is the process of aberrant folding of a protein leading to self-association that may cause the formation of oligomers and fibrils via polymerization. The resulting amyloid fibrils are rich in beta sheet structure. Physiologically, proteins undergo folding through chaperones to attain their biologically favored stable conformation. Protein structure is stabilized by covalent and non-covalent interaction between the amino acids (Dobson, 2003). In disease, structural destabilization leads to exposure of hydrophobic amino acids in the outer environment, which have an affinity to self-assemble into larger aggregates and fibrils. The basic mechanism of protein aggregation is through a misfolded or unfolded conformation of the protein monomer that leads to the exposure of hydrophobic patches into hydrophilic cellular environment (Figure 1). The adhesive nature of these patches may lead to self-association into oligomers and eventually into fibrils implicated in many neurodegenerative diseases as non-specific interactions with other cellular proteins interfere with normal cell functions. The intermediates and oligomers can interact with cellular membranes harming membrane integrity leading to the leakage of cellular material and cell death (Holmes et al., 2014).

There are several factors that lead to destabilization of protein structure (Figure 2). Genetic mutations can change the amino acid sequence, leading to altered protein conformation. Dysregulation of molecular chaperone network functions, which govern the protein quality control processes such as protein unfolding and disaggregation and targeting terminally misfolded proteins for proteolytic degradation (Kim et al., 2013). Environmental effects such as changes in pH, temperature,



infection, or chemical modification can also destabilize proteins. The larger protein aggregates accumulate in the cell or extracellularly if clearance mechanisms fail (Rubinsztein, 2006). The dysregulation in the regulatory mechanisms of the cells can lead to imbalance in the homeostasis of proteins (proteostasis) (Labbadia and Morimoto, 2015).

The neurodegenerative diseases caused by protein aggregation are termed proteinopathies. Protein aggregates are the hallmarks of several neurodegenerative disease, for example, amyloid beta and tau in Alzheimer's disease, alpha-synuclein in Parkinson's disease (PD), and huntingtin in Huntington's disease (Forman et al., 2004). ALS is a complex disease as multiple aggregating proteins such as SOD1, TDP-43, FUS, pNFH, and others have been linked to the disease (Chen et al., 2013; Brenner and Weishaupt, 2019).

**TABLE 1 |** Therapeutic protein aggregation targets in ALS.

Therapeutic candidate	Target	Process affected/checked
AAV9-ShRNA-SOD1	SOD1	Suppression of mutant SOD1 mRNA
Arimoclomol	Aggregated proteins	Enhance expression of heat-shock proteins, involved in clearance of aggregated protein
BIIB078	C9ORF72 gene	Antisense against C9ORF72 mRNA to blocks it translation
Colchicine	Proteasome and autophagy	Promotes expression of HSPB8 and autophagy-mediated removal of misfolded proteins
Macrophage migration inhibitory factor (MIF)	SOD1	Misfolding of SOD1
Molecular Tweezer (CLR01)	SOD1	Targets the self-assembly of SOD1
Myricetin	Aggregated proteins	Clearance of protein aggregates by upregulation proteasomal degradation mechanisms
Recombinant human monoclonal antibody ( $\alpha$ -miSOD1)	SOD1 Aggregates	Misfolded Sod 1
Single-chain variable fragment (scFv) derived from the 3B12A monoclonal antibody (MAb)	TDP-43	TDP-43 nuclear export signal
Single-chain variable fragment (scFv) named VH7Vk9	TDP-43	Binding of RNA recognition motif 1 (RRM1) of TDP-43
tgG-DSE2lim and tgG- DSE5b	SOD1	Vaccine against early unfolded protein for rapid clearance by immune system
Tofersen (BIIB067)	SOD1	Reduction in SOD1 protein level by antisense

## THERAPEUTIC TARGETS INVOLVING PROTEIN AGGREGATES IN ALS

### Targeting Protein Aggregates by Antibodies or Their Derived Fragments $\alpha$ -miSOD1

A recombinant human monoclonal antibody (MAb) ( $\alpha$ -miSOD1) was generated by screening human memory B cells from a large cohort of healthy elderly subjects. This antibody selectively binds to misfolded SOD1, but not to physiological SOD1 dimers. On postmortem spinal cord sections from 121 patients with ALS,  $\alpha$ -miSOD1 antibody identified misfolded SOD1 in a majority of cases, regardless of their SOD1 genotype. In transgenic mice overexpressing disease-causing human SOD1-G37R or SOD1-G93A mutations, treatment with the  $\alpha$ -miSOD1 antibody delayed the onset of motor symptoms, extended survival by up to 2 months, and reduced aggregation of misfolded SOD1 and MN degeneration (Maier et al., 2018).

### Single-Chain Variable Fragment of Antibodies

TDP-43 is a ubiquitous protein encoded by the tar-DNA binding protein 43 gene. It is an essential gene for the

development of the CNS from the earliest stages of embryonic life to adulthood. TDP-43 is associated with multiple steps of transcriptional and post-transcriptional regulation. Under physiological conditions, the majority of TDP-43 is nuclear, while a small proportion is continuously involved in nucleocytoplasmic relocation and may form aggregates in the cytoplasm (Baloh, 2011). Aggregates of wild-type TDP-43 are present in both sporadic and familial cases of ALS. Reduction in cytoplasmic TDP-43 inclusions is a promising strategy for both types of ALS. Clearance of TDP-43 was targeted using single-chain variable fragment (scFv) derived from the 3B12A MAb which can recognize a specific region of TDP-43 nuclear export signal called D247. HEK293A cells were transfected with tagged mutant TDP-43 plasmids. Using 3B12A scFv, mislocalized TDP-43 was detected to have a defective nuclear localizing signal. 3B12A scFv also accelerated proteasome-mediated degradation of aggregated TDP-43, most probably due to an endogenous proline (P), glutamic acid (E), serine (S), and threonine (T) rich sequence (PEST). Addition of the chaperone-mediated autophagy related signal to 3B12A scFv induced HSP70 transcription, which further enhanced TDP-43 aggregate clearance and cell viability. The 3B12A scFv reduced TDP-43 aggregates in embryonic mouse brain after *in utero* electroporation without any apparent side effects in postnatal brain pathology or development (Tamaki et al., 2018). In a similar approach, scFv antibody VH7Vk9 was produced against the RNA recognition motif 1 (RRM1) of TDP-43, which is responsible for abnormal protein self-aggregation and interaction with p65 NF- $\kappa$ B (Buratti, 2015). Virus-mediated delivery of VH7Vk9 in HEK293 cells and TDP-43 mice resulted in reduction of the cytoplasmic/nuclear TDP-43 ratio. Colocalization of TDP-43 with ubiquitin and microtubule associated protein 1A/1B light chain (LC-3) suggested improved clearance of the protein via proteasome and autophagosomes. Contralateral and ipsilateral cortices showed reduced microglial activation in TDP-43 mice with improvements of motor functions and cognitive deficits (Pozzi et al., 2019).

### Targeting Protein Aggregates by Vaccines

The seeding hypothesis suggests that protein aggregates can spread the disease pathology to adjacent cells and brain regions. Recent reports have indicated that misfolded SOD1 can act like prions and spread the disease (Healy, 2017; Sibilla and Bertolotti, 2017). Exogenously administered non-native misfolded or aggregated protein has been found to generate an immune response (Malik and Roy, 2011). Even if the exogenous protein is human in nature, the immune system recognizes it as foreign due to its non-native protein conformation. In this approach, the host system would generate antibodies against aggregated protein and clear them through immune response. One study in hSOD1-G37R transgenic mice used an immunological therapy with misfolded protein. Two ALS vaccines against unfolded SOD1, tgG-DSE2lim and tgG-DSE5b, were investigated (Zhao et al., 2019). Both vaccines showed rapid, robust, and well-sustained epitope-specific antibody responses

and increased the life span of treated animals. The question still remains how successfully this approach can be modified to address different mutants and conformations of SOD1 protein. The challenge is to generate antigens for multiple possible conformations of the aggregated protein which is difficult due to transient nature of certain conformations of protein aggregates.

## Targeting Self-Assembly Process by Small Molecules

### Molecular Tweezers

Small horseshoe shaped molecules termed molecular tweezers (MTs) bind reversibly to specific amino acid residues of proteins which enables targeting the process of aggregation rather than targeting a specific protein or protein conformation. MTs achieve this activity by hydrophobic and electrostatic interactions involving labile binding to positively charged amino acid residues, primarily lysine and to a lower extent arginine. Hydrophobic and electrostatic interactions are important, particularly in the early stages of the aberrant self-assembly process which are effectively interrupted by MTs (Malik et al., 2019). They do not affect the protein's bioactivity, but aberrant interactions leading to protein aggregation can be prevented. Using purified recombinant wild-type and mutant SOD1, it was found that the lead MT, CLR01, inhibited the *in vitro* aggregation of different isoforms of SOD1. In a SOD1-G93A transgenic mouse model, CLR01 treatment decreased misfolded SOD1 in the spinal cord significantly. A small, dose-dependent decrease in disease duration was found in CLR01-treated, compared to vehicle-treated animals, yet motor function did not improve in any of the treatment groups (Malik et al., 2019). The MT has been shown to be effective against multiple proteins (Malik et al., 2019) and could, thus become an ideal therapeutic candidate for ALS with its known aggregates of multiple proteins.

### Targeting Proteasome and Autophagy Colchicine

Colchicine is a plant alkaloid that interrupts microtubule formation and other cellular processes. This compound enhances the expression of heat-shock protein B8 (HSPB8) and several other autophagy factors (Crippa et al., 2016). HSPB8 recognizes and promotes the autophagy-mediated removal of misfolded mutant SOD1, as well as TDP-43 fragments from MNs and aggregating species of dipeptides produced in C9ORF72-related diseases (Crippa et al., 2016). A Phase II randomized double-blind, placebo-controlled clinical trial with colchicine in ALS (Co-ALS) was recently initiated. ALS patients will be enrolled in three groups—placebo, colchicine 0.01 mg/day, and colchicine 0.005 mg/day (Mandrioli et al., 2019). The trial will assess safety, tolerability, respiratory function, and functional ratings scale in ALS patients. The investigators will also study the cellular effects of colchicine on specific processes such as autophagy, protein aggregation, stress granules, and exosome secretion. A parallel biomarker analysis of neurofilament protein expression will be performed (Mandrioli et al., 2019).

### Arimoclomol

An investigational drug candidate, arimoclomol enhances expression of HSPs. Previous studies of transgenic SOD1 mice showed a large safety margin up to 300 mg/day. In separate studies, the effect of arimoclomol was tested in early and late stages of the disease. The compound showed promising results in both disease stages as survival was improved (Kieran et al., 2004; Kalmar et al., 2008). A double-blind, placebo-controlled trial was initiated in patients with rapidly progressive early SOD1 fALS. Arimoclomol was administered orally; it has good bioavailability as it crosses the blood–brain barrier. Primary goal of the study was to assess safety and tolerability. Secondary outcome was efficacy, with main focus on survival. The rates of decline of the Revised ALS Functional Rating Scale (ALSFRS-R), percent predicted forced expiratory volume in 6 s (FEV6), and the Combined Assessment of Function and Survival (CAFS) were also used for efficacy evaluation (Benatar et al., 2018). Arimoclomol could treat a broad range of proteinopathies as the main action of this drug involves clearance of aberrant, misfolded, degraded, and aggregated protein by activation of HSPs.

### Myricetin

The polyphenolic flavonoid, myricetin, has shown promise in targeting neurodegenerative diseases such as PD (Maher, 2019). The clear mechanism of action by which it upregulates proteasomal degradation mechanisms is not known. In ALS, cell culture studies have shown protein aggregate clearing effects of myricetin. Cos-7 cells were transfected with plasmid constructs of WT and mutant SOD1 leading to spontaneous intracellular accumulation of mutant SOD1 and WT accumulation after adding a proteasome inhibiting compound. On treatment with 10  $\mu$ M myricetin for 48 h, immunofluorescence analysis showed a decrease in the intracellular aggregation of ubiquitin-positive SOD1. Myricetin increased chaperone HSP70 level and ultimately cell survival (Joshi et al., 2019).

### Macrophage Migration Inhibitory Factor (MIF)

NSC-34 culture studies revealed that macrophage migration inhibitory factor (MIF) can reduce misfolded SOD1 and increase cell survival. One of the functions of MIF involves chaperone-like properties, which appear to change SOD1 amyloid aggregation pathways by forming disordered aggregates, which are less toxic to the cells (Shvil et al., 2018). Shvil et al. reported when NSC-34 cells are co-transfected with mutant SOD1-G93A and MIF, mutant SOD1 misfolding is affected by MIF, which prevents accumulation of mutant SOD1 in cytoplasm. MIF expression normalized the nuclear and cytoplasmic distribution of SOD1 to similar levels as wild-type SOD1 distribution (Shvil et al., 2018). Studies of MIF in animal models to investigate the therapeutic potential of MIF have not been performed.

### Targeting Aggregating Proteins by Suppressing Gene Expression Superoxide Dismutase 1

Mutations in SOD1 cause 15–20% of fALS cases. The resulting amino-acid substitutions destabilize SOD1's protein structure,



leading to its self-assembly into neurotoxic oligomers and aggregates, a process hypothesized to cause MN degeneration. The aggregates are found in the brain and spinal cord of affected individuals as intracellular inclusions. The antisense molecule tofersen (BIIB067) was designed to bind SOD1 mRNA. The artificially created DNA specifically targets the mRNA stage. Tofersen prevents translation of mRNA and ultimately the RNA degrades due to abnormal DNA-RNA strands, thereby reducing mutant SOD1 protein production. A Phase 1 clinical trial assessing the safety, tolerability, and activity of tofersen in SOD1-related fALS patients has been completed. The randomized, double-blind, placebo-controlled safety trial tested four different doses of tofersen (0.15, 0.5, 1.5, or 3 mg) in 33 patients over a 12-h period. No serious adverse effects were observed in their assessment over 28 days post-treatment (Biogen, 2019). This treatment is moving to a Phase 3 trial to evaluate its efficacy in fALS. Another gene silencing approach that targets SOD1 by using adeno-associated virus (AAV) delivered shRNA in mice, pigs, and non-human primates showed prolonged suppression of MN disease. A new device design was used for injections which enabled homogeneous delivery throughout the cervical spinal cord white and gray matter and brain motor centers after a single subpial injection (Bravo-Hernandez et al., 2020). This approach could become an efficient strategy that may be extended to other delivery vectors.

### Dipeptide Repeats of C9ORF72

The most common cause of fALS is the hexanucleotide repeat expansion in the C9ORF72 gene which is linked to 25–40% of all familial cases. Mutant C9ORF72 forms toxic DPRs (Gendron and Petrucelli, 2018). Recent studies have also demonstrated that arginine-rich DPRs (poly glycine-arginine/proline-arginine (GR/PR) are one of the major sources of neurotoxicity by targeting nucleopore complexes, thus affecting the nuclear–cytoplasmic trafficking of RNA and proteins (Zhang et al., 2015; Shi et al., 2018). Therefore, the gradual accumulation of those highly toxic DPRs, even at very low levels, could render neurons vulnerable (Lee et al., 2017). An experimental antisense oligonucleotide, BIIB078, developed by Ionis Pharmaceuticals, specifically targets C9ORF72 blocking

its translation. This reduces the DPRs burden in the cell and their toxic effects. ALS mouse model studies showed extended survival and, surprisingly in some cases, muscle function also improved indicating reversal of disease symptoms. Phase 1 trials have been initiated focusing on assessing the safety of BIIB078. The trial will enroll nearly 60 people with ALS (Clinical Trials, 2019).

## CONCLUSION

A number of different compounds that target a diverse range of mechanisms of neuronal protein aggregation pathways have demonstrated early favorable results in preclinical and early clinical ALS studies. Those include targeting mRNA—both for degradation and to inhibit translation, clearance of protein aggregates using antibodies, disruption of protein–protein interactions that lead to aggregation, preventing the formation of aggregates using vaccines, and maintaining proteostasis by activating protein clearance mechanism. This diverse list of approaches highlights the complexity and the investigational challenges of targeting protein aggregation in ALS. Although there is growing evidence that the process of protein aggregation is an important driver of neurodegeneration, a proven structure–proteotoxicity relationship based on specific protein abnormalities such as folding or aggregate state is lacking. Further basic research into the role of protein abnormalities in ALS disease mechanism is needed to guide preclinical studies toward disease specific treatments.

## AUTHOR CONTRIBUTIONS

RM contributed to writing the manuscript. MW contributed to writing and reviewing the manuscript.

## FUNDING

We thank the David Vickter Foundation for supporting this work.

## REFERENCES

- Baloh, R. H. (2011). TDP-43: the relationship between protein aggregation and neurodegeneration in amyotrophic lateral sclerosis and frontotemporal lobar degeneration. *FEBS J.* 278, 3539–3549. doi: 10.1111/j.1742-4658.2011.08256.x
- Benatar, M., Wu, J., Andersen, P. M., Atassi, N., David, W., Cudkowicz, M., et al. (2018). Randomized, double-blind, placebo-controlled trial of arimoclomol in rapidly progressive SOD1 ALS. *Neurology* 90, e565–e574. doi: 10.1212/wnl.0000000000004960
- Biogen (2019). Available online at: <http://investors.biogen.com/news-releases/news-release-details/biogen-present-new-interim-data-its-phase-12-clinical-study> (accessed September 24, 2019).
- Blokhuis, A. M., Groen, E. J., Koppers, M., van den Berg, L. H., and Pasterkamp, R. J. (2013). Protein aggregation in amyotrophic lateral sclerosis. *Acta Neuropathol.* 125, 777–794.
- Borasio, G. D., and Miller, R. G. (2001). Clinical characteristics and management of ALS. *Semin. Neurol.* 21, 155–166. doi: 10.1055/s-2001-15268
- Bravo-Hernandez, M., Tadokoro, T., Navarro, M. R., Platoshyn, O., Kobayashi, Y., Marsala, S., et al. (2020). Spinal subpial delivery of AAV9 enables widespread gene silencing and blocks motoneuron degeneration in ALS. *Nat. Med.* 26, 118–130. doi: 10.1038/s41591-019-0674-1
- Brenner, D., and Weishaupt, J. H. (2019). Update on amyotrophic lateral sclerosis genetics. *Curr. Opin. Neurol.* 32, 735–739.
- Buratti, E. (2015). Functional significance of TDP-43 mutations in disease. *Adv. Genet.* 91, 1–53. doi: 10.1016/bs.adgen.2015.07.001
- Chen, S., Sayana, P., Zhang, X., and Le, W. (2013). Genetics of amyotrophic lateral sclerosis: an update. *Mol. Neurodegener.* 8:28.
- Clinical Trials (2019). Available online at: <https://clinicaltrials.gov/ct2/show/NCT03626012> (accessed September 24, 2019).
- Crippa, V., D'Agostino, V. G., Cristofani, R., Rusmini, P., Cicardi, M. E., Messi, E., et al. (2016). Transcriptional induction of the heat shock protein B8 mediates the clearance of misfolded proteins responsible for motor neuron diseases. *Sci. Rep.* 6:22827.
- Dobson, C. M. (2003). Protein folding and misfolding. *Nature* 426, 884–890.



- Forman, M. S., Trojanowski, J. Q., and Lee, V. M. (2004). Neurodegenerative diseases: a decade of discoveries paves the way for therapeutic breakthroughs. *Nat. Med.* 10, 1055–1063. doi: 10.1038/nm1113
- Gendron, T. F., and Petrucelli, L. (2018). Disease mechanisms of C9ORF72 repeat expansions. *Cold Spring Harb. Perspect. Med.* 8:a024224. doi: 10.1101/cshperspect.a024224
- Healy, E. F. (2017). A prion-like mechanism for the propagated misfolding of SOD1 from in silico modeling of solvated near-native conformers. *PLoS One* 12:e0177284. doi: 10.1371/journal.pone.0177284
- Holmes, W. M., Klaips, C. L., and Serio, T. R. (2014). Defining the limits: Protein aggregation and toxicity in vivo. *Crit. Rev. Biochem. Mol. Biol.* 49, 294–303. doi: 10.3109/10409238.2014.914151
- Joshi, V., Mishra, R., Upadhyay, A., Amanullah, A., Poluri, K. M., Singh, S., et al. (2019). Polyphenolic flavonoid (Myricetin) upregulated proteasomal degradation mechanisms: eliminates neurodegenerative proteins aggregation. *J. Cell. Physiol.* 234, 20900–20914. doi: 10.1002/jcp.28695
- Kalmar, B., Novoselov, S., Gray, A., Cheetham, M. E., Margulis, B., Greensmith, L., et al. (2008). Late stage treatment with arimoclolel delays disease progression and prevents protein aggregation in the SOD1 mouse model of ALS. *J. Neurochem.* 107, 339–350. doi: 10.1111/j.1471-4159.2008.05595.x
- Kieran, D., Dick, J. R., Riddoch-Contreras, J., Burnstock, G., and Greensmith, L. (2004). Treatment with arimoclolel, a coinducer of heat shock proteins, delays disease progression in ALS mice. *Nat. Med.* 10, 402–405. doi: 10.1038/nm1021
- Kim, Y. E., Hipp, M. S., Bracher, A., Hayer-Hartl, M., and Hartl, F. U. (2013). Molecular chaperone functions in protein folding and proteostasis. *Annu. Rev. Biochem.* 82, 323–355. doi: 10.1146/annurev-biochem-060208-092442
- Labbadia, J., and Morimoto, R. I. (2015). The biology of proteostasis in aging and disease. *Annu. Rev. Biochem.* 84, 435–464. doi: 10.1146/annurev-biochem-060614-033955
- Lee, Y. B., Baskaran, P., Gomez-Deza, J., Chen, H. J., Nishimura, A. L., Smith, B. N., et al. (2017). C9orf72 poly GA RAN-translated protein plays a key role in amyotrophic lateral sclerosis via aggregation and toxicity. *Hum. Mol. Genet.* 26, 4765–4777. doi: 10.1093/hmg/ddx350
- Maher, P. (2019). The potential of flavonoids for the treatment of neurodegenerative diseases. *Int. J. Mol. Sci.* 20:3056. doi: 10.3390/ijms20123056
- Maier, M., Welt, T., Wirth, F., Montrasio, F., Preisig, D., McAfoose, J., et al. (2018). A human-derived antibody targets misfolded SOD1 and ameliorates motor symptoms in mouse models of amyotrophic lateral sclerosis. *Sci. Transl. Med.* 10:eah3924. doi: 10.1126/scitranslmed.aah3924
- Malik, R., Meng, H., Wongkongkathap, P., Corrales, C. I., Sepanj, N., Atlasi, R. S., et al. (2019). The molecular tweezer CLR01 inhibits aberrant superoxide dismutase 1 (SOD1) self-assembly in vitro and in the G93A-SOD1 mouse model of ALS. *J. Biol. Chem.* 294, 3501–3513. doi: 10.1074/jbc.ra118.005940
- Malik, R., and Roy, I. (2011). Probing the mechanism of insulin aggregation during agitation. *Int. J. Pharm.* 413, 73–80. doi: 10.1016/j.ijpharm.2011.04.024
- Mandrioli, J., Crippa, V., Cereda, C., Bonetto, V., Zucchi, E., Gessani, A., et al. (2019). Proteostasis and ALS: protocol for a phase II, randomised, double-blind, placebo-controlled, multicentre clinical trial for colchicine in ALS (Co-ALS). *BMJ Open* 9:e028486. doi: 10.1136/bmjopen-2018-028486
- McAlary, L., Plotkin, S. S., Yerbury, J. J., and Cashman, N. R. (2019). Prion-like propagation of protein misfolding and aggregation in amyotrophic lateral sclerosis. *Front. Mol. Neurosci.* 12:262. doi: 10.3389/fnmol.2019.00262
- Mehta, P., Kaye, W., Raymond, J., Wu, R., Larson, T., Punjani, R., et al. (2018). Prevalence of amyotrophic lateral sclerosis - United States, 2014. *MMWR Morb. Mortal. Wkly. Rep.* 67, 216–218.
- Naruse, H., Ishiura, H., Mitsui, J., Takahashi, Y., Matsukawa, T., Tanaka, M., et al. (2019). Burden of rare variants in causative genes for amyotrophic lateral sclerosis (ALS) accelerates age at onset of ALS. *J. Neurol. Neurosurg. Psychiatry* 90, 537–542. doi: 10.1136/jnnp-2018-318568
- Parakh, S., and Atkin, J. D. (2016). Protein folding alterations in amyotrophic lateral sclerosis. *Brain Res.* 1648(Pt B), 633–649. doi: 10.1016/j.brainres.2016.04.010
- Pozzi, S., Thammisetty, S. S., Codron, P., Rahimian, R., Plourde, K. V., Soucy, G., et al. (2019). Virus-mediated delivery of antibody targeting TAR DNA-binding protein-43 mitigates associated neuropathology. *J. Clin. Invest.* 129, 1581–1595. doi: 10.1172/jci123931
- Ramesh, N., and Pandey, U. B. (2017). Autophagy dysregulation in ALS: when protein aggregates get out of hand. *Front. Mol. Neurosci.* 10:263. doi: 10.3389/fnmol.2017.00263
- Ravits, J. M., and La Spada, A. R. (2009). ALS motor phenotype heterogeneity, focality, and spread: deconstructing motor neuron degeneration. *Neurology* 73, 805–811. doi: 10.1212/wnl.0b013e3181b6bbbd
- Rubinsztein, D. C. (2006). The roles of intracellular protein-degradation pathways in neurodegeneration. *Nature* 443, 780–786. doi: 10.1038/nature05291
- Seals, R. M., Hansen, J., Gredal, O., Weisskopf, M. G., et al. (2016a). Physical trauma and amyotrophic lateral sclerosis: a population-based study using danish national registries. *Am. J. Epidemiol.* 183, 294–301. doi: 10.1093/aje/kwv169
- Seals, R. M., Kioumourtoglou, M. A., Hansen, J., Gredal, O., and Weisskopf, M. G. (2016b). Amyotrophic lateral sclerosis and the military: a population-based study in the danish registries. *Epidemiology* 27, 188–193.
- Shi, Y., Lin, S., Staats, K. A., Li, Y., Chang, W. H., Hung, S. T., et al. (2018). Haploinsufficiency leads to neurodegeneration in C9ORF72 ALS/FTD human induced motor neurons. *Nat. Med.* 24, 313–325. doi: 10.1038/nm.4490
- Shvil, N., Banerjee, V., Zoltsman, G., Shani, T., Kahn, J., Abu-Hamad, S., et al. (2018). MIF inhibits the formation and toxicity of misfolded SOD1 amyloid aggregates: implications for familial ALS. *Cell Death Dis.* 9:107.
- Sibilla, C., and Bertolotti, A. (2017). Prion properties of SOD1 in amyotrophic lateral sclerosis and potential therapy. *Cold Spring Harb. Perspect. Biol.* 9:a024141. doi: 10.1101/cshperspect.a024141
- Spencer, P. S., Lagrange, E., and Camu, W. (2019). ALS and environment: clues from spatial clustering?. *Rev. Neurol.* 175, 652–663.
- Tamaki, Y., Shodai, A., Morimura, T., Hikami, R., Minamiyama, S., Ayaki, T., et al. (2018). Elimination of TDP-43 inclusions linked to amyotrophic lateral sclerosis by a misfolding-specific intrabody with dual proteolytic signals. *Sci. Rep.* 8:6030.
- Zhang, K., Donnelly, C. J., Haeusler, A. R., Grima, J. C., Machamer, J. B., Steinwald, P., et al. (2015). The C9orf72 repeat expansion disrupts nucleocytoplasmic transport. *Nature* 525, 56–61. doi: 10.1038/nature14973
- Zhao, B., Marciniuk, K., Gibbs, E., Yousefi, M., Napper, S., Cashman, N. R., et al. (2019). Therapeutic vaccines for amyotrophic lateral sclerosis directed against disease specific epitopes of superoxide dismutase 1. *Vaccine* 37, 4920–4927. doi: 10.1016/j.vaccine.2019.07.044

**Conflict of Interest:** The authors declare that the research was conducted in the absence of any commercial or financial relationships that could be construed as a potential conflict of interest.

Copyright © 2020 Malik and Wiedau. This is an open-access article distributed under the terms of the Creative Commons Attribution License (CC BY). The use, distribution or reproduction in other forums is permitted, provided the original author(s) and the copyright owner(s) are credited and that the original publication in this journal is cited, in accordance with accepted academic practice. No use, distribution or reproduction is permitted which does not comply with these terms.



# Targeting Amyloidogenic Processing of APP in Alzheimer's Disease

Jing Zhao<sup>1</sup>, Xinyue Liu<sup>1</sup>, Weiming Xia<sup>2,3</sup>, Yingkai Zhang<sup>4</sup> and Chunyu Wang<sup>1,5,6\*</sup>

<sup>1</sup> Center for Biotechnology and Interdisciplinary Studies, Rensselaer Polytechnic Institute, Troy, NY, United States,

<sup>2</sup> Geriatric Research Education Clinical Center, Edith Nourse Rogers Memorial Veterans Hospital, Bedford, MA,

United States, <sup>3</sup> Department of Pharmacology and Experimental Therapeutics, School of Medicine, Boston University,

Boston, MA, United States, <sup>4</sup> Department of Chemistry, New York University, New York, NY, United States, <sup>5</sup> Department of

Biological Sciences, Rensselaer Polytechnic Institute, Troy, NY, United States, <sup>6</sup> Department of Chemistry and Chemical

Biology, Rensselaer Polytechnic Institute, Troy, NY, United States

Alzheimer's disease (AD) is the most common type of senile dementia, characterized by neurofibrillary tangle and amyloid plaque in brain pathology. Major efforts in AD drug were devoted to the interference with the production and accumulation of amyloid- $\beta$  peptide ( $A\beta$ ), which plays a causal role in the pathogenesis of AD.  $A\beta$  is generated from amyloid precursor protein (APP), by consecutive cleavage by  $\beta$ -secretase and  $\gamma$ -secretase. Therefore,  $\beta$ -secretase and  $\gamma$ -secretase inhibition have been the focus for AD drug discovery efforts for amyloid reduction. Here, we review  $\beta$ -secretase inhibitors and  $\gamma$ -secretase inhibitors/modulators, and their efficacies in clinical trials. In addition, we discussed the novel concept of specifically targeting the  $\gamma$ -secretase substrate APP. Targeting amyloidogenic processing of APP is still a fundamentally sound strategy to develop disease-modifying AD therapies and recent advance in  $\gamma$ -secretase/APP complex structure provides new opportunities in designing selective inhibitors/modulators for AD.

**Keywords:** Alzheimer's disease, amyloid- $\beta$ ,  $\beta$ -secretase inhibitor,  $\gamma$ -secretase inhibitors,  $\gamma$ -secretase modulator, clinical trial

## OPEN ACCESS

### Edited by:

Maria Rosário Almeida,  
Universidade do Porto, Portugal

### Reviewed by:

Homira Behbahani,  
Karolinska Institutet (KI), Sweden  
Hong Qing,  
Beijing Institute of Technology, China

### \*Correspondence:

Chunyu Wang  
wangc5@rpi.edu

**Received:** 04 May 2020

**Accepted:** 08 July 2020

**Published:** 04 August 2020

### Citation:

Zhao J, Liu X, Xia W, Zhang Y and  
Wang C (2020) Targeting  
Amyloidogenic Processing of APP  
in Alzheimer's Disease.  
Front. Mol. Neurosci. 13:137.  
doi: 10.3389/fnmol.2020.00137

## INTRODUCTION

Alzheimer's disease (AD) is a progressive and incurable neurodegenerative disorder, characterized by progressive and irreversible loss of memory. AD is the leading cause of senile dementia. The number of people age 65 and older living with AD's dementia in the United States is projected to grow from 5.8 million in 2020 to 13.8 million by 2050 (Alzheimer's Association, 2020). Cognitive deficits caused by AD, such as progressive memory loss, difficulty in communication and movement disorder, significantly compromise the patients' quality of life, leading to hospitalization and eventually death due to complications. AD has been recognized as one of the most difficult medical problems with hefty economic burden (Wimo et al., 2010). Total medical expenses for Alzheimer's or other dementias in the United States are projected to be \$305 billion in 2020 (Alzheimer's Association, 2020). The cost of AD is likely to skyrocket in the near future, due to rising ageing population, increasing mortality relative to other disease and the absence of a disease-modifying drug. Therefore, there is a major unmet medical need for disease-modifying therapies for AD.

Approved drugs for AD include acetylcholinesterase inhibitors (Aricept®, Exelon®, Razadyne®) and NMDA-antagonist memantine (Namenda®). However, these drugs are not disease-modifying, only improving symptoms without slowing down or stopping AD from progressing.

In the last 30 years, a large number of drug candidates have entered clinical development but no new drug for AD has been approved since memantine in 2003. The majority of AD drug discovery focused on inhibiting the amyloid- $\beta$  peptide (A $\beta$ ) production from the amyloidogenic processing of APP.

## AMYLOID CASCADE HYPOTHESIS AND AMYLOIDOGENIC PROCESSING OF APP

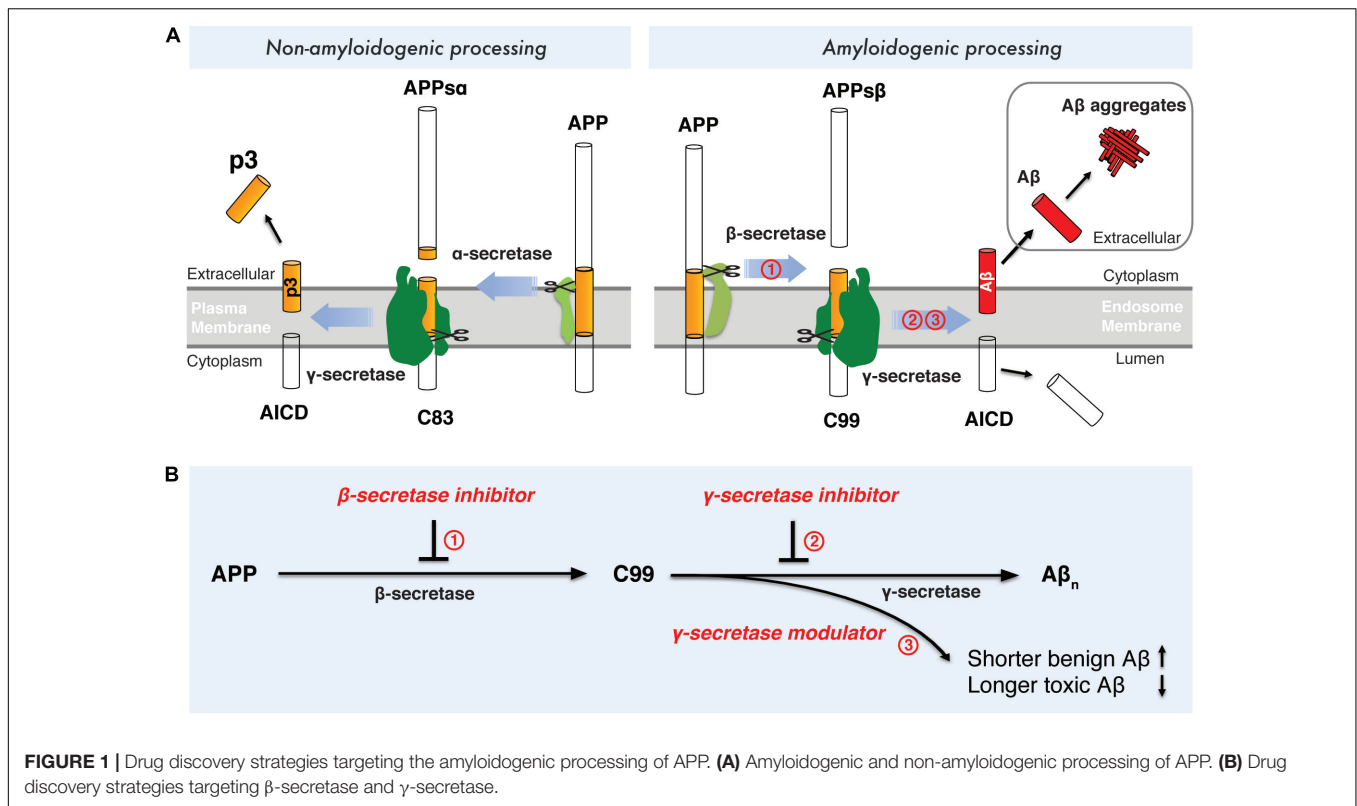
In the past 30 years, the amyloid hypothesis has been extensively tested and amyloid has been the most compelling therapeutic target for AD. Despite ongoing debates about this hypothesis in light of recent failures of anti-amyloid-based clinical trials, new evidences continue to emerge to support the idea that an imbalance between production and clearance of A $\beta$  peptides is the initiating event of AD pathogenic processes. Abnormal accumulation of amyloid eventually leads to formation of senile plaques and neurofibrillary tangles, two pathological hallmarks of AD. A $\beta$  aggregates were found to be toxic both *in vitro* and *in vivo*. Numerous studies have shown that A $\beta$  aggregates, especially soluble oligomers, impair both synaptic function and structure (Kokubo et al., 2005; Wilcox et al., 2011). Injection of soluble A $\beta$ 42 oligomers directly isolated from AD cerebral cortex into healthy rats leads to impaired memory (Selkoe et al., 2016). In addition, accumulation of A $\beta$  oligomers can not only trigger AD-type tau hyperphosphorylation and cause neurotic dystrophy (Jin et al., 2011; Stancu et al., 2014; Jacobs et al., 2018), but also activate neuroinflammation (Park et al., 2018; Henstridge et al., 2019). Apolipoprotein E4, the greatest genetic risk factor for late-onset AD, impairs A $\beta$  clearance and promotes A $\beta$  accumulation in the brain (Carter et al., 2001; Wildsmith et al., 2013). Along with tau, A $\beta$  might be transmissible through the A $\beta$  contaminants in cadaver-derived human growth hormone for the treatment of Creutzfeldt-Jakob disease (Duyckaerts et al., 2018). From human genetics, dominant mutations causing early-onset familial AD reside either in APP or presenilin (catalytic sub-unit of  $\gamma$ -secretase), which alter the proteolytic processing of APP in ways either elevating the A $\beta$ 42/A $\beta$ 40 ratio or increasing the self-aggregation propensity of resultant A $\beta$  peptides (De Jonghe, 2001; Selkoe, 2001; Chen et al., 2014). Duplication of the APP gene in Down's syndrome leads to A $\beta$  deposits in the teens, and almost invariably leads to AD at an early age (Lejeune et al., 1959; Head et al., 2012). Interestingly, three DS patients with partial trisomy that excludes the APP gene did not develop dementia (Korbel et al., 2009; Doran et al., 2016). The human genetics of DS strikingly demonstrates that increasing A $\beta$  dosage (APP duplication) causes dementia, while normalized A $\beta$  dosage in DS (partial trisomy without APP duplication) prevents dementia (albeit the sample size = 3 is low), affirming that amyloid reduction is a fundamentally sound strategy for disease-modifying treatment of AD. The failures of anti-amyloid clinical trials in recent years can be attributed to giving the therapy too late to the patients, poor clinical trial design, heterogeneity of the trial patient population etc.

A $\beta$  is a small peptide generated by proteolytic processing of APP (Figure 1A), a type-I transmembrane protein with a

large extracellular domain. APP is transported to the plasma membrane through the endoplasmic reticulum-Golgi secretory pathway. The majority of APP is processed via the non-amyloidogenic pathway at the plasma membrane (Figure 1A). In the non-amyloidogenic pathway, APP is cleaved by  $\alpha$ -secretase within the A $\beta$  domain between Lys16 and Leu17, producing a soluble N-terminal fragment (APPs  $\alpha$ ) and a membrane-bound C-terminal fragment, C83, which can be further cleaved by  $\gamma$ -secretases and generates a soluble extracellular p3 peptide, thus precluding the formation of intact A $\beta$  (Figure 1A; Anderson et al., 1991; Sisodia, 1992; Wilson et al., 1999). Unlike the non-amyloidogenic pathway, APP is internalized and delivered to endosomes in the amyloidogenic pathway (Bu, 2009). During amyloidogenic APP processing, APP is cleaved by  $\beta$ -secretase (BACE1,  $\beta$ -site APP-cleaving enzyme 1), generating a soluble N-terminal fragment (APPs $\beta$ ) and a membrane-bound C-terminal fragment (C99) (Vassar, 2004; Vassar et al., 1999). Within the membrane, C99 is subsequently cleaved by an enzymatic complex known as  $\gamma$ -secretase, releasing a cytoplasmic polypeptide termed AICD (APP intracellular domain) at the luminal side and A $\beta$  peptides (Thinakaran and Koo, 2008) at the other side of the membrane. AICD is transferred to the nucleus, where it functions as a transcriptional factor (Berridge, 2010), whereas the A $\beta$  peptides are secreted into the extracellular space when the endosome recycles to cell surface.  $\gamma$ -Secretase cleaves APP at variable sites within the transmembrane domain, generating A $\beta$  peptides ranging in length from 38 to 43 residues (Selkoe and Wolfe, 2007). Among different A $\beta$  species, A $\beta$ 42 and A $\beta$ 43 are highly self-aggregating, while A $\beta$ 40 and shorter peptides are relatively benign (Burdick et al., 1992). A $\beta$ 42 and A $\beta$ 40 are the two common A $\beta$  species in the human brain and the increased A $\beta$ 42/A $\beta$ 40 ratio is a common biochemical feature in the early-onset familial AD (FAD) caused by mutations in APP and presenilin. A $\beta$ 42 aggregates rapidly into neurotoxic oligomers, leading to fibrils and plaques. It has been proposed that A $\beta$  oligomers are more toxic than fibrils, therefore it may play a more important role than amyloid plaque in AD progression. Aberrant process of APP by  $\beta$ -secretase and  $\gamma$ -secretase may result in imbalance between production and clearance of A $\beta$  peptides, leading to toxic oligomers, fibrils and senile plaques. Interestingly, pathogenic mutations in presenilin were found to destabilize  $\gamma$ -secretase-APP interactions and thus enhance the production of longer A $\beta$  peptides (Chávez-Gutiérrez et al., 2012; Veugelen et al., 2016; Szaruga et al., 2017). These findings point to enhancing the stability of  $\gamma$ -secretase-A $\beta$ <sub>n</sub> complex as a potential therapeutic approach for AD.

## DRUG DISCOVERY TARGETING AMYLOIDOGENIC PROCESSING OF APP

Interference with the amyloidogenic processing of APP has been a major strategy to modulate A $\beta$  production. As two crucial enzymes catalyzing the intramembrane proteolysis of APP,  $\beta$ -secretase and  $\gamma$ -secretase have been the most prominent targets for AD drug discovery. In the past two decades, numerous  $\beta$ -secretase inhibitors and  $\gamma$ -secretase inhibitors/modulators



were discovered to inhibit or modulate the amyloidogenic processing of APP, either causing the reduced production of total A $\beta_n$  or shifting the production of A $\beta$  to shorter and more benign A $\beta$  species (**Figure 1B**).

## Drug Discovery Targeting $\beta$ -Secretase

### $\beta$ -Secretase

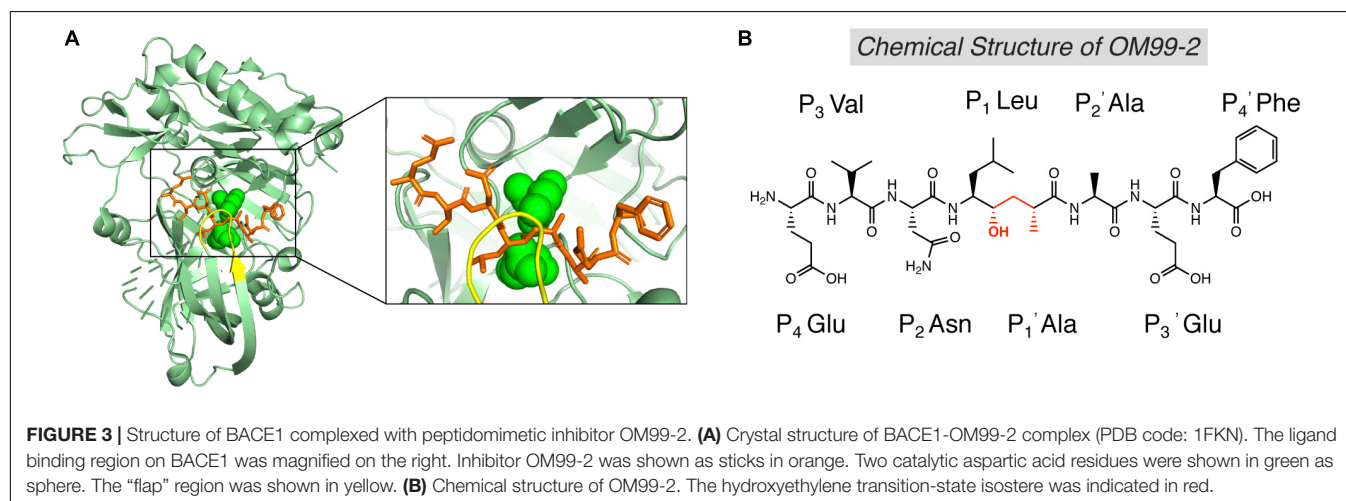
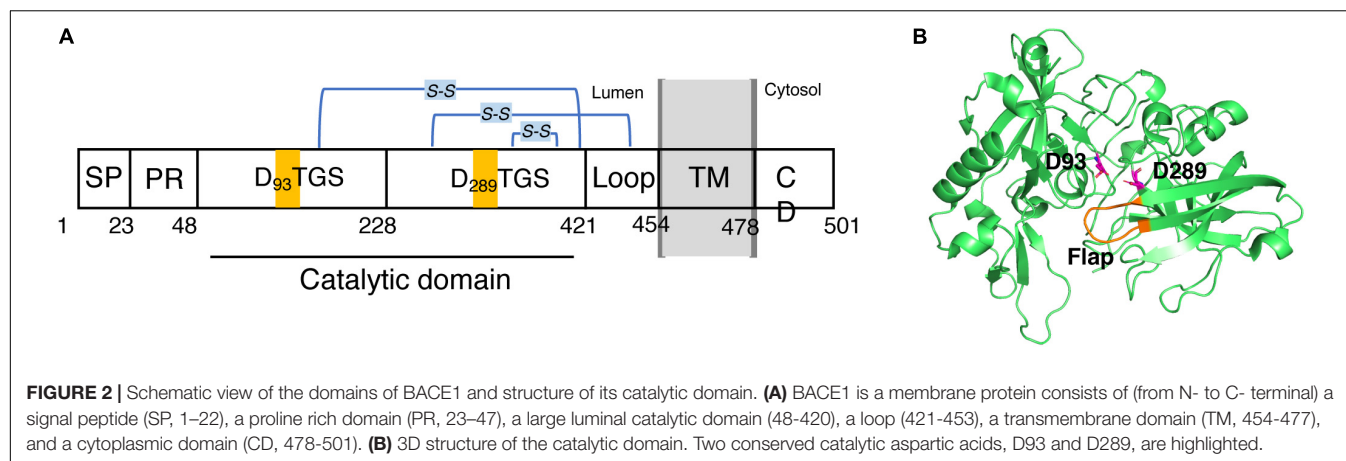
$\beta$ -secretase, also named as BACE1 ( $\beta$ -site APP-cleaving enzyme 1), was identified in 1999 (Fairbanks et al., 1999; Hussain et al., 1999; Vassar et al., 1999; Yan et al., 1999; Lin et al., 2000) as an APP-cleaving aspartyl protease. BACE1 is the principal neuronal protease for generating C99 from APP, which leads to subsequent A $\beta$  generation by  $\gamma$ -secretase. Importantly, BACE1 shedding of APP is a prerequisite for  $\gamma$ -secretase cleavage within the transmembrane domain of APP for A $\beta$  production. Secretion of A $\beta$  peptides is abolished in cultures of BACE1-deficient embryonic cortical neurons (Cai et al., 2001). Naturally, BACE1 inhibition has been a widely pursued therapeutic target for amyloid reduction.

BACE1 is a type-I membrane protein with 501 amino acid residues related to the pepsin family. It is localized within acidic subcellular compartments of the secretory pathway, primarily the Golgi apparatus and endosomes. As shown in **Figure 2A**, BACE1 has an N-terminal signal sequence (residues 1–21), a pro-peptide domain (residues 22–45), a large luminal catalytic domain (residues 46–451), a single transmembrane domain (residues 452–483), and a short cytoplasmic domain (residues 484–501) (Hussain et al., 1999; Benjannet et al., 2001). In

addition, BACE1 has several N-linked glycosylation sites and six cysteine residues that form three intramolecular disulfide bonds, C216–C420, C278–C443, and C330–C380. The N-terminal signal sequence and pro-peptide domain were removed post-translationally, so the mature BACE1 sequence begins at residue Glu46 (Creemers et al., 2001). In the luminal catalytic domain for the  $\beta$ -site cleavage of APP, BACE1 contains two motifs, DTGS (residues 93–96) and DSGT (residues 289–292), which contain the two highly conserved catalytic aspartates (Hussain et al., 1999; Bennett et al., 2000). The crystal structure of the catalytic domain (residues 56–446) of BACE1 with an inhibitor was first published by Hong et al. in 2000 (PDB code: 1FKN) (Hong et al., 2000). Like other aspartic proteases, the substrate binding cleft was located between the N- and C-terminal lobes of BACE1, together with a  $\beta$ -hairpin loop which forms the flap region. The flap opens to allow the substrate to enter and then closes down on the substrate during catalysis and reopens to release the hydrolyzed products. As shown in **Figure 2B**, the two conserved aspartate, D93 and D289, are located at the groove between the N- and C-terminal lobes, partially covered by the “flap” (residues 130–135) (Hong et al., 2000). A later substrate-free (apo) structure of BACE1 (PDB code: 1W50) showed a water molecule located between D93 and D289, which is likely involved in nucleophilic attack for peptide hydrolysis and important binding site for inhibitors (Patel et al., 2004; Ghosh and Osswald, 2014).

BACE1 cleavage is highly specific and cleaves APP only at the  $\beta$ -secretase sites of Asp1 and Glu11 of A $\beta$  (Vassar et al., 1999). As expected, BACE1 cleaves the Swedish APP mutant 10 to 100-fold more efficiently than wild-type APP. BACE1 appeared to be





an ideal target for drug discovery since its complete inhibition should shut down the amyloidogenic APP processing.

### Drug Discovery Targeting BACE1

The first generation of BACE1 inhibitors are peptidomimetic transition-state analogs, which were designed to be accommodated within the substrate-binding cleft of BACE1. In 2000, Hong et al. developed an 8-residue peptide OM99-2 utilizing the template of the  $\beta$ -cleavage site of Swedish APP, where the scissile peptide bond was replaced by a Leu-Ala hydroxyethylene transition-state isostere (**Figure 3B**; Ghosh et al., 2000). The crystal structure of BACE1 and OM99-2 complex (**Figure 3A**) provided coveted molecular insight into the ligand/enzyme interaction and significantly advanced the development of BACE1 inhibitors (Hong et al., 2000). Catalytic aspartates D93 and D289 (see **Figure 3A**, in green) are located at the center of the substrate binding pocket. There are four hydrogen bonds between the catalytic aspartates and the transition state isostere hydroxyl, and ten hydrogen bonds between the binding cleft and flap to OM99-2 backbone. As shown in **Figure 3A**, the “flap” (in yellow) closes over the top of the cleft upon the binding of the inhibitor. Further investigation led to the design of inhibitor OM00-3 by the replacement

of the P2' Ala in OM99-2 with a Val, which achieved a five-fold enhancement of inhibitory potency (Hong et al., 2002). Additional peptidomimetic inhibitors were developed, including KMI-008, KMI-420, and KMI-429 by Kiso's group (Shuto et al., 2003; Kimura et al., 2005; Asai et al., 2006), GSK188909 (Hussain et al., 2007), and compound 11 (Iserloh et al., 2008), etc. However, the big molecular size precludes the application of peptidomimetic BACE1 inhibitors *in vivo*, due to their short half-life, deficiency in crossing the BBB, and low oral availability. Therefore, later generations of BACE1 inhibitors are mostly non-peptidic small molecules.

High-throughput screening (HTS) and fragment-based drug discovery (FBDD) are two major methods employed to explore non-peptidyl small molecule BACE1 inhibitors. In contrast to traditional HTS, which uses libraries of drug-like compounds (typically 300–500 Da), FBDD screens libraries of small fragments (typically < 300 Da), allowing more thorough exploration of the chemical space and the identification of weakly binding chemical fragments. Small fragment hits can then be linked or extended into unique multi-fragment scaffold (Erlanson, 2012). Screening of 8000 fragments by Lilly Research Laboratories produced two promising fragment hits, amino-benzothiazine and amino-thiadiazine (May et al., 2011).

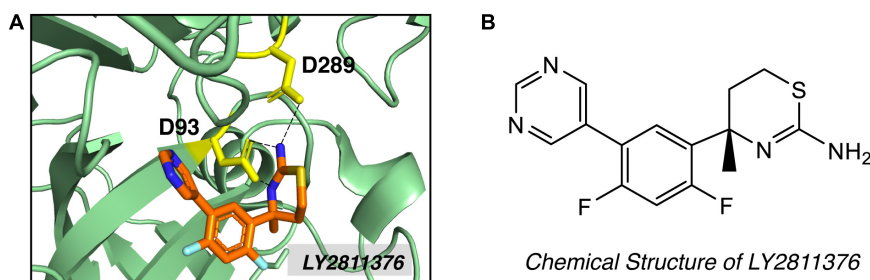


**FIGURE 4 |** Structure of BACE1 complexed with small molecule inhibitor LY2811376. **(A)** LY2811376 binds to the active site of BACE1 (PDB code: 4YBI). Inhibitor LY2811376 was shown as sticks colored with orange for carbon, blue for nitrogen, light blue for fluorine and light-orange for sulfur. The side chain of two catalytic aspartate (D93 and D289) were shown in yellow as sticks. Hydrogen bonds between aspartate side chain and LY2811376 were shown in dotted black lines. **(B)** Chemical structure of LY2811376.

Evolution of the fragment based on crystal structure produced compound LY2811376 [(S)-4-(2,4-difluoro-5-pyrimidin-5-yl-phenyl)-4-methyl-5,6-dihydro-4H-[1,3]thiazin-2-ylamine]. LY2811376 was the first orally available, non-peptidic small-molecule BACE1 inhibitor, showing satisfactory pharmacokinetic and pharmacodynamic properties in preclinical animal models and in humans (May et al., 2011). The chemical structure of LY2811376 and its complex with BACE1 were shown in **Figure 4**. LY2811376 binds to the active site of BACE1 and forms an optimal H-bonds network with the catalytic aspartates (May et al., 2011). Despite the encouraging results in preclinical animal models, LY2811376 shows toxicity in long-term studies. Other fragment-based compounds, including AZD3839 from Astra-Zeneca (Jeppsson et al., 2012) and NB-360 from Novartis (Neumann et al., 2015), also showed great potential in reducing brain A $\beta$  levels in preclinical studies.

### BACE1 Inhibitors in Clinical Trials

BACE1 inhibitors effectively reduced brain and CSF A $\beta$  levels in both animal studies and human clinical trials. In the past two decades, many potent BACE inhibitors have been developed, but only a small portion entered the clinical trials. Selectivity over other aspartic protease (BACE2, pepsin, renin, cathepsin D, and cathepsin E) and blood-brain barrier (BBB) permeability are major hurdles. The first Phase I clinical trial on a BACE1 inhibitor, CTS-21166, was conducted by CoMentis in 2008. CTS-21166 passes BBB, with high oral bio-availability and selectivity of BACE1 over other proteases. Results from clinical studies indicated a dose-dependent reduction of plasma A $\beta$  for an extended period of time, with up to 80% inhibition at the highest dosage (Gabrielle, 2008). Merck conducted phase I clinical trial on their inhibitor MK-8931 (Verubecestat) in 2012, which is well-tolerated and demonstrates a profound (up to 94%) reduction in CSF A $\beta$  (Forman et al., 2012). MK-8931 is the first BACE1 inhibitor to advance to phase II/III clinical trial in patients with mild to moderate AD. It was discontinued in 2017 (**Table 1**), due to a lack of clinical benefit in cognition (Egan et al., 2018). Subsequent phase III clinical trials of MK-8931 in patients with prodromal AD was also discontinued in 2018, because it was deemed unlikely to exhibit a positive benefit/risk ratio (Merck, 2018). Several other promising BACE1 inhibitors in late

state clinical trials also reported disappointing results, including LY2886721 (Eli Lilly), AZD3839 (AstraZeneca), atabecestat (JNJ-54,861,911, Janssen), and lanabecestat (AZD3293, LY3314814, AstraZeneca and Eli Lilly) (**Table 1**).

### Drug Discovery Targeting $\gamma$ -Secretase

$\gamma$ -secretase is a membrane protein complex composed of four essential subunits, with presenilin-1 (PS1) or presenilin-2 (PS2) as the catalytic subunit, nicastrin (Nct), anterior pharynx-defective 1 (Aph-1), and presenilin enhancer 2 (Pen-2) (De Strooper, 2003; Wolfe and Kopan, 2004; Wolfe, 2006). PS1 undergoes autocleavage through its endopeptidase activity to produce a N-terminal fragment (NTF) and a C-terminal fragment (CTF) (Thinakaran et al., 1996), each of which contributes a conserved catalytic aspartate, D257 and D385, respectively (**Figure 5A**). Nct is believed to play a role in substrate recognition and its initial docking (Shah et al., 2005). Aph-1 stabilizes the complex and Pen-2 is required for maturation of  $\gamma$ -secretase (Takasugi et al., 2003).  $\gamma$ -secretase cleaves type I transmembrane proteins and has more than 90 reported substrates (Haapasalo and Kovacs, 2011; Jurisch-Yaksi et al., 2013), of which APP and Notch are the most well-characterized. After the cleavage of APP by BACE1, a C-terminal 99-residue fragment of APP (C99) is generated and subsequently cleaved by  $\gamma$ -secretase. The initial cleavage of  $\gamma$ -secretase produces a 48-residue (A $\beta$ 48) or 49-residue (A $\beta$ 49) amyloid peptide, while at the same time the intracellular domains (AICD) are liberated into the cytoplasm (**Figure 5B**; De Strooper et al., 1998; Wolfe et al., 1999). Subsequent cleavage of A $\beta$ 49 by the C-terminal peptidase activity of  $\gamma$ -secretase leads to the generation of A $\beta$ 46, A $\beta$ 43, and A $\beta$ 40, while cleavage of A $\beta$ 48 results in A $\beta$ 45, A $\beta$ 42, and A $\beta$ 38 (Golde et al., 1992; Sano et al., 2009). Among A $\beta$  peptides with different lengths, A $\beta$ 42 and A $\beta$ 43 are most prone to aggregation, while A $\beta$ 40 and shorter peptides are relatively benign (Burdick et al., 1992).

### Drug Discovery Targeting $\gamma$ -Secretase

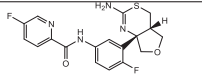
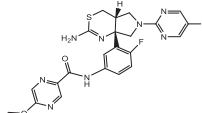
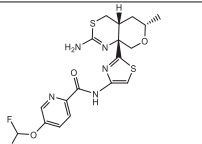
$\gamma$ -Secretase cleaves within APP transmembrane domain (APPTM) of C99 to release A $\beta$ , which aggregates to form neurotoxic oligomers and fibrils. Thus,  $\gamma$ -secretase is an obvious

**TABLE 1 |** BACE1 inhibitors in clinical trials.

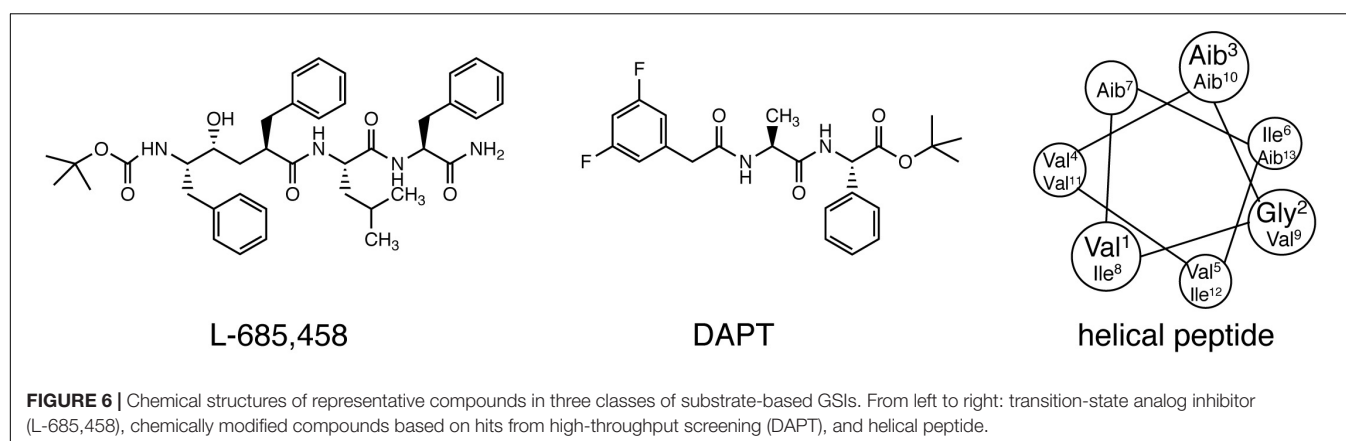
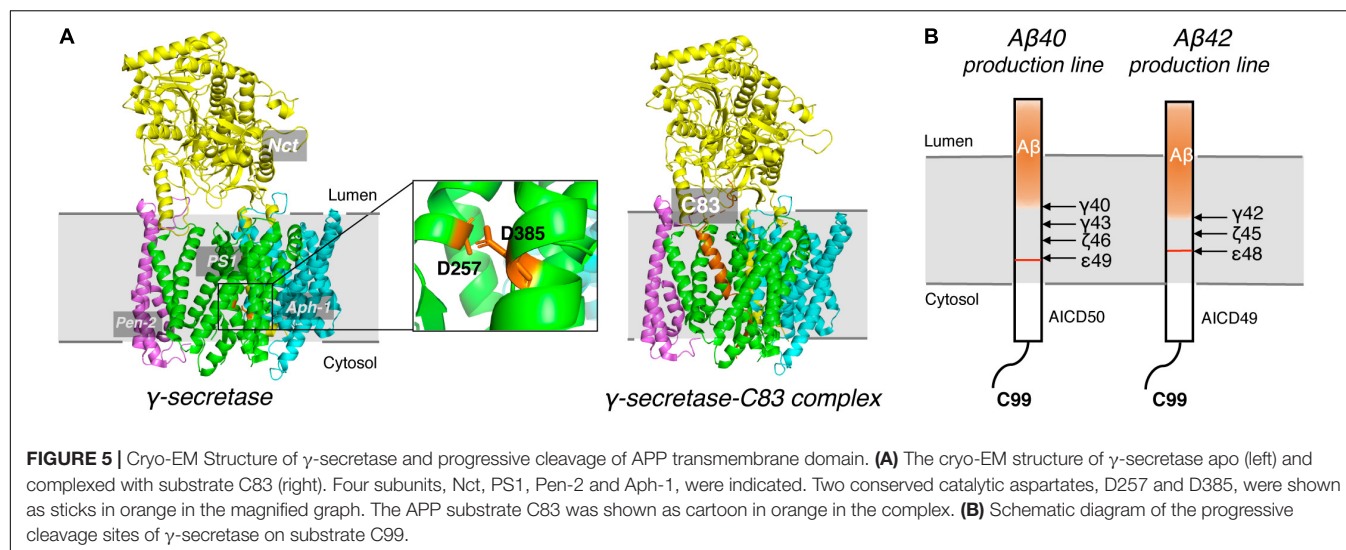
Compounds	Company	Structure	Clinical trials	Participants	Status	Outcomes	References
Verubecestat (MK-8931, MK-8931-009)	Merck Sharp & Dohme Corp.	 <chem>C17H17F2N5O3S</chem> 409.41 Da	NCT01739348 EPOCH Phase II/III 2012–2017  NCT01953601 APECS Phase III 2013–2018	<i>N</i> = 2211 People with mild to moderate AD  <i>N</i> = 1500 People with prodromal AD	Discontinued  Discontinued	No improvement in cognition  Worsening cognition in high dose (40 mg)	Kennedy et al., 2016; Scott et al., 2016
Atabecestat (JNJ-54861911)	Janssen & Shionogi Pharma	 <chem>C18H14FN5OS</chem> 367.400 Da	NCT02260674 Phase II 2014–2016 NCT02569398 Phase II/III 2015–2018  NCT02406027 Phase II 2015–2018	<i>N</i> = 114 People with early AD <i>N</i> = 596 People asymptomatic at risk for developing AD  <i>N</i> = 90 People with Early AD	Completed  Completed  Discontinued	No improvement in cognition Liver toxicity	Timmers et al., 2016, 2018
Lanabecestat (AZD3293, LY3314814)	Eli Lilly & Co., AstraZeneca	 <chem>C26H28N4O</chem> 412.54 Da	NCT02245737 Phase II/III 2014–2018  NCT02783573 Phase III 2016–2018	<i>N</i> = 7255 People with early AD  <i>N</i> = 5697 People with mild AD	Discontinued  Discontinued	lack of efficacy	Eketjäll et al., 2016; Cebers et al., 2017; Sakamoto et al., 2017; Sims et al., 2017
Elenbecestat (E2609)	Biogen, Eisai Co., Ltd.	 <chem>C19H18F3N5O2S</chem> 437.44 Da	NCT02322021 Phase II 2014–2020  NCT02956486 NCT03036280 Phase III 2016–2021	<i>N</i> = 71 People with prodromal and mild to moderate AD  <i>N</i> = 1330 People with early AD	Active  Recruiting		Albala et al., 2012; Bernier et al., 2013; Lai et al., 2017; Lynch et al., 2018
CNP520	Amgen, Inc., Novartis Pharmaceuticals	 <chem>C19H15ClF7N5O2</chem> 513.80 Da	NCT02576639 Phase II 2015–2016  NCT02565511 Phase II/III 2016–2025	<i>N</i> = 124 Healthy people ≥ 60 years old  <i>N</i> = 1340 People at risk for AD based on APOE genotype	Completed  Recruiting		Ufer et al., 2016; Neumann et al., 2018
RG7129 (RO5508887)	Hoffmann-La Roche	 <chem>C18H14F3N5O2</chem> 389.34 Da	NCT01664143 Phase I 2012 NCT01592331 Phase I 2012	<i>N</i> = 36 Healthy people <i>N</i> = 42 Healthy people	Completed Completed	Liver toxicity	
LY2811376	Eli Lilly & Co.	 <chem>C15H14F2N4S</chem> 320.36 Da	NCT00838084 Phase I 2008–2009	<i>N</i> = 61 Healthy people	Completed	Liver toxicity	Martenyi et al., 2010; May et al., 2010, 2011

(Continued)

TABLE 1 | Continued

Compounds	Company	Structure	Clinical trials	Participants	Status	Outcomes	References
LY2886721	Eli Lilly & Co.	 <chem>C18H16F2N4O2S</chem> 390.41 Da	NCT01561430 Phase I/II 2012–2013	<i>N</i> = 70 People with AD or mild AD	Discontinued	Liver toxicity	Hansen et al., 2015; Inhibitor et al., 2015; May et al., 2015
LY3202626	Eli Lilly & Co.	 <chem>C22H20F2N8O2S</chem> 498.51 Da	NCT03023826 Phase I 2017 NCT02323334 Phase I 2014–2016 NCT02791191 Phase II 2016–2019	<i>N</i> = 30 Healthy people <i>N</i> = 136 Healthy people and people with AD <i>N</i> = 316 People with mild AD dementia	Completed Completed Discontinued	Low likelihood of identifying a statistically significant treatment effect	Mckinzie et al., 2016; Willis et al., 2016
PF-06751979	Pfizer	 <chem>C18H19F2N5O3S2</chem> 455.50 Da	NCT02509117 Phase I 2015–2016 NCT03126721 Phase I 2017	<i>N</i> = 55 Healthy people and elderly people <i>N</i> = 12 Healthy people	Completed Completed	Safe and well-tolerated, reduced plasma and CSF A $\beta$	Qiu et al., 2017; Inhibitor et al., 2018
BI 1181181	Boehringer Ingelheim & Vitae Pharmaceuticals	Structure not released	NCT02044406 Phase I 2014 NCT02106247 Phase I 2014 NCT02254161 Phase I 2014–2015	<i>N</i> = 65 Healthy male  <i>N</i> = 36 Healthy male  <i>N</i> = 36 Young healthy male and elderly healthy people	Completed  Completed  Discontinued	Discontinued in favor of a second-generation compound	Firth and Tools, 2010a,b; Dorner-Ciossek et al., 2015





drug target for reducing amyloid load. Efforts have been devoted to develop  $\gamma$ -secretase targeting compounds,  $\gamma$ -secretase inhibitors (GSIs) and later  $\gamma$ -secretase modulators (GSMs).

Early studies on  $\gamma$ -secretase targeting compounds have shown an increase of the levels of substrates C99 and C83, and a reduction of the levels of the  $\gamma$ -secretase cleavage products A $\beta$  and p3 in APP-transfected cells (Higaki et al., 1995, 1999; Klafki et al., 1996). Those compounds were named as GSIs, among which dipeptide aldehydes (such as MG-132 and MDL-28170) were firstly reported (Higaki et al., 1995; Klafki et al., 1996). At the same time, substrate-based GSIs were designed, and these compounds show pharmacological effects through occupying the binding site of APP on  $\gamma$ -secretase. The substrate-based GSIs (Figure 6) includes: (1) transition-state analog inhibitor of aspartyl proteases, such as hydroxyethylene L-685,458, which was identified to target PS1 NTF and CTF (Shearman et al., 2000); (2) helical peptide (Das et al., 2003), which was found to directly bind to the PS1 NTF/CTF interface (Kornilova et al., 2005); (3) Chemically modified compounds based on hits from high-throughput screening, such as DAPT (Dovey et al., 2001), for which PS1 was identified as the direct target (Morohashi et al., 2006; Bai et al., 2015). The complex structure of

presenilin homolog PSH bound to a hydroxyethylene derivative L-682,679 was shown in Figure 7. PSH is composed of 9 transmembrane helices (TMs). L-682,679 was found to bind in the cleft surrounded by TMs 2, 6, 7, 8, and 9. The two catalytic aspartates D162 and D220 were separated by the phenol group in the amide end of L-682679 (Dang et al., 2015).

Additional non-peptidyl GSIs were developed, e.g., modification of DAPT led to a much more potent compound LY-411,575, which was further modified to be LY-450,139 (semagacestat, Table 2), a compound that was advanced to phase III clinical trials. However, the phase III clinical trial revealed severe gastrointestinal toxicity and skin cancer, which were probably due to impairment of Notch signaling.

To avoid the toxicity of GSIs, extensive efforts have been devoted toward selective  $\gamma$ -secretase inhibitors/ $\gamma$ -secretase modulators (GSMs) (Weggen et al., 2001). Some GSMs interact with  $\gamma$ -secretase through the allosteric binding site, and therefore do not interfere with the normal  $\gamma$ -secretase processing of other physiological substrates, such as Notch (called “Notch-sparing GSMs”). The first generation of GSMs is a subset of non-steroidal anti-inflammatory agents (NSAIDs), including ibuprofen, sulindac and indomethacin. These NSAIDs interact

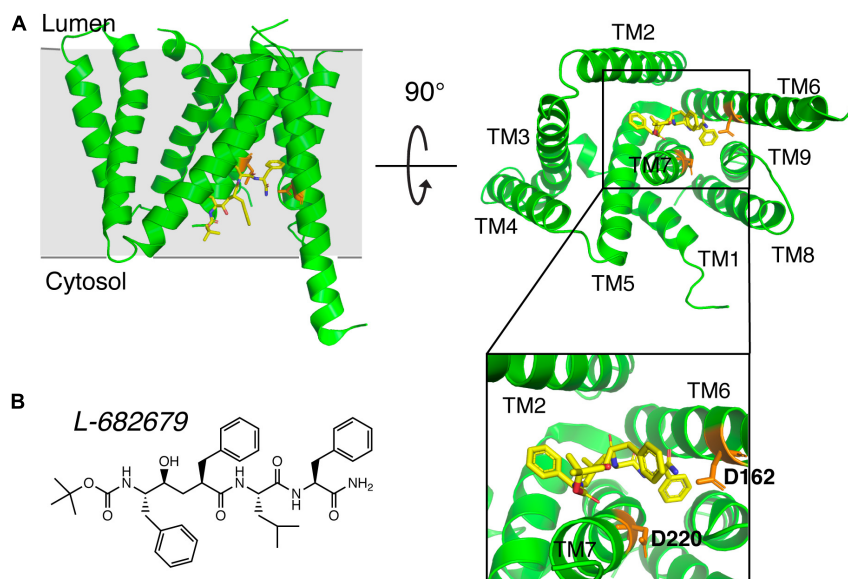


**FIGURE 7 |** The complex structure of presenilin homolog PSH bound to a hydroxyethylene derivative L-682679. **(A)** Structure of PSH bound to L-682679. The two catalytic aspartates D162 and D220 were shown in orange. L-682679 was shown in stick model with yellow for carbon, blue for nitrogen, red for oxygen (Dang et al., 2015). **(B)** Chemical structure of L-682679.

with PS at the luminal side and increase the distance between the N- and C- termini of PS, thus direct the cleavage sites toward A $\beta$ 38 instead of A $\beta$ 42, without altering total A $\beta$  production (Lleó et al., 2004; Takeo et al., 2014). The second generation of GSMs include NSAID-derived carboxylic acid analogs (Behr et al., 2004; Hall et al., 2010) and non-NSAID GSMs (Huang et al., 2012; Sun et al., 2012). The second-generation GSMs have better pharmacokinetic properties, and several of them entered clinical trials, including CHF 5074, EVP-0962, and PF-06648671 (Table 2). Natural products were also screened and characterized for their GSM activities, such as dihydroergocristine (DHEC) (Lei et al., 2015), curcumin (Goozee et al., 2016), and luteolin (Wang et al., 2016). However, the mechanism of how GSMs shift A $\beta$  production is poorly understood, partially because the complexity of the structure of  $\gamma$ -secretase.  $\gamma$ -Secretase contains 4 subunits and at least 18 transmembrane domains, structural information on this high molecular weight complex is limited until recently. Moreover, the binding sites of GSMs are still not understood. GSMs fenofibrate and tarenflurbil were initially reported to modulate  $\gamma$ -secretase cleavage by binding to the substrate APP (Kukar et al., 2008), but the specificity of this binding is questionable (Beel et al., 2009). Other GSMs have been reported to bind presenilin (Crump et al., 2011; Ohki et al., 2011).

### $\gamma$ -Secretase Inhibitors/Modulators in Clinical Trials

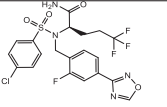
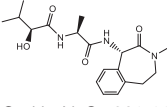
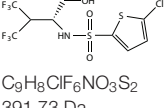
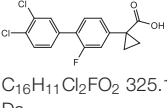
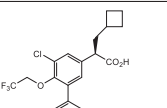
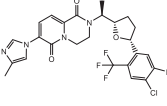
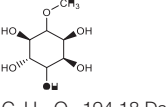
The most potent GSI semagacestat (LY450139) failed in Phase III clinical trials with more than 2600 patients from 31 countries, due to worsening cognition and increased risk of skin cancer in test patients comparing to placebo group (Kieburz et al., 2013; Tagami et al., 2017). The side effects are likely due to the impaired Notch signaling. Focus was then shifted toward “Notch-sparing” GSMs, which shift the A $\beta$  production to shorter and benign

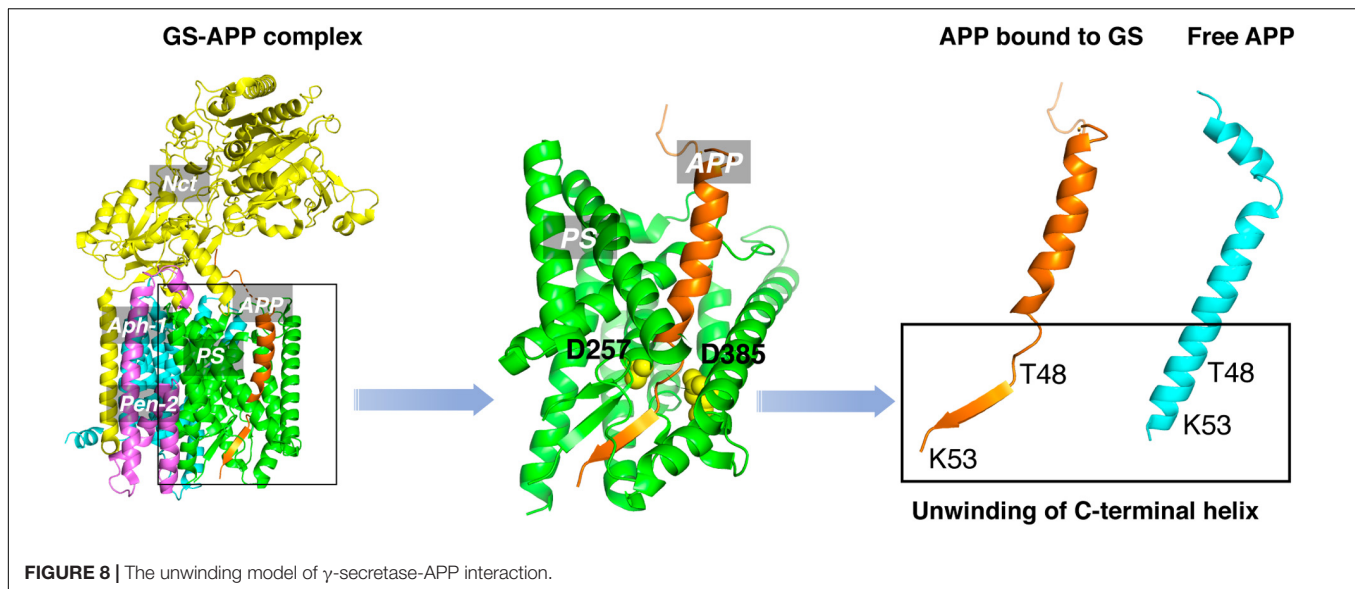
peptides without affecting the total A $\beta$  production. However, avagacestat (BMS-708163), which was claimed to be a Notch-sparing GSI, also failed in a Phase II clinical trial (Table 2) with similar side effects to those found with semagacestat (Sverdlow et al., 2012; van Dyck et al., 2012; Coric et al., 2015). Later a lack of Notch selectivity was reported for avagacestat, which may contribute to the failure of clinical trial (Crump et al., 2012). Two more GSMs entered clinical trials. EVP-0962, entered phase II clinical trial in 2012 but no results have ever been reported. NIC5-15, a naturally occurring sugar alcohol found in plants and fruits, also entered phase II clinical trial without follow-up studies.

## DISCUSSION

All clinical trials of BACE1 inhibitors and GSIs/GSMs failed, raising the question about causal role of A $\beta$  in AD pathogenesis, and the validity of amyloid cascade hypothesis in general. However, the amyloid hypothesis refers to a continuum of pathological processes at different stages of disease lasting 15–20 years before symptoms appear (Rowe et al., 2010). It is widely accepted that amyloid biomarkers (detected by reduced A $\beta$ 42 in cerebrospinal fluid (CSF) and/or positive brain amyloid PET imaging) represent the earliest evidence of AD neuropathologic change currently detectable in humans (Donohue et al., 2014; Young et al., 2014; Xiong et al., 2016). A causative role of A $\beta$  in AD pathogenesis is supported by strong evidences, including genetic of FAD (De Jonghe, 2001; Selkoe, 2001; Chen et al., 2014) and Down’s syndrome (Lejeune et al., 1959; Head et al., 2012), toxicity of A $\beta$  aggregates (Selkoe et al., 2016), A $\beta$  activation of neuron inflammation (Eng et al., 2004) and A $\beta$  potentiation of tau pathology (Jin et al., 2011). Very recently, increased

**TABLE 2 |**  $\gamma$ -secretase inhibitors/modulators in clinical trials.

Compounds	Company	Structure	Clinical trials	Participants	Status	Outcomes	References
Avagacestat (BMS-708163) GSI	Bristol-Myers Squibb	 <chem>C20H17ClF4N4O4S</chem> 520.88 Da	NCT00890890 Phase II 2009–2013	<i>N</i> = 263 People with prodromal AD	Discontinued	Lack of efficacy, Adverse effects: cerebral microbleeds, glycosuria, and nonmelanoma skin cancer	Sverdllov et al., 2012; van Dyck et al., 2012; Coric et al., 2015
Semagacestat (LY450139) GSI	Eli Lilly & Co.	 <chem>C19H27N3O4</chem> 361.44 Da	NCT01035138 Phase III 2009–2011 NCT00762411 NCT00594568 Phase III 2008–2011	<i>N</i> = 180 People with AD <i>N</i> = 1111, <i>N</i> = 1537 People with AD	Completed Completed	Lack of efficacy, increased risk of skin cancer	Dean et al., 2008; Bateman et al., 2009; Kieburz et al., 2013; Tagami et al., 2017
Begacestat (GSI-953) GSM	Pfizer	 <chem>C9H8ClF6NO3S2</chem> 391.73 Da	NCT00547560 Phase I 2007–2011 NCT00441987 Phase I 2007–2010 NCT00479219 Phase I 2007–2008	<i>N</i> = 49 Healthy elderly objects (> = 65) <i>N</i> = 96 Healthy adult <i>N</i> = 17 Healthy and AD patients	Completed Completed Completed	Lack of efficacy, Concentration of A $\beta$ in CSF not affected	
CHF 5074 GSM	CereSpir Incorporated & Chiesi Pharmaceuticals Inc.	 <chem>C16H11Cl2FO2</chem> 325.16 Da	NCT01421056 Phase II 2011–2012 NCT01602393 Phase II 2012–2013 NCT01303744 Phase II 2011–2012	<i>N</i> = 74 People with mild cognitive impairment <i>N</i> = 51 People with mild cognitive impairment <i>N</i> = 96 People with mild cognitive impairment	Completed Completed Completed	Mild diarrhea as a notable side effect Anti-inflammatory benefit Improved executive function for ApoE4 risk allele carriers	Imbimbo et al., 2009; Lanzillotta et al., 2010; Franceschi et al., 2013
EVP-0962 GSM	FORUM Pharmaceuticals Inc	 <chem>C22H19ClF6O3</chem> 480.83 Da	NCT01661673 Phase II 2012–2013	<i>N</i> = 52 People with early AD	Discontinued	Severe side effects	Rogers et al., 2012
PF-06648671 GSM	Pfizer	 <chem>C25H23ClF4N4O3</chem> 538.93 Da	NCT02407353 NCT02440100 Phase I 2015–2016 NCT02316756 Phase I 2014–2015 NCT02883114 Phase I 2016–2016	<i>N</i> = 22, <i>N</i> = 92 Healthy people <i>N</i> = 18 Healthy people <i>N</i> = 12 Healthy people	Completed Completed Completed	Dose–dependent reductions in CSF A $\beta$ 42 and A $\beta$ 40 and elevations in A $\beta$ 37 and A $\beta$ 38, with no effect on total A $\beta$ .	Qiu et al., 2016; Ahn et al., 2017, 2020
NIC5-15 Natural product	Humanetics Pharmaceuticals Corporation	 <chem>C7H14O6</chem> 194.18 Da	NCT00470418 Phase II 2007–2010 NCT01928420 Phase II 2007–2014	<i>N</i> = 15 People with AD <i>N</i> = 30 People with AD	Completed Completed	Good tolerability, Stabilization of cognition	Alzforum



A $\beta$ 42/40 ratio was shown to drive tau pathology in 3-dimensional human AD neural cell culture models (Kwak et al., 2020). These studies support the causal upstream role for A $\beta$  in the pathogenesis of AD.

Reducing A $\beta$ 42 by modulating  $\beta$ - or  $\gamma$ -secretase activity may inhibit subsequent neurodegenerative changes in the brain. It is clear that A $\beta$  alone is not sufficient for cognitive dysfunction, but it may play a crucial role in potentiating downstream tauopathy and neuroinflammation, converting a cognitively unimpaired preclinical AD subject to a patient with MCI and finally with dementia. With recent advances in ultra-sensitive quantification of pathological proteins in human plasma samples, levels of phosphorylated Tau protein (pTau181) were used to distinguish plasma samples from AD vs. control subjects (Janelidze et al., 2020; Thijssen et al., 2020). For the first time, both Tau and pTau181 can be measured in plasma to predict brain Tau load and neurodegeneration, for monitoring the efficacy of  $\beta$ - or  $\gamma$ -secretase inhibitors/modulators in clinical trials. Existing  $\beta$ -/ $\gamma$ -secretase inhibitors/modulators can then be tested in subcohorts selected by AT(N) biomarker.

One plausible explanation for negative clinical results is that BACE1 inhibitors and GSIs/GSMs were given too late, during the irreversible phase of the disease (MCI/prodromal AD, mild-to-moderate AD), and patients need to be treated at earlier stage of AD to prevent neurodegeneration. The phase III trial of BACE1 inhibitor verubecestat by Merck in patients with prodromal AD (MCI) was discontinued in 2018, similar to the phase II/III trial of atabecestat by Janssen.

In addition, side effects and toxicity account for a number of failed trials, such as the inhibition of Notch signaling by GSIs. Recent studies on BACE1 knockout mice suggested that BACE1 inhibitors may disrupt the axonal organization in the hippocampus, and impair synaptic plasticity, leading to defects in learning and memory (Ou-Yang et al., 2018; Lombardo et al., 2019). Inhibition of  $\gamma$ -secretase cleavage can lead to the accumulation of C99 fragment (Lauritzen et al., 2019a), which

was correlated to the acceleration of early neurodegenerative process in AD (Lauritzen et al., 2012; Lauritzen et al., 2019b).

An obstacle for the development of selective GSMs is the lack of information about the structural characteristics of  $\gamma$ -secretase-substrate complex. Recent cryo-EM structure of  $\gamma$ -secretase bound to the C83 fragment and Notch substrate (Yang et al., 2019; Zhou et al., 2019) started to fill this crucial knowledge gap. An  $\alpha$ -helical to  $\beta$ -strand transition was observed at the C-terminal of APPTM, forming an anti-parallel, intermolecular  $\beta$ -sheet with two induced  $\beta$ -strands from presenilin (Figure 8). The unwinding of C-terminal transmembrane helix exposes the initial  $\epsilon$ -cleavage sites (T48, L49) to interact with  $\gamma$ -secretase (Zhou et al., 2019). These are in agreement with earlier Raman and NMR spectroscopic studies carried out on APPTM and PSHs in solution, which showed that substrate binding is coupled with helical unwinding to prime the substrate for peptide bond hydrolysis (Brown et al., 2018; Clemente et al., 2018).

This unwinding model of the substrate in  $\gamma$ -secretase-APP interaction suggests that targeting APP, especially the C-terminal of APPTM, could be a new strategy in selective amyloid reduction. A substrate-specific inhibitor is not expected to affect the  $\gamma$ -secretase cleavage of other physiological substrates, the assembly of the  $\gamma$ -secretase complex, or any presenilin function (Saura et al., 2004; Wines-Samuelson et al., 2010; Watanabe et al., 2012; Barthet et al., 2013), thereby sparing the side effects associated with broad-spectrum  $\gamma$ -secretase inhibitors. A novel compound C1 was found to interact with the C-terminal juxtamembrane lysines of APP and inhibit the  $\gamma$ -secretase production of A $\beta$  both *in vitro* and in cell (Zhao et al., 2020). This study provides the first *in vitro* evidence that targeting the C-terminal juxtamembrane lysines is sufficient for reducing A $\beta$  production.

Besides cleavage by the well-known  $\alpha$ -,  $\beta$ -, and  $\gamma$ -secretases, APP can be alternatively cleaved by meprin- $\beta$ , legumain, rhomboid-like protein-4 (RHBDL4), caspases,  $\eta$ -secretase (MT-MMPs) at different sites, resulting in different APP fragments



(reviewed by García-González et al., 2019). These emerging proteinases in APP metabolism opened more possibilities for the intervention of amyloidogenic APP processing in AD. For example, cleavage of APP by meprin- $\beta$  can generate a N-terminally truncated A $\beta$  (A $\beta_{2-X}$ ), which is more prone to aggregation than A $\beta_{40}$ ; while the inhibitor of meprin- $\beta$ , fetuin-A, was reduced in CSF of AD patients (Puchades et al., 2003), indicating a potentially pathogenic role of enhanced meprin- $\beta$  activity in AD. Further investigations are needed to link the new proteinases to AD pathogenesis, which will offer novel insights and more molecular targets in AD drug discovery.

AD is a complex disease and therefore drugs with a single molecular target may not be sufficient for reversing the progression of AD. Thus, multi-target molecules able to inhibit both APP processing and tau pathology, or neuroinflammation etc., may be a promising approach for the treatment of AD. Emerging multi-targeted molecules are developed based on natural products and their derivatives, such as curcumin, berberine, and epigallocatechin gallate (EGCG) (Shan et al., 2011; Di Martino et al., 2016). Multiple AD-related clinical trials were carried out for EGCG, which is a polyphenolic flavonoid extracted from green tea. EGCG has been proposed to not only inhibit A $\beta$  misfolding and tau aggregation *in vitro* but also increase  $\alpha$ -secretase cleavage of APP and improve inflammatory in APP/PS1 transgenic mouse models (Obregon et al., 2006; Ahmed et al., 2017; Guéroux et al., 2017; Ettcheto et al., 2020). While the outcome of clinical trials on EGCG is currently inconclusive, more trials are

ongoing and it represents an intriguing multi-target strategy in AD treatment.

## SUMMARY

Drug discovery targeting A $\beta$ -producing enzymes is one of the most important strategies to develop disease modifying therapeutics for AD. Exploration of “Notch-sparing” GSMs and inhibitors targeting the substrate APP are two promising future directions. Beyond obvious significance in AD drug discovery, investigation of the  $\gamma$ -secretase and BACE inhibitors will not only provide chemical probes to study fundamental enzymatic mechanisms, but also help settling the debates on whether A $\beta$  is indeed a molecular driver in AD pathogenesis.

## AUTHOR CONTRIBUTIONS

JZ and CW conceived and wrote the manuscript. XL, WX, and YZ edited the manuscript. All authors contributed to the article and approved the submitted version.

## FUNDING

This work was supported by a grant from the Warren Alpert Foundation (to CW) and NIH grant R21-NS109926 (to CW).

## REFERENCES

- Ahmed, R., Vanschouwen, B., Jafari, N., Ni, X., Ortega, J., and Melacini, G. (2017). Molecular mechanism for the (-)-Epigallocatechin gallate-induced toxic to nontoxic remodeling of A $\beta$  oligomers. *J. Am. Chem. Soc.* 139, 13720–13734. doi: 10.1021/jacs.7b05012
- Ahn, J. E., Carrieri, C., Dela Cruz, F., Fullerton, T., Hajos-Korcsok, E., He, P., et al. (2020). Pharmacokinetic and pharmacodynamic effects of a  $\gamma$ -secretase modulator, PF-06648671, on CSF amyloid- $\beta$  peptides in randomized Phase I studies. *Clin. Pharmacol. Ther.* 107, 211–220. doi: 10.1002/cpt.1570
- Ahn, J. E., Liu, R., Trapa, P., Wood, K. M., Hajos-Korcsok, E., Fullerton, T., et al. (2017). Pharmacokinetic/Pharmacodynamic (Pk/Pd) effects of Pf-06648671, a novel gamma secretase modulator (GSM), following single and multiple dose administration in healthy volunteers. *Alzheimer's Dement.* 13:601. doi: 10.1016/j.jalz.2017.07.244
- Albala, B., Kaplow, J. M., Lai, R., Matijevic, M., Aluri, J., and Satlin, A. (2012). CSF amyloid lowering in human volunteers after 14 days' oral administration of the novel BACE1 inhibitor E2609. *Alzheimer's Dement.* 8:S743. doi: 10.1016/j.jalz.2013.08.023
- Alzheimer's Association (2020). *Alzheimer's Association 2020 Facts and Figures Report*. Available online at: <https://www.alz.org/alzheimers-dementia/facts-figures> (accessed July 24, 2020).
- Anderson, J. P., Esch, F. S., Keim, P. S., Sambamurti, K., Lieberburg, I., and Robakis, N. K. (1991). Exact cleavage site of Alzheimer amyloid precursor in neuronal PC-12 cells. *Neurosci. Lett.* 128, 126–128. doi: 10.1016/0304-3940(91)90775-O
- Asai, M., Hattori, C., Iwata, N., Saido, T. C., Sasagawa, N., Szabó, B., et al. (2006). The novel  $\beta$ -secretase inhibitor KMI-429 reduces amyloid  $\beta$  peptide production in amyloid precursor protein transgenic and wild-type mice. *J. Neurochem.* 96, 533–540. doi: 10.1111/j.1471-4159.2005.03576.x
- Bai, X. C., Rajendra, E., Yang, G., Shi, Y., and Scheres, S. H. W. (2015). Sampling the conformational space of the catalytic subunit of human  $\gamma$ -secretase. *elife* 4:e11182. doi: 10.7554/eLife.11182
- Barthet, G., Dunys, J., Shao, Z., Xuan, Z., Ren, Y., Xu, J., et al. (2013). Presenilin mediates neuroprotective functions of ephrinB and brain-derived neurotrophic factor and regulates ligand-induced internalization and metabolism of EphB2 and TrkB receptors. *Neurobiol. Aging* 34, 499–510. doi: 10.1016/j.neurobiolaging.2012.02.024
- Bateman, R. J., Siemers, E. R., Mawuenyega, K. G., Wen, G., Browning, K. R., Sigurdson, W. C., et al. (2009). A  $\gamma$ -secretase inhibitor decreases amyloid- $\beta$  production in the central nervous system. *Ann. Neurol.* 66, 48–54. doi: 10.1002/ana.21623
- Beel, A. J., Barrett, P., Schnier, P. D., Hitchcock, S. A., Bagal, D., Sanders, C. R., et al. (2009). Nonspecificity of binding of gamma-secretase modulators to the amyloid precursor protein. *Biochemistry* 48, 11837–11839. doi: 10.1021/bi901839d
- Behr, D., Clarke, E. E., Wrigley, J. D. J., Martin, A. C. L., Nadin, A., Churcher, I., et al. (2004). Selected non-steroidal anti-inflammatory drugs and their derivatives target  $\gamma$ -secretase at a novel site: evidence for an allosteric mechanism. *J. Biol. Chem.* 279, 43419–43426. doi: 10.1074/jbc.M404937200
- Benjannet, S., Elagoz, A., Wickham, L., Mamarbachi, M., Munzer, J. S., Basak, A., et al. (2001). Post-translational processing of  $\beta$ -secretase ( $\beta$ -amyloid-converting enzyme) and its ectodomain shedding: the pro- and transmembrane/cytosolic domains affect its cellular activity and amyloid- $\beta$  production. *J. Biol. Chem.* 276, 10879–10887. doi: 10.1074/jbc.M009899200
- Bennett, B. D., Denis, P., Haniu, M., Teplow, D. B., Kahn, S., Louis, J. C., et al. (2000). A furin-like convertase mediates propeptide cleavage of BACE, the Alzheimer's  $\beta$ -secretase. *J. Biol. Chem.* 275, 37712–37717. doi: 10.1074/jbc.M005339200
- Bernier, F., Sato, Y., Matijevic, M., Desmond, H., McGrath, S., Burns, L., et al. (2013). Clinical study of E2609, a novel BACE1 inhibitor, demonstrates target engagement and inhibition of BACE1 activity in CSF. *Alzheimer's Dement.* 9:886. doi: 10.1016/j.jalz.2013.08.244
- Berridge, M. J. (2010). Calcium hypothesis of Alzheimer's disease. *Pflugers Arch. Eur. J. Physiol.* 459, 441–449. doi: 10.1007/s00424-009-0736-1

- Brown, M. C., Abdine, A., Chavez, J., Schaffner, A., Torres-Arancibia, C., Lada, B., et al. (2018). Unwinding of the substrate transmembrane helix in intramembrane proteolysis. *Biophys. J.* 114, 1579–1589. doi: 10.1016/j.bpj.2018.01.043
- Bu, G. (2009). Apolipoprotein e and its receptors in Alzheimer's disease: pathways, pathogenesis and therapy. *Nat. Rev. Neurosci.* 10, 333–344. doi: 10.1038/nrn2620
- Burdick, D., Soreghan, B., Kwon, M., Kosmoski, J., Knauer, M., Henschen, A., et al. (1992). Assembly and aggregation properties of synthetic Alzheimer's A4/ $\beta$  amyloid peptide analogs. *J. Biol. Chem.* 267, 546–554.
- Cai, H., Wang, Y., McCarthy, D., Wen, H., Borchelt, D. R., Price, D. L., et al. (2001). BACE1 is the major  $\beta$ -secretase for generation of A $\beta$  peptides by neurons. *Nat. Neurosci.* 4, 233–234. doi: 10.1038/85064
- Carter, D. B., Dunn, E., McKinley, D. D., Stratman, N. C., Boyle, T. P., Kuiper, S. L., et al. (2001). Human apolipoprotein E4 accelerates  $\beta$ -amyloid deposition in APPsw transgenic mouse brain. *Ann. Neurol.* 50, 468–475. doi: 10.1002/ana.1134
- Cebers, G., Alexander, R. C., Haeblerlein, S. B., Han, D., Goldwater, R., Ereshefsky, L., et al. (2017). AZD3293: pharmacokinetic and pharmacodynamic effects in healthy subjects and patients with Alzheimer's disease. *J. Alzheimer's Dis.* 55, 1039–1053. doi: 10.3233/JAD-160701
- Chen, W., Gamache, E., Rosenman, D. J., Xie, J., Lopez, M. M., Li, Y. M., et al. (2014). Familial Alzheimer's mutations within APPTM increase A $\beta$ 42 production by enhancing accessibility of  $\epsilon$ -cleavage site. *Nat. Commun.* 5:3037. doi: 10.1038/ncomms4037
- Chávez-Gutiérrez, L., Bammens, L., Benilova, I., Vandersteen, A., Benurwar, M., Borgers, M., et al. (2012). The mechanism of  $\gamma$ -Secretase dysfunction in familial Alzheimer disease. *EMBO J.* 31, 2261–2274. doi: 10.1038/emboj.2012.79
- Clemente, N., Abdine, A., Ubarretxena-Belandia, I., and Wang, C. (2018). Coupled transmembrane substrate docking and helical unwinding in intramembrane proteolysis of amyloid precursor Protein. *Sci. Rep.* 8:12411. doi: 10.1038/s41598-018-30015-6
- Coric, V., Salloway, S., Van Dyck, C. H., Dubois, B., Andreasen, N., Brody, M., et al. (2015). Targeting prodromal Alzheimer disease with avagacestat: a randomized clinical trial. *JAMA Neurol.* 72, 1324–1333. doi: 10.1001/jamaneurol.2015.0607
- Creemers, J. W. M., Dominguez, D. I., Plets, E., Serneels, L., Taylor, N. A., Multhaup, G., et al. (2001). Processing of  $\beta$ -secretase by furin and other members of the proprotein convertase family. *J. Biol. Chem.* 276, 4211–4217. doi: 10.1074/jbc.M006947200
- Crump, C. J., Castro, S. V., Wang, F., Pozdnyakov, N., Ballard, T. E., Sisodia, S. S., et al. (2012). BMS-708,163 targets presenilin and lacks notch-sparing activity. *Biochemistry* 51, 7209–7211. doi: 10.1021/bi301137h
- Crump, C. J., Fish, B. A., Castro, S. V., Chau, D. M., Gertsik, N., Ahn, K., et al. (2011). Piperidine acetic acid based  $\gamma$ -secretase modulators directly bind to presenilin-1. *ACS Chem. Neurosci.* 2, 705–710. doi: 10.1021/cn200098p
- Dang, S., Wu, S., Wang, J., Li, H., Huang, M., He, W., et al. (2015). Cleavage of amyloid precursor protein by an archaeal presenilin homologue PSH. *Proc. Natl. Acad. Sci. U.S.A.* 112, 3344–3349. doi: 10.1073/pnas.1502150112
- Das, C., Berezovska, O., Diehl, T. S., Genet, C., Buldyrev, I., Tsai, J. Y., et al. (2003). Designed helical peptides inhibit an intramembrane protease. *J. Am. Chem. Soc.* 125, 11794–11795. doi: 10.1021/ja037131v
- De Jonghe, C. (2001). Pathogenic APP mutations near the gamma-secretase cleavage site differentially affect Abeta secretion and APP C-terminal fragment stability. *Hum. Mol. Genet.* 10, 1665–1671. doi: 10.1093/hmg/10.16.1665
- De Strooper, B. (2003). Aph-1, Pen-2, and nicastrin with presenilin generate an active  $\gamma$ -secretase complex. *Neuron* 38, 9–12. doi: 10.1109/TASL.2012.2197612
- De Strooper, B., Saftig, P., Craessaerts, K., Vanderstichele, H., Guhde, G., Annaert, W., et al. (1998). Deficiency of presenilin-1 inhibits the normal cleavage of amyloid precursor protein. *Nature* 391, 387–390. doi: 10.1038/34910
- Dean, R. A., Farlow, M. R., Galvin, J. E., Peskind, E. R., and Quinn, J. F. (2008). Phase 2 safety trial targeting amyloid N<sub>L</sub> production with a  $\gamma$ -secretase inhibitor in Alzheimer disease. *Arch. Neurol.* 65, 1031–1038.
- Di Martino, R. M. C., De Simone, A., Andrisano, V., Bisignano, P., Bisi, A., Gobbi, S., et al. (2016). Versatility of the curcumin scaffold: discovery of potent and balanced dual BACE-1 and GSK-3 $\beta$  inhibitors. *J. Med. Chem.* 59, 531–544. doi: 10.1021/acs.jmedchem.5b00894
- Donohue, M. C., Jacqmin-Gadda, H., Le Goff, M., Thomas, R. G., Raman, R., Gamst, A. C., et al. (2014). Estimating long-term multivariate progression from short-term data. *Alzheimer's Dement.* 10, S400–S410. doi: 10.1016/j.jalz.2013.10.003
- Doran, E., Small, G. W., Lott, I. T., Kim, R., Barrio, J. R., Keator, D., et al. (2016). Down syndrome, partial trisomy 21, and absence of Alzheimer's disease: the role of APP. *J. Alzheimer's Dis.* 56, 459–470. doi: 10.3233/jad-160836
- Dorner-Ciossek, C., Hobson, S., Fuchs, K., Sauer, A., Bauer, M., Morales-Ramos, A., et al. (2015). Pharmacological characterization of the new bace1 inhibitor bi 1181181. *Alzheimer's Dement.* 11:477. doi: 10.1016/j.jalz.2015.06.529
- Dovey, H. F., John, V., Anderson, J. P., Chen, L. Z., De Saint Andrieu, P., Fang, L. Y., et al. (2001). Functional gamma-secretase inhibitors reduce beta-amyloid peptide levels in brain. *J. Neurochem.* 76, 173–181. doi: 10.1046/j.1471-4159.2001.00012.x
- Duyckaerts, C., Szadovitch, V., Ando, K., Seilhean, D., Privat, N., Yilmaz, Z., et al. (2018). Neuropathology of iatrogenic Creutzfeldt–Jakob disease and immunoassay of French cadaver-sourced growth hormone batches suggest possible transmission of tauopathy and long incubation periods for the transmission of Abeta pathology. *Acta Neuropathol.* 135, 201–212. doi: 10.1007/s00401-017-1791-x
- Egan, M. F., Kost, J., Tariot, P. N., Aisen, P. S., Cummings, J. L., Vellas, B., et al. (2018). Randomized trial of verubecestat for mild-to-moderate Alzheimer's disease. *N. Engl. J. Med.* 378, 1691–1703. doi: 10.1056/NEJMoa1706441
- Eketjäll, S., Janson, J., Kaspersson, K., Bogstedt, A., Jeppsson, F., Fälting, J., et al. (2016). AZD3293: a novel, orally active BACE1 inhibitor with high potency and permeability and markedly slow Off-rate kinetics. *J. Alzheimer's Dis.* 50, 1109–1123. doi: 10.3233/JAD-150834
- Eng, J. A., Frosch, M. P., Choi, K., Rebeck, G. W., and Greenberg, S. M. (2004). Clinical manifestations of cerebral amyloid angiopathy – related inflammation. *Ann. Neurol.* 55, 250–256. doi: 10.1002/ana.10810
- Erlanson, D. A. (2012). Introduction to fragment-based drug discovery. *Top. Curr. Chem.* 317, 1–32. doi: 10.1007/128-2011-180
- Ettheto, M., Cano, A., Manzone, P. R., Busquets, O., Verdaguer, E., Castro-Torres, R. D., et al. (2020). Epigallocatechin-3-Gallate (EGCG) improves cognitive deficits aggravated by an obesogenic diet through modulation of unfolded protein response in APPsw/PS1dE9 Mice. *Mol. Neurobiol.* 57, 1814–1827. doi: 10.1007/s12035-019-01849-6
- Fairbanks, M., Leone, J., Emmons, T., Drong, R., Slightom, J., and Winterrowd, G. (1999). Purification and cloning of amyloid precursor protein  $\beta$ -secretase from human brain. *Nature* 705, 537–540.
- Firth, I. E., and Tools, M. H. (2010b). Single oral doses of the novel BACE inhibitor BI 1181181 significantly reduce concentrations of cerebrospinal fluid amyloid-beta peptides in healthy subjects. *JALZ* 11:740. doi: 10.1016/j.jalz.2015.06.1655
- Firth, I. E., and Tools, M. H. (2010a). Pharmacokinetics, pharmacodynamics, and safety of the novel bace inhibitor BI1181181 after oral administration of single ascending doses in healthy subjects. *JALZ* 11, 740–741. doi: 10.1016/j.jalz.2015.06.1656
- Forman, M., Tseng, J., Palcza, J., Leempoels, J., Ramael, S., Krishna, G., et al. (2012). The novel BACE inhibitor MK-8931 dramatically lowers CSF Abeta peptides in healthy subjects: results from a rising single dose study. *Neurology* 78:PL02.004-PL02.004. doi: 10.1212/WNL.78.1\_MeetingAbstracts.PL02.004
- Franceschi, M., Casula, D., Bottini, G., Giardino, L., Scarpini, E., Norris, D., et al. (2013). CHF5074 reduces biomarkers of neuroinflammation in patients with mild cognitive impairment: a 12-week, double-blind, placebo- controlled study. *Curr. Alzheimer Res.* 10, 742–753. doi: 10.2174/13892037113149990144
- Gabrielle, S. (2008). *Keystone Drug News: coMentis BACE Inhibitor Debuts*. Available online at: <http://www.alzforum.org/new/detail.asp?id=1790> (accessed April 5, 2018).
- García-González, L., Pilat, D., Baranger, K., and Rivera, S. (2019). Emerging alternative proteinases in APP metabolism and alzheimer's disease pathogenesis: a focus on MT1-MMP and MT5-MMP. *Front. Aging Neurosci.* 11:244. doi: 10.3389/fnagi.2019.00244
- Ghosh, A. K., and Osswald, H. L. (2014). BACE1 ( $\beta$ -Secretase) inhibitors for the treatment of Alzheimer's disease. *Chem. Soc. Rev.* 43, 6765–6813. doi: 10.1039/c3cs60460h.BACE1

- Ghosh, A. K., Shin, D., Downs, D., Koelsch, G., Lin, X., Ermolieff, J., et al. (2000). Design of potent inhibitors for human brain memapsin 2 ( $\beta$ -secretase) [1]. *J. Am. Chem. Soc.* 122, 3522–3523. doi: 10.1021/ja000300g
- Golde, T. E., Estus, S., Younkin, L. H., Selkoe, D. J., Steven, G., Golde, T. E., et al. (1992). Processing of the amyloid protein precursor to potentially amyloidogenic derivatives. *Science* 255, 728–730. doi: 10.1126/science.1738847
- Goozee, K. G., Shah, T. M., Sohrabi, H. R., Rainey-Smith, S. R., Brown, B., Verdile, G., et al. (2016). Examining the potential clinical value of curcumin in the prevention and diagnosis of Alzheimer's disease. *Br. J. Nutr.* 115, 449–465. doi: 10.1017/S0007114515004687
- Guéroux, M., Fleau, C., Slozeck, M., Laguerre, M., and Pianet, I. (2017). Epigallocatechin 3-Gallate as an inhibitor of Tau phosphorylation and aggregation: a molecular and structural insight. *J. Prev. Alzheimer's Dis.* 4, 218–225. doi: 10.14283/jpad.2017.35
- Haapasalo, A., and Kovacs, D. M. (2011). The many substrates of presenilin/ $\gamma$ -secretase. *J. Alzheimer's Dis.* 25, 3–28. doi: 10.3233/JAD-2011-101065
- Hall, A., Elliott, R. L., Giblin, G. M. P., Hussain, I., Musgrave, J., Naylor, A., et al. (2010). Piperidine-derived  $\gamma$ -secretase modulators. *Bioorgan. Med. Chem. Lett.* 20, 1306–1311. doi: 10.1016/j.bmcl.2009.08.072
- Hansen, M. M., Jarmer, D. J., Arslantas, E., Debaille, A. C., Frederick, A. L., Harding, M., et al. (2015). Synthesis of BACE inhibitor LY2886721. Part II. isoxazolidines as precursors to chiral aminothiazines, selective peptide coupling, and a controlled reactive crystallization. *Organ. Process Res. Dev.* 19, 150828123638003. doi: 10.1021/op500327t
- Head, E., Powell, D., Gold, B. T., and Schmitt, F. A. (2012). Alzheimer's disease in down syndrome. *Eur. J. Neurodegener. Dis.* 1, 353–364.
- Henstridge, C. M., Hyman, B. T., and Spires-Jones, T. L. (2019). Beyond the neuron–cellular interactions early in Alzheimer disease pathogenesis. *Nat. Rev. Neurosci.* 20, 94–108. doi: 10.1038/s41583-018-0113-1
- Higaki, J., Quon, D., Zhong, Z., and Cordell, B. (1995). Inhibition of  $\beta$ -amyloid formation identifies proteolytic precursors and subcellular site of catabolism. *Neuron* 14, 651–659. doi: 10.1016/0896-6273(95)90322-4
- Higaki, J. N., Chakravarty, S., Bryant, C. M., Cowart, L. R., Harden, P., Scardina, J. M., et al. (1999). A combinatorial approach to the identification of dipeptide aldehyde inhibitors of  $\beta$ -amyloid production. *J. Med. Chem.* 42, 3889–3898. doi: 10.1021/jm990009f
- Hong, L., Koelsch, G., Lin, X., Wu, S., Terzyan, S., Ghosh, A. K., et al. (2000). Structure of the protease domain of memapsin 2 ( $\beta$ -secretase) complexed with inhibitor. *Science* 290, 150–153. doi: 10.1126/science.290.5489.150
- Hong, L., Turner, R. T., Koelsch, G., Shin, D., Ghosh, A. K., and Tang, J. (2002). Crystal structure of memapsin 2 ( $\beta$ -secretase) in complex with an inhibitor OM00-3. *Biochemistry* 41, 10963–10967. doi: 10.1021/bi026232n
- Huang, X., Zhou, W., Liu, X., Li, H., Sun, G., Mandal, M., et al. (2012). Synthesis and SAR studies of fused oxadiazines as  $\gamma$ -secretase modulators for treatment of Alzheimer's disease. *ACS Med. Chem. Lett.* 3, 931–935. doi: 10.1021/ml300209g
- Hussain, I., Hawkins, J., Harrison, D., Hille, C., Wayne, G., Cutler, L., et al. (2007). Oral administration of a potent and selective non-peptidic BACE-1 inhibitor decreases  $\beta$ -cleavage of amyloid precursor protein and amyloid- $\beta$  production in vivo. *J. Neurochem.* 100, 802–809. doi: 10.1111/j.1471-4159.2006.04260.x
- Hussain, I., Powell, D., Howlett, D. R., Tew, D. G., Meek, T. D., Chapman, C., et al. (1999). Identification of a novel aspartic protease (Asp 2) as  $\beta$ -secretase. *Mol. Cell. Neurosci.* 14, 419–427. doi: 10.1006/mcne.1999.0811
- Imbimbo, B. P., Hutter-Paier, B., Villetti, G., Facchinetti, F., Cenacchi, V., Volta, R., et al. (2009). CHF5074, a novel  $\gamma$ -secretase modulator, attenuates brain  $\beta$ -amyloid pathology and learning deficit in a mouse model of Alzheimer's disease. *Br. J. Pharmacol.* 156, 982–993. doi: 10.1111/j.1476-5381.2008.00097.x
- Inhibitor, B., Hypopigmentation, L., Neill, B. T. O., Beck, E. M., Butler, C. R., Nolan, C. E., et al. (2018). Design and synthesis of clinical candidate PF-06751979: a potent, brain penetrant,  $\beta$ -Site amyloid precursor protein cleaving enzyme 1 (BACE1) inhibitor lacking hypopigmentation. *J. Med. Chem.* 61, 4476–4504. doi: 10.1021/acs.jmedchem.8b00246
- Inhibitor, B., Part, L. Y., Asymmetric, I. A., Kolis, S. P., Hansen, M. M., Arslantas, E., et al. (2015). Synthesis of BACE inhibitor LY2886721. Part I. An asymmetric nitron cycloaddition strategy. *Org. Process Res. Dev.* 19, 1203–1213. doi: 10.1021/op500351q
- Iserloh, U., Pan, J., Stamford, A. W., Kennedy, M. E., Zhang, Q., Zhang, L., et al. (2008). Discovery of an orally efficacious 4-phenoxypyrrrolidine-based BACE-1 inhibitor. *Bioorganic Med. Chem. Lett.* 18, 418–422. doi: 10.1016/j.bmcl.2007.10.053
- Jacobs, H. I. L., Hedden, T., Schultz, A. P., Sepulcre, J., Perea, R. D., Amariglio, R. E., et al. (2018). Structural tract alterations predict downstream tau accumulation in amyloid-positive older individuals. *Nat. Neurosci.* 21, 424–431. doi: 10.1038/s41593-018-0070-z
- Janelidze, S., Mattsson, N., Palmqvist, S., Smith, R., Beach, T. G., Serrano, G. E., et al. (2020). Plasma P-tau181 in Alzheimer's disease: relationship to other biomarkers, differential diagnosis, and longitudinal progression to Alzheimer's dementia. *Nat. Med.* 26, 379–386. doi: 10.1038/s41591-020-0755-1
- Jeppsson, F., Eketjäll, S., Janson, J., Karlström, S., Gustavsson, S., Olsson, L. L., et al. (2012). Discovery of AZD3839, a potent and selective BACE1 inhibitor clinical candidate for the treatment of Alzheimer disease. *J. Biol. Chem.* 287, 41245–41257. doi: 10.1074/jbc.M112.409110
- Jin, M., Shephardson, N., Yang, T., Chen, G., Walsh, D., and Selkoe, D. J. (2011). Soluble amyloid -protein dimers isolated from Alzheimer cortex directly induce Tau hyperphosphorylation and neuritic degeneration. *Proc. Natl. Acad. Sci. U.S.A.* 108, 5819–5824. doi: 10.1073/pnas.1017033108
- Jurisch-Yaksi, N., Sannerud, R., and Annaert, W. (2013). A fast growing spectrum of biological functions of  $\gamma$ -secretase in development and disease. *Biochim. Biophys. Acta Biomembr.* 1828, 2815–2827. doi: 10.1016/j.bbmem.2013.04.016
- Kennedy, M. E., Stamford, A. W., Chen, X., Cox, K., Cumming, J. N., Dockendorf, M. F., et al. (2016). The BACE1 inhibitor verubecestat (MK-8931) reduces CNS  $\beta$ -Amyloid in animal models and in Alzheimer's disease patients. *Sci. Transl. Med.* 8, 363ra150. doi: 10.1126/scitranslmed.aad9704
- Kieburz, K., He, F., Sun, X., Thomas, R. G., Ph, D., and Aisen, P. S. (2013). A Phase 3 trial of semagecestat for treatment of Alzheimer's disease. 369, 341–350. doi: 10.1056/NEJMoa1210951
- Kimura, T., Shuto, D., Hamada, Y., Igawa, N., Kasai, S., Liu, P., et al. (2005). Design and synthesis of highly active Alzheimer's  $\beta$ -secretase (BACE1) inhibitors, KMI-420 and KMI-429, with enhanced chemical stability. *Bioorganic Med. Chem. Lett.* 15, 211–215. doi: 10.1016/j.bmcl.2004.09.090
- Klafki, H. W., Abramowski, D., Swoboda, R., Paganetti, P. A., and Staufenbiel, M. (1996). The carboxyl termini of  $\beta$ -amyloid peptides 1–40 and 1–42 are generated by distinct  $\gamma$ -secretase activities. *J. Biol. Chem.* 271, 28655–28659. doi: 10.1074/jbc.271.45.28655
- Kokubo, H., Kaye, R., Glabe, C. G., and Yamaguchi, H. (2005). Soluble A $\beta$  oligomers ultrastructurally localize to cell processes and might be related to synaptic dysfunction in Alzheimer's disease brain. *Brain Res.* 1031, 222–228. doi: 10.1016/j.brainres.2004.10.041
- Korbel, J. O., Tirosh-Wagner, T., Urban, A. E., Chen, X.-N., Kasowski, M., Dai, L., et al. (2009). The genetic architecture of Down syndrome phenotypes revealed by high-resolution analysis of human segmental trisomies. *Proc. Natl. Acad. Sci. U.S.A.* 106, 12031–12036. doi: 10.1073/pnas.0813248106
- Kornilova, A. Y., Bihel, F., Das, C., and Wolfe, M. S. (2005). The initial substrate-binding site of  $\gamma$ -secretase is located on presenilin near the active site. *Proc. Natl. Acad. Sci. U.S.A.* 102, 3230–3235. doi: 10.1073/pnas.0407640102
- Kukar, T. L., Ladd, T. B., Bann, M. A., Fraering, P. C., Narlawar, R., Maharvi, G. M., et al. (2008). Substrate-targeting  $\gamma$ -secretase modulators. *Nature* 453, 925–929. doi: 10.1038/nature07055
- Kwak, S. S., Washicosky, K. J., Brand, E., von Maydel, D., Aronson, J., Kim, S., et al. (2020). Amyloid- $\beta$ 42/40 ratio drives tau pathology in 3D human neural cell culture models of Alzheimer's disease. *Nat. Commun.* 11:1377.
- Lai, R. Y., Darpo, B., Dayal, S., Hall, N., Chang, M.-K., Albala, B., et al. (2017). Elenbecestat, a novel oral bace inhibitor, has no clinically meaningful effect on Qtc interval up to a supratherapeutic dose of 200 Mg. *Alzheimer's Dement.* 13, 250–251. doi: 10.1016/j.jalz.2017.06.110
- Lanzillotta, A., Sarnico, I., Benarese, M., Branca, C., Baiguera, C., Hutter-Paier, B., et al. (2010). The  $\gamma$ -secretase modulator CHF5074 reduces the accumulation of native hyperphosphorylated Tau in a transgenic mouse model of Alzheimer's disease. *J. Mol. Neurosci.* 45, 22–31. doi: 10.1007/s12031-010-9482-2
- Lauritzen, I., Bécot, A., Bourgeois, A., Pardossi-Piquard, R., Biferi, M. G., Barkats, M., et al. (2019a). Targeting  $\gamma$ -secretase triggers the selective enrichment of oligomeric APP-CTFs in brain extracellular vesicles from Alzheimer cell and mouse models. *Transl. Neurodegener.* 8:35. doi: 10.1186/s40035-019-0176-6
- Lauritzen, I., Pardossi-Piquard, R., Bauer, C., Brigham, E., Abraham, J. D., Rinaldi, S., et al. (2012). The  $\beta$ -secretase-derived C-terminal fragment of  $\beta$ APP, C99, but not A $\beta$ , is a key contributor to early intraneuronal lesions in triple-transgenic



- mouse hippocampus. *J. Neurosci.* 32, 16243–16255. doi: 10.1523/JNEUROSCI.2775-12.2012
- Lauritzen, I., Pardossi-Piquard, R., Bourgeois, A., Bécot, A., and Checler, F. (2019b). Does intraneuronal accumulation of carboxyl-terminal fragments of the amyloid precursor protein trigger early neurotoxicity in Alzheimer's Disease? *Curr. Alzheimer Res.* 16, 453–457. doi: 10.2174/1567205016666190325092841
- Lei, X., Yu, J., Niu, Q., Liu, J., Fraering, P. C., and Wu, F. (2015). The FDA-approved natural product dihydroergocristine reduces the production of the Alzheimer's disease amyloid- $\beta$  peptides. *Sci. Rep.* 5:16541. doi: 10.1038/srep16541
- Lejeune, J., Gautier, M., and Turpin, R. (1959). Study of the somatic chromosomes of nine mongoloid children. *C. R. Hebd. Seances Acad. Sci.* 248, 1721–1722.
- Lin, X., Koelsch, G., Wu, S., Downs, D., Dashti, A., and Tang, J. (2000). Human aspartic protease memapsin 2 cleaves the beta -secretase site of beta -amyloid precursor protein. *Proc. Natl. Acad. Sci. U.S.A.* 97, 1456–1460. doi: 10.1073/pnas.97.4.1456
- Lleó, A., Berezovska, O., Herl, L., Raju, S., Deng, A., Bacska, B. J., et al. (2004). Nonsteroidal anti-inflammatory drugs lower A $\beta$ 42 and change presenilin 1 conformation. *Nat. Med.* 10, 1065–1066. doi: 10.1038/nm1112
- Lombardo, S., Chiacchiarretta, M., Tarr, A., Kim, W. H., Cao, T., Sigal, G., et al. (2019). BACE1 partial deletion induces synaptic plasticity deficit in adult mice. *Sci. Rep.* 9:19877. doi: 10.1038/s41598-019-56329-7
- Lynch, S. Y., Kaplow, J., Zhao, J., Dhadda, S., Luthman, J., and Albala, B. (2018). Elenbecestat, E2609, a bace inhibitor: results from a Phase-2 study in subjects with mild cognitive impairment and mild-to-moderate dementia due to Alzheimer's disease. *Alzheimer's Dement.* 14:1623. doi: 10.1016/j.jalz.2018.07.213
- Martenyi, F., Lowe, S., Dean, R. A., Monk, S. A., Gonzales, C. R., Friedrich, S., et al. (2010). Central and peripheral pharmacokinetic and pharmacodynamic effects of the  $\beta$ -site APP cleavage enzyme (BACE1) inhibitor LY2811376 in humans. *Alzheimer's Dement.* 6:e48. doi: 10.1016/j.jalz.2010.08.148
- May, P. C., Boggs, L. N., Yang, Z., Lindstrom, T., Calligaro, D., Citron, M., et al. (2010). Central and peripheral pharmacodynamic effects of BACE1 inhibition following oral administration of LY2811376 to PDAPP mice and beagle dog. *Alzheimer's Dement.* 6, S590–S591. doi: 10.1016/j.jalz.2010.05.2010
- May, P. C., Dean, R. A., Lowe, S. L., Martenyi, F., Sheehan, S. M., Boggs, L. N., et al. (2011). Robust central reduction of amyloid- in humans with an orally available, non-peptidic -secretase inhibitor. *J. Neurosci.* 31, 16507–16516. doi: 10.1523/JNEUROSCI.3647-11.2011
- May, P. C., Willis, B. A., Lowe, S. L., Dean, R. A., Monk, S. A., Cocke, P. J., et al. (2015). The potent BACE1 inhibitor LY2886721 elicits robust central A $\beta$  pharmacodynamic responses in mice, dogs, and humans. *J. Neurosci.* 35, 1199–1210. doi: 10.1523/JNEUROSCI.4129-14.2015
- Mckinzie, D. L., May, P. C., Boggs, L. N., Yang, Z., Brier, R. A., Monk, S. A., et al. (2016). Nonclinical pharmacological characterization of The BACE1 inhibitor LY3202626. *Alzheimer's Dement.* 12, 432–433. doi: 10.1016/j.jalz.2016.06.828
- Merck (2018). *Merck Announces Discontinuation of APECS Study Evaluating Verubecestat (MK-8931) for the Treatment of People with Prodromal Alzheimer's Disease*. Available online at: <https://investors.merck.com/news/press-release-details/2018/Merck-Announces-Discontinuation-of-APECS-Study-Evaluating-Verubecestat-MK-8931-for-the-Treatment-of-People-with-Prodromal-Alzheimers-Disease/default.aspx> (accessed February 13, 2018).
- Morohashi, Y., Kan, T., Tominari, Y., Fuwa, H., Okamura, Y., Watanabe, N., et al. (2006). C-terminal fragment of presenilin is the molecular target of a dipeptidic  $\gamma$ -secretase-specific inhibitor DAPT (N-[N-(3,5-difluorophenacetyl)-L-alanyl]-S-phenylglycine t-butyl ester). *J. Biol. Chem.* 281, 14670–14676. doi: 10.1074/jbc.M513012200
- Neumann, U., Rueger, H., MacHauer, R., Veenstra, S. J., Lueoend, R. M., Tintelnot-Blomley, M., et al. (2015). A novel BACE inhibitor NB-360 shows a superior pharmacological profile and robust reduction of amyloid- $\beta$  and neuroinflammation in APP transgenic mice. *Mol. Neurodegener.* 10, 1–15. doi: 10.1186/s13024-015-0033-8
- Neumann, U., Ufer, M., Jacobson, L. H., Rouzade-Dominguez, M., Huledal, G., Kolly, C., et al. (2018). The BACE-1 inhibitor CNP520 for prevention trials in Alzheimer's disease. *EMBO Mol. Med.* 10:e9316. doi: 10.15252/emmm.201809316
- Obregon, D. F., Rezai-Zadeh, K., Bai, Y., Sun, N., Hou, H., Ehrhart, J., et al. (2006). ADAM10 activation is required for green tea (-)-epigallocatechin-3-gallate-induced  $\alpha$ -secretase cleavage of amyloid precursor protein. *J. Biol. Chem.* 281, 16419–16427. doi: 10.1074/jbc.M600617200
- Ohki, Y., Higo, T., Uemura, K., Shimada, N., Osawa, S., Berezovska, O., et al. (2011). Phenylpiperidine-type  $\gamma$ -secretase modulators target the transmembrane domain 1 of presenilin 1. *EMBO J.* 30, 4815–4824. doi: 10.1038/emboj.2011.372
- Ou-Yang, M. H., Kurz, J. E., Nomura, T., Popovic, J., Rajapaksha, T. W., Dong, H., et al. (2018). Axonal organization defects in the hippocampus of adult conditional BACE1 knockout mice. *Sci. Transl. Med.* 10:eao5620. doi: 10.1126/scitranslmed.aao5620
- Park, J., Wetzel, I., Marriott, I., Dréau, D., D'Avanzo, C., Kim, D. Y., et al. (2018). A 3D human triculture system modeling neurodegeneration and neuroinflammation in Alzheimer's disease. *Nat. Neurosci.* 21, 941–951. doi: 10.1038/s41593-018-0175-4
- Patel, S., Vuillard, L., Cleasby, A., Murray, C. W., and Yon, J. (2004). Apo and inhibitor complex structures of BACE ( $\beta$ -secretase). *J. Mol. Biol.* 343, 407–416. doi: 10.1016/j.jmb.2004.08.018
- Puchades, M., Hansson, S. F., Nilsson, C. L., Andreassen, N., Blennow, K., and Davidsson, P. (2003). Proteomic studies of potential cerebrospinal fluid protein markers for Alzheimer's disease. *Mol. Brain Res.* 118, 140–146. doi: 10.1016/j.molbrainres.2003.08.005
- Qiu, R., Liu, R., He, P., Wills, A., Tankisheva, E., Alvey, C., et al. (2017). Tolerability, and pharmacokinetic and pharmacodynamic effects of PF-06751979, a potent and selective oral BACE1 inhibitor: results from Phase I single and multiple ascending dose studies in healthy young and older volunteers. *Alzheimer's Dement. J. Alzheimer's Assoc.* 13, 575–576. doi: 10.1016/j.jalz.2017.07.196
- Qiu, R., Liu, R., Wills, A., He, P., Leurent, C., Hajos-korcsok, E., et al. (2016). PF-06648671-A novel gamma secretase modulator: safety, tolerability, pharmacokinetics, and effects on plasma amyloid- $\beta$  Levels following single oral ascending doses in healthy volunteers. *Alzheimer's Dement.* 12, 611–612. doi: 10.1016/j.jalz.2016.06.1213
- Rogers, K., Felsenstein, K. M., Hrdlicka, L., Tu, Z., Albayya, F., Lee, W., et al. (2012). Modulation of  $\gamma$ -secretase by EVP-0015962 reduces amyloid deposition and behavioral deficits in Tg2576 mice. *Mol. Neurodegen.* 7:61. doi: 10.1186/1750-1326-7-61
- Rowe, C. C., Ellis, K. A., Rimajova, M., Bourgeat, P., Pike, K. E., Jones, G., et al. (2010). Amyloid imaging results from the Australian imaging, biomarkers and lifestyle (AIBL) study of aging. *Neurobiol. Aging* 31, 1275–1283. doi: 10.1016/j.neurobiolaging.2010.04.007
- Sakamoto, K., Matsuki, S., Matsuguma, K., Yoshihara, T., Uchida, N., Azuma, F., et al. (2017). BACE1 inhibitor lanabecestat (AZD3293) in a Phase 1 study of healthy Japanese subjects: pharmacokinetics and effects on plasma and cerebrospinal fluid A $\beta$  peptides. *J. Clin. Pharmacol.* 57, 1460–1471. doi: 10.1002/jcph.950
- Sano, Y., Morishima-Kawashima, M., Funamoto, S., Ihara, Y., Nagashima, Y., Ishihara, S., et al. (2009).  $\gamma$ -Secretase: successive tripeptide and tetrapeptide release from the transmembrane domain of -Carboxyl terminal fragment. *J. Neurosci.* 29, 13042–13052. doi: 10.1523/jneurosci.2362-09.2009
- Saura, C. A., Choi, S. Y., Beglopoulos, V., Malkani, S., Zhang, D., Rao, B. S. S., et al. (2004). Loss of presenilin function causes impairments of memory and synaptic plasticity followed by age-dependent neurodegeneration. *Neuron* 42, 23–36. doi: 10.1016/S0896-6273(04)00182-5
- Scott, J. D., Li, S. W., Brunskill, A. P. J., Chen, X., Cox, K., Cumming, J. N., et al. (2016). Discovery of the 3-Imino-1,2,4-thiadiazine 1,1-dioxide derivative verubecestat (MK-8931)-A  $\beta$ -site amyloid precursor protein cleaving enzyme 1 inhibitor for the treatment of Alzheimer's disease. *J. Med. Chem.* 59, 10435–10450. doi: 10.1021/acs.jmedchem.6b00307
- Selkoe, D. J. (2001). Alzheimer's disease: genes, proteins, and therapy. *Perspective* 81, 741–767.
- Selkoe, D. J., Hardy, J., Sciences, B., Hu, N.-W., Nicoll, A. J., Zhang, D., et al. (2016). Amyloid  $\beta$ -protein dimers isolated directly from Alzheimer brains impair synaptic plasticity and memory. *Nat. Med.* 7:3374. doi: 10.1038/nm1782.
- Amyloid
- Selkoe, D. J., and Wolfe, M. S. (2007). Presenilin: running with scissors in the membrane. *Cell* 131, 215–221. doi: 10.1016/j.cell.2007.10.012



- Shah, S., Lee, S. F., Tabuchi, K., Hao, Y. H., Yu, C., LaPlant, Q., et al. (2005). Nicastrin functions as a  $\gamma$ -secretase-substrate receptor. *Cell* 122, 435–447. doi: 10.1016/j.cell.2005.05.022
- Shan, W. J., Huang, L., Zhou, Q., Meng, F. C., and Li, X. S. (2011). Synthesis, biological evaluation of 9-N-substituted berberine derivatives as multi-functional agents of antioxidant, inhibitors of acetylcholinesterase, butyrylcholinesterase and amyloid- $\beta$  aggregation. *Eur. J. Med. Chem.* 46, 5885–5893. doi: 10.1016/j.ejmech.2011.09.051
- Shearman, M. S., Beher, D., Clarke, E. E., Lewis, H. D., Harrison, T., Hunt, P., et al. (2000). L-685,458, an aspartyl protease transition state mimic, is a potent inhibitor of amyloid  $\beta$ -protein precursor  $\gamma$ -secretase activity. *Biochemistry* 39, 8698–8704. doi: 10.1021/bi0005456
- Shuto, D., Kasai, S., Kimura, T., Liu, P., Hidaka, K., Hamada, T., et al. (2003). KMI-008, a novel  $\beta$ -Secretase inhibitor containing a hydroxymethylcarbonyl isostere as a transition-state mimic: design and synthesis of substrate-based octapeptides. *Bioorganic Med. Chem. Lett.* 13, 4273–4276. doi: 10.1016/j.bmcl.2003.09.053
- Sims, J. R., Selzler, K. J., Downing, A. M., Willis, B. A., Aluise, C. D., Zimmer, J., et al. (2017). Development review of the BACE1 inhibitor lanabecestat (AZD3293/LY3314814). *J. Prev. Alzheimer's Dis.* 4, 247–254. doi: 10.14283/jpad.2017.38
- Sisodia, S. S. (1992). Secretion of the  $\beta$ -amyloid precursor protein. *Ann. N. Y. Acad. Sci.* 674, 53–57. doi: 10.1111/j.1749-6632.1992.tb27476
- Stancu, I.-C., Vasconcelos, B., Terwel, D., and Dewachter, I. (2014). Models of beta-amyloid induced Tau-pathology: the long and folded road to understand the mechanism Molecular Neurodegeneration. *Mol. Neurodegener.* 9:51. doi: 10.1186/1750-1326-9-51
- Sun, Z. Y., Asberom, T., Bara, T., Bennett, C., Burnett, D., Chu, I., et al. (2012). Cyclic hydroxyamidines as amide isosteres: discovery of oxadiazolines and oxadiazines as potent and highly efficacious  $\gamma$ -secretase modulators in vivo. *J. Med. Chem.* 55, 489–502. doi: 10.1021/jm201407j
- Sverdlow, O., Berman, R. M., Castaneda, L., Li, H., Albright, C. F., Wong, O., et al. (2012). Multicenter, randomized, double-blind, placebo-controlled, single-ascending dose study of the oral  $\gamma$ -secretase inhibitor BMS-708163 (Avagacestat): tolerability profile, pharmacokinetic parameters, and pharmacodynamic markers. *Clin. Ther.* 34, 654–667. doi: 10.1016/j.clinthera.2012.01.022
- Szaruga, M., Munteanu, B., Lismont, S., Veugelen, S., Horré, K., Mercken, M., et al. (2017). Alzheimer's-causing mutations shift A $\beta$  length by Destabilizing  $\gamma$ -secretase-A $\beta$ n interactions. *Cell* 170:443–456.e14. doi: 10.1016/j.cell.2017.07.004
- Tagami, S., Yanagida, K., Kodama, T. S., Takami, M., Mizuta, N., Oyama, H., et al. (2017). Semagacestat is a pseudo-inhibitor of  $\gamma$ -secretase. *Cell Rep.* 21, 259–273. doi: 10.1016/j.celrep.2017.09.032
- Takasugi, N., Tomita, T., Hayashi, I., Tsuruoka, M., Niimura, M., Takahashi, Y., et al. (2003). The role of presenilin cofactors in the gamma-secretase complex. *Nature* 422, 438–441. doi: 10.1038/nature01506
- Takeo, K., Tanimura, S., Shinoda, T., Osawa, S., Zahariev, I. K., Takegami, N., et al. (2014). Allosteric regulation of -secretase activity by a phenylimidazole-type -secretase modulator. *Proc. Natl. Acad. Sci. U.S.A.* 111, 10544–10549. doi: 10.1073/pnas.1402171111
- Thijssen, E. H., La Joie, R., Wolf, A., Strom, A., Wang, P., Iaccarino, L., et al. (2020). Diagnostic value of plasma phosphorylated tau181 in Alzheimer's disease and frontotemporal lobar degeneration. *Nat. Med.* 26, 387–397.
- Thinakaran, G., Borchelt, D. R., Lee, M. K., Slunt, H. H., Spitzer, L., Kim, G., et al. (1996). Endoproteolysis of presenilin 1 and accumulation of processed derivatives in vivo. *Neuron* 17, 181–190. doi: 10.1016/S0896-6273(00)80291-3
- Thinakaran, G., and Koo, E. H. (2008). Amyloid precursor protein trafficking, processing, and function. *J. Biol. Chem.* 283, 29615–29619. doi: 10.1074/jbc.R800019200
- Timmers, M., Streffer, J. R., Russu, A., Tominaga, Y., Shimizu, H., Shiraishi, A., et al. (2018). Pharmacodynamics of atabecestat (JNJ-54861911), an oral BACE1 inhibitor in patients with early Alzheimer's disease: randomized, double-blind, placebo-controlled study. *Alzheimer's Res. Ther.* 10, 1–18. doi: 10.1186/s13195-018-0415-6
- Timmers, M., Van Broeck, B., Ramael, S., Slemmon, J., De Waepenaert, K., Russu, A., et al. (2016). Profiling the dynamics of CSF and plasma A $\beta$  reduction after treatment with JNJ-54861911, a potent oral BACE inhibitor. *Alzheimer's Dement. Transl. Res. Clin. Interv.* 2, 202–212. doi: 10.1016/j.trci.2016.08.001
- Ufer, M., Rouzade-Dominguez, M.-L., Huledal, G., Pezous, N., Avrameas, A., David, O., et al. (2016). Results from a first-in-human study with the bace inhibitor Cnp520. *Alzheimer's Dement.* 12:200. doi: 10.1016/j.jalz.2016.06.351
- van Dyck, C. H., Brody, M., Salloway, S., Rollin, L., Pilcher, G., Berman, R. M., et al. (2012). Safety and tolerability of the  $\gamma$ -secretase inhibitor avagacestat in a Phase 2 study of mild to moderate Alzheimer disease. *Arch. Neurol.* 69:1430. doi: 10.1001/archneurol.2012.2194
- Vassar, R. (2004). The  $\beta$ -secretase enzyme in Alzheimer's disease. *Mol. Biol.* 23, 105–113.
- Vassar, R., Bennett, B. D., Babu-Khan, S., Kahn, S., Mendiaz, E. A., Rogers, G., et al. (1999).  $\beta$ -Secretase cleavage of Alzheimer's amyloid precursor protein by the transmembrane aspartic protease BACE. *Science* 286, 735–741. doi: 10.1126/science.286.5440.735
- Veugelen, S., Saito, T., Saido, T. C., Chávez-Gutiérrez, L., and De Strooper, B. (2016). Familial Alzheimer's disease mutations in presenilin generate amyloidogenic A $\beta$  peptide seeds. *Neuron* 90, 410–416. doi: 10.1016/j.neuron.2016.03.010
- Wang, H., Wang, H., Cheng, H., and Che, Z. (2016). Ameliorating effect of luteolin on memory impairment in an Alzheimer's disease model. *Mol. Med. Rep.* 13, 4215–4220. doi: 10.3892/mmr.2016.5052
- Watanabe, H., Xia, D., Kanekiyo, T., Kelleher, R. J., and Shen, J. (2012). Familial frontotemporal dementia-associated presenilin-1 c.548G>T mutation causes decreased mRNA expression and reduced presenilin function in knock-in mice. *J. Neurosci.* 32, 5085–5096. doi: 10.1523/jneurosci.0317-12.2012
- Weggen, S., Eriksen, J. L., Das, P., Sagi, S. A., Wang, R., Pietrzik, C. U., et al. (2001). A subset of NSAIDs lower amyloidogenic A $\beta$ 42 independently of cyclooxygenase activity. *Nature* 414, 212–216. doi: 10.1038/35102591
- Wilcox, K. C., Lacor, P. N., Pitt, J., and Klein, W. L. (2011). A $\beta$  oligomer-induced synapse degeneration in Alzheimer's disease. *Cell. Mol. Neurobiol.* 31, 939–948. doi: 10.1007/s10571-011-9691-4
- Wildsmith, K. R., Holley, M., Savage, J. C., Skerrett, R., and Landreth, G. E. (2013). Evidence for impaired amyloid  $\beta$  clearance in Alzheimer's disease. *Alzheimer's Res. Ther.* 5:33. doi: 10.1186/alzrt187
- Willis, B. A., Lowe, S. L., Daugherty, L. L., Dean, R. A., English, B., Ereshefsky, L., et al. (2016). Pharmacokinetics, pharmacodynamics, safety, and tolerability of LY3202626, a novel Bace1 inhibitor, in healthy subjects and patients with Alzheimer's disease. *Alzheimer's Dement.* 12:418. doi: 10.1016/j.jalz.2016.06.791
- Wilson, C. A., Doms, R. W., and Lee, V. M. Y. (1999). Intracellular APP processing and A $\beta$  production in Alzheimer disease. *J. Neuropathol. Exp. Neurol.* 58, 787–794. doi: 10.1097/00005072-199908000-00001
- Wimo, A., Winblad, B., and Jönsson, L. (2010). The worldwide societal costs of dementia: estimates for 2009. *Alzheimer's Dement.* 6, 98–103. doi: 10.1016/j.jalz.2010.01.010
- Wines-Samuelson, M., Schulte, E. C., Smith, M. J., Aoki, C., Liu, X., Kelleher, R. J., et al. (2010). Characterization of age-dependent and progressive cortical neuronal degeneration in Presenilin conditional mutant mice. *PLoS One* 5:e10195. doi: 10.1371/journal.pone.0010195
- Wolfe, M. S. (2006). The  $\gamma$ -secretase complex: membrane-embedded proteolytic ensemble. *Biochemistry* 45, 7931–7939. doi: 10.1021/bi060799c
- Wolfe, M. S., and Kopan, R. (2004). Intramembrane proteolysis: theme and variations. *Science* 305, 1119–1123. doi: 10.1126/science.1096187
- Wolfe, M. S., Xia, W., Ostaszewski, B. L., Diehl, T. S., Kimberly, W. T., and Selkoe, D. J. (1999). Two transmembrane aspartates in presenilin-1 required for presenilin endoproteolysis and gamma-secretase activity. *Nature* 398, 513–517. doi: 10.1038/19077
- Xiong, C., Jasielec, M. S., Weng, H., Fagan, A. M., Benzinger, T. L. S., Head, D., et al. (2016). Longitudinal relationships among biomarkers for Alzheimer disease in the adult children study. *Neurology* 86, 1499–1506. doi: 10.1212/WNL.0000000000002593
- Yan, R., Blenkowski, M. J., Shuck, M. E., Miao, H., Tory, M. C., Pauley, A. M., et al. (1999). Membrane-anchored aspartyl protease with Alzheimer's disease  $\beta$ -secretase activity. *Nature* 402, 533–537. doi: 10.1038/990107
- Yang, G., Zhou, R., Zhou, Q., Guo, X., Yan, C., Ke, M., et al. (2019). Structural basis of Notch recognition by human  $\gamma$ -secretase. *Nature* 565, 192–197. doi: 10.1038/s41586-018-0813-8

- Young, A. L., Oxtoby, N. P., Daga, P., Cash, D. M., Fox, N. C., Ourselin, S., et al. (2014). A data-driven model of biomarker changes in sporadic Alzheimer's disease. *Brain* 137, 2564–2577. doi: 10.1093/brain/awu176
- Zhao, J., Xiao, Y., Liu, X., Kim, S., Wu, X., Barros, M., et al. (2020). Substrate interaction inhibits  $\gamma$ -secretase production of amyloid- $\beta$  peptides. *Chem. Commun.* 56, 2578–2581. doi: 10.1039/c9cc09170j
- Zhou, R., Yang, G., Guo, X., Zhou, Q., Lei, J., and Shi, Y. (2019). Recognition of the amyloid precursor protein by human  $\gamma$ -secretase. *Science* 363:eaaw0930. doi: 10.1126/science.aaw0930

**Conflict of Interest:** The authors declare that the research was conducted in the absence of any commercial or financial relationships that could be construed as a potential conflict of interest.

Copyright © 2020 Zhao, Liu, Xia, Zhang and Wang. This is an open-access article distributed under the terms of the Creative Commons Attribution License (CC BY). The use, distribution or reproduction in other forums is permitted, provided the original author(s) and the copyright owner(s) are credited and that the original publication in this journal is cited, in accordance with accepted academic practice. No use, distribution or reproduction is permitted which does not comply with these terms.



# Modulation of $\beta$ -Amyloid Fibril Formation in Alzheimer's Disease by Microglia and Infection

Madeleine R. Brown, Sheena E. Radford and Eric W. Hewitt\*

School of Molecular and Cellular Biology and Astbury Centre for Structural Molecular Biology, Faculty of Biological Sciences, University of Leeds, Leeds, United Kingdom

## OPEN ACCESS

### Edited by:

Sandra Macedo-Ribeiro,  
Universidade do Porto, Portugal

### Reviewed by:

Louise Charlotte Serpell,  
University of Sussex, United Kingdom  
Takashi Saito,  
Nagoya City University, Japan

### \*Correspondence:

Eric W. Hewitt  
e.w.hewitt@leeds.ac.uk

**Received:** 22 September 2020

**Accepted:** 03 November 2020

**Published:** 26 November 2020

### Citation:

Brown MR, Radford SE and  
Hewitt EW (2020) Modulation  
of  $\beta$ -Amyloid Fibril Formation  
in Alzheimer's Disease by Microglia  
and Infection.  
Front. Mol. Neurosci. 13:609073.  
doi: 10.3389/fnmol.2020.609073

Amyloid plaques are a pathological hallmark of Alzheimer's disease. The major component of these plaques are highly ordered amyloid fibrils formed by amyloid- $\beta$  (A $\beta$ ) peptides. However, whilst A $\beta$  amyloid fibril assembly has been subjected to detailed and extensive analysis *in vitro*, these studies may not reproduce how A $\beta$  fibrils assemble in the brain. This is because the brain represents a highly complex and dynamic environment, and in Alzheimer's disease multiple cofactors may affect the assembly of A $\beta$  fibrils. Moreover, *in vivo* amyloid plaque formation will reflect the balance between the assembly of A $\beta$  fibrils and their degradation. This review explores the roles of microglia as cofactors in A $\beta$  aggregation and in the clearance of amyloid deposits. In addition, we discuss how infection may be an additional cofactor in A $\beta$  fibril assembly by virtue of the antimicrobial properties of A $\beta$  peptides. Crucially, by understanding the roles of microglia and infection in A $\beta$  amyloid fibril assembly it may be possible to identify new therapeutic targets for Alzheimer's disease.

**Keywords:**  $\beta$ -amyloid, A $\beta$ , amyloid fibril, amyloid plaques, Alzheimer's disease, infection, microglia

## INTRODUCTION

Alzheimer's disease (AD) is the most common form of dementia and is characterized by brain atrophy, amyloid plaques, intracellular neurofibrillary tangles, and neuroinflammation (Braak and Braak, 1991; Jack et al., 1998; Heppner et al., 2015). The amyloid plaques are primarily composed of fibrils formed by the  $\beta$ -amyloid (A $\beta$ ) peptides (Wang et al., 1996). In AD A $\beta$  assembles into fibrils within the highly complex environment of the brain; as such multiple molecular and cellular factors may influence not only the formation the fibrils, but also their clearance. In contrast, A $\beta$  fibril formation is typically studied *in vitro* by incubating the purified peptide in simple solution conditions. This may not reproduce how A $\beta$  fibrils assemble in the AD brain, and result in the generation of fibrils that have different properties to those formed *in vivo*. Indeed, A $\beta$  fibrils made *in vitro* do not efficiently induce amyloid plaque formation when injected into the hippocampus of young AD model mice, whereas brain extracts from AD patients and aged AD model mice lead to A $\beta$  deposition into plaques (Meyer-Luehmann et al., 2006). This suggests that there are cofactors present *in vivo* that promote A $\beta$  fibril assembly and deposition in AD. This review will focus on two potential cofactors, microglia and infection, and how these modulate A $\beta$  amyloid fibril assembly and whether these can be targeted to reduce plaque formation (**Figure 1**).

## A $\beta$ AMYLOID FIBRIL ASSEMBLY

A $\beta$  is formed by the sequential cleavage of transmembrane protein amyloid precursor protein (APP) by  $\beta$ -secretase and  $\gamma$ -secretase, resulting in A $\beta$  fragments ranging from 39 to 43 residues in length (Selkoe, 1998). The predominant forms of the peptide are the 40- and 42- residue peptide variants A $\beta$ <sub>1–40</sub> and A $\beta$ <sub>1–42</sub> (Wang et al., 1996). All known dominant mutations associated with early-onset AD occur in APP or in presenilin-1 (PSEN1) and presenilin-2 (PSEN2), which are components of  $\gamma$ -secretase (Karch et al., 2014). Genome-wide association studies (GWAS) have also been used to identify genetic risk factors for late-onset AD, and this has identified genes that encode proteins involved in APP processing including SORL1, ADAM10, and APOE4 (Lambert et al., 2013; Jansen et al., 2019). This genetic evidence implicates A $\beta$  as an initiating factor in AD.

A $\beta$  peptides are intrinsically disordered in their monomeric form and assemble into highly ordered fibrils via a nucleation dependent pathway, in which monomers self-associate to form a nucleus (Knowles et al., 2014). Addition of further A $\beta$  peptides to the nucleus culminates in the formation of fibrils, which can then be elongated by end on addition of A $\beta$  peptides. An array of oligomeric forms of A $\beta$  are associated with fibril assembly reactions and many studies point to a key role for these oligomers in neurotoxicity (Shankar et al., 2008; Evangelisti et al., 2016; Serra-Batiste et al., 2016). In addition, in secondary nucleation, the surface of existing A $\beta$  fibrils can catalyze the formation of new A $\beta$  fibrils (Cohen et al., 2013). Cross-seeding can also occur in which other protein complexes, including fibrils of other amyloidogenic sequences, provide surfaces for the secondary nucleation of A $\beta$  fibril assembly (Morales et al., 2013; Ono et al., 2014; Moreno-Gonzalez et al., 2017).

A $\beta$  amyloid fibrils are highly ordered, with a common cross- $\beta$  structure, consisting of  $\beta$ -sheets in which in-register  $\beta$ -strands are oriented perpendicularly to the fibril axis, with 4.6–4.7 Å spacing between them (Eanes and Glenner, 1968). Fibrils are unbranched, typically 5–15 nm in width, can reach up to several microns in length and can consist of a number of cross- $\beta$  subunits (Iadanza et al., 2018). These subunits are protofilaments which associate to form a mature A $\beta$  fibril (Iadanza et al., 2018). While all A $\beta$  fibrils share this characteristic cross- $\beta$  structure, polymorphism refers to the different molecular structure of the peptide within this cross- $\beta$  subunit, and also the different number and arrangement of the cross- $\beta$  subunits that make up a mature fibril (Tycko, 2015). While A $\beta$  fibrils formed both *in vitro* and derived from *ex vivo* patient tissue exhibit polymorphism, the structures determined to date of fibrils derived from AD patient tissue are distinct from those formed *in vitro* (Petkova et al., 2005; Paravastu et al., 2008, 2009; Lu et al., 2013; Qiang et al., 2017; Kollmer et al., 2019). In addition, it was shown that synthetic A $\beta$  fibrils do not efficiently induce A $\beta$ -plaque formation when injected into the hippocampus of young AD model (APP23) mice, whereas brain extracts from AD patients and aged APP23 mice led to A $\beta$  deposition (Meyer-Luehmann et al., 2006). This suggests that a cofactor, or multiple cofactors within the brain, could

be required to drive A $\beta$  assembly and deposition *in vivo* (Meyer-Luehmann et al., 2006).

## MICROGLIA AND THE IMMUNE RESPONSE TO A $\beta$ AMYLOID FIBRILS

Microglia are immune cells that are resident in the brain, and depending on the region, make up 0.5–16% of all cells in the human brain (Mittelbronn et al., 2001; Ajami et al., 2007; Ginhoux et al., 2010). When in a resting state, microglia have a ramified morphology, multiple fine processes project from the cell body, which are used to monitor the central nervous system (CNS) microenvironment (Nimmerjahn et al., 2005). These cells respond to changes in the local environment and migrate to activating stimuli, adopting a more amoeboid morphology and expressing an altered repertoire of receptors (Davalos et al., 2005). Reactive microglia are observed in AD brains, in close association with A $\beta$  plaques (Itagaki et al., 1989; Yuan et al., 2016). A $\beta$  fibrils have been shown to activate the production of pro-inflammatory cytokines by microglia and thus may be a stimulus for the increased production of these cytokines, which contribute to the neurodegeneration associated with AD (Griffin et al., 1989; Bauer et al., 1991; Patel et al., 2005; Halle et al., 2008; Ojala et al., 2009). However, in addition to cytokine production, microglia may also modulate the formation of A $\beta$  amyloid fibrils and plaques. Crucially, microglia can affect both the generation and the degradation of A $\beta$  fibrils. The balance between these activities may therefore represent a key determinant in whether amyloid plaques accumulate in the AD brain.

## FORMATION OF PHYSICAL BARRIERS AROUND A $\beta$ AMYLOID PLAQUES BY MICROGLIA

In AD microglia migrate to, surround and infiltrate A $\beta$  amyloid plaques, where they come into close contact with A $\beta$  fibrils (Itagaki et al., 1989). In AD mice models this recruitment can occur as quickly as within a day of plaque formation and results in a two-fivefold increase in microglia at A $\beta$  plaques compared to the neighboring tissue (Frautschi et al., 1998; Simard et al., 2006; Meyer-Luehmann et al., 2008). Microglia have been shown to surround plaques forming a barrier that limits their outward growth by preventing the recruitment of A $\beta$  peptides (Condello et al., 2015). Plaques with less microglial coverage were less compact and had increased recruitment of soluble A $\beta$ <sub>1–42</sub>, allowing the formation of A $\beta$ <sub>1–42</sub> protofibrils (Condello et al., 2015). Similar results were found after depletion of microglia with PLX5622, an inhibitor of the essential microglial colony stimulating factor 1 receptor (CSF1R) signaling pathway (Spangenberg et al., 2019). These hotspots of A $\beta$ <sub>1–42</sub> protofibrils were found to be neurotoxic, resulting in more severe neuritic dystrophy (Condello et al., 2015). This supports the role of microglia in the formation of a physical barrier around fibrillar plaques, compacting





2014; Ulrich et al., 2018; Grieciuc et al., 2019) highlighting the importance of this process in AD.

## Secreted Microglial Proteases

Enzymes that cleave A $\beta$  include the metalloendopeptidases insulin-degrading enzyme (IDE) and neprilysin (NEP). Microglia are thought to contribute to the secretion of these enzymes, along with neurons and astrocytes, and a decrease in microglial expression of both enzymes is associated with aging in AD model mice (Leissring et al., 2003; Hickman et al., 2008; Tamboli et al., 2010). These enzymes, however, are thought to be limited to the degradation of monomeric peptide, and do not contribute to the degradation of A $\beta$  amyloid fibrils (Qiu et al., 1998; Farris et al., 2003; Leissring et al., 2003). There is also evidence on the capability of NEP to degrade some oligomeric forms of A $\beta$ . The enzyme was found to degrade oligomers formed from synthetic A $\beta$  peptide, but in another study NEP did not degrade A $\beta$  oligomers secreted from cells overexpressing APP (Kanemitsu et al., 2003; Leissring et al., 2003).

Secreted enzymes capable of cleaving fibrillar A $\beta$  have, however, been identified. Metalloprotease-9 (MMP-9) is a zinc-dependent metalloprotease expressed by neurons, astrocytes, microglia and vascular cells in the brain (Vafadari et al., 2016). It was shown that incubation of A $\beta_{1-40}$  and A $\beta_{1-42}$  fibrils with MMP-9 leads to their degradation (Yan et al., 2006). Fibril fragments produced were analyzed using mass spectrometry and this revealed species corresponding to A $\beta_{1-20}$  and A $\beta_{1-30}$ , suggesting Phe20-Ala21 and Ala30-Ile31 as cleavage sites (Yan et al., 2006). These sites must be accessible to MMP-9 in the fibril structure. MMP-9 was also found to degrade compact A $\beta$  amyloid plaques in brain sections from AD model (APP/PS1) mice (Yan et al., 2006). MMP-2 is implicated in the degradation of soluble A $\beta$ , with increased A $\beta_{1-40}$  and A $\beta_{1-42}$  identified in the soluble fraction of cortex and hippocampal brain samples of knock out MMP-2 mice compared to wild-type controls (Yin et al., 2006).

## Uptake and Degradation of A $\beta$ Fibrils by Microglia

Consistent with a role in the clearance of A $\beta$ , microglia express an array of receptors that facilitate the uptake of A $\beta$  aggregates.

### Toll-Like Receptors

One family of receptors involved in the immune response to A $\beta$  amyloid are the Toll-like receptors (TLRs) a class of pattern recognition receptors that recognize conserved microbial structures (Kawasaki and Kawai, 2014). TLRs are type I integral membrane proteins which recognize ligands with their leucine-rich repeat (LRR)-containing ectodomains. RNA sequencing revealed that the expression of six TLR genes (1,2,4,5,6,8) is upregulated in the temporal cortex of AD patients when compared to control brains, likely resulting from increased microglial activation (Chakrabarty et al., 2018). A direct interaction was identified between A $\beta$  fibrils and CD14, a TLR co-receptor previously shown to be associated with the inflammatory response to fibrillar A $\beta$  (Fassbender et al., 2004; Reed-Geaghan et al., 2009). This interaction was shown to facilitate the internalization of A $\beta$  fibrils by microglia, at lower concentrations

than that required for cell activation (Liu et al., 2005). This suggests that CD14 could be involved in the phagocytosis of A $\beta$  fibrils at low concentrations, but increased A $\beta$  levels in AD results in cellular activation. Consistent with a role in A $\beta$  uptake, TLR4 deficiency in AD mouse models results in increased fibrillar and soluble A $\beta$  deposition (Tahara et al., 2006). Conversely, stimulation of the murine microglial cell line BV-2 with TLR2 and TLR4 ligands significantly increased the internalization of A $\beta$  *in vitro*, further implicating TLR receptors in A $\beta$  uptake and clearance (Tahara et al., 2006; Song et al., 2011).

### Scavenger Receptors

Another family of receptors found to be involved in the internalization of A $\beta$  fibrils are the scavenger receptors (SRs), which are highly expressed by microglia (Christie et al., 1996; Wilkinson and El Khoury, 2012). It was found initially that class A SRs, characterized by an extracellular collagen-like domain, are involved in the binding to A $\beta$  fibrils to microglial cells (El Khoury et al., 1996). It was then shown that cocubation of microglia with SR ligands such as acetyl-low density lipoprotein (Ac-LDL) reduced A $\beta$  uptake, and CHO cells transfected with class A, or class B SRs showed enhanced A $\beta$  uptake, suggesting that SRs are important in the uptake and clearance of A $\beta$  (Paresce et al., 1996). Further investigation using microglia that are deficient in SR-A1 confirmed the role of SR-A1 and also SR-B1 in binding A $\beta$  fibrils, consistent with a role in the clearance of A $\beta$  amyloid (Husemann et al., 2001). CD36 is a class B scavenger receptor identified to form a receptor complex with the  $\alpha_6\beta_1$ -integrin and the integrin-associated protein CD47 in microglia. This complex was shown to mediate the binding of A $\beta$  fibrils to microglial cells and the subsequent activation of intracellular signaling pathways (Bamberger et al., 2003). While initial studies reported that A $\beta$  fibril binding to this complex is largely involved in the activation of an inflammatory response, it was also reported that the interaction of A $\beta$  fibrils with this complex is involved in the phagocytic uptake of fibrils by microglia (Coraci et al., 2002; Moore et al., 2002; Bamberger et al., 2003; Koenigsknecht and Landreth, 2004).

### TREM2

The deletion of TREM2 in primary microglia was shown to significantly reduce the phagocytosis of aggregated A $\beta_{1-42}$  (Kleinberger et al., 2014). Similarly, TREM2 deficiency reduced the efficacy of antibody-targeted A $\beta$  phagocytosis by microglia (Xiang et al., 2016). There is evidence for direct interactions between TREM2 and A $\beta_{1-42}$  fibrils, although no difference in binding affinity was identified for TREM2 R47H and R62H variants that are associated with an increased risk of AD (Lessard et al., 2018). However, the internalization of monomeric A $\beta$  was reduced with the expression of these TREM2 AD variants (Lessard et al., 2018). In another study, TREM2 was found to bind to A $\beta$  oligomers with a similar affinity to previously described A $\beta$  receptors, CD36 and receptor for advanced glycation end products (RAGE), and this interaction was compromised by R47H and R62H TREM2 mutations (Zhao et al., 2018). In this study, TREM2 deficiency had little effect on A $\beta$  uptake but led to significantly reduced A $\beta$  degradation once internalized by

microglia (Zhao et al., 2018). In TREM2 knock out mice injected with A $\beta$  oligomers, there was reduced microglial migration to the site of injection and reduced A $\beta$  clearance (Zhao et al., 2018). A recent study found that loss of TREM2 function led to an acceleration in early amyloidogenesis, accompanied by a reduction in microglial recruitment as previously described, again suggesting that TREM2 has a role in microglial clearance of A $\beta$  (Parhizkar et al., 2019). Together this evidence suggests that A $\beta$  is a ligand for TREM2, and that TREM2 has a role to play in both A $\beta$  clearance and A $\beta$ -stimulated microglial activation.

## A Novel Role for the Autophagy Machinery in A $\beta$ Receptor Recycling

A $\beta$  clearance by microglia may involve proteins of the autophagy machinery in a pathway distinct from their canonical function (Heckmann et al., 2019). This pathway is referred to as LC3-associated endocytosis (LANDO), with LC3 being a key protein in macroautophagy. Evidence from this study suggests that LANDO facilitates recycling of the A $\beta$  receptors CD36, TLR4 and TREM2, thus allowing cycles of A $\beta$  endocytosis to continue, promoting A $\beta$  uptake and clearance (Heckmann et al., 2019). The autophagy proteins ATG5 and Rubicon were found to be protective against A $\beta$  deposition, with their absence leading to increased pathology. The expression of autophagy proteins declines with age, which may be related to the development of A $\beta$  pathology in AD (Rubinsztein et al., 2011). It is important to note that macroautophagy has previously been implicated in the secretion of A $\beta$  into the extracellular space where it forms plaques in AD (Nilsson et al., 2013). When autophagy-related gene 7 (ATG7) was conditionally knocked out in excitatory neurons of APP transgenic mice, extracellular A $\beta$  plaque pathology was significantly decreased, and A $\beta$  instead accumulated intracellularly (Nilsson et al., 2013). Thus, a reduction in expression of proteins involved in macroautophagy could affect both A $\beta$  secretion and clearance.

## CD33

CD33, a type 1 transmembrane protein, is a sialic acid-binding immunoglobulin-like lectin (Siglec) expressed by immune cells, and was identified by GWAS to be associated with AD (Hollingworth et al., 2011). In addition, CD33-positive microglia and CD33 protein levels were found to be increased in AD brains, and CD33 was found to be associated with cognitive decline (Karch et al., 2012; Griciu et al., 2013). It was found that a rs3865444 allele that was found to be protective in AD led to a reduction in the level of insoluble A $\beta$  in the AD brain, suggesting a role for CD33 in mediating the clearance of A $\beta$  (Griciu et al., 2013). Furthermore, a risk allele of rs3865444 was associated with reduced A $\beta$ <sub>1–42</sub> internalization, and an increase in fibrillar amyloid, and neuritic amyloid pathology in AD patients, supporting the involvement of CD33 in the modulation of A $\beta$  clearance (Bradshaw et al., 2013). Recent work by Griciu et al. (2019) showed that knockout of CD33 led to mitigated A $\beta$  pathology in 5xFAD AD model mice, with genes related to phagocytosis found to be upregulated (Griciu et al., 2019). The opposite effects were found to result from TREM2

knockout (Griciu et al., 2019). Interestingly, this differential gene expression in CD33 deficient 5xFAD mice only occurred in the presence of TREM2, suggesting that TREM2 acts downstream of CD33 (Griciu et al., 2019).

## Degradation of A $\beta$ Fibrils by Lysosomal Proteases

Once internalized A $\beta$  fibrils are sorted to lysosomes, a degradative organelle which contains proteases that are capable of degrading A $\beta$  fibrils (Paresce et al., 1997). A $\beta$ <sub>1–42</sub> monomeric peptide, non-fibrillar assemblies and fibrils were all shown to be cleaved by the lysosomal cysteine protease cathepsin B, resulting in the production of A $\beta$ <sub>1–40</sub>, A $\beta$ <sub>1–38</sub> and A $\beta$ <sub>1–33</sub> in a dose-dependent manner (Mueller-Steiner et al., 2006). This suggests an anti-amyloidogenic role for cathepsin B, via the C-terminal truncation of A $\beta$ . In addition to this, cathepsin B was found to accumulate in mature amyloid plaques in AD model mice. Cathepsin B activity was highest in supernatant taken from primary microglial cell cultures, compared to neurons and astrocytes, suggesting that these cells act as a source of cathepsin B as they surround A $\beta$  plaques (Mueller-Steiner et al., 2006). The lysosomal protease, tripeptidyl peptidase 1 (TPP1) is another enzyme capable of cleaving A $\beta$  fibrils. Digestion of A $\beta$ <sub>1–42</sub> fibrils *in vitro* by TPP1 revealed a number of different cleavage sites within the  $\beta$ -sheet domains, and molecular dynamics simulations demonstrated that these cleavages lead to destabilization of the  $\beta$ -sheet fibril structure (Solé-Domènech et al., 2018).

## Failure of Microglia to Clear A $\beta$ Amyloid Fibrils in AD

Although evidence suggests that A $\beta$  amyloid fibrils can be internalized by microglia and degraded by lysosomal and secreted proteases, microglia may be limited in their capacity to clear A $\beta$ . This is evidenced by the accumulation of amyloid plaques in the AD brain despite microglial recruitment. A number of studies support this notion (Paresce et al., 1997; Majumdar et al., 2008). Fluorescently labeled A $\beta$  fibrils internalized by cultured microglia were trafficked to lysosomes, however, A $\beta$  was not degraded and was retained in microglial cells over a 3-day chase period (Majumdar et al., 2008). This was due to the inefficient delivery of chloride transporter CIC-9 to lysosomes, resulting in incomplete lysosome acidification and reduced activity of lysosomal proteases in the microglial (Majumdar et al., 2011).

Similarly, the genetic risk factor for AD, the  $\epsilon$ 4 allele of ApoE, may impair the ability of microglia to remove A $\beta$  deposits. ApoE is a key cholesterol carrier, primarily produced by astrocytes in the brain, but also to some extent by microglia, and facilitates the transport of lipids via receptors of the low-density lipoprotein receptor (LDLR) family (Bu, 2009). Three common isoforms of ApoE exist in humans;  $\epsilon$ 2  $\epsilon$ 3 and  $\epsilon$ 4 (Mahley, 1988). The  $\epsilon$ 4 allele of ApoE is the strongest genetic risk factor for late-onset AD, whereas the  $\epsilon$ 2 allele has a protective effect (Lambert et al., 2013). ApoE deletion in AD mouse models leads to reduced A $\beta$  plaque deposition, implicating ApoE in A $\beta$  amyloidogenesis and/or clearance (Bales et al., 1997; Ulrich et al., 2018). The efficiency of soluble A $\beta$  clearance from the interstitial fluid of the



brain is dependent on the ApoE isoform, with ApoE4 resulting in the least efficient clearance (Castellano et al., 2011). A number of mechanisms by which ApoE influences A $\beta$  clearance have been proposed. In microglia, it was reported that lipidated forms of ApoE stimulate the degradation of soluble A $\beta$  by NEP, with ApoE4 being the least efficient at promoting this degradation, and ApoE2 having the strongest effect (Jiang et al., 2008). There is also evidence to suggest that ApoE results in faster delivery of A $\beta$  to lysosomes in microglia, by lowering cellular cholesterol levels, and the efficiency of this cholesterol efflux activity is isoform-dependent (Hara et al., 2003; Lee et al., 2011). Furthermore, microglial-like cells derived from human induced pluripotent stem cells expressing ApoE4 displayed reduced oligomeric A $\beta_{1-42}$  phagocytosis compared to ApoE3 cells (Lin et al., 2018).

The ability of microglia to clear amyloid deposits in AD may also be diminished as a consequence of aging. Indeed, when production and clearance rates of A $\beta_{1-40}$  and A $\beta_{1-42}$  were tracked in AD patients using metabolic labeling, it was found that clearance rates for both peptides were reduced in AD compared to controls, but there were no differences in the rates of their production (Mawuenyega et al., 2010). This may be due to a reduced capacity of microglia to internalize A $\beta$  fibrils. Microglia from older AD model mice have a twofold to sixfold reduction in expression of A $\beta$ -binding receptors SR-A, CD36 and RAGE compared to wild type controls, in addition there was a significant reduction in the expression of secreted A $\beta$ -degrading enzymes IDE, NEP and MMP-9 (Hickman et al., 2008). Old AD model mice were also found to have increased expression of inflammatory cytokines tumor necrosis factor- $\alpha$  (TNF- $\alpha$ ) and interleukin-1 $\beta$  (IL-1 $\beta$ ), indicating that while clearance pathways are impaired, a damaging inflammatory response to A $\beta$  could be exacerbated (Hickman et al., 2008). A later study also found an impairment in phagocytic activity in AD mice compared to wild type controls, and this impairment correlated with an increased deposition of A $\beta$  (Krabbe et al., 2013). Reducing A $\beta$  load by administering an anti-A $\beta$  antibody restored the phagocytic capacity of microglia, suggesting that the microglial dysfunction is a result of AD pathology (Krabbe et al., 2013).

A number of subset populations of microglia have been identified in aging and AD brains, with distinct transcriptional profiles and phenotypes (Keren-Shaul et al., 2017; Krasemann et al., 2017; Marschallinger et al., 2020). These include 'damage associated microglia' (DAM) which are proposed to play a protective role in disease (Keren-Shaul et al., 2017), and microglia with a neurodegenerative phenotype, which have lost their homeostatic function (Krasemann et al., 2017). The switch of microglia to this impaired neurodegenerative phenotype was found to be dependent on APOE signaling induced by TREM2, further implicating these pathways and microglial dysfunction in AD (Krasemann et al., 2017). Furthermore, a unique population was recently identified in the aging brain, termed 'lipid-droplet-accumulating microglia' (LDAM), which show a build-up of lipid droplets, and possess a distinct transcriptional signature (Marschallinger et al., 2020). Importantly, these microglia show defects in phagocytosis, as well as increased release of pro-inflammatory cytokines (Marschallinger et al., 2020). LDAM

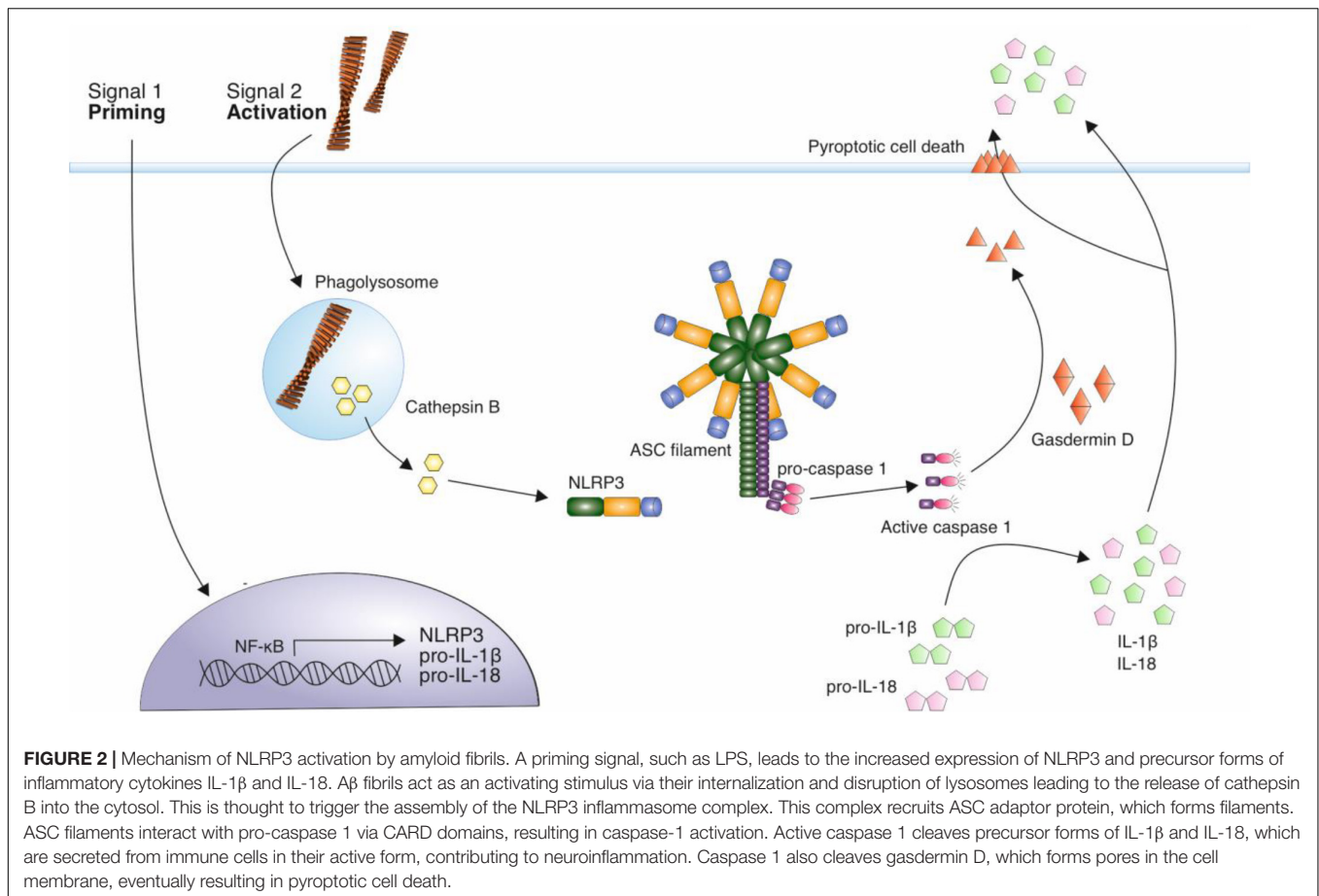
accounted for up to 50% of microglia in the hippocampus of aged mice, but have yet to be confirmed in AD models or brains (Marschallinger et al., 2020). Frigerio et al. (2019) showed that a microglial population termed 'activated response microglia' (ARMs) occur naturally in aging mice and in human brain, but the conversion to this state is accelerated in response to A $\beta$  plaques (Frigerio et al., 2019). A number of AD risk genes including ApoE were found to be upregulated in ARMs, conversely depletion of ApoE blocked the recruitment of microglia to A $\beta$  plaques (Frigerio et al., 2019). Given the association of the ApoE4 allele with AD, future studies should investigate whether this allele influences the production of ARMs (Lambert et al., 2013). Nonetheless, the implication of these data is that both aging and AD affect the phenotypes of microglia and thus their responses to A $\beta$ .

## CLEARANCE OF A $\beta$ BY ASTROCYTES

In addition to microglia, astrocytes may play a role in the clearance of A $\beta$ . Astrocytes, the most abundant glial cell in the brain, have numerous crucial roles in maintaining and regulating neuronal function and signal transmission (Perez-Nievas and Serrano-Pozo, 2018). Like microglia, astrocytes can react to pathogenesis by adopting a reactive phenotype, and this reactive astrogliosis is observed in AD brains, with a close relationship to A $\beta$  pathology (Itagaki et al., 1989; Nagele et al., 2003; Perez-Nievas and Serrano-Pozo, 2018). Moreover, astrocytes may also contribute to the clearance of A $\beta$  fibrils in AD and as discussed above the secreted protease MMP-9 is produced by a number of cell types including astrocytes (Vafadari et al., 2016). Astrocytes also secrete the MMP membrane type-1 (MT1) and kallikrein-related peptidase 7 (KLK7) (Liao and Van Nostrand, 2010; Kidana et al., 2018). MT1 is expressed by reactive astrocytes close to A $\beta$  deposits and was shown to degrade A $\beta$  plaques in an AD (APP) mouse model and cleave A $\beta_{1-42}$  fibrils *in vitro* (Liao and Van Nostrand, 2010). KLK7 was found to cleave A $\beta$  in the hydrophobic core motif of fibrils (KLVFFA), thus preventing fibril formation and promoting the degradation of pre-formed fibrils (Shropshire et al., 2014). KLK7 shows A $\beta$ -degrading activity *in vitro*, and deletion of KLK7 in AD mice resulted in increased fibrillar A $\beta$  pathology (Kidana et al., 2018). Further to this, KLK7 mRNA levels were found to be reduced in AD brains (Kidana et al., 2018).

A number of studies have also reported the ability of astrocytes to internalize A $\beta$ , resulting in the accumulation of A $\beta_{1-42}$  within activated astrocytes (Nagele et al., 2003; Wyss-Coray et al., 2003; Nielsen et al., 2010; Pihlaja et al., 2011). Cultured astrocytes were shown to migrate toward C-C motif ligand 2 (CCL2), a chemokine present at AD plaques, and subsequently bind to A $\beta$ , although the receptors involved in A $\beta$  binding were not identified (Wyss-Coray et al., 2003). ApoE deficient astrocytes are, however, less efficient in the internalization and degradation of A $\beta$  deposits compared to wild-type cells, thus implicating ApoE in astrocytic A $\beta$  clearance (Koistinaho et al., 2004). Moreover, in a study of AD brain tissue, A $\beta$  present within astrocytes was suggested to result from the phagocytosis of debris





derived from damaged neurons, as neuron-specific markers were also identified (Nagele et al., 2003).

## INFLAMMASOMES AND THE CROSS SEEDING OF A $\beta$ AGGREGATION

A role for activated microglia in the production of proinflammatory cytokines is well documented, and A $\beta$  fibrils can act as a stimulus for this activation (Halle et al., 2008; Reed-Geaghan et al., 2009; Stewart et al., 2010). However, the pathway for the production of pro-inflammatory cytokines IL-1 $\beta$  and interleukin-18 (IL-18) in microglia may also promote A $\beta$  fibril formation (Venegas et al., 2017). Thus, the relationship between microglia and A $\beta$  is complex, and instead of attempting to remove amyloid plaques, microglia may also be playing a role in the formation of A $\beta$  amyloid fibrils.

The NOD-like receptor family, pyrin domain containing 3 (NLRP3) inflammasome, is involved in the production and release of the pro-inflammatory cytokines IL-1 $\beta$  and IL-18 (Swanson et al., 2019). The activation of the inflammasome is a two-step process, requiring a priming stimulus followed by an activating stimulus. The priming stimulus can be cytokines, such as TNF- $\alpha$  and IL-1 $\beta$ , or pathogen associated molecular patterns (PAMPs) such as bacterial lipopolysaccharide

(LPS) (Bauernfeind et al., 2009; Franchi et al., 2009). This priming step results in the transcriptional upregulation of inflammasome components, NALP3 and inactive forms of IL-1 $\beta$ , IL-18 and caspase-1 (Bauernfeind et al., 2009; Franchi et al., 2009). A number of stimuli can act as a second activating stimulus, including ATP, pore-forming toxins that result in low intracellular K<sup>+</sup>, crystalline structures such as uric acid and silica, and A $\beta$  fibrils (Mariathasan et al., 2006; Martinon et al., 2006; Halle et al., 2008). The activating stimulus leads to the oligomerization of NLRP3, and the recruitment of adaptor protein apoptosis-associated speck-like protein containing a CARD (ASC). This triggers ASC polymerization into helical fibrils and subsequently assembly into micrometer-sized structures known as specks (Masumoto et al., 1999; Franklin et al., 2014; Lu et al., 2014). Caspase-1 is recruited via a caspase recruitment (CARD) domain and this results in caspase-1 autoproteolytic cleavage and activation. Caspase-1 is then responsible for the cleavage and thus activation of cytokines IL-1 $\beta$  and IL-18, which are released from cells, contributing to inflammation (Figure 2).

The activation of the inflammasome by A $\beta$  fibrils was first shown *in vitro* and was dependent on A $\beta$  phagocytosis and the subsequent damage to lysosomes, resulting in the release of cathepsin B into the cytosol (Halle et al., 2008). A further study then demonstrated that when NLRP3 or caspase-1 was

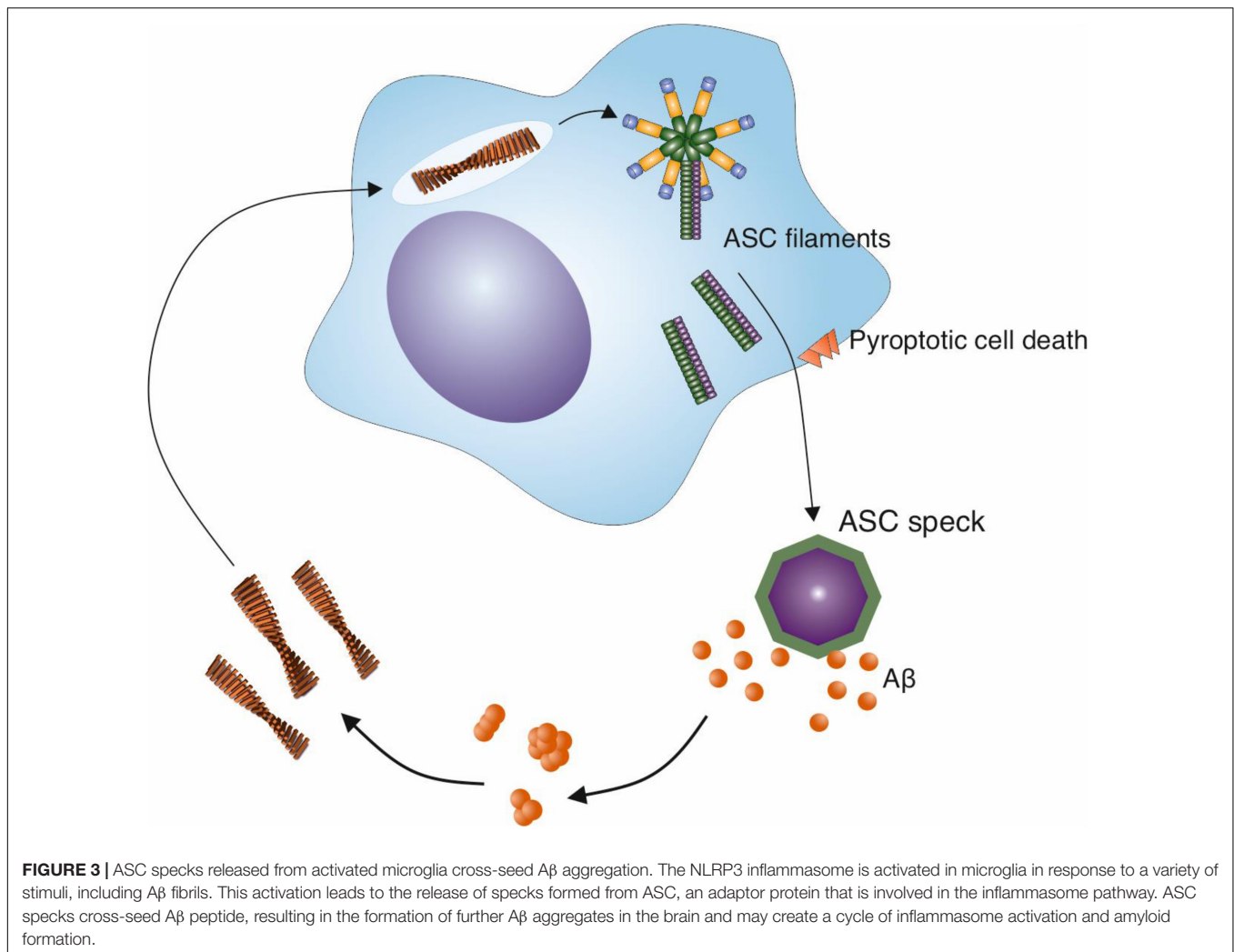


**FIGURE 3 |** ASC specks released from activated microglia cross-seed A $\beta$  aggregation. The NLRP3 inflammasome is activated in microglia in response to a variety of stimuli, including A $\beta$  fibrils. This activation leads to the release of specks formed from ASC, an adaptor protein that is involved in the inflammasome pathway. ASC specks cross-seed A $\beta$  peptide, resulting in the formation of further A $\beta$  aggregates in the brain and may create a cycle of inflammasome activation and amyloid formation.

knocked out in transgenic AD model mice, IL-1 $\beta$  activation was substantially reduced, providing support for the role of this activation pathway *in vivo* (Heneka et al., 2013). Furthermore, increased levels of cleaved caspase-1 were identified in AD patient brains compared with controls in hippocampal and cortical lysates, implicating the NLRP3 inflammasome as an important pathway in disease (Heneka et al., 2013).

Crucially, in addition to the activation of the NLRP3 inflammasome by A $\beta$  fibrils, evidence is emerging for a positive effect of the NLRP3 inflammasome on A $\beta$  aggregation (Figure 3). The activation of the NLRP3 inflammasome results in the release of ASC specks (Swanson et al., 2019). Venegas et al. (2017) demonstrated that after their release, ASC specks bind to A $\beta$ <sub>1–42</sub> peptide (Venegas et al., 2017). *In vitro* experiments revealed that ASC specks accelerate the aggregation of both A $\beta$ <sub>1–40</sub> and A $\beta$ <sub>1–42</sub> into oligomers and protofibrils, indicating a cross-seeding activity (Venegas et al., 2017). This was dependent on the PYD domain of ASC. Moreover, when purified ASC specks were injected into the hippocampus of AD model mice, more A $\beta$  deposits were observed, whereas an anti-ASC-speck antibody was capable of reducing A $\beta$  deposition (Venegas et al., 2017).

This suggests that not only do A $\beta$  fibrils act as a stimulus to trigger microglial activation, but also that the result of this activation is the formation of A $\beta$  aggregates, effectively producing a positive feedback loop (Figure 3). To compound this, in the presence of ASC-A $\beta$  composites, consisting of A $\beta$  oligomeric complexes forming in close association with ASC fibrils, the phagocytic clearance of A $\beta$  by microglia was reduced by 35%, and its degradation was reduced (Friker et al., 2020). Thus, the activation of the NLRP3 inflammasome by A $\beta$  fibrils could therefore both increase amyloid formation and reduce its clearance, contributing to the A $\beta$  deposition observed in AD.

## ANTIMICROBIAL AND ANTIVIRAL PROPERTIES OF A $\beta$ AND ITS AGGREGATION

### A $\beta$ Response to Bacteria and Fungi

Infection may be a co-factor in the aggregation of A $\beta$  into amyloid fibrils, moreover this may be related to the intrinsic

antimicrobial activities of A $\beta$  peptides. Indeed, it was found that A $\beta$  inhibits the growth of eight common microorganisms including both bacterial and fungal species, at a similar potency to the *bone fide* antimicrobial peptide LL-37 (Soscia et al., 2010). A further study reported that A $\beta$  protects against fungal and bacterial infections in mouse, *Caenorhabditis elegans* and cell culture models (Kumar et al., 2016). This was as a result of A $\beta$  binding to microbial cell wall polysaccharides via its heparin-binding domain (VHHQKL) (Kumar et al., 2016). A $\beta$  oligomers exhibited significantly increased binding compared to the monomeric peptide, and electron microscopy imaging revealed A $\beta$  fibrillation, with fibrils associating with and linking together microbial cells into clumps, a process known as agglutination (Kumar et al., 2016). Another study found that this microbial agglutination was mediated by A $\beta_{1-42}$ , but not A $\beta_{1-40}$ , suggesting that the more amyloidogenic form of this peptide has greater antimicrobial activity (Spitzer et al., 2016).

The demonstration of the antimicrobial properties of A $\beta$  suggests that AD may have an infectious etiology. A relationship has been proposed between gut microbiota and brain amyloidosis. APP AD model mice were found to have an altered gut microbiome compared to wild-type mice, and when APP mice were bred under sterile conditions, a significant reduction in cerebral A $\beta$  pathology was observed (Harach et al., 2017). Furthermore, fecal transplants from APP mice bred in standard conditions to APP mice bred in sterile conditions resulted in increased A $\beta$  pathology, whereas fecal transplants from wild-type mice did not have this effect (Harach et al., 2017). This research has been supported by studies in humans, with differences identified in the abundance of pro- and anti-inflammatory gut bacterial taxa in patients with brain amyloidosis (Cattaneo et al., 2017). When the bacterial taxonomic composition of fecal samples was compared between AD patient and control samples, a distinct microbiome composition was identified in AD samples (Vogt et al., 2017). Similarly, a number of studies have suggested a connection between the oral microbiome and AD (Ide et al., 2016; Chen et al., 2017; Dominy et al., 2019). *Porphyromonas gingivalis*, a pathogen in periodontal infections, was recently identified in AD brains and resulted in increased A $\beta$  deposition in mice (Poole et al., 2013; Dominy et al., 2019).

## A $\beta$ Response to Viruses

A number of studies have investigated the relationship between viral infections and AD. There is evidence that herpes simplex virus type-1 (HSV-1) is a risk factor for AD, when the AD patient is a carrier of the APOE- $\epsilon$ 4 allele (Itzhaki et al., 1997). Subsequent studies have found an association between HSV-1 and the risk of neurodegenerative disease, with one retrospective cohort study in Taiwan identifying a 2.56-fold increased risk of dementia with HSV infection (Tzeng et al., 2018). However, another study reported only a slightly increased risk (Chen et al., 2018). In addition to HSV-1, analysis of genomic, transcriptomic, proteomic and histopathological data from brains identified increased human herpesvirus 6A (HHV-6A) and human herpesvirus 7 (HHV-7) in AD brain tissue samples compared to controls. Viral abundance was suggested to be linked with APP metabolism networks, including the induction

of PSEN1 and BACE1 expression by HHV-6A (Readhead et al., 2018). However, the statistical robustness of this analysis was contested, and re-analysis of the data did not support a link between HHV-6A or HHV-7 and AD (Jeong and Liu, 2019).

Whilst the link between herpesvirus infections and AD may be equivocal, various studies suggest that herpesviruses and other infectious agents promote A $\beta$  aggregation into amyloid fibrils. In neuronal and glial cell cultures, infection with HSV-1 led to the accumulation of A $\beta$  within cells, and increased A $\beta$  deposits were present in mouse brains after HSV-1 infection (Wozniak et al., 2007). Further investigation revealed that in AD, HSV-1 DNA localizes with A $\beta$  plaques, with 90% of the plaques containing viral DNA (Wozniak et al., 2009). Similarly, it was shown that in a mouse model of recurrent HSV-1 infections, AD pathologies including A $\beta$  accumulation, tau hyperphosphorylation and markers of neuroinflammation were observed (De Chiara et al., 2019). These results were corroborated recently in a 3D human brain-like model formed from human-induced neural stem cells (Cairns et al., 2020). It was found that whilst high HSV-1 infection levels led to cell death, low HSV-1 infection levels led to an AD-like phenotype, including dense A $\beta$  fibrillar plaques and neuroinflammation (Cairns et al., 2020).

Both A $\beta_{1-40}$  and A $\beta_{1-42}$  inhibited the replication of HSV-1 in a number of cell lines when added to the cultures either prior to or in parallel with the virus (Bourgade et al., 2014). This effect was postulated to be a result of A $\beta$  inserting into the HSV-1 envelope (Bourgade et al., 2014). Moreover, A $\beta$  oligomers bind viral surface glycoproteins and fibrils mediate virus entrapment (Eimer et al., 2018). A recent study found that HSV-1 catalyzes the aggregation of A $\beta_{1-42}$  *in vitro* and in an AD mouse model via surface-mediated nucleation, thus providing further support for this hypothesis (Ezzat et al., 2019). Crucially, the interaction of A $\beta$  with viruses may be the same mechanism as its interaction with bacteria and fungi, namely the A $\beta$  heparin-binding domain binds carbohydrates exposed on the surface of the virus (Eimer et al., 2018).

Not only does A $\beta$  have antiviral activity, but its production may be controlled by the innate immunity protein, interferon-induced transmembrane protein 3 (IFITM3), which upregulates the activity of  $\gamma$ -secretase, resulting in the increased generation of A $\beta$  peptide (Hur et al., 2020). Furthermore, deletion of IFITM3 in the 5xFAD mouse AD model resulted in reduced A $\beta$  plaque formation, and IFITM3 expression was found to increase with aging and in mouse models expressing familial AD genes (Hur et al., 2020). IFITM3 plays a role in preventing viral infection, and its expression is induced by pro-inflammatory cytokines (Bailey et al., 2014). Thus, taken together these data support the antimicrobial and antiviral hypothesis for A $\beta$  and suggest that infection may be a cofactor for A $\beta$  aggregation *in vivo* (Jackson and Hewitt, 2017).

## HOW TO PREVENT A $\beta$ AGGREGATION AND ENHANCE REMOVAL OF A $\beta$ DEPOSITS

A $\beta$  plaque formation in AD will be a balance between the rate of amyloid fibril assembly and the rate of clearance. Given

their potential roles as cofactors in amyloid fibril assembly, targeting microglial activation and infections by viruses and bacteria may represent therapeutic approaches in AD. Similarly, enhancing the uptake and degradation of A $\beta$  fibrils may provide an additional approach to reduce A $\beta$  plaque burden in AD (Figure 1).

## Reducing the Activation of Microglia

Activated microglia are a characteristic feature of neuroinflammation in AD (Frautschy et al., 1998; Felsky et al., 2019). However, despite a decreased risk of AD associated with long-term non-steroidal anti-inflammatory drugs (NSAID) treatment, clinical trials of anti-inflammatory drugs to treat AD have not yet been successful (Aisen et al., 2003; Meyer et al., 2019; Howard et al., 2020). Minocycline, an anti-inflammatory tetracycline capable of crossing the blood-brain barrier (BBB), was found to reduce inflammatory markers and reverse cognitive impairment in an AD-like mouse model, induced by the administration of A $\beta$ <sub>1–42</sub> oligomers to the brain (Garcez et al., 2017). However, in clinical trials no improvement in cognitive impairment was identified with minocycline treatment (Howard et al., 2020). Similarly, treatment with naproxen did not slow disease progression in patients with mild-moderate, or reduce the progression of pre-symptomatic AD (Aisen et al., 2003; Meyer et al., 2019).

Whilst the aforementioned anti-inflammatories may be ineffective in the treatment of AD, the inflammasome may prove to be a better target. Indeed, a small molecule inhibitor of the NLRP3 inflammasome, MCC950, was found to stimulate A $\beta$  phagocytosis *in vitro*, and reduce A $\beta$  deposition in AD (APP/PS1) model mice (Dempsey et al., 2017). This was also associated with an improvement in cognitive function (Dempsey et al., 2017). Similarly, MCC950 prevented  $\alpha$ -synuclein aggregate pathology and the degeneration of dopaminergic neurons in multiple rodent models of Parkinson's disease (Gordon et al., 2018). These results are supported by a study in which NLRP3 components were knocked out in AD model mice, and this led to enhanced A $\beta$  clearance and decreased A $\beta$  deposition (Heneka et al., 2013). Importantly, these results support the clinical development of inflammasome inhibitors as a treatment for neurodegenerative amyloid diseases such as AD.

## Targeting Viral and Bacterial Infections

The demonstration that A $\beta$  interacts with viruses may provide new routes of clinical intervention in AD patients; targeting viral infection could prevent the A $\beta$  aggregation associated with AD. Two population cohort studies found that those taking anti-herpetic treatments for HSV infections had a reduced risk of dementia (Chen et al., 2018; Tzeng et al., 2018). In addition, in a recent study in 3D brain-like structures, HSV-1 infection induced an AD-like phenotype, and antiviral medication was successful in abrogating this phenotype, suggesting that antivirals could be utilized to treat AD patients (Cairns et al., 2020). An antiviral drug, Valacyclovir, is currently in Phase II clinical trials for the treatment of

AD (ClinicalTrials.gov, ID# NCT03282916). Similarly, targeting bacterial infections could be used to prevent A $\beta$  aggregation in AD. For example, inhibition of gingipains, toxic proteases from *P. gingivalis*, using small molecule inhibitors led to reduced A $\beta$ <sub>1–42</sub> production, neuroinflammation and neuronal death (Dominy et al., 2019). Consequently, a small molecule inhibitor of gingipains, COR388, is currently in Phase II clinical trials for the treatment of AD (ClinicalTrials.gov, ID# NCT03823404).

## Enhancing the Uptake and Degradation of Amyloid by Microglia

Whilst a role for TLR receptors in A $\beta$  uptake by microglia has been suggested, these receptors also have a central role in the activation of inflammation (Reed-Geaghan et al., 2009; Stewart et al., 2010). Thus, targeting these receptors in the treatment of AD is not straight forward, as a detrimental inflammatory response could also be activated. Treatment with an LPS-derived TLR4 agonist, monophosphoryl lipid A (MPL) in a murine AD model led to reduced A $\beta$  load and enhanced cognitive function, but a 'low level' inflammatory response was also triggered (Michaud et al., 2013). However, the AAV-mediated expression of the human TLR5 ectodomain as a 'decoy' receptor was explored, and found to result in the attenuation of A $\beta$  plaque formation in a mouse model (Chakrabarty et al., 2018). The human TLR5 ectodomain was fused to human IgG4 Fc (sTLR5Fc), and this was found to bind to A $\beta$  fibrils strongly, and to other forms of A $\beta$ <sub>1–40</sub> and A $\beta$ <sub>1–42</sub>, to lesser extents. Therefore, the reduction in A $\beta$  deposition into plaques could be due to the sequestration of fibrils by the TLR5 ectodomain (Chakrabarty et al., 2018). Furthermore, *in vitro* incubation with sTLR5Fc resulted in increased uptake of A $\beta$ <sub>1–40</sub> fibrils by microglia without activating TLR5 signaling (Chakrabarty et al., 2018), thus suggesting it as a safe method of immunomodulation in AD.

TREM2 is upregulated in response to increased A $\beta$  levels in an AD mouse model (Jiang et al., 2014). Importantly, upregulating TREM2 significantly reduced A $\beta$  deposition, neuroinflammation, synapse loss and led to improvements in cognitive function (Jiang et al., 2014). A monoclonal antibody targeting TREM2, AL002a, was found to activate TREM2 signaling *in vitro* (Price et al., 2020). Furthermore, treatment of 5xFAD mice with this antibody led to increased microglial recruitment to A $\beta$  plaques, and reduced A $\beta$  deposition (Price et al., 2020). TREM2 could therefore be a potential target for clinical intervention in the treatment of AD, and AL002 is currently being tested in Phase I clinical trials in patients with mild to moderate Alzheimer's disease (ClinicalTrials.gov, ID#NCT03635047). Another monoclonal antibody, 4D9, was recently found to increase microglial uptake of A $\beta$  *in vitro* and reduce A $\beta$  deposits in the APP NL-G-F knock-in AD mouse model (Schlepckow et al., 2020). This antibody enhances TREM2 activity by competing for binding to the  $\alpha$ -secretase cleavage site, therefore preventing TREM2 cleavage and subsequent shedding, whilst also enhancing TREM2 signaling (Schlepckow et al., 2020).



Macrophage colony stimulating factor (M-CSF) upregulates the transcription of the chloride transporter CIC-7 by microglia, increasing lysosomal acidification and enhancing the degradation of A $\beta$  amyloid fibrils (Majumdar et al., 2011). This suggests that M-CSF could be used to promote A $\beta$  amyloid clearance in AD. Indeed, in APP<sub>(Swe)</sub>/PS1 transgenic AD model mice M-CSF treatment resulted in a reduced number of A $\beta$  deposits, a higher ratio of microglia with evidence of A $\beta$  internalization, and reduced cognitive decline (Boissonneault et al., 2009). However, M-CSF is a hematopoietic cytokine that has been implicated in a number of inflammatory and autoimmune diseases and as a consequence M-CSF treatment could have deleterious inflammatory effects (Hamilton et al., 2016).

An alternative to enhancing pathways for fibril uptake and degradation is to inhibit negative regulators of these pathways. Evidence points toward a role for CD33 as a negative modulator of A $\beta$  fibril clearance (Bradshaw et al., 2013; Griciu et al., 2013, 2019), and inhibition of CD33 may represent a therapeutic strategy. A phase I clinical trial is underway for the monoclonal antibody, AL003, which targets and inhibits CD33 (ClinicalTrials.gov, NCT03822208). With evidence suggesting that CD33 deletion in mice reduces A $\beta$  pathology and increases microglial expression of genes relating to phagocytosis, AL003 administration aims to inhibit CD33, thus increasing the clearance activity of microglia and reducing A $\beta$  deposition (Griciu et al., 2019). Similarly, CD22 could be targeted in AD. A recent study used CRISPR-Cas9 with RNA sequencing analysis to identify genes that are related to aging and lead to changes in microglial phagocytosis (Pluvinage et al., 2019). CD22 was identified as a receptor that negatively regulates phagocytosis and is upregulated in aged microglia. It was found that inhibiting CD22 with a CD22 blocking antibody improved the phagocytosis of A $\beta$  oligomers and  $\alpha$ -synuclein fibrils *in vivo*, supporting the hypothesis that AD results from age-related changes in microglia that reduce their amyloid clearing ability (Pluvinage et al., 2019). Similarly, manipulating microglia in order to favor a switch from dysfunctional phenotypes to a protective phenotype such as DAM could be used as future approach to restore microglial function and enhance the clearance of Keren-Shaul et al. (2017); Krasemann et al. (2017), and Marschallinger et al. (2020).

## DISCUSSION

Multiple different cofactors may influence A $\beta$  assembly *in vivo*, including inflammation and infection. Moreover, the extent of amyloid plaques formation in AD will be dependent on the balance between A $\beta$  fibril formation and the clearance and degradation of these deposits. Evidence points to microglia playing roles in both amyloid formation and its clearance (Lee and Landreth, 2010; Venegas et al., 2017), as such the balance between these microglial activities may be a factor in the accumulation of amyloid plaques. Yet, despite their recruitment to plaques, microglia do not appear to be able to halt the formation A $\beta$  fibrils in AD. In the aging AD brain a

reduction in the uptake and degradation of A $\beta$  amyloid fibrils by microglia may cause these cells to be overwhelmed by the amyloid deposits (Hickman et al., 2008; Mawuenyega et al., 2010; Krabbe et al., 2013). Enhancement of the degradative activity of microglia therefore represent potential targets for therapeutic intervention in AD (Boissonneault et al., 2009; Majumdar et al., 2011).

Neuroinflammation is a damaging process in AD (Heppner et al., 2015), but via production of the inflammasome specks microglia could be exacerbating the disease by cross seeding A $\beta$  amyloid formation (Venegas et al., 2017). Moreover, A $\beta$  fibrils can themselves stimulate inflammasome formation and this raises the intriguing possibility that A $\beta$  fibrils promote A $\beta$  aggregation via microglia activation, resulting in a vicious cycle (Halle et al., 2008; Heneka et al., 2013; Venegas et al., 2017; Friker et al., 2020). As such the inflammasome may be a good target for AD therapeutics (Heneka et al., 2013; Dempsey et al., 2017; Gordon et al., 2018), as both inflammation and inflammasome-dependent A $\beta$  fibril assembly could be reduced.

Whilst, A $\beta$  aggregation has been thought of as being a pathological process, A $\beta$  has properties consistent with it being an antimicrobial peptide (Soscia et al., 2010; Bourgade et al., 2014; Kumar et al., 2016; Spitzer et al., 2016; Hur et al., 2020). Indeed, there are a number of key similarities with the antimicrobial peptide LL-37, which can also assemble into amyloid fibrils (Sood et al., 2008; Jackson and Hewitt, 2017). Whilst a role for A $\beta$  *in vivo* as an antimicrobial peptide is unclear, *in vitro* it can agglutinate viruses, bacteria and fungi by assembling into amyloid like structures on the surface of these infectious agents. This provides an additional mechanism by which A $\beta$  assembly could be promoted *in vivo*, by virtue of its interaction with the surfaces of infectious agents (Kumar et al., 2016; Eimer et al., 2018; Ezzat et al., 2019). Moreover, infection would also be predicted to activate inflammation and could promote A $\beta$  aggregation via the inflammasome (Swanson et al., 2019). Although, bacteria, fungi, viruses and inflammasome specks can cross seed A $\beta$  aggregation, little is known about the structure and properties of the fibrils produced. Crucially, both *in vitro* and *in vivo* A $\beta$  fibrils can assemble into multiple different fibril polymorphs, in which the A $\beta$  peptides have different arrangements in the fibril structure (Petkova et al., 2005; Paravastu et al., 2008, 2009; Lu et al., 2013; Colvin et al., 2015; Gremer et al., 2017; Kollmer et al., 2019). Little is known about the molecular structure of the A $\beta$  aggregates produced by cross seeding by either specks and microorganisms *in vitro* nor how they relate to those formed *in vivo* in AD brain. This is important to know because A $\beta$  fibril polymorphism *in vivo* is related to the type of AD presented (Lu et al., 2013; Qiang et al., 2017; Rasmussen et al., 2017). Similarly, whilst A $\beta$  fibrils can be internalized and degraded by microglia, at least to some extent *in vitro* (Husemann et al., 2001; Tahara et al., 2006; Reed-Geaghan et al., 2009; Song et al., 2011) it is not known if polymorphism affects clearance of amyloid fibrils *in vivo*. It is plausible that A $\beta$  fibril polymorphism could affect the affinity for microglial A $\beta$  receptors and how the fibrils are degraded by microglial

proteases. Thus, any fibril polymorphs that can escape microglial clearance may accumulate more in an AD brain.

In summary, *in vivo* multiple different cofactors, including microglia and infection, may influence the assembly of A $\beta$  amyloid fibrils, and thus could represent targets for therapeutic intervention in AD.

## AUTHOR CONTRIBUTIONS

MB, EH, and SR wrote and edited the manuscript. All authors contributed to the article and approved the submitted version.

## REFERENCES

- Aisen, P. S., Schafer, K. A., Grundman, M., Pfeiffer, E., Sano, M., Davis, K. L., et al. (2003). Effects of Rofecoxib or Naproxen vs placebo on alzheimer disease progression: a randomized controlled trial. *J. Am. Med. Assoc.* 289, 2819–2826. doi: 10.1001/jama.289.21.2819
- Ajami, B., Bennett, J. L., Krieger, C., Tetzlaff, W., and Rossi, F. M. V. (2007). Local self-renewal can sustain CNS microglia maintenance and function throughout adult life. *Nat. Neurosci.* 10, 1538–1543. doi: 10.1038/nn2014
- Bailey, C. C., Zhong, G., Huang, I. C., and Farzan, M. (2014). IFITM-Family proteins: the cell's first line of antiviral defense. *Annu. Rev. Virol.* 1, 261–283. doi: 10.1146/annurev-virology-031413-085537
- Bales, K. R., Verina, T., Dodel, R. C., Du, Y., Altstiel, L., Bender, M., et al. (1997). Lack of apolipoprotein E dramatically reduces amyloid  $\beta$ -peptide deposition. *Nat. Genet.* 17, 263–264. doi: 10.1038/ng1197-263
- Bamberger, M. E., Harris, M. E., McDonald, D. R., Husemann, J., and Landreth, G. E. (2003). A cell surface receptor complex for fibrillar  $\beta$ -amyloid mediates microglial activation. *J. Neurosci.* 23, 2665–2674. doi: 10.1523/JNEUROSCI.23-07-02665.2003
- Bauer, J., Strauss, S., Schreiter-Gasser, U., Ganter, U., Schlegel, P., Witt, I., et al. (1991). Interleukin-6 and  $\alpha$ -2-macroglobulin indicate an acute-phase state in Alzheimer's disease cortices. *FEBS Lett.* 285, 111–114. doi: 10.1016/0014-5793(91)80737-N
- Bauernfeind, F. G., Horvath, G., Stutz, A., Alnemri, E. S., MacDonald, K., Speert, D., et al. (2009). Cutting Edge: NF- $\kappa$ B activating pattern recognition and cytokine receptors license NLRP3 inflammasome activation by regulating NLRP3 expression. *J. Immunol.* 183, 787–791. doi: 10.4049/jimmunol.0901363
- Boissonneault, V., Filali, M., Lessard, M., Relton, J., Wong, G., and Rivest, S. (2009). Powerful beneficial effects of macrophage colony-stimulating factor on  $\beta$ -amyloid deposition and cognitive impairment in Alzheimer's disease. *Brain* 132, 1078–1092. doi: 10.1093/brain/awn331
- Bourgade, K., Garneau, H., Giroux, G., Le Page, A. Y., Bocti, C., Dupuis, G., et al. (2014).  $\beta$ -Amyloid peptides display protective activity against the human Alzheimer's disease-associated herpes simplex virus-1. *Biogerontology* 16, 85–98. doi: 10.1007/s10522-014-9538-8
- Braak, H., and Braak, E. (1991). Neuropathological staging of Alzheimer-related changes. *Acta Neuropathol.* 82, 239–259. doi: 10.1007/BF00308809
- Bradshaw, E. M., Chibnik, L. B., Keenan, B. T., Ottoboni, L., Raj, T., Tang, A., et al. (2013). CD33 Alzheimer's disease locus: altered monocyte function and amyloid biology. *Nat. Neurosci.* 16, 848–850. doi: 10.1038/nn.3435
- Bu, G. (2009). Apolipoprotein e and its receptors in Alzheimer's disease: pathways, pathogenesis and therapy. *Nat. Rev. Neurosci.* 10, 333–344. doi: 10.1038/nrn2620
- Cairns, D. M., Rouleau, N., Parker, R. N., Walsh, K. G., Gehrke, L., and Kaplan, D. L. (2020). A 3D human brain-like tissue model of herpes-induced Alzheimer's disease. *Sci. Adv.* 6:eay8828. doi: 10.1126/sciadv.aay8828
- Castellano, J. M., Kim, J., Stewart, F. R., Jiang, H., DeMattos, R. B., Patterson, B. W., et al. (2011). Human apoE isoforms differentially regulate brain amyloid- $\beta$  peptide clearance. *Sci. Transl. Med.* 3:89ra57. doi: 10.1126/scitranslmed.3002156
- Cattaneo, A., Cattane, N., Galluzzi, S., Provasi, S., Lopizzo, N., Festari, C., et al. (2017). Association of brain amyloidosis with pro-inflammatory gut bacterial taxa and peripheral inflammation markers in cognitively impaired elderly. *Neurobiol. Aging* 49, 60–68. doi: 10.1016/j.neurobiolaging.2016.08.019
- Chakrabarty, P., Li, A., Ladd, T. B., Strickland, M. R., Koller, E. J., Burgess, J. D., et al. (2018). TLR5 decoy receptor as a novel anti-amyloid therapeutic for Alzheimer's disease. *J. Exp. Med.* 215, 2247–2264. doi: 10.1084/jem.20180484
- Chen, C. K., Wu, Y. T., and Chang, Y. C. (2017). Association between chronic periodontitis and the risk of Alzheimer's disease: a retrospective, population-based, matched-cohort study. *Alzheimers Res. Ther.* 9:56.
- Chen, V. C. H., Wu, S. I., Huang, K. Y., Yang, Y. H., Kuo, T. Y., Liang, H. Y., et al. (2018). Herpes zoster and dementia: a nationwide population-based cohort study. *J. Clin. Psychiatry* 79:16m11312. doi: 10.4088/JCP.16m11312
- Chih Jin, S., Benitez, B. A., Karch, C. M., Cooper, B., Skorupa, T., Carrell, D., et al. (2014). Coding variants in TREM2 increase risk for Alzheimer's disease. *Hum. Mol. Genet.* 23, 5838–5846. doi: 10.1093/hmg/ddu277
- Christie, R. H., Freeman, M., and Hyman, B. T. (1996). Expression of the macrophage scavenger receptor, a multifunctional lipoprotein receptor, in microglia associated with senile plaques in Alzheimer's disease. *Am. J. Pathol.* 148, 399–403.
- Cohen, S. I. A., Linse, S., Luheshi, L. M., Hellstrand, E., White, D. A., Rajah, L., et al. (2013). Proliferation of amyloid- $\beta$ 42 aggregates occurs through a secondary nucleation mechanism. *Proc. Natl. Acad. Sci. U.S.A.* 110, 9758–9763. doi: 10.1073/pnas.1218402110
- Colvin, M. T., Silvers, R., Frohm, B., Su, Y., Linse, S., and Griffin, R. G. (2015). High Resolution Structural Characterization of A $\beta$ 42 Amyloid Fibrils by Magic Angle Spinning NMR. *J. Am. Chem. Soc.* 137, 7509–7518. doi: 10.1021/jacs.5b03997
- Condello, C., Yuan, P., Schain, A., and Grutzendler, J. (2015). Microglia constitute a barrier that prevents neurotoxic protofibrillar A $\beta$ 42 hotspots around plaques. *Nat. Commun.* 6:6176. doi: 10.1038/ncomms7176
- Coraci, I. S., Husemann, J., Berman, J. W., Hulette, C., Dufour, J. H., Campanella, G. K., et al. (2002). CD36, a class B scavenger receptor, is expressed on microglia in Alzheimer's disease brains and can mediate production of reactive oxygen species in response to  $\beta$ -amyloid fibrils. *Am. J. Pathol.* 160, 101–112. doi: 10.1016/s0002-9440(10)64354-4
- Davalos, D., Grutzendler, J., Yang, G., Kim, J. V., Zuo, Y., Jung, S., et al. (2005). ATP mediates rapid microglial response to local brain injury *in vivo*. *Nat. Neurosci.* 8, 752–758. doi: 10.1038/nn1472
- De Chiara, G., Piacentini, R., Fabiani, M., Mastrodonato, A., Marcocci, M. E., Limongi, D., et al. (2019). Recurrent herpes simplex virus-1 infection induces hallmarks of neurodegeneration and cognitive deficits in mice. *PLoS Pathog.* 15:e1007617. doi: 10.1371/journal.ppat.1007617
- Dempsey, C., Rubio Araiz, A., Bryson, K. J., Finucane, O., Larkin, C., Mills, E. L., et al. (2017). Inhibiting the NLRP3 inflammasome with MCC950 promotes non-phlogistic clearance of amyloid- $\beta$  and cognitive function in APP/PS1 mice. *Brain Behav. Immun.* 61, 306–316. doi: 10.1016/j.bbi.2016.12.014
- Dominy, S. S., Lynch, C., Ermini, F., Benedyk, M., Marczyk, A., Konradi, A., et al. (2019). Porphyromonas gingivalis in Alzheimer's disease brains: evidence for disease causation and treatment with small-molecule inhibitors. *Sci. Adv.* 5:eaa3333. doi: 10.1126/sciadv.aau3333
- Eanes, E. D., and Glenner, G. G. (1968). X-ray diffraction studies on amyloid filaments. *J. Histochem. Cytochem.* 16, 673–677. doi: 10.1177/16.11.673
- Eimer, W. A., Vijaya Kumar, D. K., Navalpur Shanmugam, N. K., Rodriguez, A. S., Mitchell, T., Washicosky, K. J., et al. (2018). Alzheimer's disease-associated

## FUNDING

MB was supported by a studentship from the MRC Discovery Medicine North (DiMeN) Doctoral Training Partnership (MR/N013840/1). SR acknowledges funding from the Wellcome Trust (204963).

## ACKNOWLEDGMENTS

We thank members of the Hewitt and Radford laboratories for insightful discussions.

- $\beta$ -amyloid is rapidly seeded by herpesviridae to protect against brain infection. *Neuron* 99, 56–63.e3. doi: 10.1016/j.neuron.2018.06.030
- El Khoury, J., Hickman, S. E., Thomas, C. A., Cao, L., Silverstein, S. C., and Loike, J. D. (1996). Scavenger receptor-mediated adhesion of microglia to  $\beta$ -amyloid fibrils. *Nature* 382, 716–719. doi: 10.1038/382716a0
- Evangelisti, E., Cascella, R., Becatti, M., Marrazza, G., Dobson, C. M., Chiti, F., et al. (2016). Binding affinity of amyloid oligomers to cellular membranes is a generic indicator of cellular dysfunction in protein misfolding diseases. *Sci. Rep.* 6:32721. doi: 10.1038/srep32721
- Ezzat, K., Pernemalm, M., Pålsson, S., Roberts, T. C., Järver, P., Dondalska, A., et al. (2019). The viral protein corona directs viral pathogenesis and amyloid aggregation. *Nat. Commun.* 10:2331.
- Farris, W., Mansourian, S., Chang, Y., Lindsley, L., Eckman, E. A., Frosch, M. P., et al. (2003). Insulin-degrading enzyme regulates the levels of insulin, amyloid  $\beta$ -protein, and the  $\beta$ -amyloid precursor protein intracellular domain *in vivo*. *Proc. Natl. Acad. Sci. U.S.A.* 100, 4162–4167. doi: 10.1073/pnas.0230450100
- Fassbender, K., Walter, S., Kühl, S., Landmann, R., Ishii, K., Bertsch, T., et al. (2004). The LPS receptor (CD14) links innate immunity with Alzheimer's disease. *FASEB J.* 18, 203–205. doi: 10.1096/fj.03-0364fje
- Felsky, D., Roostaei, T., Nho, K., Risacher, S. L., Bradshaw, E. M., Petyuk, V., et al. (2019). Neuropathological correlates and genetic architecture of microglial activation in elderly human brain. *Nat. Commun.* 10:409.
- Franchi, L., Eigenbrod, T., and Núñez, G. (2009). Cutting Edge: TNF- $\alpha$  Mediates Sensitization to ATP and Silica via the NLRP3 Inflammasome in the Absence of Microbial Stimulation. *J. Immunol.* 183, 792–796. doi: 10.4049/jimmunol.0900173
- Franklin, B. S., Bossaller, L., De Nardo, D., Ratter, J. M., Stutz, A., Engels, G., et al. (2014). The adaptor ASC has extracellular and “prionoid” activities that propagate inflammation. *Nat. Immunol.* 15, 727–737. doi: 10.1038/ni.2913
- Frautschy, S. A., Yang, F., Irrizarry, M., Hyman, B., Saido, T. C., Hsiao, K., et al. (1998). Microglial response to amyloid plaques in APPsw transgenic mice. *Am. J. Pathol.* 152, 307–317.
- Frigerio, C. S., Wolfs, L., Fattorelli, N., Perry, V. H., Fiers, M., and De Strooper, B. (2019). The major risk factors for alzheimer's disease: age, sex, and genes modulate the microglia response to A $\beta$  Plaques. *Cell Rep.* 27, 1293–1306.e6. doi: 10.1016/j.celrep.2019.03.099
- Friker, L. L., Scheiblich, H., Hochheiser, I. V., Latz, E., Geyer, M., and Heneka, M. T. (2020).  $\beta$ -Amyloid Clustering around ASC fibrils boosts its toxicity in microglia. *Cell Rep.* 30, 3743–3754.e6. doi: 10.1016/j.celrep.2020.02.025
- Garcez, M. L., Mina, F., Bellettini-Santos, T., Carneiro, F. G., Luz, A. P., Schiavo, G. L., et al. (2017). Minocycline reduces inflammatory parameters in the brain structures and serum and reverses memory impairment caused by the administration of amyloid  $\beta$  (1–42) in mice. *Prog. Neuropsychopharmacol. Biol. Psychiatry* 77, 23–31. doi: 10.1016/j.pnpbp.2017.03.010
- Ginhoux, F., Greter, M., Leboeuf, M., Nandi, S., See, P., Gokhan, S., et al. (2010). Fate mapping analysis reveals that adult microglia derive from primitive macrophages. *Science* 330, 841–845. doi: 10.1126/science.1194637
- Gordon, R., Albornoz, E. A., Christie, D. C., Langley, M. R., Kumar, V., Mantovani, S., et al. (2018). Inflammasome inhibition prevents -synuclein pathology and dopaminergic neurodegeneration in mice. *Sci. Transl. Med.* 10:ea4066. doi: 10.1126/scitranslmed.aah4066
- Gremer, L., Schölzel, D., Schenk, C., Reinartz, E., Labahn, J., Ravelli, R. B. G., et al. (2017). Fibril structure of amyloid-beta(1–42) by cryo – electron microscopy. *Science* 358, 116–119. doi: 10.1042/BJ20081572
- Griciuc, A., Patel, S., Federico, A. N., Choi, S. H., Innes, B. J., Oram, M. K., et al. (2019). TREM2 Acts downstream of CD33 in MODULATING MICROGLIAL PATHOLOGY in Alzheimer's Disease. *Neuron* 103, 820–835.e7. doi: 10.1016/j.neuron.2019.06.010
- Griciuc, A., Serrano-Pozo, A., Parrado, A. R., Lesinski, A. N., Asselin, C. N., Mullin, K., et al. (2013). Alzheimer's disease risk gene cd33 inhibits microglial uptake of amyloid beta. *Neuron* 78, 631–643. doi: 10.1016/j.neuron.2013.04.014
- Griffin, W. S. T., Stanley, L. C., Ling, C., White, L., MacLeod, V., Perrot, L. J., et al. (1989). Brain interleukin 1 and S-100 immunoreactivity are elevated in Down syndrome and Alzheimer disease. *Proc. Natl. Acad. Sci. U.S.A.* 86, 7611–7615. doi: 10.1073/pnas.86.19.7611
- Halle, A., Hornung, V., Petzold, G. C., Stewart, C. R., Monks, B. G., Reinheckel, T., et al. (2008). The NALP3 inflammasome is involved in the innate immune response to amyloid- $\beta$ . *Nat. Immunol.* 9, 857–865. doi: 10.1038/ni.1636
- Hamerman, J. A., Jarjoura, J. R., Humphrey, M. B., Nakamura, M. C., Seaman, W. E., and Lanier, L. L. (2006). Cutting Edge: inhibition of TLR and FcR Responses in Macrophages by Triggering Receptor Expressed on Myeloid Cells (TREM)-2 and DAP12. *J. Immunol.* 177, 2051–2055. doi: 10.4049/jimmunol.177.4.2051
- Hamerman, J. A., Tchao, N. K., Lowell, C. A., and Lanier, L. L. (2005). Enhanced Toll-like receptor responses in the absence of signaling adaptor DAP12. *Nat. Immunol.* 6, 579–586. doi: 10.1038/ni1204
- Hamilton, J. A., Cook, A. D., and Tak, P. P. (2016). Anti-colony-stimulating factor therapies for inflammatory and autoimmune diseases. *Nat. Rev. Drug Discov.* 16, 53–70. doi: 10.1038/nrd.2016.231
- Hara, M., Matsushima, T., Satoh, H., Iso-o, N., Noto, H., Togo, M., et al. (2003). Isoform-dependent cholesterol efflux from macrophages by apolipoprotein E is modulated by cell surface proteoglycans. *Arterioscler. Thromb. Vasc. Biol.* 23, 269–274. doi: 10.1161/01.ATV.0000054199.78458.4B
- Harach, T., Marungu, N., Duthilleul, N., Cheatham, V., Mc Coy, K. D., Frisoni, G., et al. (2017). Reduction of A $\beta$  amyloid pathology in APPPS1 transgenic mice in the absence of gut microbiota. *Sci. Rep.* 7:41802. doi: 10.1038/srep41802
- Heckmann, B. L., Teubner, B. J. W., Tummers, B., Boada-Romero, E., Harris, L., Yang, M., et al. (2019). LC3-Associated Endocytosis Facilitates  $\beta$ -Amyloid Clearance and Mitigates Neurodegeneration in Murine Alzheimer's Disease. *Cell* 178, 536–551.e14. doi: 10.1016/j.cell.2019.05.056
- Heneka, M. T., Kummer, M. P., Stutz, A., Delekate, A., Schwartz, S., Vieira-Saecker, A., et al. (2013). NLRP3 is activated in Alzheimer's disease and contributes to pathology in APP/PS1 mice. *Nature* 493, 674–678. doi: 10.1038/nature11729
- Heppner, F. L., Ransohoff, R. M., and Becher, B. (2015). Immune attack: the role of inflammation in Alzheimer disease. *Nat. Rev. Neurosci.* 16, 358–372. doi: 10.1038/nrn3880
- Hickman, S. E., Allison, E. K., and El Khoury, J. (2008). Microglial dysfunction and defective  $\beta$ -amyloid clearance pathways in aging alzheimer's disease mice. *J. Neurosci.* 28, 8354–8360. doi: 10.1523/JNEUROSCI.0616-08.2008
- Hollingworth, P., Harold, D., Sims, R., Gerrish, A., Lambert, J. C., Carrasquillo, M. M., et al. (2011). Common variants at ABCA7, MS4A6A/MS4A4E, EPHA1, CD33 and CD2AP are associated with Alzheimer's disease. *Nat. Genet.* 43, 429–436. doi: 10.1038/ng.803
- Howard, R., Zubko, O., Bradley, R., Harper, E., Pank, L., O'Brien, J., et al. (2020). Minocycline at 2 Different Dosages vs Placebo for Patients with Mild Alzheimer disease: a randomized clinical trial. *JAMA Neurol.* 77, 164–174. doi: 10.1001/jamaneurol.2019.3762
- Hsieh, C. L., Koike, M., Spusta, S. C., Niemi, E. C., Yenari, M., Nakamura, M. C., et al. (2009). A role for TREM2 ligands in the phagocytosis of apoptotic neuronal cells by microglia. *J. Neurochem.* 109, 1144–1156. doi: 10.1111/j.1471-4159.2009.06042.x
- Hur, J. Y., Frost, G. R., Wu, X., Crump, C., Pan, S. J., Wong, E., et al. (2020). The innate immunity protein IFITM3 modulates  $\gamma$ -secretase in Alzheimer's disease. *Nature* 586, 735–740. doi: 10.1038/s41586-020-2681-2
- Husemann, J., Loike, J. D., Kodama, T., and Silverstein, S. C. (2001). Scavenger receptor class B type I (SR-BI) mediates adhesion of neonatal murine microglia to fibrillar beta-amyloid. *J. Neuroimmunol.* 114, 142–150. doi: 10.1016/s0165-5728(01)00239-9
- Iadanza, M. G., Jackson, M. P., Hewitt, E. W., Ranson, N. A., and Radford, S. E. (2018). A new era for understanding amyloid structures and disease. *Nat. Rev. Mol. Cell Biol.* 19, 755–773. doi: 10.1038/s41580-018-0060-8
- Ide, M., Harris, M., Stevens, A., Sussams, R., Hopkins, V., Culliford, D., et al. (2016). Periodontitis and cognitive decline in Alzheimer's disease. *PLoS One* 11:e0151081. doi: 10.1371/journal.pone.0151081
- Itagaki, S., McGeer, P. L., Akiyama, H., Zhu, S., and Selkoe, D. (1989). Relationship of microglia and astrocytes to amyloid deposits of Alzheimer disease. *J. Neuroimmunol.* 24, 173–182. doi: 10.1016/0165-5728(89)90115-X
- Itzhaki, R. F., Lin, W. R., Shang, D., Wilcock, G. K., Faragher, B., and Jamieson, G. A. (1997). Herpes simplex virus type 1 in brain and risk of Alzheimer's disease. *Lancet* 349, 241–244. doi: 10.1016/s0140-6736(96)10149-5
- Jack, C. R., Petersen, R. C., Xu, Y., O'Brien, P. C., Smith, G. E., Ivnik, R. J., et al. (1998). The rate of medial temporal lobe atrophy in typical aging and Alzheimer's disease. *Neurology* 51:993–999. doi: 10.1212/wnl.51.4.993
- Jackson, M. P., and Hewitt, E. W. (2017). Why are functional amyloids non-toxic in humans? *Biomolecules* 7:71. doi: 10.3390/biom7040071



- Jansen, I. E., Savage, J. E., Watanabe, K., Bryois, J., Williams, D. M., Steinberg, S., et al. (2019). Genome-wide meta-analysis identifies new loci and functional pathways influencing Alzheimer's disease risk. *Nat. Genet.* 51, 404–413.
- Jeong, H. H., and Liu, Z. (2019). Are HHV-6A and HHV-7 Really More Abundant in Alzheimer's Disease? *Neuron* 104, 1034–1035. doi: 10.1016/j.neuron.2019.11.009
- Jiang, Q., Lee, C. Y. D., Mandrekar, S., Wilkinson, B., Cramer, P., Zelcer, N., et al. (2008). ApoE Promotes the Proteolytic Degradation of A $\beta$ . *Neuron* 58, 681–693. doi: 10.1016/j.neuron.2008.04.010
- Jiang, T., Tan, L., Zhu, X. C., Zhang, Q. Q., Cao, L., Tan, M. S., et al. (2014). Upregulation of TREM2 ameliorates neuropathology and rescues spatial cognitive impairment in a transgenic mouse model of Alzheimer's disease. *Neuropsychopharmacology* 39, 2949–2962. doi: 10.1038/npp.2014.164
- Jonsson, T., Stefansson, H., Steinberg, S., Jonsson, P. V., Snaedal, J., et al. (2013). Variant of TREM2 associated with the risk of Alzheimer's disease. *N. Engl. J. Med.* 368, 107–116. doi: 10.1056/NEJMoa1211103
- Kanemitsu, H., Tomiyama, T., and Mori, H. (2003). Human neprilysin is capable of degrading amyloid  $\beta$  peptide not only in the monomeric form but also the pathological oligomeric form. *Neurosci. Lett.* 350, 113–116. doi: 10.1016/S0304-3940(03)00898-X
- Karch, C. M., Cruchaga, C., and Goate, A. M. (2014). Alzheimer's disease genetics: from the bench to the clinic. *Neuron* 83, 11–26. doi: 10.1016/j.neuron.2014.05.041
- Karch, C. M., Jeng, A. T., Nowotny, P., Cady, J., Cruchaga, C., and Goate, A. M. (2012). Expression of novel Alzheimer's disease risk genes in control and Alzheimer's disease brains. *PLoS One* 7:e50976. doi: 10.1371/journal.pone.0050976
- Kawasaki, T., and Kawai, T. (2014). Toll-like receptor signaling pathways. *Front. Immunol.* 5:461. doi: 10.3389/fimmu.2014.00461
- Keren-Shaul, H., Spinrad, A., Weiner, A., Matcovitch-Natan, O., Dvir-Szternfeld, R., Ulland, T. K., et al. (2017). A Unique microglia type associated with restricting development of Alzheimer's disease. *Cell* 169, 1276–1290.e17. doi: 10.1016/j.cell.2017.05.018
- Kidana, K., Tatebe, T., Ito, K., Hara, N., Kakita, A., Saito, T., et al. (2018). Loss of kallikrein-related peptidase 7 exacerbates amyloid pathology in Alzheimer's disease model mice. *EMBO Mol. Med.* 10:e8184. doi: 10.15252/emmm.201708184
- Kleinberger, G., Yamanishi, Y., Suárez-Calvet, M., Czirr, E., Lohmann, E., Cuyvers, E., et al. (2014). TREM2 mutations implicated in neurodegeneration impair cell surface transport and phagocytosis. *Sci. Transl. Med.* 6:243ra86. doi: 10.1126/scitranslmed.3009093
- Knowles, T. P. J., Vendruscolo, M., and Dobson, C. M. (2014). The amyloid state and its association with protein misfolding diseases. *Nat. Rev. Mol. Cell Biol.* 15, 384–396. doi: 10.1038/nrm3810
- Koenigsnecht, J., and Landreth, G. (2004). Microglial phagocytosis of fibrillar  $\beta$ -amyloid through a  $\beta$ 1 integrin-dependent mechanism. *J. Neurosci.* 24, 9838–9846. doi: 10.1523/JNEUROSCI.2557-04.2004
- Koistinaho, M., Lin, S., Wu, X., Esterman, M., Koger, D., Hanson, J., et al. (2004). Apolipoprotein E promotes astrocyte colocalization and degradation of deposited amyloid- $\beta$  peptides. *Nat. Med.* 10, 719–726. doi: 10.1038/nm1058
- Kollmer, M., Close, W., Funk, L., Rasmussen, J., Bsoul, A., Schierhorn, A., et al. (2019). Cryo-EM structure and polymorphism of A $\beta$  amyloid fibrils purified from Alzheimer's brain tissue. *Nat. Commun.* 10:4760.
- Krabbe, G., Halle, A., Matyash, V., Rinnenthal, J. L., Eom, G. D., Bernhardt, U., et al. (2013). Functional impairment of microglia coincides with beta-amyloid deposition in mice with Alzheimer-like pathology. *PLoS One* 8:e60921. doi: 10.1371/journal.pone.0060921
- Krasemann, S., Madore, C., Cialic, R., Baufeld, C., Calcagno, N., El Fatimy, R., et al. (2017). The TREM2-APOE pathway drives the transcriptional phenotype of dysfunctional microglia in neurodegenerative diseases. *Immunity* 47, 566–581.e9. doi: 10.1016/j.immuni.2017.08.008
- Kumar, D. K. V., Choi, H. S., Washicosky, K. J., Eimer, W. A., Tucker, S., Ghofrani, J., et al. (2016). Amyloid- $\beta$  peptide protects against microbial infection in mouse and worm models of Alzheimer's disease. *Sci. Transl. Med.* 8:340ra72. doi: 10.1126/scitranslmed.aaf1059
- Lambert, J. C., Ibrahim-Verbaas, C. A., Harold, D., Naj, A. C., Sims, R., Bellenguez, C., et al. (2013). Meta-analysis of 74,046 individuals identifies 11 new susceptibility loci for Alzheimer's disease. *Nat. Genet.* 45, 1452–1458. doi: 10.1038/ng.2802
- Lee, C. Y. D., and Landreth, G. E. (2010). The role of microglia in amyloid clearance from the AD brain. *J. Neural Transm.* 117, 949–960. doi: 10.1007/s00702-010-0433-4
- Lee, C. Y. D., Tse, W., Smith, J. D., and Landreth, G. E. (2011). Apolipoprotein E promotes-amyloid trafficking and degradation by modulating microglial cholesterol levels. *J. Biol. Chem.* 287, 2032–2044. doi: 10.1074/jbc.M111.295451
- Leissring, M. A., Farris, W., Chang, A. Y., Walsh, D. M., Wu, X., Sun, X., et al. (2003). Enhanced proteolysis of  $\beta$ -amyloid in APP transgenic mice prevents plaque formation, secondary pathology, and premature death. *Neuron* 40, 1087–1093. doi: 10.1016/S0896-6273(03)00787-6
- Lessard, C. B., Malnik, S. L., Zhou, Y., Ladd, T. B., Cruz, P. E., Ran, Y., et al. (2018). High-affinity interactions and signal transduction between A $\beta$  oligomers and TREM 2. *EMBO Mol. Med.* 10:e9027. doi: 10.15252/emmm.201809027
- Liao, M.-C., and Van Nostrand, W. E. (2010). Degradation of Soluble and Fibrillar Amyloid  $\beta$ -Protein by Matrix Metalloproteinase (MT1-MMP) in Vitro†. *Biochemistry* 49:1127. doi: 10.1021/bi901994d
- Lin, Y.-T., Seo, J., Ko, T., Yankner, B. A., and Correspondence, L.-H. T. (2018). APOE4 causes widespread molecular and cellular alterations associated with Alzheimer's disease phenotypes in human iPSC-Derived brain cell types. *Neuron* 98, 1141. doi: 10.1016/j.neuron.2018.05.008
- Liu, Y., Walter, S., Stagi, M., Cherny, D., Letiembre, M., Schulz-Schaeffer, W., et al. (2005). LPS receptor (CD14): a receptor for phagocytosis of Alzheimer's amyloid peptide. *Brain* 128, 1778–1789. doi: 10.1093/brain/awh531
- Lu, A., Magupalli, V. G., Ruan, J., Yin, Q., Atianand, M. K., Vos, M. R., et al. (2014). Unified polymerization mechanism for the assembly of asc-dependent inflammasomes. *Cell* 156, 1193–1206. doi: 10.1016/j.cell.2014.02.008
- Lu, J. X., Qiang, W., Yau, W. M., Schwieters, C. D., Meredith, S. C., and Tycko, R. (2013). X-Molecular structure of  $\beta$ -amyloid fibrils in Alzheimer's disease brain tissue. *Cell* 154:10.1016/j.cell.2013.08.035. doi: 10.1016/j.cell.2013.08.035
- Mahley, R. W. (1988). Apolipoprotein E: cholesterol transport protein with expanding role in cell biology. *Science* 240, 622–630. doi: 10.1126/science.3283935
- Majumdar, A., Capetillo-Zarate, E., Cruz, D., Gouras, G. K., and Maxfield, F. R. (2011). Degradation of Alzheimer's amyloid fibrils by microglia requires delivery of ClC-7 to lysosomes. *Mol. Biol. Cell* 22, 1664–1676. doi: 10.1091/mbc.e10-09-0745
- Majumdar, A., Chung, H., Dolios, G., Wang, R., Asamoah, N., Lobel, P., et al. (2008). Degradation of fibrillar forms of Alzheimer's amyloid  $\beta$ -peptide by macrophages. *Neurobiol. Aging* 29, 707–715. doi: 10.1016/j.neurobiolaging.2006.12.001
- Mariathasan, S., Weiss, D. S., Newton, K., McBride, J., O'Rourke, K., Roose-Girma, M., et al. (2006). Cryopyrin activates the inflammasome in response to toxins and ATP. *Nature* 440, 228–232. doi: 10.1038/nature04515
- Marschallinger, J., Iram, T., Zardeneta, M., Lee, S. E., Lehallier, B., Haney, M. S., et al. (2020). Lipid-droplet-accumulating microglia represent a dysfunctional and proinflammatory state in the aging brain. *Nat. Neurosci.* 23, 194–208. doi: 10.1038/s41593-019-0566-1
- Martinon, F., Pétrilli, V., Mayor, A., Tardivel, A., and Tschopp, J. (2006). Gout-associated uric acid crystals activate the NALP3 inflammasome. *Nature* 440, 237–241. doi: 10.1038/nature04516
- Masumoto, J., Taniguchi, S., Ayukawa, K., Sarvotham, H., Kishino, T., Niikawa, N., et al. (1999). ASC, a novel 22-kDa protein, aggregates during apoptosis of human promyelocytic leukemia HL-60 cells. *J. Biol. Chem.* 274, 33835–33838. doi: 10.1074/jbc.274.48.33835
- Mawuenyega, K. G., Sigurdson, W., Ovod, V., Munsell, L., Kasten, T., Morris, J. C., et al. (2010). Decreased clearance of CNS  $\beta$ -amyloid in Alzheimer's disease. *Science* 330:1774. doi: 10.1126/science.1197623
- Meyer, P. F., Tremblay-Mercier, J., Leoutsakos, J., Madjar, C., Lafaille-Maignan, M. E., Savard, M., et al. (2019). A randomized trial of naproxen to slow progress of presymptomatic Alzheimer disease. *Neurology* 92, E2070–E2080. doi: 10.1212/WNL.0000000000007232
- Meyer-Luehmann, M., Coomaraswamy, J., Bolmont, T., Kaeser, S., Schaefer, C., Kilger, E., et al. (2006). Exogenous induction of cerebral  $\beta$ -amyloidogenesis is governed by agent and host. *Science* 313, 1781–1784. doi: 10.1126/science.1131864



- Meyer-Luehmann, M., Spires-Jones, T. L., Prada, C., Garcia-Alloza, M., De Calignon, A., Rozkalne, A., et al. (2008). Rapid appearance and local toxicity of amyloid- $\beta$  plaques in a mouse model of Alzheimer's disease. *Nature* 451, 720–724. doi: 10.1038/nature06616
- Michaud, J. P., Hallé, M., Lampron, A., Thériault, P., Préfontaine, P., Filali, M., et al. (2013). Toll-like receptor 4 stimulation with the detoxified ligand monophosphoryl lipid A improves Alzheimer's disease-related pathology. *Proc. Natl. Acad. Sci. U.S.A.* 110, 1941–1946. doi: 10.1073/pnas.1215165110
- Mittelbronn, M., Dietz, K., Schluesener, H. J., and Meyermann, R. (2001). Local distribution of microglia in the normal adult human central nervous system differs by up to one order of magnitude. *Acta Neuropathol.* 101, 249–255. doi: 10.1007/s004010000284
- Moore, K. J., El Khoury, J., Medeiros, L. A., Terada, K., Geula, C., Luster, A. D., et al. (2002). A CD36-initiated signaling cascade mediates inflammatory effects of  $\beta$ -amyloid. *J. Biol. Chem.* 277, 47373–47379. doi: 10.1074/jbc.M208788200
- Morales, R., Moreno-Gonzalez, I., and Soto, C. (2013). Cross-seeding of misfolded proteins: implications for etiology and pathogenesis of protein misfolding diseases. *PLoS Pathog.* 9:e1003537. doi: 10.1371/journal.ppat.1003537
- Moreno-Gonzalez, I., Edwards, G., Salvadores, N., Shahnawaz, M., Diaz-Espinoza, R., and Soto, C. (2017). Molecular interaction between type 2 diabetes and Alzheimer's disease through cross-seeding of protein misfolding. *Mol. Psychiatry* 22, 1327–1334. doi: 10.1038/mp.2016.230
- Mueller-Stainer, S., Zhou, Y., Arai, H., Roberson, E. D., Sun, B., Chen, J., et al. (2006). Anti-amyloidogenic and neuroprotective functions of cathepsin b: implications for Alzheimer's disease. *Neuron* 51, 703–714. doi: 10.1016/j.neuron.2006.07.027
- Nagele, R. G., D'Andrea, M. R., Lee, H., Venkataraman, V., and Wang, H. Y. (2003). Astrocytes accumulate A $\beta$ 42 and give rise to astrocytic amyloid plaques in Alzheimer disease brains. *Brain Res.* 971, 197–209. doi: 10.1016/s0006-8993(03)02361-8
- Nielsen, H. M., Mulder, S. D., Beliën, J. A. M., Musters, R. J. P., Eikelenboom, P., and Veerhuis, R. (2010). Astrocytic A $\beta$ 1-42 uptake is determined by A $\beta$ -aggregation state and the presence of amyloid-associated proteins. *Glia* 58, 1235–1246. doi: 10.1002/glia.21004
- Nilsson, P., Loganathan, K., Sekiguchi, M., Matsuba, Y., Hui, K., Tsubuki, S., et al. (2013). A $\beta$  secretion and plaque formation depend on autophagy. *Cell Rep.* 5, 61–69. doi: 10.1016/j.celrep.2013.08.042
- Nimmerjahn, A., Kirchhoff, F., and Helmchen, F. (2005). Neuroscience: resting microglial cells are highly dynamic surveillants of brain parenchyma *in vivo*. *Science* 308, 1314–1318. doi: 10.1126/science.1110647
- Ojala, J., Alafuzoff, I., Herukka, S. K., van Groen, T., Tanila, H., and Pirttilä, T. (2009). Expression of interleukin-18 is increased in the brains of Alzheimer's disease patients. *Neurobiol. Aging* 30, 198–209. doi: 10.1016/j.neurobiolaging.2007.06.006
- Ono, K., Takahashi, R., Ikeda, T., Mizuguchi, M., Hamaguchi, T., and Yamada, M. (2014). Exogenous amyloidogenic proteins function as seeds in amyloid  $\beta$ -protein aggregation. *Biochim. Biophys. Acta Mol. Basis Dis.* 1842, 646–653. doi: 10.1016/j.bbdis.2014.01.002
- Paravastu, A. K., Leapman, R. D., Yau, W. M., and Tycko, R. (2008). Molecular structural basis for polymorphism in Alzheimer's  $\beta$ -amyloid fibrils. *Proc. Natl. Acad. Sci. U.S.A.* 105, 18349–18354. doi: 10.1073/pnas.0806270105
- Paravastu, A. K., Qahwash, I., Leapman, R. D., Meredith, S. C., and Tycko, R. (2009). Seeded growth of  $\beta$ -amyloid fibrils from Alzheimer's brain-derived fibrils produces a distinct fibril structure. *Proc. Natl. Acad. Sci. U.S.A.* 106, 7443–7448. doi: 10.1073/pnas.0812033106
- Paresce, D. M., Chung, H., and Maxfield, F. R. (1997). Slow degradation of aggregates of the Alzheimer's disease amyloid  $\beta$ -protein by microglial cells. *J. Biol. Chem.* 272, 29390–29397. doi: 10.1074/jbc.272.46.29390
- Paresce, D. M., Ghosh, R. N., and Maxfield, F. R. (1996). Microglial cells internalize aggregates of the Alzheimer's disease amyloid  $\beta$ -protein via a scavenger receptor. *Neuron* 17, 553–565. doi: 10.1016/s0896-6273(00)80187-7
- Parhizkar, S., Arzberger, T., Brendel, M., Kleinberger, G., Deussing, M., Focke, C., et al. (2019). Loss of TREM2 function increases amyloid seeding but reduces plaque-associated ApoE. *Nat. Neurosci.* 22, 191–204. doi: 10.1038/s41593-018-0296-9
- Patel, N. S., Paris, D., Mathura, V., Quadros, A. N., Crawford, F. C., and Mullan, M. J. (2005). Inflammatory cytokine levels correlate with amyloid load in transgenic mouse models of Alzheimer's disease. *J. Neuroinflammation* 2:9.
- Perez-Nievas, B. G., and Serrano-Pozo, A. (2018). Deciphering the astrocyte reaction in Alzheimer's disease. *Front. Aging Neurosci.* 10:114. doi: 10.3389/fnagi.2018.00114
- Petkova, A. T., Leapman, R. D., Guo, Z., Yau, W. M., Mattson, M. P., and Tycko, R. (2005). Self-propagating, molecular-level polymorphism in Alzheimer's  $\beta$ -amyloid fibrils. *Science* 307, 262–265. doi: 10.1126/science.1105850
- Piccio, L., Buonsanti, C., Mariani, M., Cella, M., Gilfillan, S., Cross, A. H., et al. (2007). Blockade of TREM-2 exacerbates experimental autoimmune encephalomyelitis. *Eur. J. Immunol.* 37, 1290–1301. doi: 10.1002/eji.200636837
- Pihlaja, R., Koistinaho, J., Kauppinen, R., Sandholm, J., Tanila, H., and Koistinaho, M. (2011). Multiple cellular and molecular mechanisms are involved in human A $\beta$  clearance by transplanted adult astrocytes. *Glia* 59, 1643–1657. doi: 10.1002/glia.21212
- Pluvinage, J. V., Haney, M. S., Smith, B. A. H., Sun, J., Iram, T., Bonanno, L., et al. (2019). CD22 blockade restores homeostatic microglial phagocytosis in ageing brains. *Nature* 568, 187–192. doi: 10.1038/s41586-019-1088-4
- Poole, S., Singhrao, S. K., Kesavalu, L., Curtis, M. A., and Crean, S. J. (2013). Determining the presence of periodontopathic virulence factors in short-term postmortem Alzheimer's disease brain tissue. *J. Alzheimers Dis.* 36, 665–677. doi: 10.3233/JAD-121918
- Price, B. R., Sudduth, T. L., Weekman, E. M., Johnson, S., Hawthorne, D., Woolums, A., et al. (2020). Therapeutic Trem2 activation ameliorates amyloid- $\beta$  deposition and improves cognition in the 5XFAD model of amyloid deposition. *J. Neuroinflammation* 17:238.
- Qiang, W., Yau, W.-M., Lu, J.-X., Collinge, J., and Tycko, R. (2017). Structural variation in amyloid- $\beta$  fibrils from Alzheimer's disease clinical subtypes. *Nature* 541, 217–221. doi: 10.1038/nature20814
- Qiu, W. Q., Walsh, D. M., Ye, Z., Vekrellis, K., Zhang, J., Podlisny, M. B., et al. (1998). Insulin-degrading enzyme regulates extracellular levels of amyloid  $\beta$ -protein by degradation. *J. Biol. Chem.* 273, 32730–32738. doi: 10.1074/jbc.273.49.32730
- Rasmussen, J., Mahler, J., Beschoner, N., Kaeser, S. A., Häslér, L. M., Baumann, F., et al. (2017). Amyloid polymorphisms constitute distinct clouds of conformational variants in different etiological subtypes of Alzheimer's disease. *Proc. Natl. Acad. Sci. U.S.A.* 114, 13018–13023. doi: 10.1073/pnas.1713215114
- Readhead, B., Haure-Mirande, J. V., Funk, C. C., Richards, M. A., Shannon, P., Haroutunian, V., et al. (2018). Multiscale analysis of independent Alzheimer's cohorts finds disruption of molecular, genetic, and clinical networks by human herpesvirus. *Neuron* 99, 64–82. doi: 10.1016/j.neuron.2018.05.023
- Reed-Geaghan, E. G., Savage, J. C., Hise, A. G., and Landreth, G. E. (2009). CD14 and toll-like receptors 2 and 4 are required for fibrillar A $\beta$ -stimulated microglial activation. *J. Neurosci.* 29, 11982–11992. doi: 10.1523/JNEUROSCI.3158-09.2009
- Rogers, J., Strohmeier, R., Kovelowski, C. J., and Li, R. (2002). Microglia and inflammatory mechanisms in the clearance of amyloid  $\beta$  peptide. *Glia* 40, 260–269. doi: 10.1002/glia.10153
- Rubinsztein, D. C., Mariño, G., and Kroemer, G. (2011). Autophagy and aging. *Cell* 146, 682–695. doi: 10.1016/j.cell.2011.07.030
- Schlepckow, K., Monroe, K. M., Kleinberger, G., Cantuti-Castelvetri, L., Parhizkar, S., Xia, D., et al. (2020). Enhancing protective microglial activities with a dual function TREM 2 antibody to the stalk region. *EMBO Mol. Med.* 12:e11227. doi: 10.15252/emmm.201911227
- Selkoe, D. J. (1998). The cell biology  $\beta$ -amyloid precursor protein and presenilin in Alzheimer's disease. *Trends Cell Biol.* 8, 447–453. doi: 10.1016/s0962-8924(98)01363-4
- Serra-Batiste, M., Ninot-Pedrosa, M., Bayoumi, M., Gairí, M., Maglia, G., and Carulla, N. (2016). A $\beta$ 42 assembles into specific  $\beta$ -barrel pore-forming oligomers in membrane-mimicking environments. *Proc. Natl. Acad. Sci. U.S.A.* 113, 10866–10871. doi: 10.1073/pnas.1605104113
- Shankar, G. M., Li, S., Mehta, T. H., Garcia-Munoz, A., Shepardson, N. E., Smith, I., et al. (2008). Amyloid- $\beta$  protein dimers isolated directly from Alzheimer's brains impair synaptic plasticity and memory. *Nat. Med.* 14, 837–842. doi: 10.1038/nm1782
- Shropshire, T. D., Reifert, J., Rajagopalan, S., Baker, D., Feinstein, S. C., and Daugherty, P. S. (2014). Amyloid  $\beta$  peptide cleavage by kallikrein 7 attenuates fibril growth and rescues neurons from A $\beta$ -mediated toxicity *in vitro*. *Biol. Chem.* 395, 109–118. doi: 10.1515/hsz-2013-0230

- Simard, A. R., Soulet, D., Gowing, G., Julien, J. P., and Rivest, S. (2006). Bone marrow-derived microglia play a critical role in restricting senile plaque formation in Alzheimer's disease. *Neuron* 49, 489–502. doi: 10.1016/j.neuron.2006.01.022
- Solé-Domènech, S., Rojas, A. V., Maisuradze, G. G., Scheraga, H. A., Lobel, P., Maxfield, F. R., et al. (2018). Lysosomal enzyme tripeptidyl peptidase 1 destabilizes fibrillar A $\beta$  by multiple endoproteolytic cleavages within the  $\beta$ -sheet domain. *Proc. Natl. Acad. Sci. U.S.A.* 115, 1493–1498. doi: 10.1073/pnas.1719808115
- Song, M., Jin, J. J., Lim, J. E., Kou, J., Pattanayak, A., Rehman, J. A., et al. (2011). TLR4 mutation reduces microglial activation, increases A $\beta$  deposits and exacerbates cognitive deficits in a mouse model of Alzheimer's disease. *J. Neuroinflammation* 8:92. doi: 10.1186/1742-2094-8-92
- Sood, R., Domanov, Y., Pietiäinen, M., Kontinen, V. P., and Kinnunen, P. K. J. (2008). Binding of LL-37 to model biomembranes: insight into target vs host cell recognition. *Biochim. Biophys. Acta Biomembr.* 1778, 983–996. doi: 10.1016/j.bbamem.2007.11.016
- Soscia, S. J., Kirby, J. E., Washicosky, K. J., Tucker, S. M., Ingelsson, M., Hyman, B., et al. (2010). The Alzheimer's disease-associated amyloid  $\beta$ -protein is an antimicrobial peptide. *PLoS One* 5:e9505. doi: 10.1371/journal.pone.0009505
- Spangenberg, E., Severson, P. L., Hohsfield, L. A., Crapser, J., Zhang, J., Burton, E. A., et al. (2019). Sustained microglial depletion with CSF1R inhibitor impairs parenchymal plaque development in an Alzheimer's disease model. *Nat. Commun.* 10:3758. doi: 10.1038/s41467-019-11674-z
- Spitzer, P., Condic, M., Herrmann, M., Oberstein, T. J., Scharin-Mehlmann, M., Gilbert, D. F., et al. (2016). Amyloidogenic amyloid- $\beta$ -peptide variants induce microbial agglutination and exert antimicrobial activity. *Sci. Rep.* 6:32228. doi: 10.1038/srep32228
- Stewart, C. R., Stuart, L. M., Wilkinson, K., Van Gils, J. M., Deng, J., Halle, A., et al. (2010). CD36 ligands promote sterile inflammation through assembly of a Toll-like receptor 4 and 6 heterodimer. *Nat. Immunol.* 11, 155–161. doi: 10.1038/ni.1836
- Swanson, K. V., Deng, M., and Ting, J. P. Y. (2019). The NLRP3 inflammasome: molecular activation and regulation to therapeutics. *Nat. Rev. Immunol.* 19, 477–489. doi: 10.1038/s41577-019-0165-0
- Tahara, K., Kim, H.-D., Jin, J.-J., Maxwell, J. A., Li, L., and Fukuchi, K.-I. (2006). Role of toll-like receptor signalling in Ab uptake and clearance. *Brain* 129, 3006–3019. doi: 10.1093/brain/awl249
- Takahashi, K., Rochford, C. D. P., and Neumann, H. (2005). Clearance of apoptotic neurons without inflammation by microglial triggering receptor expressed on myeloid cells-2. *J. Exp. Med.* 201, 647–657. doi: 10.1084/jem.20041611
- Tamboli, I. Y., Barth, E., Christian, L., Siepmann, M., Kumar, S., Singh, S., et al. (2010). Statins promote the degradation of extracellular amyloid  $\beta$ -peptide by microglia via stimulation of exosome-associated insulin-degrading enzyme (IDE) secretion. *J. Biol. Chem.* 285, 37405–37414. doi: 10.1074/jbc.M110.149468
- Tycko, R. (2015). Amyloid polymorphism: structural basis and neurobiological relevance. *Neuron* 86, 632–645. doi: 10.1016/j.neuron.2015.03.017
- Tzeng, N. S., Chung, C. H., Lin, F. H., Chiang, C. P., Yeh, C.-B., Huang, S. Y., et al. (2018). Anti-herpetic medications and reduced risk of dementia in patients with herpes simplex virus infections—a nationwide, population-based cohort study in Taiwan. *Neurotherapeutics* 15, 417–429. doi: 10.1007/s13311-018-0611-x
- Ulrich, J. D., Finn, M. B., Wang, Y., Shen, A., Mahan, T. E., Jiang, H., et al. (2014). Altered microglial response to A $\beta$  plaques in APPPS1-21 mice heterozygous for TREM2. *Mol. Neurodegener.* 9:20. doi: 10.1186/1750-1326-9-20
- Ulrich, J. D., Ulland, T. K., Mahan, T. E., Nyström, S., Peter Nilsson, K., Song, W. M., et al. (2018). ApoE facilitates the microglial response to amyloid plaque pathology. *J. Exp. Med.* 215, 1047–1058. doi: 10.1084/jem.20171265
- Vafadari, B., Salamian, A., and Kaczmarek, L. (2016). MMP-9 in translation: from molecule to brain physiology, pathology, and therapy. *J. Neurochem.* 139, 91–114. doi: 10.1111/jnc.13415
- Venegas, C., Kumar, S., Franklin, B. S., Dierkes, T., Brinkschulte, R., Tejera, D., et al. (2017). Microglia-derived ASC specks crossseed amyloid- $\beta$  in Alzheimer's disease. *Nature* 552, 355–361. doi: 10.1038/nature25158
- Vogt, N. M., Kerby, R. L., Dill-McFarland, K. A., Harding, S. J., Merluzzi, A. P., Johnson, S. C., et al. (2017). Gut microbiome alterations in Alzheimer's disease. *Sci. Rep.* 7, 13537. doi: 10.1038/s41598-017-13601-y
- Wang, R., Sweeney, D., Gandy, S. E., and Sisodia, S. S. (1996). The profile of soluble amyloid  $\beta$  protein in cultured cell media. Detection and quantification of amyloid  $\beta$  protein and variants by immunoprecipitation-mass spectrometry. *J. Biol. Chem.* 271, 31894–31902. doi: 10.1074/jbc.271.50.31894
- Wang, Y., Ulland, T. K., Ulrich, J. D., Song, W., Tzaferis, J. A., Hole, J. T., et al. (2016). TREM2-mediated early microglial response limits diffusion and toxicity of amyloid plaques. *J. Exp. Med.* 213, 667–675. doi: 10.1084/jem.20151948
- Wilkinson, K., and El Khoury, J. (2012). Microglial scavenger receptors and their roles in the pathogenesis of Alzheimer's disease. *Int. J. Alzheimers Dis.* 2012:489456. doi: 10.1155/2012/489456
- Wozniak, M., Mee, A. P., and Itzhaki, R. F. (2009). Herpes simplex virus type 1 DNA is located within Alzheimer's disease amyloid plaques. *J. Pathol.* 217, 131–138. doi: 10.1002/path.2449
- Wozniak, M. A., Itzhaki, R. F., Shipley, S. J., and Dobson, C. B. (2007). Herpes simplex virus infection causes cellular  $\beta$ -amyloid accumulation and secretase upregulation. *Neurosci. Lett.* 429, 95–100. doi: 10.1016/j.neulet.2007.09.077
- Wyss-Coray, T., Loike, J. D., Brionne, T. C., Lu, E., Anankov, R., Yan, F., et al. (2003). Adult mouse astrocytes degrade amyloid- $\beta$  in vitro and in situ. *Nat. Med.* 9, 453–457. doi: 10.1038/nm838
- Xiang, X., Werner, G., Bohrmann, B., Liesz, A., Mazaheri, F., Capell, A., et al. (2016). TREM2 deficiency reduces the efficacy of immunotherapeutic amyloid clearance. *EMBO Mol. Med.* 8, 992–1004. doi: 10.15252/emmm.201606370
- Yan, P., Hu, X., Song, H., Yin, K., Bateman, R. J., Cirrito, J. R., et al. (2006). Matrix Metalloproteinase-9 Degrades Amyloid-Fibrils in Vitro and Compact Plaques in Situ. *J. Biol. Chem.* 281, 24566–24574. doi: 10.1074/jbc.M602440200
- Yin, K. J., Cirrito, J. R., Yan, P., Hu, X., Xiao, Q., Pan, X., et al. (2006). Matrix metalloproteinases expressed by astrocytes mediate extracellular amyloid- $\beta$  peptide catabolism. *J. Neurosci.* 26, 10939–10948. doi: 10.1523/JNEUROSCI.2085-06.2006
- Yuan, P., Condello, C., Keene, C. D., Wang, Y., Bird, T. D., Paul, S. M., et al. (2016). TREM2 haploinsufficiency in mice and humans impairs the microglia barrier function leading to decreased amyloid compaction and severe axonal dystrophy. *Neuron* 90, 724–739. doi: 10.1016/j.neuron.2016.05.003
- Zhang, B., Gaiteri, C., Bodea, L. G., Wang, Z., McElwee, J., Podtelezhnikov, A. A., et al. (2013). Integrated systems approach identifies genetic nodes and networks in late-onset Alzheimer's disease. *Cell* 153, 707–720. doi: 10.1016/j.cell.2013.03.030
- Zhao, Y., Wu, X., Li, X., Jiang, L. L., Gui, X., Liu, Y., et al. (2018). TREM2 is a receptor for  $\beta$ -Amyloid that Mediates Microglial Function. *Neuron* 97, 1023–1031.e7. doi: 10.1016/j.neuron.2018.01.031

**Conflict of Interest:** The authors declare that the research was conducted in the absence of any commercial or financial relationships that could be construed as a potential conflict of interest.

Copyright © 2020 Brown, Radford and Hewitt. This is an open-access article distributed under the terms of the Creative Commons Attribution License (CC BY). The use, distribution or reproduction in other forums is permitted, provided the original author(s) and the copyright owner(s) are credited and that the original publication in this journal is cited, in accordance with accepted academic practice. No use, distribution or reproduction is permitted which does not comply with these terms.



# MIRRAGGE – Minimum Information Required for Reproducible AGGregation Experiments

Pedro M. Martins<sup>1,2†</sup>, Susanna Navarro<sup>3†</sup>, Alexandra Silva<sup>1</sup>, Maria F. Pinto<sup>1</sup>, Zsuzsa Sárkány<sup>1</sup>, Francisco Figueiredo<sup>1,2,4</sup>, Pedro José Barbosa Pereira<sup>1</sup>, Francisca Pinheiro<sup>3</sup>, Zuzana Bednarikova<sup>5</sup>, Michał Burdukiewicz<sup>6</sup>, Oxana V. Galzitskaya<sup>7,8</sup>, Zuzana Gazova<sup>5</sup>, Cláudio M. Gomes<sup>9</sup>, Annalisa Pastore<sup>10</sup>, Louise C. Serpell<sup>11</sup>, Rostislav Skrabana<sup>12,13</sup>, Vytautas Smirnovas<sup>14</sup>, Mantas Ziaunys<sup>14</sup>, Daniel E. Otzen<sup>15</sup>, Salvador Ventura<sup>3\*</sup> and Sandra Macedo-Ribeiro<sup>1\*</sup>

<sup>1</sup> Instituto de Biologia Molecular e Celular and Instituto de Investigação e Inovação em Saúde, Universidade do Porto, Porto, Portugal, <sup>2</sup> Instituto de Ciências Biomédicas Abel Salazar, Universidade do Porto, Porto, Portugal, <sup>3</sup> Institut de Biotechnologia i Biomedicina – Departament de Bioquímica i Biologia Molecular, Universitat Autònoma de Barcelona, Bellaterra, Spain, <sup>4</sup> International Iberian Nanotechnology Laboratory – Department of Atomic Structure – Composition of Materials, Braga, Portugal, <sup>5</sup> Department of Biophysics, Institute of Experimental Physics, Slovak Academy of Sciences, Kosice, Slovakia, <sup>6</sup> Faculty of Mathematics and Information Science, Warsaw University of Technology, Warsaw, Poland, <sup>7</sup> Institute of Protein Research, Russian Academy of Sciences, Pushchino, Russia, <sup>8</sup> Institute of Theoretical and Experimental Biophysics, Russian Academy of Sciences, Pushchino, Russia, <sup>9</sup> Biosystems and Integrative Sciences Institute and Departamento de Química e Bioquímica, Faculdade de Ciências, Universidade de Lisboa, Lisbon, Portugal, <sup>10</sup> UK-DRI Centre at King's College London, the Maurice Wohl Clinical Neuroscience Institute, London, United Kingdom, <sup>11</sup> Sussex Neuroscience, School of Life Sciences, University of Sussex, Brighton, United Kingdom, <sup>12</sup> Department of Neuroimmunology, Axon Neuroscience R&D Services SE, Bratislava, Slovakia, <sup>13</sup> Institute of Neuroimmunology, Slovak Academy of Sciences, Bratislava, Slovakia, <sup>14</sup> Institute of Biotechnology, Life Sciences Center, Vilnius University, Vilnius, Lithuania, <sup>15</sup> Interdisciplinary Nanoscience Center (iNANO) and Department of Molecular Biology and Genetics, Aarhus University, Aarhus, Denmark

## OPEN ACCESS

### Edited by:

Serena Carra,  
University of Modena and Reggio  
Emilia, Italy

### Reviewed by:

Fabrizio Chiti,  
University of Florence, Italy  
Ehud Cohen,  
Hebrew University of Jerusalem, Israel

### \*Correspondence:

Salvador Ventura  
salvador.ventura@uab.cat  
Sandra Macedo-Ribeiro  
sribeiro@ibmc.up.pt

†These authors share first authorship

**Received:** 12 July 2020

**Accepted:** 23 October 2020

**Published:** 27 November 2020

### Citation:

Martins PM, Navarro S, Silva A, Pinto MF, Sárkány Z, Figueiredo F, Pereira PJB, Pinheiro F, Bednarikova Z, Burdukiewicz M, Galzitskaya OV, Gazova Z, Gomes CM, Pastore A, Serpell LC, Skrabana R, Smirnovas V, Ziaunys M, Otzen DE, Ventura S and Macedo-Ribeiro S (2020) MIRRAGGE – Minimum Information Required for Reproducible AGGregation Experiments. *Front. Mol. Neurosci.* 13:582488. doi: 10.3389/fnmol.2020.582488

Reports on phase separation and amyloid formation for multiple proteins and aggregation-prone peptides are recurrently used to explore the molecular mechanisms associated with several human diseases. The information conveyed by these reports can be used directly in translational investigation, e.g., for the design of better drug screening strategies, or be compiled in databases for benchmarking novel aggregation-predicting algorithms. Given that minute protocol variations determine different outcomes of protein aggregation assays, there is a strong urge for standardized descriptions of the different types of aggregates and the detailed methods used in their production. In an attempt to address this need, we assembled the Minimum Information Required for Reproducible Aggregation Experiments (MIRRAGGE) guidelines, considering first-principles and the established literature on protein self-assembly and aggregation. This consensus information aims to cover the major and subtle determinants of experimental reproducibility while avoiding excessive technical details that are of limited practical interest for non-specialized users. The MIRRAGGE table (template available in **Supplementary Information**) is useful as a guide for the design of new studies and as a checklist during submission of experimental reports for publication. Full disclosure of relevant information also enables other researchers to reproduce results correctly and facilitates systematic data deposition into curated databases.

**Keywords:** amyloid, reproducible data, protein, peptide, phase separation

## INTRODUCTION

Aggregation of misfolded proteins and peptides is associated with common and rare neurodegenerative disorders and with amyloidoses (Aguzzi and O'Connor, 2010; Chiti and Dobson, 2017; Benson et al., 2018). Classical neuropathological hallmarks such as neurofibrillary tangles in Alzheimer's disease (AD), Lewy bodies in Parkinson's disease (PD), or inclusion bodies in Huntington's disease, have as main constituent characteristic polypeptides aggregated in the form of insoluble highly-ordered structures named amyloid fibrils (Westermarck et al., 2007; Gremer et al., 2017). The definition of amyloid encompasses morphological (**Figure 1A**), structural (**Figure 1B**) and histological (**Figure 1C**) aspects. Amyloid polymorphs are associated with different clinical sub-types of the same disease (Guo et al., 2013; Qiang et al., 2017; Goedert et al., 2018), and they exhibit structural differences that can be characterized at atomic resolution using solid-state nuclear magnetic resonance with magic angle spinning (ss-NMR) and cryo-electron microscopy (cryo-EM) techniques (Fitzpatrick et al., 2013; Qiang et al., 2017; Rasmussen et al., 2017; Iadanza et al., 2018b). When the amyloid fold is exploited by nature for functional purposes, the structural variability is less evident than in disease-related aggregates, thus suggesting that functional amyloids are the result of naturally evolved amino acid sequences (Otzen and Riek, 2019). The analogy of a low-energy "black hole" has been used to illustrate the propensity of proteins to form amyloid fibrils after incomplete native folding or if subjected to appropriate denaturing conditions; under mildly denaturing conditions, native interactions and intrachain interactions are in competition, so that the occurrence of transiently stable, non-native conformations may trigger amyloid fibril formation (Zheng et al., 2013). However, there are other energetically stable structures into which proteins self-assemble irrespectively of, prior to, or concomitantly with the formation of amyloid fibrils (**Figure 1D**). Of these, the soluble aggregates of amyloidogenic proteins attract a particular interest justified by the cytotoxic properties attributed to amyloid- $\beta$  (A $\beta$ ) oligomers in AD (Ahmed et al., 2010; Yang et al., 2017) and  $\alpha$ -synuclein oligomers in PD (Lorenzen et al., 2014; Ingelsson, 2016). Liquid-liquid phase separation is now recognized as having a central role in cell physiology and disease (Shin and Brangwynne, 2017). For example, membraneless compartments of concentrated proteins/nucleic acids are implicated in diverse processes, including RNA metabolism, ribosome assembly, DNA repair and intracellular signaling (Banani et al., 2017). When the capacity of protein quality control by the proteasome is exceeded, misfolded proteins are sequestered into intracellular compartments such as the aggresome, a perinuclear deposit destined to autophagy (Johnston et al., 1998), or the CytoQ and INQ, which are deposition sites of misfolded proteins in the cytosol and the nucleus, respectively (Miller et al., 2015). On the other hand, a neuropathological hallmark of sporadic and inherited forms of amyotrophic lateral sclerosis and frontotemporal dementia is the deposition of poorly soluble assemblies of mutated RNA-binding proteins in the nucleus and cytoplasm of neurons (Patel et al., 2015). The pathogenic

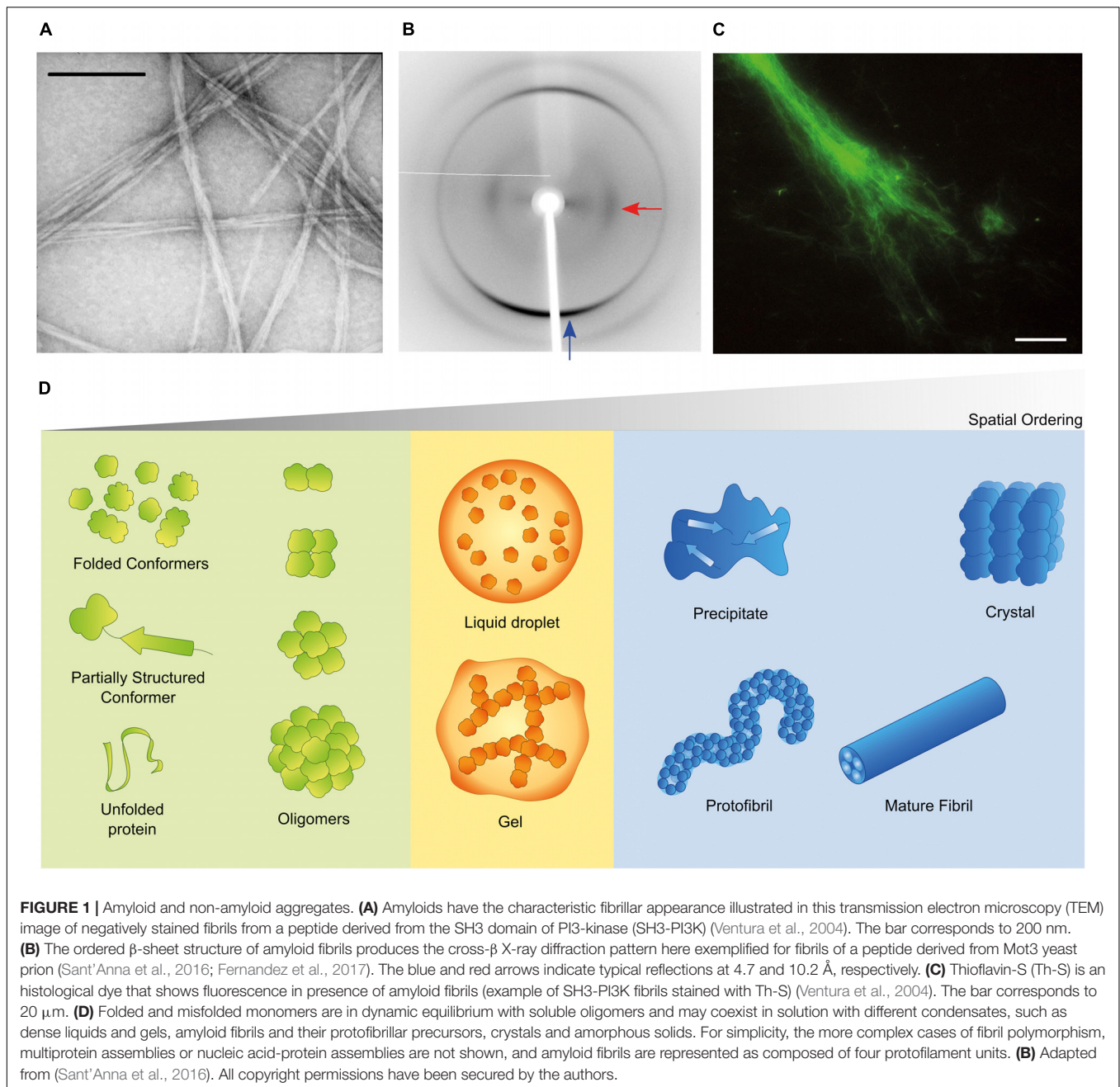
mutants are characterized by a diminished ability to reiteratively shift between dispersed and condensed phases consisting of dense liquids and gels (Murakami et al., 2015). The physical properties of the different polypeptide assemblies (summarized in **Figure 1D**) are determined by the degrees of molecular and supramolecular order. Although denser liquid phases relax more slowly in response to shear deformation, they still lack the long-range translational order characteristic of solids (Falahati and Haji-Akbari, 2019). The maximal organization provided by crystal lattices allows the structure of folded proteins to be solved using X-ray crystallography. Naturally occurring microcrystals are also used by living cells for protein storage, protection and stabilization (Schönherr et al., 2018), whereas in crystallopathies such as eosinophilic inflammation, protein crystals have been reported as promising drug targets (Persson et al., 2019).

## THERMODYNAMIC AND KINETIC OBSTACLES TO REPRODUCIBILITY

According to the phase rule of thermodynamics, the maximum number of stable phases that can coexist within a mixture is limited to  $k + 2$ , with  $k$  being the number of non-reactive components present in the mixture (Falahati and Haji-Akbari, 2019). The reduced number of accessible microstates due to demixing implies an entropic penalty of  $-T\Delta S > 0$  reflecting the disorder-to-order transition (Shin and Brangwynne, 2017; Falahati and Haji-Akbari, 2019). This entropic cost, which is higher at higher temperature ( $T$ ), can be compensated by the enthalpic contribution ( $\Delta H < 0$ ) provided that the new intermolecular interactions are sufficiently strong to decrease the Gibbs free energy  $\Delta G = \Delta H - T\Delta S$ . Whether a given protein undergoes a phase separation or not is, therefore, predictable according to the information of temperature and composition given in phase diagrams. In practice, however, differences in the protein source and sample manipulation generate aggregation states that are not readily duplicated among distinct laboratories, a problem that was highlighted in the editorial entitled "State of Aggregation" of Nature Neuroscience in April, 2011. The difficulties in reproducing protein self-assembly experiments are correlated with the occurrence of metastable states of protein folding (Sohl et al., 1998) and phase separation (Gazit, 2002; Baldwin et al., 2011) consisting of local free energy minima whose evolution toward the global minimum takes place over too long timescales to be biologically realistic. Partially unfolded states that are more stable than the native fold (Giri Rao and Gosavi, 2018) and the kinetic trapping of condensates into oligomeric (Miti et al., 2015) and gel-like states (Alberti, 2017) accentuate the need for a clear description of the initial state of the protein, its source and how it was manipulated.

The interplay between protein folding, oligomerization and metastable phase separation adds uncertainty to the dynamic distribution of the different species during test-tube experiments. How cells spatiotemporally regulate these processes is additionally determined by the occurrence of post-translational modifications (Boeynaems et al., 2018; González et al., 2019), chaperone recruitment (Mateju et al., 2017) and macromolecular





crowding (Aguzzi and Altmeyer, 2016; Rivas and Minton, 2016). For the molecular-level understanding of protein aggregation, kinetic results obtained under tightly controlled conditions and in the presence of specific dyes, such as Thioflavin-T (Th-T), Thioflavin-S (Th-S) and Congo red (CR), are analyzed using different nucleation-and-growth models (Crespo et al., 2012; Meisl et al., 2016; Chatani and Yamamoto, 2018). A combination of complementary techniques including (but not limited to) chromatography, light scattering, and advanced microscopy is required to validate complex mechanisms that may comprise the formation of intermediate phases (Ianiro et al., 2019), precursor oligomers (Pieri et al., 2016), reversible

oligomerization (Silva et al., 2017), irreversible oligomerization (Silva et al., 2018), and conformational transitions (Ruff et al., 2019), to cite but a few examples. As a stochastic process, primary nucleation is itself a source of variability in which stable clusters are formed occasionally as the result of random molecular collisions (Vekilov, 2010; Sleutel and Van Driessche, 2018). When nucleation is a rare event, the emergence of measurable amounts of protein aggregates is preceded by a lag phase whose variable duration reflects the probability distribution of a successful event (Crespo et al., 2012; Michaels et al., 2016). During amyloid fibril formation, prior addition of > 1% of preformed fibrils (or seeds) is often sufficient to eliminate the

lag phase and the intrinsic uncertainty associated to primary nucleation (Sárkány et al., 2019). Conversely, protein samples containing residual, yet variable, amounts of preformed seeds may not be suitable for “unseeded” assays due to irreproducible lag times (Crespo et al., 2012, 2016). In these cases, a final step of sample polishing immediately before the aggregation assay is recommended to eliminate vestigial assemblies formed during storage or upon thawing (Mahler et al., 2009; Silva et al., 2017; Weinbuch et al., 2018).

## AN ONTOLOGICAL APPROACH TO PROTEIN AGGREGATION

As new published data on protein aggregation and phase separation proliferate, they increase the risk that different semantics are adopted to characterize the same entities, or else, that different entities end up having the same designation. Motivated by a similar concern, the International Society of Amyloidosis has created a nomenclature committee whose periodical reports try to keep pace with the ever-increasing knowledge of amyloid disorders in humans and animals (Westermarck et al., 2007; Benson et al., 2018). Recent efforts toward a controlled vocabulary were also taken in the context of phase separation in living cells (Alberti, 2017; Shin and Brangwynne, 2017; Boeynaems et al., 2018), or while establishing guidelines to the use of Th-T in the presence of non-amyloid species (Gade Malmos et al., 2017). We now propose an ontological roadmap (Figure 2) and a systematized terminology (Table 1), considering the established nomenclature and the fundamental concepts of physical-chemical equilibrium. We depart from the definition of phase as a region in space with uniform density and composition at a given pressure and temperature (Prausnitz et al., 1998). Phase separation, therefore, refers to a change in density and/or composition that culminates in the formation of a new phase. The transition of a molecule  $i$  from phase  $A$  to the new phase  $B$  is driven by the difference in chemical potential  $\Delta\mu = \mu_i^B - \mu_i^A$  that results from the different values of mole fraction  $x_i$  and activity coefficient  $\gamma_i$  within the two phases. Recall that

$$\mu_i = \mu_i^0 + RT \ln(x_i \gamma_i) \quad (1)$$

with  $\mu_i^0$  being the standard chemical potential and  $R$  the universal gas constant. The depletion of phase  $A$  (and the concomitant enrichment of phase  $B$ ) in component  $i$  proceeds until the equilibrium condition  $\mu_i^A = \mu_i^B$  is verified, so that

$$x_i^A \gamma_i^A = x_i^B \gamma_i^B \quad (2)$$

The formation of a new phase can occur instantaneously by spinodal decomposition, or via the energy-activated process of nucleation. In the latter case, thermal and compositional fluctuations result in the generation of embryos of phase  $B$  with non-zero surface free energy in the phase boundary. The thermodynamically unstable embryos tend to disintegrate back to phase  $A$ , unless they are larger than the critical size of the primary nucleus (Vekilov, 2010; Falahati and Haji-Akbari, 2019). Once

this free energy barrier is overcome, phase transition will proceed at a faster rate if catalyzed by the secondary steps of growth (or elongation) and templated nucleation (or secondary nucleation) (Padrick and Miranker, 2002; Crespo et al., 2012; Meisl et al., 2016; Chatani and Yamamoto, 2018). Alternatively, the initially homogeneous phase  $A$  can be further destabilized by increasing  $x_i$  and/or by decreasing  $T$  to a point of spinodal decomposition where phase separation occurs by spontaneous amplification of infinitesimal phase fluctuations (Falahati and Haji-Akbari, 2019). The absence of a visible lag phase in aggregation progress curves does not necessarily mean that the critical nucleus has reached the minimum size of 1 molecule required for spinodal decomposition (Vekilov, 2010). Instead, it may happen that the presence of a nucleation barrier is concealed by (comparatively) fast elongation and secondary nucleation steps, thus originating the hyperbolic curves typical of downhill polymerization (Hurshman et al., 2004; Crespo et al., 2012).

As discussed above, the occurrence of kinetically trapped species is one of the obstacles for reproducible reporting of aggregation experiments. While corresponding to an unstable, high-energy state, the short-lived nucleation embryos are not included in the catalog of such intermediates. Primary nuclei, on the contrary, may have a fixed, well-ordered structure at the moment of their formation, or pass through local spatial ordering and structural annealing until a free energy minimum is eventually reached (Murray et al., 2017; Boeynaems et al., 2018). The sizes of primary and secondary nuclei can be estimated from the concentration dependences of kinetic parameters such as the duration of the lag phase and the limit aggregation rates (Cohen et al., 2013; Dovidchenko et al., 2014; Silva et al., 2018), but also through direct measurements using dynamic light scattering (Walters and Murphy, 2011; Silva et al., 2017) and small-angle X-ray scattering techniques (Vestergaard et al., 2007). In the hierarchy of amyloid fibril assembly, protofilaments are the primordial insoluble species and the fibrillar subunit of the  $\beta$ -sheet stacking (Teplow, 1998; Rochet and Lansbury, 2000; Khurana et al., 2003; Makin and Serpell, 2005). Protofilaments intertwine to form small and flexible protofibrils, which are classified as worm-like, rod-like or fuzzy, according to the morphological features displayed in, e.g., EM micrographs (Gosal et al., 2005; Gade Malmos et al., 2017). The elongation and intertwining of protofibrils give rise to typically straight and SDS-resistant mature fibrils with length often exceeding 1  $\mu\text{m}$  and diameter around 10–20 nm (Rochet and Lansbury, 2000; Eisenberg and Sawaya, 2017; Gade Malmos et al., 2017). Instead of mature fibrils, the end product of amyloid assembly may consist of protofibrils, as in the cases of the L55P mutant of transthyretin at physiological (instead of acidic) pH (Lashuel et al., 1999), and of ataxin-3 containing a non-expanded (fewer than ca. 30 glutamine residues) polyglutamine tract (Carvalho et al., 2018). Equally, dense liquid droplets nucleated after local enrichment of aggregation-prone proteins can either mediate new disorder-to-order transitions during crystallization and amyloid fibril formation (Vorontsova et al., 2015; Aguzzi and Altmeyer, 2016), or develop into gel-like states with reduced fluidity and protein movement (Aguzzi and Altmeyer, 2016; Banani et al., 2017; Boeynaems et al., 2018). Pathway 1 in

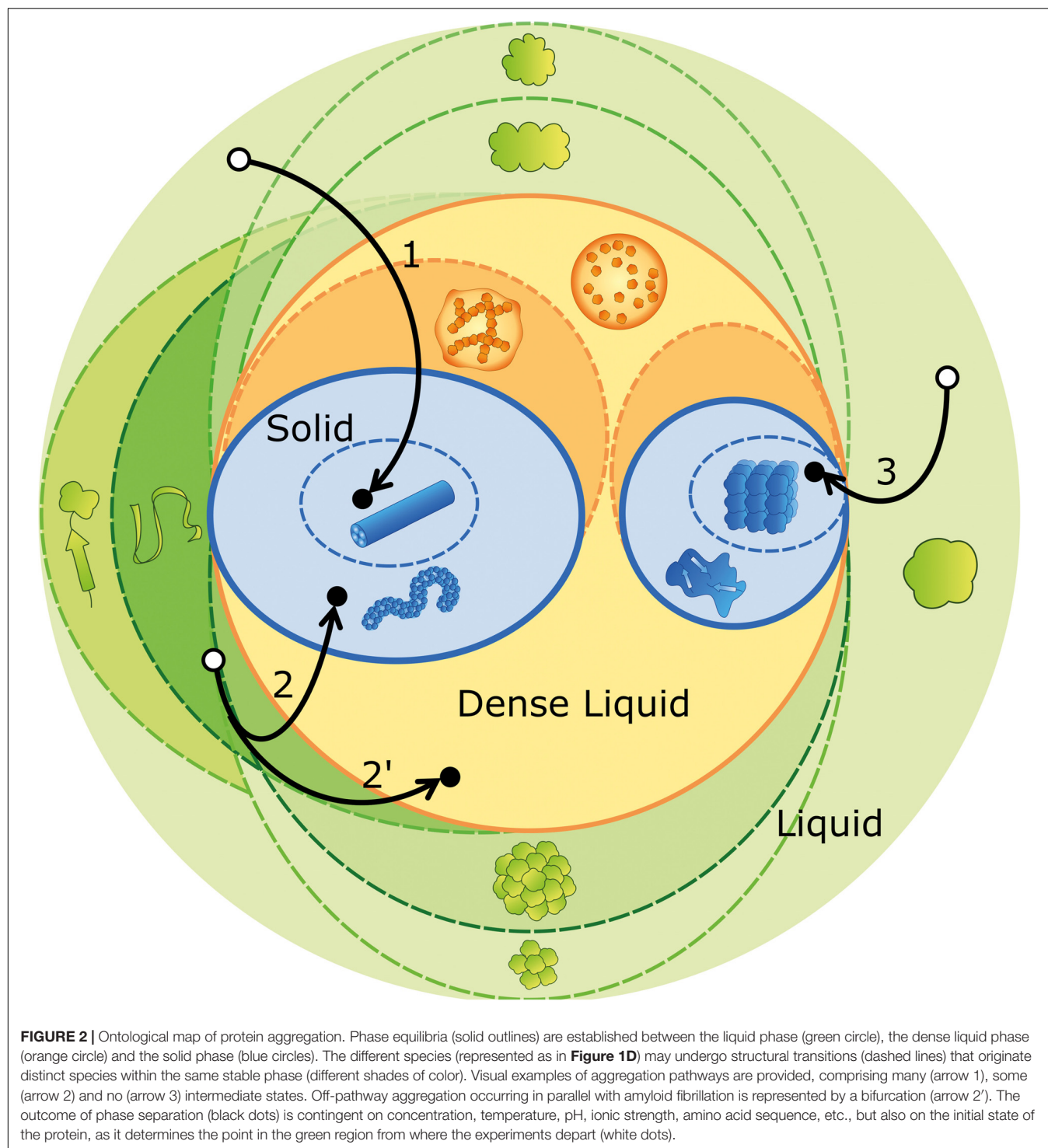


**Figure 2** illustrates the formation of mature fibrils preceded by the occurrence of several intermediate states, including liquid droplets, gels, and protofibrils. Pathways 2 and 2' show the possible coexistence of kinetically arrested states that, in this illustrative example, correspond to protofibrils and liquid droplets, respectively. Pathway 3 corresponds to the direct formation of protein crystals from globular protein.

Protein unfolding and oligomerization (represented in **Figure 2** by green dashed lines) involve the interconversion between native, partially unfolded, denatured and oligomeric states of the protein. The equilibrium composition of these structurally distinct entities results, as in phase separation, from the balance of chemical potentials; however, each state of the protein is now characterized by different values of the



**TABLE 1 |** Glossary of terms used in protein aggregation phenomena.

Amyloid fibril	Insoluble, protease resistant aggregate with characteristic (i) fibrillar electron microscopic appearance, (ii) X-ray fiber diffraction pattern and (iii) histological staining reactions, including Th-T fluorescence and green birefringence in the presence of Congo red.
Amyloidosis	Any disease associated with the formation of amyloid deposits, i.e., deposits that have amyloid fibrils as main constituent.
Condensate	The denser phase formed upon phase separation.
Embryo	A metastable cluster formed as the result of random molecular collisions; embryos will tend to disintegrate if smaller than the critical nucleus size.
Liquid demixing	Separation of a solution into two coexisting liquid phases (compare with phase separation); also known as “liquid-liquid demixing.”
Mature amyloid fibril	A long, fully stable amyloid fibril consisting of intertwined protofilament units producing a wound structure that is resistant to 2% (w/v) sodium dodecyl sulfate (SDS) treatment.
Nucleation	The stochastic process by which nuclei are formed; primary nucleation occurs in the homogeneous bulk solution; secondary nucleation occurs on the surface of an already existing aggregate; heterogeneous nucleation occurs on the surface of a foreign substance.
Nucleus	A cluster formed as the result of random molecular collisions and with the ability to elongate into a fibril (compare with embryo).
Off-pathway oligomer	Stable oligomer that coexists with amyloid fibrils but is not an amyloid precursor; off-pathway oligomerization and amyloid fibrillation are competitive processes.
Oligomer	Multimeric species lacking the morphology and properties of amyloid fibrils.
On-pathway oligomer	A precursor of amyloid fibrils; the addition of pre-formed on-pathway oligomers accelerates the formation of amyloid fibrils without affecting the total amyloid conversion.
Phase separation	The formation of a new region with uniform density and composition; it can occur instantaneously by spinodal decomposition, or via the energy-activated process of nucleation.
Protofibril	Beaded chain with ~5 nm diameter and <150 nm length that matures into amyloid fibrils.
Protofilament	Subunit of amyloid fibrils; smaller protofilaments with ~1 nm diameter entwine to form larger protofilament units with 2.5–3.5 nm diameter.
Seed	Preformed amyloid particle able to accelerate the assembly of amyloid fibrils.

standard chemical potential  $\mu_i^0$  (Eq. 1) (Tanford, 1970). Although occurring within the same liquid phase, structural transitions might trigger subsequent phase separations as in the general case of protein misfolding diseases in which pathologic protein aggregation arises from the failure of a specific protein or peptide to adopt its native conformation (Chiti and Dobson, 2006). Also, insulin amyloid fibril formation is preceded by the aggregation of a precursor helical oligomer that later becomes the repeating unit of mature fibrils (Vestergaard et al., 2007), whereas several of the key proteins present in membraneless organelles have oligomerization domains that drive liquid demixing through multiplicative sticky interactions (Boeynaems et al., 2018). In a different example, amyloid fibrillation of non-expanded ataxin-3 decreases the concentration of soluble monomers, thus causing the dissociation of off-pathway oligomers to monomeric species (Silva et al., 2017). Because the different states of protein aggregation are in dynamic equilibrium, a possible rescue mechanism includes the sequestration of harmful species into less toxic aggregates or in phase separated compartments of the cell (Gosal et al., 2005; Haass and Selkoe, 2007; Boeynaems et al., 2018). Illustrating this protection mechanism, amyloid plaques isolated from AD cortex do not elicit toxic effects in rodent hippocampus unless they are solubilized to release toxic A $\beta$  dimers (Shankar et al., 2008).

Systematizing protein folding intermediates and oligomeric species into organized categories is a challenging task due to the heterogeneity and elusive nature of both populations. Moreover, many proteins naturally occur as an ensemble of more than one polypeptide chain folded into a characteristic oligomeric conformation (Doyle et al., 2013), while others, known as intrinsically disordered proteins, can sample a continuum of conformations (Jarosz and Khurana, 2017; Darling et al., 2018).

Folding intermediates have been detected for a limited number of proteins by measuring the exchange rates of hydrogen atoms between the main-chain amides and water (Englander et al., 2016), or by combining  $^1\text{H}$  liquid-state NMR and multivariate analysis (Malmendal et al., 2010). **Figure 2** necessarily simplifies the folding landscape that is associated with pathogenic protein aggregation as different protein-protein interactions are required to maintain proteostasis in living cells. For example, the correct folding of prion protein (PrP) is assured by chaperones of the endoplasmic reticulum such as calnexin (Wang et al., 2010) and the proline cis/trans isomerase cyclophilin B (Ben-Gedalya et al., 2015). Conformational variations between the normal (PrP<sup>C</sup>) and the infectious (PrP<sup>SC</sup>) isoforms are responsible for the recruitment of PrP<sup>C</sup> by PrP<sup>SC</sup> during amyloid polymerization (Prusiner, 2001). The self-templating properties of PrP<sup>SC</sup> are the basis for ultrasensitive tests for prion infections in biological fluids and tissues (Saborio et al., 2001; Orru et al., 2012). Likewise, the amplification of seeding-competent aggregates of A $\beta$  peptide (Salvadores et al., 2014),  $\alpha$ -synuclein (Fairfoul et al., 2016) and tau (Saijo et al., 2017) is a promising technological principle for the diagnosis of AD, PD, and tauopathies, respectively (Soto and Pritzkow, 2018). Amyloid seeding capacity can be used to evaluate whether a given intermediate is on-pathway or off-pathway to form amyloid fibrils. The maximal seeding potency is achieved upon the addition of pre-formed, sonicated fibrils. Conversely, off-pathway oligomers (Farmer et al., 2017; Hasecke et al., 2018), fibril polymorphs (Kodali and Wetzel, 2007; Falcon et al., 2015; Cao et al., 2019), and seeds pre-treated with aggregation inhibitors (Arimon et al., 2008; Oskarsson et al., 2018; Saelices et al., 2018) are expected to have lower seeding potencies. Amyloid fibrils produced from distinct proteins can be tested for conformational



complementarity in cross-seeding experiments, also known as heterologous or heterogeneous seeding (Harper and Peterand Lansbury, 1997; O’Nuallain et al., 2004; Soto and Pritzkow, 2018).

## METHODS TO EXPERIMENTALLY EVALUATE GENERAL AGGREGATION AND AMYLOID FORMATION

Significant experimental evidence must be gathered by complementary biophysical methods to determine if a protein or peptide does aggregate and if it is specifically able to form amyloid assemblies. Several computational approaches have been developed to predict aggregation-prone regions in (poly)peptide sequences (Belli et al., 2011; Pallarès and Ventura, 2019), but often experimental validation of aggregation propensity represents a considerable bottleneck (Grishin et al., 2020). Protein self-assembly is a complex process that might result in the formation of amorphous aggregates, different oligomers or amyloid fibrils, heterogeneous species that often coexist during the aggregation process. In this section, the methodological approaches required to identify general protein aggregation (see section “Monitoring the Presence of Protein Aggregates”) and to distinguish amyloid fibril formation specifically (see sections “Methods to Monitor the Conformational Properties of Amyloid Aggregates,” “Morphology of Amyloid Fibrils,” and “Fluorescence Techniques and Tinctorial Properties of Amyloids”) are summarized. In particular, we focus on the study of amyloid fibril formation, which can be addressed from the structural (see section “Morphology of Amyloid Fibrils”) and the kinetic point of view (see section “Fluorescence Techniques and Tinctorial Properties of Amyloids”). A minimum set of experiments is suggested to satisfy the criteria that generally define amyloid aggregates according to their conformational, morphological and tinctorial properties.

### Monitoring the Presence of Protein Aggregates

The formation of protein aggregates can be detected by a collection of orthogonal methods that report on different properties of these macromolecular assemblies.

#### Light Scattering and Turbidimetry

The aggregated states of proteins or peptides scatter the light passing through the aggregate solution proportionally to the size of aggregated particles. Therefore, the course of aggregation can be monitored by the measurement of an attenuation of incident light beam (turbidimetry) or by integration of an angle-specific scattering [static light scattering, SLS (Zhao et al., 2016)]. Turbidimetry is often taken as a linear descriptor of the kinetics of aggregation reactions; however, caution should be taken when comparing different proteins or conditions, since light is scattered as a function of both aggregate size and shape. SLS is able to determine the relative size of an aggregate by measuring the time-averaged intensity of scattered light, usually employing the same wavelength for excitation and detection at an

angle of 90°. It reports on the molar mass (weight-average) and concentration of the aggregate.

#### Dynamic Light Scattering

Dynamic light scattering (DLS), also known as photon correlation spectroscopy or quasi-elastic light scattering, is a spectroscopy technique that measures the fluctuation of intensity of scattered light with time and is routinely applied to detect protein aggregates, as well as other nanoparticles (Zaccai et al., 2017).

Dynamic light scattering allows to derive two basic characteristics from a protein population. First, the mean hydrodynamic size, assuming a spherical geometry of the particle, and second, the polydispersity index of the solution. DLS is highly sensitive to the presence of aggregates because light scattering intensity scales with the second power of the mass of the light scattering particle. Therefore, low amounts of protein aggregates can be detected when the hydrodynamic radii are large enough. When the sample contains both monomeric and aggregated species, the monomer can only be adequately detected when the polydispersity index is low and the protein concentration is high. In this case, the particle size distribution plot shows multiple peaks indicative of a multimodal distribution.

#### Size Exclusion Chromatography

Size-exclusion chromatography (SEC) offers the possibility to identify, collect and determine the relative molecular weight of the different assemblies in an aggregated sample (Striegel et al., 2009; Burgess, 2018). Extra care must be exerted when dealing with labile oligomers. These can be potentially disrupted during the fractionation process, shifting the equilibrium between species as a function of the protein concentration. Moreover, large insoluble aggregates should be filtered out before analysis to prevent column clogging.

Size-exclusion chromatography becomes a versatile technique when coupled to multiangle light scattering (MALS) and differential refractive index (dRI) detectors, which allow to determine protein concentration, molecular weight (MW), size and conformation (Folta-Stogniew, 2006). The SEC-MALS instrument is calibrated independently of the column and does not depend on commercial reference standards, becoming the default method for the estimation of native MW on heterogeneous samples (Sahin and Roberts, 2012).

#### Intrinsic Fluorescence Spectroscopy

The sensitivity of the intrinsic fluorescence signal of tyrosine and tryptophan residues to their local environment has been extensively used to study protein conformation by fluorescence spectroscopy. A steady-state fluorescence spectrum is obtained by recording the emission fluorescence intensity of a sample excited at a fixed wavelength. In proteins, tryptophan fluorescence is owed to the side-chain indole group, displaying an absorption maximum at 280 nm and a fluorescence peak that is solvatochromic, ranging from 300 to 350 nm. Depending on the polarity of the local environment, the fluorescence emission maximum ranges from ~308 nm for a tryptophan

fully embedded in a hydrophobic pocket to  $\sim 348\text{--}352\text{ nm}$  for a tryptophan fully exposed to solvent (Ghisaidoobe and Chung, 2014). Thus, the fluorescence of tryptophan in monomeric and aggregated states of proteins is significantly different (Bobone and van de Weert, 2014). The fluorescence of tyrosine is due to its side-chain phenolic ring, with excitation and emission maxima at 260 nm and 305 nm, respectively. When compared to tryptophan, the fluorescence signal of tyrosine is less sensitive to environmental changes, as a consequence of the lack of dipole reorientation in the excited phenol. Still, since tyrosine is on average three times more abundant than tryptophan in polypeptides, its signal also differs significantly between the aggregated and soluble states of proteins.

## Methods to Monitor the Conformational Properties of Amyloid Aggregates

Although the nature and self-assembly mechanisms of protein amyloids differ, most of them share a final fibrillar morphology highly enriched in intermolecular cross- $\beta$  structure, whose presence can be confirmed by different biophysical methods.

### Circular Dichroism Spectroscopy

Circular dichroism (CD) relies on the differential absorption of left and right circularly polarized light. Optically active chiral molecules and chemical groups absorb preferentially in one direction of the light. Thus, peptide bonds, aromatic amino acid side chains and disulfide bonds in proteins act as conformation reporters, providing information about the secondary structure composition ( $\alpha$ -helix,  $\beta$ -sheet, disorder). In the far UV region of the spectrum (190–260 nm) a maximum at 196 nm and a single minimum at 218 nm is attributed to a  $\beta$ -sheet conformation; meanwhile, a maximum at 192 nm and two minima at 208 nm and 222 nm are indicative of  $\alpha$ -helical content, whereas a minimum at 198 nm correlates with the presence of disordered regions (Cristovao et al., 2019). The shift from an initial native conformation to an amyloid  $\beta$ -sheet structure often exacerbates the minimum at 218 nm (Kelly et al., 2005; Vadukul et al., 2019). The presence of additional molecules in the sample, such as reducing agents, organic molecules and excipients, should be taken into account since they might interfere with the measurement, precluding detection of the expected transition.

The far UV spectra of aggregated samples are usually complex and require the use of deconvolution algorithms (SELCON, VARSLC, CDSSTR, K2d2, K2d3, BeStSel, DICHROWEB server) (Provencher and Glockner, 1981; Manavalan and Johnson Jr., 1987; Andrade et al., 1993; Sreerama and Woody, 2000; Whitmore and Wallace, 2004; Micsonai et al., 2015) to quantify the contribution of the different secondary structure elements to the signal. However, care should be taken with these estimates, even in the analysis of the variation of secondary structure content, which should be favored over absolute determinations. The presence of aggregates often leads to distortions in the CD spectra (differential absorption flattening) that might lead to errors in the estimation of secondary structure content, as most algorithms are optimized for soluble proteins. Of note, one

algorithm – BeStSel – is especially suited for secondary structure determination of proteins with high  $\beta$ -sheet content, such as those found in amyloid protein aggregates (Micsonai et al., 2015).

The CD spectrum in the near UV region (260–320 nm) arises from the contribution from aromatic amino acids and provides information on the tertiary structure, complementary to that gathered from intrinsic fluorescence measurements.

### Fourier-Transform Infrared Spectroscopy

Fourier transform infrared (FTIR) spectroscopy is especially suitable to determine the existence of  $\beta$ -sheet secondary structures in aggregated samples. The presence of a band at  $1620\text{--}1640\text{ cm}^{-1}$  in the amide I region of the infrared spectrum is a signature of  $\beta$ -strands. Intramolecular (native  $\beta$ -sheet) signals fall typically in the  $1630\text{--}1640\text{ cm}^{-1}$  range, whereas the intermolecular  $\beta$ -sheets characteristic of aggregates usually peak at  $1620\text{--}1630\text{ cm}^{-1}$  or even lower wavenumbers (Hiramatsu and Kitagawa, 2005).

The FTIR spectrum is particularly sensitive to the presence of additives in the sample, such as TFA, DMSO and reducing agents; therefore, the signal of the buffer should be subtracted from that of the sample. Because the vibration signal of water maps in the amide I region ( $1630\text{ cm}^{-1}$ ), the FTIR spectrum must be obtained by drying out the sample to an hydrated protein film when using Attenuated Total Reflection sampling devices or by exchanging  $\text{H}_2\text{O}$  with  $\text{D}_2\text{O}$  for transmission experiments when using DTGS (deuterated triglycine sulfate) and MCT (mercuric cadmium telluride) detectors (Cristovao et al., 2019).

The peaks in the FTIR spectrum are identified by curve fitting using Fourier self-deconvolution, or/and by analysis of the inflection points in the second derivative of the spectrum curve. Fitting of the FTIR spectrum does not provide a unique solution and thus the fitting parameters become critical: a minimum number of peaks should be used, the maxima of the curve-fitted peaks should correspond to the evident maxima in the raw data, and, generally, curve-fitted peaks should present similar full-width and half-height values. This technique can be used to study and compare protein aggregates obtained *in vivo* and *in vitro* (Shivu et al., 2013). Traditional FTIR analysis only reports on bulk composition and even FTIR microspectrometers, despite their extensive applications [e.g., in cell biology (Bouyanfif et al., 2018)], only provide resolution down to  $2\text{--}5\text{ }\mu\text{m}$ , which is insufficient for the analysis of individual fibrils. However, by combining IR with atomic force microscopy in Infrared Nanospectroscopy it is possible to acquire both morphological, nanomechanical and nanoscale-level (10–20 nm) chemical IR absorption spectra and maps from protein aggregates, single cells and liquid-liquid phase condensates (Ruggeri et al., 2020). This approach is particularly useful in analyzing complex mixtures with co-existing amyloid, amorphous aggregates and pre-fibrillar aggregates with different secondary structure (Ruggeri et al., 2015, 2016; Galante et al., 2016; Waeytens et al., 2020).

### Proteinase K and Mixture of Proteases Digestion

Complementary to the techniques mentioned above, the relative resistance of amyloid fibrils to proteinase K digestion is

commonly used for their characterization, especially in the case of prionic proteins. Proteinase K is a serine protease that cleaves peptide bonds on the carboxy-terminal side of aromatic and aliphatic amino acids. Despite the high processivity of proteinase K in disordered and regular secondary structures, its proteolytic activity is rather limited in cross- $\beta$ -sheet structures, which are characteristic of amyloid fibrils (Kushnirov et al., 2020). The identification of proteinase K-resistant amyloid cores can be achieved by two main approaches: adding different proteinase K concentrations at the end-times of aggregation reactions or following the time-course of the digestion at a given proteinase K concentration. The results of the digestion experiments can be monitored with several techniques, such as SDS-PAGE and protein immunoblotting, mass spectrometry, or electron microscopy. In some cases, a mixture of proteases can be used instead of proteinase K to identify the core of amyloid fibrils (Selivanova et al., 2016; Surin et al., 2020).

### X-Ray Diffraction and Scattering Techniques

X-ray diffraction and small-angle scattering techniques, including small-angle X-ray scattering (SAXS) and small-angle neutron scattering (SANS) are considered gold standard techniques for the analysis of the structural properties of amyloid fibrils.

The X-ray fiber diffraction pattern of partially aligned amyloid fibrils displays a characteristic arrangement with a meridional reflection (vertical axis) at 4.7–4.8 Å and an equatorial reflection (horizontal axis) at 10–12 Å (**Figure 1B**), which report on the distances between  $\beta$ -strands that are associated via hydrogen-bonding perpendicular to the fibril axis and between the adjacent  $\beta$ -sheets running parallel to the axis, respectively. The meridional signal is generally very sharp and intense due to the repeating nature of the  $\beta$ -strands along the fiber axis. The equatorial signal is generally weaker and more diffuse and its position can vary depending on the amino acid composition of a constituent peptide (e.g., large aromatic side chains will result in a larger sheet spacing). This is the reason why the common amyloid fold is known as cross- $\beta$  (Morris and Serpell, 2012). Low angle signals are often also observed, which arise from chain length and/or protofilament packing.

Small-angle scattering techniques are one of the best-suited biophysical approaches to study the conformational properties of the different oligomeric forms appearing along an amyloidogenic process and how they evolve into mature fibrils. In theory, one can decompose the time-resolved SAXS and SANS data into the scattering intensity profiles of the individual forms (structural information), along with their relative populations (kinetic information), without the need to isolate the transient or co-existing species (Langkilde et al., 2015). Nonetheless, the use of this technique is limited to specific cases because it requires highly concentrated and stable samples, containing only a few oligomeric species simultaneously.

### Sedimentation Techniques: Separation and Size Distribution

While complex mixtures of aggregated protein can be imaged by a variety of different techniques (see section “Morphology

of Amyloid Fibrils”), separation of insoluble species is not straightforward. An increase in particle mass during protein aggregation can be exploited for detection, isolation and characterization of both high-molecular weight intermediates and final filaments. Several ultracentrifugation protocols have been adopted for analyzing protein aggregates in cellular and animal models of various human proteinopathies including prion protein amyloidosis (Vey et al., 1996), a familial tauopathy (Berger et al., 2007) or sporadic AD (Skrabana et al., 2017). The ability to differentially isolate protein conformers with distinct physical properties by sedimentation at high speed can be used also in *in vitro* experiments of protein aggregation. Insoluble fibrils and larger aggregates pellet quickly around 14,000–16,000  $\times g$  in aqueous buffers, but smaller species such as oligomers or shorter fibril fragments sediment more slowly even under high-speed centrifugation above 50,000  $\times g$  (Mok and Howlett, 2006). It is sometimes possible to separate different fibrils based on their morphology. Straight fibrils of human apolipoprotein ApoC-II, which dominate in the presence of phospholipid micelles, sediment more rapidly than flexible ribbons formed in the absence of lipids, making it possible to pellet the two populations at 14,500  $\times g$  and 350,000  $\times g$ , respectively (Mok et al., 2015). Similar approaches have separated linear versus closed-loop fibrils of ApoC-II (Yang et al., 2012), while complex mixtures of huntingtin aggregates have more simply been fractionated by pelleting a mixture of inclusions, soluble but large oligomers and cell debris from lysed cells (14,000  $\times g$  for 10 min) followed by centrifugation of the resuspended pellet through a desalting column, which allows separating the soluble oligomers from the insoluble material (Ormsby et al., 2013). Just as importantly, if the relationship between the molecular weight of fibrillar species and their diffusion coefficient is known (MacRaild et al., 2003), it is possible to estimate the size distribution of fibrils using sedimentation velocity analysis (Yang et al., 2012), which measures how quickly fibrils move through a centrifugal field. It is even possible to selectively monitor fibril sizes in the presence of non-fibrillar components (e.g., chaperones) using fluorescence detection and fluorophore-labeled fibrils; this allows to assess changes in the size distribution and lateral association of a given protein (Binger et al., 2013). As an alternative approach, OptiPrep gradients have been used to isolate and characterize protein aggregates associating with membrane-like domains (Vey et al., 1996).

### Morphology of Amyloid Fibrils

Once the  $\beta$ -sheet content has been confirmed by the methods above, the morphology of the amyloid fibrils should be examined by imaging techniques.

### Transmission Electron Microscopy

The visualization of transmission electron microscope (TEM) images at high resolution provides information on the morphology, homogeneity and size of the amyloid fibrils. In order to obtain high-quality TEM data, samples deposited on carbon-coated copper grids should be negatively stained with a heavy metal solution [typically 2% (w/v) uranyl acetate solution in water] to increase contrast. It should, however, be taken into



account that TEM images may display structural artifacts due to dehydration and staining during the sample preparation process (Gras et al., 2011).

### Atomic Force Microscopy

Atomic force microscopy (AFM) allows direct visualization of amyloid fibrils in aqueous solutions, providing information about their structural and mechanical properties under physiological-like conditions (Ruggeri et al., 2019). AFM images have nanometer-resolution, allowing to assess the fibril contour length, width, height and periodicity or the high-order assembly of single protofilaments into mature fibrils (Adamcik et al., 2012). These properties can be measured at final time-points or directly during the assembly reaction. Besides, it is possible to define the packing scheme and polymorphic state of the amyloid fibrils (e.g., twisted, helical ribbon) by measuring the height profile of fibrils along their contour length and the shape of height profile. An advantage of AFM, when compared to TEM, is that it allows measuring forces and elastic properties of amyloid assemblies with piconewton resolution.

Several additional methods, such as solid-state NMR and cryo-EM, provide valuable information about the morphology and structural features of amyloid fibrils at high resolution. These methods and their applications to uncover the atomic structures of amyloid fibrils have been extensively covered in recent reviews (Iadanza et al., 2018a; Fitzpatrick and Saibil, 2019). Although key to explore correlations between structure and toxicity, they need advanced equipment and go beyond a *minimum requirement* for determining that a polypeptide assembles into amyloid fibrils.

### Fluorescence Techniques and Tinctorial Properties of Amyloids

It is well established that regular fibrillar structures have the ability to bind small molecules at their surfaces and cavities with a concomitant alteration of the optical properties of the binding compounds. Th-T and CR are two of these molecules, and have been extensively used for the detection of amyloid structure in fibrils and deposits.

#### Thioflavines

The Th-T assay measures the increase in emission fluorescence signal of Th-T as amyloid fibrils grow. The enhanced fluorescence can be detected by spectroscopy or visualized by epifluorescence or confocal microscopy. In all techniques, the molecule is excited at 445 nm and emission fluorescence is recorded in the 470–500 nm range, usually with a maximum around 482 nm (Biancalana and Koide, 2010).

Th-T fluorescence enhancement is not a quantitative parameter since it is strongly dependent on the fibril morphology. In some cases, amyloid fibrils may be present, but do not display fluorescence because the rotation movement of the Th-T molecule is not sufficiently impeded. On these occasions, Th-T fluorescence anisotropy provides an alternative technique for the study of amyloid aggregation (Sabate and Saupe, 2007). Also, the maximum excitation and emission wavelengths may

change slightly depending on each particular amyloid structure (Sabate et al., 2013).

Th-S is a mixture of compounds that results from the methylation of dehydrothiitoluidine with sulfonic acid. As such, its molar concentration cannot be accurately calculated, which in addition to its high fluorescence background make this dye sub-optimal for spectroscopic measurements *in vitro* (Espargaro et al., 2012). However, Th-S presents the advantage of being able to permeate through cell membranes, thus allowing to detect intracellular amyloid aggregates, even in living cells. Accordingly, it has been vastly used in the histological staining of amyloids and to image purified amyloid material (Figure 1C).

#### Congo Red

The CR dye has been broadly used to detect amyloid aggregates in tissues and *in vitro*. The absorption spectra of CR alone and in the presence of amyloids are recorded in the visible region of the light spectrum (300–700 nm) and compared (Yakupova et al., 2019). The binding of CR to amyloids induces a spectral red shift, with maximum absorbance change occurring around 540 nm. As in the case of Th-T assays, the CR spectrophotometric assay is not quantitative.

Birefringence originates from the decomposition of a ray of light into two rays when it passes through certain anisotropic materials, such as crystals. The fixation of CR molecules along the axis of the amyloid fibrils usually causes apple-green birefringence when viewed through cross-polarized light, providing an assessment of the amyloid nature of protein aggregates complementary to CR absorbance measurements.

#### Other Amyloid-Staining Molecules

The use of Th-T and CR for amyloid detection has limitations. Many non-amyloid molecules can also exhibit birefringence under cross-polarized light in the presence of CR, such as phosphate salts, urea, and other types of fibers like hair. Moreover, CR is a pH indicator and, accordingly, its absorbance spectrum is strongly dependent on the solution pH, being useless under acidic conditions. The absorption and emission spectra of some molecules, such as flavins and reduced NAD(P)H overlap with that of Th-T. Also, some polyphenolic anti-aggregational compounds, such as curcumin or epigallocatechin, exhibit fluorescent properties similar to those of Th-T (Hudson et al., 2009). In a similar way, the auto-fluorescence generated by some aldehyde compounds used as tissue fixatives significantly interferes with the histological detection of amyloids using this dye. In light of these problems (Viegas et al., 2007), novel fluorescent dyes with improved sensitivity and specificity properties have been developed.

As Th-T, the ProteoStat dye is a rotor molecule that intercalates into the cross- $\beta$  structure, leading to a strong red fluorescence with excitation and emission maxima at 500 nm and 600 nm, respectively (Shen et al., 2011; Navarro and Ventura, 2014). Compared to Th-T, ProteoStat staining produces a stronger fluorescent signal with a wider linear dynamic range in a broad range of pH values (4–10) and avoids spectral



**TABLE 2 |** Experimental details that should be reported for protein aggregation assays.

Reported parameter		Information that should be reported
Sample stock	Sample source and storage conditions	Description of protein source – commercial (supplier and reference), recombinant (including expression and purification), or other (e.g., extracted from tissue); description of how the protein or peptide stock was preserved (lyophilized or stored in solution); if stored in solution indicate storage buffer, sample concentration, storage temperature, freezing/thawing conditions, as well as material and supplier of vials used for sample storage.
	Sample purity and concentration	Indicate the methods (SDS-PAGE, HPLC, etc.) used to determine sample purity, as well as those used to determine the exact concentration of the stock sample in the assay. The purity of the sample stock as evaluated by SDS-PAGE should be indicated and higher than 95%. Indicate whether the sample was tested for the presence of “invisible” components such as nucleic acids.
	Sample concentration	Indicate the final concentration of the sample in the assay.
	Sample preparation prior to assay	Mention if the protein/peptide stocks were pre-treated, filtered or centrifuged; these procedures are recommended to remove pre-aggregated forms.
	Assay buffer	Indicate the composition, concentrations and pH value of the buffer or solvent stock.
	Assay volume	The final volume of the sample, as well as the volume of the tube/well in which the aggregation assay is performed should be reported since interfaces (liquid-solid and liquid-air) influence protein aggregation. The method used to prevent sample evaporation should also be mentioned when using small sample volumes.
Experimental procedures, type of equipment used and system-dependent parameters	Additives	List ALL components that could be found in the aggregation assay (even those that may exist in minute amounts). For example, if an aggregation modulator is dissolved in DMSO, it is important that all samples (including control) contain the same final concentration of DMSO.
	Plate or vial	Report the type of material and geometry of the vial or microplate well (binding versus non-binding surface, bottom versus top-reading, square versus round bottom, etc.) used in the assay. Include information on the microplate/vial material, including supplier and reference code.
	Temperature	Report the assay temperature. In particular, mention if samples/buffer are preincubated at the assay temperature: fluorescence drifts may be observed at the beginning of the experiment resulting from temperature shifts.
	Agitation	Indicate whether an orbital shaker, a thermomixer or magnetic stirring was used (describing shape, size and material of stirrers), the type of shaking (orbital, linear, etc.) and speed. If applicable, indicate if beads were included (material, size, number of beads). Measurement cycles and the pre-shaking agitation procedures should be clearly specified.
	Time	The total duration of the aggregation reaction should be reported.
	Equipment for measuring aggregation kinetics and its settings	Indicate the device make and model, control software, and general settings used (e.g., filter bandpass and bandwidth/monochromator settings).
	Reporters	Provide the exact amount of reporter (if used) employed for measurement and any pre-treatment of the sample.
	Data analysis and raw data that should be preserved for publication	Indicate the software (including version) used for image and data analysis and specify the equation applied for fitting kinetic data obtained from aggregation assays.

overlap with the autofluorescence signal of membranes and co-factors. ProteoStat is particularly indicated if working in the presence of RNA, when the use of Th-T is unsuited, because it produces huge distortions of the baseline (Sugimoto et al., 2015; Liu et al., 2017).

Heptamer-formyl thiophene acetic acid (hFTAA) is yet another amyloid detection dye. hFTAA exhibits distinct shifts in its emission spectra when bound to different amyloid species and polymorphs, finding application in the differentiation of amyloid (sub)types *in vivo* and in monitoring changes of amyloid structure and composition over time (Klingstedt et al., 2011, 2013; Sjolander et al., 2016).

Molecules such as 1-anilinonaphthalene-8-sulfonate (ANS) and its dimeric analog 4,4'-bis-1-anilinonaphthalene-8-sulfonate (Bis-ANS) are barely fluorescent in polar solvent, but become highly fluorescent in an apolar environment. In the presence of aggregates a blue shift and an increase of their emission

maxima occur, due to their binding to the hydrophobic clusters exposed in such assemblies. ANS and bis-ANS are particularly useful in the detection of the low concentrations of protein aggregates populating the early stages of the reaction (de Groot et al., 2007).

A Th-T derivative, called Pittsburgh compound B (PiB) is able to enter the brain and is used as a radioactive tracer for *in vivo* PET imaging of amyloid beta pathology in AD (Klunk et al., 2004).

**GUIDELINES FOR REPORTING PROTEIN AGGREGATION EXPERIMENTS: THE MIRRAGGE TABLE**

Given the diversity of oligomeric species and folding states, the choice of protein purification and handling procedures

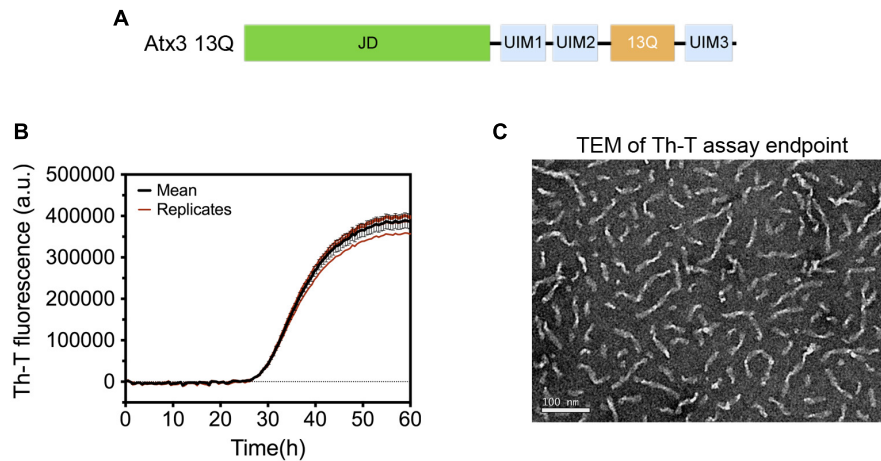


**FIGURE 3 |** Aggregation of human ataxin-3 (UniProt accession code: P54252-2). **(A)** Schematic representation of the structural organization of ataxin-3, with the N-terminal globular Josephin domain (JD) and the flexible C-terminal tail encompassing the ubiquitin-interacting motifs (UIMs) and the polyQ tract containing 13 glutamine residues (13Q); **(B)** Representative graph of human ataxin-3 aggregation at 37°C monitored by Th-T fluorescence. **(C)** TEM image of ataxin-3 protofibrils at the end of the aggregation assay (~60 h).

plays a crucial role in determining where in the aggregation map (**Figure 2**) are the departing and arrival points located, and by what pathways are they connected. Therefore, we propose a set of guidelines for presentation and publication of data related to polypeptide aggregation that ensure an adequate and accurate description of the experimental results. The relevant information that we propose to be reported is divided into two parts: sample preparation and quality and incubation conditions. Ideally, the methods section of each publication should contain the information briefly described in **Table 2**.

A pre-filled MIRRAGGE table using the aggregation of the protein ataxin-3 (**Figure 3**) (Gales et al., 2005; Almeida et al., 2015) and of a peptide from the Mot3 yeast prion (Sant'Anna et al., 2016; Fernandez et al., 2017) as examples is provided as **Supplementary Information (Supplementary File MIRRAGGE\_template.xls)** illustrating the minimum information that we suggest should be included to ensure reproducible (poly)peptide aggregation experiments. A large part of the minimum information required in the MIRRAGGE table concerns the sample preparation steps that precede the aggregation assay itself. Starting by the unambiguous identification of the protein molecule, it is particularly important for curators of public databases that the UniProt accession number, the species of origin and, if applicable, the presence of affinity tags are provided for the molecules under investigation (Orchard et al., 2007; Trewthella et al., 2017). For synthetic peptides, the chemical nature of the N and C termini (whether capped or uncapped) should be made clear as well as the buffering salt (e.g., TFA). Besides the essential information about the sample source, namely the protein expression system, the purification and polishing protocols, or, in the case of samples obtained from commercial sources, the catalog number and the name and location of the supplier, the MIRRAGGE table can also encompass any additional

information or experimental detail found to be important for the outcome of aggregation. This is achieved by including a flexible field of “additional key information” at the end of the tabular descriptions of the purification protocol and of the aggregation assay, wherein relevant remarks concerning the aggregation state of the protein, sample collection procedures in gel filtration chromatography, the occurrence of contaminants or co-solvents, the procedure adopted for removal of air bubbles, a critical sequence of reagent addition, etc., can be emphasized. A comprehensive characterization of the aggregation assay in terms of the total volume of reaction, plate/cuvette/vial geometry and material, method of evaporation control, size and material of beads (if present), and type of agitation is required on account of the effects of interfaces and shear flow on protein aggregation (Giehm and Otzen, 2010; Bekard et al., 2011; Yoshimura et al., 2012; Ferreira et al., 2016; Koepf et al., 2018). As a major determinant of phase separation, protein concentration is discriminated (i) before storage of the purified protein, (ii) immediately before aggregation, e.g., after the final filtration step, and (iii) during aggregation. The concentration of protein or peptide is provided, together with the information about MW, extinction coefficient and the quantification method adopted. Freeze-thawing stress can lead to the cold denaturation of the protein, its adsorption at the ice-liquid interface with subsequent partial denaturation and aggregation, or to drastic pH changes in buffers like sodium phosphate or succinate (Hawe et al., 2009). It is recommended to control the quality of thawed samples to judge whether additional polishing steps are required before the aggregation assay. Cohen et al. (2013) reported two rounds of gel filtration post-thawing on purified A $\beta$ 42 peptide to ensure pure monomer at the beginning of the kinetic assay. In the case of ataxin-3, increased reproducibility is achieved by adding a re-polishing step immediately before the aggregation assay, separating the predominant monomer from contaminant oligomeric

species putatively formed during the freezing-thawing process (Silva et al., 2017).

In conclusion, this review aims to provide an overview of the biophysical principles underlying protein self-assembly in its multiple shapes, and compiles detailed information on the experimental validation of polypeptide aggregation, with a focus on amyloid fibril formation. It results from several discussions on this topic in the context of the COST action BM1405 [Non-globular proteins – from sequence to structure, to applications in molecular physiopathology (NGP-net)]. We aim to endow both experienced researchers and newcomers to the field with a set of guidelines to enhance reproducibility in (poly)peptide aggregation experiments. The MIRRAGGE table template compiles a recommended reporting framework that is expected to provide a minimum set of information required for replicating protein aggregation experiments and swiftly discriminate protein assembly into amyloid fibrils from amorphous protein aggregation.

## AUTHOR CONTRIBUTIONS

PMM and SN revised the literature and wrote the manuscript. AS, ZS, FF, and MFP designed the template MIRRAGGE table, with contributions from all authors. PJB, FP, ZB, MB, OVG, ZG, CMG, AP, LCS, RS, VS, MZ, and DEO participated in the discussion of the minimum requirements for publication of experimental data on (poly)peptide aggregation, and contributed for the preparation of the list of experimental methods and details that should be reported for protein aggregation assays. SM-R and SV designed the review focus and finalized the manuscript. All authors contributed to the article and approved the submitted version.

## REFERENCES

- Adamcik, J., Lara, C., Usov, I., Jeong, J. S., Ruggeri, F. S., Dietler, G., et al. (2012). Measurement of intrinsic properties of amyloid fibrils by the peak force QNM method. *Nanoscale* 4, 4426–4429. doi: 10.1039/c2nr30768e
- Aguzzi, A., and Altmeyer, M. (2016). Phase separation: linking cellular compartmentalization to disease. *Trends Cell Biol.* 26, 547–558. doi: 10.1016/j.tcb.2016.03.004
- Aguzzi, A., and O'Connor, T. (2010). Protein aggregation diseases: pathogenicity and therapeutic perspectives. *Nat. Rev. Drug Discov.* 9, 237–248. doi: 10.1038/nrd3050
- Ahmed, M., Davis, J., Aucoin, D., Sato, T., Ahuja, S., Aimoto, S., et al. (2010). Structural conversion of neurotoxic amyloid- $\beta$ 1–42 oligomers to fibrils. *Nat. Struct. Mol. Biol.* 17, 561–567. doi: 10.1038/nsmb.1799
- Alberti, S. (2017). The wisdom of crowds: regulating cell function through condensed states of living matter. *J. Cell Sci.* 130, 2789–2796. doi: 10.1242/jcs.200295
- Almeida, B., Abreu, I. A., Matos, C. A., Fraga, J. S., Fernandes, S., Macedo, M. G., et al. (2015). SUMOylation of the brain-predominant Ataxin-3 isoform modulates its interaction with p97. *Biochim. Biophys. Acta* 1852, 1950–1959. doi: 10.1016/j.bbdis.2015.06.010
- Andrade, M. A., Chacon, P., Merelo, J. J., and Moran, F. (1993). Evaluation of secondary structure of proteins from UV circular dichroism spectra using an

## FUNDING

This work was supported by (i) the European Regional Development Fund (ERDF) through the COMPETE 2020—Operacional Programme for Competitiveness and Internationalisation (POCI), Portugal 2020, and by Portuguese funds through FCT—Fundação para a Ciência e a Tecnologia (FCT/MCTES) in the framework of grants POCI-01-0145-FEDER-031173, POCI-01-0145-FEDER-007274, POCI-01-0145-FEDER-031323 (“Institute for Research and Innovation in Health Sciences”), UID/Multi/04046/2013 (BioISI) and PTDC/NEU-NMC/2138/2014 (to CMG). SV was funded by the Spanish Ministry of Economy and Competitiveness (BIO2016-78310-R) and by ICREA (ICREA-Academia 2015). ZG and ZB were funded by Slovak research agencies VEGA 02/0145/17, 02/0030/18 and APVV-18-0284. RS was funded by VEGA 02/0163/19. DEO was funded by the Lundbeck Foundation (grant no. R276-2018-671) and the Independent Research Foundation Denmark | Natural Sciences (grant no. 8021-00208B). AP research was supported by UK Dementia Research Institute (RE1 3556) and by ARUK (ARUK-PG2019B-020).

## ACKNOWLEDGMENTS

The authors acknowledge the fruitful discussions with the scientists that participated in NGP-net (COST Action BM1405) scientific activities.

## SUPPLEMENTARY MATERIAL

The Supplementary Material for this article can be found online at: <https://www.frontiersin.org/articles/10.3389/fnmol.2020.582488/full#supplementary-material>

- unsupervised learning neural network. *Protein Eng.* 6, 383–390. doi: 10.1093/protein/6.4.383
- Arimon, M., Grimminger, V., Sanz, F., and Lashuel, H. A. (2008). Hsp104 targets multiple intermediates on the amyloid pathway and suppresses the seeding capacity of A $\beta$  fibrils and protofibrils. *J. Mol. Biol.* 384, 1157–1173. doi: 10.1016/j.jmb.2008.09.063
- Baldwin, A. J., Knowles, T. P. J., Tartaglia, G. G., Fitzpatrick, A. W., Devlin, G. L., Shammass, S. L., et al. (2011). Metastability of native proteins and the phenomenon of amyloid formation. *J. Am. Chem. Soc.* 133, 14160–14163. doi: 10.1021/ja2017703
- Banani, S. F., Lee, H. O., Hyman, A. A., and Rosen, M. K. (2017). Biomolecular condensates: organizers of cellular biochemistry. *Nat. Rev. Mol. Cell Biol.* 18, 285–298. doi: 10.1038/nrm.2017.7
- Bekard, I. B., Asimakis, P., Bertolini, J., and Dunstan, D. E. (2011). The effects of shear flow on protein structure and function. *Biopolymers* 95, 733–745. doi: 10.1002/bip.21646
- Belli, M., Ramazzotti, M., and Chiti, F. (2011). Prediction of amyloid aggregation *in vivo*. *EMBO Rep.* 12, 657–663. doi: 10.1038/embor.2011.116
- Ben-Gedalya, T., Moll, L., Bejerano-Sagie, M., Frere, S., Cabral, W. A., Friedmann-Morvinski, D., et al. (2015). Alzheimer's disease-causing proline substitutions lead to presenilin 1 aggregation and malfunction. *EMBO J.* 34, 2820–2839. doi: 10.15252/embj.201592042
- Benson, M. D., Buxbaum, J. N., Eisenberg, D. S., Merlini, G., Saraiva, M. J. M., Sekijima, Y., et al. (2018). Amyloid nomenclature 2018:

- recommendations by the International Society of Amyloidosis (ISA) nomenclature committee. *Amyloid* 25, 215–219. doi: 10.1080/13506129.2018.1549825
- Berger, Z., Roder, H., Hanna, A., Carlson, A., Rangachari, V., Yue, M., et al. (2007). Accumulation of pathological tau species and memory loss in a conditional model of tauopathy. *J. Neurosci.* 27, 3650–3662. doi: 10.1523/jneurosci.0587-07.2007
- Biancalana, M., and Koide, S. (2010). Molecular mechanism of Thioflavin-T binding to amyloid fibrils. *Biochim. Biophys. Acta* 1804, 1405–1412. doi: 10.1016/j.bbapap.2010.04.001
- Binger, K. J., Ecroyd, H., Yang, S., Carver, J. A., Howlett, G. J., and Griffin, M. D. W. (2013). Avoiding the oligomeric state:  $\alpha$ B-crystallin inhibits fragmentation and induces dissociation of apolipoprotein C-II amyloid fibrils. *FASEB J.* 27, 1214–1222. doi: 10.1096/fj.12-220657
- Bobone, S., and van de Weert, M. (2014). A reassessment of synchronous fluorescence in the separation of Trp and Tyr contributions in protein emission and in the determination of conformational changes. *J. Mol. Struct.* 1077, 68–76. doi: 10.1016/j.molstruc.2014.01.004
- Boeynaems, S., Alberti, S., Fawzi, N. L., Mittag, T., Polymenidou, M., Rousseau, F., et al. (2018). Protein phase separation: a new phase in cell biology. *Trends Cell Biol.* 28, 420–435. doi: 10.1016/j.tcb.2018.02.004
- Bouyanfif, A., Liyanage, S., Hequet, E., Moustaid-Moussa, N., and Abidi, N. (2018). Review of FTIR microspectroscopy applications to investigate biochemical changes in *C. elegans*. *Vib. Spectrosc.* 96, 74–82. doi: 10.1016/j.vibspec.2018.03.001
- Burgess, R. R. (2018). A brief practical review of size exclusion chromatography: rules of thumb, limitations, and troubleshooting. *Protein Expr. Purif.* 150, 81–85. doi: 10.1016/j.pep.2018.05.007
- Cao, Q., Boyer, D. R., Sawaya, M. R., Ge, P., and Eisenberg, D. S. (2019). Cryo-EM structures of four polymorphic TDP-43 amyloid cores. *Nat. Struct. Mol. Biol.* 26, 619–627. doi: 10.1038/s41594-019-0248-4
- Carvalho, A. L., Silva, A., and Macedo-Ribeiro, S. (2018). “Polyglutamine-Independent Features in Ataxin-3 Aggregation and Pathogenesis of Machado-Joseph Disease,” in *Polyglutamine Disorders*, eds C. Nóbrega and L. Pereira De Almeida. (Cham: Springer), 275–288. doi: 10.3389/fphar.2020.01311
- Chatani, E., and Yamamoto, N. (2018). Recent progress on understanding the mechanisms of amyloid nucleation. *Biophys. Rev.* 10, 527–534. doi: 10.1007/s12551-017-0353-8
- Chiti, F., and Dobson, C. M. (2006). Protein misfolding, functional amyloid, and human disease. *Annu. Rev. Biochem.* 75, 333–366. doi: 10.1146/annurev.biochem.75.101304.123901
- Chiti, F., and Dobson, C. M. (2017). Protein misfolding, amyloid formation, and human disease: a summary of progress over the last decade. *Annu. Rev. Biochem.* 86, 27–68. doi: 10.1146/annurev-biochem-061516-045115
- Cohen, S. I. A., Linse, S., Luheshi, L. M., Hellstrand, E., White, D. A., Rajah, L., et al. (2013). Proliferation of amyloid- $\beta$ 42 aggregates occurs through a secondary nucleation mechanism. *Proc. Natl. Acad. Sci. U.S.A.* 110, 9758–9763. doi: 10.1073/pnas.1218402110
- Crespo, R., Rocha, F. A., Damas, A. M., and Martins, P. M. (2012). A generic crystallization-like model that describes the kinetics of amyloid fibril formation. *J. Biol. Chem.* 287, 30585–30594. doi: 10.1074/jbc.m112.375345
- Crespo, R., Villar-Alvarez, E., Taboada, P., Rocha, F. A., Damas, A. M., and Martins, P. M. (2016). What can the kinetics of amyloid fibril formation tell about off-pathway aggregation? *J. Biol. Chem.* 291, 2018–2032. doi: 10.1074/jbc.m115.699348
- Cristovao, J. S., Henriques, B. J., and Gomes, C. M. (2019). Biophysical and spectroscopic methods for monitoring protein misfolding and amyloid aggregation. *Methods Mol. Biol.* 1873, 3–18. doi: 10.1007/978-1-4939-8820-4\_1
- Darling, A. L., Liu, Y., Oldfield, C. J., and Uversky, V. N. (2018). Intrinsically disordered proteome of human membrane-less organelles. *Proteomics* 18:e1700193. doi: 10.1002/pmic.201700193
- de Groot, N. S., Parella, T., Aviles, F. X., Vendrell, J., and Ventura, S. (2007). Ile-phe dipeptide self-assembly: clues to amyloid formation. *Biophys. J.* 92, 1732–1741. doi: 10.1529/biophysj.106.096677
- Dovidchenko, N. V., Finkelstein, A. V., and Galzitskaya, O. V. (2014). How to determine the size of folding nuclei of protofibrils from the concentration dependence of the rate and lag-time of aggregation. I. Modeling the amyloid protofibril formation. *J. Phys. Chem. B* 118, 1189–1197. doi: 10.1021/jp4083294
- Doyle, C. M., Rumpf, J. A., Broom, H. R., Broom, A., Stathopoulos, P. B., Vassall, K. A., et al. (2013). Energetics of oligomeric protein folding and association. *Arch. Biochem. Biophys.* 531, 44–64. doi: 10.1016/j.abb.2012.12.005
- Eisenberg, D. S., and Sawaya, M. R. (2017). Structural studies of amyloid proteins at the molecular level. *Annu. Rev. Biochem.* 86, 69–95. doi: 10.1146/annurev-biochem-061516-045104
- Englander, S. W., Mayne, L., Kan, Z.-Y., and Hu, W. (2016). Protein folding—how and why: by hydrogen exchange, fragment separation, and mass spectrometry. *Annu. Rev. Biophys.* 45, 135–152. doi: 10.1146/annurev-biophys-062215-011121
- Espargaro, A., Sabate, R., and Ventura, S. (2012). Thioflavin-S staining coupled to flow cytometry. A screening tool to detect in vivo protein aggregation. *Mol. Biosyst.* 8, 2839–2844. doi: 10.1039/c2mb25214g
- Fairfoul, G., McGuire, L. I., Pal, S., Ironside, J. W., Neumann, J., Christie, S., et al. (2016). Alpha-synuclein RT-QuIC in the CSF of patients with alpha-synucleinopathies. *Ann. Clin. Transl. Neurol.* 3, 812–818. doi: 10.1002/acn3.338
- Falahati, H., and Haji-Akbari, A. (2019). Thermodynamically driven assemblies and liquid-liquid phase separations in biology. *Soft Matter* 15, 1135–1154. doi: 10.1039/c8sm02285b
- Falcon, B., Cavallini, A., Angers, R., Glover, S., Murray, T. K., Barnham, L., et al. (2015). Conformation determines the seeding potencies of native and recombinant tau aggregates. *J. Biol. Chem.* 290, 1049–1065. doi: 10.1074/jbc.m114.589309
- Farmer, K., Gerson, J. E., and Kaye, R. (2017). Oligomer formation and cross-seeding: the new frontier. *Isr. J. Chem.* 57, 665–673. doi: 10.1002/ijch.201600103
- Fernandez, M. R., Battle, C., Gil-Garcia, M., and Ventura, S. (2017). Amyloid cores in prion domains: key regulators for prion conformational conversion. *Prion* 11, 31–39. doi: 10.1080/19336896.2017.1282020
- Ferreira, C., Rocha, F. A., Damas, A. M., and Martins, P. M. (2016). The finding of nondissolving lysozyme crystals and its significance for the study of hard-to-crystallize biological macromolecules. *Cryst. Growth Des.* 16, 4285–4291. doi: 10.1021/acs.cgd.6b00334
- Fitzpatrick, A. W., and Saibil, H. R. (2019). Cryo-EM of amyloid fibrils and cellular aggregates. *Curr. Opin. Struct. Biol.* 58, 34–42. doi: 10.1016/j.sbi.2019.05.003
- Fitzpatrick, A. W. P., Debelouchina, G. T., Bayro, M. J., Clare, D. K., Caporini, M. A., Bajaj, V. S., et al. (2013). Atomic structure and hierarchical assembly of a cross- $\beta$  amyloid fibril. *Proc. Natl. Acad. Sci. U.S.A.* 110, 5468–5473. doi: 10.1073/pnas.1219476110
- Folta-Stogniew, E. (2006). Oligomeric states of proteins determined by size-exclusion chromatography coupled with light scattering, absorbance, and refractive index detectors. *Methods Mol. Biol.* 328, 97–112. doi: 10.1385/1-59745-026-x:97
- Gade Malmos, K., Blancas-Mejia, L. M., Weber, B., Buchner, J., Ramirez-Alvarado, M., Naiki, H., et al. (2017). ThT 101: a primer on the use of thioflavin T to investigate amyloid formation. *Amyloid* 24, 1–16. doi: 10.1080/13506129.2017.1304905
- Galante, D., Ruggeri, F. S., Dietler, G., Pellistri, F., Gatta, E., Corsaro, A., et al. (2016). A critical concentration of N-terminal pyroglutamylation amyloid beta drives the misfolding of Ab1-42 into more toxic aggregates. *Int. J. Biochem. Cell Biol.* 79, 261–270. doi: 10.1016/j.biocel.2016.08.037
- Gales, L., Cortes, L., Almeida, C., Melo, C. V., Costa, M. C., Maciel, P., et al. (2005). Towards a structural understanding of the fibrillation pathway in Machado-Joseph's disease: trapping early oligomers of non-expanded ataxin-3. *J. Mol. Biol.* 353, 642–654. doi: 10.1016/j.jmb.2005.08.061
- Gazit, E. (2002). The “Correctly Folded” state of proteins: Is it a metastable state? *Angew. Chem. Int. Ed. Engl.* 41, 257–259. doi: 10.1002/1521-3773(20020118)41:2<257::aid-anie257>3.0.co;2-m
- Ghisaidoobe, A. B., and Chung, S. J. (2014). Intrinsic tryptophan fluorescence in the detection and analysis of proteins: a focus on Förster resonance energy transfer techniques. *Int. J. Mol. Sci.* 15, 22518–22538. doi: 10.3390/ijms151222518
- Giehm, L., and Otzen, D. E. (2010). Strategies to increase the reproducibility of protein fibrillization in plate reader assays. *Anal. Biochem.* 400, 270–281. doi: 10.1016/j.ab.2010.02.001



- Giri Rao, V. V. H., and Gosavi, S. (2018). On the folding of a structurally complex protein to its metastable active state. *Proc. Natl. Acad. Sci. U.S.A.* 115, 1998–2003. doi: 10.1073/pnas.1708173115
- Goedert, M., Falcon, B., Zhang, W., Ghetti, B., and Scheres, S. H. W. (2018). Distinct conformers of assembled Tau in Alzheimer's and Pick's diseases. *Cold Spring Harb. Symp. Quant. Biol.* 83, 163–171. doi: 10.1101/sqb.2018.83.037580
- González, N., Arcos-López, T., König, A., Quintanar, L., Menacho Márquez, M., Outeiro, T. F., et al. (2019). Effects of alpha-synuclein posttranslational modifications on metal binding. *J. Neurochem.* 150, 507–521. doi: 10.1111/jnc.14721
- Gosal, W. S., Morten, I. J., Hewitt, E. W., Smith, D. A., Thomson, N. H., and Radford, S. E. (2005). Competing pathways determine fibril morphology in the self-assembly of  $\beta$ 2-microglobulin into amyloid. *J. Mol. Biol.* 351, 850–864. doi: 10.1016/j.jmb.2005.06.040
- Gras, S. L., Waddington, L. J., and Goldie, K. N. (2011). Transmission electron microscopy of amyloid fibrils. *Methods Mol. Biol.* 752, 197–214. doi: 10.1007/978-1-60327-223-0\_13
- Gremer, L., Schölzel, D., Schenk, C., Reinartz, E., Labahn, J., Ravelli, R. B. G., et al. (2017). Fibril structure of amyloid- $\beta$ (1–42) by cryo-electron microscopy. *Science* 358, 116–119. doi: 10.1126/science.aao2825
- Grishin, S. Y., Deryusheva, E. I., Machulin, A. V., Selivanova, O. M., Glyakina, A. V., Gorbunova, E. Y., et al. (2020). Amyloidogenic propensities of ribosomal S1 proteins: bioinformatics screening and experimental checking. *Int. J. Mol. Sci.* 21:5199. doi: 10.3390/ijms21155199
- Guo, J. L., Covell, D. J., Daniels, J. P., Iba, M., Stieber, A., Zhang, B., et al. (2013). Distinct alpha-synuclein strains differentially promote tau inclusions in neurons. *Cell* 154, 103–117. doi: 10.1016/j.cell.2013.05.057
- Haass, C., and Selkoe, D. J. (2007). Soluble protein oligomers in neurodegeneration: lessons from the Alzheimer's amyloid  $\beta$ -peptide. *Nat. Rev. Mol. Cell Biol.* 8, 101–112. doi: 10.1038/nrm2101
- Harper, J. D., and Peter, T., and Lansbury, J. (1997). Models of amyloid seeding in Alzheimer's disease and scrapie: mechanistic truths and physiological consequences of the time-dependent solubility of amyloid proteins. *Annu. Rev. Biochem.* 66, 385–407. doi: 10.1146/annurev.biochem.66.1.385
- Hasecke, F., Miti, T., Perez, C., Barton, J., Schölzel, D., Gremer, L., et al. (2018). Origin of metastable oligomers and their effects on amyloid fibril self-assembly. *Chem. Sci.* 9, 5937–5948. doi: 10.1039/c8sc01479e
- Hawe, A., Kasper, J. C., Friess, W., and Jiskoot, W. (2009). Structural properties of monoclonal antibody aggregates induced by freeze–thawing and thermal stress. *Eur. J. Pharm. Sci.* 38, 79–87. doi: 10.1016/j.ejps.2009.06.001
- Hiramatsu, H., and Kitagawa, T. (2005). FT-IR approaches on amyloid fibril structure. *Biochim. Biophys. Acta* 1753, 100–107. doi: 10.1016/j.bbapap.2005.07.008
- Hudson, S. A., Ecroyd, H., Kee, T. W., and Carver, J. A. (2009). The thioflavin T fluorescence assay for amyloid fibril detection can be biased by the presence of exogenous compounds. *FEBS J.* 276, 5960–5972. doi: 10.1111/j.1742-4658.2009.07307.x
- Hurshman, A. R., White, J. T., Powers, E. T., and Kelly, J. W. (2004). Transthyretin aggregation under partially denaturing conditions is a downhill polymerization. *Biochemistry* 43, 7365–7381. doi: 10.1021/bi049621l
- Iadanza, M. G., Jackson, M. P., Hewitt, E. W., Ranson, N. A., and Radford, S. E. (2018a). A new era for understanding amyloid structures and disease. *Nat. Rev. Mol. Cell Biol.* 19, 755–773. doi: 10.1038/s41580-018-0060-8
- Iadanza, M. G., Silvers, R., Boardman, J., Smith, H. I., Karamanos, T. K., Debelouchina, G. T., et al. (2018b). The structure of a  $\beta$ 2-microglobulin fibril suggests a molecular basis for its amyloid polymorphism. *Nat. Commun.* 9:4517. doi: 10.1038/s41467-018-06761-6
- Ianiri, A., Wu, H., Van Rij, M. M. J., Vena, M. P., Keizer, A. D. A., Esteves, A. C. C., et al. (2019). Liquid–liquid phase separation during amphiphilic self-assembly. *Nat. Chem.* 11, 320–328. doi: 10.1038/s41557-019-0210-4
- Ingelsson, M. (2016). Alpha-synuclein oligomers—neurotoxic molecules in Parkinson's disease and other lewy body disorders. *Front. Neurosci.* 10:408. doi: 10.3389/fnins.2016.00408
- Jarosz, D. F., and Khurana, V. (2017). Specification of physiologic and disease states by distinct proteins and protein conformations. *Cell* 171, 1001–1014. doi: 10.1016/j.cell.2017.10.047
- Johnston, J. A., Ward, C. L., and Kopito, R. R. (1998). Aggresomes: a cellular response to misfolded proteins. *J. Cell Biol.* 143, 1883–1898. doi: 10.1083/jcb.143.7.1883
- Kelly, S. M., Jess, T. J., and Price, N. C. (2005). How to study proteins by circular dichroism. *Biochim. Biophys. Acta* 1751, 119–139. doi: 10.1016/j.bbapap.2005.06.005
- Khurana, R., Ionescu-Zanetti, C., Pope, M., Li, J., Nielson, L., Ramírez-Alvarado, M., et al. (2003). A general model for amyloid fibril assembly based on morphological studies using atomic force microscopy. *Biophys. J.* 85, 1135–1144. doi: 10.1016/s0006-3495(03)74550-0
- Klingstedt, T., Aslund, A., Simon, R. A., Johansson, L. B., Mason, J. J., Nystrom, S., et al. (2011). Synthesis of a library of oligothiophenes and their utilization as fluorescent ligands for spectral assignment of protein aggregates. *Org. Biomol. Chem.* 9, 8356–8370. doi: 10.1039/c1ob05637a
- Klingstedt, T., Blechschmidt, C., Nogalska, A., Prokop, S., Haggqvist, B., Danielsson, O., et al. (2013). Luminescent conjugated oligothiophenes for sensitive fluorescent assignment of protein inclusion bodies. *ChemBiochem* 14, 607–616. doi: 10.1002/cbic.201200731
- Klunk, W. E., Engler, H., Nordberg, A., Wang, Y., Blomqvist, G., Holt, D. P., et al. (2004). Imaging brain amyloid in Alzheimer's disease with Pittsburgh Compound-B. *Ann. Neurol.* 55, 306–319. doi: 10.1002/ana.20009
- Kodali, R., and Wetzel, R. (2007). Polymorphism in the intermediates and products of amyloid assembly. *Curr. Opin. Struct. Biol.* 17, 48–57. doi: 10.1016/j.sbi.2007.01.007
- Koepf, E., Eisele, S., Schroeder, R., Brezesinski, G., and Friess, W. (2018). Notorious but not understood: how liquid-air interfacial stress triggers protein aggregation. *Int. J. Pharm.* 537, 202–212. doi: 10.1016/j.ijpharm.2017.12.043
- Kushnirov, V. V., Dergalev, A. A., and Alexandrov, A. I. (2020). Proteinase K resistant cores of prions and amyloids. *Prion* 14, 11–19. doi: 10.1080/19336896.2019.1704612
- Langkilde, A. E., Morris, K. L., Serpell, L. C., Svergun, D. I., and Vestergaard, B. (2015). The architecture of amyloid-like peptide fibrils revealed by X-ray scattering, diffraction and electron microscopy. *Acta Crystallogr. Sect. D Biol. Crystallogr.* 71, 882–895. doi: 10.1107/s1399004715001674
- Lashuel, H. A., Wurth, C., Woo, L., and Kelly, J. W. (1999). The most pathogenic transthyretin variant, L55P, forms amyloid fibrils under acidic conditions and protofibrils under physiological conditions. *Biochemistry* 38, 13560–13573. doi: 10.1021/bi991021c
- Liu, S., Peng, P., Wang, H., Shi, L., and Li, T. (2017). Thioflavin T binds dimeric parallel-stranded GA-containing non-G-quadruplex DNAs: a general approach to lighting up double-stranded scaffolds. *Nucleic Acids Res.* 45, 12080–12089. doi: 10.1093/nar/gkx942
- Lorenzen, N., Nielsen, S. B., Buell, A. K., Kaspersen, J. D., Arosio, P., Vad, B. S., et al. (2014). The role of stable  $\alpha$ -synuclein oligomers in the molecular events underlying amyloid formation. *J. Am. Chem. Soc.* 136, 3859–3868. doi: 10.1021/ja411577t
- MacRaid, C. A., Hatters, D. M., Lawrence, L. J., and Howlett, G. J. (2003). Sedimentation velocity analysis of flexible macromolecules: self-association and tangling of amyloid fibrils. *Biophys. J.* 84, 2562–2569. doi: 10.1016/s0006-3495(03)75061-9
- Mahler, H.-C., Friess, W., Grauschopf, U., and Kiese, S. (2009). Protein aggregation: pathways, induction factors and analysis. *J. Pharm. Sci.* 98, 2909–2934. doi: 10.1002/jps.21566
- Makin, O. S., and Serpell, L. C. (2005). Structures for amyloid fibrils. *FEBS J.* 272, 5950–5961. doi: 10.1111/j.1742-4658.2005.05025.x
- Malmendal, A., Underhaug, J., Otzen, D. E., and Nielsen, N. C. (2010). Fast mapping of global protein folding states by multivariate NMR: a GPS for proteins. *PLoS One* 5:e10262. doi: 10.1371/journal.pone.0010262
- Manavalan, P., and Johnson, W. C. Jr. (1987). Variable selection method improves the prediction of protein secondary structure from circular dichroism spectra. *Anal. Biochem.* 167, 76–85. doi: 10.1016/0003-2697(87)90135-7
- Mateju, D., Franzmann, T. M., Patel, A., Kopach, A., Boczek, E. E., Maharana, S., et al. (2017). An aberrant phase transition of stress granules triggered by misfolded protein and prevented by chaperone function. *EMBO J.* 36, 1669–1687. doi: 10.15252/embj.201695957
- Meisl, G., Kirkegaard, J. B., Arosio, P., Michaels, T. C. T., Vendruscolo, M., Dobson, C. M., et al. (2016). Molecular mechanisms of protein aggregation from

- global fitting of kinetic models. *Nat. Protoc.* 11, 252–272. doi: 10.1038/nprot.2016.010
- Michaels, T. C. T., Dear, A. J., Kirkegaard, J. B., Saar, K. L., Weitz, D. A., and Knowles, T. P. J. (2016). Fluctuations in the kinetics of linear protein self-assembly. *Phys. Rev. Lett.* 116:258103. doi: 10.1103/PhysRevLett.116.258103
- Miconai, A., Wien, F., Kerna, L., Lee, Y. H., Goto, Y., Refregiers, M., et al. (2015). Accurate secondary structure prediction and fold recognition for circular dichroism spectroscopy. *Proc. Natl. Acad. Sci. U.S.A.* 112, E3095–E3103. doi: 10.1073/pnas.1500851112
- Miller, S. B., Ho, C.-T., Winkler, J., Khokhrina, M., Neuner, A., Mohamed, M. Y., et al. (2015). Compartment-specific aggregates direct distinct nuclear and cytoplasmic aggregate deposition. *EMBO J.* 34, 778–797. doi: 10.15252/embj.201489524
- Miti, T., Mulaj, M., Schmit, J. D., and Muschol, M. (2015). Stable, metastable, and kinetically trapped amyloid aggregate phases. *Biomacromolecules* 16, 326–335. doi: 10.1021/bm501521r
- Mok, Y.-F., and Howlett, G. J. (2006). Sedimentation velocity analysis of amyloid oligomers and fibrils. *Methods Enzymol.* 413, 199–217. doi: 10.1016/s0076-6879(06)13011-6
- Mok, Y.-F., Howlett, G. J., and Griffin, M. D. W. (2015). Sedimentation velocity analysis of the size distribution of amyloid oligomers and fibrils. *Methods Enzymol.* 562, 241–256. doi: 10.1016/bs.mie.2015.06.024
- Morris, K. L., and Serpell, L. C. (2012). X-ray fibre diffraction studies of amyloid fibrils. *Methods Mol. Biol.* 849, 121–135. doi: 10.1007/978-1-61779-551-0\_9
- Murakami, T., Qamar, S., Lin, J. Q., Schierle, G. S. K., Rees, E., Miyashita, A., et al. (2015). ALS/FTD mutation-induced phase transition of FUS liquid droplets and reversible hydrogels into irreversible hydrogels impairs RNP granule function. *Neuron* 88, 678–690. doi: 10.1016/j.neuron.2015.10.030
- Murray, D. T., Kato, M., Lin, Y., Thurber, K. R., Hung, I., Mcknight, S. L., et al. (2017). Structure of FUS protein fibrils and its relevance to self-assembly and phase separation of low-complexity domains. *Cell* 171, 615–627. doi: 10.1016/j.cell.2017.08.048
- Navarro, S., and Ventura, S. (2014). Fluorescent dye ProteoStat to detect and discriminate intracellular amyloid-like aggregates in *Escherichia coli*. *Biotechnol. J.* 9, 1259–1266. doi: 10.1002/biot.201400291
- O’Nuallain, B., Williams, A. D., Westermarck, P., and Wetzel, R. (2004). Seeding specificity in amyloid growth induced by heterologous fibrils. *J. Biol. Chem.* 279, 17490–17499. doi: 10.1074/jbc.m311300200
- Orchard, S., Salwinski, L., Kerrien, S., Montecchi-Palazzi, L., Oesterheld, M., Stümpflen, V., et al. (2007). The minimum information required for reporting a molecular interaction experiment (MIMIX). *Nat. Biotechnol.* 25, 894–898. doi: 10.1038/nbt1324
- Ormsby, A. R., Ramdhan, Y. M., Mok, Y.-F., Jovanoski, K. D., and Hatters, D. M. (2013). A platform to view huntingtin Exon 1 aggregation flux in the cell reveals divergent influences from chaperones hsp40 and hsp70. *J. Biol. Chem.* 288, 37192–37203. doi: 10.1074/jbc.m113.486944
- Orru, C. D., Wilham, J. M., Vascellari, S., Hughson, A. G., and Caughey, B. (2012). New generation QuIC assays for prion seeding activity. *Prion* 6, 147–152. doi: 10.4161/pri.19430
- Oskarsson, M. E., Hermansson, E., Wang, Y., Welsh, N., Presto, J., Johansson, J., et al. (2018). BRICHOS domain of Bri2 inhibits islet amyloid polypeptide (IAPP) fibril formation and toxicity in human beta cells. *Proc. Natl. Acad. Sci. U.S.A.* 115, E2752–E2761. doi: 10.1073/pnas.1715951115
- Otzen, D., and Riek, R. (2019). Functional amyloids. *Cold Spring Harb. Perspect. Biol.* 11:a033860. doi: 10.1101/cshperspect.a033860
- Padrick, S. B., and Miranker, A. D. (2002). Islet amyloid: phase partitioning and secondary nucleation are central to the mechanism of fibrillogenesis. *Biochemistry* 41, 4694–4703. doi: 10.1021/bi0160462
- Pallarès, I., and Ventura, S. (2019). Advances in the prediction of protein aggregation propensity. *Curr. Med. Chem.* 26, 3911–3920. doi: 10.2174/0929867324666170705121754
- Patel, A., Lee, H. O., Jawerth, L., Maharana, S., Jähnel, M., Hein, M. Y., et al. (2015). A liquid-to-solid phase transition of the ALS protein FUS accelerated by disease mutation. *Cell* 162, 1066–1077. doi: 10.1016/j.cell.2015.07.047
- Persson, E. K., Verstraete, K., Heyndrickx, I., Gevaert, E., Aegerter, H., Percier, J.-M., et al. (2019). Protein crystallization promotes type 2 immunity and is reversible by antibody treatment. *Science* 364:eaaw4295. doi: 10.1126/science.aaw4295
- Pieri, L., Madiona, K., and Melki, R. (2016). Structural and functional properties of prefibrillar  $\alpha$ -synuclein oligomers. *Sci. Rep.* 6:24526. doi: 10.1038/srep24526
- Prausnitz, J. M., Lichtenthaler, R. N., and De Azevedo, E. G. (1998). *Molecular Thermodynamics of Fluid-Phase Equilibria*. London: Pearson Education.
- Provencher, S. W., and Glockner, J. (1981). Estimation of globular protein secondary structure from circular dichroism. *Biochemistry* 20, 33–37. doi: 10.1021/bi00504a006
- Prusiner, S. B. (2001). Neurodegenerative Diseases and Prions. *N. Engl. J. Med.* 344, 1516–1526. doi: 10.1056/NEJM200105173442006
- Qiang, W., Yau, W.-M., Lu, J.-X., Collinge, J., and Tycko, R. (2017). Structural variation in amyloid- $\beta$  fibrils from Alzheimer’s disease clinical subtypes. *Nature* 541, 217–221. doi: 10.1038/nature20814
- Rasmussen, J., Mahler, J., Beschoner, N., Kaeser, S. A., Häslér, L. M., Baumann, F., et al. (2017). Amyloid polymorphisms constitute distinct clouds of conformational variants in different etiological subtypes of Alzheimer’s disease. *Proc. Natl. Acad. Sci. U.S.A.* 114, 13018–13023. doi: 10.1073/pnas.1713215114
- Rivas, G., and Minton, A. P. (2016). Macromolecular crowding *in vitro*, *in vivo*, and in between. *Trends Biochem. Sci.* 41, 970–981. doi: 10.1016/j.tibs.2016.08.013
- Rochet, J.-C., and Lansbury, P. T. (2000). Amyloid fibrillogenesis: themes and variations. *Curr. Opin. Struct. Biol.* 10, 60–68. doi: 10.1016/s0959-440x(99)00049-4
- Ruff, K. M., Pappu, R. V., and Holehouse, A. S. (2019). Conformational preferences and phase behavior of intrinsically disordered low complexity sequences: insights from multiscale simulations. *Curr. Opin. Struct. Biol.* 56, 1–10. doi: 10.1016/j.sbi.2018.10.003
- Ruggeri, F. S., Longo, G., Faggiano, S., Lipiec, E., Pastore, A., and Dietler, G. (2015). Infrared nanospectroscopy characterization of oligomeric and fibrillar aggregates during amyloid formation. *Nat. Commun.* 6:7831. doi: 10.1038/ncomms8831
- Ruggeri, F. S., Mannini, B., Schmid, R., Vendruscolo, M., and Knowles, T. P. J. (2020). Single molecule secondary structure determination of proteins through infrared absorption nanospectroscopy. *Nat. Commun.* 11:2945. doi: 10.1038/s41467-020-16728-1
- Ruggeri, F. S., Sneideris, T., Vendruscolo, M., and Knowles, T. P. J. (2019). Atomic force microscopy for single molecule characterisation of protein aggregation. *Arch. Biochem. Biophys.* 664, 134–148. doi: 10.1016/j.abb.2019.02.001
- Ruggeri, F. S., Vieweg, S., Cendrowska, U., Longo, G., Chiki, A., Lashuel, H. A., et al. (2016). Nanoscale studies link amyloid maturity with polyglutamine diseases onset. *Sci. Rep.* 6:31155. doi: 10.1038/srep31155
- Sabate, R., Rodriguez-Santiago, L., Sodupe, M., Saupe, S. J., and Ventura, S. (2013). Thioflavin-T excimer formation upon interaction with amyloid fibers. *Chem. Commun.* 49, 5745–5747. doi: 10.1039/c3cc42040j
- Sabate, R., and Saupe, S. J. (2007). Thioflavin T fluorescence anisotropy: an alternative technique for the study of amyloid aggregation. *Biochem. Biophys. Res. Commun.* 360, 135–138. doi: 10.1016/j.bbrc.2007.06.063
- Saborio, G. P., Permann, B., and Soto, C. (2001). Sensitive detection of pathological prion protein by cyclic amplification of protein misfolding. *Nature* 411, 810–813. doi: 10.1038/35081095
- Saelices, L., Chung, K., Lee, J. H., Cohn, W., Whitelegge, J. P., Benson, M. D., et al. (2018). Amyloid seeding of transthyretin by ex vivo cardiac fibrils and its inhibition. *Proc. Natl. Acad. Sci. U.S.A.* 115, E6741–E6750. doi: 10.1073/pnas.1805131115
- Sahin, E., and Roberts, C. J. (2012). Size-exclusion chromatography with multi-angle light scattering for elucidating protein aggregation mechanisms. *Methods Mol. Biol.* 899, 403–423. doi: 10.1007/978-1-61779-921-1\_25
- Saijo, E., Ghetti, B., Zanusso, G., Oblak, A., Furman, J. L., Diamond, M. I., et al. (2017). Ultrasensitive and selective detection of 3-repeat tau seeding activity in Pick disease brain and cerebrospinal fluid. *Acta Neuropathol.* 133, 751–765. doi: 10.1007/s00401-017-1692-z
- Salvadores, N., Shahnawaz, M., Scarpini, E., Tagliavini, F., and Soto, C. (2014). Detection of misfolded A $\beta$  oligomers for sensitive biochemical diagnosis

- of Alzheimer's disease. *Cell Rep.* 7, 261–268. doi: 10.1016/j.celrep.2014.02.031
- Sant'Anna, R., Fernandez, M. R., Batlle, C., Navarro, S., De Groot, N. S., Serpell, L., et al. (2016). Characterization of amyloid cores in prion domains. *Sci. Rep.* 6:34274. doi: 10.1038/srep34274
- Sárány, Z., Rocha, F., Damas, A. M., Macedo-Ribeiro, S., and Martins, P. M. (2019). Chemical kinetic strategies for high-throughput screening of protein aggregation modulators. *Chem. Asian J.* 14, 500–508. doi: 10.1002/asia.201801703
- Schönherr, R., Rudolph Janine, M., and Redecke, L. (2018). Protein crystallization in living cells. *Biol. Chem.* 399, 751–772. doi: 10.1515/hsz-2018-0158
- Selivanova, O. M., Surin, A. K., Marchenkov, V. V., Dzhus, U. F., Grigorashvili, E. I., Suvorina, M. Y., et al. (2016). The mechanism underlying amyloid polymorphism is opened for Alzheimer's disease amyloid- $\beta$  peptide. *J. Alzheimers Dis.* 54, 821–830. doi: 10.3233/jad-160405
- Shankar, G. M., Li, S., Mehta, T. H., Garcia-Munoz, A., Shepardson, N. E., Smith, I., et al. (2008). Amyloid- $\beta$  protein dimers isolated directly from Alzheimer's brains impair synaptic plasticity and memory. *Nat. Med.* 14, 837–842. doi: 10.1038/nm1782
- Shen, D., Coleman, J., Chan, E., Nicholson, T. P., Dai, L., Sheppard, P. W., et al. (2011). Novel cell- and tissue-based assays for detecting misfolded and aggregated protein accumulation within aggresomes and inclusion bodies. *Cell Biochem. Biophys.* 60, 173–185. doi: 10.1007/s12013-010-9138-4
- Shin, Y., and Brangwynne, C. P. (2017). Liquid phase condensation in cell physiology and disease. *Science* 357:eaf4382. doi: 10.1126/science.aaf4382
- Shivu, B., Seshadri, S., Li, J., Oberg, K. A., Uversky, V. N., and Fink, A. L. (2013). Distinct beta-sheet structure in protein aggregates determined by ATR-FTIR spectroscopy. *Biochemistry* 52, 5176–5183. doi: 10.1021/bi400625v
- Silva, A., Almeida, B., Fraga, J. S., Taboada, P., Martins, P. M., and Macedo-Ribeiro, S. (2017). Distribution of amyloid-like and oligomeric species from protein aggregation kinetics. *Angew. Chem. Int. Ed.* 56, 14042–14045. doi: 10.1002/anie.201707345
- Silva, A., Sárány, Z., Fraga, J. S., Taboada, P., Macedo-Ribeiro, S., and Martins, P. M. (2018). Probing the occurrence of soluble oligomers through amyloid aggregation scaling laws. *Biomolecules* 8:108. doi: 10.3390/biom8040108
- Sjolander, D., Rocken, C., Westermarck, P., Westermarck, G. T., Nilsson, K. P., and Hammarstrom, P. (2016). Establishing the fluorescent amyloid ligand h-FTAA for studying human tissues with systemic and localized amyloid. *Amyloid* 23, 98–108. doi: 10.3109/13506129.2016.1158159
- Skrabana, R., Kovacech, B., Filipcik, P., Zilka, N., Jadhav, S., Smolek, T., et al. (2017). Neuronal expression of truncated Tau efficiently promotes neurodegeneration in animal models: pitfalls of toxic oligomer analysis. *J. Alzheimers Dis.* 58, 1017–1025. doi: 10.3233/jad-161124
- Seutel, M., and Van Driessche, A. E. (2018). Nucleation of protein crystals—a nanoscopic perspective. *Nanoscale* 10, 12256–12267. doi: 10.1039/c8nr02867b
- Sohl, J. L., Jaswal, S. S., and Agard, D. A. (1998). Unfolded conformations of  $\alpha$ -lytic protease are more stable than its native state. *Nature* 395, 817–819. doi: 10.1038/27470
- Soto, C., and Pritzkow, S. (2018). Protein misfolding, aggregation, and conformational strains in neurodegenerative diseases. *Nat. Neurosci.* 21, 1332–1340. doi: 10.1038/s41593-018-0235-9
- Sreerama, N., and Woody, R. W. (2000). Estimation of protein secondary structure from circular dichroism spectra: comparison of CONTIN, SELCON, and CDSSTR methods with an expanded reference set. *Anal. Biochem.* 287, 252–260. doi: 10.1006/abio.2000.4880
- Striegel, A. M., Yau, W. W., Kirkland, J. J., and Bly, D. D. (2009). *Modern Size-Exclusion Liquid Chromatography: Practice of Gel Permeation and Gel Filtration Chromatography*. Hoboken, NJ: John Wiley & Sons, Inc. doi: 10.1002/9780470442876
- Sugimoto, S., Arita-Morioka, K., Mizunoe, Y., Yamanaka, K., and Ogura, T. (2015). Thioflavin T as a fluorescence probe for monitoring RNA metabolism at molecular and cellular levels. *Nucleic Acids Res.* 43:e92. doi: 10.1093/nar/gkv338
- Surin, A. K., Grishin, S. Y., and Galzitskaya, O. V. (2020). Determination of amyloid core regions of insulin analogues fibrils. *Prion* 14, 149–162. doi: 10.1080/19336896.2020.1776062
- Tanford, C. (1970). "Protein Denaturation: Part C.\*Parts A and B were published in Volume 23 of Advances in Protein Chemistry (1968), starting on p. 121 Theoretical Models for The Mechanism of Denaturation," in *Advances in Protein Chemistry*, eds C. B. Anfinsen, J. T. Edsall, and F. M. Richards (Cambridge, MA: Academic Press), 1–95. doi: 10.1016/s0065-3233(08)60241-7
- Teplow, D. B. (1998). Structural and kinetic features of amyloid  $\beta$ -protein fibrillogenesis. *Amyloid* 5, 121–142. doi: 10.3109/13506129808995290
- Trewhella, J., Duff, A. P., Durand, D., Gabel, F., Guss, J. M., Hendrickson, W. A., et al. (2017). 2017 publication guidelines for structural modelling of small-angle scattering data from biomolecules in solution: an update. *Acta Crystallogr. Sect. D Biol. Crystallogr.* 73, 710–728. doi: 10.1107/S2059798317011597
- Vadukul, D. M., Al-Hilaly, Y. K., and Serpell, L. C. (2019). Methods for structural analysis of amyloid fibrils in misfolding diseases. *Methods Mol. Biol.* 1873, 109–122. doi: 10.1007/978-1-4939-8820-4\_7
- Vekilov, P. G. (2010). Phase transitions of folded proteins. *Soft Matter* 6, 5254–5272. doi: 10.1039/c0sm00215a
- Ventura, S., Zurdo, J., Narayanan, S., Parreno, M., Mangues, R., Reif, B., et al. (2004). Short amino acid stretches can mediate amyloid formation in globular proteins: the Src homology 3 (SH3) case. *Proc. Natl. Acad. Sci. U.S.A.* 101, 7258–7263. doi: 10.1073/pnas.0308249101
- Vestergaard, B., Groenning, M., Roessle, M., Kastrop, J. S., De Weert, M. V., Flink, J. M., et al. (2007). A helical structural nucleus is the primary elongating unit of insulin amyloid fibrils. *PLoS Biol.* 5:e134. doi: 10.1371/journal.pbio.0050134
- Vey, M., Pilkuhn, S., Wille, H., Nixon, R., Dearmond, S. J., Smart, E. J., et al. (1996). Subcellular colocalization of the cellular and scrapie prion proteins in caveolae-like membranous domains. *Proc. Natl. Acad. Sci. U.S.A.* 93, 14945–14949. doi: 10.1073/pnas.93.25.14945
- Viegas, M. S., Martins, T. C., Seco, F., and Do Carmo, A. (2007). An improved and cost-effective methodology for the reduction of autofluorescence in direct immunofluorescence studies on formalin-fixed paraffin-embedded tissues. *Eur. J. Histochem.* 51, 59–66. doi: 10.4081/1013
- Vorontsova, M. A., Maes, D., and Vekilov, P. G. (2015). Recent advances in the understanding of two-step nucleation of protein crystals. *Faraday Discuss.* 179, 27–40. doi: 10.1039/c4fd00217b
- Waeytens, J., Van Hemelryck, V., Deniset-Besseau, A., Ruyschaert, J.-M., Dazzi, A., and Raussens, V. (2020). Characterization by nano-infrared spectroscopy of individual aggregated species of amyloid proteins. *Molecules* 25:2899. doi: 10.3390/molecules25122899
- Walters, R. H., and Murphy, R. M. (2011). aggregation kinetics of interrupted polyglutamine peptides. *J. Mol. Biol.* 412, 505–519. doi: 10.1016/j.jmb.2011.07.003
- Wang, W., Chen, R., Luo, K., Wu, D., Huang, L., Huang, T., et al. (2010). Calnexin inhibits thermal aggregation and neurotoxicity of prion protein. *J. Cell. Biochem.* 111, 343–349. doi: 10.1002/jcb.22698
- Weinbuch, D., Hawe, A., Jiskoot, W., and Friess, W. (2018). "Introduction into formulation development of biologics," in *Challenges in Protein Product Development*, eds N. W. Warne and H.-C. Mahler (Cham: Springer), 3–22. doi: 10.1007/978-3-319-90603-4\_1
- Westermarck, P., Benson, M. D., Buxbaum, J. N., Cohen, A. S., Frangione, B., Ikeda, S.-I., et al. (2007). A primer of amyloid nomenclature. *Amyloid* 14, 179–183. doi: 10.1080/13506120701460923
- Whitmore, L., and Wallace, B. A. (2004). DICHROWEB, an online server for protein secondary structure analyses from circular dichroism spectroscopic data. *Nucleic Acids Res.* 32, W668–W673. doi: 10.1093/nar/gkh371
- Yakupova, E. I., Bobyleva, L. G., Vikhlyantsev, I. M., and Bobylev, A. G. (2019). Congo Red and amyloids: history and relationship. *Biosci. Rep.* 39:BSR20181415. doi: 10.1042/BSR20181415

- Yang, S., Griffin, M. D. W., Binger, K. J., Schuck, P., and Howlett, G. J. (2012). An equilibrium model for linear and closed-loop amyloid fibril formation. *J. Mol. Biol.* 421, 364–377. doi: 10.1016/j.jmb.2012.02.026
- Yang, T., Li, S., Xu, H., Walsh, D. M., and Selkoe, D. J. (2017). Large soluble oligomers of amyloid  $\beta$ -protein from Alzheimer brain are far less neuroactive than the smaller oligomers to which they dissociate. *J. Neurosci.* 37, 152–163. doi: 10.1523/jneurosci.1698-16.2017
- Yoshimura, Y., Lin, Y., Yagi, H., Lee, Y.-H., Kitayama, H., Sakurai, K., et al. (2012). Distinguishing crystal-like amyloid fibrils and glass-like amorphous aggregates from their kinetics of formation. *Proc. Natl. Acad. Sci. U.S.A.* 109, 14446–14451. doi: 10.1073/pnas.1208228109
- Zaccai, N. R., Serdyuk, I. N., and Zaccai, J. (2017). *Methods in Molecular Biophysics: Structure, Dynamics, Function for Biology and Medicine*. Cambridge: Cambridge University Press. doi: 10.1017/9781107297227
- Zhao, R., So, M., Maat, H., Ray, N. J., Arisaka, F., Goto, Y., et al. (2016). Measurement of amyloid formation by turbidity assay-seeing through the cloud. *Biophys. Rev.* 8, 445–471. doi: 10.1007/s12551-016-0233-7
- Zheng, W., Schafer, N. P., and Wolynes, P. G. (2013). Frustration in the energy landscapes of multidomain protein misfolding. *Proc. Natl. Acad. Sci. U.S.A.* 110, 1680–1685. doi: 10.1073/pnas.1222130110

**Conflict of Interest:** The authors declare that the research was conducted in the absence of any commercial or financial relationships that could be construed as a potential conflict of interest.

Copyright © 2020 Martins, Navarro, Silva, Pinto, Sárkány, Figueiredo, Pereira, Pinheiro, Bednarikova, Burdukiewicz, Galzitskaya, Gazova, Gomes, Pastore, Serpell, Skrabana, Smirnovas, Ziaunys, Otzen, Ventura and Macedo-Ribeiro. This is an open-access article distributed under the terms of the Creative Commons Attribution License (CC BY). The use, distribution or reproduction in other forums is permitted, provided the original author(s) and the copyright owner(s) are credited and that the original publication in this journal is cited, in accordance with accepted academic practice. No use, distribution or reproduction is permitted which does not comply with these terms.





# Modulation of the Mechanisms Driving Transthyretin Amyloidosis

Filipa Bezerra<sup>1,2</sup>, Maria João Saraiva<sup>1,2</sup> and Maria Rosário Almeida<sup>1,2\*</sup>

<sup>1</sup> Molecular Neurobiology Group, IBMC—Instituto de Biologia Molecular e Celular, i3S—Instituto de Investigação e Inovação em Saúde, Porto, Portugal, <sup>2</sup> Department of Molecular Biology, ICBAS—Instituto de Ciências Biomédicas Abel Salazar, Universidade do Porto, Porto, Portugal

Transthyretin (TTR) amyloidoses are systemic diseases associated with TTR aggregation and extracellular deposition in tissues as amyloid. The most frequent and severe forms of the disease are hereditary and associated with amino acid substitutions in the protein due to single point mutations in the *TTR* gene (ATTRv amyloidosis). However, the wild type TTR (TTR wt) has an intrinsic amyloidogenic potential that, in particular altered physiologic conditions and aging, leads to TTR aggregation in people over 80 years old being responsible for the non-hereditary ATTRwt amyloidosis. In normal physiologic conditions TTR wt occurs as a tetramer of identical subunits forming a central hydrophobic channel where small molecules can bind as is the case of the natural ligand thyroxine (T<sub>4</sub>). However, the TTR amyloidogenic variants present decreased stability, and in particular conditions, dissociate into partially misfolded monomers that aggregate and polymerize as amyloid fibrils. Therefore, therapeutic strategies for these amyloidoses may target different steps in the disease process such as decrease of variant TTR (TTRv) in plasma, stabilization of TTR, inhibition of TTR aggregation and polymerization or disruption of the preformed fibrils. While strategies aiming decrease of the mutated TTR involve mainly genetic approaches, either by liver transplant or the more recent technologies using specific oligonucleotides or silencing RNA, the other steps of the amyloidogenic cascade might be impaired by pharmacologic compounds, namely, TTR stabilizers, inhibitors of aggregation and amyloid disruptors. Modulation of different steps involved in the mechanism of ATTR amyloidosis and compounds proposed as pharmacologic agents to treat TTR amyloidosis will be reviewed and discussed.

**Keywords:** transthyretin, amyloidosis, mechanism of disease, therapy, amyloid inhibitors

## OPEN ACCESS

### Edited by:

Christian Gonzalez-Billault,  
University of Chile, Chile

### Reviewed by:

Violaine Plante-Bordeneuve,  
Hôpitaux Universitaires Henri  
Mondor, France  
Yifat Miller,  
Ben-Gurion University of the  
Negev, Israel

### \*Correspondence:

Maria Rosário Almeida  
ralmeida@ibmc.up.pt

**Received:** 07 August 2020

**Accepted:** 18 November 2020

**Published:** 11 December 2020

### Citation:

Bezerra F, Saraiva MJ and  
Almeida MR (2020) Modulation of the  
Mechanisms Driving Transthyretin  
Amyloidosis.  
Front. Mol. Neurosci. 13:592644.  
doi: 10.3389/fnmol.2020.592644

## INTRODUCTION

Amyloidosis comprises a group of diseases which are characterized by extracellular deposition of protein aggregates, with a structure mainly composed of cross  $\beta$ -sheets, insoluble and toxic, in a range of tissues leading to the dysfunction of normal surrounding tissue (Galant et al., 2017). This review summarizes the current knowledge concerning TTR amyloidosis (ATTR amyloidosis) modulation aiming therapy and discusses the influence of other processes and factors such as proteolysis and extracellular chaperones, respectively, on TTR amyloidogenesis in order to contribute for better understanding the disease pathophysiology and for the development of new therapeutic approaches.

## TRANSTHYRETIN (TTR) STRUCTURE AND FUNCTION

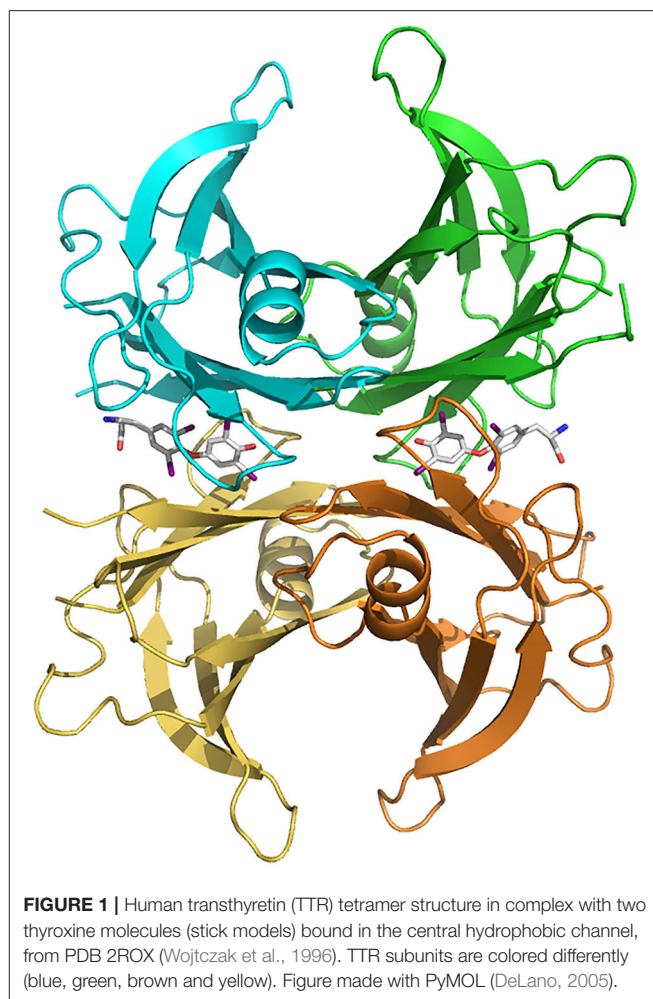
Transthyretin (TTR) is a 55 kDa homotetrameric globular protein constituted by four monomers of 127 amino acid residues (Kanda et al., 1974). It is mainly produced by the liver and choroid plexus of the brain, being then secreted into the blood and cerebrospinal fluid (CSF), respectively. However, TTR synthesis has also been described in other tissues, such as the retinal pigment epithelia (RPE), a monolayer of cells acting as a blood barrier for the retina, which in turn secretes TTR to the vitreous humor (Richardson, 2009). Low levels of TTR expression were also found in Schwann cells of the sciatic nerve, as described by Murakami et al. (2010).

TTR structure was firstly determined in the seventies by Blake and collaborators (Blake et al., 1978), who described that each TTR monomer is organized into two four-stranded anti-parallel  $\beta$ -sheets (A through H) and a short  $\beta$ -helix located on  $\beta$ -strand E (Blake et al., 1978); two monomers are connected through hydrogen bonds between the two H strands of neighboring monomers resulting in a very stable dimer. The association of two dimers, mainly through hydrophobic interactions between residues of the AB to GH loops results in the formation of the TTR tetramer (Blake et al., 1978; Yokoyama et al., 2012).

TTR mainly functions as a carrier protein (Buxbaum and Reixach, 2009; Vieira and Saraiva, 2014). The homotetrameric structure of native TTR forms a central hydrophobic channel that harbors two thyroxine ( $T_4$ ) binding sites at the dimer-dimer interface (Blake et al., 1974) (**Figure 1**). However, due to negative cooperativity, only one molecule of  $T_4$  is transported by TTR (Andrea et al., 1980). In humans, around 15% of plasma  $T_4$  is transported by TTR, whereas in rodents this percentage increases to 50% (Vieira and Saraiva, 2014). In the CSF, TTR is the major carrier of  $T_4$ , transporting around 80% of the hormone in both humans and rodents (Hu et al., 2006), being recently described as essential for the retention of  $T_4$  in the CSF (Chen et al., 2016).

The TTR tetramer has four additional binding sites at the protein's surface for retinol-binding protein (RBP), two in each dimer. Due to steric hindrance, only two RBP molecules may effectively bind to TTR but, since the RBP levels in plasma are lower than TTR, only one RBP molecule is effectively bound to the TTR tetramer (Folli et al., 2010). The assembly of this TTR-RBP complex is essential for the transport of retinol (or vitamin A), allowing its delivery to the cells (Raghu and Sivakumar, 2004). Indeed, studies in TTR knockout mice revealed a decrease in both retinol and RBP levels in plasma (van Bennekum et al., 2001), as well as an accumulation of hepatic RBP (Wei et al., 1995), comparatively to wild-type mice. Altogether these results suggest the pivotal role of TTR as a carrier of the retinol-RBP complex preventing its glomerular filtration by the kidney (Wei et al., 1995; van Bennekum et al., 2001; Gaetani et al., 2002).

Besides its functions as carrier protein, a proteolytic activity has been attributed to TTR. A small fraction of plasma TTR (1–2%) was found associated with high density lipoproteins (HDL) via apolipoprotein AI (apoA-I) (Sousa et al., 2000) and,



later, the capacity of TTR to cleave apoA-I carboxyl terminal domain *in vitro* was also demonstrated (Liz et al., 2004). In addition to apoA-I, TTR is also involved on the cleavage of both neuropeptide Y (NPY) (Liz et al., 2009) and A $\beta$  peptide (Costa et al., 2008), suggesting an important role of TTR-mediated proteolysis either in physiologic or pathologic conditions, with major impacts on the biology of nervous system and Alzheimer's disease, respectively (Liz et al., 2010).

A neuroprotective role of TTR has also been described under conditions of cerebral ischemia in mice deficient for heat shock transcription factor 1 (HSF1), an activator of heat-shock proteins. Under conditions of compromised heat-shock response, TTR from CSF contributes to control neuronal cell death, edema and inflammation, thereby influencing the survival of endangered neurons in cerebral ischemia (Santos et al., 2010). More recent work, indicates that TTR acts as neurotrophic factor, through interaction with megalin, stimulating neurite outgrowth and promoting neuroprotection in ischemic conditions (Gomes et al., 2016, 2019).

## TRANSTHYRETIN-RELATED AMYLOIDOSIS

Transthyretin amyloidosis (ATTR amyloidosis) is a group of diseases in which TTR variants (ATTRv) or even the wild-type protein (ATTRwt) aggregate and form amyloid fibrils that deposit extracellularly in tissues (Sipe et al., 2016). These are, respectively, hereditary and non-hereditary forms of the disease. The non-hereditary form is related to alterations of environmental conditions and aging leading to the aggregation and fibril formation of wild type TTR, ATTRwt (Sipe et al., 2016). Thus, ATTRwt amyloidosis is mainly an age-related disorder, affecting 12–25% of the population over 80 years-old and is characterized by ATTRwt deposition, particularly in the heart, affecting cardiac functions (Westermarck et al., 2003). In contrast, the hereditary forms of the disease, ATTRv amyloidosis result from single point mutations in the coding region of the *TTR* gene, mainly producing less stable variant proteins with an altered amino acid in the polypeptide chain, ATTRv (Saraiva, 1995). Accordingly, to date, more than 140 mutations on the *TTR* gene have been described (<http://amyloidosismutations.com/mut-attr.php>) (Connors et al., 2003). Among these, only about 15 TTR variants are reported as non-amyloidogenic, while most TTR point mutations induce systemic amyloidosis with predominant neuropathic (Plante-Bordeneuve and Said, 2011), or cardiac phenotypes (Rapezzi et al., 2010). However, most of the variants have been associated with a mixed phenotype, characterized by varying degrees of neurological and cardiac involvement (Conceicao et al., 2019). Less frequently, manifestations of ATTR amyloidosis include vitreous opacities (Ando et al., 1997) and, in rare cases, leptomeningeal amyloidosis (Maia et al., 2015).

The substitution of valine for methionine at position 30 (V30M) in the TTR polypeptide chain was the first mutation to be identified and, is the most common mutation associated with ATTR polyneuropathy (ATTR-PN) (previously designated familial amyloid polyneuropathy—FAP) (Saraiva et al., 1984). This life-threatening disease, first described by Corino de Andrade (Andrade, 1952) mainly affects both peripheral and autonomic nervous system, being sensorimotor polyneuropathy, autonomic dysfunction and gastrointestinal tract disturbances the major clinical manifestations which may lead to death within 10 years after disease onset if not treated (Ando et al., 2005; Conceicao et al., 2016).

The prevalence of ATTR V30M amyloidosis is estimated to be 0.87–1.1 per 1 000 000 individuals (Adams et al., 2014) and the disease has been considered endemic in the north of Portugal (Sousa et al., 1995), Japan (Kato-Motozaki et al., 2008), and Sweden (Sousa et al., 1993). Individuals from Portugal and some provinces in Japan typically manifest early-onset and high-penetrance phenotype, whereas people in Sweden and, also in other Japanese regions usually present late-onset and low-penetrance disease (Plante-Bordeneuve and Said, 2011).

Besides peripheral neuropathy, cardiomyopathy is also one of the major clinical manifestations of ATTR amyloidosis (ATTR-CM) (Suhr et al., 2003). In addition to ATTRwt, which is the

main cause of ATTR-CM, as mentioned above, some non-V30M mutations on *TTR* gene also lead to the development of cardiac symptoms (Westermarck et al., 1990). In particular, TTR V122I is the most common variant responsible for ATTR-CM being almost exclusively found in 3–4% of African-Americans and, the predominant phenotype associated with this mutation is severe restrictive cardiomyopathy with late-onset, i.e., occurs mainly after the age of 60, without neurological symptoms (Jacobson et al., 1997; Quarta et al., 2015; Buxbaum and Ruberg, 2017). There are also other TTR variants responsible for the development of cardiac amyloidosis, such as T49A, S50I, T60A, I68L, and L111M (Rapezzi et al., 2015; Sekijima, 2015).

In patients with ATTR-CM, amyloid fibrils can infiltrate any or all cardiovascular structures including conduction system, the atrial and ventricular myocardium, valvular tissue and, the coronary and large arteries (Falk and Dubrey, 2010). Myocardial infiltration results in progressive increase in the thickness of left and right ventricular walls and of the interatrial septum, ultimately leading to heart failure (Rapezzi et al., 2010).

The diagnosis of ATTR-CM firstly includes echocardiogram and electrocardiogram (Donnelly and Hanna, 2017). However, myocardial scintigraphy using bone avid tracers, in particular, technetium-based isotopes, such as <sup>99m</sup>technetium 3,3-diphosphono-1,2-propanodicarboxylic acid, pyrophosphate and hydroxymethylene diphosphonate revealed high sensitivity and specificity to cardiac ATTR amyloid deposits. In fact, these agents allow to identify deposits before increasing myocardial wall thickness, contributing to early diagnosis of ATTR-CM (Maurer et al., 2019). In addition, alterations in the values of cardiac biomarkers have also been increasingly helpful on the management of ATTR-CM. Indeed, clinical data from Patel and Hawkins indicate that substantial ATTR amyloid deposits accumulating in the cardiac tissue are accompanied by a moderate increase in serum levels of NT-proBNP concentration (Patel and Hawkins, 2015).

Approximately, one-fourth of the amyloidogenic *TTR* mutations originates vitreous amyloid, namely F33I, R34G, L35T, I84S, and T114C (Sekijima, 2015). It has been postulated that vitreous amyloid is the result of local TTR synthesis in the RPE cells in the eye (Ando et al., 1997). Similarly to vitreous, also leptomeningeal amyloidosis may be related to local TTR synthesis, in this case by choroid plexus and, amyloid deposition mainly occurs in the media and adventitia of medium-sized and small arteries, arterioles and veins of the cortex and leptomeninges. These amyloid infiltrations induce cerebral infarction, cerebral hemorrhage, subarachnoid hemorrhage and hydrocephalus, ultimately leading to serious central nervous dysfunctions, namely ataxia and dementia (Maia et al., 2015; Sekijima, 2015). Till now, leptomeningeal amyloidosis is mainly associated with D18G, A25T, and T114C TTR mutations (Sekijima, 2015). However, in some cases, leptomeningeal amyloidosis may also develop in patients with V30M mutation (Maia et al., 2015).



## TTR AMYLOID FORMATION

The hallmark of ATTR amyloidosis is the extracellular deposition of aggregated TTR or TTR fibrils in tissues. The process of TTR aggregation and fibril formation is not completely elucidated however biochemical and biophysical evidences indicate that the tetrameric form of TTR becomes unstable and the protein dissociates into dimers and monomers presenting a partially unfolded conformation which self-assemble into toxic non-fibrillar aggregates and, later into amyloid fibrils that accumulate as amyloid deposits throughout the body (Quintas et al., 2001; Cardoso et al., 2002).

*In vivo* the amyloid deposits are composed also by other proteins such as serum amyloid P component (SAP) and proteoglycans (Benson et al., 2018a). In the case of ATTR amyloidosis, TTR in the amyloid deposits might be in its intact form meaning as full-length protein and as TTR fragments suggesting that proteolysis might contribute as a mechanism of amyloid formation.

Knowledge of the mechanisms involved in TTR amyloid formation allows establishing therapeutic targets to avoid and/or halt the progression of disease. In this sense several therapeutic strategies have been pursued targeting different stages of the process of amyloid formation or clearance of pre-formed fibrils. The main targets have been lowering or silencing TTR, TTR stabilization, inhibition of TTR fibril formation and fibril disruption that will be discussed below.

## ATTR AMYLOIDOSIS THERAPIES TARGETING TTR SYNTHESIS

TTR variants are the main component of amyloid deposits in ATTRv amyloidosis, therefore abolishment of TTR synthesis was one of the first proposed therapeutic approaches in these diseases. Since the liver is the main organ producing and secreting TTR into blood, liver transplant emerged as a possible therapeutic strategy for ATTR amyloidosis (Lewis et al., 1994). Indeed, orthotopic liver transplant (OLT) was shown to arrest disease progression through suppression of mutant TTR from circulation and has been the most effective treatment for ATTR amyloidosis (Benson, 2013; Ericzon et al., 2015). Despite the favorable prognosis observed in transplanted patients, there are still some concerns and long-term complications since the previously existing hereditary amyloid deposits may recruit newly circulating TTR wt promoting amyloid growth and, ultimately resulting in disease progression (Maurer et al., 2016; Saelices et al., 2018). Additionally, there are reports of continuous amyloid deposition even after liver transplantation, mainly in cardiac tissue of transplanted TTR V30M carriers (Okamoto et al., 2011), as well as in the vitreous humor (Munar-Ques et al., 2000; Ando et al., 2001) and leptomeninges (Sekijima et al., 2016). This may be due to the recruitment of newly circulating TTR wt by the previously existing amyloid deposits, mainly in the heart or due to the local TTR synthesis in the eye and choroid plexus of the brain, in either case this might result in amyloid

growth and disease progression (Maurer et al., 2016; Saelices et al., 2018). On the other hand, in the case of domino liver transplant (DLT), in which the liver excised from ATTRv patient is transplanted to patients with severe liver disease, the recipients developed symptoms related to ATTR amyloidosis (Stangou et al., 2005; Goto et al., 2006; Barreiros et al., 2010). In addition, post-mortem analysis indicated that systemic amyloid deposition occurred before the appearance of the symptoms (Koike et al., 2011). Interestingly, the clinical manifestations of acquired ATTR amyloidosis after DLT are predominantly related to sensory deficits contrary to the predominant autonomic symptoms in the donors (Stangou et al., 2005; Goto et al., 2006; Barreiros et al., 2010).

The previous findings of continuous amyloid deposition, even after OLT, as well as the knowledge that TTR wt may also aggregate into amyloid fibrils (Westermarck et al., 2003), led to an increasing interest in less invasive treatments aiming also to arrest TTR synthesis through gene silencing as a new strategy for the treatment of ATTR amyloidosis. Two different gene-silencing approaches have been developed. One is based on antisense nucleotides (ASOs) and the other on small-interfering RNA (siRNA) (Gertz et al., 2019).

TTR specific siRNAs were firstly tested in mouse models of ATTR amyloidosis and a reduction on amyloid deposition was observed, inducing ATTR amyloid regression (Butler et al., 2016). Different siRNAs with similar mechanism of action were further assessed, in particular patisiran and revusiran, being patisiran the one selected for phase III clinical trials (Coelho et al., 2013). Prolonged administration of patisiran in an open-label study for an extended period of 29 months demonstrated a consistent lowering of plasma TTR levels resulting in disease stabilization and absence of major safety concerns, confirming its indication for ATTR amyloidosis therapy (Adams et al., 2018).

More recently, a novel liver-directed siRNA conjugate, vutrisiran, has been formulated. Vutrisiran is a GalNAc-siRNA conjugate presenting improved pharmacokinetic and pharmacodynamic properties allowing potent and sustained TTR reduction and an acceptable safety profile with mild treatment-related adverse effects as found in a phase I clinical trial enrolling healthy individuals (Habtemariam et al., 2020). These improved characteristics suggest vutrisiran as a novel promising therapy for the treatment of ATTR amyloidosis.

Furthermore, a second-generation ASOs (e.g., IONIS-TTRRx or Inotersen) was reported to be effective by decreasing TTR plasma levels in both monkeys and ATTR I84S transgenic mice. Experiments in healthy humans also revealed a decrease in TTR wt plasma concentrations in a dose-dependent manner (Ackermann et al., 2016). More recent results from phase 3 clinical trial studies with these two gene silencers, patisiran and inotersen, reveal that both are able to efficiently reduce TTR synthesis and arrest disease progression though with some differences in the form and frequency of the therapeutic administration and safety monitoring (Adams et al., 2018; Benson et al., 2018b; Gertz et al., 2019; Koike and Katsuno, 2020).



## ATTR AMYLOIDOSIS THERAPIES TARGETING AMYLOID FORMATION

Several compounds have been suggested for the treatment of ATTR amyloidosis by targeting different steps of the amyloid formation. The main steps include TTR stabilization, inhibition of oligomerization and fibril disruption. The most relevant compounds are listed in **Table 1** and will be discussed in the following sections. In the recent years, computational studies, such as molecular dynamics (MD) simulations, molecular docking and quantitative structural-activity relationships (SAR) have been used as complement of experimental approaches to better understand TTR monomer misfolding mechanisms-driving TTR amyloidogenesis (Zhou et al., 2019), as well as the binding of small molecules to TTR (Dessi et al., 2020). Indeed, these *in silico* experiments have been essential to obtain a more detailed information about structural changes in biomolecules and, have been used to determine the structural dynamics of TTR (Ortore and Martinelli, 2012; Zhao and Lei, 2014), which in turn will be particularly relevant to the development of more targeted and effective therapies for the treatment of ATTR amyloidosis.

### TTR Stabilization

TTR tetramer stability is a determinant factor conditioning tetramer disassembly, the rate-limiting step for aggregation and amyloid fibrils formation (McCutchen et al., 1993; Quintas et al., 1999). Accordingly, the development of small molecules able to stabilize the TTR tetramer, preventing its dissociation into monomers, has been recognized as a great therapeutic strategy for the treatment of ATTR amyloidosis. The design of these molecules was based on the affinity of T<sub>4</sub> to bind to the central pocket of the TTR tetramer inhibiting its dissociation (Mirov et al., 1996). Based on the capacity of the nonsteroidal anti-inflammatory drugs (NSAIDs), to bind to the T<sub>4</sub>-binding channel in TTR (Baures et al., 1999; Miller et al., 2004), the first drug to be tested was diflunisal, which was reported as an effective stabilizer of the TTR tetramer in plasmas from ATTR-PN patients (Tojo et al., 2006). Then, ATTRv patients were randomly assigned to receive diflunisal for 2 years and, in fact, the use of diflunisal reduced the rate of progression in neurologic impairment and preserved the quality of life of patients comparatively to placebo group (Berk et al., 2013) and ameliorated the autonomic symptoms in ATTRv patients (Takahashi et al., 2014). However, diflunisal administration to these patients induced long-term side effects, namely impaired renal function and thrombocytopenia (Sekijima et al., 2015), which may compromise its clinical value.

Following, other pharmacologic molecules, such as tafamidis (a benzoxazole derivative) (Vyndaqel®) have been proposed through a structure-based drug design approach to select compounds to occupy these T<sub>4</sub>-binding sites, kinetically stabilizing the TTR tetramer, and ultimately resulting in a decrease in the rate of amyloid fibril formation *in vitro* (Bulawa et al., 2012). One of the major concerns about the use of tafamidis in ATTRv patients is related to potential metabolic side effects, since it could interfere with T<sub>4</sub> delivery throughout the body. However, clinical trials have found minimal evidences

about this concern because thyroxine binding globulin (TBG), rather than TTR, transports the majority of the circulating T<sub>4</sub> (~75%) (Refetoff, 2000; Coelho et al., 2012). Tafamidis has gained approval for the treatment of ATTRv amyloidosis in several countries, including in the European Union, Mexico, Argentina, Japan and more recently also in the USA for the treatment of ATTR-CM (Coelho et al., 2016). Moreover, an open-label extension study for 6 years also revealed the slowing of neuropathy progression without unexpected adverse effects (Barroso et al., 2017). Recently, the effects of tafamidis on ATTR-CM were also evaluated in both ATTRv and ATTRwt patients in a phase III clinical trial significantly reducing mortality and cardiovascular-related hospitalizations (Maurer et al., 2018).

Most studies for the development of efficient TTR stabilizers were based on rational ligand design and, thus most of the stabilizers are, in general, halogenated biaryl analogs of T<sub>4</sub>, many resembling NSAIDs. However, these molecules act as cyclooxygenase (COX) inhibitors increasing the risk of severe cardiovascular events therefore being contraindicated in patients with ATTR-CM (Mukherjee et al., 2001). Moreover, high-throughput screening studies pointed out a new compound, AG10, as an effective and selective stabilizer of the cardiac TTRwt and TTR V122I protecting human cardiomyocytes from TTR amyloid toxicity (Alhamadsheh et al., 2011; Penchala et al., 2013). Interestingly, structural studies revealed that AG10 is unique in its capacity to form hydrogen bonds with the same serine residues at position 117 that stabilize the non-amyloidogenic TTR T119M variant (Miller et al., 2018). Recent results from phase II clinical trials revealed that AG10 has the potential to be safe and effective for the treatment of ATTR-CM patients either carrying mutant or TTR wt. Phase III clinical trials with AG10 are ongoing (Judge et al., 2019).

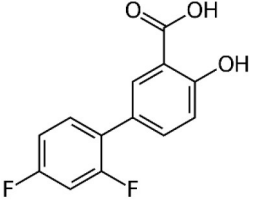
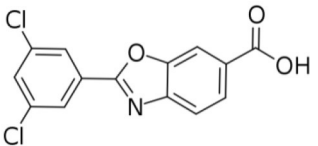
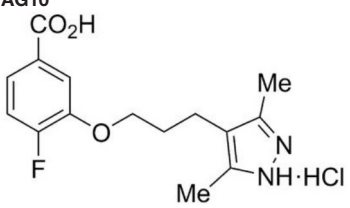
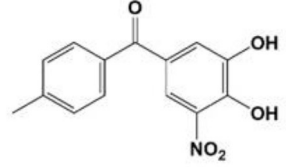
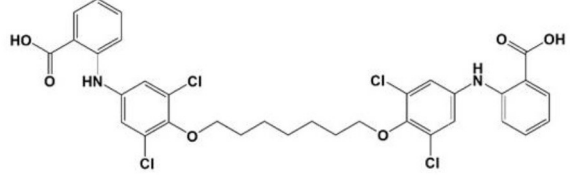
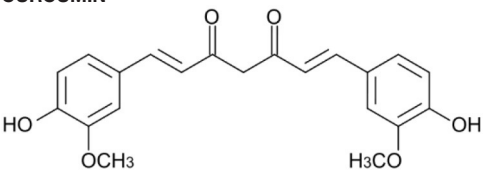
In addition, based in its molecular structure, tolcapone, an FDA-approved drug for the treatment of Parkinson's disease, has been repurposed for the treatment of ATTR amyloidosis. Tolcapone specifically binds to TTR in human plasma and, stabilizes the native TTR tetramer *in vivo* in mice and humans. Furthermore, it was also demonstrated that the binding of tolcapone to the recombinants TTR wt and TTR V122I, at the T<sub>4</sub>-binding channel is stronger comparatively to tafamidis (Sant'Anna et al., 2016). These results pointed-out tolcapone as a strong candidate for the treatment of ATTR polyneuropathy and, in fact, it has gained clinical interest and it already passed phase I/II clinical trials (Gamez et al., 2019). A very recent work on the structural characterization of Tolcapone-TTR complexes demonstrates high stabilization and binding affinity of Tolcapone to TTR variants associated with leptomeningeal amyloidosis. These characteristics in association with its ability to cross the blood-brain barrier suggests its particular indication for therapeutic intervention in this type of amyloidosis (Pinheiro et al., 2020).

Contrarily to the above-mentioned compounds, palindromic ligands, such as mds84, rapidly bind simultaneously to both T<sub>4</sub>-binding sites in each tetrameric TTR molecule, which would overcome the problems of negative cooperativity of the binding of the existing drugs, such as tafamidis. Mds84 binds to the native TTR wt in whole serum and, more effectively to

the amyloidogenic TTR variants, promoting the stabilization of the TTR tetramer (Kolstoe et al., 2010; Corazza et al., 2019).

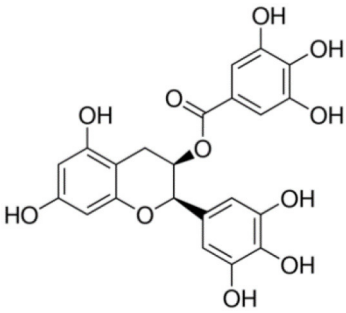
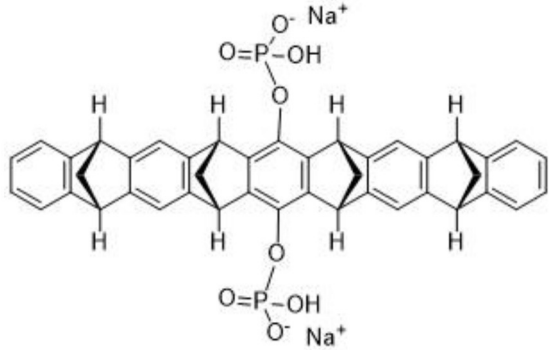
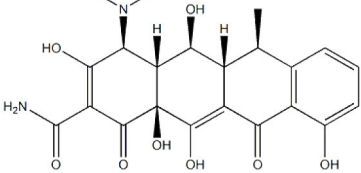
Some plant polyphenols which may be part of our diet have also been reported as TTR tetrameric stabilizers. In particular, epigallocatechin-3-gallate (EGCG) and curcumin, the major

**TABLE 1** | Compounds proposed for the treatment of ATTR amyloidosis.

Compound/structure	Activity	References
<b>DIFLUNISAL</b> 	Binding at the thyroxine binding sites/TTR stabilization	Tojo et al., 2006; Berk et al., 2013; Takahashi et al., 2014
<b>TAFAMIDIS</b> 	Binding at the thyroxine binding sites/TTR stabilization	Bulawa et al., 2012; Coelho et al., 2016; Barroso et al., 2017; Maurer et al., 2018
<b>AG10</b> 	Binding at the thyroxine binding sites/TTR stabilization	Alhamadsheh et al., 2011; Penchala et al., 2013; Miller et al., 2018; Judge et al., 2019
<b>TOLCAPONE</b> 	Binding at the thyroxine binding sites/TTR stabilization	Sant'Anna et al., 2016; Gamez et al., 2019; Pinheiro et al., 2020
<b>mds84</b> 	Binding at the thyroxine binding sites-bivalent ligand/TTR stabilization	Kolstoe et al., 2010; Corazza et al., 2019
<b>CURCUMIN</b> 	Binding at the thyroxine binding sites/TTR stabilization	Ferreira et al., 2011, 2013, 2016, 2019

(Continued)

TABLE 1 | Continued

Compound/structure	Activity	References
<b>EGCG</b> 	TTR stabilization /inhibition of aggregation (oligomerization)/Disruption of aggregates	Ferreira et al., 2009, 2011, 2012
<b>Molecular tweezer CLR01</b> 	Inhibition of aggregation (oligomerization)/Disruption of aggregates	Sinha et al., 2011; Ferreira et al., 2014
<b>DOXYCYCLINE</b> 	Disruption of TTR aggregates	Cardoso et al., 2003, 2008; Cardoso and Saraiva, 2006

components of green tea and turmeric, respectively, were able to effectively stabilize the TTR tetramer in human plasmas from both V30M carriers and controls (Ferreira et al., 2011), as well as in plasmas from transgenic mice carrying human TTR V30M variant (HM30 mice) (Ferreira et al., 2012, 2013). It should be noted that these compounds exhibit different ways of action. Curcumin competes with T<sub>4</sub> for the binding to TTR, meaning that it binds at the T<sub>4</sub> binding sites, whereas EGCG stabilizes TTR through binding at the surface of the TTR molecule in particular at two binding sites at the dimer-dimer interface exerting an effect similar to a cross-linker. Low bioavailability and low specificity of binding seem to be relevant conditioning factors of their effects *in vivo* in humans (Kristen et al., 2012; aus dem Siepen et al., 2015; Cappelli et al., 2018).

### Inhibition of TTR Aggregation Into Amyloid Fibril

TTR stabilizers, as the above-mentioned small molecule compounds, including EGCG, curcumin, tolcapone and mds84

have also been reported as inhibitors of TTR amyloid formation as consequence of their effect on the first step of TTR aggregation.

Ferreira *et al.* firstly described EGCG as a strong inhibitor of TTR aggregation *in vitro* (Ferreira et al., 2009), by maintaining most of the protein in a non-aggregated soluble form. EGCG also suppressed the amyloid fibril formation pathway in a cell culture system (Ferreira et al., 2009). Later, the role of EGCG on the inhibition of amyloid fibril formation *in vivo* using a well-characterized transgenic murine model of ATTR-PN was also demonstrated. EGCG reduced, in about 50%, the deposition of TTR toxic aggregates in the gastro-intestinal tract and peripheral nervous system (PNS), with a concomitant decrease in the expression of both non-fibrillar-related biomarkers and amyloid deposition markers (Ferreira et al., 2012).

Similar studies using curcumin demonstrated suppression of fibril formation *in vitro* through the generation of small “off-pathway” oligomers (Ferreira et al., 2011) and inhibited this process in transgenic mice carrying human TTR V30M variant. In fact, immunohistochemical analysis of mice tissues revealed

that dietary curcumin decreased TTR load in as much as 70% and lowered the cytotoxicity associated with TTR aggregation (Ferreira et al., 2013). Later, it has been shown that dietary curcumin decreases TTR deposition and associated toxicity in the dorsal root ganglia and stomach of aged mice carrying human TTR V30M variant (Ferreira et al., 2016).

Furthermore, synthetic compounds such as tolcapone and mds84 effectively inhibited the process of TTR fibril formation *in vitro* (Kolstoe et al., 2010; Sant'Anna et al., 2016) and, tolcapone was also able to suppress TTR toxicity in cellular models (Sant'Anna et al., 2016).

However, some inhibitors of amyloid formation might act on a different step of the cascade leading to fibril formation that includes, for instance, the polymerization of the intermediate species originating aggregates that evolve to amyloid fibrils. That is the case of the molecular tweezer CLR01 (Sinha et al., 2011). This is a synthetic compound that through binding to positively charged amino acids, in particular lysine and arginine residues in the terminal beta-strands of TTR, inhibit the tight alignment of protofilaments characteristic of amyloid formation. Thus, the molecular tweezer CLR01 inhibited TTR aggregation *in vitro* and also *in vivo* as demonstrated in a study in which TTR V30M mice treated with CLR01 presented decrease of TTR deposition and of associated biomarkers (Ferreira et al., 2014). However, this compound presents limitations related to the low binding affinity to proteins and to its formulation needing improvement of pharmacologic properties.

## Disruption of Aggregates

The role of anthracyclines and, in particular of 4'-iodo-4'-deoxydoxorubicin on the reabsorption of amyloid deposits was related to the almost planar structure of these compounds and the cross  $\beta$ -pleated structure characteristic of all amyloid fibrils (Merlini et al., 1995). Furthermore, doxycycline, a member of tetracycline antibiotics family, structurally homologous to the anthracyclines, was found to be particularly effective on the disruption of TTR amyloid fibrils *in vitro* (Cardoso et al., 2003). In addition, *in vivo* studies on transgenic mice carrying human TTR V30M variant supported the previous *in vitro* findings. Doxycycline was administered to old transgenic mice and, tissue analysis revealed Congo red positive staining only for the non-treated animals from the control group. Additionally, a decrease in several markers associated with TTR amyloid deposition was also reported (Cardoso and Saraiva, 2006; Cardoso et al., 2008). The recent development of doxycycline conjugates, namely polyglutamate-doxycycline, demonstrated an enhanced effect in the clearance of fibrils comparatively to non-conjugated doxycycline only (Conejos-Sanchez et al., 2015).

Since doxycycline has effect only in advanced phases of the amyloidogenic cascade it has been proposed that it could be combined with another drug targeting an earlier phase of the amyloid fibrils assembly (Cardoso et al., 2010). In this sense, tauroursodeoxycholic acid (TUDCA), a hydrophilic biliary acid derivative, gained particular clinical interest for the treatment of ATTR amyloidosis since it has been previously referred to cause a decrease in the deposition of toxic pre-fibrillar TTR oligomers and to reduce the expression of several apoptotic and

oxidative biomarkers associated with ATTR amyloid deposition in transgenic murine models treated with TUDCA (Macedo et al., 2008; Cardoso et al., 2010). Clinical trials of combined doxycycline and TUDCA are underway and preliminary results indicate positive effects though more results are necessary to evaluate the impact of this therapeutic approach in disease progression (Obici and Merlini, 2014).

Moreover, some therapeutic compounds are classified as multi-target disease agents, performing a role in different steps of amyloid fibril formation. For instance, compounds such as EGCG and curcumin besides its effects as inhibitors of aggregation act also as disruptors of TTR amyloid deposits. In fact, both natural polyphenols, EGCG and curcumin, efficiently disaggregated pre-formed TTR amyloid fibrils (Ferreira et al., 2011) (Ferreira et al., 2019). Recent studies using transgenic murine models pointed out both curcumin and TUDCA as modulators of cellular autophagy processes, which are involved in the clearance of large protein aggregates (Teixeira et al., 2016).

## Immunotherapy

Immunotherapy is another therapeutic strategy for the treatment of ATTR amyloidosis, which still remains under investigation. Specific antibodies targeting TTR monomers, oligomers or amyloid aggregates may prevent TTR fibrillogenesis. As a first approach, a structure-based strategy was used to develop a TTR conformation-specific antibody targeting pre-fibrillar, misfolded TTR intermediates without recognizing native tetrameric TTR. This is achieved since the antibody (misTTR) targets the residues 89–97 in the polypeptide chain, which are buried in the TTR tetramer, but it is exposed in the monomer, inhibiting fibrillogenesis of misfolded TTR under micromolar concentrations (Galant et al., 2016). This antibody has already entered into phase I clinical trials in ATTRv patients (Macedo et al., 2020).

## CONTRIBUTION OF TTR PROTEOLYSIS TO AMYLOID FORMATION

Since a long time ago, TTR proteolysis has been suggested to be involved in the mechanisms driving TTR-related amyloidosis (Pitkanen et al., 1984). Therefore, by understanding in detail the molecular mechanisms implicated in the pathophysiology of ATTR amyloidosis, it would be possible to develop new targeted therapies to improve the patients' outcomes.

Several evidences suggest the existence of different types of TTR amyloid fibrils in a range of tissues. In fact, amyloid deposits might be composed by a mixture of both cleaved and full-length TTR (type A) or full-length TTR only (type B). The resulting amyloid deposits are different. Type A fibrils are shorter and exhibit weaker affinity for Congo Red staining than type B fibrils, which are longer, slender and strongly stain with Congo Red (Bergstrom et al., 2005; Ihse et al., 2008, 2011).

Different amyloidogenic fragments may be found in different tissues and could be associated either with ATTRwt or ATTRv amyloidosis (Suhr et al., 2017). Vitreous TTR appeared to be fragmented between the residues Lys48-Thr49, whereas cardiac



TTR may be cleaved at multiple sites between the 46–52 amino acid residues in polypeptide chain (Liepnieks et al., 2006). However, peptide 49–127 C-terminal fragment is the main component of *ex vivo* TTR amyloid fibrils in tissue biopsies of cardiac deposits, which is further associated with poor clinical prognosis, often with rapidly progressive cardiac involvement, even after liver transplantation (Gustafsson et al., 2012; Ihse et al., 2013).

The protease responsible for TTR cleavage has not yet been identified. However, the highly specific fragmentation pattern suggests that it could be a trypsin-like serine protease. The three-dimensional structure of this protein region is solvent exposed and potentially accessible for cleavage. In accordance, all amyloidogenic TTR variants showed an increased main chain solvent exposure comparatively to both native and non-amyloidogenic variants, which may result in increased susceptibility to proteolysis (Schormann et al., 1998).

Recent *in vitro* studies, using recombinant trypsin, revealed that the proteolysis/fibrillogenesis pathway is common to several amyloidogenic TTR variants and, the process of cleavage and release of the 49–127 TTR fragment is faster for the highly amyloidogenic variant, TTR S52P, than for the other TTR variants analyzed (Mangione et al., 2014; Marcoux et al., 2015). It requires the action of biomechanical forces provided by shear stress of physiological fluid flow and, importantly, the non-amyloidogenic TTR T119M is neither cleaved nor generates amyloid fibrils under these conditions. These studies also demonstrated that the TTR stabilizers, mds84, tolcapon, diflunisal and tafamidis, inhibited TTR proteolysis resulting in the inhibition of aggregation. However, the maximum inhibition is only achieved when both T<sub>4</sub>-binding sites in central hydrophobic channel are simultaneously occupied by small ligands (Mangione et al., 2014; Verona et al., 2017). In opposition, natural TTR ligands, T<sub>4</sub> and RBP, were not able to inhibit TTR cleavage. Nevertheless, binding of RBP, but not T<sub>4</sub>, effectively inhibited the subsequent formation of amyloid fibrils (Mangione et al., 2014).

Due to the exclusive duodenal location of trypsin, it is unlikely that it may contribute to the development of systemic TTR amyloidosis *in vivo*. In *silico* studies recently pointed out plasmin as a plausible pathophysiological candidate protease involved in the process of TTR amyloid formation (Mangione et al., 2018). Furthermore, the ubiquitous distribution of plasmin, its structural similarities to trypsin (Mangione et al., 2018) and the reported activation of plasminogen activation system (PAS) in other amyloid-related disorders, such as Alzheimer's disease (Tucker et al., 2000) and immunoglobulin light chain (AL) amyloidosis (Mumford et al., 2000; Bouma et al., 2007; Uchiba et al., 2009) also indicate that this protease could perform a key role in TTR amyloidogenesis.

Recent studies showed that amorphous protein aggregates are degraded by plasmin, releasing smaller soluble protein fragments, which are cytotoxic *in vitro* for both endothelial and microglial cells (Constantinescu et al., 2017).

Plasmin, similarly to trypsin, selectively cleaves TTR S52P variant, at Lys48-Thr49 peptide bond under physiological conditions *in vitro* being, both the TTR fragments and

full-length protomers readily released from the homotetramer and incorporated into amyloid fibrils, morphologically identical to *ex vivo* TTR amyloid (Mangione et al., 2018). Concerning these observations, a hypothetical model for the role of plasmin-mediated proteolysis on TTR fibrillogenesis has been proposed. In this model, circulating TTR can diffuse toward the extracellular compartment, be entrapped in the fibrin clot or escape from it. Upon plasminogen activation, TTR may be cleaved and then dissociate into a mixture of both truncated and full-length TTR, which ultimately assemble into amyloid fibrils and deposit at the extracellular space (Mangione et al., 2018).

Altogether these evidences seem to point out the importance of lysine (Lys) residues for the pathogenicity of ATTR amyloidosis as it has been described for other amyloid disorders (Sinha et al., 2011). By targeting the Lys residues using synthetic Lys specific molecular tweezers (e.g., CLR01), the process of TTR proteolysis could be effectively inhibited through its binding to Lys48, which seem to be target of the protease responsible for TTR cleavage. This could be particularly important for the treatment of both ATTR-CM and vitreous amyloidosis, since the 49–127 TTR fragment has been frequently encountered in the amyloid deposits in both cases.

Despite the increasing interest on TTR proteolysis as leading mechanism-driving ATTR amyloidosis, some questions remain to be answered. Though, it is still unknown whether TTR fragmentation occurs prior or after aggregation and, where it occurs, in circulation or at the site of deposition, an increase of the proteolytic activity in plasmas from ATTR patients comparatively to healthy controls, suggesting that the process occurs in the bloodstream before fibril formation (da Costa et al., 2015).

## EXTRACELLULAR CHAPERONES AS REGULATORS OF ATTR AMYLOIDOSIS

The disruption of the protein folding quality control mechanisms is also an underlying cause of ATTR amyloidosis. Recently, some studies revealed the existence of a growing family of extracellular chaperones in body fluids, which selectively bind to exposed hydrophobic residues in misfolded proteins in order to prevent their toxicity upon aggregation into insoluble deposits (Wyatt et al., 2013).

Among those extracellular chaperones, haptoglobin, alpha-2-microglobulin (A2M) and clusterin were found to be increased in plasmas from ATTR patients (da Costa et al., 2015). While haptoglobin and A2M, were previously described as effective in the inhibition of stress-induced aggregation of a number of unrelated target proteins (Yerbury et al., 2005; French et al., 2008), clusterin is an ubiquitous highly conserved secreted protein (Wyatt et al., 2009), which inhibits protein aggregation in an ATP-independent manner upon its binding to misfolded proteins, such as  $\alpha$ -synuclein and  $\beta$ -amyloid peptide, producing soluble, high molecular complexes (Matsubara et al., 1996; Poon et al., 2000; Yerbury et al., 2007).

The role of clusterin on the clearance of extracellular aggregates has also been investigated in ATTR-PN (Lee et al.,

2009; Magalhaes and Saraiva, 2011). *In vitro* studies using neuroblastoma cells incubated with TTR oligomers revealed intracellular clusterin overexpression and increased levels of clusterin secreted to the culture medium. An overexpression of clusterin in tissues with TTR deposition was found in mice carrying human TTR V30M in HSF-1 null background, which exhibit early and extensive non-fibrillar TTR deposition in the gastrointestinal tract and in the peripheral and autonomic nervous system. In addition, in human nerve, clusterin co-localizes either with fibrillar or non-fibrillar TTR deposits as detected by double immunostaining (Magalhaes and Saraiva, 2011).

Clusterin was also found in cardiac TTR amyloid deposits from patients with ATTRwt and ATTRv (Greene et al., 2011) and, later, experiments using circular dichroism spectroscopy revealed that clusterin preferentially stabilizes monomeric TTR leading to the appearance of increasingly stable conformations under acid stress. Additionally, clusterin interacts also with high molecular weight TTR aggregated species and, these interactions with both monomeric and oligomeric TTR proceed

in a cooperative manner in the presence of the TTR tetramer stabilizer, diflunisal. Altogether these observations suggest a novel synergistic treatment for ATTR amyloidosis using both diflunisal and clusterin for the removal of misfolded and aggregated TTR (Greene et al., 2015). Accordingly, preliminary data revealed a temporal increase in serum clusterin levels in patients treated with diflunisal at 1-year follow-up compared to baseline. In opposition, patients who were not treated with diflunisal demonstrated decreased clusterin levels at annual evaluation. Interestingly, a positive correlation between clusterin and TTR levels was found at baseline suggesting that soluble tetrameric TTR decreases as more of the native protein dissociates and forms species, overwhelming the protein folding capacity of clusterin leading to a reduction in circulating levels of this molecular chaperone and, the treatment of the ATTR patients with diflunisal lead to a partial recovery of serum clusterin levels (Torres-Arancibia and Connors, 2019). These results are in accordance with previous studies reporting the beneficial effects of diflunisal for the treatment of ATTRv amyloidosis.

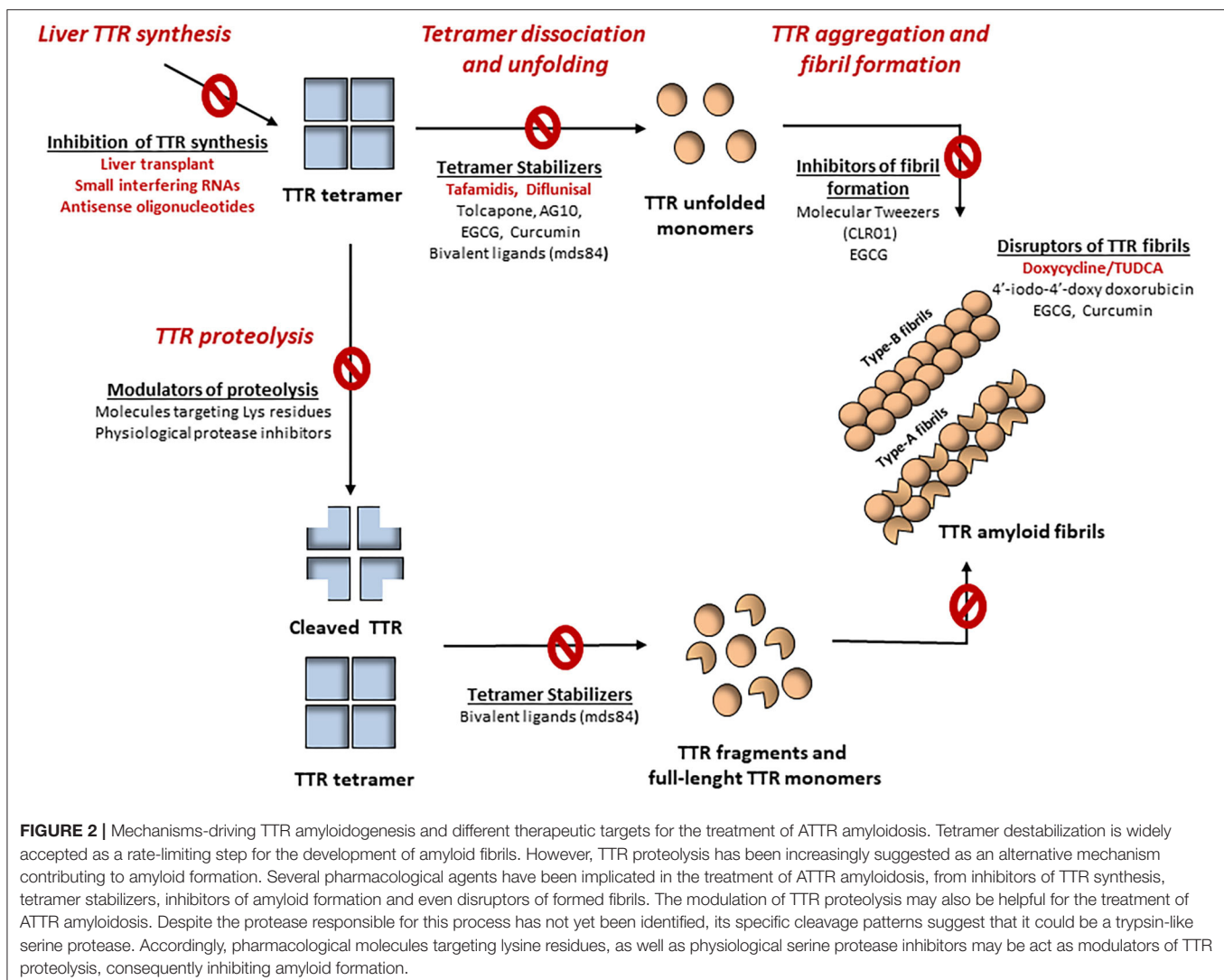


**FIGURE 2 |** Mechanisms-driving TTR amyloidogenesis and different therapeutic targets for the treatment of ATTR amyloidosis. Tetramer destabilization is widely accepted as a rate-limiting step for the development of amyloid fibrils. However, TTR proteolysis has been increasingly suggested as an alternative mechanism contributing to amyloid formation. Several pharmacological agents have been implicated in the treatment of ATTR amyloidosis, from inhibitors of TTR synthesis, tetramer stabilizers, inhibitors of amyloid formation and even disruptors of formed fibrils. The modulation of TTR proteolysis may also be helpful for the treatment of ATTR amyloidosis. Despite the protease responsible for this process has not yet been identified, its specific cleavage patterns suggest that it could be a trypsin-like serine protease. Accordingly, pharmacological molecules targeting lysine residues, as well as physiological serine protease inhibitors may be act as modulators of TTR proteolysis, consequently inhibiting amyloid formation.

## CONCLUSION AND FUTURE PERSPECTIVES

ATTR amyloidosis is an under-recognized disease which is characterized by extracellular deposition of TTR aggregates in several organs, being polyneuropathy and cardiomyopathy the major clinical manifestations. The mechanism by which the tetramer disassembles and aggregates into amyloid fibrils has been considered the main driver of the disease. However, TTR proteolysis, namely occurring in the cardiac tissue, as well as its modulation have been increasingly documented as fundamental for understanding the development and progression of ATTR amyloidosis.

Many therapeutic approaches have been suggested for the treatment of ATTR amyloidosis targeting different steps of the pathology. Those therapies include interventions from the synthesis of the TTR variants through liver transplant or gene silencing therapies, to TTR stabilization, inhibition of aggregation, disruption of amyloid fibrils and clearance of amyloid deposits. The main targets for intervention on TTR amyloid formation are summarized in **Figure 2**. Although some of the available therapies are more efficient than others, it becomes increasingly evident that combination of different therapies may improve the therapeutic outcome. In this sense, it would be interesting to test TTR gene silencing therapies in combination with protein stabilizers or disruptors of pre-existing amyloid

deposits. It is also important to obtain more efficient and targeted therapies specific to organ and tissues with limited drug access as is the case of the eye and brain, that are particularly relevant in some forms of the disease. Moreover, it is crucial to continue with studies that can contribute to a better understanding of the mechanisms involved in the disease, in particular, TTR proteolysis, which has been mainly valued in the case of ATTR-CM and, also at the extracellular level involving either interactions with components of the extracellular matrix or with molecular and chemical chaperones acting as disease modulators.

Overall, detailed knowledge of the mechanisms of amyloid formation and the availability of different approaches allows directed and personalized interventions aiming higher specificity and efficacy of chosen therapeutic solutions.

## AUTHOR CONTRIBUTIONS

FB, MS, and MA wrote and discussed the manuscript. All authors contributed to the article and approved the submitted version.

## FUNDING

FB was supported by FCT- Fundação para a Ciência e Tecnologia/MEC - Ministério da Educação e Ciência with a Ph.D. fellowship (SFRH/BD/123674/2016).

## REFERENCES

- Ackermann, E. J., Guo, S., Benson, M. D., Booten, S., Freier, S., Hughes, S. G., et al. (2016). Suppressing transthyretin production in mice, monkeys and humans using 2nd-Generation antisense oligonucleotides. *Amyloid* 23, 148–157. doi: 10.1080/13506129.2016.1191458
- Adams, D., Gonzalez-Duarte, A., O'Riordan, W. D., Yang, C. C., Ueda, M., Kristen, A. V., et al. (2018). Patisiran, an RNAi Therapeutic, for Hereditary Transthyretin Amyloidosis. *N. Engl. J. Med.* 379, 11–21. doi: 10.1056/NEJMoa1716153
- Adams, D., Theaudin, M., Cauquil, C., Algalarrondo, V., and Slama, M. (2014). FAP neuropathy and emerging treatments. *Curr. Neurol. Neurosci. Rep.* 14:435. doi: 10.1007/s11910-013-0435-3
- Alhamadsheh, M. M., Connelly, S., Cho, A., Reixach, N., Powers, E. T., Pan, D. W., et al. (2011). Potent kinetic stabilizers that prevent transthyretin-mediated cardiomyocyte proteotoxicity. *Sci. Transl. Med.* 3:97ra81. doi: 10.1126/scitranslmed.3002473
- Ando, E., Ando, Y., and Haraoka, K. (2001). Ocular amyloid involvement after liver transplantation for polyneuropathy. *Ann. Intern. Med.* 135, 931–932. doi: 10.7326/0003-4819-135-10-200111200-00026
- Ando, E., Ando, Y., Okamura, R., Uchino, M., Ando, M., and Negi, A. (1997). Ocular manifestations of familial amyloidotic polyneuropathy type I: long-term follow up. *Br. J. Ophthalmol.* 81, 295–298. doi: 10.1136/bjo.81.4.295
- Ando, Y., Nakamura, M., and Araki, S. (2005). Transthyretin-related familial amyloidotic polyneuropathy. *Arch. Neurol.* 62, 1057–1062. doi: 10.1001/archneur.62.7.1057
- Andrade, C. (1952). A peculiar form of peripheral neuropathy; familial atypical generalized amyloidosis with special involvement of the peripheral nerves. *Brain* 75, 408–427. doi: 10.1093/brain/75.3.408
- Andrea, T. A., Cavalieri, R. R., Goldfine, I. D., and Jorgensen, E. C. (1980). Binding of thyroid hormones and analogues to the human plasma protein prealbumin. *Biochemistry* 19, 55–63. doi: 10.1021/bi00542a009
- aus dem Siepen, F., Bauer, R., Aurich, M., Buss, S. J., Steen, H., Altland, K., et al. (2015). Green tea extract as a treatment for patients with wild-type transthyretin amyloidosis: an observational study. *Drug Des. Devel. Ther.* 9, 6319–6325. doi: 10.2147/DDDT.S96893
- Barreiros, A. P., Post, F., Hoppe-Lotichius, M., Linke, R. P., Vahl, C. F., Schafers, H. J., et al. (2010). Liver transplantation and combined liver-heart transplantation in patients with familial amyloid polyneuropathy: a single-center experience. *Liver Transpl.* 16, 314–323. doi: 10.1002/lt.21996
- Barroso, F. A., Judge, D. P., Ebade, B., Li, H., Stewart, M., Amass, L., et al. (2017). Long-term safety and efficacy of tafamidis for the treatment of hereditary transthyretin amyloid polyneuropathy: results up to 6 years. *Amyloid* 24, 194–204. doi: 10.1080/13506129.2017.1357545
- Baures, P. W., Oza, V. B., Peterson, S. A., and Kelly, J. W. (1999). Synthesis and evaluation of inhibitors of transthyretin amyloid formation based on the non-steroidal anti-inflammatory drug, flufenamic acid. *Bioorg. Med. Chem.* 7, 1339–1347.
- Benson, M. D. (2013). Liver transplantation and transthyretin amyloidosis. *Muscle Nerve* 47, 157–162. doi: 10.1002/mus.23521
- Benson, M. D., Buxbaum, J. N., Eisenberg, D. S., Merlini, G., Saraiva, M. J. M., Sekijima, Y., et al. (2018a). Amyloid nomenclature 2018: recommendations by the International Society of Amyloidosis (ISA) nomenclature committee. *Amyloid* 25, 215–219. doi: 10.1080/13506129.2018.1549825
- Benson, M. D., Waddington-Cruz, M., Berk, J. L., Polydefkis, M., Dyck, P. J., Wang, A. K., et al. (2018b). Inotersen treatment for patients with hereditary transthyretin amyloidosis. *N. Engl. J. Med.* 379, 22–31. doi: 10.1056/NEJMoa1716793
- Bergstrom, J., Gustavsson, A., Hellman, U., Sletten, K., Murphy, C. L., Weiss, D. T., et al. (2005). Amyloid deposits in transthyretin-derived amyloidosis: cleaved transthyretin is associated with distinct amyloid morphology. *J. Pathol.* 206, 224–232. doi: 10.1002/path.1759
- Berk, J. L., Suhr, O. B., Obici, L., Sekijima, Y., Zeldenrust, S. R., Yamashita, T., et al. (2013). Repurposing diflunisal for familial amyloid polyneuropathy: a randomized clinical trial. *JAMA* 310, 2658–2667. doi: 10.1001/jama.2013.283815
- Blake, C. C., Geisow, M. J., Oatley, S. J., Rerat, B., and Rerat, C. (1978). Structure of prealbumin: secondary, tertiary and quaternary interactions determined by Fourier refinement at 1.8 Å. *J. Mol. Biol.* 121, 339–356.

- Blake, C. C., Geisow, M. J., Swan, I. D., Rerat, C., and Rerat, B. (1974). Structure of human plasma prealbumin at 2.5 Å resolution. A preliminary report on the polypeptide chain conformation, quaternary structure and thyroxine binding. *J. Mol. Biol.* 88, 1–12.
- Bouma, B., Maas, C., Hazenberg, B. P., Lokhorst, H. M., and Gebbink, M. F. (2007). Increased plasmin-alpha2-antiplasmin levels indicate activation of the fibrinolytic system in systemic amyloidosis. *J. Thromb. Haemost.* 5, 1139–1142. doi: 10.1111/j.1538-7836.2007.02457.x
- Bulawa, C. E., Connelly, S., Devit, M., Wang, L., Weigel, C., Fleming, J. A., et al. (2012). Tafamidis, a potent and selective transthyretin kinetic stabilizer that inhibits the amyloid cascade. *Proc. Natl. Acad. Sci. U S A* 109, 9629–9634. doi: 10.1073/pnas.1121005109
- Butler, J. S., Chan, A., Costelha, S., Fishman, S., Willoughby, J. L., Borland, T. D., et al. (2016). Preclinical evaluation of RNAi as a treatment for transthyretin-mediated amyloidosis. *Amyloid* 23, 109–118. doi: 10.3109/13506129.2016.1160882
- Buxbaum, J. N., and Reixach, N. (2009). Transthyretin: the servant of many masters. *Cell. Mol. Life Sci.* 66, 3095–3101. doi: 10.1007/s00018-009-0109-0
- Buxbaum, J. N., and Ruberg, F. L. (2017). Transthyretin V122I (pV142I)\* cardiac amyloidosis: an age-dependent autosomal dominant cardiomyopathy too common to be overlooked as a cause of significant heart disease in elderly African Americans. *Genet. Med.* 19, 733–742. doi: 10.1038/gim.2016.200
- Cappelli, F., Martone, R., Taborchi, G., Morini, S., Bartolini, S., Angelotti, P., et al. (2018). Epigallocatechin-3-gallate tolerability and impact on survival in a cohort of patients with transthyretin-related cardiac amyloidosis. A single-center retrospective study. *Intern. Emerg. Med.* 13, 873–880. doi: 10.1007/s11739-018-1887-x
- Cardoso, I., Brito, M., and Saraiva, M. J. (2008). Extracellular matrix markers for disease progression and follow-up of therapies in familial amyloid polyneuropathy V30M TTR-related. *Dis. Markers* 25, 37–47. doi: 10.1155/2008/549872
- Cardoso, I., Goldsbury, C. S., Muller, S. A., Olivieri, V., Wirtz, S., Damas, A. M., et al. (2002). Transthyretin fibrillogenesis entails the assembly of monomers: a molecular model for in vitro assembled transthyretin amyloid-like fibrils. *J. Mol. Biol.* 317, 683–695. doi: 10.1006/jmbi.2002.5441
- Cardoso, I., Martins, D., Ribeiro, T., Merlini, G., and Saraiva, M. J. (2010). Synergy of combined doxycycline/TUDCA treatment in lowering Transthyretin deposition and associated biomarkers: studies in FAP mouse models. *J. Transl. Med.* 8:74. doi: 10.1186/1479-5876-8-74
- Cardoso, I., Merlini, G., and Saraiva, M. J. (2003). 4'-iodo-4'-deoxydoxorubicin and tetracyclines disrupt transthyretin amyloid fibrils in vitro producing noncytotoxic species: screening for TTR fibril disrupters. *FASEB J.* 17, 803–809. doi: 10.1096/fj.02-0764com
- Cardoso, I., and Saraiva, M. J. (2006). Doxycycline disrupts transthyretin amyloid: evidence from studies in a FAP transgenic mice model. *FASEB J.* 20, 234–239. doi: 10.1096/fj.05-4509com
- Chen, R., Chen, C. P., and Preston, J. E. (2016). Effects of transthyretin on thyroxine and beta-amyloid removal from cerebrospinal fluid in mice. *Clin. Exp. Pharmacol. Physiol.* 43, 844–850. doi: 10.1111/1440-1681.12598
- Coelho, T., Adams, D., Silva, A., Lozeron, P., Hawkins, P. N., Mant, T., et al. (2013). Safety and efficacy of RNAi therapy for transthyretin amyloidosis. *N. Engl. J. Med.* 369, 819–829. doi: 10.1056/NEJMoa1208760
- Coelho, T., Maia, L. F., Martins da Silva, A., Waddington Cruz, M., Plante-Bordeneuve, V., Lozeron, P., et al. (2012). Tafamidis for transthyretin familial amyloid polyneuropathy: a randomized, controlled trial. *Neurology* 79, 785–792. doi: 10.1212/WNL.0b013e3182661eb1
- Coelho, T., Merlini, G., Bulawa, C. E., Fleming, J. A., Judge, D. P., Kelly, J. W., et al. (2016). Mechanism of Action and Clinical Application of Tafamidis in Hereditary Transthyretin Amyloidosis. *Neurol. Ther.* 5, 1–25. doi: 10.1007/s40120-016-0040-x
- Conceicao, I., Coelho, T., Rapezzi, C., Parman, Y., Obici, L., Galan, L., et al. (2019). Assessment of patients with hereditary transthyretin amyloidosis - understanding the impact of management and disease progression. *Amyloid* 26, 103–111. doi: 10.1080/13506129.2019.1627312
- Conceicao, I., Gonzalez-Duarte, A., Obici, L., Schmidt, H. H., Simoneau, D., Ong, M. L., et al. (2016). “Red-flag” symptom clusters in transthyretin familial amyloid polyneuropathy. *J. Peripher. Nerv. Syst.* 21, 5–9. doi: 10.1111/jns.12153
- Conejos-Sanchez, I., Cardoso, I., Oteo-Vives, M., Romero-Sanz, E., Paul, A., Sauri, A. R., et al. (2015). Polymer-doxycycline conjugates as fibril disrupters: an approach towards the treatment of a rare amyloidotic disease. *J. Control Release* 198, 80–90. doi: 10.1016/j.jconrel.2014.12.003
- Connors, L. H., Lim, A., Prokaeva, T., Roskens, V. A., and Costello, C. E. (2003). Tabulation of human transthyretin (TTR) variants, 2003. *Amyloid* 10, 160–184. doi: 10.3109/13506120308998998
- Constantinescu, P., Brown, R. A., Wyatt, A. R., Ranson, M., and Wilson, M. R. (2017). Amorphous protein aggregates stimulate plasminogen activation, leading to release of cytotoxic fragments that are clients for extracellular chaperones. *J. Biol. Chem.* 292, 14425–14437. doi: 10.1074/jbc.M117.786657
- Corazza, A., Verona, G., Waudby, C. A., Mangione, P. P., Bingham, R., Uings, I., et al. (2019). Binding of monovalent and bivalent ligands by transthyretin causes different short- and long-distance conformational changes. *J. Med. Chem.* 62, 8274–8283. doi: 10.1021/acs.jmedchem.9b01037
- Costa, R., Ferreira-da-Silva, F., Saraiva, M. J., and Cardoso, I. (2008). Transthyretin protects against A-beta peptide toxicity by proteolytic cleavage of the peptide: a mechanism sensitive to the Kunitz protease inhibitor. *PLoS ONE* 3:e2899. doi: 10.1371/journal.pone.0002899
- da Costa, G., Ribeiro-Silva, C., Ribeiro, R., Gilberto, S., Gomes, R. A., Ferreira, A., et al. (2015). Transthyretin amyloidosis: chaperone concentration changes and increased proteolysis in the pathway to disease. *PLoS ONE* 10:e0125392. doi: 10.1371/journal.pone.0125392
- DeLano, W. (2005). *The PyMOL Molecular Graphics System*. San Carlos: DeLano Scientific.
- Dessi, A., Peluso, P., Dallochio, R., Weiss, R., Andreotti, G., Allocca, M., et al. (2020). Rational design, synthesis, characterization and evaluation of iodinated 4,4'-bipyridines as new transthyretin fibrillogenesis inhibitors. *Molecules* 25:2213. doi: 10.3390/molecules25092213
- Donnelly, J. P., and Hanna, M. (2017). Cardiac amyloidosis: an update on diagnosis and treatment. *Cleve. Clin. J. Med.* 84 (12 Suppl. 3), 12–26. doi: 10.3949/ccjm.84.s3.02
- Ericzon, B. G., Wilczek, H. E., Larsson, M., Wijayatunga, P., Stangou, A., Pena, J. R., et al. (2015). Liver transplantation for hereditary transthyretin amyloidosis: after 20 years still the best therapeutic alternative? *Transplantation* 99, 1847–1854. doi: 10.1097/TP.0000000000000574
- Falk, R. H., and Dubrey, S. W. (2010). Amyloid heart disease. *Prog. Cardiovasc. Dis.* 52, 347–361. doi: 10.1016/j.pcad.2009.11.007
- Ferreira, N., Cardoso, I., Domingues, M. R., Vitorino, R., Bastos, M., Bai, G., et al. (2009). Binding of epigallocatechin-3-gallate to transthyretin modulates its amyloidogenicity. *FEBS Lett.* 583, 3569–3576. doi: 10.1016/j.febslet.2009.10.062
- Ferreira, N., Goncalves, N. P., Saraiva, M. J., and Almeida, M. R. (2016). Curcumin: a multi-target disease-modifying agent for late-stage transthyretin amyloidosis. *Sci. Rep.* 6:26623. doi: 10.1038/srep26623
- Ferreira, N., Pereira-Henriques, A., Attar, A., Klarner, F. G., Schrader, T., Bitan, G., et al. (2014). Molecular tweezers targeting transthyretin amyloidosis. *Neurotherapeutics* 11, 450–461. doi: 10.1007/s13311-013-0256-8
- Ferreira, N., Santos, S. A., Domingues, M. R., Saraiva, M. J., and Almeida, M. R. (2013). Dietary curcumin counteracts extracellular transthyretin deposition: insights on the mechanism of amyloid inhibition. *Biochim. Biophys. Acta* 1832, 39–45. doi: 10.1016/j.bbdis.2012.10.007
- Ferreira, N., Saraiva, M. J., and Almeida, M. R. (2011). Natural polyphenols inhibit different steps of the process of transthyretin (TTR) amyloid fibril formation. *FEBS Lett.* 585, 2424–2430. doi: 10.1016/j.febslet.2011.06.030
- Ferreira, N., Saraiva, M. J., and Almeida, M. R. (2012). Epigallocatechin-3-gallate as a potential therapeutic drug for TTR-related amyloidosis: “in vivo” evidence from FAP mice models. *PLoS ONE* 7:e29933. doi: 10.1371/journal.pone.0029933
- Ferreira, N., Saraiva, M. J., and Almeida, M. R. (2019). Uncovering the neuroprotective mechanisms of curcumin on transthyretin amyloidosis. *Int. J. Mol. Sci.* 20:1287. doi: 10.3390/ijms20061287
- Folli, C., Favilla, R., and Berni, R. (2010). The interaction between retinol-binding protein and transthyretin analyzed by fluorescence anisotropy. *Methods Mol. Biol.* 652, 189–207. doi: 10.1007/978-1-60327-325-1\_11
- French, K., Yerbury, J. J., and Wilson, M. R. (2008). Protease activation of alpha2-macroglobulin modulates a chaperone-like action with broad specificity. *Biochemistry* 47, 1176–1185. doi: 10.1021/bi701976f



- Gaetani, S., Bellovino, D., Aprea, M., and Devirgiliis, C. (2002). Hepatic synthesis, maturation and complex formation between retinol-binding protein and transthyretin. *Clin. Chem. Lab. Med.* 40, 1211–1220. doi: 10.1515/CCLM.2002.211
- Galant, N. J., Bugyei-Twum, A., Rakshit, R., Walsh, P., Sharpe, S., Arslan, P. E., et al. (2016). Substoichiometric inhibition of transthyretin misfolding by immune-targeting sparsely populated misfolding intermediates: a potential diagnostic and therapeutic for TTR amyloidosis. *Sci. Rep.* 6:25080. doi: 10.1038/srep25080
- Galant, N. J., Westermarck, P., Higaki, J. N., and Chakrabarty, A. (2017). Transthyretin amyloidosis: an under-recognized neuropathy and cardiomyopathy. *Clin. Sci.* 131, 395–409. doi: 10.1042/CS20160413
- Gamez, J., Salvado, M., Reig, N., Sune, P., Casasnovas, C., Rojas-García, R., et al. (2019). Transthyretin stabilization activity of the catechol-O-methyltransferase inhibitor tolcapone (SOM0226) in hereditary ATTR amyloidosis patients and asymptomatic carriers: proof-of-concept study(). *Amyloid* 26, 74–84. doi: 10.1080/13506129.2019.1597702
- Gertz, M. A., Mauermann, M. L., Grogan, M., and Coelho, T. (2019). Advances in the treatment of hereditary transthyretin amyloidosis: a review. *Brain Behav.* 9:e01371. doi: 10.1002/brb3.1371
- Gomes, J. R., Nogueira, R. S., Vieira, M., Santos, S. D., Ferraz-Nogueira, J. P., Relvas, J. B., et al. (2016). Transthyretin provides trophic support via megalin by promoting neurite outgrowth and neuroprotection in cerebral ischemia. *Cell Death Differ* 23, 1749–1764. doi: 10.1038/cdd.2016.64
- Gomes, J. R., Sarkany, Z., Teixeira, A., Nogueira, R., Cabrito, I., Soares, H., et al. (2019). Anti-TTR nanobodies allow the identification of TTR neurotogenic epitope associated with TTR-megalin neurotrophic activities. *ACS Chem. Neurosci.* 10, 704–715. doi: 10.1021/acchemneuro.8b00502
- Goto, T., Yamashita, T., Ueda, M., Ohshima, S., Yoneyama, K., Nakamura, M., et al. (2006). Iatrogenic amyloid neuropathy in a Japanese patient after sequential liver transplantation. *Am. J. Transplant* 6, 2512–2515. doi: 10.1111/j.1600-6143.2006.01484.x
- Greene, M. J., Klimtchuk, E. S., Seldin, D. C., Berk, J. L., and Connors, L. H. (2015). Cooperative stabilization of transthyretin by clusterin and diflunisal. *Biochemistry* 54, 268–278. doi: 10.1021/bi5011249
- Greene, M. J., Sam, F., Soo Hoo, P. T., Patel, R. S., Seldin, D. C., and Connors, L. H. (2011). Evidence for a functional role of the molecular chaperone clusterin in amyloidotic cardiomyopathy. *Am. J. Pathol.* 178, 61–68. doi: 10.1016/j.ajpath.2010.11.015
- Gustafsson, S., Ihse, E., Henein, M. Y., Westermarck, P., Lindqvist, P., and Suhr, O. B. (2012). Amyloid fibril composition as a predictor of development of cardiomyopathy after liver transplantation for hereditary transthyretin amyloidosis. *Transplantation* 93, 1017–1023. doi: 10.1097/TP.0b013e31824b3749
- Habtemariam, B. A., Karsten, V., Attarwala, H., Goel, V., Melch, M., Clausen, V. A., et al. (2020). Single-dose pharmacokinetics and pharmacodynamics of transthyretin targeting n-acetylgalactosamine-small interfering ribonucleic acid conjugate, vutrisiran, in healthy subjects. *Clin. Pharmacol. Ther.* doi: 10.1002/cpt.1974. [Epub ahead of print].
- Hu, S., Loo, J. A., and Wong, D. T. (2006). Human body fluid proteome analysis. *Proteomics* 6, 6326–6353. doi: 10.1002/pmic.200600284
- Ihse, E., Rapezzi, C., Merlini, G., Benson, M. D., Ando, Y., Suhr, O. B., et al. (2013). Amyloid fibrils containing fragmented ATTR may be the standard fibril composition in ATTR amyloidosis. *Amyloid* 20, 142–150. doi: 10.3109/13506129.2013.797890
- Ihse, E., Suhr, O. B., Hellman, U., and Westermarck, P. (2011). Variation in amount of wild-type transthyretin in different fibril and tissue types in ATTR amyloidosis. *J. Mol. Med.* 89, 171–180. doi: 10.1007/s00109-010-0695-1
- Ihse, E., Ybo, A., Suhr, O., Lindqvist, P., Backman, C., and Westermarck, P. (2008). Amyloid fibril composition is related to the phenotype of hereditary transthyretin V30M amyloidosis. *J. Pathol.* 216, 253–261. doi: 10.1002/path.2411
- Jacobson, D. R., Pastore, R. D., Yaghoubian, R., Kane, I., Gallo, G., Buck, F. S., et al. (1997). Variant-sequence transthyretin (isoleucine 122) in late-onset cardiac amyloidosis in black Americans. *N. Engl. J. Med.* 336, 466–473. doi: 10.1056/NEJM199702133360703
- Judge, D. P., Heitner, S. B., Falk, R. H., Maurer, M. S., Shah, S. J., Witteles, R. M., et al. (2019). Transthyretin Stabilization by AG10 in Symptomatic Transthyretin Amyloid Cardiomyopathy. *J. Am. Coll. Cardiol* 74, 285–295. doi: 10.1016/j.jacc.2019.03.012
- Kanda, Y., Goodman, D. S., Canfield, R. E., and Morgan, F. J. (1974). The amino acid sequence of human plasma prealbumin. *J. Biol. Chem* 249, 6796–6805.
- Kato-Motozaki, Y., Ono, K., Shima, K., Morinaga, A., Machiya, T., Nozaki, I., et al. (2008). Epidemiology of familial amyloid polyneuropathy in Japan: Identification of a novel endemic focus. *J. Neurol. Sci.* 270, 133–140. doi: 10.1016/j.jns.2008.02.019
- Koike, H., and Katsuno, M. (2020). Transthyretin amyloidosis: update on the clinical spectrum, pathogenesis, and disease-modifying therapies. *Neurol. Ther.* 1–17. doi: 10.1007/s40120-020-00210-7. [Epub ahead of print].
- Koike, H., Kiuchi, T., Iijima, M., Ueda, M., Ando, Y., Morozumi, S., et al. (2011). Systemic but asymptomatic transthyretin amyloidosis 8 years after domino liver transplantation. *J. Neurol. Neurosurg. Psychiatr.* 82, 1287–1290. doi: 10.1136/jnnp.2010.218958
- Kolstoe, S. E., Mangione, P. P., Bellotti, V., Taylor, G. W., Tennent, G. A., Deroo, S., et al. (2010). Trapping of palindromic ligands within native transthyretin prevents amyloid formation. *Proc. Natl. Acad. Sci. U.S.A.* 107, 20483–20488. doi: 10.1073/pnas.1008255107
- Kristen, A. V., Lehrke, S., Buss, S., Mereles, D., Steen, H., Ehlermann, P., et al. (2012). Green tea halts progression of cardiac transthyretin amyloidosis: an observational report. *Clin. Res. Cardiol.* 101, 805–813. doi: 10.1007/s00392-012-0463-z
- Lee, K. W., Lee, D. H., Son, H., Kim, Y. S., Park, J. Y., Roh, G. S., et al. (2009). Clusterin regulates transthyretin amyloidosis. *Biochem. Biophys. Res. Commun.* 388, 256–260. doi: 10.1016/j.bbrc.2009.07.166
- Lewis, W. D., Skinner, M., Simms, R. W., Jones, L. A., Cohen, A. S., and Jenkins, R. L. (1994). Orthotopic liver transplantation for familial amyloidotic polyneuropathy. *Clin Transplant* 8(2 Pt 1), 107–110.
- Liepnies, J. J., Wilson, D. L., and Benson, M. D. (2006). Biochemical characterization of vitreous and cardiac amyloid in Ile84Ser transthyretin amyloidosis. *Amyloid* 13, 170–177. doi: 10.1080/13506120600877003
- Liz, M. A., Faro, C. J., Saraiva, M. J., and Sousa, M. M. (2004). Transthyretin, a new cryptic protease. *J. Biol. Chem* 279, 21431–21438. doi: 10.1074/jbc.M402212200
- Liz, M. A., Fleming, C. E., Nunes, A. F., Almeida, M. R., Mar, F. M., Choe, Y., et al. (2009). Substrate specificity of transthyretin: identification of natural substrates in the nervous system. *Biochem. J.* 419, 467–474. doi: 10.1042/BJ20082090
- Liz, M. A., Mar, F. M., Franquinho, F., and Sousa, M. M. (2010). Aboard transthyretin: From transport to cleavage. *IUBMB Life* 62, 429–435. doi: 10.1002/iub.340
- Macedo, A. V. S., Schwartzmann, P. V., de Gusmao, B. M., Melo, M. D. T., and Coelho-Filho, O. R. (2020). Advances in the Treatment of Cardiac Amyloidosis. *Curr. Treat. Options Oncol.* 21:36. doi: 10.1007/s11864-020-00738-8
- Macedo, B., Batista, A. R., Ferreira, N., Almeida, M. R., and Saraiva, M. J. (2008). Anti-apoptotic treatment reduces transthyretin deposition in a transgenic mouse model of Familial Amyloidotic Polyneuropathy. *Biochim. Biophys. Acta* 1782, 517–522. doi: 10.1016/j.bbdis.2008.05.005
- Magalhaes, J., and Saraiva, M. J. (2011). Clusterin overexpression and its possible protective role in transthyretin deposition in familial amyloidotic polyneuropathy. *J. Neuropathol. Exp. Neurol.* 70, 1097–1106. doi: 10.1097/NEN.0b013e31823a44f4
- Maia, L. F., Magalhaes, R., Freitas, J., Taipa, R., Pires, M. M., Osorio, H., et al. (2015). CNS involvement in V30M transthyretin amyloidosis: clinical, neuropathological and biochemical findings. *J. Neurol. Neurosurg. Psychiatr.* 86, 159–167. doi: 10.1136/jnnp-2014-308107
- Mangione, P. P., Porcari, R., Gillmore, J. D., Pucci, P., Monti, M., Porcari, M., et al. (2014). Proteolytic cleavage of Ser52Pro variant transthyretin triggers its amyloid fibrillogenesis. *Proc. Natl. Acad. Sci. U.S.A.* 111, 1539–1544. doi: 10.1073/pnas.1317488111
- Mangione, P. P., Verona, G., Corazza, A., Marcoux, J., Canetti, D., Giorgetti, S., et al. (2018). Plasminogen activation triggers transthyretin amyloidogenesis in vitro. *J. Biol. Chem.* 293, 14192–14199. doi: 10.1074/jbc.RA118.003990
- Marcoux, J., Mangione, P. P., Porcari, R., Degiacomi, M. T., Verona, G., Taylor, G. W., et al. (2015). A novel mechano-enzymatic cleavage mechanism underlies transthyretin amyloidogenesis. *EMBO Mol. Med.* 7, 1337–1349. doi: 10.15252/emmm.201505357

- Matsubara, E., Soto, C., Governale, S., Frangione, B., and Ghiso, J. (1996). Apolipoprotein J and Alzheimer's amyloid beta solubility. *Biochem. J.* 316 (Pt 2), 671–679.
- Maurer, M. S., Bokhari, S., Damy, T., Dorbala, S., Drachman, B. M., Fontana, M., et al. (2019). Expert consensus recommendations for the suspicion and diagnosis of transthyretin cardiac amyloidosis. *Circ. Heart Fail.* 12:e006075. doi: 10.1161/CIRCHEARTFAILURE.119.006075
- Maurer, M. S., Hanna, M., Grogan, M., Dispenzieri, A., Witteles, R., Drachman, B., et al. (2016). Genotype and phenotype of transthyretin cardiac Amyloidosis: THAOS (transthyretin amyloid outcome survey). *J. Am. Coll. Cardiol.* 68, 161–172. doi: 10.1016/j.jacc.2016.03.596
- Maurer, M. S., Schwartz, J. H., Gundapaneni, B., Elliott, P. M., Merlini, G., Waddington-Cruz, M., et al. (2018). Tafamidis treatment for patients with transthyretin amyloid cardiomyopathy. *N. Engl. J. Med.* 379, 1007–1016. doi: 10.1056/NEJMoa1805689
- McCutchen, S. L., Colon, W., and Kelly, J. W. (1993). Transthyretin mutation Leu-55-Pro significantly alters tetramer stability and increases amyloidogenicity. *Biochemistry* 32, 12119–12127. doi: 10.1021/bi00096a024
- Merlini, G., Ascarei, E., Amboldi, N., Bellotti, V., Arbustini, E., Perfetti, V., et al. (1995). Interaction of the anthracycline 4'-iodo-4'-deoxydoxorubicin with amyloid fibrils: inhibition of amyloidogenesis. *Proc. Natl. Acad. Sci. U.S.A.* 92, 2959–2963. doi: 10.1073/pnas.92.7.2959
- Miller, M., Pal, A., Albusairi, W., Joo, H., Pappas, B., Haque Tuhin, M. T., et al. (2018). Enthalpy-driven stabilization of transthyretin by AG10 mimics a naturally occurring genetic variant that protects from transthyretin amyloidosis. *J. Med. Chem.* 61, 7862–7876. doi: 10.1021/acs.jmedchem.8b00817
- Miller, S. R., Sekijima, Y., and Kelly, J. W. (2004). Native state stabilization by NSAIDs inhibits transthyretin amyloidogenesis from the most common familial disease variants. *Lab. Invest.* 84, 545–552. doi: 10.1038/labinvest.3700059
- Miroy, G. J., Lai, Z., Lashuel, H. A., Peterson, S. A., Strang, C., and Kelly, J. W. (1996). Inhibiting transthyretin amyloid fibril formation via protein stabilization. *Proc. Natl. Acad. Sci. U.S.A.* 93, 15051–15056.
- Mukherjee, D., Nissen, S. E., and Topol, E. J. (2001). Risk of cardiovascular events associated with selective COX-2 inhibitors. *JAMA* 286, 954–959. doi: 10.1001/jama.286.8.954
- Mumford, A. D., O'Donnell, J., Gillmore, J. D., Manning, R. A., Hawkins, P. N., and Laffan, M. (2000). Bleeding symptoms and coagulation abnormalities in 337 patients with AL-amyloidosis. *Br. J. Haematol.* 110, 454–460. doi: 10.1046/j.1365-2141.2000.02183.x
- Munar-Ques, M., Salva-Ladaria, L., Mulet-Perera, P., Sole, M., Lopez-Andreu, F. R., and Saraiva, M. J. (2000). Vitreous amyloidosis after liver transplantation in patients with familial amyloid polyneuropathy: ocular synthesis of mutant transthyretin. *Amyloid* 7, 266–269. doi: 10.3109/13506120009146440
- Murakami, T., Ohsawa, Y., Zhenghua, L., Yamamura, K., and Sunada, Y. (2010). The transthyretin gene is expressed in Schwann cells of peripheral nerves. *Brain Res.* 1348, 222–225. doi: 10.1016/j.brainres.2010.06.017
- Obici, L., and Merlini, G. (2014). An overview of drugs currently under investigation for the treatment of transthyretin-related hereditary amyloidosis. *Expert Opin. Investig. Drugs* 23, 1239–1251. doi: 10.1517/13543784.2014.922541
- Okamoto, S., Zhao, Y., Lindqvist, P., Backman, C., Ericzon, B. G., Wijayatunga, P., et al. (2011). Development of cardiomyopathy after liver transplantation in Swedish hereditary transthyretin amyloidosis (ATTR) patients. *Amyloid* 18, 200–205. doi: 10.3109/13506129.2011.615872
- Ortore, G., and Martinelli, A. (2012). Computational Studies on Transthyretin. *Curr. Med. Chem.* 19, 2380–2387. doi: 10.2174/092986712800269344
- Patel, K. S., and Hawkins, P. N. (2015). Cardiac amyloidosis: where are we today? *J. Intern. Med.* 278, 126–144. doi: 10.1111/joim.12383
- Penchala, S. C., Connelly, S., Wang, Y., Park, M. S., Zhao, L., Baranczak, A., et al. (2013). AG10 inhibits amyloidogenesis and cellular toxicity of the familial amyloid cardiomyopathy-associated V122I transthyretin. *Proc. Natl. Acad. Sci. U.S.A.* 110, 9992–9997. doi: 10.1073/pnas.1300761110
- Pinheiro, F., Varejao, N., Esperante, S., Santos, J., Velazquez-Campoy, A., Reverter, D., et al. (2020). Tolcapone, a potent aggregation inhibitor for the treatment of familial leptomeningeal amyloidosis. *FEBS J.* doi: 10.1111/febs.15339. [Epub ahead of print].
- Pitkanen, P., Westermark, P., and Cornwell, G. G. III. (1984). Senile systemic amyloidosis. *Am. J. Pathol.* 117, 391–399.
- Plante-Bordeneuve, V., and Said, G. (2011). Familial amyloid polyneuropathy. *Lancet Neurol.* 10, 1086–1097. doi: 10.1016/S1474-4422(11)70246-0
- Poon, S., Easterbrook-Smith, S. B., Rybchyn, M. S., Carver, J. A., and Wilson, M. R. (2000). Clusterin is an ATP-independent chaperone with very broad substrate specificity that stabilizes stressed proteins in a folding-competent state. *Biochemistry* 39, 15953–15960. doi: 10.1021/bi002189x
- Quarta, C. C., Buxbaum, J. N., Shah, A. M., Falk, R. H., Claggett, B., Kitzman, D. W., et al. (2015). The amyloidogenic V122I transthyretin variant in elderly black Americans. *N. Engl. J. Med.* 372, 21–29. doi: 10.1056/NEJMoa1404852
- Quintas, A., Saraiva, M. J., and Brito, R. M. (1999). The tetrameric protein transthyretin dissociates to a non-native monomer in solution. A novel model for amyloidogenesis. *J. Biol. Chem.* 274, 32943–32949. doi: 10.1074/jbc.274.46.32943
- Quintas, A., Vaz, D. C., Cardoso, L., Saraiva, M. J., and Brito, R. M. (2001). Tetramer dissociation and monomer partial unfolding precedes protofibril formation in amyloidogenic transthyretin variants. *J. Biol. Chem.* 276, 27207–27213. doi: 10.1074/jbc.M101024200
- Raghu, P., and Sivakumar, B. (2004). Interactions amongst plasma retinol-binding protein, transthyretin and their ligands: implications in vitamin A homeostasis and transthyretin amyloidosis. *Biochim. Biophys. Acta* 1703, 1–9. doi: 10.1016/j.bbapap.2004.09.023
- Rapezzi, C., Lorenzini, M., Longhi, S., Milandri, A., Gagliardi, C., Bartolomei, I., et al. (2015). Cardiac amyloidosis: the great pretender. *Heart Fail. Rev.* 20, 117–124. doi: 10.1007/s10741-015-9480-0
- Rapezzi, C., Quarta, C. C., Riva, L., Longhi, S., Gallelli, I., Lorenzini, M., et al. (2010). Transthyretin-related amyloidoses and the heart: a clinical overview. *Nat. Rev. Cardiol.* 7, 398–408. doi: 10.1038/nrcardio.2010.67
- Refetoff, S. (2000). "Thyroid hormone serum transport proteins," in *Endotext* [Internet], eds K. R. Feingold, B. Anawalt, A. Boyce, et al. South Dartmouth, MA: MDText.com, Inc.
- Richardson, S. J. (2009). Evolutionary changes to transthyretin: evolution of transthyretin biosynthesis. *FEBS J.* 276, 5342–5356. doi: 10.1111/j.1742-4658.2009.07244.x
- Saelices, L., Chung, K., Lee, J. H., Cohn, W., Whitelegge, J. P., Benson, M. D., et al. (2018). Amyloid seeding of transthyretin by ex vivo cardiac fibrils and its inhibition. *Proc. Natl. Acad. Sci. U.S.A.* 115, E6741–E6750. doi: 10.1073/pnas.1805131115
- Sant'Anna, R., Gallego, P., Robinson, L. Z., Pereira-Henriques, A., Ferreira, N., Pinheiro, F., et al. (2016). Repositioning tolcapone as a potent inhibitor of transthyretin amyloidogenesis and associated cellular toxicity. *Nat. Commun.* 7:10787. doi: 10.1038/ncomms10787
- Santos, S. D., Lambertsen, K. L., Clausen, B. H., Akinc, A., Alvarez, R., Finsen, B., et al. (2010). CSF transthyretin neuroprotection in a mouse model of brain ischemia. *J. Neurochem.* 115, 1434–1444. doi: 10.1111/j.1471-4159.2010.07047.x
- Saraiva, M. J. (1995). Transthyretin mutations in health and disease. *Hum. Mutat.* 5, 191–196. doi: 10.1002/humu.1380050302
- Saraiva, M. J., Birken, S., Costa, P. P., and Goodman, D. S. (1984). Amyloid fibril protein in familial amyloidotic polyneuropathy, Portuguese type. Definition of molecular abnormality in transthyretin (prealbumin). *J. Clin. Invest.* 74, 104–119. doi: 10.1172/JCI11390
- Schormann, N., Murrell, J. R., and Benson, M. D. (1998). Tertiary structures of amyloidogenic and non-amyloidogenic transthyretin variants: new model for amyloid fibril formation. *Amyloid* 5, 175–187.
- Sekijima, Y. (2015). Transthyretin (ATTR) amyloidosis: clinical spectrum, molecular pathogenesis and disease-modifying treatments. *J. Neurol. Neurosurg. Psychiatr.* 86, 1036–1043. doi: 10.1136/jnnp-2014-308724
- Sekijima, Y., Tojo, K., Morita, H., Koyama, J., and Ikeda, S. (2015). Safety and efficacy of long-term diflunisal administration in hereditary transthyretin (ATTR) amyloidosis. *Amyloid* 22, 79–83. doi: 10.3109/13506129.2014.997872
- Sekijima, Y., Yazaki, M., Oguchi, K., Ezawa, N., Yoshinaga, T., Yamada, M., et al. (2016). Cerebral amyloid angiopathy in posttransplant

- patients with hereditary ATTR amyloidosis. *Neurology* 87, 773–781. doi: 10.1212/WNL.0000000000003001
- Sinha, S., Lopes, D. H., Du, Z., Pang, E. S., Shanmugam, A., Lomakin, A., et al. (2011). Lysine-specific molecular tweezers are broad-spectrum inhibitors of assembly and toxicity of amyloid proteins. *J. Am. Chem. Soc.* 133, 16958–16969. doi: 10.1021/ja206279b
- Sipe, J. D., Benson, M. D., Buxbaum, J. N., Ikeda, S. I., Merlini, G., Saraiva, M. J., et al. (2016). Amyloid fibril proteins and amyloidosis: chemical identification and clinical classification International Society of Amyloidosis 2016 Nomenclature Guidelines. *Amyloid* 23, 209–213. doi: 10.1080/13506129.2016.1257986
- Sousa, A., Andersson, R., Drugge, U., Holmgren, G., and Sandgren, O. (1993). Familial amyloidotic polyneuropathy in Sweden: geographical distribution, age of onset, and prevalence. *Hum. Hered.* 43, 288–294. doi: 10.1159/000154146
- Sousa, A., Coelho, T., Barros, J., and Sequeiros, J. (1995). Genetic epidemiology of familial amyloidotic polyneuropathy (FAP)-type I in Povoá do Varzim and Vila do Conde (north of Portugal). *Am. J. Med. Genet.* 60, 512–521. doi: 10.1002/ajmg.1320600606
- Sousa, M. M., Berglund, L., and Saraiva, M. J. (2000). Transthyretin in high density lipoproteins: association with apolipoprotein A-I. *J. Lipid Res.* 41, 58–65.
- Stangou, A. J., Heaton, N. D., and Hawkins, P. N. (2005). Transmission of systemic transthyretin amyloidosis by means of domino liver transplantation. *N. Engl. J. Med.* 352:2356. doi: 10.1056/NEJM200506023522219
- Suhr, O. B., Lundgren, E., and Westermark, P. (2017). One mutation, two distinct disease variants: unravelling the impact of transthyretin amyloid fibril composition. *J. Intern. Med.* 281, 337–347. doi: 10.1111/joim.12585
- Suhr, O. B., Svendsen, I. H., Andersson, R., Danielsson, A., Holmgren, G., and Ranlov, P. J. (2003). Hereditary transthyretin amyloidosis from a Scandinavian perspective. *J. Intern. Med.* 254, 225–235. doi: 10.1046/j.1365-2796.2003.01173.x
- Takahashi, R., Ono, K., Shibata, S., Nakamura, K., Komatsu, J., Ikeda, Y., et al. (2014). Efficacy of diflunisal on autonomic dysfunction of late-onset familial amyloid polyneuropathy (TTR Val30Met) in a Japanese endemic area. *J. Neurol. Sci.* 345, 231–235. doi: 10.1016/j.jns.2014.07.017
- Teixeira, C. A., Almeida Mdo, R., and Saraiva, M. J. (2016). Impairment of autophagy by TTR V30M aggregates: in vivo reversal by TUDCA and curcumin. *Clin. Sci.* 130, 1665–1675. doi: 10.1042/CS20160075
- Tojo, K., Sekijima, Y., Kelly, J. W., and Ikeda, S. (2006). Diflunisal stabilizes familial amyloid polyneuropathy-associated transthyretin variant tetramers in serum against dissociation required for amyloidogenesis. *Neurosci. Res.* 56, 441–449. doi: 10.1016/j.neures.2006.08.014
- Torres-Arancivia, C., and Connors, L. H. (2019). Effect of diflunisal on clusterin levels in ATTRwt amyloidosis. *Amyloid* 26, 49–50. doi: 10.1080/13506129.2019.1582515
- Tucker, H. M., Kihiko-Ehmann, M., Wright, S., Rydel, R. E., and Estus, S. (2000). Tissue plasminogen activator requires plasminogen to modulate amyloid-beta neurotoxicity and deposition. *J. Neurochem.* 75, 2172–2177. doi: 10.1046/j.1471-4159.2000.0752172.x
- Uchiba, M., Imamura, T., Hata, H., Tatetsu, H., Yonemura, Y., Ueda, M., et al. (2009). Excessive fibrinolysis in AL-amyloidosis is induced by urokinase-type plasminogen activator from bone marrow plasma cells. *Amyloid* 16, 89–93. doi: 10.1080/13506120902879269
- van Bennekum, A. M., Wei, S., Gamble, M. V., Vogel, S., Piantadosi, R., Gottesman, M., et al. (2001). Biochemical basis for depressed serum retinol levels in transthyretin-deficient mice. *J. Biol. Chem.* 276, 1107–1113. doi: 10.1074/jbc.M008091200
- Verona, G., Mangione, P. P., Raimondi, S., Giorgetti, S., Faravelli, G., Porcari, R., et al. (2017). Inhibition of the mechano-enzymatic amyloidogenesis of transthyretin: role of ligand affinity, binding cooperativity and occupancy of the inner channel. *Sci. Rep.* 7:182. doi: 10.1038/s41598-017-00338-x
- Vieira, M., and Saraiva, M. J. (2014). Transthyretin: a multifaceted protein. *Biomol. Concepts* 5, 45–54. doi: 10.1515/bmc-2013-0038
- Wei, S., Episkopou, V., Piantadosi, R., Maeda, S., Shimada, K., Gottesman, M. E., et al. (1995). Studies on the metabolism of retinol and retinol-binding protein in transthyretin-deficient mice produced by homologous recombination. *J. Biol. Chem.* 270, 866–870. doi: 10.1074/jbc.270.2.866
- Westermark, P., Bergstrom, J., Solomon, A., Murphy, C., and Sletten, K. (2003). Transthyretin-derived senile systemic amyloidosis: clinicopathologic and structural considerations. *Amyloid* 10 Suppl 1, 48–54.
- Westermark, P., Sletten, K., Johansson, B., and Cornwell, G. G. III. (1990). Fibril in senile systemic amyloidosis is derived from normal transthyretin. *Proc. Natl. Acad. Sci. U.S.A.* 87, 2843–2845.
- Wojtczak, A., Cody, V., Luft, J. R., and Pangborn, W. (1996). Structures of human transthyretin complexed with thyroxine at 2.0 Å resolution and 3',5'-dinitro-N-acetyl-L-tyrosine at 2.2 Å resolution. *Acta Crystallogr D Biol Crystallogr* 52(Pt 4), 758–765. doi: 10.1107/S0907444996003046
- Wyatt, A., Yerbury, J., Poon, S., Dabbs, R., and Wilson, M. (2009). Chapter 6: The chaperone action of Clusterin and its putative role in quality control of extracellular protein folding. *Adv. Cancer Res.* 104, 89–114. doi: 10.1016/S0065-230X(09)04006-8
- Wyatt, A. R., Yerbury, J. J., Ecroyd, H., and Wilson, M. R. (2013). Extracellular chaperones and proteostasis. *Annu. Rev. Biochem.* 82, 295–322. doi: 10.1146/annurev-biochem-072711-163904
- Yerbury, J. J., Poon, S., Meehan, S., Thompson, B., Kumita, J. R., Dobson, C. M., et al. (2007). The extracellular chaperone clusterin influences amyloid formation and toxicity by interacting with prefibrillar structures. *FASEB J.* 21, 2312–2322. doi: 10.1096/fj.06-7986com
- Yerbury, J. J., Rybchyn, M. S., Easterbrook-Smith, S. B., Henriques, C., and Wilson, M. R. (2005). The acute phase protein haptoglobin is a mammalian extracellular chaperone with an action similar to clusterin. *Biochemistry* 44, 10914–10925. doi: 10.1021/bi050764x
- Yokoyama, T., Mizuguchi, M., Nabeshima, Y., Kusaka, K., Yamada, T., Hosoya, T., et al. (2012). Hydrogen-bond network and pH sensitivity in transthyretin: Neutron crystal structure of human transthyretin. *J. Struct. Biol.* 177, 283–290. doi: 10.1016/j.jsb.2011.12.022
- Zhao, L. J., and Lei, M. (2014). Computational Chemical Studies on Transthyretin. *Progress Chem.* 26, 193–202. doi: 10.7536/PC130612
- Zhou, S., Cheng, J., Yang, T., Ma, M., Zhang, W., Yuan, S., et al. (2019). Exploration of the misfolding mechanism of transthyretin monomer: insights from hybrid-resolution simulations and markov state model analysis. *Biomolecules* 9:889. doi: 10.3390/biom9120889

**Conflict of Interest:** The authors declare that the research was conducted in the absence of any commercial or financial relationships that could be construed as a potential conflict of interest.

Copyright © 2020 Bezerra, Saraiva and Almeida. This is an open-access article distributed under the terms of the Creative Commons Attribution License (CC BY). The use, distribution or reproduction in other forums is permitted, provided the original author(s) and the copyright owner(s) are credited and that the original publication in this journal is cited, in accordance with accepted academic practice. No use, distribution or reproduction is permitted which does not comply with these terms.

# Advantages of publishing in Frontiers



## OPEN ACCESS

Articles are free to read  
for greatest visibility  
and readership



## FAST PUBLICATION

Around 90 days  
from submission  
to decision



## HIGH QUALITY PEER-REVIEW

Rigorous, collaborative,  
and constructive  
peer-review



## TRANSPARENT PEER-REVIEW

Editors and reviewers  
acknowledged by name  
on published articles

## Frontiers

Avenue du Tribunal-Fédéral 34  
1005 Lausanne | Switzerland

**Visit us:** [www.frontiersin.org](http://www.frontiersin.org)

**Contact us:** [frontiersin.org/about/contact](http://frontiersin.org/about/contact)



## REPRODUCIBILITY OF RESEARCH

Support open data  
and methods to enhance  
research reproducibility



## DIGITAL PUBLISHING

Articles designed  
for optimal readership  
across devices



## FOLLOW US

@frontiersin



## IMPACT METRICS

Advanced article metrics  
track visibility across  
digital media



## EXTENSIVE PROMOTION

Marketing  
and promotion  
of impactful research



## LOOP RESEARCH NETWORK

Our network  
increases your  
article's readership